Abdul Shakoor
Kerry Cato   *Editors*

IAEG/AEG Annual Meeting Proceedings, San Francisco, California, 2018—

Volume 6

Advances in Engineering Geology:
Education, Soil and Rock Properties, Modeling

Springer

IAEG/AEG Annual Meeting Proceedings,
San Francisco, California, 2018—Volume 6

Abdul Shakoor • Kerry Cato
Editors

IAEG/AEG Annual Meeting Proceedings, San Francisco, California, 2018—Volume 6

Advances in Engineering Geology: Education, Soil and Rock Properties, Modeling

Springer

Editors
Abdul Shakoor
Department of Geology
Kent State University
Kent, OH, USA

Kerry Cato
Department of Geological Sciences
California State University
San Bernardino, CA, USA

Cover illustration: Golden Gate Bridge at night. © Frederic Prochasson 123rf.com

Preface

The XIII IAEG Congress and 61st AEG Annual Meeting, San Francisco, USA, chose *Engineering Geology for a Sustainable World* as the theme for 2018. Based on the topical symposia and technical sessions, the proceedings are organized into six volumes and sub-categories as follows:

Volume 1: Slope Stability: Case Histories, Landslide Mapping, Emerging Technologies
Volume 2: Geotechnical and Environmental Site Characterization
Volume 3: Mining, Aggregates, Karst
Volume 4: Dams, Tunnels, Groundwater Resources, Climate Change
Volume 5: Geologic Hazards: Earthquakes, Land Subsidence, Coastal Hazards, and
          Emergency Response
Volume 6: Advances in Engineering Geology: Education, Soil and Rock Properties, Modeling

Participants of this joint meeting had the option to submit either a full paper or only an abstract. The editors would like to thank the authors for their valuable contributions. One hundred eighty-six full papers were submitted for the review, and 153 papers successfully completed the process. Each paper submitted for the proceedings was peer-reviewed by two reviewers. Authors revised their papers in accordance with reviewers' comments. The reviewers, from across the globe, included professional experts as well as authors of other papers. The editors greatly appreciate the help provided by reviewers. A list of reviewers follows.

The editors are also very grateful to Karen Smith and Paisley Cato for their assistance throughout the review process.

Kent, OH, USA   Abdul Shakoor
San Bernardino, CA, USA   Kerry Cato
2018

Organization

General Meeting Chairs

Sarah Kalika, Cornerstone Earth Group
Gary Luce, Resource Concepts, Inc.
Coralie Wilhite, United States Army Corps of Engineers

Field Course Chairs

Chase White, California Geological Survey
Drew Kennedy, Sage Engineers

IAEG Planning Committee Heads

Scott Burns, Portland State University
Jeffrey R. Keaton, Wood

Proceedings Editors

Abdul Shakoor, Kent State University
Kerry Cato, Cato Geoscience, Inc./California State University, San Bernardino

Editorial Assistants

Karen Smith, Kent State University
Paisley Cato, Cato Geoscience, Inc.

Short Course Chairs

E. Morley Beckman, Kleinfelder
Byron Anderson, Kleinfelder
Chrissey Villeneuve, Shannon & Wilson, Inc.

Technical Program Committee

Abdul Shakoor, Kent State University
Kerry Cato, Cato Geoscience, Inc./California State University, San Bernardino
William Godwin, Consulting Geologist
Sarah Kalika, Cornerstone Earth Group

Symposium Chairs

Robert E. Tepel, Retired Professional Geologist and Certified Engineering Geologist
Brian H. Greene, United States Army Corps of Engineers
Donald Bruce, Geosystems, L.P.
Holly Nichols, California Department of Water Resources
Keith Turner, Colorado School of Mines
Fred Baynes, Consulting Engineering Geologist
Kevin McCoy, Colorado Geological Survey

Hilary Whitney, Environmental Resources Management
Michelle Sneed, United States Geological Survey
Thomas Oommen, Michigan Technological University
Julien Waeber, AECOM
Ed Medley, Consulting Geological Engineer
Mark Bailey, Asbestos TEM Labs
Atiye Tugrul, Istanbul University, Avcilar Campus, Turkey
Lindsay Swain, Dudek
Ike Isaacson, Brierley Associates
Mike Piepenburg, Aldea Services, LLC
Bruce Hilton, Kleinfelder
Anne Rosinski, California Geological Survey
Steve Parry, Parry Engineering Geological Services
Jan Novotny, Ceska Geologicka Sluzba, Czech Republic
Xiaolei Liu, Shandong Provincial Key Laboratory of Marine Environment and Geological
Engineering (Ocean University of China), China

Field Course Leaders and Contributors

William Godwin, Consulting Geologist
William McCormick, Kleinfelder
Bradley Erskine, Kleinfelder
Marina Mascorro, Langan
Frank Rollo, Rollo & Ridley
John Egan, Sage Engineers
Ken Johnson, WSP
John Wallace, Cotton, Shires and Associates, Inc.
Ryan Seelbach, Geosyntec
Tom Barry, California Department of Conservation, Division of Oil, Gas and Geothermal
Resources
John Wakabayashi, Fresno State University
Greg Stock, Yosemite National Park
Janet Sowers, Fugro
Jim Lienkaemper, United States Geological Survey
Keith Kelson, United States Army Corps of Engineers
Carol Prentice, United States Geological Survey
Gordon Seitz, California Department of Conservation
Chris Madugo, Pacific Gas & Electric Company
Mike Jewett, Miller Pacific Engineers
Ray Sullivan, San Francisco State University
George Ford, Geosyntec
Wayne Akiyama, APTIM
Ryan Coe, Terracon
Kate Zeiger, AECOM
John Murphy, California State Water Resources Control Board
Jennifer Gomez, Syar Industries
Mike George, BGC Engineering
Nick Sitar, University of California, Berkeley
Peter Holland, California Geological Survey
Chris Hundemer, C2earth
Jake Hudson, Holdrege & Kull/NV5
Shane Cummings, Holdrege & Kull/NV5
Chris Hitchcock, InfraTerra
Roxanne Renedo, BSK Associates
Tim Dawson, California Department of Conservation

Margaret Doolittle, Kleinfelder
Kevin Clahan, Lettis Consultants
Donald Wells, AMEC/Foster Wheeler
Jennifer Dean, California State Water Resources Control Board
Felix Desperrier, Lettis Consultants
Karen Grove, San Francisco State University

Guest Tour Chairs

Alice Tepel
Linda Upp

Publicity Committee

Nathan Saraceno, DiGioia Gray & Associates
Courtney Johnson, Sage Engineers
Maggie Parks, ENGEO

Sponsorship Chair

Courtney Johnson, Sage Engineers

Technical Session Editing

Bill Yu, Case Western Reserve University

Guidebook App

Clayton Johnson, Golder Associates
Nathan Saraceno, DiGioia Gray & Associates

Fed IGS

Jean-Louis Briaud, Texas A&M University

K-12 Teacher Workshop

Cynthia Pridmore, California Geological Survey

Special Event

E. Morley Beckman, Kleinfelder

AEG Meeting Manager

Heather Clark, Association of Environmental & Engineering Geologists

AEG Headquarters

AMR Management

List of Reviewers

David Abbott, USA
Biljana Abolmasov, Serbia
Okechukwu Aghamelu, Nigeria
M. Farooq Ahmed, Pakistan
Paolo Allasia, Italy
Priyanthi Amarasinghe, USA
Sofia Anagnostopoulou, Greece
Pedro Andrade, Portugal
Luis Bacellar, Brazil
Marco Baldo, Italy
Elizabeth Beckman, USA
Zbigniew Bednarczyk, Poland
Eduardo Bergillos Navarro, Spain
David Bieber, USA
Candan BíLen, Turkey
Andrée Blais-Stevens, Canada
Peter Bobrowsky, Canada
Nana Bolashvili, Georgia
James Borchers, USA
Anika Braun, Germany
Stephanie Briggs, USA
Luke Brouwers, United Arab Emirates
Brian Bruckno, USA
Matthias Brugger, Germany
Fintan Buggy, Ireland
Domenico Calcaterra, Italy
Michael Carpenter, USA
Kerry Cato, USA
Andrea Cevasco, Italy
Hannah Chapella, USA
Xiaoli Chen, China
Sibonakaliso Chiliza, South Africa
Jeff Coe, USA
Mike Collins, USA
Brian Conway, USA
Jasper Cook, UK
Isabela Coutinho, Brazil
John Cripps, UK
Balázs Czinder, Hungary
Ranjan Kumar Dahal, Nepal
Jerome De Graff, USA
Rachael Delaney, USA
Artem Demenev, Russia

Diego Di Martire, Italy
Matthys Dippenaar, South Africa
Angelo Doglioni, Italy
Anastasia Dorozhko, Russia
Peter Ellecosta, Germany
Selman Er, Turkey
Olga Eremina, Russia
Georg Erharter, Austria
Moises Failache, Brazil
Andrew Farrant, UK
Zhen Feng, China
Clark Fenton, New Zealand
Maria Ferentinou, South Africa
Kenneth Fergason, USA
Isabel Fernandes, Portugal
Paz Fernandez, Spain
Mohammad Feruj Alam, Bangladesh
Phil Flentje, Australia
Yannis Fourniadis, UK
Edwin Friend, USA
Irina Galitskaya, Russia
George Gaprindashvili, Georgia
George Gardner, USA
Jesus Garrido Manrique, Spain
Eldon Gath, USA
Ben Gilson, UK
Daniele Giordan, Italy
William Godwin, USA
Robert Goldsmith, Australia
Dick Gray, USA
Brian Greene, USA
James Hamel, USA
Hans-Balder-Havenith, Belgium
Greg Hempen, USA
Egerton Hingston, South Africa
Peter Hudec, Canada
Matthew Huebner, USA
Maria Ingunza, Brazil
Upali De Silva Jayawardena, Sri Lanka
Filipe Jeremias, Portugal
Brendon Jones, South Africa
Frank Jordan, USA
Kumud Raj Kafle, Nepal
Sarah Kalika, USA
Efstratios Karantanellis, Greece
Ekaterina Karfidova, Russia
Hamza Karrad, Algeria
Heiko Käsling, Germany
Brian Katz, USA
Katerina Kavoura, Greece
Andrey Kazeev, Russia
Jeffrey Keaton, USA
Klaus-Peterkeilig, Germany
Alexey Kindler, Russia
Matheus Klein Flach, Brazil

Aliki Kokkala, Greece
Goh Thian Lai, Malaysia
Hana Lee, Austria
Nkopane Lefu, South Africa
Leticia Lescano, Argentina
Cheng Li, China
Wenping Li, China
Qian Liu, Austria
José Lollo, Brazil
Silvina Marfil, Argentina
Vassilis Marinos, Greece
Milos Marjanovic, Serbia
Kristofer Marsch, Germany
Pedro Martins, New Zealand
Flora Menezes, Germany
Amira Merchichi, Algeria
Olga Meshcheriakova, Russia
Stuart Millis, Hong Kong
Omar Mimouni, Algeria
Oleg Mironov, Russia
Matthew Morris, USA
Tim Mote, Australia
Elena Mraz, Germany
Marcos Musso, Uruguay
Masashi Nakaya, Japan
Arpita Nandi, USA
Marivaldo Dos Nascimento, Brazil
Monique Neves, Brazil
Holly Nichols, USA
Vanessa Noveletto, Brazil
Takehiro Ohta, Japan
Kazuhiro Onuma, Japan
Thomas Oommen, USA
Rolando Orense, New Zealand
Ibrahim Oyediran, Nigeria
George Papathanasiou, Greece
Steve Parry, UK
Darren Paul, Australia
Osni Jose Pejon, Brazil
Giacomo Pepe, Italy
Regina Pläsken, Germany
Lindsay Poluga, USA
Joaquim Pombo, Portugal
Martin Potten, Germany
Constantin Prins, Germany
Mário Quinta-Ferreira, Portugal
Rute Ramos, Portugal
Emanuele Raso, Italy
Liana Rocha, Brazil
Valéria Rodrigues, Brazil
Michael Rucker, USA
Nicholas Sabatakakis, Greece
Rosanna Saindon, USA
Mahin Salimi, Iran
Ligia Sampaio, Brazil

Paul Santi, USA
Regiane Sbroglia, Brazil
David Scarpato, USA
Malcolm Schaeffer, USA
William Schulz, USA
Jorge Sfragulla, Argentina
Sachin Shah, USA
Abdul Shakoor, USA
Timothy Shevlin, USA
Anna Shidlovskaya, Russia
Roy Shlemon, USA
Zachary Simpson, South Africa
Alessandra Siqueira, Brazil
Young-Suk Song, South Korea
Georg Stockinger, Germany
Alexander Strom, Russia
Wanghua Sui, China
Valentina Svalova, Russia
Debora Targa, Brazil
Ashley Tizzano, USA
Ákos Török, Hungary
Emil Tsereteli, Georgia
Ryosuke Tsuruta, Japan
Atiye Tugrul, Turkey
Alan Keith Turner, USA
Anatilii Tushev, Ukraine
Resat Ulusay, Turkey
Isabella Magalhães Valadares, Brazil
Lazaro Valezuquette, Brazil
J. Louis Van Rooy, South Africa
Ioannis Vazaios, Canada
Marlene Villeneuve, New Zealand
Nicholas Vlachopoulos, Canada
Yasuhiko Wakizaka, Japan
Chester (Skip) Watts, USA
Luke Weidner, USA
Baoping Wen, China
Charles Wilk, USA
Stephen Wilkinson, UK
John Williams, USA
Louis Wong, Hong Kong
Martin Woodard, USA
Richard Wooten, USA
Yang Yang, China
Katherine Yates, New Zealand
Julia Yeakley, USA
Murat Yilmaz, Turkey
Zelin Zhang, China

Contents

Territorial Zoning by Natural Conditions as a Nature-Like Technology in Engineering Geology

Victor Osipov, Nadezda Rumyantseva, and Olga Eremina

Abstract

The strategy of human-nature interaction is considered, which is based on two kinds of anthropogenic activities: (a) nature consumption, i.e., extraction and consumption of natural resources necessary for civilization survival and (b) nature use or nature management in the course of economic activity, which is aimed at providing comfortable and safe living on the Earth. Implementation of the first principle depends on the technological level of civilization development, whereas the second principle presumes adapting the economic activity to natural conditions. The paper discusses the principles of adaptive nature-use technologies and it cites cases of their application to civil construction and waste management. The nature-like technologies based on the adaptation principle are aimed at mitigating the adverse impact of construction sites on the environment and at providing safety of engineering structures.

1 Adaptation as a Nature-Like Technology

People interact with nature through two kinds of activities: (a) extraction and consumption of natural resources, which is vital for maintaining their living; (b) nature use in the course of economic activity aimed at creation of comfortable and safe living conditions. Both approaches are usually regarded as nature management, although they differ radically in their conceptual essence. The former approach is based on the consumption (often irreversible) of life-supporting resources, i.e., foodstuff, energy, water, pure air, etc. The latter approach implies living in agreement with nature; its resources being used for creating comfortable living conditions and improving the quality of life.

Proceeding from this idea, the principles and methods of nature consumption and nature management are different. Nature consumption is inevitably accompanied by the withdrawal of natural resources from the Earth, resulting in their shortage. Therefore, nature consumption should be based on the principle of rational withdrawal and reproduction of the Earth resources in order to preserve their plentiful amount for the future generations of people. The implementation of this principle is a matter of technology. It involves the development of innovative techniques for reprocessing and utilization of mineral, energy, water, agricultural, forest and other resources, waste recycling and waste involvement in the general cycle of matter.

Nature management implies not the consumption of natural resources, but their use in the economic activity aimed, above all, at the creation of social and economic infrastructure. In doing so, the main idea lies in the preservation of healthy environment and minimizing its transformation and degradation.

At present, the humankind has reached the level of technological development permitting us to keep the balance between maintaining the ecological safety and the use of natural environment for improving the living standards. The strategic aim in nature management is the involvement of economic activity in the modern integral process of nature and society development. Application of nature-conservation (nature-like) technologies based on the scientific achievements plays an important role in solving this problem. These technologies are based on the adaptive principle and two major requirements: (a) a man should adjust to the environment rather that transform it, and (b) a man should not induce the development of hazardous natural processes.

Adaptation appears to be an efficient co-evolution mechanism of nature-use control permitting us to save the nature and simultaneously to use it for creating comfortable

V. Osipov · N. Rumyantseva · O. Eremina (✉)
Sergeev Institute of Environmental Geoscience RAS, Ulansky lane 13, Moscow, Russia
e-mail: sci-council@geoenv.ru

living conditions for people. Therefore, adaptation is considered to be one of the most important principles in ecological strategy.

Adaptation does not mean the total refusal from the use of natural resources. This is impossible. Adaptation means the turn to the rational nature use, upon which the nature consumption by people aimed at the creation of the necessary infrastructure on the Earth does not exceed the permissible limits, beyond which the nature loses its ability to self-restoration. This goal can be achieved, if the human activity will not oppose the nature laws, but it will be "adjusted" to natural processes not causing their radical changes. In other words, a man should create the infrastructure necessary for his existence in line with the laws of nature.

2 Cases of Applying Nature-Like Technologies to Nature Management

Nature-like technologies for nature management are widely applied to different kinds of economic activities. Below, we describe the cases of their application to civil construction practice and waste management.

Almost any construction (urban, industrial, transport, etc.) is accompanied by the substantial impact on the environment components (the lithosphere, the atmosphere and the hydrosphere). The operation time, the reliability, and the cost of engineering structures is controlled by the environmental conditions in many respects influencing the strength and deformability of ground massifs, possible geohazard development, etc.

Geological conditions are formed in the course of long-lasting geological history of the region and they show a great diversity due to spatial-temporal variability of the geological environment. Therefore, selecting places for allocation of engineering structures appears to be one of the most important tasks in civil construction. The nature-like technologies based on the adaptive principle permit experts to provide safety of constructed objects with the minimal hazardous impact on the natural environment.

Despite the construction norms and standards, the particular site for allocating an engineering structure is often decided without taking options in consideration, i.e., making no allowance for the variability of geological and other natural conditions in the territory. These decisions often result in the inappropriate allocation of objects, endangering their safety.

Territory zoning by natural conditions and selecting the most favorable sites for construction (alternative projecting) appears to be one of the simplest and efficient methods of "adjusting" engineering structures to the environment. Zoning should be carried out at the early (pre-project) stage of construction, i.e., at the stage of planning. It should

consist in the preliminary assessment of geoenvironmental conditions of construction, i.e., the assessment of geological properties of ground massifs, as well as their geodynamic, geomorphological, hydrogeological and other conditions. The optimal place for the construction site is selected proceeding from this assessment. The detailed engineering geological survey is carried out for the chosen variant to come up with the project parameters for future engineering structure.

Most often, the comprehensive estimation of geological conditions in the studied areas is taken as the chief criterion for zoning. In addition, the territories prone to geohazards may be zoned by such parameters as seismicity, slope stability, karstification, subsidence, permeability and adsorption properties of soil and rock layers, etc. Hence, different types of zoning may be used.

The zoning technology appears to be a very efficient tool for scientifically grounded allocation of engineering structures proceeding from the adaptive principle. Based on zoning, the construction may be performed with the minimal disturbance of nature; and the desired socio-economic benefit and the safety of engineering objects may be achieved with the minimal expenses.

2.1 Engineering Geological Zoning

Engineering geological zoning is necessary for the comprehensive assessment of geological conditions in the areas. Engineering geological zoning implies subdivision of the studied area into a series of taxonomic hierarchical units on the basis of estimation of structural-geodynamic, geomorphological, and hydrogeological peculiarities, lithology and structure of geological cross-section, physical and physico-mechanical properties of soils and rocks, as well as development of geohazards (Golodkovskaya and Lebedeva 1984; Popov 1950; Trofimov and Krasilova 2007).

Taxon names are based on the idea about a ground massif, which means a geological body with certain dynamics, structure, lithology, state, and properties (Osipov 2011). The hierarchical system of taxonomic units includes mega-, macro-, meso-, and engineering geological massifs, permitting us to subdivide territories successively from the major to minor territorial unit. The massifs of different levels are successively distinguished proceeding from the certain identification features, which are essential for the engineering geological conditions in the studied area (see Table 1). The final taxon, i.e., an engineering geological massif, is distinguished in line with the construction standards and rules proceeding from the expert assessment of composition, thickness, state and properties of lithological-stratigraphic ground complexes, hydrogeological conditions and geohazards development. According to their appropriateness for

Table 1 The hierarchical system of taxonomic geological massifs for engineering geological zoning

Taxon name	Identification features
Megamassif	Structural-geodynamic
Macromassif	Geomorphological
Mesomassif	Lithological stratigraphic
Engineering geological massif	Engineering geological

construction, all engineering geological massifs are united into three groups, i.e., of (a) low, (b) moderate, and (c) high complexity.

The map of engineering geological zoning of Moscow built at IEG RAS to a scale 1:10,000 is a case of application of the above-described technology (Osipov 2011; Osipov and Antipov 2009). In the Moscow city territory equal to 1082 km², a total of 2 mega- , 8 macro- , 50 mesomassifs, and 3658 engineering geological massifs are distinguished differing in the construction conditions. Taxons of the first order, i.e., megamassifs, are distinguished proceeding from the tendency to tectonic uplifting (A) or sinking (B) of the area. Using a specially developed computer code, all engineering geological massifs are united into three groups according to their suitability for construction, i.e., of low, medium, and high complexity (Fig. 1). The engineering geological massifs of low complexity cover 44% of Moscow territory; those of medium complexity, 45%; and those of

high complexity, 11% of the city territory. The compiled map appears to be a fundamental document for the scientifically grounded nature use proceeding from the adaptive mechanism upon the urban construction. This map divides the city territory into sites according to their favorability for construction, permitting users to outline the optimal location for residential, industrial and recreational zones, to develop the general scheme of engineering protection of the territory and thereby to adopt the optimal decisions on safety, cost, and environmental comfort.

Mapping permits planners to allocate dwelling districts and urban life-supporting infrastructure at the most geologically stable urban sites devoid of geohazards. Geologically unfavorable for construction sites are used in recreational purposes, the more so, these sites are often attractive in terms of natural landscape. In addition, engineering geological zoning permits us to make the preliminary assessment of geological conditions at the planned construction sites at the investment and tender stages. It is no less important upon working out the requirements specification, engineering survey program and feasibility study of construction projects.

2.2 Seismic Microzoning

Seismic microzoning as another example of applying adaptive nature-use technologies to engineering geology. In seismic regions, construction is often accompanied by the possible catastrophic destruction of technogenic objects and death of people. Thousands of such disasters happened on the Earth during the humankind history (Drumya and Shebalin 1985). To reduce the catastrophic consequences in earthquake-prone regions; cities, settlements and other technogenic objects should be allocated in the areas of minimal seismicity. For this purpose, maps of general, detailed and seismic microzoning are compiled. The latter appear to be the most informative, since they are built to a large scale and in addition to the background seismicity they make allowance for geomorphology, lithology and hydrology of the region.

As an example, we may describe the case of seismic microzoning in the Imeretinskaya depression at the Black Sea coast in the vicinity of Sochi, Caucasus, performed at the Sergeev Institute of Environmental Geoscience RAS (IEG RAS) upon planning the Olympic facilities there.

Fig. 1 Map of engineering geological zoning of Moscow territory. Designations: complexity for civil construction (1) low, (2) medium; (3) high; (4) boundary between megamassifs
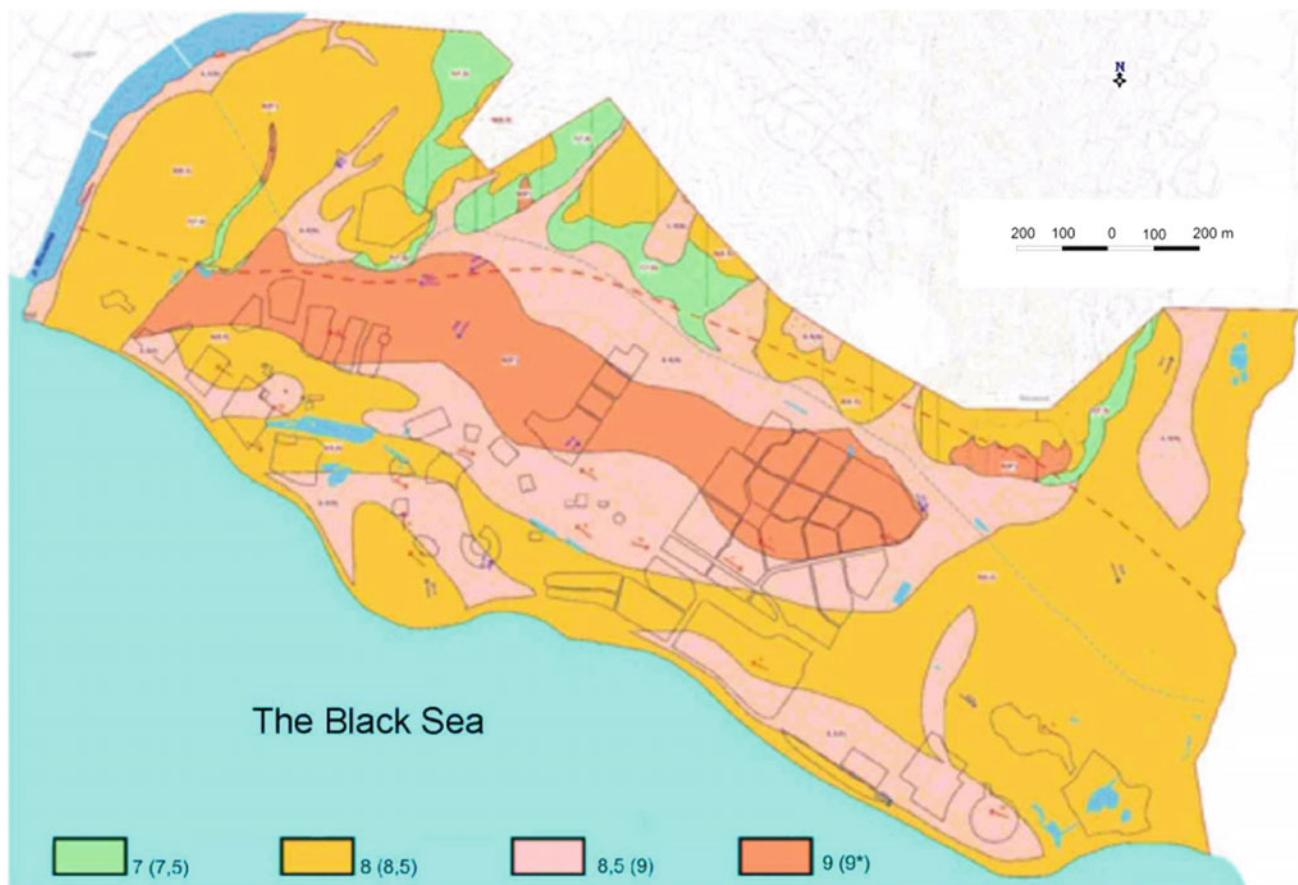
Fig. 2 The map of seismic microzoning of the Imeretinskaya depression. The distinguished sites and their seismicity in scores for the recurrence intervals of 500 and 1000 years (in parentheses) are shown in color

Construction in the Imeretinskaya depression is complicated by high seismicity in this area. It was estimated to range from 7 to 9 (MSK-64 scale) within a relatively small area for the recurrence intervals of 500 and 1000 years (Fig. 2). The use of seismic microzoning map permitted planners to allocate the sport facilities at the sites with the minimal seismicity and thus to raise the construction safety and to optimize its cost.

2.3 Zoning of Territories for the Disposal Sites of Solid Municipal and Industrial Wastes

Waste management is one of the most important issues in ensuring ecological safety of Russia, with solid municipal wastes (SMW) being the main concern. Fifty-six million tons SMW are accumulated in Russia annually, of which 5.5 million tons coming from Moscow. According to the official data, waste storage sites and landfills cover a total area of 107,000 ha.

A quickly growing amount of industrial and domestic wastes exerting a harmful effect on the environment and population health poses the task of creating a virtually new branch of industry dealing with the collection, sorting, temporary storage, recycling and the secondary use of recycled waste, as well as the disposal of non-utilizable waste. This is a very important interdisciplinary ecological problem, for solving which in addition to the application of innovative recycling technologies, a scientifically grounded approach to the landfill allocation within the entire Russia's territory is needed, which takes the environment conservation into consideration.

The landfill site allocation should meet the following requirements:

– waste disposal sites should be situated beyond the boundaries of sanitary-hygienic zones around settlements and industrial facilities;
– waste disposal sites should not be situated within the nature-conservation areas;
– waste disposal sites should manifest high natural isolating properties preventing the contaminant penetration to the environment upon the collection, sorting, and recycling of waste, as well as upon the disposal of non-utilizable waste.

The latter requirement should be based on the adaptive technologies. For this purpose, the engineering geological zoning of territories is performed with outlining sites favorable for allocation of waste landfill sites in line with the afore-mentioned requirements.

Upon the engineering geological zoning, tectonically inactive sites are chosen with no traces of geodynamic stress, deformations or fracturing. In terms of lithology, the sites composed of low-permeable clayey soils are preferable. For assessing the hydrogeological conditions, the permeability of different soil and rock strata is taken into account, as well as the presence of aquifers, their interconnection,

distribution, etc. In addition, the possible development of hazardous natural processes is also analyzed.

For instance, Fig. 3 shows the scheme of zoning of the Central region of Russia compiled at the Sergeev Institute of Environmental Geoscience RAS to a scale 1:25,000. Eighteen types of geological cross-sections were distinguished in the studied territory differing in their geological structure to the studied depth of 50–60 m, which are characterized by different combinations of clayey and nonclayey deposits. By the favorability degree for the storage of domestic waste, the distinguished types of geological cross-sections were united in 5 groups. All rock massifs were subdivided into favorable,
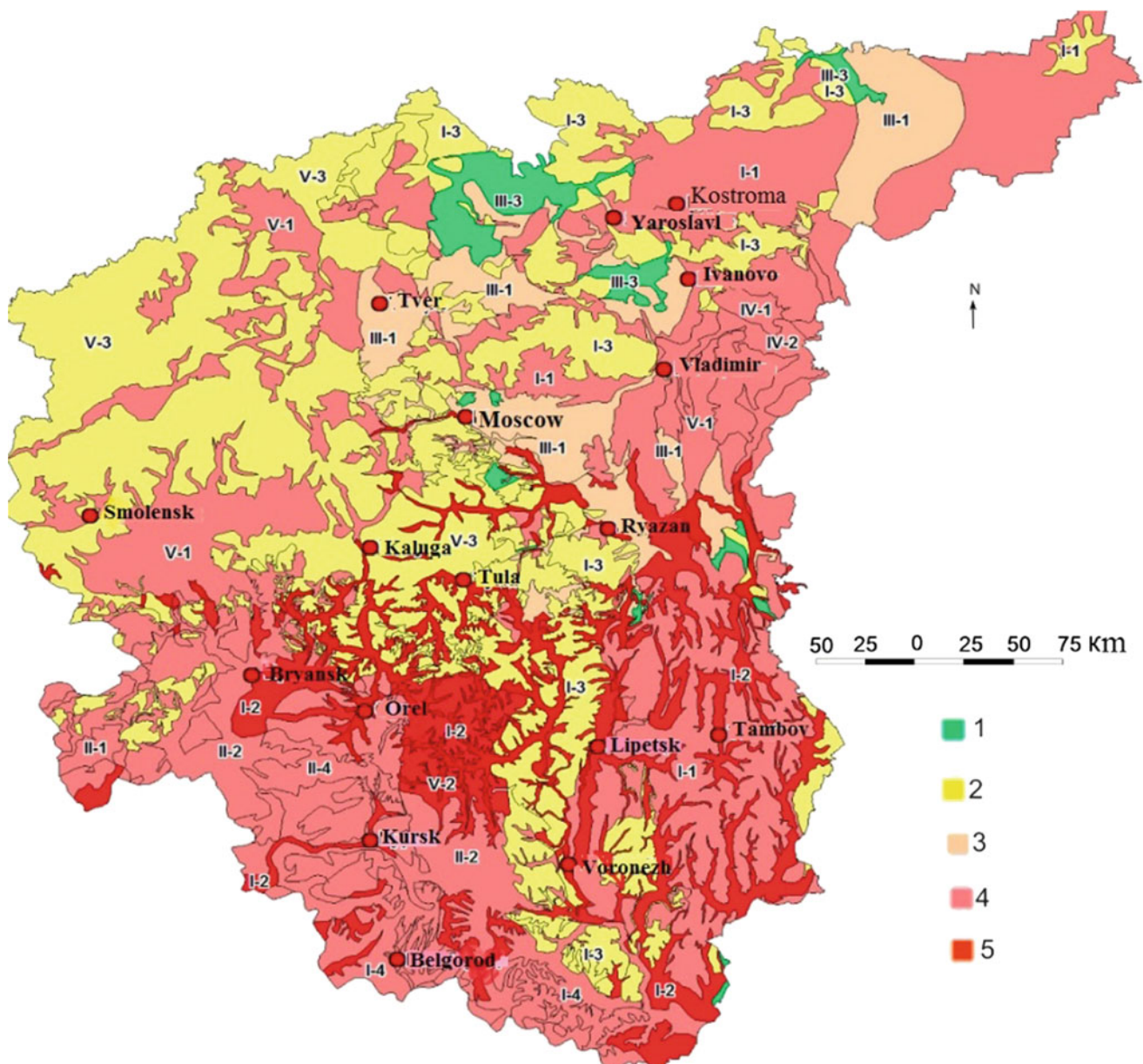
Fig. 3 The map of zoning the Central region of the European part of Russia by the conditions of solid domestic waste disposal: (1) favorable; (2) conventionally favorable; (3) conventionally unfavorable; (4) unfavorable; and (5) very unfavorable

conventionally favorable, conventionally unfavorable, unfavorable, and very unfavorable categories (Fig. 3).

The first group (favorable) includes massifs with two aquitards in their geological cross-section, i.e., the Quaternary moraine loam and the Jurassic marine clay, which protect the Quaternary and Mesozoic aquifers, respectively. Conventionally favorable massifs are considered those with the Quaternary moraine loam occurring at the top of the geological cross-section underlain by high permeable Quaternary and Mesozoic deposits. Within these sites, the degree of geoenvironment protection from the surface contamination is controlled by the thickness of moraine loam only. Conventionally unfavorable areas include those composed of sandy-clayey Quaternary deposits without any continuous low permeable strata. The screening horizon in these massifs is represented by Jurassic clay underlying the Quaternary deposits. The groundwater horizon is subjected to contamination, and the contamination degree of deep strata depends on the Jurassic clay thickness. The massifs are considered to be unfavorable for allocating waste disposal sites, in case they are composed of high permeable Quaternary and preQuaternary deposits with local discontinuous interlayers of impermeable glacial or Jurassic clay. These massifs show poor geological protection from the surface contaminants.

If the geological cross-section consists of well-permeable strata only, the massif is classified as of very unfavorable conditions. In this case, the geoenvironment is not protected from the surface pollutants at all. In the Central region of European Russia, these massifs are usually confined to the present-day river valleys, where the alluvial deposits occur immediately above Paleogene-Neogene sand or Carboniferous limestone.

The experience obtained by us upon performing this mapping based on the adaptive principle for selecting sites for storage, sorting, and utilization of municipal and industrial waste as well as for the disposal of unrecyclable waste residue should be used in elaborating the governmental policy in waste management aimed at minimizing negative ecological consequences.

3 Conclusion

The adaptive principle is a promising branch in nature-use development permitting people to carry out the economic activity on the Earth with the minimal impact on the environment and the biosphere degradation. This principle forms a basis for the development of nature-like technologies, such as zoning of territories intended for different types of human-environment interaction. Such zoning permits us to obtain the preliminary data about the geological structure and hydrogeological conditions of the studied area, to reveal hazardous geological processes, to substantiate at the early stage the necessity of engineering protection measures, and to develop the program on detailed engineering geological survey. Adaptation is regarded as a nature-like technology, since it is based on the principle of adjusting to nature and natural processes without disturbing them. Engineering geological and microseismic zoning as well as the zoning for selecting optimal sites for the waste landfill allocation testify to the high efficiency of adaptive principle in application to engineering geology.

References

Drumya, A.V., Shebalin, N.V.: Earthquake: where and why? In: Sadovskii, M.A. (ed.) Shtiintsa Press, Chisinau (1985)

Golodkovskaya, G.A., Lebedeva,N.A.: Engineering geological zoning of Moscow territory. Inzhenernayageologiya(Engineering geology) **3**, 87–102 (1984)

Osipov, V.I., Antipov, A.V.: Principles of engineering geological zoning of Moscow territory. Geoekologiya (Environ. Geosci.) **1**, 3–13 (2009)

Osipov, V.I.: Large-scale geological mapping of Moscow territory. Proektirovanieiinzhenernyeizyskaniya (Projecting and Engineering Survey), **3**(12), 12–18 (2011)

Popov, I.V.: Technique of compiling engineering geological maps. USSR Minsitry of Geology Press, Moscow (1950)

Trofimov, V.T., Krasilova, N.S.: Engineering geological maps. KDU Publ., Moscow (2007)

Registration of Ground Engineering Professionals—A European Perspective

Fintan Buggy, Kurosch Thuro, Gunilla Franzen, and Michael de Freitas

Abstract

Registration of professionals involved in ground engineering including the disciplines of soil mechanics, rock mechanics, geo-environmental science and engineering geology has slowly evolved over the past decade. The paper discusses the history and current status of national registration systems in Europe and provides commentary on the need for and advantages of such systems. The variation in attitudes and legal implications for national registration within Europe is large and some discussion contrasting the various systems, traditions and experience to date is presented. The potential advantages to be gained from ultimately gaining adoption of a "common platform" as a legal definition consistent with the European Directive 2005/36/EC on Recognition of Professional Qualifications are outlined. Lastly, the anticipated development of an Informative Annex to the revised Eurocode EN 1997 (expected to be formally adopted in 2022) is described, which defines the term "appropriately qualified and experienced personnel" cited in the code by means of national registration. Member countries of CEN may each choose to adopt or ignore the Informative Annex.

1 Introduction

Registration of professionals involved in ground engineering including the disciplines of soil mechanics, rock mechanics, geo-environmental science and engineering geology has slowly evolved over the past decade. Several countries in Europe either currently operate or are actively considering and developing national registration systems. Around 13 European member societies of the International Society of Soil Mechanics and Geotechnical Engineering (ISSMGE) currently participate in a working group formed following the ECSMGE held in Edinburgh, Scotland in 2015. The working group has convened two workshops in Leuven, Belgium 2016 and in Oslo, Norway 2017, each attended by 10 European member societies and their activities are the primary focus of this paper.

Previous attempts have been made to unify professional qualifications and competence standards in ground engineering both in Europe and Internationally. A Joint European Working Group (JEWG) was commissioned by the three international professional bodies IAEG, ISRM and ISSMGE, who set terms of reference in 2003. The JEWG Report (2008) identified a "common scientific and professional platform" of the disciplines of soil mechanics, rock mechanics and engineering geology. Professional competencies of all three primary disciplines (soil and rock mechanics and engineering geology) were summarised in terms of the following:

- Key Competence—fundamental understanding of relevant material behaviour or geological processes; site investigation and geo-hazard identification; setting up site specific Ground or Geologic Models; analysis and

F. Buggy (✉)
Geotechnical Society of Ireland, Associate, Roughan & O'Donovan, Dublin, Ireland
e-mail: fintan.buggy@rod.ie

K. Thuro
Chair of Engineering Geology, Technical University of Munich, Munich, Germany

G. Franzen
President Swedish Geotechnical Society, Geoverkstan, Kungsbacka, Sweden

M. de Freitas
Emeritus Reader in Engineering Geology, Imperial College, London, UK

design; soils and rock improvement techniques; construction supervision.

- General Competence—familiarity with pertinent scientific methods, knowledge of terminology, working methods, geomechanics and design methods;
- Specialised Fields—laboratory and field testing methods, site mapping and observation of geological data, GIS, numerical modelling, design construction and contractual procedures adjusted to geotechnical uncertainty, fractured, slaking and ageing materials, geological risk scenarios.

Competencies for each discipline were more broadly described in three attachments to the report. The interaction of separate disciplines within ground engineering and the need for an integrated approach required to meet EN 1997 was explicitly acknowledged, paricularly for Geotechnical Category 2 and 3 projects as defined in EN 1997-1 (Eurocode 7). One of the terms of reference of JEWG was to "prepare… recommendations for European model curricula in higher education, including post-graduate training and professional experience" but this goal was not realised.

VanDine (2016) discusses the variation in definitions of and competencies for ground engineering professionals citing currently operational, voluntary registration systems in Canada, USA and UK plus the work of the Joint Technical Committee on Education and Training (JTC-3) established by the Federation of International Geo-engineering Societies (FedIGS) and reported by Turner and Rengers (2010). The JTC-3 reported four conceptual competency profiles demonstrating how the differing disciplines within ground engineering each have a distinct set of required competencies generally characterised as foundational; technical-engineering science and design plus a set of common professional outcomes in terms of communication, public policy, leadership, teamwork, lifelong learning, professional ethics etc. VanDine (2016) concludes that a world-wide consensus on definitions and competencies is desirable to better protect the public, geotechnical professionals and the profession.

The Institution of Professional Engineers New Zealand (IPENZ) has operated Regulations for Competence Registers for various professionals including engineering geologists since 2015. Extensive guidelines are available for 12 elements covering a broad range of both technical and professional competence IPENZ (2013). A consultation document has been developed for geotechnical engineers in New Zealand IPENZ (2016) and the Australian Geomechanics Society (AGS) is developing a similar framework for their National Engineering Register informed by both the UK and NZ models.

In Asia a Geotechnical Engineers' Register was established by the Hong Kong government in the 1970s, largely driven by public safety concerns related to development impacts on natural slope stability, currently with around 100 members. This is a mandatory requirement for all engineers working in this field in Hong Kong. The Japanese Geotechnical Society operates a 2 tier voluntary system for Professional Engineers for Geotechnical Evaluation and other professional bodies in Japan offer similar systems for Geological Surveys and Information Management.

2 Why Is Registration for Ground Engineering Professionals Beneficial or Necessary?

Given the critical role of ground engineering professionals in the planning, design and construction of major infrastructure, industrial, mining, commercial and residential development in the modern world, it is readily apparent that the interests of both public safety and to minimise economic losses from failure are served by having qualified and competent persons perform these services. VanDine (2016) argues that current self or peer opinion regulated practices are no longer adequate for a global marketplace where professionals practice in many jurisdictions. ISSMGE TC304-TF3 (2013) Risk Management reported the top six recommendations for integrating geotechnical and project risk management. Four of these could be directly supported or enhanced by registration systems requiring minimum education, communication and risk management skills and continuous education standards. The national professional institution IPENZ (2016) has identified that "the geotechnical engineering profession in New Zealand has a poorly defined body of learning. … Concerns have also been raised about the quality standard of the CPEng qualification, particularly with regard to specialist fields of engineering like Geotechnics." The proposed remedy for this is to define the core knowledge and skills that a Chartered Professional Engineer (Geotechnical) is expected to have and to inform the competence assessment process used by the Registration Authority.

The main beneficiaries of introducing a common international consensus for national registration of Ground Engineering Professionals as suggested by VanDine (2016) could be divided into three categories: society as a whole; the construction industry; and the individual engineer or geologist. For the society a well developed and adequately regulated system to enforce that the responsible professional is registered, ensures a minimum level of competence within the project to ensure the public safety and minimise economic losses.

For the construction and professional consulting firms that employ such professionals, it is necessary that there is some tangible return, if they invest time and money in their

employees by supporting them to get continuing education and experience to fulfil the requirements of registration. This return only occurs if clients use registration as one of the evaluation criteria in the tender process and it would inevitably lead to an increased interest in education and competence within the relevant professions. Requirements for specialist registration in the tender could also promote competition on an equal basis, where less competent companies with inexperienced professional staff would have reduced possibilities to win. The profession may need to consider what further inducements it can offer to both firms and individuals to encourage registration, particularly in its early years before the longer term benefits have been realised.

For the individual engineer or geologist, registration would be a recognition of their competence that would open up opportunities to work not only in their own country but also abroad. This latter aspect would increase the possibilities for ground engineering professionals to get a wide experience from different countries, and hence different geology and geotechnical difficulties. For some, it might also be an important tool in the discussion within their company, to motivate the need for time and training activities to achieve the need of continuous professional development.

A common objection voiced by professionals in related professions such as civil and structural engineering and by wider society is that specialist registration of ground engineering is inherently protectionist and anti competitive. The authors personal view and typical response is to point out that many failures in ground engineering have resulted from the activities of non specialist professionals who have become involved in ground investigations, geotechnical designs and construction in challenging or complex ground conditions for which they have inadequate training and experience (Bracegirdle 2017). There is however acknowledgement that simple, non complex ground conditions can be adequately addressed by non specialist professionals with sufficient experience in and knowledge of the local geologic conditions. These projects and conditions would generically all fall within Geotechnical Category 1 of EN 1997-1.

Another issue that is often voiced is the difficulty to find qualified persons that could evaluate the applications for registration. On what bases are these persons selected and by what right may they evaluate the experience and competence of their peers? From the authors point of view, this difficulty is mainly an issue in the initial start-up phase of a registration system and in the training of assessors. After a couple of years, there should be a sufficient number of senior professionals that, together with their own registration and further training, should be experienced enough to evaluate younger and other peer colleagues. It should be recognised that it might be beneficial to make the introduction of a system as a process, avoiding introducing a mandatory registration, but

this approach cannot be applied in all countries where differing legal standards apply.

3 Review of Current Status and Common Aspects of National Registration Systems in Europe

The characteristics of current and proposed or draft registration systems in 8 European states are summarised in Table 1 under the general column headings of Professional Designation, Education, Experience, CPD and Legal Status. This table was updated at the ISSMGE working group workshop held in Oslo in May 2017. A map showing the current status of these countries is shown in Fig. 1. The contrasting characteristics of two prominent national registration systems currently operated in UK and Germany are described by Bock et al. (2014).

In the UK the Register of Ground Engineering Professionals (RoGEP) has been operational since 2011 and currently has circa 525 members. The three tier UK RoGEP system aims to be broadly inclusive of all ground engineering professionals and is voluntary. Registration is not a mandatory requirement of any public or statute law, but it can be made a stated requirement in contracts for professional services. RoGEP is user driven by the professions and their clients and adaptable to new demands whether coming from regulatory change or industry. RoGEP is endorsed by The Welsh Government, London Underground (Transport for London), United Utilities, Highways Agency and Network Rail in the UK. Clients were initially concerned with regards to the availability of sufficient registrants for the workload required in the UK, but this is now somewhat diminishing as the number if registrants has increased.

Chartered status is the common entry point to join RoGEP for professionals of all disciplines. One of the important contributions RoGEP has brought to the profession in the UK is the harmonisation of relevant backgrounds, so that teams from different backgrounds and contributing different skills can work as equals. Each candidate is assessed for their activity and level of responsibility in six areas; innovation, technical solutions, integration, risk management, sustainability and management. Three levels of registration were formed, the lowest (Professional) is suitable for those just chartered who, under direction, can perform and manage as required. As experience is gained so the management role increases and the second level (Specialist) can be gained; this would typically be held by those in middle-management. Those that eventually become responsible for highly complex projects including the risks of all sorts associated with them will be recognised as the highest grade (Adviser). RoGEP is considering extending registration to those in the industry holding technical grade

Table 1 Summary of national registration systems for ground engineering professionals in Europe

Country	Professional designation	Educational qualification (ECTS credit points) (see NOTE 1)		Professional experience (see NOTE 3)	CPD	Remarks registration legal status (p) = under private (contract) law (P) = under public law (see NOTE 4)
Austria	Registered engineer ("*Ziviltechniker*") (geo-engineering at large)	Master in civil or Mining engineering or Natural sciences		3 years	3-week course and examination on law, technical. standards and management	(**P**) mandatory: – registration with chamber of engineers ("*Ziviltechnikerkammer*") – liability insurance
Belgium	Geotechnical (2 tiers) Specialist and expert (draft; to comply with EN 1997)	B.Eng./B.Sc. (180–240)		Specialist G1, G2, G4, D1: 5 years	Acknowledged but not quantified	(p) intended: through Belgian member body of the ISSMGE
		MEng./MSc. (300)		Expert G3, D1–D4: 10 years		
Germany	Geotechnical expert ("*Sachsverständiger für Geotechnik*" EASV) (to comply with EN 1997)	B.Eng./ B.Sc. (180–240)	Note (2)	GC2: 4 years GC3: 7 years	8 hrs/year (ma ndatory)	(p) self assessment; in operation since 2013 Objective: (**P**) registration with state chamber of engineers
		M.Eng./ M.Sc. (300)		GC2: 2 years GC3: 5 years		
	Checking expert ("*Prüfsachver-ständiger*") (ground engineering at large)	Master in civil or geotechnical engineering or engineering geology		9 years in-depth and specialized knowledge	"shall be up to date with the developments in ground engineering"	(**P**) Federal German chamber of engineers ("*Bundesingenieur-kammer*")
Ireland	Objective: joint UK and Ireland RoGEP-scheme (see UK below)	Minimum: B.Eng./ B.Sc. *plus*: C Eng or P Geol title (membership with EI or IGI)		Variable number of years of working experience, depending on the registration grade	40–60 hrs/year (mandatory)	(p) RoGEP (registration of ground engineering professionals) scheme sponsors EI (engineers of Ireland) and IGI (institute of geologists of Ireland) mutual agreement between UK & Irish institutions signed in June 2018
FYR Macedonia	Geotechnical expert (to comply with EN 1997 and mining requirements)	B.Eng. (Civil or mining)/B.Sc. (180–240)		Level B: GC 1-2: 2 years	Not defined	(**P**) Macedonian chamber of certified architects and Certified engineers 2 sponsors
		M.Eng. (Civil or Mining)/MSc. (300		Level A: GC 1-3: 5 years	Required, but hours not defined	
Netherlands	Geotechnical (3 tiers) Professional; specialist and adviser (draft; to comply with EN 1997)	B.Eng./B.Sc. note 2. (180–240)		Variable number of years of working experience in the field, depending on the grade of registration (minimum 5 years after M.Sc.)	8 hrs/year (mandatory)	(p) Pending adjustment of the Charter of the KIVI ("*Koninklijk Instituut Van Ingenieurs*") to include Geotechnics Mutual Agreement between UK & Irish institutions signed in June 2018.
		M.Eng./M.Sc. (300)				

(continued)

Table 1 (continued)

Country	Professional designation	Educational qualification (ECTS credit points) (see NOTE 1)		Professional experience (see NOTE 3)	CPD	Remarks registration legal status (p) = under private (contract) law (P) = under public law (see NOTE 4)
Sweden	Three levels of competence: L-1: aware; L-2: apply and understand; L-3: evaluate (matrix of competence)	Bachelor or Master		Variable number of years of working experience in the field, depending on the area of competence	Acknowledged but not defined	(p) self assessment of competence
U.K.	Geotechnical (3 tiers) professional; specialist and adviser (ground engineering at large)	B.Sc./B. Eng. M. Eng./ M.Sc. *plus*: Chartered title C Eng or C Geol (membership with GSL or ICE or IoM³)	Note (2)	Variable number of years of working experience in the field, depending on the grade of registration	40–60 hrs/year (mandatory)	(p) RoGEP (registration of ground engineering professionals) joint scheme of GSL—the geological society of London ICE—institution of civil engineers IoM³—Institute of materials, minerals and mining, administered by the ICE, 2 sponsors , in operation since 2011

NOTE 1 Traditional university degrees such as Dipl.-Ing. or Dipl.-Geol. (in Austria and Germany) or the diploma Industrial Engineer (in Belgium and Netherlands), are not considered. The EASV-Recommendations of the German Geotechnical Society DGGT provides guidelines for assessing tertiary studies outside of the ECTS System

NOTE 2 Geotechnical core subjects such as soil mechanics, foundation engineering and engineering geology are required as part of the university studies

NOTE 3 The professional experience is measured by a variety of criteria, such as the number of years spent on a geotechnical construction site, the Geotechnical Category (GC) of the project, the level and field of competence and application of geotechnical methods.

NOTE 4 Common features in the registration process of geotechnical professionals are: Lodging of an application form together with a CV and other documents in support of the application, assessment and examination of the applicant by an independent professional panel and, if the application was successful, a revalidation of the registration after 5 years
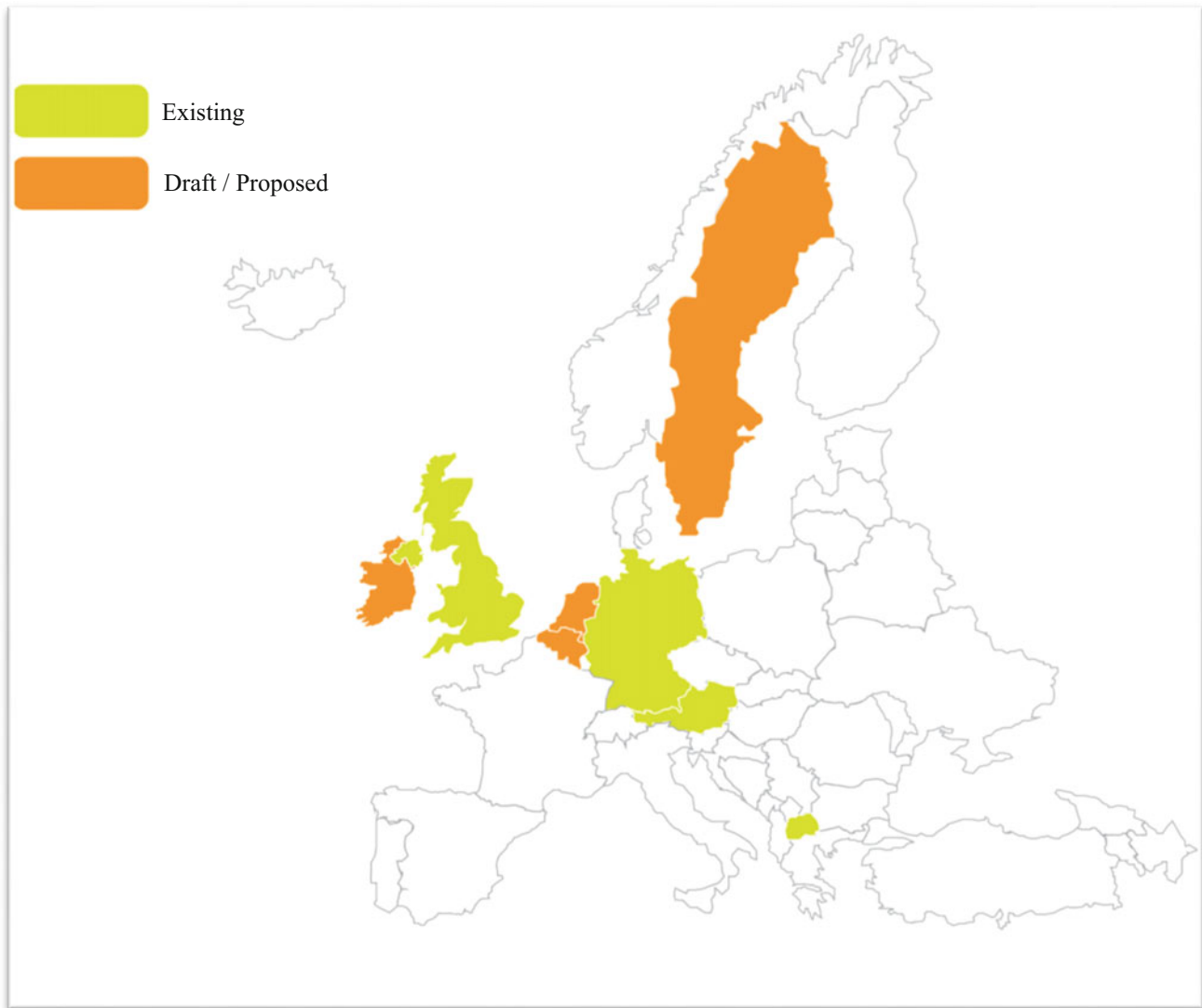
Fig. 1 Map of European states with existing and draft/proposed registration systems

qualifications, especially those in the construction sector (e.g. investigation drilling, piling, field monitoring and testing etc.)

The single tier German system developed by the German Geotechnical Society DGGT is being introduced incrementally into the public law of individual states within the Federal Republic since 2013. It is currently adopted in 2 states (North Rhine Westphalia and Berlin) and is actively in negotiation in Bavaria but has a low uptake to date of 60 members due to its very recent promotion. The German system is primarily focussed on defining the minimum competence to meet the specific requirements of EN 1997 and is a mandatory requirement of state law in those jurisdictions that have formally adopted it. There is also an existing higher tier of Checking Expert in Germany who is separately registered through the Federal Chamber of Engineers.

This same contrast in focus on either geo-engineering at large or the more specific requirements of EN 1997 and the use of mandatory public law versus voluntary private (contract) law is reflected in the diverse cultural, professional organisation and legal practices of the other European countries. Austria has a mandatory single tier system which operates in tandem with other civil engineers with a broad focus on geo-engineering at large while FYR Macedonia operates a mandatory 2 tier system focussed on EN 1997 and mining engineering. In terms of developing registration systems, Ireland and the Netherlands are expected to have operating registers in 2018. Ireland expects to achieve this by means of the mutually agreed expansion of RoGEP and the Netherlands is adopting a 3 tier system which closely resembles RoGEP. Belgium has developed a 2 tier draft system but is a little further from formal adoption.

Although there is some general interest elsewhere in Europe, other states have not yet developed draft systems for ground engineering specialists. Sweden has chosen to initially focus on the broader education of professionals involved in ground engineering design and construction, including non specialists, rather than developing a professional ground engineering register. Finally, there are countries such as France and Norway with little interest in the professional registration of individuals, primarily because professional competence is traditionally addressed in those states by the registration of companies or organisations.

Educational qualifications are stated in terms of ECTS credit points and a distinction is frequently made between B.Sc. or B.Eng. and M.Sc. or M.Eng. level degrees, with geotechnical core subjects also being required as a part of university studies. Professional experience is usually defined in terms of minimum years of post graduate experience and varies with the level of degree obtained and in terms of the Geotechnical Complexity of the project for those national registration systems with focus on EN 1997 (e.g. Belgium, Germany, FYR Macedonia). Minimum requirements for Continuing Professional Development (CPD) are frequently mandatory, although the definition of what activities are acceptable as CPD is not always well defined or consistent between the various systems. Competence requirements vary greatly and are not included in Table 1 due to space limitations. Details of the UK and German competency requirements can be found in published literature e.g. DGGT (2013, 2016) and ICE (2017). A distinctive feature of RoGEP is its requirements for competence in broader areas of innovation, integration, risk management, sustainability and management in addition to technical expertise. The application process for registration is also quite variable between states, sometimes relying of self assessment but more typically an independent body such as government organisation or professional learned society assesses individual's competence following a formal submission, which sometimes requires sponsors to attest the candidate's experience and level of professional responsibility held.

4 EU Directive 2005/36/EC Recognition of Professional Qualifications: "Common Platform"

The objective of EU Directive 2005/36/EC is to facilitate the mobility of EU citizens in the single market by defining a set of rules allowing professionals qualified in one Member State to exercise their profession in another. An evaluation of the functioning of the rules was published by the EU (2011) which acknowledged that the most benefits to date have been derived by mutual recognition in health, architecture, teaching, social/cultural professions and craftsmen. The variation in engineering disciplines and national organisations between Member States resulting in significant differences in duration and content of training was cited as a difficulty in applying the regulation. Engineering organisations also concluded that the complexity of implementing a common platform was simply too great.

A "Common Platform" is defined by the Directive as a set of criteria such as training, adaptation periods, aptitude tests, professional practice, or combinations which compensate for variations in individual state practices. A professional who satisfies all of its criteria would be waived of any individual compensatory measure in a Member State. No common platform has yet been achieved for the engineering profession within the EU. The common platform can be initiated by a Member State or by professional organisations representative at national and European level and requires two-thirds of EU member states to agree i.e. 18 states from a total of 27 EU states (following UK departure in 2019). An inventory of legal situations is required in two-thirds of EU states.

Table 2 is a draft of a common platform developed by the ISSMGE working group which tries to reach a common basis for minimum professional competence within ground engineering. One of the agreed minimum target competencies in developing this common platform was to be able to develop a Geotechnical Investigation Report (GIR) or Geotechnical Design Report (GDR) for a Geotechnical Category 2 project within the meaning of EN 1997. The idea of having a second higher tier for Geotechnical Category 3 projects in the common platform was also considered but abandoned by the working group as impractical. There has been broad agreement following much discussion within the group on the minimum educational qualifications, duration of post academic experience, CPD and application requirements. Defining minimum competency has proven more difficult, with a diverse range of opinions being expressed.

The goal of attaining agreement of 18 EU member states to a common platform for ground engineering professionals is clearly a long term aspiration. A further potential difficulty lies in the fact that a common platform would require approval by the national representative engineering bodies. These national organisations are at least one level and often two levels above the ISSMGE member societies and they may or may not support the ultimate goals of the EU Directive or those of specialist ground engineering professionals.

Table 2 Summary of draft common platform registration characteristics (EN 1997 GC2 project)

Objectives	Professions geotech eng/eng geologist/mining/rock mechanics	Educational qualifications (ECTS credit points)	Professional qualifications	Public (statute) law	Expected post academic experience	Technical competencies	Continuing profession development (CPD) (hrs/year)	Application/review
Informative annex of revised EC7 Professional recognition across Europe for ground engineering at large Minimum complexity as per EN 1997 GC2	All	B.Sc./B.Eng. (180–240) M.Sc./M.Eng. (300) (1) majors in civil engineering/geology/earth sciences plus specialist subjects e.g. soil mechanics and engineering geology, etc.	Varies with national practice	No	B.Sc./B.Eng. 5 years–GC2 M.Sc./M.Eng. 3 years—GC2 and demonstrated appropriate competence	To be agreed	Content to be specified by national body ≥ 20 h/year	Documented independent assessment, statement and CV Revalidation at 5 year intervals

5 Informative Annex G to prEN 1997-1

Despite the many problems and hurdles to be overcome to achieve a legally binding common platform compliant with the EU Directive, there is a second goal which can serve a similar consensus through the current revisions to the Eurocode 7 (EN 1997). Work on updating the current code commenced in 2016 and is expected to be substantially complete by 2020. It will then be published for public comment before a formal vote by European national standards authorities on its adoption, expected in 2022.

Both the core Eurocode EN 1990: Basis of Structural Design and EN 1997: Geotechnical Design make references in Clause 1.3 Assumptions to design by "appropriately qualified and experienced personnel". The same language is currently retained in the draft code revisions but critically no further guidance or definition of the qualifications or experience of these personnel is given. The ISSMGE working group identified that national registration systems for ground engineering professions could play a valuable role in providing this definition, at least on a voluntary basis for those countries who either had active registers or were developing them. The mechanism by which this is being proposed is as an Informative Annex to the revised code. It is important to note that all Informative Annexes can be either adopted or excluded by each member country. Any national standards authority can choose not to adopt the definition offered in the Annex, in which case the code requirements revert to the existing rather vague description given in Clause 1.3.

A draft Informative Annex proposal was submitted to the CEN TC250 SC7 meeting held in Oslo in May 2017 for consideration and comment by national representatives and SC7 Task Groups. The Annex contained two optional tables, essentially reflecting Table 1 "national listing" and Table 2 "draft common platform" described earlier in this paper, with a recommendation to select one of these formats for further development. The majority decision by the ISSMGE and SC7 Task Groups was to try to develop Table 2 common platform into an agreed content, but this was not unanimous and some countries argued strongly in favour of the national listing approach. Work on developing the Annex G has been slowly progressing and is expected to reach a conclusion in Spring 2018. Agreeing on a common definition for technical competency remains a significant hurdle which may default to permit individual states provide a definition consistent with their own registration systems in their National Annex to the Eurocode. While not ideal for ultimate use in a true "common platform", this arrangement gives maximum flexibility to each state and is the preferred choice for those countries with existing registers.

6 Conclusions

Registration of ground engineering professionals on a national basis is increasing in Europe by means of a combination of voluntary and mandatory practices. By 2020 at least seven European jurisdictions are expected to have operating registers. Although there is very significant diversity in national practices and the characteristics of individual registration systems, the development and adoption of an Informative Annex to the revised EN 1997 based on a common platform is actively being pursued. It is hoped that this recommended minimum standard would be adopted as a baseline for all future national registration systems in Europe and perhaps also serve as a useful reference for consideration of a more global approach to registration in due course. Adoption of a common platform fully compliant with EU Directive 2005/36/EC is a much more distant aspiration which requires many more countries to participate and is unlikely to be achieved in the short term.

References

Bock, H., Herten, M., Schwerter, R., Thuro, K.: Unified qualification requirements for ground engineering and engineering geology professionals. Eng. Geol. Soc. Territory **7**, 207–211 (2014)

Bracegirdle, T.: "Grounds for Dispute" Engineers Ireland, Geotechnical Society of Ireland Presentation (Apr 2017)

DGGT: EASV Sachverständige für Geotchnik: Anforderungen an Sachkunde und Erfahrung. Empfehlung des Arbeitskreises AK 2.11 der Fachsektion Erd- und Grundbau der Deutschen Gesellschaft für Geotechnik e.V. Recommendation EASV geotechnical consultants —requirements regarding expertise and professional experience. Recommendation of the working group 2.11 of the section of ground engineering of the German geotechnical society (draft version). Geotechnik **36**, 51–57 (2013)

DGGT: EASV Sachverständige für Geotchnik: Anforderungen an Sachkunde und Erfahrung. Empfehlung des Arbeitskreises AK 2.11 der Fachsektion Erd- und Grundbau der Deutschen Gesellschaft für Geotechnik e.V. Recommendation EASV geotechnical consultants —requirements regarding expertise and professional experience. Recommendation of the working group 2.11 of the section of ground engineering of the German geotechnical society (final version). 18 p., DGGT Essen (2016). http://www.dggt.de/images/PDF-Dokumente/Arbeitskreise/ak_2-11_empfehlung_2016.pdf

EN (1997) Eurocode 7: Geotechnical Design CEN 2009

EU: Evaluation of the Professional Qualifications Directive (2005/36/EC), Brussels 5 July 2011, 89 p

ICE RoGEP: (2017). https://www.ice.org.uk/careers-and-training/careers-advice-for-civil-engineers/specialist-professional-registers#RoGEP

IPENZ: Guidelines for Engineering Geologists. Version 1.0, 14 p (2013)

ISSMGE TC304-TF3: Integration of Geotechnical Risk Management and Project Risk Management. Part 1, 51 p (Nov 2013)

JEWG Report: Professional Tasks, Responsibilities and Cooperation in Geo-Engineering. IAEG, ISRM and ISSMGE, 30 p (2008)

NZ Geomechanics News December 2016: Evolution of the CPEng (Geotechnical) Body of Knowledge and Skills, pp. 98–107 (2016). IPENZ Institute od Professional Engineers New Zealand

Turner, A.K., Rengers, N.: A Report Proposing the Adaptation of the ASCE Body of Knowledge Competency-based Approach to the Assessment of Education and Training Needs in Geo-Engineering, a progress report, FedIGS, Joint Technical Committee (JTC-3: Education and Training), 37 p (2010)

VanDine, D.F.: What is a geotechnical professional? In: 17th Nordic Geotechnical Meeting, Reykjavik, Iceland, pp. 43–52 (2016)

Engineering Geology Research and Rural Access in Support of United Nations Sustainable Development Goals

Jasper Cook

Abstract

Improved rural transportation is recognised as a key driver of increased rural socio-economic transformation through poverty eradication, increased food security, hunger elimination and social integration. In this context, rural transport plays a vital role in supporting progress towards many of the UN 2030 Sustainable Development Goals (SDGs).

These Sustainable Development Goals (SDGs) form the ambitious internationally agreed plan of action for eradicating poverty and taking the bold and transformative steps which are needed to shift the world onto a sustainable and resilient path. The 17 Sustainable Development Goals build on the Millennium Development Goals and aim to complete (by 2030) what these did not achieve.

Getting to zero poverty by 2030, means doing more and larger economic infrastructure investments in the poorest countries. It means reaching the remote rural poor and working in the most difficult environments.

Within the context of IAEG Commission C32 (Engineering Geology and Rural Infrastructure) it is the contention of this paper that research, and in this case Engineering Geological Research, plays a key role in advancing sustainable rural transport by providing evidence to inform the key decisions on strengthening cost effective rural access processes. This improved transport infrastructure needs to be soundly based on well-informed design, construction and management principles and procedures. The role of research in rural access is recognised in the recent Vientiane Declaration on Sustainable Rural Transport towards Achieving the 2030 Agenda for Sustainable Development, which was recently adopted by representatives of 23 member and 14 observer countries of the 10th Regional Environmentally Sustainable Transport (EST) Forum in Asia. The Declaration speaks to the link between research and improved rural access by a requirement to "utilize the outputs of research for innovative methodologies to provide more sustainable and appropriately-engineered rural connectivity."

This research in the engineering geological context has a focus on:

- Cost effective use of local resources
- Appropriate climate resilience adaptation options
- Sustainable earthworks
- Supporting rural access indicators

This paper provides examples of the application and uptake of research, particularly in terms of the projects in the framework of the current Research for Community Access Partnership (ReCAP), funded by UKAID as well as previous related programmes. It links the examples with contributions to the achievement of specific SDGs. The paper also discusses the role of engineering geological research in cooperating with such initiatives such as Sustainable Mobility for All (SuM4All) and the Rural Access Index (RAI) as the proportion of a population living within 2 km of an all-season road (SDG 9.1.1).

J. Cook (✉)
Research for Community Access Partnership (ReCAP), London, UK
e-mail: jaspcook@btinternet.com

1 Introduction

1.1 Background

In rural areas, where the vast majority of poor people live, limited rural access is a critical constraint to economic and social development. Rural transport and rural access can be directly associated with 4 of the 17 recently adopted United Nations Sustainable Development Goals (SDG) for 2030 and indirectly associated with 3 others, (Peet 2015):

Direct Targets

- Target 1.4: Equal access to economic resources/basic services
- Target 2.1: End hunger and ensure access to safe, nutritious food
- Target 9.1: Develop regional and trans-border infrastructure
- Target 11.2: Provide access to safe and sustainable transport systems

Indirect Targets

- Target 6.1: Access to safe drinking water
- Target 12.3: Reduction of postharvest food losses
- Target 13.1: Climate change adaptation and mitigation

The SDGs outline the global framework for the International Community. Within this framework transport has a number of targets and indicators. These focus on regional infrastructure and economic development, rural transport and poverty reduction, urban and low carbon transport. It is a challenging time for the transport sector globally and for the rural transport sector in particular. The SDG Indicator 9.1.1 (Proportion of the population living within 2 km of an all-season road) is key to monitoring progress on rural access.

The requirement within the Engineering Geological sector is to be agile in our response to these significant global challenges and to align our efforts around climate smart infrastructure design, emerging technologies, rural poverty and infrastructure resilience.

Within the context of IAEG Commission C32 (Engineering Geology and Rural Infrastructure) it is the contention of this paper that Engineering Geological research, plays a key role in advancing sustainable rural transport by providing the evidence to inform the key decisions on strengthening cost effective rural access and aiding sustainable economic and social development in Lower Income Countries (LICs).

The Vientiane Declaration (2017) signed by 23 developing countries stated that essential steps to achieve the SDGs in the rural sector include "developing and maintaining rural transport infrastructure (e.g. footpaths, tracks, trails, farm and feeder roads, railroads, waterways, bridges and drainage systems)". At the same it emphasizes the link between research and improved rural access by a requirement to "utilize the outputs of research for innovative methodologies to provide more sustainable and appropriately-engineered rural connectivity." The ability of engineers and engineering geologists to identify problems and to devise solutions that provide sustainable cost-effective access for the rural poor is a key factor in overarching aims of poverty reduction and socio-economic development. The application of sound engineering geological principles to the uptake and embedment of innovative and cost-beneficial rural access solutions is an essential element in this process (Cook et al. 2014).

1.2 Transport Research Initiatives

Over the last few decades, the UK's Department for International Development (DFID) and others have committed significant resources into researching relevant themes and optimum solutions to increase rural access in developing countries. The Research for Community Access Partnership (ReCAP) is a DFID funded initiative comprising AsCAP (Asian Community Access Partnership and AfCAP (African Community Access Partnership) and the previous South East Asian Community Access Programme (SEACAP). Its aim is to improve accessibility of the rural poor in Africa and Asia to economic opportunities through applied research and by strengthening the evidence base on more cost effective and reliable low volume roads and transport services. Many of its projects incorporate significant elements of Engineering Geology.

2 Access, Research and Engineering Geology

To underscore the critical role of rural transport in achieving the SDGs, a set of key messages has been developed by ReCAP, (SLoCaT 2017). Table 1 outlines these messages.

The role of Engineering Geology in responding to these messages can gauged by considering the factors that impact upon the sustainability of rural access networks. It is now recognised that the life-time performance of rural access roads are influenced to a greater extent than higher volume roads by the impacts of what collectively are termed the 'Road Environment', Fig. 1. In a sector that is under significant pressure with regard to budgets and resources, the importance of the "Road Environment" factors with respect to the sustainable rural access becomes crucial. An examination of the factors making up the Road Environment when taken within the context of the Key Messages illustrates the relevance of Engineering Geological related research to achieving SDGs, Table 2.

Table 1 Key SDG messages

No.	Message	The rationale
1	Improved rural transport drives sustainable rural development and national growth	Road infrastructure promotes connectivity and social cohesion, drives commercial activities as well as accessibility to social and economic facilities
2	Better rural transport is key for food security and zero hunger	Improving rural access can lead to lower costs for farm inputs and lower transport costs for marketed outputs thus increasing agricultural production
3	Poor rural transport condemns the poor to stay disconnected and poor	Access to markets and employment opportunities through better rural transport infrastructure and services is an essential pre-condition to generating rural income and thus reducing poverty
4	Additional money and commitment is needed to build and maintain rural road networks	Funding sources need to be expanded and new funding sources need to be developed, piloted and implemented not only for building but also for maintaining the asset
5	Better rural transport calls for local solutions for local challenges	Rural access challenges require local resource-based solutions that are compatible with the local road environment conditions

Fig. 1 The road environment factors (Cook et al. 2013)
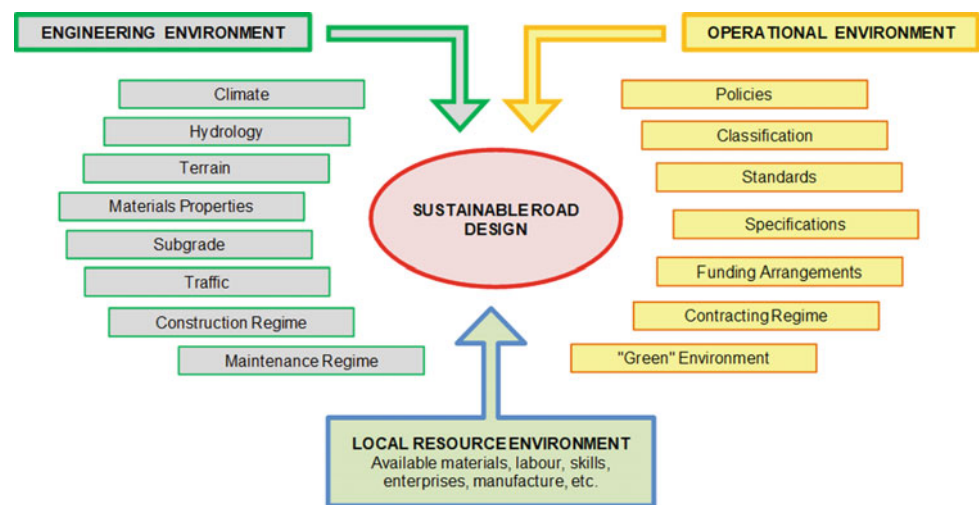
3 Examples of Engineering Geological Research Related to Access

3.1 General

The largest rural transport research programme in sub-Saharan Africa and South Asia is ReCAP. RECAP (and its predecessors) continue to be involved in a number of projects involving key aspects of Engineering Geology. The following sections have drawn on this body of work to illustrate the relationships between Engineering Geology, rural access and the delivery of rural mobility as defined by the SDGs. The following topics are dealt with in particular:

- Natural construction materials
- Climate resilience
- Earthwork protection
- "First Mile" agricultural access

3.2 Cost Effective Use of Local Materials Resources

Research focused around the specified use of local materials that would normally be classified as "marginal" is of great significance in terms of cost-effective and sustainable rural road networks. In defining the appropriate use of marginal materials an appreciation of the geological environments of formation of potential construction materials is an essential pre-requisite for understanding their likely behaviour and in deriving appropriate specifications and limits to their use.

Table 3 lists some of the recent and current research under both the overall ReCAP umbrella and the previous DFID-funded Knowledge and Research (KaR) programme.

Some points to come out of this body of work are:

1. The limiting criteria (compacted strength, plasticity and grading) set out in traditional specifications for road-base

Table 2 Relevance of engineering geological research within the road environment

Impact factor	Relevance of engineering geological research
Primary relevance	
Climate	Methodologies for assessing climate impacts and prioritising appropriate geotechnical adaptation options
Hydrology	Research into interaction of water and its movement within and adjacent to the road structure which has an over-arching impact on the performance of the pavement and drainage structures
Terrain	Research related to the assessment of terrain and its interaction with constraints on horizontal and vertical geometry for basic access alignments and the requirements for natural and earthwork slope protection
Materials	Research into the appropriate use of materials to ensure that they are neither sub-standard nor wastefully above the standards demanded by their engineering task. The use of local materials implies a priority in defining limits to the use of "marginal" pavement and earthwork materials
Sub-grade	The nature of the foundation, or subgrade, is a fundamental input into access road design and research into methods of assessment and procedures for dealing with problem sub-grades (e.g. swelling or collapsible soils) is an important issue
Secondary relevance	
Policies	Research frequently provides basic key evidence for appropriate policies on rural access; e.g. climate resilience; use of materials; road asset management
Specifications	Specifications appropriate to the local engineering environment are an essential element of an effective enabling environment for rural access. Engineering Geological research provides important evidence for drafting these locally based specifications
Maintenance	All roads, however designed and constructed, require regular maintenance to ensure that their basic task is delivered throughout the design life. Engineering geology provides important support in terms of materials, earthworks and drainage monitoring and performance

Table 3 Recent and current DFID-funded materials-related research

Topic	Research	Reference
Marginal material	Review of marginal road construction materials and their appropriate use in developing countries	Cook et al. (2001)
Performance gravel wearing course materials	Recommendation on the limitations of the use of unsealed roads in a high rainfall environment (Vietnam)	Cook and Petts (2005)
Use of calcretes	Review of calcrete properties and suggestion technical specifications	TRL (2014)
Use of Ethiopian cinder gravels	Review of cinder gravel properties and suggestions as to their use as road construction materials	Hearn et al. (2017)
Back analysis of material performance	Comprehensive capture of existing rural road performance data and recommendations on improved specifications	Rolt et al. (2017)

and sub-base materials are based on universal standards applied to all traffic levels. Where the materials fail to meet these criteria they are termed "marginal" or "sub-standard". However, research advances have introduced the concept of "appropriate" local use of materials rather than selection on the basis of comparison to an overarching international standard applicable to all traffic levels.

2. An important principle is to look for and adopt access road designs that suits local materials rather than look for materials to suit standard designs.

3. Materials that have undergone tropical (chemical) in situ weathering and/or pedogenesis (laterites, calcretes and gypcretes for instance) may need to be treated slightly differently from traditional materials. Standard test methods often do not produce results applicable to the materials as conventional sample preparation techniques (oven drying, soaking, etc.) can affect the results.

4. Appropriate road construction materials need to be selected on a "fitness for purpose" basis and that this is related to the service performance expectations for the material. This approach needs to recognize the impacts of the governing road environment.

5. A key objective in sustainable rural access provision is to best match the available construction material to its road task and its local environment

6. Conflicts can also arise between material acceptability as defined by the specification and material suitability in terms of its actual engineering performance as a road making material. This occurs because of:
   - Inappropriate application or misplaced interpretation of test methods

- Testing materials that are not in the final compacted/as-built state
- Inability to measure or assess the environmental influences
- Inherently non-standard engineering characteristics.

3.3 Appropriate Climate Resilience (CR) Adaptation Options

ReCAP commissioned a project in April 2016 to produce regional guidance on the development of climate-resilient rural access in Sub Saharan Africa through research and knowledge sharing within and between participating countries. The study covers threats and adaptation for both existing and new infrastructure. It addresses the issues of appropriate and economic methodologies for vulnerability and risk assessments; prioritisation of adaptation interventions; and optimisation of asset resilience in the context of low volume rural access roads. A key output is a Guideline on Engineering Adaptation which discusses the expected effects of different climate change attributes on low volume access roads and highlights possible adaptive solutions, (CSIR 2017). Table 4 summarises the relevance of Engineering Geology within a logical series of steps associated with an effective CR assessment for a rural road or rural road network.

3.4 Natural and Earthwork Slopes

Natural and earthworks slopes along rural access alignments constructed in hilly and mountainous areas may require to be stabilised and protected from erosion using low-cost engineering and bio-engineering techniques.

Recent DFID funded research in Lao PDR produced practical manuals for the use of low cost techniques, including bio-engineering (Scott-Wilson 2009). The demonstration used grass and shrub planting, both with and without the contribution of small-scale engineering structures to stabilise erosion and shallow instability on earthworks slopes. It was important to ensure that the mechanisms of instability were fully understood before decisions were made as to how to invest in stabilisation and protection. Experience gained on the project in Lao PDR has shown that a combination of small scale engineering works and grass and shrub planting can have rapid positive effects on slope stability.

Appropriately selected bio-engineering options may also be effectively used for the protection of roadside erosion-vulnerable embankments adjacent to river and delta channels or in low-lying coastal zones. Options here also need to be designed as carefully as any other engineered structure, and hence take account of engineering geological models as reported in Cambodia by SeaCAP, (Howell 2008).

3.5 "First Mile" Agricultural Access

The primary transport segment (the "first mile") between the farm and an all-season access road is where the initial stages of crop movement in many developing countries is most expensive (tonne/km), and provide the biggest transport constraints in terms of post-harvest losses and agricultural marketing An understanding of the relationship between low standard, frequently earth, roads and constraints to rural economic development is an important research issue. The general approach for dealing with such access requirements is to employ earth road technology and apply spot improvements in sections likely to encounter seasonal problems.

A crucial element of research in this area is appreciating the nature (the geology) of the materials providing the earth

Table 4 Engineering geology and CR assessment

Step	Description	Engineering geology research input
1	Identification of the relevant climate threats and/or impacts	Limited application
3	Definition of the road assets at risk from climate impacts	Engineering geological procedure for identification and characterisation of road assets
4	Assessment of the vulnerability of these assets	Engineering geological assessment of condition and the consequence of climate impact of road assets
6	Prioritisation of the importance of climate impact hazards in terms of risk	Concepts of hazard and risk within the engineering geological- geotechnical context
7	Identification of engineering options to deal with prioritised risks	Research into the development and application of a range of cost-effective geotechnical options within the broad groups of avoid; remove and adaptation
8	Definition of actual options to be implemented	Research into the appropriate engineering geological parameters to be used within specific road environments

road running surface and how they perform under varying conditions of moisture and remoulding leading to roughness and rutting under combined impacts of traffic and climate.

A current ReCAP project (Bradbury et al. 2017) is researching the cost-benefits of the improvement of 'First Mile' access and the transport services associated with transferring harvest produce on the initial stages of movement from the farm to established road access in Sub-Saharan Africa. The research also explores the specific elements of the transport system that can be improved in order to unlock growth in the smallholder value chain. Rolt et al. (2008) focussed more on the engineering and geological factors around earth roads being sustainable option for rural access in Cambodia. The research defined simple key factors on the effective use of earth materials on these roads based on a number of criteria:

- Grading Coefficient
- Remoulded shear strength (with links to clay mineralogy)
- Compact strength (using CBR as an index).

4 Mobility and the Rural Access Index (RAI)

A new initiative—Sustainable Mobility for All (SuM4All)—is a global partnership that acts collectively to help unify and transform the transport sector (World Bank 2017). Its ambition is to make mobility: (i) equitable—ensuring that everyone has access to jobs and markets through good quality transport regardless of their economic or social status; (ii) efficient— to allow people and goods to move from place to place quickly and seamlessly; (iii) safe—by halving the number of global deaths and injuries from road traffic accidents and other modes of transportation; and (iv) green —by lowering the environmental footprint of the sector to combat climate change and pollution.

SuM4All has been identified by ReCAP as a focus for its transport research. ReCAP will explore how to work most effectively with SuM4ALL to support the necessary supply of scientific data and evidence that SuM4All requires for its monitoring function through a global tracking framework. Elements of engineering geological research are included in this. One aspect will be through the Rural Access Index (RAI) which is the principal indicator for universal access in rural areas proposed for SDG target 9.1.1 and is defined as the proportion of the population that lives within 2 km of an all-season road (Roberts et al. 2006).

In 2015 the World Bank (with funding from DFID) developed a new methodology that uses detailed geospatial road network, road quality, and population data to measure the RAI. Many low-income countries have no (or very limited) information, in terms of the inventory and condition

of their rural network of predominantly low-volume roads. To circumvent this issue, DFID has been exploring further development of the RAI data capture methodology through ReCAP, using satellite imagery (Workman 2017). The significant technological advances over the past ten years mean there are opportunities for utilization of remote sensing technologies and methodologies to make significant advances in the data for the sector and the effectiveness of the sector.

High-resolution satellite imagery is now available worldwide, and covers many of these inaccessible areas. The research has shown the potential exits to provide inventory data and condition assessments of entire networks. It is important to investigate the suitability of cost-effective, sustainable, high-technology solutions that can be used to gather appropriate information on a country's rural network for maintenance and management purposes. The ReCAP research has indicated that inventory and condition of roads can be established relatively accurately using satellite imagery. Tentative condition indicators from satellite imagery have been developed through correlations with manual assessments. Draft guidelines have been produced as part of this ongoing research.

5 Conclusions

Engineering Geological research has an important role to play in the sustainable development of fit-for-purpose rural access which in turn is key to achieving several of the 2030 Sustainable Development Goals (SDGs). Through Engineering Geology related research a wide range of rural access issues: construction materials; slope stability; climate resilience; and agricultural development are potentially impacted. Engineering Geology has an important role to play in providing the tools to deliver an holistic approach to strengthening rural access within an environment of low budgets and low resource allocation.

Uptake of this research through targeted design guides and low volume road manuals and specifications add considerable value to the research and enhance its value to road network development (Sampson et al. 2014).

The benefits of Engineering Geological Research have started to be quantified in economic terms. A recently completed Cost Benefit Analysis (CBA) of research was undertaken by ReCAP on previous DFID funded work on the impact of materials and rural pavement research and the improvements of rural access in Vietnam (Petts et al. 2017). Conclusions were that the CBA of the research (key elements such as materials properties were Engineering Geology related) provided an approximate Economic Internal Rate of Return (EIRR) of at least 20%, using worst case scenarios, and Net Present Value (NPV) of US$465 million.

Additional work to compliment these figures gave a Benefit Cost Ratio of at least 3%. Whilst further work continues to be undertaken on this project these results are very positive in terms of demonstrating the benefits of research.

This work has underscored the benefits of research in the rural transport sector. The Cost/Benefit Analysis has been carried out for Commune Roads only in Vietnam. The additional benefits for paving District and other Roads in Vietnam, and the uptake of the paving and gravel research knowledge in other countries in the region were not included.

References

Bradbury, A., Hine, J., Njenga, P., Otto, A., Muhia, G., Willilo, S.: Evaluation of the Effect of Road Condition on the Quality of Agricultural Produce, TRL-IFRTD Progress report for ReCAP. ReCAP for DFID, London (2017). http://research4cap.org/Library

Cook, J.R., Bishop, E.C., Gourley, C.S., Elsworth, N.E.: Promoting the Use of Marginal Materials. KaR report PR/INT/205/2001/R6887 for DFID (2001)

Cook, J.R., Petts, R.C., Rolt, J.: Low Volume Rural Road Surfacing and Pavements: A Guide to Good Practice. Research Report for AfCAP and DFID (2013). http://research4cap.org/Library

Cook, J.R., Petts, R.C.: Rural Road Gravel Assessment Programme. Draft Final Report, SEACAP report for DFID (2005)

Cook, J., Hearn, G., Paige-Green, P., Hagues, D.: An Overview of Engineering Geology and Sustainable Rural Infrastructure Development. IAEG Congress, Turin (2014)

CSIR et al.: Climate Adaptation: Risk Management and Resilience Optimisation for Vulnerable Road Access in Africa Project GEN2014C; Series of Technical Reports. London: ReCAP for DFID (2016–17). http://research4cap.org/Library

Hearn, G.J., Otto, A., Greening, P.A.K.: Investigation of the Use of Cinder Gravels in Pavement Layers for Low-Volume Roads. Ongoing series of ReCAP Progress and Technical Reports. London: ReCAP for DFID. http://research4cap.org/Library

Howell, J.: Study of Road Embankment Erosion and Protection. DFID Technical paper SEACAP19/06 for Royal Government of Cambodia (2008). www.gtkp.com. EST 2017. Transport Towards Achieving the 2030 Agenda for Sustainable Development. Adopted at the 10th Regional Environmentally Sustainable Transport (EST) Forum in Asia, 14–16 March 2017, Vientiane, Lao PDR

Peet, K.: Accelerated Action on Rural Transport in Asia-Pacific Region. Presentation to 9th UNCRD EST Forum Kathmandu, Nepal November 2015 (2015). Available from: http://slocat.net/sites/default/files/uncrd_-_9est_-_rural_transport_-_slides_-_2015-11-18_-_flash.pdf

Petts, R., Hine, J., Nguyen, T.P.H., Pham, G.T.: Cost/Benefit Analysis of SEACAP trials in Vietnam. ReCAP for DFID. Draft Final Report, London (2017)

Roberts, P., Shyam, K.C., Rastogi, C.: Rural Access Index: A Key Development Indicator. Transport Papers TP-10. The World Bank Group (2006)

Rolt, J., Cook, J.R., Kackada, H.: Behaviour of Engineered Natural Surfaced Roads: Experimental Evidence in Cambodia. TRL Ltd Report for SEACAP (2008). http://research4cap.org/Library

Rolt, J., Mukura, K., Buckland, T., Otto, A., Mayanja, M., Zihni, J.: Development of Guidelines and Specifications for Low Volume Sealed Roads through Back Analysis: Phase 1 Final Report. ReCAP for DFID, London (2017). http://research4cap.org/Library

Sampson, L.R., Geddes, R.N., Negussie, B., Asrat, A.: Low volume road research into practice: the Ethiopian experience. In: Proceedings of the South African Road Federation (SARF) 5th Regional Conference for Africa, Pretoria, 2014

Scott-Wilson.: Slope Maintenance Manual for Ministry of Public Works, Lao PDR (2009). http://research4cap.org/Library

SLoCaT.: Partnership on Sustainable, Low Carbon Transport.: Promotion of Sustainable Rural Access in the implementation of the 2030 Global Agenda on Sustainable Development: Key Messages Consultation Analysis (2017). ReCAP for DFID, London. http://research4cap.org/Library

TRL Ltd.: Identification and Mapping of Calcrete Deposits in Inhambane Province and Preparation of a Calcrete Classification System and Specifications for the Use of Calcrete in Road Construction in Mozambique. AFCAP/MOZ/091 (2014)

The Vientiane Declaration.: Vientiane Declaration on Sustainable Rural Transport. Towards Achieving the 2030 Agenda for Sustainable Development (2017). http://www.uncrd.or.jp/content/documents/5099Final%20Adopted%20Vientiane%20Declaration-16March2017-(Unedited).pdf

Workman, R.: The Use of Appropriate High-Tech Solutions for Road Network and Condition Analysis, with a Focus on Satellite Imagery: Technical Status Report. ReCAP for DFID, London (2017). http://research4cap.org/Library

World Bank: Global Mobility Report 2017 (GMR) (2017). http://wrld.bg/ezWj30fWUOC

World Bank: Rural Access Index: Access to Rural Transport (2017). Available at: http://bit.ly/2rg8k1J

South Asian Perspectives in Understanding Role of Engineering Geology for Geodisaster Management

Ranjan Kumar Dahal

Abstract

Loss associated with geodisasters is immense in South Asia, not only in terms of human lives but also in terms of property destroyed. Despite increasing geodisaster risk in the South Asian Region, awareness and understanding of georisks among people and governments remains low. Exposure and vulnerability to geohazards and their consequential impacts are not yet at the forefront of development agendas in the all South Asian countries. Situations are worst in Nepal, India, Pakistan and Bangladesh. In many cases, the disaster management authorities in these countries could not accept the fact that the geohazards in this region are directly associated with fragile geological settings and weak understanding of engineering geology of the region. This paper describes importance of engineering geological study in south Asia for geodisaster management.

1 Introduction

The losses caused by geodisasters, such as landslides, floods, earthquakes, and tsunamis are immense in south Asia (Fig. 1), not only in terms of human lives, but also in terms of property destroyed. The regional ratio of the number of the earthquake and tsunami disasters and of the number of casualties during the last two decades is very critical. In the last two decades, 16 events in the Asian region claimed about 500,000 lives, which is almost 90% of the total number of global casualties (Hamada 2009), and the proportion of South Asia is very alarming.

The International Disaster Database (2017) reveals that South Asian Region is facing high number of geodisasters per year over the past four decades, and the cost of damages have accumulated to over US$25 billion in the period of 2007–2012 alone. The human impact of geodisasters is also high in this region in the last 40 years; approximately 850,000 people have lost their lives in South Asia due to natural disasters.

It is important to understand the role of the engineering geologist when considering construction and planning of engineering projects. This is especially important for the case for the South Asian region because of its relatively very complex geological setting from young Himalayan mountains to Precambrian Indian Shield along with alluvial plains and coastlines. Engineering geologists employ scientific method essentially required in civil engineering; firstly, for the observation and classification of physical conditions of the site, second, for the formation of a hypothesis to explain those engineering geological conditions, and third, for experimented qualitative and quantitative results to validate hypothesis and support sustainable engineering projects. A detailed and precise knowledge of engineering geology is an essential part of construction projects and hazard analysis (Prakash et al. 2015). In the South Asian context, geologists are still limited to mine and rock sciences. Governmental and non-governmental agencies in South Asian region are still unable to understand the precise role of engineering geologists in civil engineering works such as dams, bridges, roads, and large buildings together with residential development. Agencies are still unaware that safety in land development requires the expertise of both the engineering geologist and engineer. It is hard to convince governmental agencies that the engineering geologist has an important role in managing geologic hazards along with civil engineering designs.

Despite increasing geodisaster risk in the South Asian Region, awareness and understanding of georisks among

R. K. Dahal (✉)
Central Department of Geology, Tribhuvan University, Kritipur, Kathmandu, Nepal
e-mail: rkdahal@gmail.com

Fig. 1 Regional map of the south Asian region. The locations mentioned in the map are described in the various sections of this paper. M–N road is the Mugling-Narayangadh road of Nepal

people and governments remains low. Exposure and vulnerability to geohazards and their consequential impacts are not yet at the forefront of development agendas in all South Asian countries. Situations are worst in Nepal, India, Pakistan and Bangladesh. In many cases, the disaster management authorities in these countries could not accept the fact that the geohazards in these regions are directly associated with fragile geological settings and poor understanding of engineering geology of the region. Following paragraphs describe few cases of geodisasters in South Asian regions and role of engineering geology in the mitigation and management of geodisasters.

With these understandings, this paper gives a brief synopsis of few major geodisasters of South Asia and describes the status of engineering geology in geodisaster mitigation.

2 2015 Gorkha Earthquake—Nepal

Nepal is central part of the Himalayan ranges, and it is regarded as one of the earthquake-prone countries in the South Asian region. Earthquakes in Nepal have been reported since 1255 while major earthquakes were recorded in 1408, 1681, 1810, 1833, and 1866, 1934, 1980, 1988, 2011 and 2015. The 2015 Gorkha Earthquake measuring Mw 7.8, killed about 9000 people and injured thousands

of people. The 2015 Gorkha Earthquake occurred at 11:56 AM Nepal Standard Time on 25 April 2015 with an epicenter 77 km northwest of Kathmandu at Barpak village. This earthquake was one of the most powerful earthquakes and it was estimated that more than eighty-five million people have been affected which is equal to a quarter of Nepal's population (Dahal 2015).

Earthquakes are a major concern for Nepal because of poor land use planning, precarious settlement patterns, and poorly implemented building codes. Within these understandings, the Government of Nepal has started reconstruction and resettlement work in the earthquake affected areas. Government of Nepal has announced 17 model houses, and the second edition of these houses is already published (DUDBC 2017). The government clearly mentioned that the model houses were prepared with architectural designs, structural detailing and material estimates. There was nothing about the consideration of engineering geology of the construction sites. In fact, the earlier investigations already confirmed that topographic features are basically responsible for dissipation of seismic energy, and extremely high accelerations are usually observed at sites located on topographic ridges (Gilbert and Knopoff 1960; Davis and West 1973; Geli et al. 1988; Ambraseys and Srbulov 1995; Chávez-García et al. 1996; Miles and Keefer 2000; Dahal et al. 2013). Observations of the damage patterns of 2015 Gorkha Earthquakes, 1987 Whittier Narrows California Earthquake, the 1989 Loma Prieta (California) Earthquake, the 1999 Chi–Chi Earthquake of Taiwan, the 2004 Chuetsu Earthquake of Japan and the 2005 Kashmir Earthquake of Pakistan also indicate the occurrence of intense shaking in elevated ridges of rugged topography. Geli et al. (1988) have reported that buildings on crests suffer more damage than those located at the base. In the case of 2015 Gorkha Earthquake, the observations of Geli et al. (1988) were well noticed in northern part of central Nepal, such as Chautara, Sangachowk, Charikot, and Nawalpur town. These situations were well elaborated by local scientists after visiting damaged areas. But, while preparing 17 model houses, such ground variations were not considered. One can construct the same model house on top of the hill or ridge (rocky terrain) as well as on the mountain base (alluvial plain) without any change in design consideration. This clearly disregarded role of engineering geology in the reconstruction process. Although there were many more technical gatherings and visits in Kathmandu, reconstruction work did not realize the need to prepare seismic hazard map of the affected areas prior to reconstruction work to make earthquake safe settlements for the future.

3 2013 Uttarakhand Flood—India

An unexpected cloudburst, centered on the north Indian state of Uttarakhand, caused devastating floods and landslides in third week of July, 2013. This disastrous event is India's worst natural disaster of this decade so far. The rainfall received by the area was much larger than the regular rainfall. The debris flow and landslide blocked up the rivers, causing major overflow. The main day of the disaster was on 16 June 2013 and as of the official data of 26 June 2013 showed that more than 20,000 people were dead; many pilgrims were the victims and many people were reported missing.

Many villages settled either at river banks or on the debris flow fans faced extensive damages. The famous Hindu temple Kedarnath and surrounding settlements faced huge debris flow events after melting of ice and snow together with floods in Charbari lake (upstream). Although the Kedarnath Temple itself had not been damaged, its base was inundated with water, mud and boulders. But the settlement around the temple were severally damaged, resulting in several casualties.

This Kedarnath incident was directly linked with settlement on flood plain. The government could not regulate the settlement criteria based on the geological engineering site investigation for debris flow hazard assessment. People constructed hotels on the big boulders at Kedarnath. The site conditions and geomorphological settings clearly suggest the debris flow risk associated in the area, but no remedies were considered while constructing hotels and other residential units.

Although, the Government of India announced that the Uttrakhand disaster was a natural calamity caused by cloudbursts and unprecedented heavy monsoon rainfall, the true causes of this epic tragedy were in fact, associated with the unplanned tourism industry, construction of commercial and residential buildings and roads without any geologic engineering investigation study as well as without any hazard and risk analysis.

4 2005 Kashmir Earthquake—Pakistan

On October 8, 2005, a magnitude 7.6 earthquake affected the Kashmir region of Pakistan and India. The shaking was experienced in Pakistan, India and Afghanistan. More than 80,000 people were killed by this earthquake, and more than 4 million lost their homes.

The Kashmir earthquake took place at 8:50 AM Pakistan Standard Time and the epicenter was centered about 20 km northeast of Muzaffarabad, the capital of Pakistan-administered Kashmir. The Kashmir region is active belt of Himalaya making this region prone to intense seismic activity. 2005 Kashmir Earthquake was one of the worst earthquakes to hit in the region, and it caused extensive destruction in both Pakistan- and India- administered Kashmir, North–West Frontier Province of Pakistan, and Northern Pakistan. A few damages were also reported in Afghanistan and China. The secondary disaster after the earthquake were landslides that damaged many roads, settlements and infrastructures. The reconstruction processes were started, but they were basically driven with few technical assistances and supervisions by engineers from government and non-governmental organizations. The reconstruction works mostly concentrated to ensure compliance with seismic resistant building construction guidelines. The designs were more specifically prepared with thumb rules of structural engineering and ground response. As mentioned in earlier section, same type of practice was repeated during the reconstruction work after the 2015 Gorkha Earthquake in Nepal.

5 Role of Engineering Geologist in Disaster Mitigation

The major role of the engineering geologist for natural disaster reduction is to understand geological issues during planning and design of infrastructures, hazard and risk mapping as well as early warning of hazard and risk for sustainable economic development. Likewise, the engineering geologist can participate in the restoration and reconstruction works after natural disasters.

In many cases of South Asian region, the traditional geological site investigation practices dominate engineering geological evaluation of a site. A notable example is the recent road improvement project (Mugling-Narayangadh Road, Fig. 2) of central Nepal. Detailed site investigation report prepared as per the classical concept of geological study contained rock mass study, joint analysis, rock type study and geological description of the area. But, the report missed large-scale landslide masses in the road alignment; nearly 60% of road out of 36 km stretch is passing through old landslide masses (Yatabe et al. 2005; Hasegawa et al. 2009). During excavation of road for widening, toe of creeping landmass was cut. As a result, slope failures due to construction have claimed lives of more than 50 passengers within 2 years. Further, blockade of the road in this critical stretch is a common phenomenon. This is probably the most exemplary project of South Asian region where engineering geology was grossly neglected, and the project faced lots of damages in terms of wealth and lives.

Similarly, another example can be taken from the Gorkha Earthquake. The 2015 Gorkha Earthquake destroyed a huge number of infrastructures in central Nepal. Therefore,
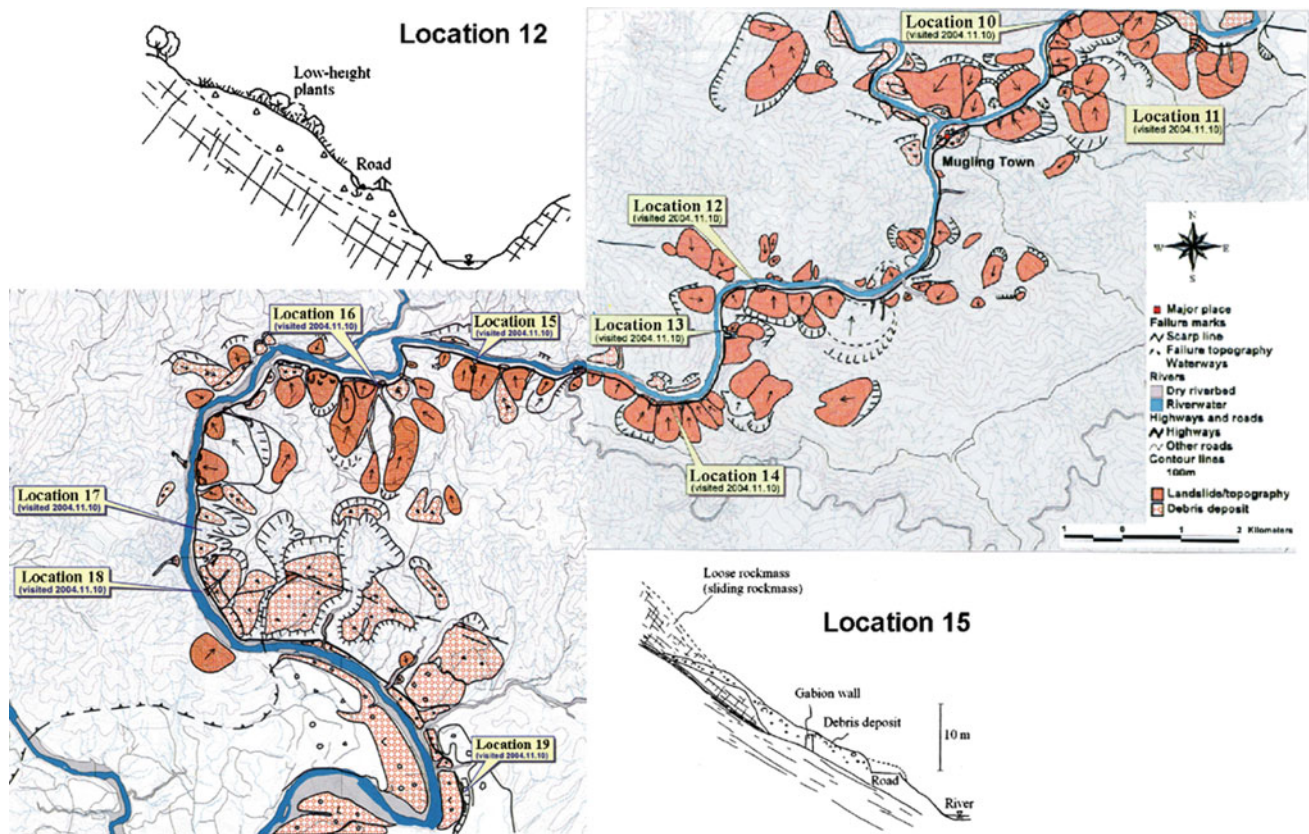
Fig. 2 Distribution of large-scale landslide mass in the Mugling-Narayangadh road of Nepal. Now this route has road widening project and facing serious problems due to many toe failures. After Yatabe et al. (2005)

engineering geologists have been advocating for consideration of ground properties in construction of new infrastructures considering future earthquakes. However, Nepal started reconstruction work without proper engineering geological site evaluations. Simply, qualitative observations have been done by geologists to finalize reconstruction plans. A major part of the reconstruction program was concentrated on earthquake safe building construction without considering ground characteristics. A large number of infrastructures such as highways, bridges, dams and public infrastructures were not evaluated in terms of future earthquake disasters. Gross conclusions have been drawn that these structures survived during the Gorkha Earthquake, so they will survive in another earthquakes and perform well in future! An utter disregard to engineering geology is repeated even in the aftermath of a disaster.

6 Proposals for Changes

From observations of various geodisasters of last 20 years in South Asia, it is realized that certain changes and interventions are necessary for sustainable development planning in

the region. Following proposals are made through this discussion paper for consideration of engineering geology in disaster risk management in South Asia.

In the South Asian context, the traditional concept of dealing with geological issues is only limited to regional geological study of rock identification, rock mass study, kinematic analysis, soil identification and so on during the infrastructure project study. The birds eye view of the site in terms of engineering geomorphological study is always lacking. The natural environment is not a permanent entity, and it is changing with time, and it is changing as per its utilization plan of social systems. The government should consider paradigm shift in policies for natural disaster mitigation and the role of engineering geology. Policies should be away from a short-term perspective focusing on sustainable economic growth and towards the long-term creation of safe and secure infrastructures.

National land utilization plan should be more balanced with the engineering geological study for geodisaster mitigation. Likewise, making engineering geological study compulsory in the process of assessment of vulnerability and potential risks of populated areas can help to save lives and properties in the communities. Specialized education on

engineering geology (preferably graduate programs) and focusing on geodisaster mitigation can help younger geologists to acquire mechanisms of disaster occurrence in terms of geological settings, and it will also help to obtain a proper understanding and judgment for geodisaster mitigation. Realizing this fact, an M.Sc. in Engineering Geology program has already been started in Nepalese university, and the program is first of its kind the South Asian region.

Improvement of observation and monitoring systems help to predict large-scale geodisasters, such as major earthquakes, tsunamis, landslides and floods. The impact and characteristics of large-scale geodisasters, which may occur once in several hundreds or even thousands of years should be studied by engineering geological and geophysical surveys. Engineering geology based numerical modeling for prediction of geodisaster can be attained by utilizing the data obtained from engineering geological site investigation and the results of computer simulations. In the meantime, uncertainties in the predictions and forecasting of geodisasters should be identified and should be taken into account in the planning of geodisaster mitigation measures.

7 Concluding Remarks

Geodisasters such as earthquakes, landslides, floods, tsunamis, and storms have been increasing during the last three decades in the South Asian region. Moreover, rapidly changing natural and social environments are expanding the scale of the geodisasters in south Asia. For the mitigation of the future geodisasters, the roles and the responsibilities of engineering geologists are increasing. The recent geodisasters in the south Asian region clearly pointed out that the development and application of technologies and knowledges for geodisaster mitigation are the urgent topic for engineering geologists working in South Asia.

References

Ambraseys, N., Srbulov, M.: Earthquake induced displacement of slopes. Soil Dyn. Earthq. Eng. **14**, 59–71 (1995)

Chávez-García, F.J., Sanchez, L.R., Hatzfeld, D.: Topographic site effects and HVSR, a comparison between observation and theory. Bull. Seismol. Soc. Am. **86**(5), 1559–1573 (1996)

Dahal, R.K.: Engineering geological issues after Gorkha earthquake 2015 in Nepal—a preliminary understanding. In: Paper Presented in 10th Asian Regional Conference of IAEG, Kyoto, Japan (2015)

Dahal, R.K., Bhandary, N.P., Timilsina, M., Yatabe, R., Hasegawa, S.: Earthquake induced landslides in the roadside slopes of East Nepal after recent September 18, 2011. In: Ugai, K., Yagi, H., Wakai, A. (eds.) Earthquake Induced Landslides. Springer Berlin Heidelberg, pp. 149–157 (2013)

Davis, L.L., West, L.R.: Observed effects of topography on ground motion. Bull. Seismol. Soc. Am. **63**, 283–298 (1973)

DUDBC: Catalogue for Reconstruction of Earthquake Resistant House, vol. II. Department of Urban Development and Building Construction, Government of Nepal (2017)

Geli, L., Bard, P.Y., Jullien, B.: The effect of topography on earthquake ground motion: a review and new results. Bull. Seismol. Soc. Am. **78**(1), 42–63 (1988)

Gilbert, F., Knopoff, L.: Seismic scattering from topographic irregularities. J. Geophys. Res. **65**, 3437–3444 (1960)

Hamada, M.: Roles of civil engineers for disaster mitigation under changes of natural and social environments and policies for the creation of a safe and secure society. In: Tankut, A.T. (eds.) Earthquakes and Tsunamis. Geotechnical, Geological, and Earthquake Engineering, vol. 11. Springer, Dordrecht (2009)

Hasegawa, S., Dahal, R.K., Yamanaka, M., Bhandary, N.P., Yatabe, R., Inagaki, H.: Causes of large-scale landslides in the Lesser Himalaya of central Nepal. Environ. Geol. **57**(6), 1423–1434 (2009)

International Disaster Database: Published in (2017). http://emdat.be/emdat_db/ and accessed on 2017/10/01

Miles, S.B., Keefer, D.K.: Evaluation of seismic slope-performance models using a regional case study. Environ. Eng. Geosci. **6**(1), 25–39 (2000)

Prakash, S., Singh, S.K., Jain, P.A., Dwivedi, N., Dwivedi, S., Mishra, V.K., Pundir, V.S.: Importance of geology in construction and prevent the hazards. Adv. Appl. Sci. Res. Pelagia Res. Libr. **6**(6), 75–80 (2015)

Yatabe, R., Bhandary, N.P., Bhattarai, D.: Landslide Hazard Mapping along Major Highways of Nepal. Ehime University and Nepal Engineering College, 164 p (2005)

Action Research to Enhance Student Engagement in Geotechnical Engineering

Maria Ferentinou and Zach Simpson

Abstract

In recent decades, much attention has been given to students' classroom participation, with many academicians and institutions arguing that the traditional lecture format is no longer conducive to student learning in higher education. This has prompted much investigation into alternative methods of teaching, including online learning, and others. This research takes places in a large university in Johannesburg, South Africa, where student exam results, as well as feedback obtained through teaching and module evaluations, indicate that undergraduate students lacked interest in geotechnical engineering and felt that course content was poorly communicated. In order to address problems of teaching and learning, this study applies an action research methodology aimed at enhancing student engagement in geotechnical engineering study. Action research is a cyclical approach to research, in which a series of interventions are designed, implemented and assessed, before being re-designed. Generally, a number of such iterations are undertaken. In this study, these interventions were aimed at improving teaching practice, enhancing student satisfaction, instilling confidence within the students, and improving the teaching and learning experience for both the lecturer and students. The interventions designed include: in-class participation, interactive lecturing, strategies to relate current learning to future practice, increased use of software applications, and weekly quizzes. The interventions were assessed through student surveys, teaching evaluations, and the lecturer's personal reflection journal. In this paper, the results of the first iteration of this action research are presented, wherein the preliminary results are encouraging regarding increased student engagement in geotechnical engineering study.

1 Introduction

In order to address of teaching and learning, much attention has been given to students' classroom participation, with many academics and institutions arguing that the traditional lecture format is no longer conducive to student learning in higher education. This has prompted investigation into alternative methods of teaching, including online learning (Clarke 2011), 'flipped classroom' approaches (Kostaris et al. 2017), and myriad others. In engineering education, specifically, lecturers face varied challenges in the classroom, these being compounded by diminishing credit hours, increased workload, programme accreditation bodies, assessment, and decreased student engagement.

In this study, the focus is on students' engagement in the area of geotechnical engineering. Geotechnical engineering is a major component of civil engineering curricula. The underlying principles of geotechnical engineering education, according to Burland (1987) and Orr and Farrell (1999) are:

M. Ferentinou (✉) · Z. Simpson
Faculty of Engineering and the Built Environment, University of Johannesburg, Johannesburg, South Africa
e-mail: mferentinou@uj.ac.za

- to develop good understanding of soil and its behaviour;
- to perform appropriate investigations and tests so that the soil profile and the properties of soil strata may be determined;
- to teach appropriate models for analysing soil behaviour and predicting the behaviour of different types of geotechnical structures, such as spread foundations, piles, retaining structures and slopes;
- to provide guidance on the design and construction of common geotechnical design;
- and impart a liking and enthusiasm for geotechnical engineering.

As a discipline, geotechnical engineering involves uncertainty, both epistemic and aleatory uncertainty. To address this inherent problem, geotechnical engineers apply probabilistic analysis methods. This raises challenges for student learning, as they must come to realise that there is no one superior truth and they need to move themselves away from dualistic ways of thinking. In order to enable students to apply theoretical knowledge to complex engineering problems, they have to be confronted with real engineering problems as part of their learning.

At University at which this research was conducted, around 70 students are registered in the final year of studies at any given time, and around 10 of these pursue their final year capstone research project in a geotechnical engineering subject. Students prefer other areas, such as construction management or structural engineering. A possible reason for this is that geotechnical subjects are perceived as too difficult. This difficulty emanates from the fact that the students need to apply non-linear mechanics, which is not what they have been taught in structural mechanics and/or strength of materials. However, once students understand uncertainty as legitimate and inherent to geotechnical engineering science, they can gain greater levels of comprehension.

This paper seeks to overcome these challenges by describing the initial iteration of an action research project aimed at enhancing student engagement in geotechnical engineering study. The decision to use action research was informed by the fact that it is generally accepted that action research is "a suitable research model for engineering educators who wish to do research on active learning in engineering education" (Christie and de Graaff 2017: 9). Action research is a cyclical approach to research, in which a series of interventions are designed, implemented and assessed, before being re-designed. In this study, these interventions were aimed at improving teaching practice, enhancing student satisfaction, instilling confidence within the students, and improving the teaching and learning experience for both the lecturer and students. Action research is characterised by multiple iterations of intervention: this paper reports on the

initial iteration of the project and reflects on the ways forward for subsequent iterations.

The paper is structured such that it begins by describing the problems evident in higher education, generally, and the specific site at which this action research was undertaken, namely a large university in Johannesburg, South Africa, where student exam results, as well as feedback obtained through teaching and module evaluations, indicate that undergraduate students lacked interest in geotechnical engineering and felt that course content was poorly communicated. Thereafter, the particular interventions deployed are described: these interventions were aimed at addressing the problems previously mentioned. The preliminary results of these interventions are then presented; this is based on lecturer reflection as well as student data. Finally, reflection on the design of subsequent interventions is presented, before conclusions are drawn as to the need for action research to inform teacher practice in higher education and at all levels of education. This structure follows the traditional approach to action research.

2 Sketching the Problem: Higher Education, Student Engagement and the Need for Action Research

Traditionally, teaching in higher education (and at other levels) has been conceived of as an exercise in knowledge transfer (Konstantinou-Katzi et al. 2013). Within such a view, students are conceptualised as empty vessels that passively receive the information that educators impart. However, this traditional view of teaching, "where the teacher is always the one delivering the material" is becoming increasingly ineffective (Konstantinou-Katzi et al. 2013: 332). Indeed, such traditional teaching is seen to foster what Marton and Säljö (1976) term 'surface learning'. Instead, students create knowledge for themselves, rather than it being imposed upon them by teachers (Biggs 2003).

This is closely linked to another problem often encountered, particularly in engineering education, namely that students are often able to follow procedures without understanding basic concepts, and without being able to apply those concepts across multiple contexts and scenarios (Konstantinou-Katzi et al. 2013). For example, Konstantinou-Katzi et al. (2013: 337) argue that this is commonly observed in mathematics classrooms targeted at engineering students: "students often do not see the usefulness and applications of mathematics in their field of study, and thus lose their motivation". This accords with Perkins' (1992) argument that students not only need to be taught content, but also need to be taught how to understand and apply that content, as well as how to demonstrate their understanding of content.

Of course, these challenges are not universal: many students are fully capable of understanding and applying knowledge within the current education system. However, one of the main challenges faced by higher education instructors is effectively dealing with students' differing educational backgrounds (Konstantinou-Katzi et al. 2013). Inequalities across society are made manifest in the resources that students bring with them to the educational sphere, and this means that there is a range of prior knowledge in any given classroom. This was particularly apparent in the context in which the present research was undertaken, as South Africa is recognised as one of the most unequal societies in the world, which is made manifest in its basic education system.

The challenges described above necessitate active learning on the part of students. This requires that educators direct learners' experiences and organise the conditions upon which effective learning depends (Christie and de Graaff 2017). This is a difficult proposition, as university students have already been exposed to many years of formal education and have therefore been 'programmed' to learn in particular ways; nonetheless, there is a need to incorporate active learning into engineering education as "an inquiry-based education that distributes the responsibility for learning between the individual student, the group and the teacher/facilitator" (Christie and de Graaff 2017: 8). This requires the deployment of formal and informal learning experiences across various settings, including classrooms, laboratories, online spaces, and in the real world (Christie and de Graaff 2017).

Such learning experiences may be more likely to engage and motivate learners; moreover, they may accommodate a more diverse group of students (Christie and de Graaff 2017). This is important as, too often, teaching addresses the needs of an imagined 'average student', with the result that students with low levels of preparedness are left to fail, while 'strong' students are left without challenge and become demotivated (Konstantinou-Katzi et al. 2013). Thus, in addition to active learning, there is a need for differentiated learning. Such an approach to teaching involves incorporation of a wider variety of learning activities that appeal to diverse learning styles and which challenge individual learners based on their own prior knowledge and abilities. One example of such an approach is the use of mini-projects undertaken by 'learning companies' (Cancela et al. 2016). Such mini-projects are "carried out in the classroom [but are] similar to the activities that exist in real companies … [and lead to] more cooperative learning and a different style of experimentation" (Cancela et al. 2016: 23).

However, the implementation of such strategies requires that educators be willing to experiment, to take risks, and potentially fail. It also necessitates that educators engage in scholarly reflection on their teaching practice. To this end,

action research is "a simple and straightforward methodology for engineering educators interested in pursuing their own scholarship of teaching and learning (Christie and de Graaff 2017: 8). Action research was selected as appropriate for use in this project because it encourages scholarly reflection on any new strategies introduced in the classroom. It also allows for trial and error, creativity and experimentation, as it involves multiple iterations.

More importantly, action research recognises that the teaching and learning process is complex "and that neither small, 'one off' course development prototypes nor tightly controlled experiments will be sufficient to solve challenges facing engineering education" (Olds et al. 2012: 408). Instead, it acknowledges that such change requires concerted and co-ordinated effort over time. As such, this paper represents the initial attempts at addressing the challenges that were evident in modules on geotechnical engineering at a large, public university in Johannesburg, South Africa. As has already been mentioned, these challenges included poor student engagement, low motivation, and dissatisfaction on the part of both the students and lecturer. These challenges were addressed by designing, evaluating and reflecting upon a number of teaching and learning interventions.

3 Implementing an Action Research Intervention

In order to address the challenges described above, a number of intervention strategies were identified. These were aimed at: enhanced in-class participation, interactive lecturing, application of strategies to relate current learning to future practice, increased use of software applications, and weekly quizzes.

Enhanced in-class participation

The lecturer sought to implement strategies aimed at motivating students. This included delivering course material with increased enthusiasm and energy, and sharing with the students her own interest in the material. Moreover, the lecturer tried to get to know the students in order to tailor the material to their concerns. To this end, long PowerPoint presentations and monologues were avoided. The lecturer also sought to learn and use all the students' names. The lecturer explained to students how to take good class notes. The lecturer designed the course with care and explained the organisation of the content to the students, both in class and through the study guide. Matching teaching methods to learning outcomes was a key approach to providing clarity to students, and student learning was enhanced though incrementally presenting what would be covered during the semester through a course map. The lecturer did more to

explain the reasoning behind selecting certain teaching methods or assignments or class activities. Student-centred teaching formats were introduced, including discussion, problem-based learning, case methods, and in-class problem solving.

Application of Interactive lecturing methods

The lecturer developed a lecture plan, supported by questions, and practical examples which were given to the students. This enabled a student-centred learning experience. Questions were used to guide students' thinking about problem components and goals.

Strategies to relate current learning to future practice

Two particular strategies were introduced in order to relate students' learning in class to their future practice. First, a guest lecture by a professional engineer was arranged, during which this guest shared his experience on various projects in Southern Africa. Second, a technical visit was arranged. This saw the students visit a major infrastructure project, owned by a state-owned company. The scale of the project was such that students were able to apprehend various aspects, from design to construction, across various disciplines of civil engineering.

Emphasize increased use of software applications

The lecturer encouraged the use of standard geotechnical analysis tools in order to introduce students to computer-based data analysis, synthesis and design. After a short demonstration of the software suite, students were asked to go through tutorial examples, and practice problem solving.

Weekly quizzes

Short quizzes were given to ensure that students were adequately prepared for class. This is a method that enhances student's weekly engagement with the content.

4　Preliminary Results

The interventions were assessed through analysis of student pass rates in the two semester tests, as well as through teaching evaluations. These statistical measures were supported by data from the lecturer's personal reflection journal.

One of the earliest observations made was that the students were keen to participate in class discussions, once the stereotype of the lecturer-centred classroom was broken. This was evident in the fact that there was a steady 70% participation in class throughout the semester.

The pass rates in the two semester tests also rose. In fact, there was a 100% pass rate in both tests, with 60% of the students obtaining a distinction in the first test. In the second test, 35% obtained distinctions.

There was a third assessment opportunity in the module, in the form of a term paper. This form of assignment requires development of academic writing skill. However, students found this assignment demanding and also appeared to not manage their time effectively, failing to leave sufficient time for adequate research, or revision.

The results were particularly promising regarding the student teaching evaluations. The teaching evaluation questionnaire was distributed in the year prior to the commencement of the action research interventions (2016), and to the subsequent cohort who benefitted from the implementation of the first cycle of intervention (in 2017). The teaching evaluation questionnaire is administered by the University, and lecturers are required to have their teaching evaluated on a regular basis (usually, once per year). The aim of the questionnaire is to gather feedback from students regarding certain aspects of teaching, learning and assessment. The questionnaire consisted of 12 mandatory quantitative questions, 12 quantitative questions selected by the lecturer (from a bank of possible questions), and one qualitative question. The teaching evaluation questionnaires were completed by 40 out of 76 students in 2016, and 41 out of 96 students in 2017. Students recorded their responses to the questions using the following response set: Strongly agree (4), Agree (3), Disagree (2), Strongly disagree (1), Not applicable (0).

The results of both the mandatory and selected additional questions, for both 2016 and 2017, are shown in Figs. 1 and 2 respectively. Figures 1 and 2 show the percentage of student responses per category. As can be seen in the Figures, there was a clear increase in the percentage of responses in the categories 'agree' (green) and 'strongly agree' (blue), and a concomitant decrease in the proportion of students that 'disagreed' (red) or 'strongly disagreed' (white) with each statement.

In particular, the responses suggest significant increase in the proportion of students that agreed that the purpose of learning was made clear (from fewer than 50% to over 90%), that the lecturer encouraged student involvement (from approximately 65% to over 90%), and that the lecturer encouraged critical thinking (again, from approximately 65% to over 90%).

It is anticipated that a next cycle of action research based on reflections from the current cycle will continue to improve the teaching and learning experience. The qualitative question in the teaching evaluation questionnaire revealed that students perceive a need for more examples, and additional problem solving in class, in combination with the further use of the geotechnical software available. Some of the students indicated that continuous assessment through
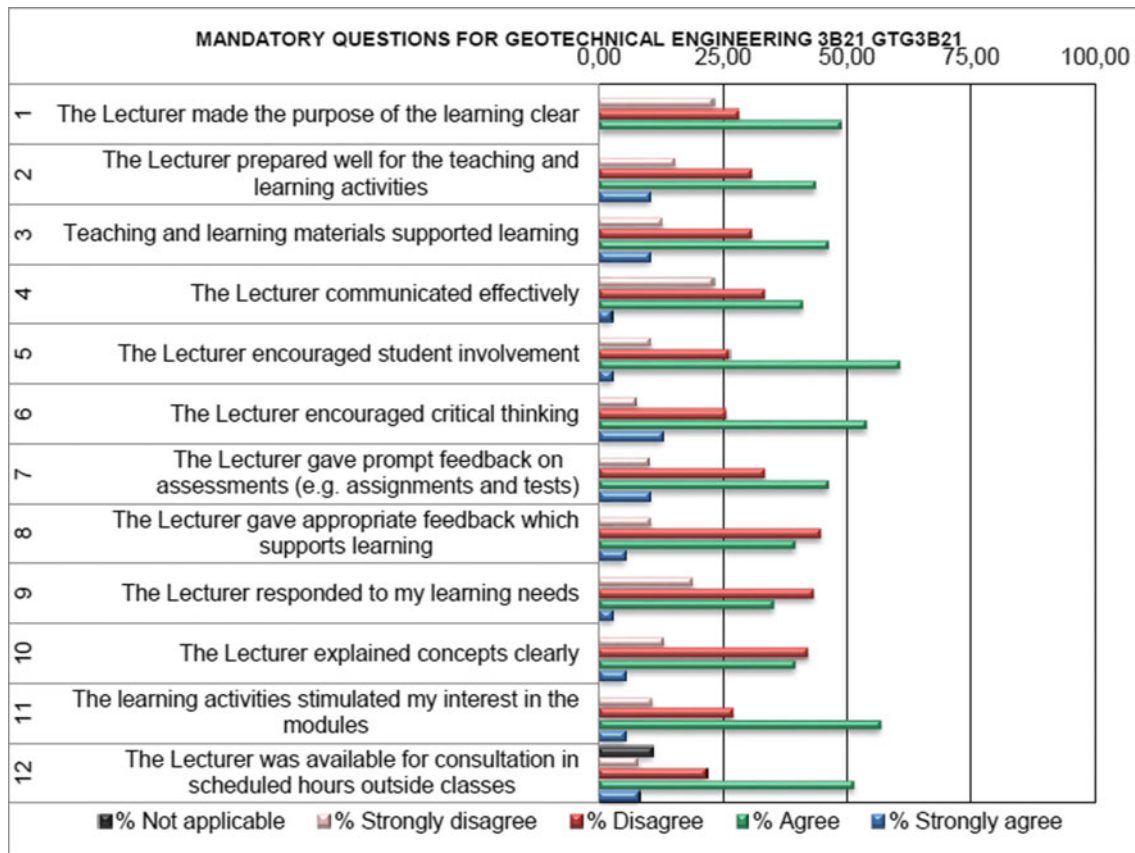
Fig. 1 Selected teaching evaluation questions and students response, in 2016

quizzes, and tests assisted them in organising their reading and studying. The comments also supported the further use of a variety of teaching styles.

In summary, the lecturer reflected that the initial cycle of interventions succeeded in increasing class attendance and class participation, and that there was a significantly more positive response evident in the teaching evaluations. The lecturer identified a need to continue to work toward applying methods that can deepen the learning experience of the students, while the students also seemed to appreciate the revisions made by the lecturer.

5 The Next Cycle

As evident in the first iteration of this action research intervention, strategies to enhance student participation were successful and should be continued. The application of interactive lecturing methods is becoming a minimum requirement for successful teaching and learning, and there is a myriad of such strategies which can be implemented in the future, such as homework classroom, the 'flipped' classroom, blended learning, etc.

Moreover, the guest lecture and technical site visit were highly welcomed by students and were found to assist with building knowledge and motivation regarding future professional practice standards and expectations.

Further emphasis needs to be placed on the use of software. This can be achieved through the requirement of mini projects. It was noted that students appeared to appreciate teaching and learning initiatives that link to their future progression through the academic and professional environment. To this end, mini projects can assist students to apply their knowledge, and the tools of analysis, in order to solve real world problems. These mini projects could be similar to those described by Cancela et al. (2016).

6 Conclusion: Student Engagement and Teacher Reflection

This paper has reported on the initial iteration of an action research project aimed at enhancing student engagement in modules in geotechnical engineering at a large, public university in Johannesburg, South Africa. Prior to the initiation of the action research, student engagement with these
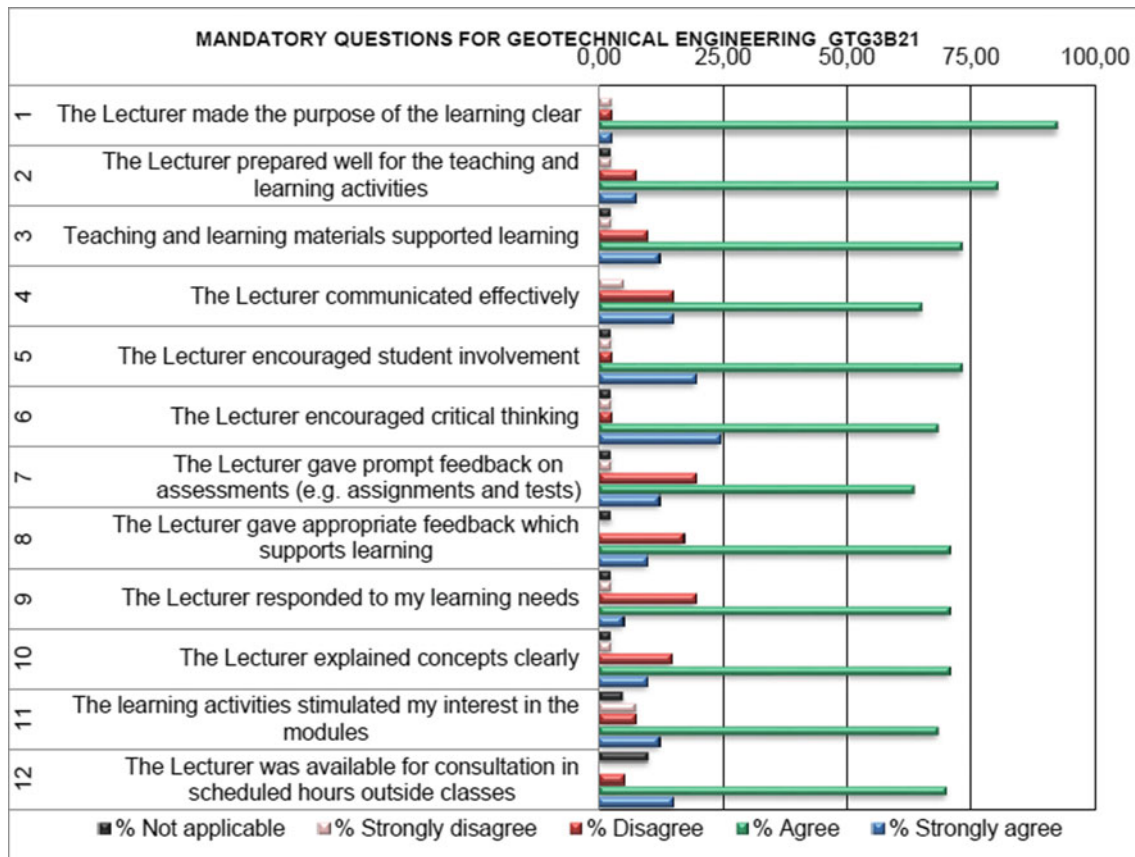
Fig. 2 Selected teaching evaluation questions, and student's response, in 2017

modules was poor, and feedback obtained from teaching and module evaluations was neutral to negative. A variety of teaching and learning interventions were designed in order to overcome these problems. Preliminary results from the action research study suggest some improvement regarding student engagement and satisfaction.

Moreover, the initiation of this action research study has demonstrated the importance of reflection on the part of lecturers. Teaching and learning is a complex process and reflection is important as it assists lecturers to "be able to handle a certain degree of chaos, uncertainty and messiness" (Brydon-Miller et al. 2003: 21). Reflection is built into the demands of action research and "action research is meant to expand the space of the possible, not only in relation to teachers' classroom practices but also in relation to reflection" (Luttenberg et al. 2017: 11). It is for this reason that action research is a useful methodology that teaching professionals can use to implement educational theory within their teaching practice, but also to generate theory from their practice. After all, "theory is really only useful insofar as it is put in the service of a practice focused on achieving positive social change" (Brydon-Miller et al. 2003: 15).

References

Biggs, J.: Teaching for quality learning at University. Open University Press, Buckingham (2003)

Burland, J.B.: Nash lecture: the teaching of soil mechanics—a personal view. In: Proceedings of the 9th European Conference on Soil Mechanics and Foundation Engineering, Dublin, vol. 3, pp. 1427–1447 (1987)

Brydon-Miller, M., Greenwood, D., Maguire, P.: Why action research. Action Res. **1**(1), 9–28 (2003)

Cancela, A., Maceiras, R., Sánchez, A., Izquierdo, M., Urréjola, S.: Use of learning miniprojects in a chemistry laboratory for engineering. Eur. J. Eng. Educ. **41**(1), 23–33 (2016)

Christie, M., de Graaff, E.: The philosophical and pedagogical underpinnings of active learning in engineering education. Eur. J. Eng. Educ. **42**(1), 5–16 (2017)

Clarke, S.: Peer interaction and engagement through online discussion forums: a cautionary tale. Liverpool Law Rev. **32**, 149–163 (2011)

Konstantinou-Katzi, P., Tsolaki, E., Meletiou-Mavrotheris, M., Koutselini, M.: Differentiation of teaching and learning mathematics: an action research study in tertiary education. Int. J. Math. Educ. Sci. Technol. **44**(3), 332–349 (2013)

Kostaris, C., Sergis, S., Sampson, D.G., Giannakos, M.N., Pelliccione, L.: Investigating the potential of the flipped classroom model in K-12 ICT teaching and learning: an action research study. Educ. Technol. Soc. **20**(1), 261–273 (2017)

Luttenberg, J., Oolbekkink-Marchand, H., Meijer, P.: Exploring scientific, artistic, moral and technical reflection in teacher action research. Educ. Action Res. [online] (2017). http://dx.doi.org/10.1080/09650792.2017.1295875

Marton, F., Säljö, R.: On qualitative differences in learning. I—outcome and process. Br. J. Educ. Psychol. **46**, 4–11 (1976)

Olds, B.M., Borrego, M., Besterfield-Sacre, M., Cox, M.: Continuing the dialog: possibilities for community action research in engineering education. J. Eng. Educ. **101**(3), 407–411 (2012)

Orr, T., Farrell, E.: Geotechnical design to Eurocode 7, Springer. In: Conference: 9th European Conference on Soil Mechanics and Foundation Engineering At: Dublin, Ireland Volume: 3 (1999)

Perkins, D.: Smart Schools: From Training Memories to Educating Minds. The Free Press, New York (1992)

Active Learning Teaching in Geotechnical Courses in Uruguay

Marcos Musso and Leonardo Behak

Abstract

Since 1960, different teaching approaches have been developed based on how the people learn. All of these show that learning is an active, contextualized and personal process where students construct their own knowledge from experience and activities and reflecting about them. This background encouraged us to introduce changes in how we were performing teaching activities. The Soil Mechanics course for the geology degree was modified. First, the goals were reformulated to include, in addition to soil mechanics practice and theory, skills as group work, writing and oral presentation. Second, field and laboratory experiences were reformated to be done as a group. Third, lectures were developed to include problem solving, student oral presentations from laboratory results and congress or journal paper. Finally, each group composed and defended a report about field and laboratory data and activities, including background and methods used during the investigation. Each student also completed an oral theoretical evaluation. The experience was a challenge for professors and students. In this course, the student groups worked similar to their future work as geotechnical geologists. They had a project that they needed to understand what to do, how to obtain laboratory and field data, analyze, write and defend a report. Our evaluation was positive because the students gained some useful tools for their professional future.

Keywords

Active learning • Geologist • Soil mechanics

M. Musso (✉) · L. Behak
Geotécnica, Facultad de Ingeniería, Universidad de la República,
J.H. Reissig 565, 11300 Montevideo, Uruguay
e-mail: mmusso@fing.edu.uy

L. Behak
e-mail: lbehak@fing.edu.uy

1 Introduction

Education and research are milestones in the University life. In general teaching activities are developed by professors who obtain a doctoral degree in a specific area and they conduct researches to improve and create new knowledge in their area. Sometimes in engineering, they teach as their professors taught them, using the same resources as blackboard and exercise list, or increasingly they used a software to create and edit presentation for slideshows (as Impress, Prezi, Powerpoint). However it is not common that the professors have undertaken didactics and pedagogy courses in their doctoral studies, meaning that they often do not have the tools for effective teaching. Often they are not aware of other methodologies other than traditional lectures.

In Uruguay the Universidad de la República was founded in 1836, is the most important university in the country and until 2014 was the only public university. Public education in Uruguay is free for all students. In university courses the enrolment is open; the students do not need to take any admission test to begin to study law, medicine, economics or engineering. Engineering courses were created more than 100 years ago, but the geology degree is only 40 year old. Nearly 100 geologists have graduated since the 1980's. The soil mechanics course is an optional course in the geology degree, however geotechnical work need the collaboration and interaction between geologists and geotechnical engineers to obtain knowledge about soil and rock behaviour. This collaboration gives to achieve the best performance in civil and environmental works.

In the last few decades the education model has been changing around the world. The students have different motivations, incentives, curiosity and they can access to non traditional information sources. In the traditional teaching style, the professor teaches a lecture and the student is bored and inattentive, hearing and writing what the professor says. This style does not take into account the fact that the students have different talents and styles of learning

(Felder and Silverman 1988). This education model is not suitable by this epoch, but this cannot only be solved with the develop of information and communication technology. Since middle of 20th century a constructivist approach of education shows other style in which the student is the an active participant in his or her own learning. Different approaches have been developed using this conceptual model. In the 1960's in Canada a Problem Based Learning (PBL) was developed using the constructivist approach. Later, other approaches have been developed as Collaborative Learning (Smith 2011; Johnson et al. 1998), Deep Learning (Millis 2011), and Significative Learning (Fick 2015). All have in common to change the education focus to the student. For that, different skills are developed: learning to cooperate and share information, promote oral and written communication, learning how learn, critical thinking, and personal development, among others (Middendorf and Kalish 1996; Mills and Treagust 2003).

The aim of this paper is to show an experience developed in 2016 and 2017 to develop the best teaching-learning procedures in the geotechnical area, and to generate discussion and synergy about education practices with colleagues, which could be used or adapted in other countries. The course had 6–10 students by year and in 15 weeks the students acquired skills such as group working, oral and written communication, planned work, produced and analyzed laboratory and field results.

2 Materials and Methods

The soil mechanics course was carried out with active learning methodologies combining: teacher-led lectures, student oral presentations, field investigations, laboratory tests and writing a report. Two professors with doctoral degrees in geotechnics participated: a geologist and a civil engineer.

The students were divided in groups, of 2 or 3, to develop a project during the course. In the beginning of the course they chose a project and they conducted a literature survey about the background of site, both geological and geotechnical.

During field work, observation and sampling was carrying out on a slope (a quarry, along a road) or using hand augers to sample the subsurface. Soil samples were collected at each site for laboratory testing. Typical soil tests such as grain size, atterberg limits were commonly use by all groups, and additional tests were carrying out according to needs of each project as identified by the student group. All tests (laboratory and field) were performed after reading and understanded the standard procedures, mainly the ASTM standard.

Examples of different that projects were proposed include hydraulic conductivity (field and laboratory) in clayey and sandy soils, expansive properties of clayey soil and mechanical behavior of soil for pavements.

In the middle of the course each project group did an oral presentation to show their lab results and at the end of the course they wrote a report and defended it in front of the professors and colleagues. The overall assessment was individual, where the students were required to show the theory.

3 Results and Discussion

The course has some traditional, teacher-led lectures where soil mechanic topics such as soil classification, hydraulic conductivity and consolidation theory, stress-strain properties and behavior, pavements, foundation, earth slopes and retaining structures were presented. Exercise lists in each chapter of the course notes were available to help students further develop their understanding of the concepts as self-directed learning.

In the fourth week the students conducted their first field work, with samples collected by each group. Three or four disturbed samples were collected by the groups, some of collecting undisturbed samples to measure physical soil properties such as porosity, bulk and dry weight, moisture, degree of saturation.

The students worked 4–6 h per week during weeks 5 and 6 weeks to obtain grain size distribution, Atterberg limits to use Unified Soil Classification System (USCS). All groups also determined weight-volume relations and optimum moisture content using the compaction test. After this, the groups carry out specific test in accordance with their project needs. The results were monitored and evaluated by the professor to guide the group in the analysis and discussion of the project data.

If any group must do field test (infiltration, dynamic cone penetration, etc.), in the 7–9 week all students go to do and learn how conduct the test is carry out.

Some difficulties occurred with respect to the testing schedule because some tests such as grain size distribution by hydrometer analysis, consolidation and expansive test required up to a full day to complete. This problem was overcome by alternating the members of the group to make the measurements during the day. Some groups took significant time to solve this difficulty; in this case the professors suggested some options for them to choose from. We consider this as part of the learning process, and provide students with exposure to the way and the time necessary to obtain this data, to analyse and do complete report.

During the oral presentations the initial results from all students groups were presented. During this event, all participants were motivated to ask questions of and provide suggestions to other groups. This feedback provided an

opportunity for the students improve their knowledge and competence.

At the end of the semester, the individual course assessment was conducted by oral defense, where students demonstrated their understanding and assimilation of soil mechanics theory.

4 Conclusion

The students completed a group project focussed on field and laboratory activities. They achieved a widespread understanding of soil mechanics theory, laboratory and field test through the work themselves on a real geotechnical problem. They also learned to work in groups, where they had to learn how to distributions the tasks and take responsibility for their contribution to the group project. They defended in oral their written report individually to assess their mastery of the course material. These professional skills must continue to be developed and perfected in other courses in the program.

In this active learning course the student showed better performance than the traditional lecture course where they showed that can integrate theory and practice with a real geotechnical site investigation.

The authors encourage colleagues to create, develop and share experiences in active learning course in the geotechnical area.

References

Fick, D.: http://www.designlearning.org/. Accessed 10 Mar 2015

Felder, R.M., Silverman, L.K.: Learning and teaching styles in engineering education. Engr. Educ. **78**(7), 674–681 (1988)

Johnson, D.W., Johnson, R.T., Smith, K.A.: Cooperative learning returns to college: what evidence is there that it works? Change, 27–35 (1998)

Middendorf, J., Kalish, A.: The "Change-up" in lectures. Natl. Teach. Learn. Forum **5**(2) (1996)

Mills, J.E., Treagust, D.F.: Engineering Education—is problem-based or project-based learning the answer. Australas. J. Eng. Educ. 2–16, ISSN 1324-5821 (2003)

Millis, B.J.: Promoting deep learning through cooperative learning. In: Cooper, J.L., Robinson, P. (eds.) Small Group Learning in Higher Education: Research and Practice, pp. 25–30. New Forums Press, Stillwater, OK (2011)

Smith, K.A.: Preparing students for an interdependent world: the role of cooperation and social interdependence theory. In : Cooper, J.L., Robinson, P. (eds.) Small Group Learning in Higher Education: Research and Practice (2011)

Engineering Geology Education in Australasia

Marlène C. Villeneuve

Abstract

Recent geohazard events, continued urban, infrastructure and resource development, and climate change in Australasia and internationally highlight the need for engineering geologists. In Australasia engineering geology is gaining recognition as a distinct profession that provides the link between engineering and geology. An important aspect of engineering geology training is through tertiary education aimed at providing the industry with work-ready graduates who are knowledgeable in the principles of engineering geology. This is achieved through a variety of programs, each with a different approach and level of proficiency upon graduation. The most common format is a single, introductory course offered in the final year of a Bachelor of Science (B.Sc.) in geology (or geoscience, earth science, etc.) available at many tertiary institutes that have a geology program. Also common are the several postgraduate courses that either build upon introductory undergraduate courses, or are stand-alone courses that form part of a taught postgraduate degree (B.Sc. (Honours), postgraduate diploma or Masters) or are combined with a thesis focused on research in engineering geology (M.Sc.). There is one postgraduate program with a comprehensive curriculum specifically aimed at educating and training engineering geologists through coursework and dissertation. Finally, engineering geology education and training is offered through geotechnical professional societies. The courses vary between institutions based on the structure of the programs and the expertise of the academic staff. This paper provides an overview of the types of courses, their learning outcomes, pedagogy, and how they form the different programs addressing engineering geology education in Australasia.

1 Introduction

This paper details the various education and training in Australasia. These are presented in four categories according to the education level and student types:

1. Undergraduate geologists
2. Postgraduate geologists
3. Professional development geologists
4. Civil engineers at all education levels

The purpose is to provide an overview of the different ways engineering geology is incorporated into tertiary curricula. Each category in this paper will summarize the typical content, and, where possible, the teaching and learning activities, and assessment types. The focus is to highlight the education pathways that exist in Australasia as an example for other countries and universities. Professional chartering of engineering geologists is possible in New Zealand and will soon be in Australia. The final section of this paper presents the competence standards on which chartering is based.

The overview of the state of engineering geology education in Australasia provided in this paper is based on a combination of review of institutional websites and discussions with course and program coordinators, where possible. Many program structures and course outlines are available online, providing a wealth of information regarding learning outcomes, delivery methods and assessments. More in-depth information was obtained from coordinators who could provide details about the course objectives in addition to what can be found in course outlines. Finally, the author is the program coordinator for the Professional Masters of

M. C. Villeneuve (✉)
University of Canterbury, Christchurch, New Zealand
e-mail: marlene.villeneuve@canterbury.ac.nz

Engineering Geology at the University of Canterbury, and has direct knowledge of that particular program.

The term "Australasia" is typically used to define Australia, New Zealand and the Pacific Islands. To the author's best knowledge there is no engineering geology education in the Pacific Islands, thus, this paper focuses on Australia and New Zealand.

2 Undergraduate Education

2.1 Single Course Occurrences

Single courses at undergraduate level tend to focus on basic engineering geological skills, including the basics of soil and rock mechanics, behavior of soil and rock, slope stability and site investigation. All of the courses referenced here incorporate some aspects of field work and used case studies to support the fundamentals. The courses range from a part course (University of Canterbury 2017a) to entire courses (Waikato University 2017a; University of Auckland 2017) dedicated to the topic. The course at the University of Canterbury is only a part course because the University also offers a fully dedicated postgraduate program in engineering geology.

The teaching and learning activities consist of conventional lectures, practicals, and invigilated exams worth 40% of the course grade. Most courses focus on the technical aspects of engineering geology to provide students with the skills they will need to perform engineering geology tasks upon entering the workforce. The part course at the University of Canterbury differs, in that its objective is to build on students' prior knowledge and skills in geology to develop engineering geology models. Eggers (2017) argues that the engineering geology model can be a powerful tool not just for communicating factual data and input parameters, but with which to frame the entire engineering project. The University of Canterbury part course embraces this viewpoint and emphasizes the development of the engineering geology model over more detailed instruction in soil and rock mechanics. The course at the University of Waikato will include components of geological models and communication as of 2019 (Vicki Moon, pers. comm.).

2.2 Undergraduate Programs

One undergraduate program in geological engineering exists in Australasia. While not strictly engineering geology, we can nevertheless learn from this example from Monash University (2017). This program is a specialization of the Resources Engineering program, and follows the same curriculum for the first two years. The 3rd and 4th year of the program are also very resource focused, with topics associated with mining and geothermal energy, a result of the strong Resources Engineering program. To complete the geological engineering aspect of the program, it includes courses in rock mechanics, numerical modeling and project, risk and safety management. The key learning from this program is that by leveraging from a pre-existing, related, program it is possible to offer a unique program like geological engineering through the introduction of a few subject-specific courses. A similar program could be developed in universities with civil/geotechnical engineering and engineering geology programs.

3 Postgraduate Education

3.1 Single Course Occurrences

Universities with single courses in engineering geology either build on a course offering in undergraduate or are true single occurrences. Regardless of whether they build on undergraduate courses, they tend to focus on particular aspects of engineering geology, especially slope stability (e.g., University of Waikato 2017b), engineering geology mapping (e.g., University of Auckland 2017) and hydrogeology (e.g., University of Auckland 2017; Curtin University 2017), or provide an advanced course in engineering geology that builds on the basics that were introduced in the undergraduate course (e.g., University of Auckland 2017). The key difference between the postgraduate and undergraduate offerings tends to be the emphasis on independent work, critical thinking, literature search and interpretation, in keeping with general expectations of postgraduate students. All courses include some aspect of fieldwork, whether directed or independent, with many also offering laboratory testing, stability analysis and even introduction to numerical modeling (e.g., University of Auckland 2017). A variety of assessments are used, depending on the nature of the course, including reports, critical reviews, seminars, and commonly final exams worth up to 40%.

3.2 Postgraduate Programs

New Zealand
The University of Canterbury provides the only program in engineering geology, the Professional Masters of Engineering Geology (PMEG). It builds on the geological knowledge and skills students obtain in an undergraduate degree. The PMEG is delivered as an 8-course plus dissertation program over three semesters (nominally 12 months). The objective of the program is professional (rather than academic or foundational) development. Students in the PMEG form two groups: recent

B.Sc. graduates continuing a postgraduate degree and industry professionals who wish to up skill.

The PMEG program includes a combination of lectures, tutorials, labs and field trips in different proportions for different courses. The structure of the program is in block-module format in order to better accommodate working professionals. Block-module courses comprise an intense 3–6 weeks of class time preceded and followed by off-campus reading, preparation and assessment. Alternative delivery techniques, such as Inverted Classroom (IC), have been shown to promote technical competencies better than traditional methods (Mason et al. 2013). Thus different delivery modes are incorporated within several of the eight courses using a variety of techniques to deliver lecture material, practical material and assessments: self-directed learning, group work, field work and blended online learning.

The PMEG block-module courses are titled: Engineering Geology Field Methods, Engineering Construction Practice, Rock Mechanics and Rock Engineering, Soil Mechanics and Soil Engineering, Applied Hydrogeology, Engineering Geomorphology, Natural Hazard Risk Assessment and Engineering Geology Synthesis and Project Preparation. These courses were selected under guidance of a technical advisory committee consisting of industry and academic professionals and closely follow the recommendations of the Joint Technical Committee 3 (JTC3) of the International Society for Rock Mechanics (ISRM), International Association of Engineering Geologists (IAEG) and the International Society for Soil Mechanics and Geotechnical Engineering (ISSMGE) as outlined in Turner and Regners (2010).

The Engineering Geology Project Portfolio consists of a design or research project (dissertation) and may be primarily field based, it could be mostly a laboratory study, and there are aspects of literature review and project planning involved. The emphasis is on developing technical and professional skills by working on: progress presentations, progress reporting, project management, poster presentation and manuscript writing, all of which constitute a portfolio. Some projects are of such high quality as to warrant publication in peer-reviewed journals (e.g., Monk et al. 2016).

In general the PMEG program balances technical knowledge and skills with professional skills and higher order thinking skills (as per Bloom's taxonomy), suitable for a postgraduate professional program. Emphasis is placed on clear communication, whether it be written, oral or visual, team work for large projects and independent research/ design work. Technical skills are developed by field, laboratory, analytical and interpretive work through directed and independent field and laboratory work followed by engineering analysis and design recommendations. This is achieved through a combination of individual and group projects. The goal is for graduates to be work ready in the engineering geology industry with a wide background of skills and knowledge and transferrable skills. Students may also wish to continue and complete a research-based M.Sc. in engineering geology.

Australia

The University of New South Wales (UNSW) offers a postgraduate degree program in geotechnical engineering and engineering geology. The program is aimed mostly at engineers and engineering graduates who wish to specialize in geotechnical engineering and engineering geology. Students from a geology background may be able to enter the program, depending on their experience. There have been a number of examples of students entering the UNSW program after completion of the PMEG at the University of Canterbury.

The program at UNSW (University of New South Wales 2017) is more focused on geotechnical engineering than the PMEG, offering courses in earthquake, concrete and structural engineering alongside courses in rock and slope engineering. Students take a total of 16 courses over 2 years, or 8 courses over 1 year if they have previous postgraduate studies, and select their courses from a large list of mostly advanced geotechnical engineering courses. Some undergraduate-level courses are available for students who do not have sufficient fundamental background in geotechnical engineering. Students must also complete masters research project courses. This program is designed for accessibility to full time students and working professionals and many components are either delivered in block-module format or as online courses.

3.3 Postgraduate Research

Many universities in Australasia have research programs that focus on or include aspects of engineering geology. Some are closely related to geological processes, such as the volcano slope stability research at Massey University (e.g., Proctor et al. 2014), while others are closely linked to geotechnical (e.g., Ranjith et al. 2012 from Monash University) or mining (e.g., Salvoni and Dight 2016 from University of Western Australia) engineering or other fields related to engineering geology, such as hydrogeology research at University of Western Australia (e.g., Boronina et al. 2015) or tunneling research at University of Canterbury (e.g., Villeneuve 2017). Still there are some that focus on more classic engineering geology issues such as landslide research at University of Wollongong (e.g., Flentje et al. 2016), complex soil behavior at University of Waikato (e.g., Moon and Churchman 2016) and geomorphology at University of Auckland (e.g., Brook et al. 2017).

This is only an overview of some of the types of research available to postgraduate students. While most of the research highlighted here is conducted at universities with strong engineering geology teaching, the fact that some research is on topics related to resource, mining and geotechnical engineering means that students can conduct research with engineering geology aspects in civil and mining engineering departments as well as geology and earth science departments.

4 Professional Development

4.1 New Zealand

The New Zealand Geotechnical Society initiated a two-day engineering geology professional development course in 2017. This course provides an overview of the basic principles underpinning the practical application of engineering geology. Students gain increased knowledge of the geoscientific methodologies and practices required for successful interpretation of ground conditions and a greater understanding of "how to get the geology right" (NZGS 2017). The course provides a mix of classroom teaching with exercises and opportunity to practice observational skills in the field. This combination is intended to enhance how an engineering geologist recognizes and documents geological and geotechnical information. Benefits are in the provision and communication of engineering geological contributions to the investigation, design and construction phases of ground engineering projects. This course is aimed at engineering geologists with two to six years' experience.

4.2 Australia

The Australian Geomechanics Society offers several engineering geology related professional development courses (AGS 2017). It offers one-day techniques courses in rock and soil logging as well as in geotechnical mapping. These provide field education with lectures and exercises targeted at developing these specific skills.

They also offer multi-day professional development courses. The field technique for landslide assessment course teaches students how to collect information and make observations in the field to support effective landslide risk assessments using guided field exercises, in which the students learn by carrying out realistic project related work in the field. The engineering geology course teaches students, typically engineering geologists and geologists, how to apply geological skills in the field to help solve engineering

problems. The geology for engineers course gives students, typically engineers, sufficient basic geological knowledge and skills to have the confidence to apply geological principles and methods in their work. This course also provides a framework for students to keep learning about geology so that they can make better engineering judgments and decisions. Teaching is based primarily on guided field exercises, supported by class exercises and case histories. All of these courses are aimed at early-career geotechnical engineers, geologists, geo-technicians and civil engineers to gain or reinforce their skills for continued professional development.

5 Engineering Geology for Civil Engineers

Engineering geology in Civil Engineering curricula is variable in Australasia. Where engineering geology courses do exist, the most modest offering consists of 3 weeks of lectures with lab or assignment, with the learning outcome to "describe the geological and geomorphological processes responsible for the formation of soils, and relate geological processes to the likely nature and distribution of soils in different environments" (University of Canterbury 2017b). The most comprehensive consist of undergraduate and postgraduate courses focused on engineering geology for engineers.

The undergraduate courses introduce geological concepts, including basic field mapping and rock and soil description, description of rock and soil materials and their implications for engineering projects (University of Auckland 2017; University of South Australia 2017; University of Western Australia 2017). In New Zealand basic seismology and geohazards are also a significant component. The postgraduate course addresses soil and rock mechanics, natural hazards and their implications for infrastructure, mapping and core logging, air photo interpretation and basic laboratory tests (University of Auckland 2017).

In a geologically active setting, such as New Zealand, the study of engineering geology should be a critical component of Civil Engineering curricula. In recent years, at least at the University of Canterbury, engineering geology education has been curtailed as a result of Civil Engineering program reorganization. This is despite the clear link between engineering geology and the performance of the ground and infrastructure during the 2010–2011 Canterbury Earthquake Sequence (Cubrinovski et al. 2010, 2011) and more recently the 2016 Kaikōura earthquake (Stringer et al. 2017; Orense et al. 2017). It is imperative that civil engineers develop the necessary judgment to identify how geological processes and materials will impact infrastructure and to critically assess geological input parameters, understand their limitations, and know when and how to work with engineering geologists.

6 Chartering of Professional Engineering Geologists

6.1 New Zealand

Engineering geologists in New Zealand can apply for chartered status through a robust peer assessment against a competence standard based on a candidate's portfolio. The competence standard has twelve elements (Engineering New Zealand 2017):

1. Comprehend, and apply knowledge of, accepted principles underpinning widely applied good practice for professional engineering geology.
2. Comprehend and apply knowledge of accepted principles underpinning good practice for professional engineering geology that is specific to New Zealand.
3. Recognize, define and investigate complex engineering geological problems in accordance with good practice for professional engineering geology.
4. Analyze and communicate complex engineering geological problems in order to inform development of engineering solutions and design in accordance with good professional practice.
5. Be responsible for making decisions on part or all of one or more complex engineering geological activities.
6. Manage part or all of one or more complex engineering geological activities in accordance with good engineering management practice.
7. Identify, assess and manage engineering geological uncertainty and geotechnical risk.
8. Conduct engineering geological activities to an ethical standard at least equivalent to the relevant code of ethical conduct.
9. Recognize the reasonably foreseeable social, cultural and environmental effects of professional engineering geological and engineering activities generally.
10. Communicate clearly with other engineering geologists, engineers and those that he or she is likely to deal with in the course of his or her professional engineering geological activities.
11. Maintain the currency of his or her professional engineering geological/geotechnical knowledge and skills.
12. Exercise sound professional judgment in engineering geology.

The candidate's portfolio will demonstrate the practice area, which is determined by: (a) the area within which he or she has engineering geological knowledge and skills; and (b) the nature of his or her professional engineering geological activities.

6.2 Australia

Australia is in the process of establishing a registered status for engineering geologists. Candidates for registration will also be assessed against competence elements (Engineers Australia, unpublished draft):

1. Design, supervise and interpret geotechnical investigation.
2. Perform geotechnical engineering computations.
3. Have knowledge of key geotechnical standards, references and case studies.
4. Conduct engineering activities to an ethical standard.
5. Recognize the reasonably foreseeable social, cultural and environmental effects of professional geotechnical engineering activities generally.
6. Communicate clearly with other geotechnical professionals and those that he or she is likely to deal with in the course of his or her professional activities.
7. Maintain the currency of his or her professional engineering geological and geotechnical engineering knowledge and skills.
8. Identify, assess and manage geotechnical uncertainty and risk.
9. Be responsible for making decisions on part or all of one or more complex geotechnical activities.
10. Exercise sound professional judgment.
11. Manage part or all of one or more complex geotechnical engineering or engineering geological activities in accordance with good engineering management practice.

In addition, candidates will be responsible for demonstrating technical competence in three out of a large list of pre-defined competency areas. The candidate's portfolio will also demonstrate the practice area, which is determined by: (a) the area within which he or she has specialist knowledge and skills; and (b) the nature of his or her professional engineering geological or geotechnical engineering activities.

7 Summary

Engineering geology is a well-recognized and respected discipline in New Zealand, with dedicated postgraduate study programs and professional chatership. Australia is working towards a stronger focus on engineering geology as a distinct discipline, and developing professional chartership. This overview shows the different models available in New Zealand and Australia and at different universities for providing engineering geology education ranging from

portions of courses to fully dedicated postgraduate programs and can provide models for other countries and universities. One aspect to highlight is the importance of engineering geology awareness for civil and geotechnical engineers, which is better provided at some universities than others.

References

Australian Geomechanics Society: Courses. https://australiangeomechanics.org/course_post/. Last accessed 7 Nov 2017

Boronina, A., Clayton, R., Gwynne, C.: Recommended methodology for determination of design groundwater levels. Aust. Geomech. J. **50**(3), 11–21 (2015)

Brook, M., Hagg, W., Winkler, S.: Contrasting medial moraine development at adjacent temperate, maritime glaciers: Fox and Franz Josef Glaciers, South Westland, New Zealand. Geomorphology **290**, 58–68 (2017)

Cubrinovski, M., Bradley, B., Wotherspoon, L., Green, R., Bray, J., Wood, C., Pender, M., Allen, J., Bradshaw, A., Rix, G., Taylor, M., Robinson, K., Henderson, D., Giorgini, S., Ma, K., Winkley, A., Zupan, J., O'Rourke, T., DePascale, G., Wells, D.: Geotechnical aspects of the 22 February 2011 Christchurch earthquake. Bull. N. Z. Soc. Earthq. Eng. **44**(4), 205–222 (2011)

Cubrinovski, M., Green, R.A., Allen, J., Ashford, S., Bowman, E., Bradley, B., Cox, B., Hutchinson, T., Kavazanjian, E., Orense, R., Pender, M., Quigley, M., Wotherspoon, L.: Geotechnical reconnaissance of the 2010 Darfield (Canterbury) earthquake. Bull. N. Z. Soc. Earthq. Eng. **43**(4), 243–320 (2010)

Curtin University: GEOL5010 (v.1) Hydrogeology and Engineering Geology unit outline. http://handbook.curtin.edu.au/units/31/318673.html. Last accessed 02 Nov 2017

Eggers, M.: Importance of engineering geological models in rock slope engineering. Bull. Eng. Geol. Environ., in prep, (2018)

Engineering New Zealand: https://www.engineeringnz.org. Last accessed 07 Nov 2017

Flentje, P., Miner, T., Stirling, D., Palamakumbure, D., Windle, D.: Landslide inventory and susceptibility zoning across SE Australia. In Eggers, M.J., Griffiths, J.S., Parry, S., Culshaw, M.G. (eds.) Developments in Engineering Geology, pp. 119–133. Geological Society of London, London (2016)

Mason, G.S., Shuman, T.R., Cook, K.E.: Comparing the effectiveness of an inverted classroom to a traditional classroom in an upper-division engineering course. IEEE Trans. Educ. **56**(4), 430–435 (2013)

Monash University: Geological Engineering. https://www.monash.edu/engineering/future-students/undergraduate-study/specialisations/geological-engineering. Last accessed 02 Nov 2017

Monk, C.B., van Ballegooy, S., Hughes, M.W., Villeneuve, M.: Liquefaction vulnerability increase at North New Brighton due to subsidence, sea level rise, and reduction in thickness of the non-liquefying layer. Bull. N. Z. Soc. Earthq. Eng. **49**(4), 334–340 (2016)

Moon, V., Churchman, J.: Halloysite behaving badly: geomechanics and slope behaviour of halloysite-rich soils. Clay Min. **51**(3), 517–528 (2016)

New Zealand Geotechnical Society: Principles and Practice of Engineering Geology. https://fl-nzgs-media.s3.amazonaws.com/uploads/2017/06/NZGS_2Day-AugSeptember2017_OUTeditable.pdf. Last accessed 7 Nov 2017

Orense, R.P., Mirjafari, Y., Asadi, S., Naghibi, M., Chen, X., Altaf, O., Asadi, B.: Ground performance in wellington waterfront area following the 2016 kaikōura earthquake. Bull. N. Z. Soc. Earthq. Eng. **50**(2), 142–151 (2017)

Procter, J.N., Cronin, S.J., Zernack, A.V., Lube, G., Stewart, R.B., Nemeth, K., Keys, H.: Debris flow evolution and the activation of an explosive hydrothermal system; Te Maari, Tongariro, New Zealand. J. Volc. Geotherm. Res. **286**, 303–316 (2014)

Ranjith, P.G., Viete, D.R., Chen, B.J., Perera, M.S.A.: Transformation plasticity and the effect of temperature on the mechanical behaviour of Hawkesbury sandstone at atmospheric pressure. Eng. Geol. **151**, 120–127 (2012)

Salvoni, M., Dight, P.M.: Rock damage assessment in a large unstable slope from microseismic monitoring—MMG Century mine (Queensland, Australia) case study. Eng. Geol. **210**, 45–56 (2016)

Stringer, M.E., Bastin, S., McGann, C.R., Cappellaro, C., El Kortbawi, M., McMahon, R., Wotherspoon, L.M., Green, R.A., Aricheta, J., Davis, R., McGlynn, L., Hargraves, S., Van Ballegooy, S., Cubrinovski, M., Bradley, B.A., Bellagamba, X., Foster, K., Lai, C., Ashfield, D., Baki, A., Zekkos, A., Lee, R., Ntritsos, N.: Geotechnical aspects of the 2016 Kaikōura earthquake on the South Island of New Zealand. Bull. N. Z. Soc. Earthq. Eng. **50**(2), 117–141 (2017)

Turner, A.K., Rengers, N.: A report proposing the adaptation of the ASCE body of knowledge competency-based approach to the assessment of education and training needs in geo-engineering. In: Progress Report to the: Joint Technical Committee JTC-3: Education and Training (2010)

University of Auckland: CIVIL 220, CIVIL 726, EARTHSCI 372, EARTHSCI 770, EARTHSCI 771 course descriptions. Courtesy of Dr. Martin Brook, course coordinator

University of Canterbury: ENCN 253 Soil Mechanics Course Outline. http://www.canterbury.ac.nz/courseinfo/GetCourseDetails.aspx?course=ENCN253&occurrence=17S2(C)&year=2017. Last accessed 02 Nov 2017 (2017a)

University of Canterbury: ENCN 338 Engineering and Mining Geology Course Outline. http://www.canterbury.ac.nz/courseinfo/GetCourseDetails.aspx?course=GEOL338&occurrence=17S2(C)&year=2017. Last accessed 02 Nov 2017 (2017b)

University of New South Wales: Geotechnical Engineering and Engineering Geology Master of Engineering Science. https://www.engineering.unsw.edu.au/study-with-us/postgraduate-degrees/geotechnical-engineering-and-engineering-geology. Last accessed 08 Nov 2017

University of South Australia: EART 3012 Engineering and Environmental Geology Course Outline. Courtesy of Dr. Tom Raimondo, course coordinator

University of Waikato: ERTH352-17A Engineering Geology Course Outline. https://paperoutlines.waikato.ac.nz/outline/ERTH352-17A%20(HAM). Last accessed 02 Nov 2017 (2017a)

University of Waikato: ERTH552-17B Rock Slope Engineering Course Outline. https://paperoutlines.waikato.ac.nz/outline/ERTH552-17B%20(HAM). Last accessed 02 Nov 2017 (2017b)

University of Western Australia: ENSC3009 Geomechanics Unit Description. http://handbooks.uwa.edu.au/units/unitdetails?code=ENSC3009. Last accessed 02 Nov 2017

Villeneuve, M.C.: Hard rock tunnel boring machine penetration tests as an indicator of chipping process efficiency. J. Rock Mech. Geotech. Eng. **9**, 611–622 (2017)

A Low Cost Alternative Approach to Geological Discontinuity Roughness Quantification

Abdul Ghani Rafek, Goh Thian Lai, and Ailie Sofyiana Serasa

Abstract

The surface roughness of geological discontinuities can be considered a key parameter in the evaluation of the stability of structures constructed within rock masses. Several different methodologies can be applied to determine this parameter and they vary in their complexity. The aim of this study is to correlate the peak friction angle (ϕ_p) of discontinuity planes of fresh bedrock with the Joint Roughness Coefficient, JRC. A simple low cost approach is presented based on the determination of JRC and the application of derived polynomial equations to determine the peak friction angle, ϕ_p from the surface roughness from geological discontinuities for the major lithologies found in Peninsula Malaysia. Eight thousand six hundred and seven tilt tests were conducted to obtain the correlations between peak friction angles with JRC of granite, schist, limestone, quartzite and sandstone. The respective polynomial equations are as follows:

for granite $\phi_p = -0.071 \text{ JRC}^2 + 3.56 \text{ JRC} + 35.6°$
for schist $\phi_p = -0.022 \text{ JRC}^2 + 3.21 \text{ JRC} + 28.1°$
for limestone $\phi_p = -0.0635 \text{ JRC}^2 + 3.95 \text{ JRC} + 25.2°$
for quartzite $\phi_p = -0.083 \text{ JRC}^2 + 4.17 \text{ JRC} + 27.6°$
for sandstone $\phi_p = 0.0424 \text{ JRC}^2 + 1.13 \text{ JRC} + 29.2°$

A. G. Rafek
Department of Geosciences, University Technology PETRONAS, Bandar Seri Iskander, Malaysia
e-mail: ghani.rafek@utp.edu.my

G. T. Lai (✉)
Geology Program, Faculty of Science & Technology, Universiti Kebangsaan Malaysia, Bangi, Malaysia
e-mail: gdsbgoh@gmail.com

A. S. Serasa
School of Engineering (Petroleum), Asia Pacific University of Technology & Innovation (APU), Technology Park Malaysia, Bukit Jalil, 57000 Kuala Lumpur, Malaysia

G. T. Lai
OST Slope Protection Engineering (M) Sdn Bhd, Bangi, Malaysia

For all the derived polynomials, the coefficient of determination, R^2 was greater than 0.9. The JRC can be determined as part of an engineering geological investigation and the respective polynomial applied to determine the peak friction angle, ϕ_p for the specific lithology.

Keywords

Discontinuity Surface Roughness • Joint Roughness Coefficient (JRC) • Tilt test • Polynomial equations

1 Introduction

The surface roughness of geological discontinuities plays a significant role in influencing the peak friction angle, ϕ_p of these discontinuities. Its determination is of considerable importance in the determination of the stability of open cut excavations as well as underground openings. The most accurate method to determine the peak friction angle, ϕ_p is to conduct direct shear tests on natural (rough) discontinuities. However, this approach has a number of technical complications such as difficulties sampling undisturbed discontinuities, test sample encapsulation and also the testing itself. As an alternative approach for the determination of this important parameter, Barton and Choubey (1977) introduced the concept of Joint Roughness Coefficient, JRC. In Malaysia less research studies have been conducted to quantify the surface roughness of discontinuities. The local researchers were focused more on rock mass classification such as using Geological Strength Index (Norbert et al. 2016) and assessment of rock fall potential at limestone hills (Norbert et al. 2015). Some research studies on the quantification of joint roughness have been undertaken by Ailie et al. (2017), Ailie et al. (2016), Ghani Rafek et al. (2012), Ghani Rafek and Goh (2012) and Goh et al. (2014). In these studies, a simple low cost approach using the tilt test, JRC determinations and derived polynomial equations has been developed to determine the peak friction angle, ϕ_p.

This presentation is the result of correlation of the peak friction angle, (ϕ_p) of discontinuity planes of fresh rocks with the Joint Roughness Coefficient, JRC and the derivation of polynomial equations correlating these two parameters for granite, schist, limestone, quartzite and sandstone. The proposed polynomial equations offer a possibility of estimating the peak friction angle, (ϕ_p) of rough discontinuity planes based on JRC for similar lithologies.

2 Materials and Methods

The location of the 12 study sites are shown in Fig. 1. The study sites were Bukit Cherakah, Selangor, Bukit Semanggol, Perak, Gunung Lang, Perak, Gunung Rapat, Perak, Gua Tempurung, Perak, Gua Kandu, Perak, along the Pos Selim-Kg. Raja road, Cameron Highlands, Perak, Bukit Penggorak, Kuantan, Pahang, Kuala Kubu Baru-Bukit Fraser road, Pahang, Gua Damai, Selangor, Ukay Perdana, Selangor, Silk Kajang Highway, Selangor and Kajang Rock Quarry, Semenyih, Selangor. More than 30 individual rock slopes, either as road cuts along major roads and highways or within quarries both active and abandoned were investigated at these sites. The major lithologies, i.e. granites, schists, limestones, quartzite and sandstone were studied.

2.1 Geology

Granite. The granitic rocks were sampled along the Pos Selim-Kg. Raja road, Cameron Highland, Perak, Bukit Penggorak, Kuantan, Pahang, Silk Highway and Kajang Rock Quarry, Selangor. The respective ages of granite along Pos Selim-Kg. Raja road and Bukit Penggorak are Late Triassic and Late Permian to Early Triassic (Bignell and Snelling 1977). Gobbett and Hutchison (1973) reported the age of granitic rock along the Silk Highway and in Kajang Rock Quarry as Triassic. These granites are medium to coarse grained, occasionally porphyritic with biotite as the main mafic mineral. In terms of rock material strength, the uniaxial compressive strength ranged from as low as 78 MPa to a maximum value of 254 MPa. The mean value was 114 MPa.

Schist. The rock samples of schist were collected at Kuala Kubu-Bukit Fraser road, Pahang, Ukay Perdana, Selangor and along the Pos Selim-Kg. Raja road, Cameron Highland in the states of Perak and Pahang. The schist along the Kuala Kubu-Bukit Fraser road as an amphibole schist. This schist is medium grained and banded with exceptionally high strength. It's uniaxial compressive strength exceeds 200 MPa, with a maximum of 248 MPa. The Dinding schist at Ukay Perdana ranges in age from Cambrian to Ordovician (Gobbett 1964). This is a fine grained banded rock

composed of quartz and muscovite with minor amounts of relict microcline. Rock material strength can be considered as moderately high with a range of values between 80 and 120 MPa and an average value of 100 MPa. All values were determined perpendicular to foliation. Schists that occur along Pos Selim-Kg. Raja road are mainly quartz-mica schist and quartz schist with the age ranges from Ordovician to Silurian. Rock material strength can be considered moderately high with a mean value of 137 MPa, and a range from 70 to 130 MPa.

Limestone. Limestones were sampled at Gunung Lang, Gunung Rapat, Gua Tempurung, Gua Kandu, in the state of Perak and Gua Damai in Selangor. Gua Damai is part of the Kuala Lumpur Limestone with age ranges from Middle-Upper Silurian (Gobbett 1964). Gunung Lang, Gunung Rapat, Gua Tempurung and Gua Kandu in Perak are part of the Kinta Limestone with an age of Silurian to Permian (Foo 1990). These rocks have been metamorphosed to marble with a mean uniaxial compressive strength of 80 MPa and a range of values from 40 to 104 MPa.

Quartzite. The quartzite collected from Bukit Cherakah in Selangor is part of Formation Kenny Hill with an age from Carboniferous to Permian (Tjia 1976). This rock is composed almost entirely of medium grained quartz, with a mean uniaxial compressive strength of 99 MPa and a range from 72 to 133 MPa.

Sandstone. The sandstone from Bukit Semanggol in the state of Perak is part of Semanggol Formation with a Permo-Triassic age (Basir and Zaiton 2007). This a fine to medium grained sandstone composed almost entirely of quartz. It's mean uniaxial compressive strength is 82 MPa, with a range from 71 to 90 MPa. Therefore, it can be classified as having moderate strength.

Tilt Test. At each site, scanline surveys were conducted to quantify the discontinuity parameters. Rock blocks containing natural discontinuity planes were carefully collected using hand tools such as a geological hammer and chisel. The collected block was then separated along the discontinuity plane into two blocks. The roughness of the discontinuity was determined using a comb profiler which is often also referred to as a Barton comb in accordance to the recommendations of Barton and Choubey (1977). The JRC was determined by visual comparison with the standard chart of Barton and Choubey (1977). After the determination of JRC, the peak friction angle, ϕ_p of the discontinuity surface was determined using a self-fabricated tilt testing apparatus (Fig. 2) constructed based on the recommendations of Priest (1993). The natural discontinuity sample, consisting of an upper and lower block was positioned on the plane of the testing apparatus and tilted until sliding of the upper block occurred. The angle of inclination was measured using a clinometer. Since this sliding does not involve cohesion between the upper and lower blocks, the angle of inclination

Fig. 1 Location of study sites, Peninsula Malaysia
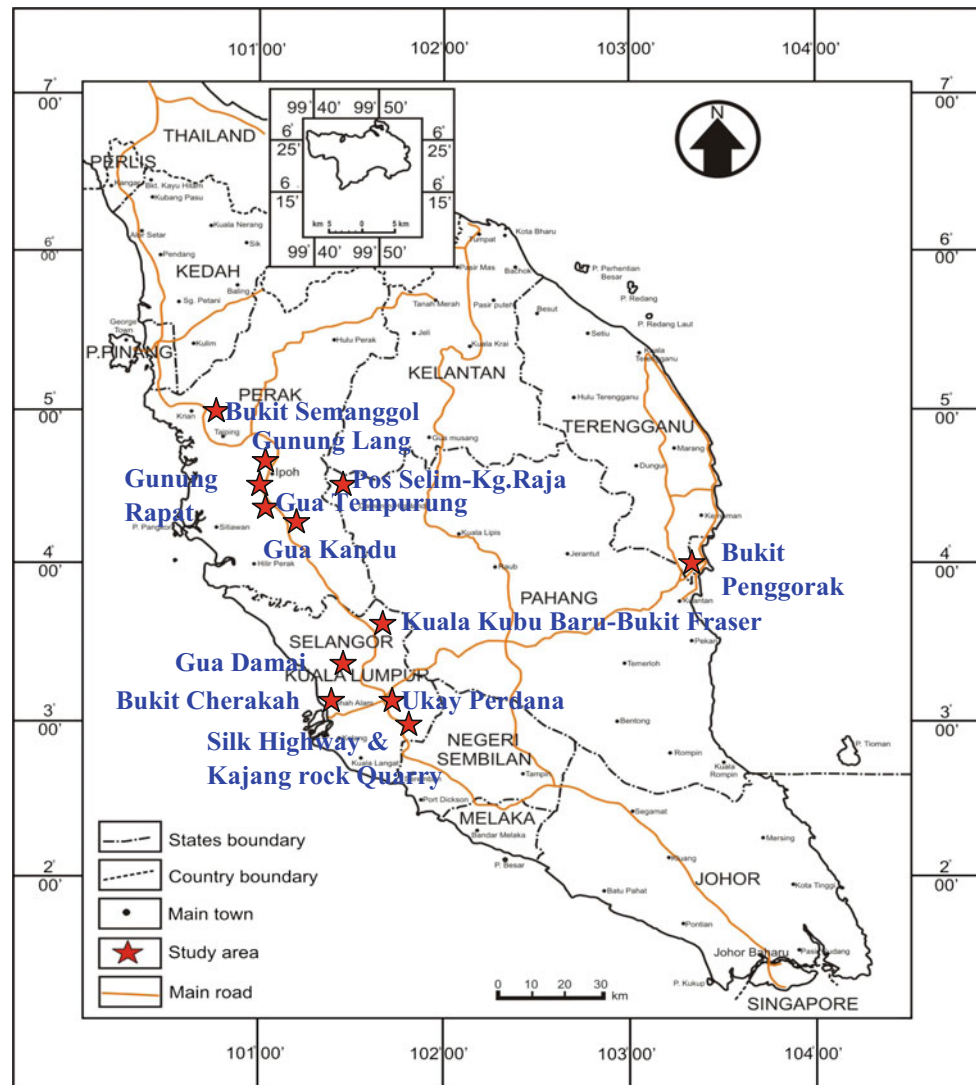
represents the peak friction angle, ϕ_p of the discontinuity surface. The tilt test for each pair of blocks was conducted in four different directions in order to take into consideration the possible variations of JRC for different directions of sliding. In addition, the tilt test was repeated five times for each direction to reduce possible errors during the measurements. The stress levels for these tests are low. The normal stress is the weight component perpendicular to the inclination plane and the shear stress is the weight component parallel to the inclination plane. This experimental set-up is shown in Fig. 2.

3 Results and Discussion

8607 tilt tests were conducted to obtain the correlations between peak friction angle with JRC of granite, schist, limestone, quartzite and sandstone samples. A total of 4080

and 2200 tilt tests were conducted on fresh granite and schists samples from the six different locations. A total of 1967 tilt tests were conducted on fresh limestone samples from the six different locations. Due to limited suitable outcrops of sandstone and quartzite, especially fresh outcrops, 140 and 220 tilt tests were conducted for these two lithologies respectively. The results of mean, median, standard deviation and skewness values from the testing are summarized in Table 1. The results were analyzed at 95% confidence level using the statistical software package IBM SPSS Statistics Version 16.

The boxplots of the tilt angles and corresponding discontinuity surface roughness for respective lithologies are shown in Fig. 3. Negative skewness implies that more test results have higher values of peak friction angle compared to the mean value, while positive skewness implies that more test results have lower values of peak friction angle compared to the mean value. The tilt test results reveal that the

Fig. 2 The tilt test apparatus,
modeled after Priest (1993)
employed for the determination of
peak friction angle, ϕ_p **a** position
of upper block before and after
sliding **b** peak friction angle (ϕ_p)
is measured after sliding of upper
block *Source* Modified after
Ghani Rafek and Goh (2015)

Fig. 2 The tilt test apparatus, modeled after Priest (1993) employed for the determination of peak friction angle, ϕ_p **a** position of upper block before and after sliding **b** peak friction angle (ϕ_p) is measured after sliding of upper block *Source* Modified after Ghani Rafek and Goh (2015)
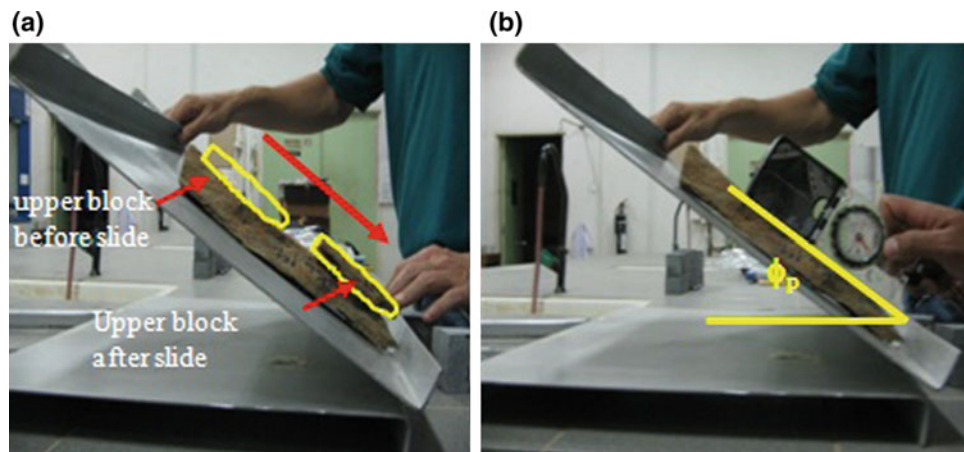
peak friction angles, ϕ_p increase with increasing JRC values and imply positive correlation. This increase in peak friction angle, ϕ_p and a corresponding increase in surface roughness contributes to an increase in the resistance to sliding of rock blocks along the discontinuity plane, resulting in an increase in stability to potential plane failure. For all the tested natural discontinuities, the statistical software package, IBM SPSS Statistics Version 16 was employed and analyzed at 95% confidence level to generate polynomial equations correlating the mean values of peak friction angle, ϕ_p with the joint roughness coefficient, JRC. The values of JRC were taken as the midpoint values of the respective JRC ranges. The respective polynomial equations are:

(i)   for granite $\phi_p = -0.071 \, JRC^2 + 3.56 \, JRC + 35.6°$
(ii) for schist $\phi_p = -0.022 \, JRC^2 + 3.21 \, JRC + 28.1°$
(iii) for limestone $\phi_p = -0.0635 \, JRC^2 + 3.95 \, JRC + 25.2°$
(iv) for quartzite $\phi_p = -0.083 \, JRC^2 + 4.17 \, JRC + 27.6°$
(v)   for sandstone $\phi_p = 0.0424 \, JRC^2 + 1.13 \, JRC + 29.2°$

For all the derived polynomials, there is a strong correlation between the values of JRC and peak friction angle measured by conducting tilt tests as shown by the coefficient of determination, R^2 that was greater than 0.9. The respective polynomial plots of peak friction angle with JRC for granite, schist, limestone, quartzite and sandstone are shown in Fig. 4. These results revealed that the peak friction angles for sandstone were relatively lower than granite, schist, limestone and quartzite. The basic friction angle values obtained when the JRC value is set as zero are 35.6°, 28.1°, 25.2°, 27.6° and 29.2° for granite, schist, limestone, quartzite and sandstone respectively. For granite and sandstone the values are comparable with those reported by Hoek and Bray (1981) whereas for

limestone the value is lower. For schist and quartzite the values obtained in this study are within their reported range. Hoek and Bray (1981) reported that the basic friction angles for granite, sandstone and limestone were 29° to 35°, 25° to 35° and 33° to 40° respectively. For schist and quartzite, the respective values are 20° to 28° and 27° to 34° respectively.

4   Conclusion

8607 tilt tests were conducted to obtain the correlations between the mean peak friction angle with JRC of granite, schist, limestone, quartzite and sandstone samples. Five (5) polynomial equations have been developed in this study to estimate the values of peak friction angle of discontinuity surface from JRC measurement for granite, schist, limestone, quartzite and sandstone in Malaysia. These equations are as follows:

(i)   for granite $\phi_p = -0.071 \, JRC^2 + 3.56 \, JRC + 35.6°$
(ii) for schist $\phi_p = -0.022 \, JRC^2 + 3.21 \, JRC + 28.1°$
(iii) for limestone $\phi_p = -0.0635 \, JRC^2 + 3.95 \, JRC + 25.2°$
(iv) for quartzite $\phi_p = -0.083 \, JRC^2 + 4.17 \, JRC + 27.6°$
(v)   for sandstone $\phi_p = 0.0424 \, JRC^2 + 1.13 \, JRC + 29.2°$

This study and its findings offer a reliable, low cost option for the determination of the peak friction angle, ϕ_p of rough geological discontinuity surfaces. These equations are applicable to granite, schist, limestone, quartzite and sandstone in Malaysia at low stress situations for rock slope stability analysis. Since pore water pressures are not accounted for, the conditions should be dry. The developed methodology can also be applied elsewhere to establish similar correlations for other regions.

Table 1 Summary of the statistical results of peak friction angle (ϕ_p) with the respective JRC values

Lithology	JRC Midpoint	No. of tests	Mean (°)	Median (°)	Standard deviation (°)	Skewness
Granite	1	2180	30.7±0.1	31	2	Normal
	3	60	53.7±2.6	52	10.1	Positive
	5	360	54.5±0.6	56	6.1	Negative
	7	170	60.5±1.0	60	6.3	Normal
	9	50	59.6±1.3	60	4.6	Normal
	11	440	65.7±0.6	64	6.9	Positive
	13	90	66.7±2.3	67	11.1	Normal
	15	60	68.4±2.0	70	7.8	Negative
	17	520	76.3±0.6	76	7.4	Normal
	19	150	81.2±0.8	80	5.0	Positive
Schist	1	920	29.6±0.1	30	2.2	Negative
	3	130	37.9±0.6	38	3.4	Normal
	5	110	44.3±1.2	42	6.1	Positive
	7	330	51.9±0.7	52	6.2	Normal
	9	140	56.6±0.8	57	5.1	Negative
	11	90	58.5±1.1	58	5.4	Positive
	13	140	67.5±0.9	68	5.5	Negative
	15	120	66.3±1.0	66	5.5	Normal
	19	220	83.3±0.7	84	5.2	Negative
Limestone	1	665	30.1 ± 0.1	30	3.1	Normal
	3	200	34.4 ± 0.2	34	2.7	Normal
	5	35	43.1 ± 0.9	42	5.2	Positive
	7	90	50.5 ± 0.7	50	6.9	Normal
	9	285	57.6± 0.5	58	8.7	Normal
	11	220	61.2± 0.5	60	7.6	Positive
	13	170	65.1± 0.6	64	7.7	Positive
	15	105	68.8± 0.9	70	8.7	Negative
	17	72	73.5 ± 1.1	72	9.7	Positive
	19	125	78.4 ± 0.5	80	6.0	Negative
Quartzite	1	60	31.7±0.2	32	0.9	Normal
	9	40	58.2±0.9	58	2.7	Normal
	15	60	71.7±0.7	72	2.7	Normal
	17	60	74.2±1.3	76	5.2	Negative
Sandstone	3	20	32.4±2.1	32	4.6	Normal
	5	30	36.8±1.4	37	3.7	Normal
	7	20	38.9±1.3	39	2.9	Normal
	9	30	42.4±1.8	41	4.8	Positive
	11	30	46.3±2.7	48	7.2	Negative
	13	10	49.9±7.1	50	9.9	Negative
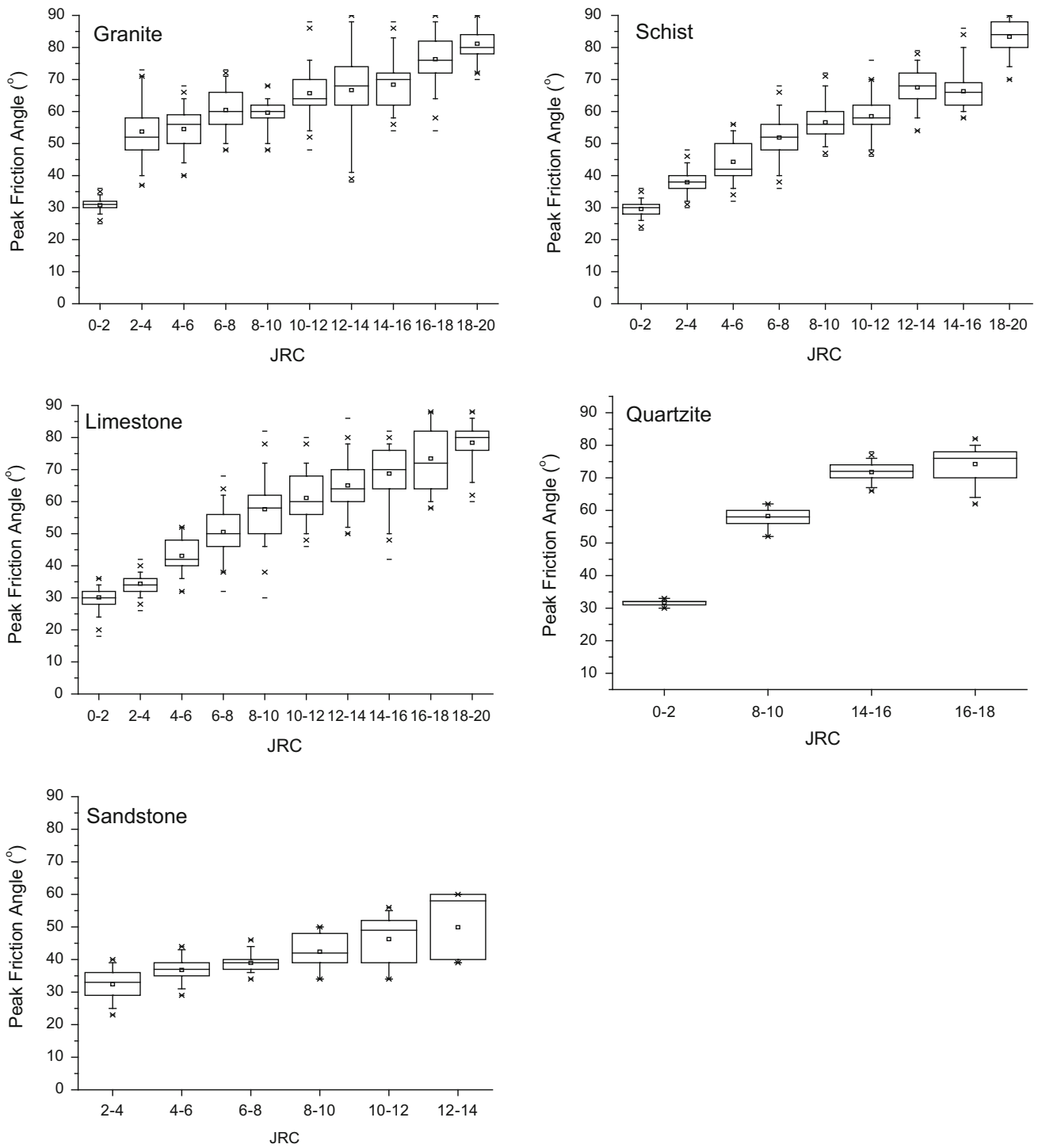
Fig. 3 Boxplots of peak friction angles, (ϕ_p) and corresponding JRC (surface roughness) values for granite, schist, limestone, quartzite and sandstone
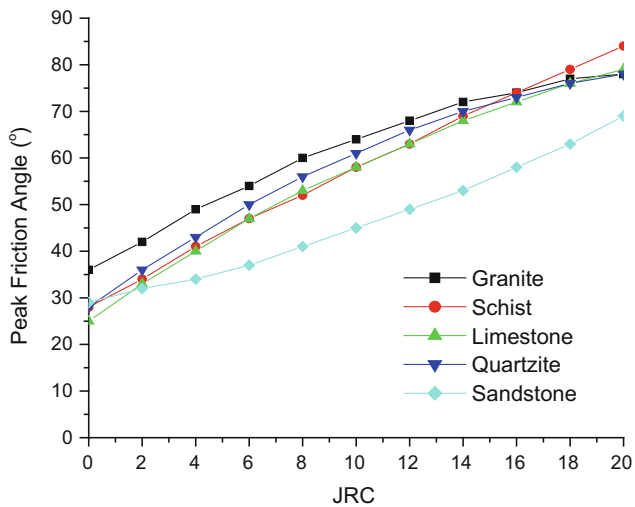
Fig. 4 Polynomial correlations of peak friction angle with JRC for granite, schist, limestone, quartzite and sandstone, Peninsula Malaysia, with coefficient of determination (R^2) more than 0.9

References

Ailie, S.S., Goh, T.L., Abdul Ghani, R., Norbert, S., Azimah, H., Lee, K.E., Noraini, S., Tuan Rusli, M.: Development of empirical correlation of peak friction angle with surface roughness of discontinuities using tilt test. In: AIP Conference Proceedings, 060033-1- 060033-18 (2016)

Ailie, S.S., Goh, T.L., Abdul Ghani, R., Azimah, H., Lee, K.E., Tuan Rusli, M.: Peak friction angle estimation from joint roughness coefficient of discontinuities of limestone in Peninsular Malaysia. Sains Malaysiana **46**(2), 181–188 (2017)

Barton, N., Choubey, V.: The shear strength of joints in theory and practice. Rock Mech. **10**, 1–54 (1977)

Basir, J., Zaiton, H.: Stratigraphy and sedimentology of the chert unit of the Semanggol Formation. Bull. Geol. Soc. Malays. **53**, 103–109 (2007)

Bignell, J.D., Snelling, N.J.: Geochronology of Malayan granites. Overseas Geol. Min. Resour. **47**, 77 (1977)

Foo, K.Y.: Geology and mineral resources of the Taiping-Kuala Kangsar Area, Perak Darul Ridzuan. Geol. Surv. Malays. Map Rep. **1**, 1–145 (1990)

Ghani Rafek, A., Goh, T.L.: Correlation of joint roughness coefficient (JRC) and peak friction angles of discontinuities of Malaysian schists. Earth Sci. Res. **1**(1), 57–63 (2012)

Ghani Rafek, A., Goh,T.L., Hariri Arifin, M.: Correlation of joint roughness coefficient with peak friction angle of discontinuity planes of schists, Peninsular Malaysia. Sains Malaysiana **41**(3), 293–297 (2012)

Ghani Rafek, A., Goh, T.L.: A systematic approach for the quantification of rock slope stability. In: Lollino, G., Giordan, D., Crosta, G.B., Corominas, J., Azzam, R., Wasowski, J., Scirra, N. (eds.) Engineering Geology for Society and Territory, vol. 2. Springer, London (2015)

Gobbett, D.J.: The lower paleozoic rocks of Kuala Lumpur, Malaysia. Fed. Museum's J. **9**, 67–79 (1964)

Gobbett, D.J., Hutchison, C.S.: Geology of the Malay Peninsula. Wiley, New York (1973)

Goh, T.L., Ghani Rafek, A., Hariri Arifin, M.: Correlation of joint roughness coefficient with peak friction angles of discontinuity planes of granite, Peninsular Malaysia. Sains Malaysiana **43**(5), 751–756 (2014)

Hoek, E., Bray, J.E.: Rock Slope Engineering, 3rd edn. Institution of Mining and Metallurgy, London (1981)

Norbert, S., Muhammad Fahmi, A.G., Goh, T.L., Abdul Ghani, R., Azimah, H., Rodeano, R., Lee, K.E.: Assessment of rockfall potential of limestone hills in the Kinta Valley. J. Sustain. Sci. Manage. **10**(2), 24–34 (2015)

Norbert, S., Rodeano, R., Abdul Ghani, R., Goh, T.L., Noran, N.N.A., Kamilia, S., Nightingle, L.M., Azimah, H., Lee, K.E.: Rock mass assessment using Geological Strength Index (GSI) along the Ranau-Tambunan Road, Sabah, Malaysia. Res. J. Appl. Sci. Eng. Technol. **12**(1), 108–115 (2016)

Priest, S.D.: Discontinuity Analysis for Rock Engineering. Chapman & Hall, London (1993)

Tjia, H.D.: Overturned structures in Kenny Hill formation, Selangor. Warta Geologi **2**(4), 63–65 (1976)

Preliminary Investigation of the Soil-Water Characteristics of Loess Soils in Canterbury, New Zealand

K. Yates and C. Fenton

Abstract

Loess and loess-derived soils cover much of Canterbury, New Zealand. When dry, these deposits exhibit an undrained shear strength up to 200 kPa and are stable in vertical cut slopes. Small increases in moisture content (2–3%), particularly near the plastic limit, lead to weakening of the soil matrix and a large reduction in shear strength. This sensitivity to moisture contributes to the susceptibility of loess slopes to failure during rainfall events. Consequently the detail of the relationship between shear strength and moisture content is important to understand. Canterbury loess soils are typically situated above the water table and therefore behave as a partially saturated soil. As such, the shear strength is influenced by negative pore pressure and interparticle bonding. Historically, the relative contribution of these mechanisms to the overall soil strength of loess soils in Canterbury is not well understood. This paper outlines the methodology for investigating the soil-water characteristics of Canterbury loess soils. Preliminary observations of the soil-water characteristics are presented.

Keywords

Loess • Slope stability • Soil suction

1 Introduction

Much of the Canterbury region, in the South Island, New Zealand, is covered by loess and loess-derived soils. These materials can be problematic for development and infrastructure due to their sensitivity to changes in moisture content and susceptibility to slope instability during high intensity rainfall events. Previous research has focused on the classification of geotechnical index properties, with limited consideration of the material as a partially saturated soil and the intrinsic relationship between water and soil behaviour. The purpose of this paper is to provide a brief introduction to loess soils in Canterbury and present an outline of ongoing research into the soil-water relationship in these soils. Preliminary results from this research are also presented.

2 Loess Soils in Canterbury

Loess and loess-derived soils greater than 1 m thick cover approximately 10% of the South Island, New Zealand (Fig. 1). These windblown deposits are yellowish-brown in colour and range from Late Pleistocene to Post Glacial (Holocene) in age (e.g., Raeside 1964; Bell et al. 1986; Bell and Trangmar 1987; Ives 1973). The thickest deposits reach up to 40 m and overlie Pliocene age Cannington Gravels and Timaru Basalt in South Canterbury, and Miocene age volcanics on Banks Peninsula (Tonkin et al. 1974; Bell and Trangmar 1987).

Loess deposits are typically divided into in situ loess and loess-derived deposits that include fluvial-, marine-, and colluvial-reworked materials. Loess and loess-derived deposits in Canterbury are primarily silt (Fig. 2) but generally behave as low plasticity clay. Table 1 provides a summary of the geotechnical index properties. When dry, loess slopes can stand vertically. However, these slopes are susceptible to failure as a result of rapid decrease in shear strength upon relatively small increases in moisture content (2–3%) (McDowell 1989; Goldwater 1990; Jowett 1995; Hughes 2002). This, along with a susceptibility to clay dispersion and erosion, make the loess vulnerable to instability during rainfall events. Mechanisms of slope failure include shallow slides, debris flow and tunnel gullying (internal erosion) (Bell et al. 1986; Hutchinson 1975; Bell and Trangmar 1987).

K. Yates (✉) · C. Fenton
Department of Geological Sciences, University of Canterbury, Christchurch, New Zealand
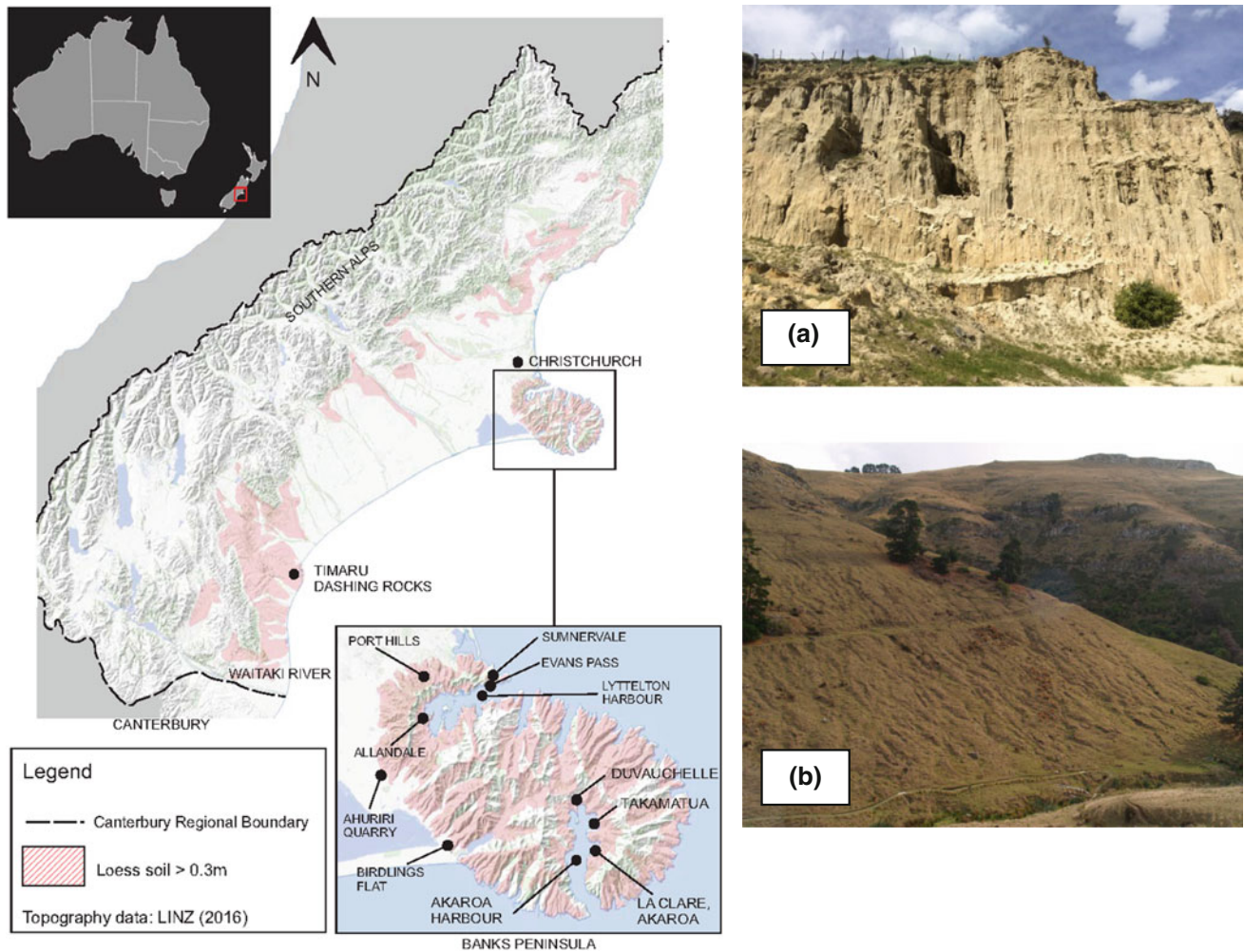e-mail: katherine.yates@pg.canterbury.ac.nz

C. Fenton
e-mail: clark.fenton@canterbury.ac.nz

Fig. 1 Distribution of loess > 300 mm thick across the South Island, New Zealand (Yates et al. 2017) **a** vertical loess cutting with erosion features, Birdlings Flat, Banks Peninsula; and **b** collapsed tunnel gullies across a loess colluvium slope, Sumnervale

Although previous research has identified a clear shear strength-moisture content relationship (e.g., Hughes 2002), the material has not yet been examined in the context of a partially saturated material. Therefore, the relationship between soil suction, water content and shear strength has not yet been investigated.

3 Research Methodology

Current research at the University of Canterbury aims to develop a better understanding of soil-water characteristics of loess and loess-derived soils in Canterbury. The results of this research will inform future development in loess-covered areas, and will improve the understanding of the behaviour of loess deposits with respect to changes in moisture content and shear strength. Research is being conducted using both field monitoring and laboratory testing techniques to allow both detailed observation of shear

strength characteristics and global examination of these mechanisms in situ.

3.1 Field Investigation

The field component of this research includes installation of twenty-four subsurface sensors in a north-facing 22° loess slope in Takamatua, Banks Peninsula (Figs. 2 and 3), for a minimum six-month period over winter, spring and summer. Twelve CS-616 sensors are used to measure volumetric water content. These sensors measure the volumetric water content by indirect methods. The probe produces an electromagnetic pulse which travels down the probe rods. The time taken for the electromagnetic pulse to propagate down the rod (wave period) is dependent on the dielectric permittivity of the soil. As the water content in the soil increases, the propagation time decreases due to the increase in the number of water molecules that need to be polarised.
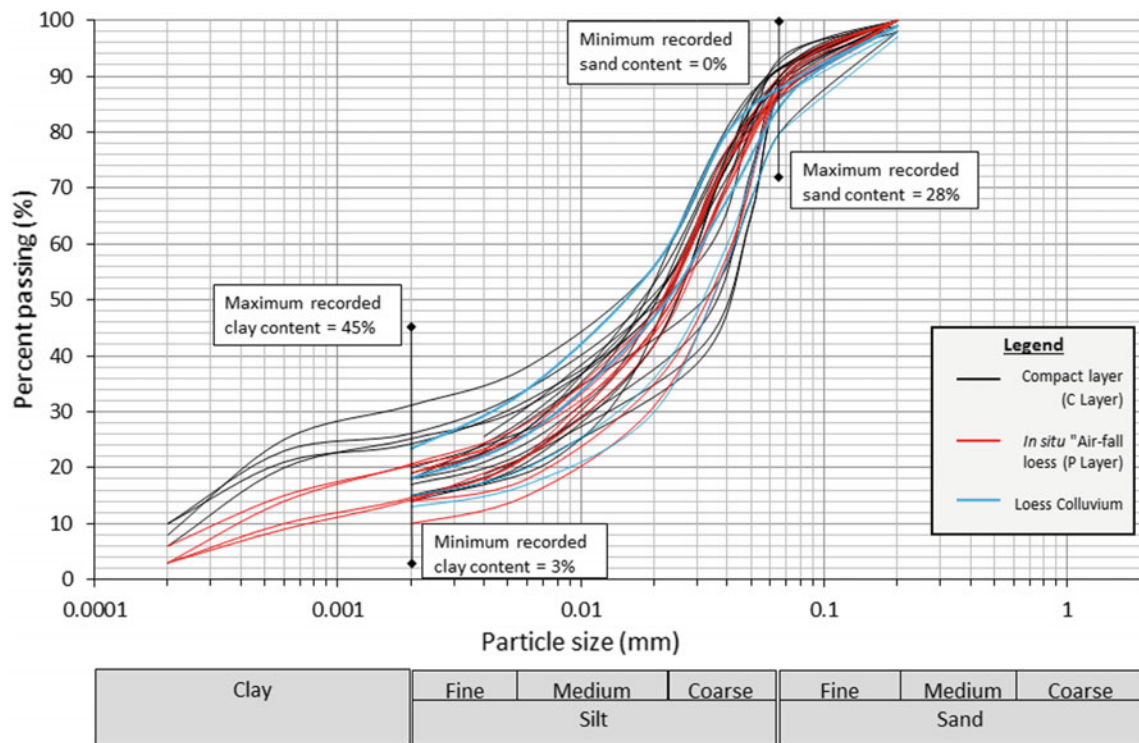
Fig. 2 Particle size distribution for loess soils in Canterbury, New Zealand (Yates et al. 2017)

Table 1 Summary of geotechnical characteristics for in situ *loess* (Yates et al. 2017)

Dry density	Atterberg limits	Shear strength
1.45–1.90 t/m^3 (average 1.70 t/m^3)	Liquid limit 20–30 Plastic limit 15–20 Plasticity index 4–12	c' 0–200 kPa φ 30–65°

Campbell Scientific provide a standard calibration equation to convert wave period to volumetric water content, however, it is important to define a site specific calibration equation that considers the specific dielectric permittivity of the loess soil. This was achieved by inserting the probes into a sample of loess compacted to in situ density. Periodically water was added to increase the volumetric water content. The known volumetric water contents and the wave period outputs from the CS 616 probes were used to develop a specific quadratic calibration equation for to allow accurate conversion of output data to volumetric water content for Canterbury loess soils.

The remaining twelve sensors are used to measure soil suction and temperature within the soil. These sensors measure suction indirectly by allowing two ceramic discs, with a known soil water characteristic curve, to equilibrate with the soil. A sensor adjacent to the ceramic discs measures the water content and provides a suction value.

MPS6 and CS616 sensors will be installed in four probe arrays (Fig. 3). Each array will have three of each sensor. Probes will be installed in individual auger holes at 0.5, 1.0 and 2.0 m depths. The advantage of using both the CS616 and MPS6 sensors are that they can be left on site for long-term monitoring—no re-calibration or maintenance is required for either of these sensors. In addition to the below ground sensors, a rain gauge is installed at surface on site to gather precipitation data. This allows assessment of the effect of precipitation on water content and soil suction.

3.2 Laboratory Testing

A soil-water characteristic curve (SWCC) is developed using the filter paper method (ASTM D5298-16). Triaxial testing is used to determine the shear strength of the loess soil at various moisture contents encountered in situ. Using the
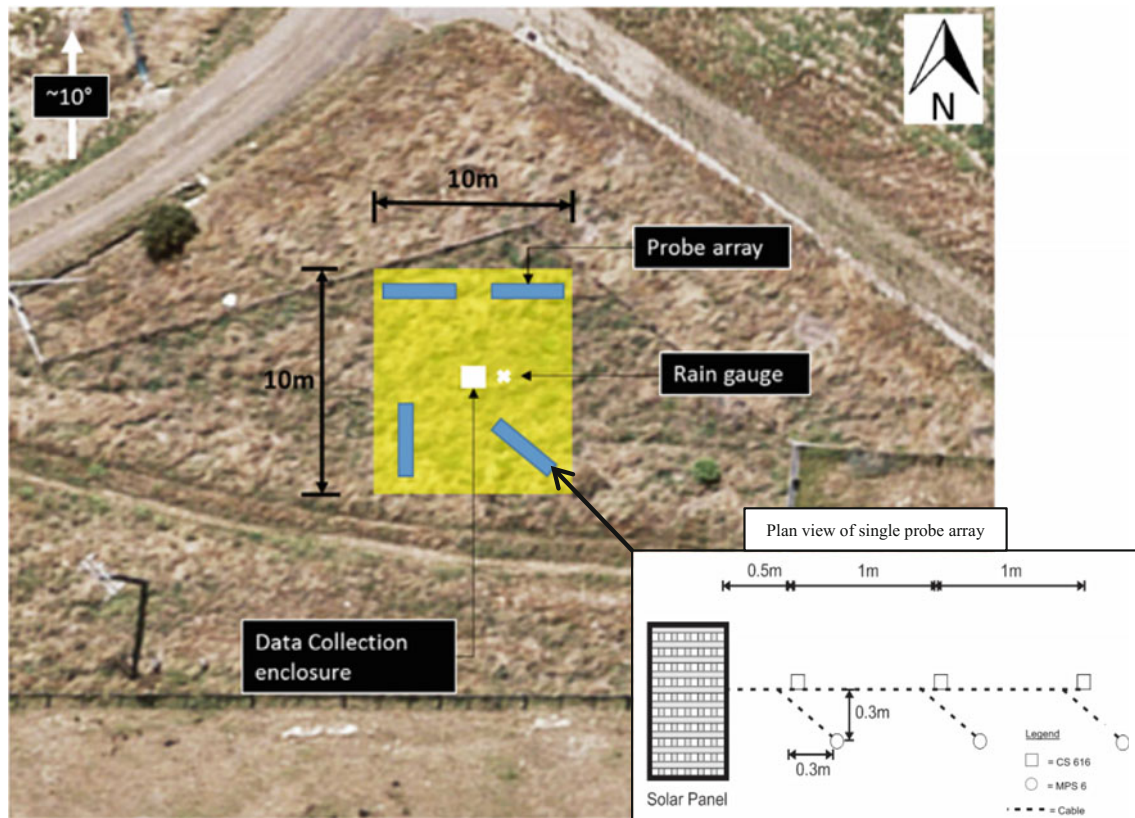
Fig. 3 Schematic of field monitoring configuration at Takamatua showing the approximate locations of the in situ instrument arrays

soil-water characteristics curve it will be possible to correlate the appropriate suction values in loess samples during triaxial testing, allowing the relationship between the shear strength and initial suction values to be examined in detail. Table 2 outlines the laboratory testing schedule for this research.

4 Preliminary Results

Initial testing of the soil-water characteristics of Canterbury loess soils has been undertaken using the Filter Paper method for testing suction. The filter paper test was conducted on 50 mm Ø samples carved from undisturbed block samples collected from Duvauchelle, Banks Peninsula (Fig. 2). Once the samples were wetted to the required moisture content they were then left for four days to equilibrate before commencing the test. Figure 4 compares the preliminary results of the Filter Paper test with SWCC from loess soils in China. The soil-water characteristic curve for Canterbury loess follows a similar trend to the Chinese loess, despite the higher sand content (Table 3).

Although there are several factors affecting the shape of the SWCC (e.g., stress history, plasticity), an obvious contributing factor is the particle size distribution for each loess deposit (Table 3). SWCCs for soil samples of varying particle size distributions (from clay through to sand) show that the coarser samples typically exhibit a steeper curve in the transition zone and lower suction values over all (Fig. 5) (Fredlund 2012; Fredlund and Xing 1994). It is interesting to note that although the loess soils from Canterbury have a slightly higher sand content, the suction values are similar to Chinese loess.

These preliminary data provide initial observations of the geometry of the SWCC for loess in Canterbury, and provides progress toward better understanding the soil-water-shear strength behaviour of these soils. Further development of the SWCC for Canterbury loess is required to confirm the shape of the curve. Furthermore, due to frequent hysteresis observed in soil-water characteristic curves, the drying portion of the curve should also be tested. Further work will also be undertaken to compare these results with SWCCs developed for the same material via different test methods (e.g. pressure plate test).

Table 2 Laboratory testing schedule

Category	Test	Purpose
Geotechnical index testing	Atterberg limits	Examine relationship between particle size grading, clay mineralisation and plasticity of loess
	Particle size distribution and clay content (hydrometer method)	
	Clay mineralogy (XRD testing)	
	Moisture content (at start and end of field trials)	Examine change in gravimetric water content throughout field trials
	Dry density	Inform relationships between density and other geotechnical characteristics
	Specific gravity	Characterisation and calculation of initial void ratio
	Oedometer test (stress history)	Examine consolidation state and infer impacts of stress state on soil consolidation Examine the possibility of collapse failure in loess
Soil water characteristics	Filter paper test and Pressure plate test	Determine the soil-water characteristic curve for both drying and wetting of the loess
Triaxial testing on in situ and Remoulded Loess	Isotropically Consolidated Drained Test (ICD) and Isotropically Consolidated Undrained Test (ICU) (Monotonic loading)	Examine stress-strain relationship, volumetric change, dilatancy, pore water pressure, critical state line and stress paths for loess
	Anisotropically Consolidated drained test (ACD) and Anisotropically Consolidated undrained test (ACU) (Monotonic loading)	Examine the influence of slope effects on the shear strength of loess
	Constant deviator stress test (CQS)	Simulate the stress paths of saturated soil in a loess slope with a rise in groundwater level. Deviator stress kept constant but pore water pressure varied
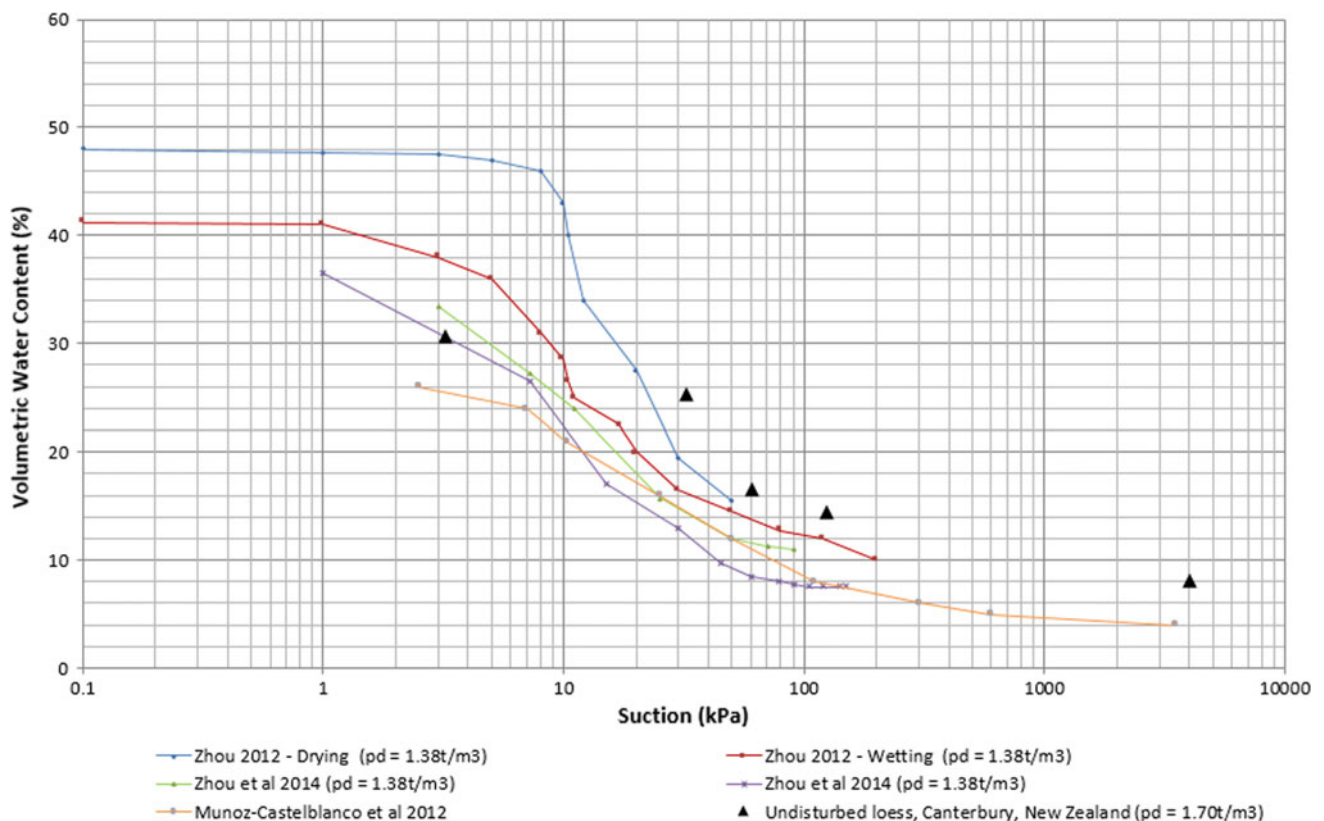
Fig. 4 Preliminary soil-water characteristic curve (wetting) for Canterbury loess compared with soil-water characteristic curves from Chinese loess (Zhou et al. 2014; Zhou 2012; Tu et al. 2009; Muñoz-Castelblanco et al. 2012)

Table 3 Physical properties of loess soils used to develop the SWCC in Fig. 4

	Duvachelle Loess, Canterbury, NZ (Marshall 2016)	Zhou (2012)	Zhou et al. (2014)	Muñoz-Castelblanco et al. (2012)
Sand content (%)	15	8	8	2
Silt content (%)	58	72	72	82
Clay content (%)	27	20	20	16
Plastic limit	18	18.3	18.3	19–21
Liquid limit	25	26.5	26.5	28–30
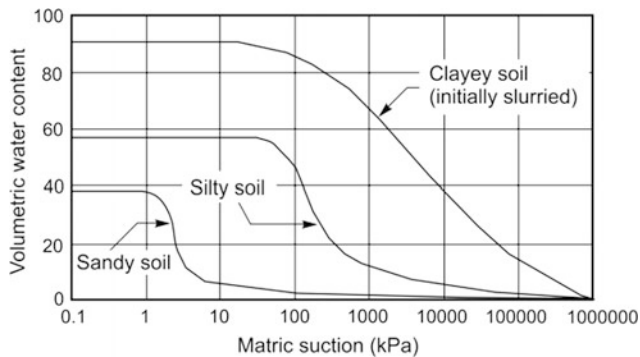
Fig. 5 Soil-water characteristic curves for clayey soil, silty soil and sandy soil (Fredlund and Xing 1994)

5 Summary

This paper presents preliminary results of the soil-water characteristics for loess soils in Canterbury, New Zealand. The motivation of this research is to investigate the sensitivity of the loess soils to moisture which contributes to the susceptibility of loess slopes to failure during rainfall events. A preliminary soil-water characteristic curve has been presented for Canterbury loess soils. This data indicates a similarity in soil-water characteristic behaviour to loess from China. These results are the beginning of a programme of research to examine the soil-water behaviour of this material. This on-going research includes the long-term observation of suction and water content in a loess slope in Canterbury to examine the relationship between rainfall infiltration and suction observed in the material. Further laboratory work will be undertaken to further develop the soil-water characteristic curve, and examine the strength characteristics of the loess with change in moisture contents.

References

Bell, D.H., Glassey, P.J., Yetton, M.D.: Chemical stabilisation of dispersive loessical soils, Banks Peninsula, Canterbury, New Zealand. In: 5th International IAEG Congress, Buenos Aires, pp. 2193–2208 (1986)

Bell, D.H., Trangmar, B.: Regolith materials and erosion processes on the Port Hills, Christchurch, New Zealand. In: 5th International Conference & Field Workshop on Landslides. Christchurch, pp. 93–105 (1987)

Fredlund, D.G.: Unsaturated soil mechanics in engineering practice. J. Geotech. Geoenviron. Eng. **132**, 286–321 (2012)

Fredlund, D.G., Xing, A.: Equations for the soil-water characteristic curve. Can. Geotech. J. **31**(6), 1026 (1994)

Goldwater, S.: Slope Failure in Loess, a Detailed Investigation, Allendale, Banks Peninsula. MSc Thesis, Department of Geological Sciences, University of Canterbury (1990)

Hughes, T.J.: A Detailed Study of Banks Peninsula Shear Strength. MSc Thesis, Department of Geological Sciences, University of Canterbury (2002)

Hutchinson, G.: Akaroa Harbour suffers extensive earth movements. Soil Water **12**, 6–7 (1975)

Ives, D.: Nature and distribution of loess in Canterbury, New Zealand. N. Z. J. Geol. Geophys. **16**(3), 587–610 (1973)

Jowett, T.W.D.: An Investigation of the Geotechnical Properties of Loess from Canterbury and Marlborough. MSc Thesis, Department of Geological Sciences, University of Canterbury. Available at: http://ir.canterbury.ac.nz/handle/10092/7580 (1995)

Marshall, S.: Laboratory Modelling of Tunnel Gully Erosion Development. Unpublished Professional Masters in Engineering Geology Report, University of Canterbury (2016)

McDowell, B.J.: Site Investigations for Residential Development on the Port Hills, Christchurch. MSc Thesis, Department of Geological Sciences, University of Canterbury (1989)

Muñoz-Castelblanco, J.A., et al.: The water retention properties of a natural unsaturated loess from Northern France. Géotechnique **62**(2), 95–106 (2012)

Raeside, J.D.: Loess deposits of the South Island, New Zealand, and Soils Formed on them. N. Z. J. Geol. Geophys. 7, 811–838 (1964)

Tonkin, P.J., Runge, E., Ives, D.: A study of late pleistocene loess deposits, South Canterbury, New Zealand. Quat. Res. **4**, 217–231 (1974)

Tu, X.B., et al.: Field monitoring of rainfall infiltration in a loess slope and analysis of failure mechanism of rainfall-induced landslides. Eng. Geol. **105**(1–2), 134–150. (2009). Available at: http://dx.doi.org/10.1016/j.enggeo.2008.11.011

Yates, K., Fenton, C.H., Bell, D.H.: A review of the geotechnical characteristics of loess and loess-derived soils from Canterbury, South Island, New Zealand. Eng. Geol. (October 2016), pp. 0–1 (2017). Available at: http://linkinghub.elsevier.com/retrieve/pii/S0013795216304422

Zhou, Y.: Study on Landslides in Loess Slope Due to Infiltration. University of Hong Kong (2012)

Zhou, Y.F., et al.: Laboratory study on soil behavior in loess slope subjected to infiltration. Eng. Geol. 183, 31–38 (2014)

Comparison of Mechanically Determined with Profile-Based Joint Roughness Coefficients

Kristofer Marsch and Tomás M. Fernandez-Steeger

Abstract

The most popular index for the geometrical characterization of rock discontinuities in rock mechanics is the Joint Roughness Coefficient (JRC). Direct shear tests or mechanical index tests such as tilt- and/or push-tests are most suitable to determine the coefficient. In engineering practice, the JRC is often set according to standard-profiles by visual matching or calculation using correlations with statistical or fractal parameters. However, this method implies that profiles can represent a surface. Naturally, different profile directions and starting points on the surface lead to different JRC values even when quantitative statistical or fractal methods are used. This study elucidates the question whether it is possible to determine a reasonable representative JRC for a surface from profiles. For that purpose, fresh mated samples were tested in push-tests from which their JRC was back-calculated. Additionally, 3D models of the surfaces were assembled as a basis for the calculation of the JRC from statistical parameters. Numerous profiles were extracted from the 3D data. The amount of more than 8000 profiles per sample offers the possibilities to define a JRC according to its variation and to assess its variability on the surface. Based on a comparison of the population of JRC values from all possible 10 cm-profiles with the mechanically determined index it can be stated, that it is not feasible to define a reliable JRC from a few profile measurements only. Moreover, there exists no connection between the experimental results of the aforementioned differing measurement approaches.

Keywords

Joint roughness • Push-test • Profilometer •
JRC • Photogrammetry

K. Marsch (✉) · T. M. Fernandez-Steeger
Institute for Applied Geosciences, Technische Universität Berlin,
Berlin, Germany
e-mail: kristofer.marsch@tu-berlin.de

1 Introduction

The empirical shear strength criterion from Barton (1973) forms a well-established constitutive model for rock joints. The relationship between normal and shear stress (σ_n and τ, respectively) in dependence of joint wall strength (JCS), residual friction angle (φ_r) and joint roughness coefficient (JRC) is as follows:

$$\tau = \sigma_n \tan\left[JRC \log\left(\frac{JCS}{\sigma_n}\right) + \varphi_r\right] \qquad (1)$$

Preferably, JRC is back-calculated from direct shear tests or mechanical index tests such as tilt- and/or push-tests. Due to the complexity of these tests, usually visual matching of surface traces with ten standard-profiles introduced by Barton and Choubey (1977) provides an estimation of JRC. Tse and Cruden (1979) criticized this rather subjective method and proposed a correlation of JRC with the statistical parameter Z_2 for the ten standard-profiles. Since the 1980s, many researchers published a variety of functions, which use different statistical parameters (Li and Zhang 2015). Besides, there exist correlations between JRC and the fractal dimension Turk et al. (1987) are the first who calculated D for the standard-profiles and linked it to JRC. Depending on the method of calculating D, different equations are available (Li and Huang 2015).

The above-mentioned popular approach of JRC estimation and calculation based on profiles essentially reduces the three-dimensional phenomenon of shear strength to a two dimensional problem. This reduction seems reasonable against the background of insufficient availability of accurate 3D measuring devices in the 1970es but should not hold in present high-technology times. However, more crucial is the fact that JRC determination through profilometry solely rests upon the ten standard-profiles. Barton and Choubey (1977) state, "an attempt was […] made to select the most typical profiles", therefore, the ten standard-profiles themselves are highly subjective. Naturally, different profile directions and

starting points on the surface lead to different JRC even when quantitative statistical or fractal methods are used. This makes their procedure of measuring only three profiles per specimen even more questionable.

In this paper, the relationship between JRC derived from mechanical push-tests and JRC calculated from the topography of profiles is studied. For that purpose, manually split rock blocks provided fresh tensile fractures, which were digitized using photogrammetry. The rock material parameters JCS and φ_r were determined through index tests, namely Schmidt Hammer and tilt-tests. The overall research program therefore resembles the original procedure.

2 Sample Material

Three different rock types were used in this study, namely basalt, granite and sandstone. The sandstone showed a medium to coarse grainsize and was poorly cemented by silica. For all rock types, the induced fractures proceeded along grain boundaries as no anisotropy was seen within the rock blocks.

2.1 Basic Friction Angle (φ_b)

All tests were performed on unweathered samples. Therefore, the residual basic friction angle φ_r in Eq. (1) has to be replaced by the basic friction angle φ_b. There exists no standardized procedure for the determination of the basic friction angle yet. Stimpson (1981) proposed to use rock cores in a tilt test where one core slides on the other two. However, this method is sensitive to the linearity of the core's skin surface and according to Alejano et al. (2012) overestimates φ_b. In contrast, they suggest using saw-cut surfaces of at least 50 cm^2 size and Length/Height ratio of 2 in 3 consecutive tilt-tests. Their approach was adopted in this study.

For the basalt, 24 tilt-tests were performed and provided basic friction angles between 21.9° and 32.2°. Due to the great range of 10.3°, the median value of $\varphi_b = 26.6°$ was used. The standard deviation for the test results of 3.3° is within the commonly expected range. The granite behaved in a similar way concerning standard deviation (3.7°) and range (21.2°–34.7°). However, its median value for φ_b amounts to 31.9°. Instead, the sandstone produced a narrower range of 25.8°–31.3° with a median value of $\varphi_b = 28.2°$. The standard deviation is the lowest with 1.7° compared to the other two rock types.

2.2 Joint Wall Strength (JCS)

By default, the joint wall compressive strength is determined by the Schmidt Hammer (Barton and Choubey 1977). In knowledge of the rock's density, the JCS is calculated from the rebound value. For fresh unweathered rock, JCS equals the uniaxial compressive strength (UCS.) In general, determination of JCS by means of Schmidt Hammer or point load test without comparison to uniaxial compression tests is error-prone (see Aydin 2009).

Prior to splitting the rock blocks, Schmidt Hammer (SH) rebound measurements were carried out on the outside faces of the blocks, which were cut using a diamond saw. The ambiguity of this measuring approach is exemplified by the results of the basalt sample: from 270 SH blows a mean rebound value of 82.2 was received. Assuming a density of 2.9 g/cm^3 an unrealistic value for JCS of about 1200 MPa would emerge.

Therefore, JCS for the basalt was set to 250 MPa according to common values. For the granite, JCS was set to 175 MPa and for the sandstone, JCS was defined as 50 MPa. The estimation of JCS/UCS according to literature values is acceptable as the push-tests were performed under very low normal stress of approximately 0.003 MPa. At this stress level, a variation of JCS of 50 MPa results in marginal increase/decrease of the JRC of approximately 0.2 points on the JRC scale. Furthermore, during all tests only minor failure of asperities occurred. Hence, the effect of JCS on the results is negligible.

3 Push-Tests

The push-tests were performed with the experimental setup depicted in Fig. 1. One half of the sample is clamped to a frame, whereas the upper half lies loosely on top. Accordingly, the normal stress originates from the self-weight of the upper block and if applicable additional balance weight. To ensure that the shearing direction is parallel to the measured profiles, guardrails made of more or less frictionless Teflon were installed. Initially, the sample is fit in the frame with a gap of 2 mm to the lateral guiderails. The shear force is applied to the upper half by means of a hydraulic hand pump. Besides shear displacement and shear force, the vertical displacement is recorded at two locations, at the front and at the end of the sample, to gather information about dilation and potential rotation of the upper sample half.

The back-calculation of JRC was carried out according to the recorded shear force and the material parameters

Fig. 1 Push-test setup

mentioned above. For the normal stress calculation, the projection of the rough surface onto the xy-plane was used. Therefore, the normal stress corresponds to the engineering stress, as the real contact area is unknown. JRC is calculated by re-arranging Eq. (1), leading to:

$$JRC = \frac{\arctan(\tau/\sigma_n) - \varphi_b}{\log(JCS/\sigma_n)} \tag{2}$$

4 Digital 3D Models

Many methods for gathering topographic information of rock surfaces, e.g. terrestrial laser scanning (TLS), structured light scanning (SLS) or photogrammetric approaches, are available. As high accuracy scanners are often very costly, digital imagery captured by off-the-shelf cameras is an alternative. Marsch and Wujanz (2016) showed that 3D-models acquired with structure-from-motion (SfM) and dense-image-matching (DIM) techniques yield acceptable deviations to high quality SLS scans. Hence, SfM and DIM were applied in this study.

An uncalibrated camera was used to gather images of the samples. The photos comprised a geometric norm that allows reliable scaling. No specific pattern was adopted; instead the photos were shot from various positions. Based on the images, point clouds were assembled from which triangulated surfaces were produced. For all samples, the point cloud resolution amounted to approximately 15 points per square millimeter (pts/mm^2) at least. Differences in

resolution can be explained by the randomness of photo-shoot positions and distances to the samples.

As an example, the model of the granite sample is shown in Fig. 2. The height is color-coded and exaggerated with a factor of 2. For clarity, only every 5th profile is displayed (for more information see next chapter). All models were rotated in space according to best-fit planes and moved to positive coordinates.

5 JRC Calculation

To calculate JRC from the 3D models an algorithm was implemented in *Matlab* ©. First, profiles are extracted by defining cutting planes in the favored spacing. This allows slicing the surface in arbitrary directions, which also permits investigation of anisotropy if desired. Second, all profiles are rotated according to least-squares regression and interpolated linearly in a predefined sampling interval. These steps are required as most of the statistical parameters are based on height differences or slopes between adjacent points, therefore, a datum must be established. In this study, a sampling interval of 1 mm (also for the spacing of the profiles) was used since the standard-profiles were also captured with 1 mm steps. Finally, based on the statistical parameter Z_2 (Myers 1962) (Eq. 3) the JRC is calculated using Yu and Vayssade's (1991) correlation (Eq. 4).

$$Z_2 = \sqrt{\frac{1}{L} \int_{x=0}^{x=L} \left(\frac{dy}{dx}\right)^2 dx} \tag{3}$$
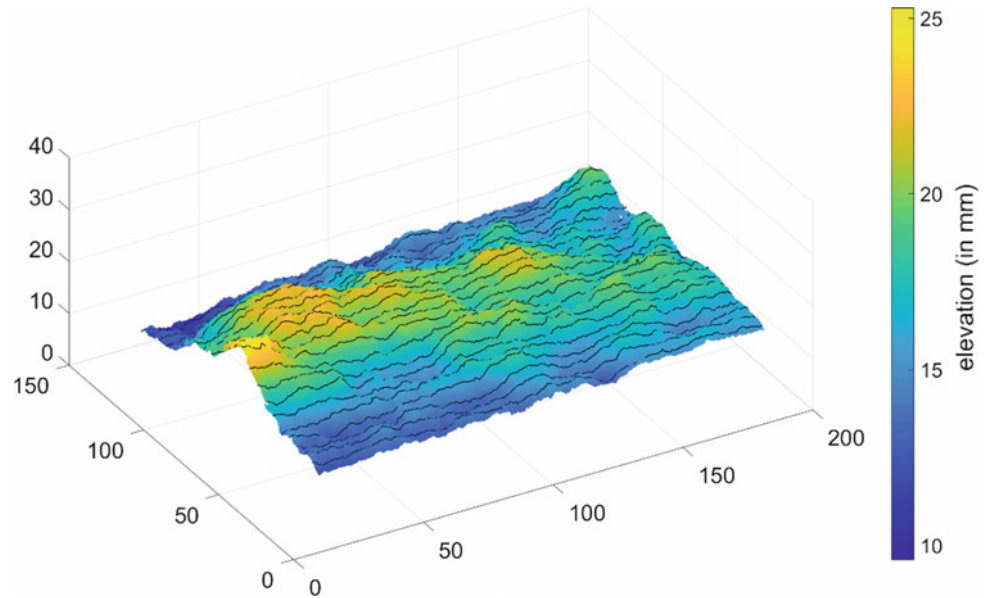
$$JRC = 64.22Z_2 - 2.31 \qquad (4)$$

For this study, on one hand profiles were extracted in the shearing direction over the whole length of the samples. Since they had lengths between 15 and 22 cm, these profiles were corrected according to Barton and Bandis (1982):

$$JRC_n \cong JRC_0 \left(\frac{L_n}{L_0}\right)^{-0,02JRC_0} \qquad (5)$$

Here, JRC_0 stands for the value measured on a 10 cm profile. The relationship between JRC_n and JRC_0 follows a power law decay using the quotient of the length in question L_n to the standard-length L_0. By rearranging Eq. (5), JRC_0 is iteratively determined for profiles longer than 10 cm.

On the other hand, all possible 10 cm profiles of the surface were evaluated. Moving an imaginary profilometer (of 10 cm and 1 mm sampling step) over the surface, just like the profile gauge used for the standard-profiles, resulted in a large amount of profiles of the same length. This marks an improvement since JRC can be evaluated statistically.

Furthermore, no correction for scale effects is necessary, which technically also applies to profiles with low deviation from the standard-length of 10 cm.

6 Results

To begin with, the results of the push-test are given. A total of 30 push-tests were conducted in this study, 10 for each sample. The results are summarized in Table 1. Note the discrimination between the first and subsequent 5 tests. Although, theoretically no failure of asperities should occur at the applied low stress level abrasion was seen during the tests. This is reflected in the slight decrease of back-calculated JRC with increasing test number as the samples were reused. Nevertheless, the standard deviation for all tests is very low.

Since profilometry by means of a simple tactile profile gauge, also referred to as profile comb, is common practice in the field and laboratory, the method was also applied in

Table 1 Median JRC of push-tests

Sample	First 5 tests	Next 5 tests	Total	Stdev.
Basalt	10.3	9.9	10.1	0.27
Granite	9.6	8.6	8.9	0.65
Sandstone	8.6	8.0	8.2	0.45

Table 2 JRC from profile gauge measurements

Sample	JRC median	Band width
Basalt	10.6	9.3–13.7
Granite	13.3	11.7–15.6
Sandstone	8.1	7.0–11.1
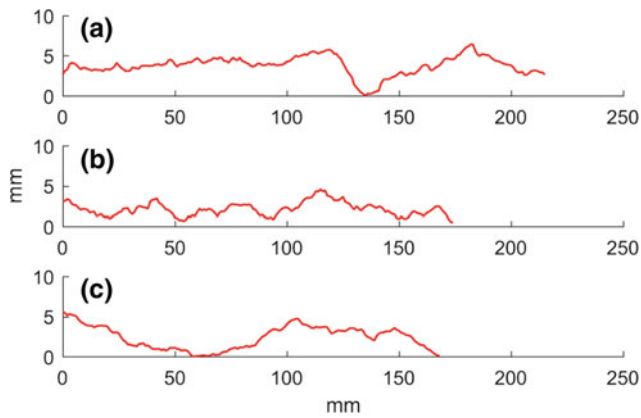
Fig. 3 Example profiles, **a** basalt, **b** granite, **c** sandstone

this study. For each sample, 10 profiles were taken over the whole length. The JRC values are summarized in Table 2. Example profiles are given in Fig. 3.

The effect of the Bandis-correction is compiled in Table 3. When profiles over the whole length of the samples are evaluated, as expected, the original distributions are shifted to higher JRC. For example, the median JRC of the basalt sample increases from 12.8 to 16.1 and also the width of the distribution increases (stdev. from 1.74 to 2.79). Essentially, Bandis' correction is a downscaling of the original data. Due to the correction JRC values of greater than 20 appear. This is clearly inconsistent with Barton's original JRC scale. The Bandis-correction might lead to values beyond the domain of definition. The above is at least valid on laboratory scale and for profiles around 10 cm longer than the standard-profiles. The same effects, namely increase in JRC and widening of the distribution, are seen for the basalt and sandstone samples. However, the effect is not as pronounced for the sandstone sample since the surface was shaped rather like a trapezoid resulting in many profiles of only 15 cm length. Thus, they did not deviate much from the standard-length.

Not only because the standard-profiles are 10 cm but also because of the scale effects discussed above, it is reasonable to directly evaluate profiles of the standard-length. The data of the granite sample is utilized for the presentation of results. In Fig. 4, distributions of JRC are displayed. A total of 8664 profiles of 10 cm length were extracted from the 3D model for

which a median JRC of 13.7 was calculated. When using a profilometer in the field or laboratory to measure the topography, the user practically randomly picks samples from this basic population. To investigate the effect of this practice, 5, 10, 15 and 100 profiles were taken likewise randomly from the basic population. A repetition of 10 times resulted in a new distribution of median JRC values (red dotted lines in Fig. 4). In matters of this particular example, a bandwidth of 12.4–15.1 evolves for 5 profiles which is larger than for 15 profiles (12.9–14.2). The bandwidth for 100 profiles is 13.6–14.0, which approaches the median of the basic population of 13.7. Therefore, a sample size of 100 profiles adequately depicts the surface. In conclusion, JRC values determined only by a few random profilometer measurements should be treated with caution as they are highly arbitrary and do not depict the basic population.

To compare the mechanically determined with profile-based JRC, in a nutshell, Fig. 5 illustrates the outcome. For all 3 samples the push-test results show little variation, they serve as a benchmark for the profile-based JRC. Most obvious, the Bandis-correction increases the gap to the benchmark value and thus should not be used on laboratory scale. Comparing the medians of the standard-length profiles (sL) and the profiles over the whole length (wL), it appears that their values are quite similar. Consequently, profiles of comparable length and even up to 10 cm longer than the standard-length can readily be used for JRC calculation. Nonetheless, when Barton's theory is strictly followed only taking 10 cm-profiles into account, the enormous variation of up to 10 JRC points (meaning 5 roughness classes) necessitates a reasonable sample size (see Fig. 4). The greatest similarity between push-test results and profile-based JRC is seen for the profile gauge measurements over the whole sample length, unsurprisingly, as this procedure was applied when the JRC concept was introduced by Barton (1973). The difference for the granite sample between push-test results and calculated JRC originates from height differences of the front part of the sample to the rear part in terms of the shear direction (as visible in Fig. 2). The shearing took place from left to right and also from left to right the elevation decreases. Therefore, during the push tests the actual contact area decreased rapidly resulting in a decreased shear strength and hence smaller back-calculated JRC.
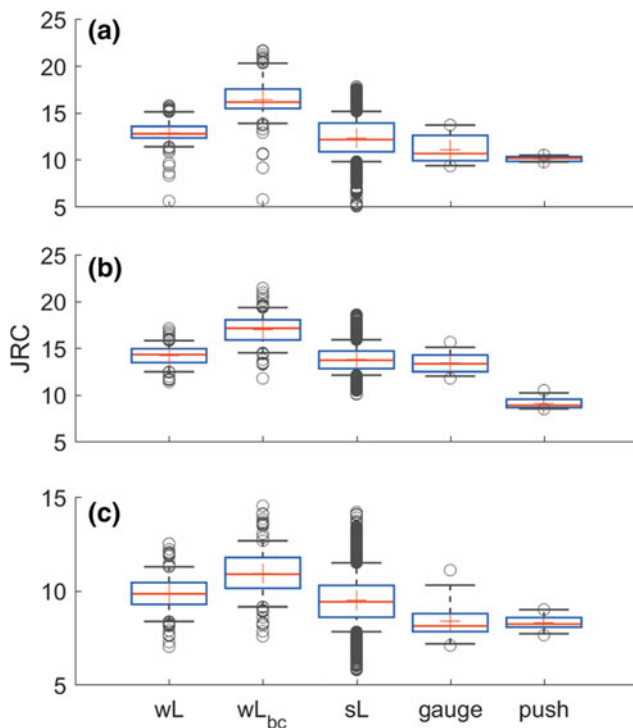
Table 3 JRC correction according to Barton and Bandis (1982)

Sample	Avg. profile length (cm)	# of profiles	Original median	Stdev.	Corrected median	Stdev.
Basalt	21.3	118	12.8	1.74	16.1	2.79
Granite	17.4	117	14.3	1.20	17.1	1.79
Sandstone	16.9	128	9.8	1.09	10.9	1.36
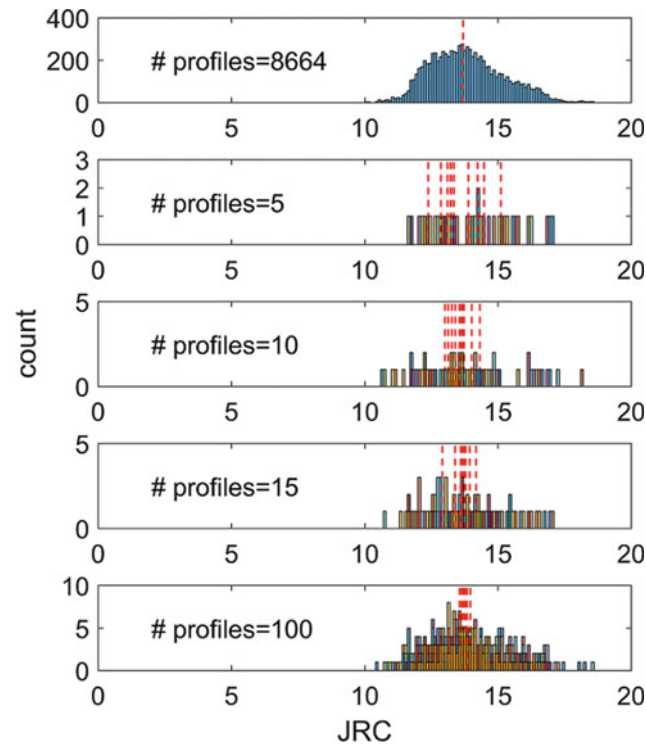
Fig. 4 Distribution of JRC with varying sample size, median as red lines (granite sample)

Fig. 5 Boxplots JRC populations, **a** basalt, **b** granite, **c** sandstone, wL = whole length, wL$_{bc}$ = whole length Bandis-corrected, sL = standard-length 10 cm

7   Conclusion

In the paper at hand, push-test results were compared with calculated JRC. As stated in Sect. 2.1, the values for the basic friction angle show considerable variation. A deviation of ±5° causes a change of JRC of approximately 10%. Hence, there exists an uncertainty of a least one JRC class for the push-test results and improvements of the determination method for the basic friction angle are needed.

In General, it was seen that the best agreement was achieved when using a tactile profile gauge, just as Barton did. For laboratory sample sizes, no correction for scale effects is necessary. Nevertheless, profilometry provides ambiguous results, which clearly asks for a reasonable sample size. The great benefit of analyzing 3D digital data lies in the possibility of extracting huge amounts of profiles in varying sampling steps, directions and virtually everywhere on the surface. As a result, the approach introduced here offers an insight into the variability of JRC and a means of statistical analysis.

References

Alejano, L.R., González, J., Muralha, J.: Comparison of different techniques of tilt testing and basic friction angle variability

assessment. Rock Mech. Rock Eng. **45**, 1023–1035 (2012). https://doi.org/10.1007/s00603-012-0265-7

Aydin, A.: ISRM Suggested method for determination of the Schmidt hammer rebound hardness: Revised version. Rock Mech. Min. Sci. **46**, 627–634 (2009)

Barton, N.: Review of a new shear-strength criterion for rock joints. Eng. Geol. **7**, 287–332 (1973)

Barton, N., Bandis, S.: Effects of block size on the shear behavior of jointed rock. In: Proceedings 23th US Symposium Rock Mechanics, pp. 739–760. Berkeley/California (1982)

Barton, N., Choubey, V.: The shear strength of rock joints in theory and practice. Rock Mech. **10**, 1–54 (1977)

Li, Y., Huang, R.: Relationship between joint roughness coefficient and fractal dimension of rock fracture surfaces. Rock Mech. Min. Sci. **75**, 15–22 (2015). https://doi.org/10.1016/j.ijrmms.2015.01.007

Li, Y., Zhang, Y.: Quantitative estimation of joint roughness coefficient using statistical parameters. Rock Mech. Min. Sci. **77**, 27–35 (2015). https://doi.org/10.1016/j.ijrmms.2015.03.016

Marsch, K., Wujanz, D.: Determination of roughness parameters based on dense image matching and structured light scanning. In: Proceedings 2nd Virtual Geoscience Conference, p. 75. Uni Research, Bergen/Norway (2016)

Myers, N.O.: Characterization of surface roughness. Wear **5**, 182–189 (1962)

Stimpson, B.: A suggested technique for determining the basic friction angle of rock surfaces using core. Rock Mech. Min. Sci. **18**, 63–65 (1981)

Tse, R., Cruden, D.M.: Estimating joint roughness coefficients. Rock Mech. Min. Sci. **16**, 303–307 (1979)

Turk, N., Greig, M.J., Dearman, W.R., Amin, F.F.: Characterization of rock joint surfaces by fractal dimension. In: Proceedings 28th US Symposium Rock Mechanics, pp. 1223–1236. University of Arizona, Tucson (1987)

Yu, X., Vayssade, B.: Joint profiles and their roughness parameters. Rock Mech. Min. Sci. **28**, 333–336 (1991)

Influence of Fine Content on the Mechanical Properties of Sand Subjected to Local Particle Loss by Piping

Yang Yang and Chao Xu

Abstract

Detachment and migration of soil particles from its skeleton under the action of seepage force, known as internal erosion, place a great risk on the stability of hydraulic structures. Despite the comprehensive research aiming to assess the onset condition and development of piping, there is little experimental research regarding the mechanical properties of soil at post erosion state. This paper presents an experimental method of reproducing piping erosion by dissolution of pre-installed glucose column inside cylindrical specimen. A series of triaxial compression tests was conducted on sand with different fines content to investigate the piping effect on mechanical behavior of sandy soil. Due to loss of finite particles, obvious variations were observed between eroded specimens and the intact ones in deformation characteristics and small strain stiffness, while the overall shear strength of the disturbed specimens appeared to be less affected.

1 Introduction

Reference to soil erosion due to piping can be found in many reports related to dam and levee failures and landslides (Foster et al. 2000). As one of the most common mechanisms of internal erosion, the term "piping" is commonly used to describe the process that a subsurface preferential path is formed and enlarged under the seepage force.

Loss of soil particles due to internal erosion can lead to a change in the microstructure of soil, which as a result, affects the strength and stiffness of soil. A variety of experimental methods have been proposed in previous studies to identify the key parameters associated with soil erosion, such as the pinhole test (Sherard et al. 1976; Acciardi 1982), the hole erosion test (Wan and Fell 2004; Benahmed and Bonelli 2012) and jet erosion test (Hanson 2004). Two major concerns in most of these approaches were the onset condition (critical shear stress) and the erosion rate. However, since little attention has been paid on the disturbed soil at post-erosion state, it is still a subject of great uncertainty as to exactly how the change of soil fabric due to particle removal would affect the mechanical properties of soil.

In the past few years, using water soluble material to simulate the erodible particles has become a common way in the study of internal erosion (Shin and Santamarina 2009; Truong et al. 2010). Element experiments on sand-salt mixtures were performed, and consequences of particle dissolution in the strength and deformation behaviour of soils have been widely investigated. It has been reported that particle loss will lead to marked settlement strain, increase in the void ratio and weakening of the overall strength. In these uniformly mixed sand-salt specimens, it was always assumed that internal volumetric strains caused by particle dissolution would follow a random spatial distribution. However, for soils subjected to piping erosion, nonhomogeneous fabric would be generated due to the localized discontinuous macropores. To our knowledge, there have been no recent studies on the mechanical properties of soil possessing piping-induced anisotropic fabric.

In this study, with the aim to reproduce internal erosion in the form of piping, particle loss was induced by saturating specimens with pre-installed glucose shaped in a column acting as the preferential erodible path. The main objective is to clarify how the particle detachment would influence the

Y. Yang (✉) · C. Xu
Department of Geotechnical Engineering, College of Civil Engineering, Tongji University, Shanghai, 200092, China
e-mail: 2011yang@tongji.edu.cn

Y. Yang · C. Xu
Key Laboratory of Geotechnical and Underground Engineering of the Ministry of Education, Tongji University, Shanghai, 200092, China

engineering properties of soils. Young's modulus was checked at the initial dry state and after the piping erosion with the help of local displacement transducers by conducting small cyclic loadings. The strength variations between the eroded specimen and non-eroded one were also obtained by monotonically shearing the specimen into failure.

2 Test Apparatus, Specimen and Procedures

2.1 Txiaxial Apparatus

A small size, gear driven, strain controlled triaxial apparatus developed at the Institute of Industrial Science, University of Tokyo was employed in this study, as is shown in Fig. 1. The apparatus mainly consists of a cell, loading system and measurement devices. The axial loading system consists of an AC servo-motor, a reduction gear system, electronic magnetic clutches and brakes. Axial load is measured by an internal load cell placed inside the triaxial cell, with a capacity of 200 kg. Cell pressure is applied through an electro-pneumatic transducer (E/P) with a capacity of 1000 kPa and adjusted by accurate regulators. High capacity differential pressure transducer (HCDPT) was used to measure the effective confining pressure, by detecting the pressure difference between the two chambers, with the positive side connected to the inside of the specimen and the negative side to the triaxial cell. In this study, all tests were conducted under drained condition, and the positive side of HCDPT was open to atmosphere.

2.2 Specimen

Two kinds of soil are used: Toyoura sand (specific gravity $G_s = 2.64$, maximum void ratio $e_{max} = 0.992$, minimum void ratio $e_{min} = 0.678$) and Edosaki sand ($G_s = 2.71$, $e_{max} = 1.383$, $e_{min} = 0.868$). The grading distributions of the materials are depicted in Figs. 2 and 3. Toyoura sand is mostly sub-angular in shape and consisting mainly of quartz and limestone, with negligible fines content. Edosaki sand contains about 20% fines and is considered as unstable material, i.e., the coarser fractions are unable to prevent the transportation of its finer fractions (Kenny and Lau; 1985; Kenny et al. 1985).

Firstly, a plastic pipe with inner diameter of 7 mm was placed in the middle, along the longitudinal axis of the cylinder specimen (7.5 cm in diameter and 15 cm in height). For dry Toyoura sand, air-pluvation method was used and sand was poured into the mould using a funnel with appropriate opening. The falling height was decided by the desired densities, and the same height was maintained from
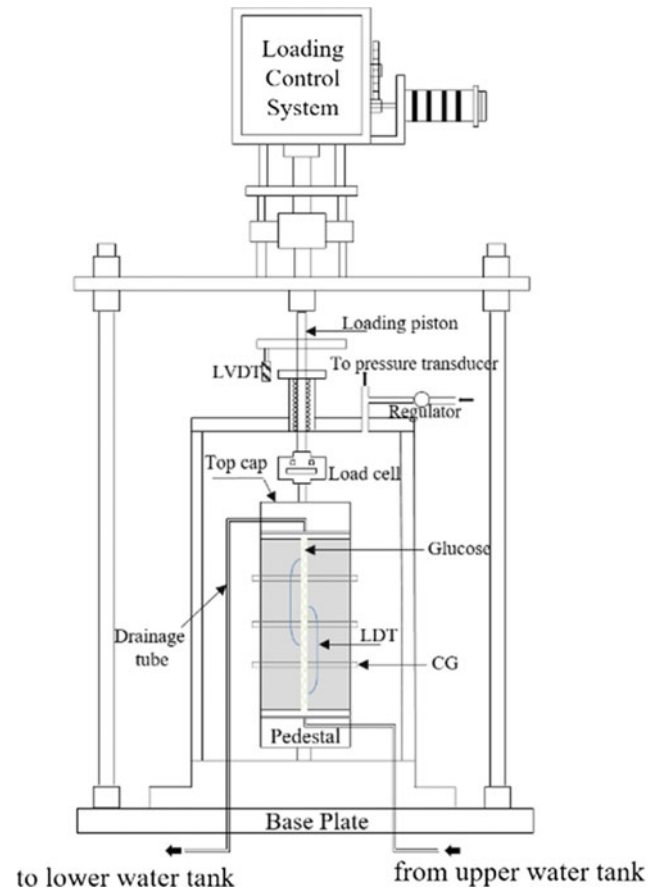
Fig. 1 Cylindrical specimen and transducers in Triaxial apparatus
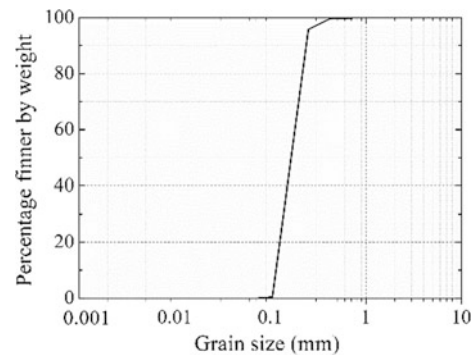
Fig. 2 Grain size distribution of Toyoura sand

the funnel opening to the sand surface. In order to make a uniform specimen, pouring direction was changed from clockwise to anti-clockwise circumferentially. For Edosaki sand, specimen was prepared by moisture tamping method. 15 layers with the height of 1 cm for each layer were tamped from the bottom to the top gradually under the water content around 6%.

After the completion of sand preparation, dry glucose powder was filled into the plastic straw with great care. Then
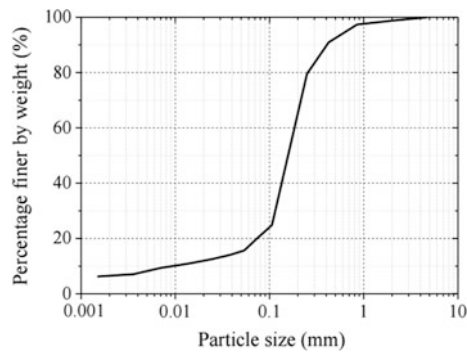
Fig. 3 Grain size distribution of Edosaki sand

the straw was removed slowly so as to minimize disturbance of the surrounding sand. Connections were made through tubes between the bottom pedestal and the upper water tank, as well as the top cap to the lower water tank. Two load cells are mounted on both upstream and downstream to measure the mass of inflow and outflow, and thus, to evaluate the infiltration rate to the soil sample. In total around 1500 ml of water was infiltrated into the sand to ensure a complete dissolution of glucose pipe. In order to dissolve the glucose in a gentle manner, the speed was set to 14–16 ml/min. Before and after the water infiltration, small cyclic loadings were conducted axially with peak to peak strain amplitude of 0.001% on the specimen in order to obtain the Young's modulus. Then the specimen was allowed to undergo a creeping process under drained conditions until it reached stability. Finally, the monotonic shearing with strain rate of 0.1% per minute under drained condition was conducted.

Due to difficulties in obtaining the non-uniform volumetric deformation during glucose dissolving, local displacement transducers (LDT) with the size of 70 mm × 3 mm × 0.2 mm (L/W/T) were used, which could measure very small strain between 10^{-6} and 10^{-2}. Two pairs of LDTs were fixed at the upper and lower half of the specimen separately on the opposite side, which could detect bending deformations caused by axial compression or extension. In addition, three clip gauges (CG) were attached on the lower, middle and upper part of the specimen to measure the radial strains. The arrangement and location of these local sensors, which were supported by hinges made of thin copper strip and small aluminum blocks glued outside the membrane, were shown in Fig. 4.

Furthermore, linear variable differential transformer (LVDT) is fixed externally to measure the vertical displacement of the specimen during shearing period.

2.3 Test Conditions

Test conditions for each specimen are summarized in Table 1, where "NP" and "P" stand for no-pipe and pipe respectively. Drini represents the initial relative density of dry sand, $e$ini is the corresponding void ratio and σc is the isotropic confining pressure during water infiltration.

3 Results and Discussions

3.1 Axial and Radial Strains During Piping Erosion

Figures 5 and 6 showed the axial strains calculated from LDTs before the final shear-ing. Generally there were two obvious increments of εa (contraction of the specimen). The first growth of εa occurred due to isotropic stress increment from 25 kPa (during specimen preparing) to 50 kPa. For the test cases with internal artificial pipes, more obvious increase of εa was observed during water infiltration, indicating the development of internal erosion. Compared with Toyoura sand, much larger settlement was found in Edosaki sand during the water infiltration even for the specimen without glucose. Similar tendency was also noticed in the variation of radial strains εr for all the specimens, seen in Figs. 7 and 8. In both specimens with glucose pipes, contraction of sand in horizontal direction was more significant than the deformation in vertical.

Based on the axial and radial strains, the volumetric strain ε_{vol} could be computed. Given the same amount of initial glucose (0.87% in volume of the whole specimen), it could be inferred that different volumetric strains observed among specimens indicated that the scope of disturbance during the generation and propagation of piping was influenced by the content of fines. Growth in volumetric strain was around 0.36% in test case of Toyoura_P during glucose dissolution, and change in ε_{vol} in Edosaki sand were found to be around 0.80%. For simplicity, the amount of eroded voids in the specimen could be considered as the difference between the initial glucose volume and the variation in volumetric strain ε_{vol} during water infiltration. It then could be inferred that more piping-induced voids were generated in Toyoura sand. These local concentrated voids would in turn have great influence on the mechanical behavior of the soil. Further evaluation on stiffness characteristics is presented below.

Fig. 4 Arrangement of local sensors (Left: side view; Right: front view)
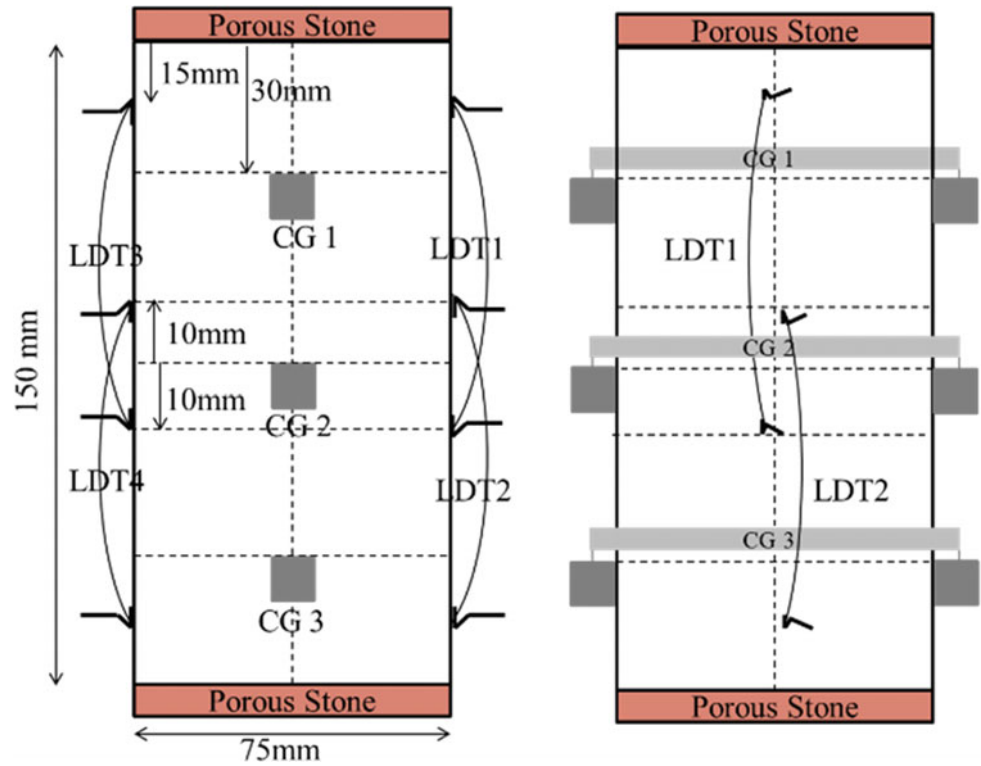
Table 1 Test conditions

No.	Test ID	Pipe condition	D_{rini} (%)	σ_c (kPa)	e_{ini}
1	Toyoura_NP	Middle	73	50	0.757
2	Toyoura_P	Middle	72	50	0.761
3	Edosaki_NP	Middle	66	50	1.042
4	Edosaki _P	Middle	70	50	1.036
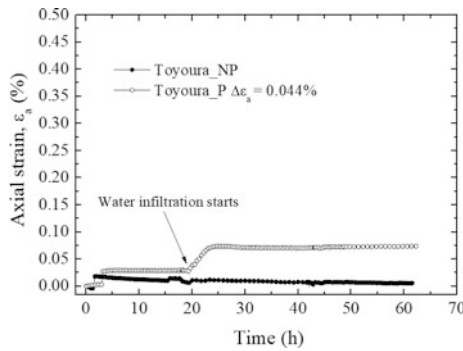
Fig. 5 Axial strain variation in Toyoura sand
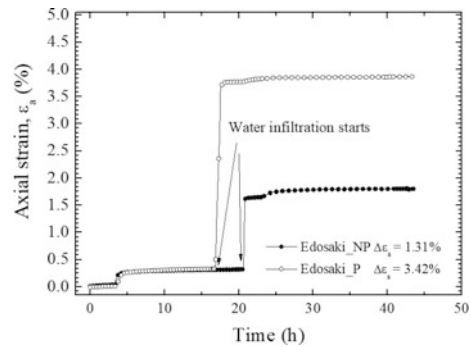
Fig. 6 Axial strain variation in Edosaki sand

3.2 Variation of Young's Modulus

In order to investigate the effect of particle dissolution during erosion on stiffness properties of sand, Young's modulus E was evaluated at the initial dry state (E_0), and after the water infiltration (E_1). E was calculated by Eq. 1, in which

$\Delta\sigma_a$ is the variation of axial stress, and $\Delta\varepsilon_{\text{axial}}$ refers to the variation of axial strain.

Figure 9 showed the calculation of E from the result of LDT before water infiltration in the case of Toyoura_NP, where the stress-strain curve during the 10th cycle was selected.
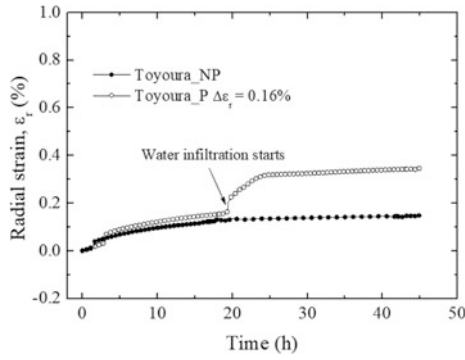
Fig. 7 Radial strain variation in Toyoura sand
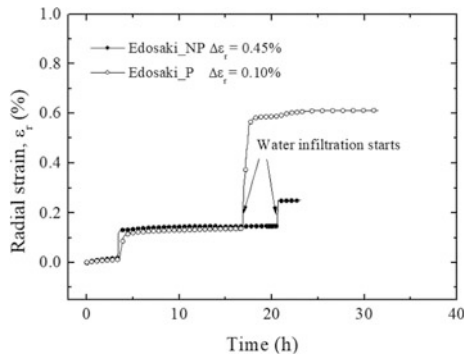
Fig. 8 Radial strain variation in Edosaki sand
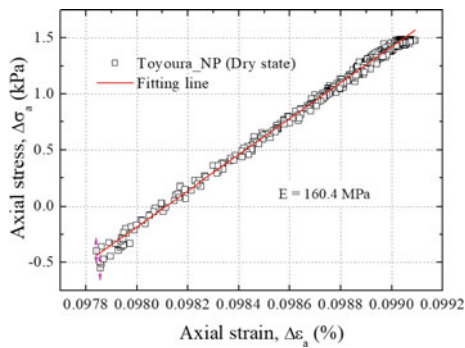
Fig. 9 Evaluation of E based on LDTs

$$E = \frac{\Delta\sigma_a}{\Delta\varepsilon_{axial}} \qquad (1)$$

Figure 10 presents the variations in the average Young's modulus for all the test cases, where open marks represent results for eroded samples and solid ones for intact specimens. It can be found that obvious reduction in E was induced after the dissolution of glucose. For non-eroded specimen, a small decrease in E was also observed. In cases of Toyoura sand, E_1 reduced by around 14.5% of the dry value, and a rather limited reduction of 5.8% was observed in case of eroded Edosaki sand.
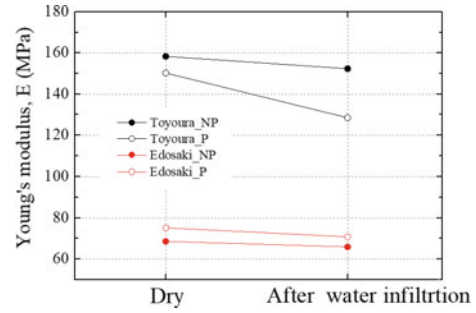

Fig. 10 Variation of E before/after glucose dissolution

3.3 Shear Strength

Figure 11 shows the stress-strain curves for all the test cases during the monotonic shearing. Although a large degree of variability of Young's modulus during piping erosion was confirmed in Toyoura sand, the limited erosion in the current study had no evident influence on either the peak or the residual shear strength. Since the glucose used in this experiment was rather limited (0.87% in volume proportion), it could be concluded that removal of particles in such a small amount and area had little impact on the overall strength of soil, which meant the force chains around the induced voids and the load-carrying structure might not be influenced. Another reason might be the disturbances caused by erosion diminished during shearing as continuous increase in the effective pressure would cause compression and clogging of those erosion-induced voids.

For Edosaki sand, fine particles were more likely to migrate or collapse into the eroded voids and refill them, leading to a fines-concentrated area with fewer voids inside. On the contrary, for Toyoura sand, the disturbance and loosening effect would propagate and thus more eroded voids were likely to be left. It was foreseeable that these interior voids would result in an unstable soil structure. Based on the current result, it was confirmed that such a small amount of dissolving particles was sufficient to trigger

Fig. 11 Stress-strain relationship during shearing for both intact specimens and eroded ones

significant degradation in small strain properties, especially in Toyoura sand. Therefore, small-strain parameters, which assess the specimen at particle level, are supposed to be more effective in detecting and quantifying the nonhomogeneous fabric changes associated with particle loss.

4   Conclusions

In this study, by introducing the water soluble material (glucose) into soil specimen, the effect of piping erosion was observed by infiltration and drainage. Detailed quantitative investigation on the deformation ch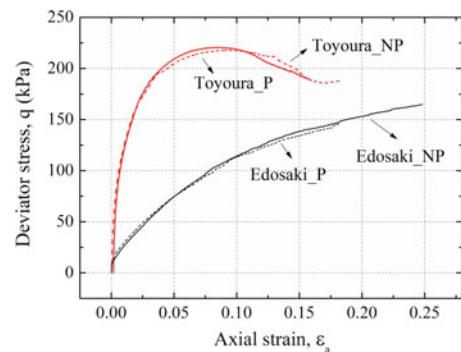aracteristics and mechanical properties of sandy soil subjected to piping was achieved through triaxial compression tests. As a first step to evaluate properties of soil subjected to particle loss, the glucose pipe in the current element specimen, to some extent, could be regarded as the loose sandy layer with high porosity and vulnerable to erosion. Although the artificial specimen sacrificed some accuracy in representing piping erosion in situ due to its special boundary condition, it could still provide beneficial insight into the microstructural behavior of soils containing soluble particles. Conclusions obtained from the present study are listed as follows.

1. Larger volumetric strains were observed in Edosaki sand due to the migration of fines and refilling of eroded voids.
2. Compared with intact specimen, Young's modulus tended to decrease for eroded specimen.
3. Dissolution of glucose pipe in Edosaki sand resulted in an area with concentrated fines; while for Toyoura sand, a more unstable structure was caused due to the presence of more interior voids.
4. Shear strength was not significantly influenced by the limited disturbance of piping effect, due possibly to the

continuously increasing pressure level during shearing and the end restrain effect of the top cap and the pedestal.

References

Acciardi, R.G.: Quantification of pinhole test equipment by hydraulic characteristics. U.S. Bureau of Reclamation, Denver, CO, Technical Report REC-ERC-82-15 (1982)

Benahmed, N., Bonelli, S.: Investigating concentrated leak erosion behaviour of cohesive soils by performing hole erosion test. Eur. J. Environ. Civil Eng. **16**(1), 43–58 (2012)

Foster, M.A., Fell, R., Spannangle, M.: The statistic of embankment dam failures and accidents. Can. Geotech. J. **37**(5), 100–124 (2000)

Hanson, G.J.: Cook. K.R.: Apparatus, test procedures, and analytical methods to measure soil erodibility in situ. ASAE Appl. Eng. Agric. **4**(20), 455–462 (2004)

Kenny, T.C., Lau., D.: Internal stability of granular filters. Can. Geotech. J. **22**, 215–225 (1985)

Kenny, T.C., Chahal, E., Chiu, E., Ofoegbu, G.I., Omange, G.N., Ume, C.A.: Controlling constriction sizes of granular filters. Can. Geotech. J. **22**, 32–43 (1985)

Sherard, J.L., Dunnigan, L.P., Decker, R.S., Steele, E.F.: Pinhole test for identifying dispersive soils. J. Geotech. Eng. Div. ASCE (GTI) **102**, 69–85 (1976)

Shin, H., Santamarina, J.C.: Mineral dissolution and the evolution of k_0. J. Geotech. Geoenviron. Eng. **134**(8), 1141–1147 (2009)

Truong, Q.H., Eom, Y.H., Lee, J.S.: Stiffness characteristics of soluble mixtures. Géotechnique **60**(4), 293–297 (2010)

Wan, C.F., Fell, R.: Investigation of rate of erosion of soils in embankment dams. J. Geotech. Geoenviron. Eng. **4**(30), 373–380 (2004)

An Electron Microscope Study of Biomineralisation for Geotechnical Engineering Purposes

Stephen Wilkinson and Adharsh Rajasekar

Abstract

Directed biomineralisation, or using microorganisms to cause the formation of minerals, has been proposed as an effective method for permeability reduction and ground improvement. Where the precipitated mineral is a carbonate, heavy metal carbonates (e.g. otavite, malachite/azurite, cerussite, smithsonite, clearcreekite) can form, locking in heavy metal contamination. Where calcium carbonate forms there is an additional benefit of a high pH which, due to the buffering effect, can greatly reduce the mobility of heavy metal ions. Seven bacteria obtained from the soil & landfill leachate environments in Suzhou China, were induced to precipitate calcium carbonate under laboratory conditions within a medium consisting of a calcium source, urea and nutrient broth in a conical flask. Trials within clean sand columns resulted in a permeability which was 1/5 of that of a non-microbial column in addition to relative increases in strength of X3-5. On this basis, it is suggested that some geotechnical works using biomineralisation may be achieved without requiring external sources bacteria. This may be achieved either by isolating and growing the bacteria for application in the ground, or where growth can be achieved, by stimulating the bacteria in situ. An electron microscope assessment of the mineral structures formed by the bacteria indicates that a variety of different crystal forms are generated by the biomineralisation process. Some crystal structures, especially the open crystal structures, are of less use for engineering purposes. This indicates that not all bacteria that can precipitate carbonates would be of use for achieving geotechnical aims.

S. Wilkinson (✉)
Department of Civil Engineering, University of Wolverhampton, Wolverhampton, WV1 1LY, UK
e-mail: S.Wilkinson4@wlv.ac.uk

A. Rajasekar
Nanjing University of Information Science and Technology-Reading Academy, 219 Ningliu road, Nanjing, 210044, Jiangsu, China

1 Introduction

Microbial Geotechnology is a field of study that has been steadily expanding over the last 15 years. With a growing global focus on sustainability in engineering, assessments have been made of the potential for utilising natural processes to achieve engineering goals. Microbial processes have received particular attention and success especially for structural applications (Qian et al. 2015).

One of the more popular microbial interventions in geotechnical engineering is microbially induced carbonate precipitation (MICP), and this process has been put forward for a wide range of geotechnical applications (Ivanov and Chu 2008). These include stabilising soil against liquefaction (retaining walls, embankments, dams, slopes), strengthening the ground (tunnelling, bearing capacity), preventing slope erosion, constructing permeability barriers for containment of contamination, controlling river erosion, to name a few possibilities.

The MICP process involves injecting the carbonate precipitating bacteria into a sand system, alongside a calcium source, urea and a nutrient broth (Fig. 1i). Variations in the concentration of components can produce differing results. Early experiments conducted by the authors, with low concentrations indicated the formation of carbonate bridging structures between particles (Fig. 1ii). The process ultimately results in a solidified sand structure (Fig. 1iii). The ultimate goals in using biomineralisation can be summarised as permeability reduction and/or ground improvement (Rajasekar et al. 2017a). MICP has been studied by a very wide range of authors (e.g. Harkes et al. 2010; Martinez et al. 2013; Neupane et al. 2013; DeJong et al. 2013;

Chu et al. 2014). Given that MICP is a biologically driven process whose main input materials are waste products, it has the potential to be a highly sustainable approach (Rajasekar et al. 2017b).

2 Experimental Methods

Biomineralising organisms were isolated (using the spread plate method, purified with repeated streaking) from samples of landfill leachate and groundwater obtained from a landfill in Suzhou, China (Fig. 2). The bacteria were grown in a biomineralising medium in order to preferentially select for organisms with a higher propensity towards biomineralisation. The isolated organisms were identified, and those that were hazardous (1 of 8), were destroyed. The following 7 organisms were retained for testing: *Bacillus licheniformis SZH2015_A, Bacillus pumilus szhxjlu2015, Bacillus sp. xjlu_herc15, Bacillus licheniformis adseedstjo15, Bacillus aerius rawirorabr15, Pseudomonas nitroreducens szh_asesj15* and *Sphingopyxis* sp. szh_adharsh. Initially, experiments were carried out by placing the 25 mM Calcium chloride, 333 mM Urea, nutrient broth and bacteria into a

conical flask which was then placed in a rotary shaker inside an incubator. Samples of this liquid were studied under the optical microscope in order to assess the crystals formed.

As outlined below, the results of the flask experiments implied that the identified micro-organisms were able to enhance the production of calcium carbonate. With some of the more successful bacteria, further experiments aimed at the cementation of sand columns were carried out. Sand was placed, without compaction, into a column made from a section of drain pipe, the base of which is an end cap with a tap installed at the base. The system was made watertight using mastic (based on the design of Harkes et al. 2010). The biomineralizing media was added into the column and replaced every 24 h during the experiment. The experiment continued for approximately 9 days. Following this, the permeability of the soil columns were calculated (in relation to a non-microbial blank column) based on the rate of downward flow of liquid placed in the top of each the column. Relative differences in strength were also measured using a pocket penetrometer (as an approximation). Finally, samples of the cemented material were transported to the, electron microscope imaging lab at Xi'an Jiaotong-Liverpool University, where microstructural images were
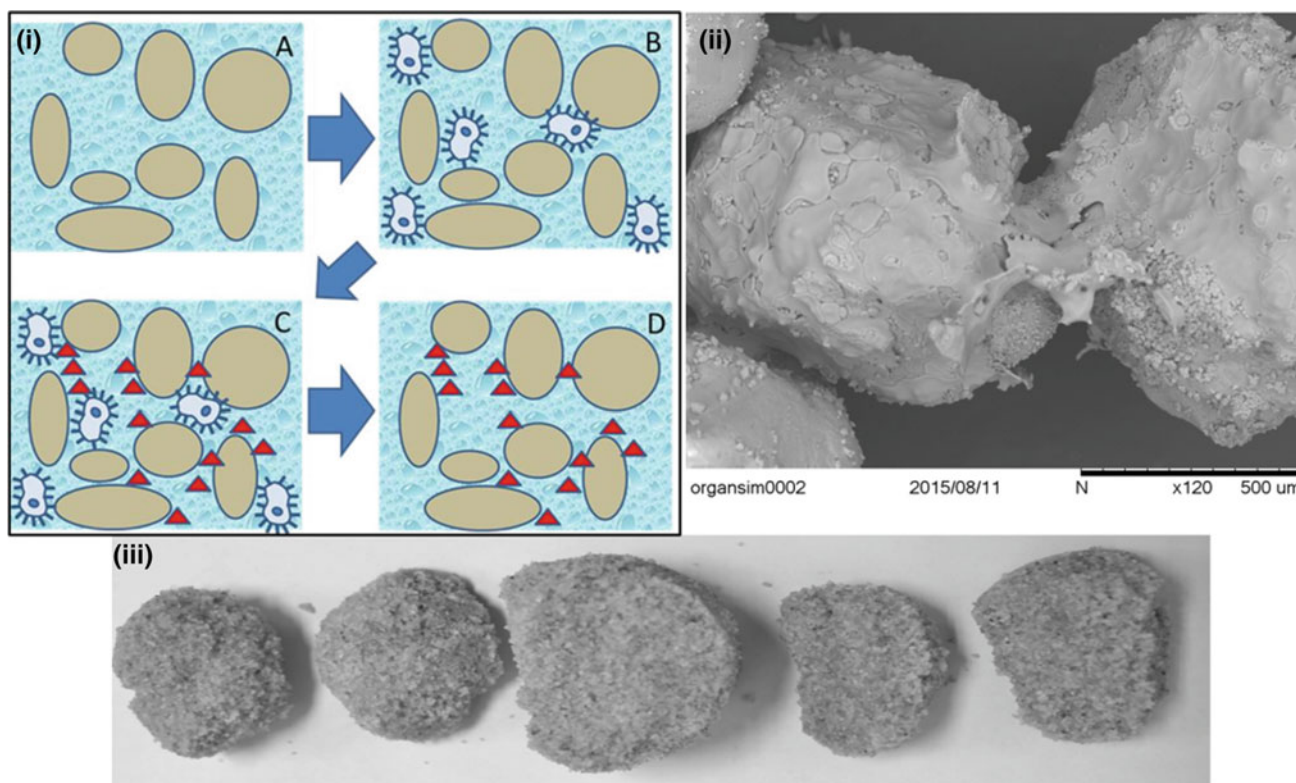
Fig. 1 The process for the biomineralisation of a soil specimen undertaken is summarised as: **i** The original soil is injected with a biomineralisation medium that contains bacteria, a calcium source, urea and nutrients. The bacterial generate the environmental conditions in which CaCO₃ can be deposited on the particle surfaces. The bacteria either die, are transported out of the system or are encased inside the minerals that they form. **ii** Early experiments with low concentrations of biomineralising fluids, showing the produced connections between particles. **iii** Broken sections from a biomineralised sand column sample, produced during this research project

Fig. 2 Approximate map showing the sampling location in relation to major local geographical features
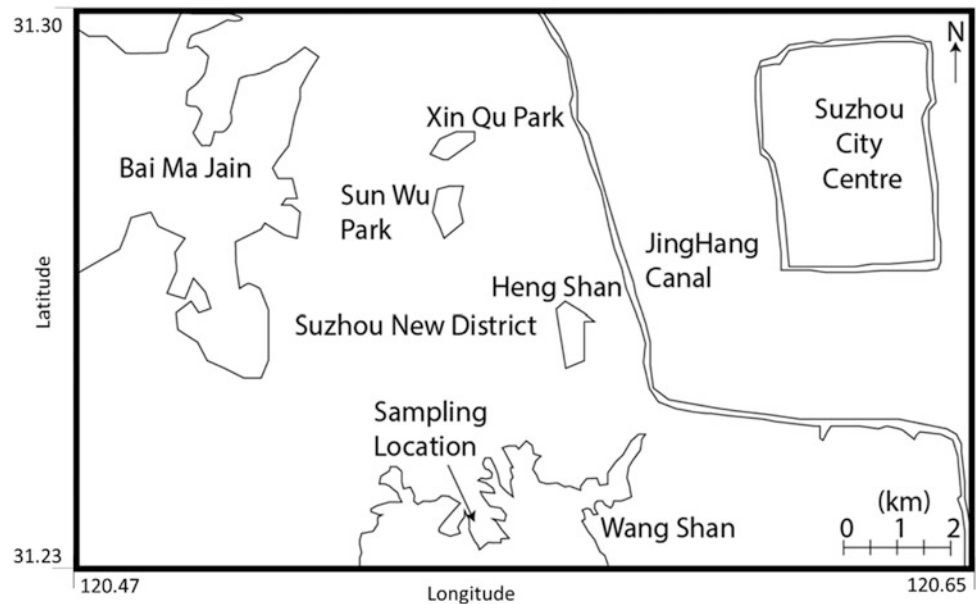
taken, in order to assess the distribution of cementation between the sand grains.

3 Results and Discussion

Due to drying, which causes supersaturation, calcium carbonate crystals could form in layers aligned to the glass slide (Fig. 3a). As a result, imaging of slides must occur rapidly. Typically, crystals formed due to biomineralisation take a more blocky form, often growing outwards from a central nucleation site (Fig. 3b). Note that the bright points in the image (Fig. 3b) were examined at a higher magnification and appeared to be the bacteria. Crystals were also observed being produced by *Bacillus licheniformis* adseedstjo15 (Fig. 3c). Due to their birefringence colour, they are thought to be calcite, which implies they have formed during the MICP process. They were however not observed in all samples and so are likely to be related to the particular organism. Other combinations of crystals were also observed (Fig. 3c).

The measured permeability was $\sim 5 \times 10^{-5}$ m/s for all of the microbial samples, the non-microbial sample being 5 times higher at 2.5×10^{-4} m/s. The strength of the samples varied from approximately 150–250 kPa (UCS) in comparison to ~ 50 kPa for the non-microbial sample. Thus the UCS was improved by a factor of 3–5X.

Early experiments were carried out to assess the effects of drying of the biomineralising fluid on the sand grains. In the same way as in the optical microscope (Fig. 3a) the drying process within the electron microscope resulted in a supersaturation of the fluid causing the formation of skeletal calcium carbonate crystals (Fig. 4a). Experiments with different organisms generated variations in the size and distribution of calcium carbonate crystals (Fig. 4). The size of the holes between particles is important for determining the resulting reduction in permeability that is achieved by the biomineralisation process. Generating an even groundmass between particles (Fig. 4b) is useful as this will generate an even reduction in permeability across the soil. Increases in strength are generated through the formation of bridging crystals between particles (Fig. 4c) which allow the transfer of stress through the soil. For some of the microbial samples, nucleation of crystals appears to be concentrated around grain contacts, which allows cementing borings to form, but may allow the more open spaces between particles to remain open, reducing the impact on permeability. In cases where the crystals formed by the organisms are large (Fig. 4d), the gaps between the crystals may also be large, enhancing this potential effect.

4 Conclusions

Experimentation with biomineralisation has resulted in the identifications of several potential applications within geotechnical engineering. The utilisation of locally sourced bacteria presents a potentially beneficial approach, as such bacteria are naturally present in the environment. Production of carbonate crystals within the abiotic media was found to be possible due to drying or through the natural hydrolysis of urea (which occurs much more slowly than in the presence of the bacterial enzyme urease). Note that calcium carbonate crystals can also form in a fluid rich in calcium due to the presence of atmospheric CO_2. The extent of biomineralisation and the distribution of the products of biomineralisation varied with each organism. However, all
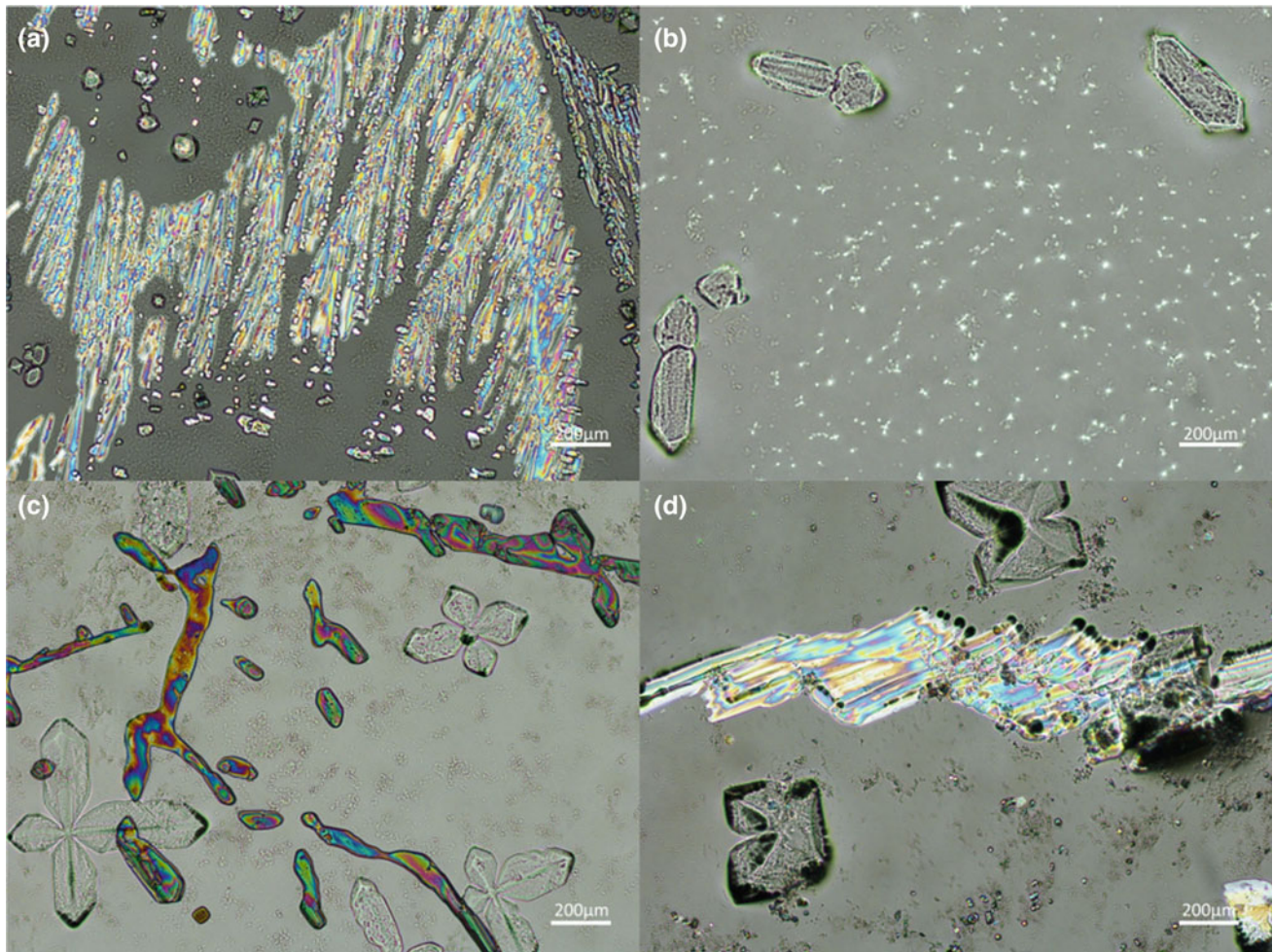
Fig. 3 Optical microscopic analysis of the final biomineralisation media, images are at $\times100$ magnification, imaged in cross polarised light. **a** Sample of calcite crystalisation caused by evaporation; **b** crystals generated due to biomineralisation; **c** & **d** combinations of different types of crystals, coloured crystals in (**c**) are thought to be related to the micro-organisms, but are of unknown origin

produced a good enhancement in the cementing of the soil. The results indicate that within a soil bacteria with the potential to allow biomineralisation to some extent may be present. Coarse scale regional mapping of the presence or absence of geotechnically beneficial bacteria, would allow the use of in situ bacteria to be applied with excessive prior investigation, allowing this more sustainable technique to be appropriately and more readily applied.
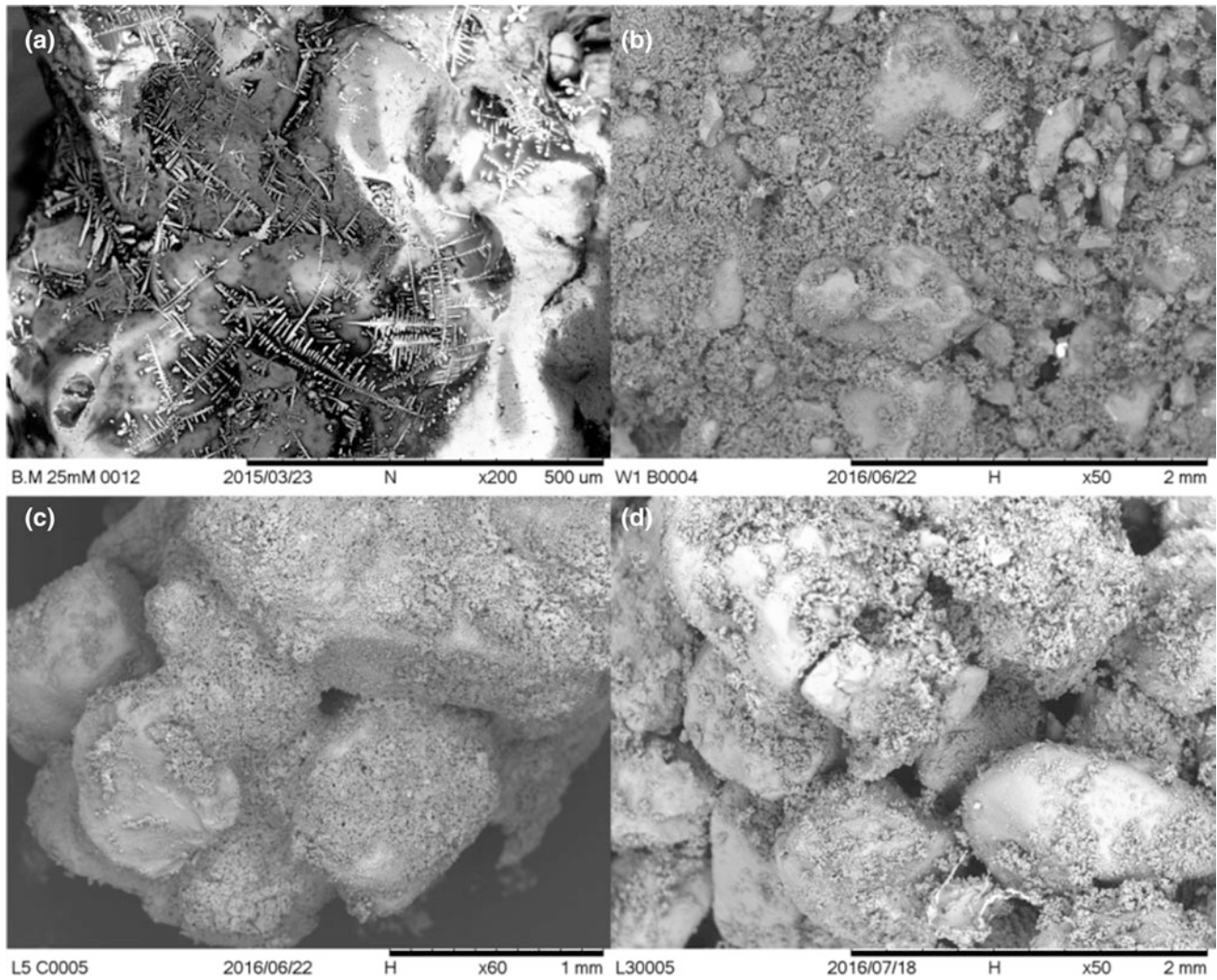
Fig. 4 Scanning Electron Microscope (SEM) images of sand samples (**a**) supersaturation during drying causing the rapid formation of skeletal calcium carbonate crystals. **b**, **c**, & **d** all show cemented particles generated by different organisms. **b** Groundmass of crystals formed between particles, a few larger quartz sand grains are visible. **c** Cluster of grains held together by MICP generated calcium carbonate crystals, some large voids between particles are present. **d** Larger, but more well-spaced crystals are formed, the surface of some particles are visible and larger gaps can be seen between particles

References

Chu, J., Ivanov, V., Naeimi, M., Stabnikov, V., Liu, H.L.: Optimization of calcium-based bioclogging and biocementation of sand. Acta Geotech. **9**, 277–285 (2014)

DeJong, J.T., Soga, K., Kavazanjian, E., Burns, S., Van Paassen, L.A., Al Qabany, A., Aydilek, A., Bang, S.S., Burbank, M., Caslake, L. F., Chen, C.Y., Cheng, X., Chu, J., Ciurli, S., Esnault-filet, A., Fauriel, S., Hamdan, N., Hata, T., Inagaki, Y., Jefferis, S., Kuo, M., Laloui, L., Larrahondo, J., Manning, D.A.C., Martinez, B., Montoya, B.M., Nelson, D.C., Palomino, A., Renforth, P., Santamarina, J.C., Seagren, E.A., Tanyu, B., Tsesarsky, M., Weaver, T.: Biogeochemical processes and geotechnical applications: progress, opportunities and challenges. Géotechnique **63**(4), 287–301 (2013)

Harkes, M.P., van Paassen, L.A., Booster, J.L., Whiffin, V.S., van Loosdrecht, M.C.M.: Fixation and distribution of bacterial activity in sand to induce carbonate precipitation for ground reinforcement. Ecol. Eng. **36**(2), 112–117 (2010)

Ivanov, V., Chu, J.: Applications of microorganisms to geotechnical engineering for bioclogging and biocementation of soil in situ. Rev. Environ. Sci. Bio/Technol. **7**(2), 139–153 (2008)

Martinez, B.C., DeJong, J.T., Ginn, T.R., Montoya, B.M., Barkouki, T.H., Hunt, C., Tanyu, B., Major, D.: Experimental optimization of microbial-induced carbonate precipitation for soil improvement. J. Geotech. Geoenviron. Eng. **139**(4), 587–598 (2013)

Neupane, D., Yasuhara, H., Kinoshita, N., Unno, T.: Applicability of enzymatic calcium carbonate precipitation as a soil-strengthening technique. J. Geotech. Geoenviron. Eng. **139**(12), 2201–2211 (2013)

Qian, X.Y., Zhang, Q., Wilkinson, S., Achal, V.: Cleaning of historic monuments: looking beyond the conventional approach? J. Clean. Prod. **101**, 180–181 (2015)

Rajasekar, A., Moy, C.K.S., Wilkinson, S.: Stimulation of indigenous carbonate precipitating bacteria for ground improvement. IOP Conf. Ser. Earth Environ. Sci. **68**(1), 012010 (2017a)

Rajasekar, A., Moy, C.K.S., Wilkinson, S.: MICP and advances towards eco-friendly and economical applications. IOP Conf. Ser. Earth Environ. Sci. **78**(1), 012016 (2017b)

An Assessment of Particle Characteristics for the Analysis of Wind Turbulence Generated Gas Transport

Stephen Wilkinson and Alireza Pourbakhtiar

Abstract

Gas flow through porous media is an important process for engineers to assess as a part of the design process. It can be modelled physically and numerically. Hazardous gases ranging from flammable vapours to radioactive gases can migrate through soil and are a concern on contaminated sites. Wind turbulence, which can be caused by the presence of man-made structures, can generate 20–70 times the amount of gas dispersion compared to calm conditions. The extent and rate of gas flow through a soil medium is dependent on the properties of the soil, including particle characteristics and the boundary conditions of the soil which includes flow rate and turbulence (gustiness). Such boundary effects may be strongly influenced by local site conditions. The important particle characteristics for gas flow through soils include primarily particle size, with minor contributions from shape and roughness. Many standardised methods for particle size measurement assume that the particles are spherical and so become much less accurate for elongate and irregular particles. Imaging techniques in combination with computational analysis allow more accurate quantification. An analysis of particle shape in two and three dimensions has been undertaken allowing the measurement of particle size and roughness. This can be used to inform models of soil behaviour. The data from this analysis includes roughness measurements from 453 particles. This data is available on request.

S. Wilkinson (✉)
Department of Civil Engineering, University of Wolverhampton, Wolverhampton, WV1 1LY, UK
e-mail: S.Wilkinson4@wlv.ac.uk

A. Pourbakhtiar
School of Engineering Sciences, University of Liverpool, Liverpool, L69 3BX, UK

1 Introduction

Gases present within soils interact with engineering structure. In environments where the gas is hazardous this interaction is undesirable, for example where the gas is radon (Wang and Ward 2002) landfill gas (Poulsen et al. 2006) or methane (Topp and Pattey 1997). Gas flow can occur due to molecular diffusion or when a pressure gradient exists. The effect of pressure variations on the ground surface caused by gustiness, or air turbulence, on gas flow has received less attention. An experimental apparatus to assess the impacts of surface gas flow on vertical gas transport in porous media was designed (Fig. 1). This apparatus measures the concentration of oxygen (which is released at a constant rate at the base of the column) as it changes through the column of soil given different wind speeds/conditions. Sensors were placed in different locations around the interior of the column to account for localized effects. Overall for a coarse granular porous media dispersions of up to seventy times those of calm conditions were observed (Pourbakhtiar et al. 2017).

2 Particle Analysis

Initial assessments were carried out using white quartz gravel. These particles were assessed to isolate the parameters which are the most important in determining the effects of surface wind turbulence. The process for the automated measurement of particles (Tang et al. 2017) involves initial selection of the particles to be assessed based on image parameters (saturation, hue, brightness). Ideally the original imaging conditions are set for easy partition. The gravel was placed on a scanner bed, and the top surface of the scanner was covered with a piece of black paper. This produced the best contrast between the particles and the surrounding medium (Fig. 2). With the resulting image, the particles could be easily separated on the basis of brightness or

Fig. 1 Diagram of the experimental set-up showing section and plan views and key elements of the measurement and data collection system, modified from Pourbakhtiar et al. (2017). Units are in centimetres, gasses enter the column from the base. Oxygen sensors are located in different areas of the sol column (see plan view and section)
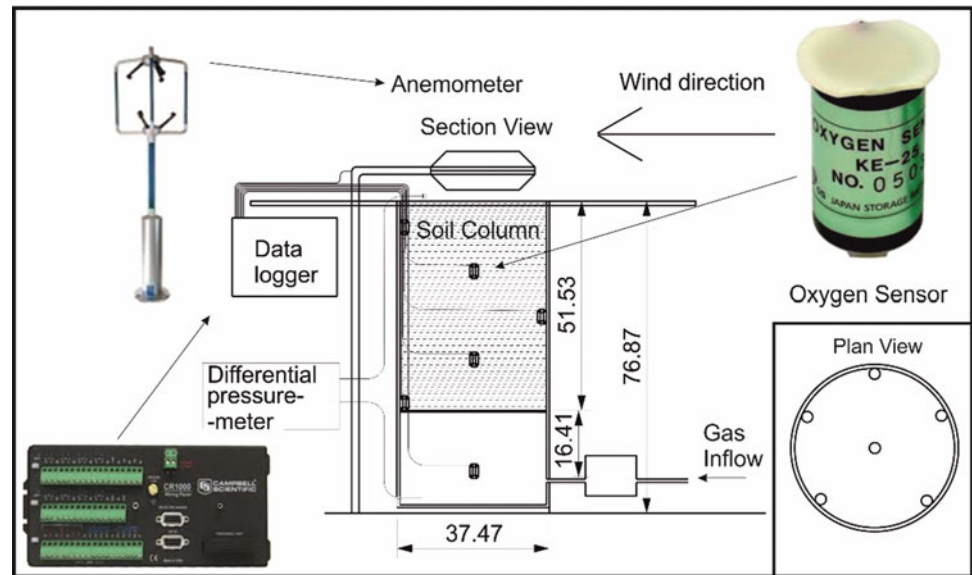
colour. This generates a binary image from which measurements can be made (Fig. 2). The images are then reviewed for errors (e.g. combined particles) and these can be removed from the data prior to analysis. At this scale, the major measurements that can be made are of particle scale characteristics. These relate to particle size (area, perimeter), particle shape (circularity, ferret lengths, aspect ratio, roundness) and presence absence of holes (solidity). Averages of these values for the populations shown in Fig. 2 are presented (Table 1).

In a two dimensional image only a single cross-section of a particle is measured. For particles with one axis shorter than the others, the measurements may be biased by the way the particles naturally lay on the scanner. However for reasonably spherical particles this provides a quick and easy method for quantification.

Through empirical, observational studies, it has been established for over 100 years that there is a relationship between particle size parameters and gas flow, e.g. Hazen's formula (Hazen 1911). The relationship between other

Fig. 2 Left, a scanned image of gravel particles. Black paper was affixed to the scanner top to increase the contrast. Right, auto-identification of particles using a binary threshold program prior to analysis. An example of a combined particle error is identified. The binary figure was generated for this project using Image
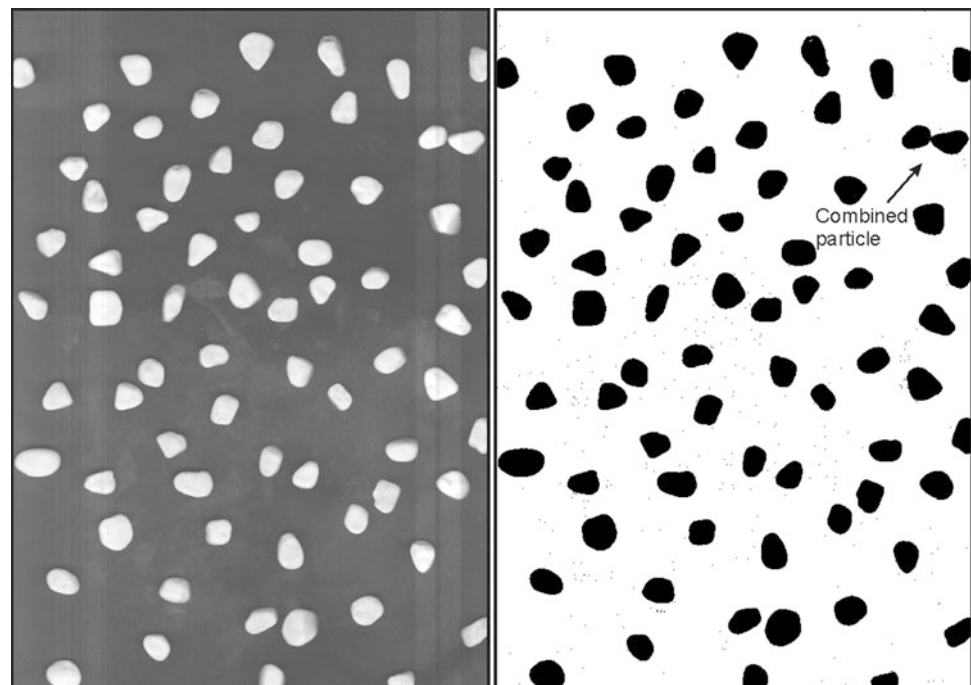
Table 1 Example: average measurements from the analysis of the particles shown in Fig. 2

Number of particles	Area (cm²)	Perimeter	Circularity	Maximum Feret dimension	Minimum feret dimension	Aspect ratio	Roundness	Solidity
60	0.184	2.037	0.563	0.566	0.428	1.317	0.774	0.978

particle parameters and flow is much less dominant, and difficult to measure. The key impact of variations in particle shape is to create variations in packing and openness of the voids (hence influencing the void ratio). Roughness has been shown to influence flow (Natrajan and Christensen 2010), by altering laminar to turbulent flow. Within the interstices of a soil the gas flow will arguably already be turbulent, and so the real effects of roughness are unclear.

The roughness of 453 particles across 5 grain sizes were quantified as a part of the Xian Jiaotong-Liverpool University (XJTLU) surface roughness project carried out by the authors. This project created a library of particle roughness measurements for the standard construction sand used for a wide range of research projects. Each individual particle is imaged using an optical microscope with a stepping motor (Fig. 3).

By identifying the in focus pixels at different focal lengths in a series of microscope images a height map can be generated for the surface of the particles. By comparing the height of pixels with the heights of their immediate neighbours, gradient maps (Fig. 3a) and aspect maps (Fig. 3b) were generated. This allows a visual assessment and categorisation of any large scale roughness features prior to measurement. Precise measurements of the roughness of
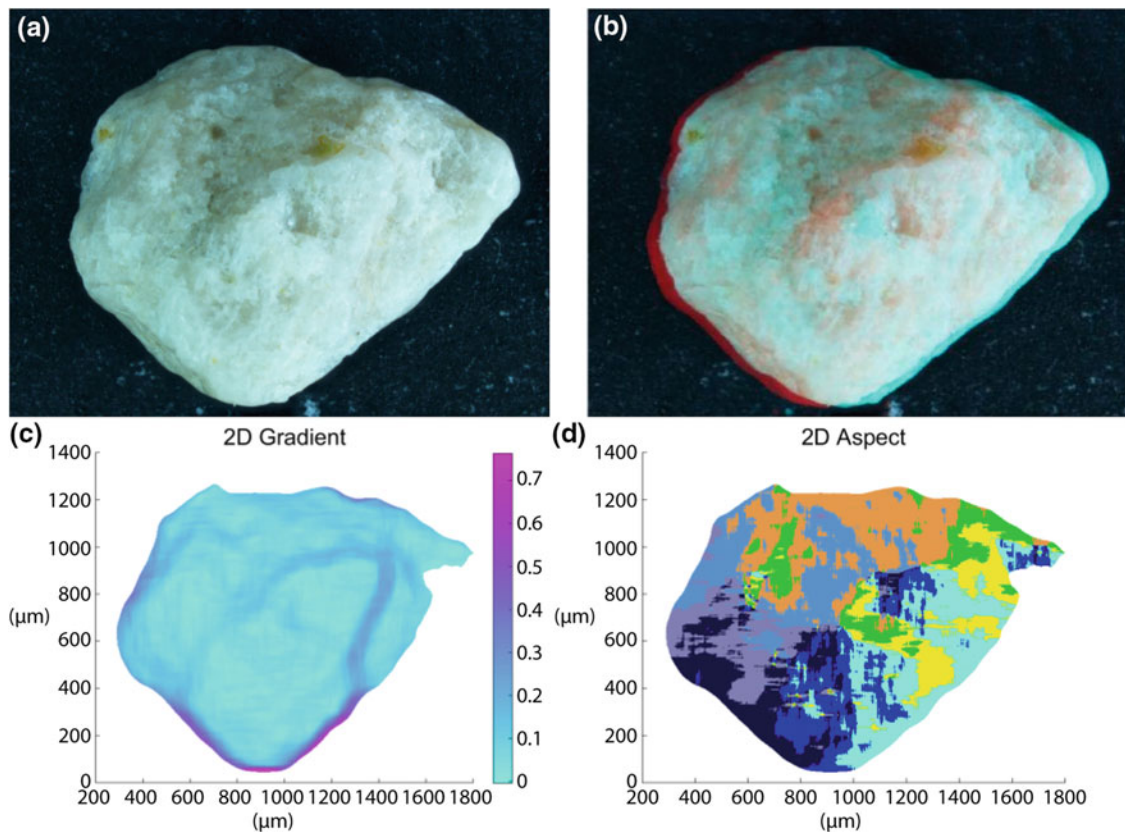
Fig. 3 Sample 3D analysis of a single grain of sand. **a** image of the surface of the sand grain taken in the optical microscope. **b** 3D surface view of the sand grain using a red cyan filter. **c** Gradient map of the surface of the sand grain. **d** Aspect map of the surface of the sand grain

particles were made from the surface measurements. The standard roughness measurements are outlined in the following equations:

$$R_a = \frac{1}{n} \sum_{i=1}^{n} |y_i| \tag{1}$$

where R_a is the mean deviation, n is the total number of pixels in each line and y_i is the residual between the datum and the particle surface

$$R_q = \sqrt{\frac{1}{n} \sum_{i=1}^{n} y_i^2} \tag{2}$$

R_q being the root mean squared

$$R_v = \min y_i \tag{3}$$

$$R_p = \max y_i \tag{4}$$

R_v being the max valley depth and R_p being the max peak height, both measured as differences from the datum

$$R_t = R_p - R_v \tag{5}$$

R_t is the max height profile

$$R_{sk} = \frac{1}{nR_q^3} \sum_{i=1}^{n} y_i^3 \tag{6}$$

$$R_{ku} = \frac{1}{nR_q^4} \sum_{i=1}^{n} y_i^4 \tag{7}$$

R_{sk} and R_{ku} being skewness and kutosis respectively.

For these roughness measurements, the selection of a datum (reference plane) is important. A best fit parabola was used as the datum for roughness measurements in this work (Fig. 4). Several other reference plane options, such as circular or locally smoothed (Gaussian filter), are available alternatives. However, as long as the same approach to the reference plane is used; valid comparisons can be made between particles and with their application in soils. The roughness measurements for the sample particle are shown (Fig. 4). The complete particle library (453 particles) is available on request.

In bulk the measured roughness parameter can be related to rates of gas flow. However due to the dominant effect of particle size on the results a large number of different

Ra	Rq	Rv	Rp	Rt	Rsk	Rku
40.3803	2.2221e+03	-107.1868	94.3318	201.5185	4.9265e-07	4.0426e-07
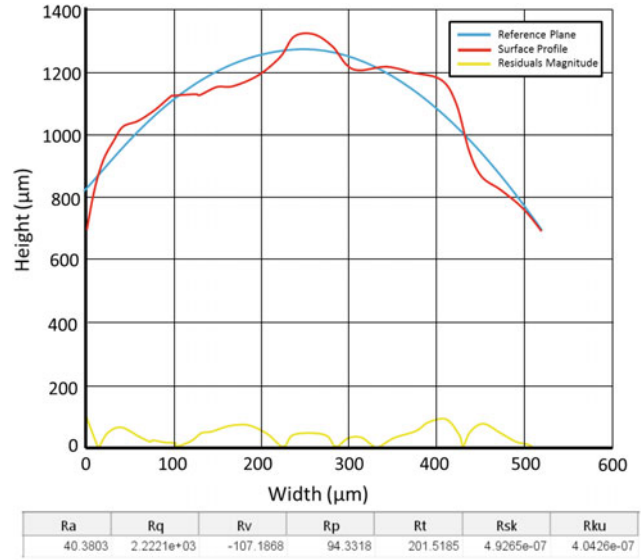
Fig. 4 Measurement of the roughness of the midplane of the surface of the sand grain shown in Fig. 3. Only the top of the particle is shown, all values are in micrometre. In this approach the reference plan used is the best fit parabola. The magnitude of residuals is shown. The measurements of different types of roughness based on these residuals from left to right are: mean deviation (R_a), root mean squared (R_q), max valley depth (R_v), max peak height(R_p), max height profile(R_t), skewness (R_{sk}) and kutosis (R_{ku})

samples with different properties need to be analysed to identify the significance of the effect of particle roughness, this research is ongoing.

3 Conclusions

Measurements of gas flow within a soil column have shown that wind turbulence can have a significant effect on the amount of gas that flows through the column. The amount of gas flow is also a function of the particle characteristics of the soil. The most dominant of these measurements, at least for coarse particles, on gas flow is particle size. The effect of shape and roughness on gas flow is far more difficult to quantify as it requires measurements with multiple soils with different characteristics. This paper provides details of the automated measurement of particle characteristics including shape and roughness for large numbers of particles. The use of binary images for 2D characterisation is an important tool

for automated measurement. For 3D surfaces there are many options for the selection of a reference plane to make roughness measurements. The use of a parabola as a datum in this work highlights the wide range of possibilities.

References

Hazen, A.: Discussion: dams on sand foundations. Trans. Am. Soc. Civ. Eng. **73**, 199 (1911)

Natrajan, V.K., Christensen, K.T.: The impact of surface roughness on flow through a rectangular microchannel from the laminar to turbulent regimes. Microfluid. Nanofluid. **9**(1), 95–121 (2010)

Poulsen, T.G., Moldrup, P., Yoshikawa, S., Komatsu, T.: Bimodal probability law model for unified description of water retention, air and water permeability, and gas diffusivity in variably saturated soil. Vadose Zone J. **5**, 1119–1128 (2006)

Pourbakhtiar, A., Poulsen, T.G., Wilkinson, S., Bridge, J.W.: Effect of wind turbulence on gas transport in porous media: experimental method and preliminary results. Eur. J. Soil Sci. **68**, 48–56 (2017)

Tang, K., Wilkinson, S., Beattie, G.: Effects of curing temperature on the hydration of GGBS concrete and the use of electron microscope particle analysis. Adv. Cem. Res. **29**(8), 322–335 (2017)

Topp, E., Pattey, E.: Soils as sources and sinks for atmospheric methane. Can. J. Soil Sci. **77**, 167–178 (1997)

Wang, F., Ward, I.C.: Radon entry, migration and reduction in houses with cellars. Build. Environ. **37**, 1153–1165 (2002)

Beneath the Sands: A Glimpse of Engineering Geological Conditions of Dubai, UAE

Luke Bernhard Brouwers

Abstract

Recent large-scale civil infrastructure developments in Dubai have led to the completion of remarkable engineering feats. These achievements are only matched by the aspirations of future projects, which continue to push the boundaries of engineering by seeking bigger, stronger and deeper developments while simultaneously being more economical. However, future ground development in Dubai faces unique challenges and information currently available to assist engineers in solving these problems is limited. To combat this, this paper presents results from 87 boreholes drilled throughout Dubai. The general lithographic sequence comprises of Quarternary Aeolian sand deposits overlying the thinly bedded calcareous sandstones of the Ghayathi Formation underlain by interbedded conglomerates and siltstones of the Barzaman Formation before encountering the thinly bedded claystones of the Gachsaran Formation. Laboratory results show that 90% of all unconfined compressive strength (UCS) results classify as very weak or weaker with an overall average UCS value and elastic modulus of 2.24 and 2058 MPa, respectively. The average bulk and dry densities are 1960 and 1630 kg/m³, respectively, with an average moisture content of 19%. Discussion of the laboratory results illustrates some engineering geology challenges currently being faced in site investigations for Dubai and identify the important role engineering geologists and geotechnical engineers play in ensuring that suitable site investigation methods and techniques are performed correctly to ensure that an accurate and thorough understanding of subsurface conditions is obtained to minimize the associated risk of development.

1 Introduction

The ever increasing and demanding civil infrastructure development within Dubai and the United Arab Emirates provide engineering geologists and geotechnical engineers' with unique hazards and challenges. Information available to combat these hazards and challenges is however sorely lacking despite being of paramount importance in pushing the boundaries of engineering for future aspiring projects. This paper attempts to illustrate some of the challenges currently being faced in Dubai and it is hoped that more collaboration and research is inspired from this paper.

1.1 Regional Setting

The Arabian Gulf is a shallow elongated basin of Late Pliocene to Early Pleistocene age and currently has water depths rarely exceeding 100 m. The basin is asymmetric, with a gentle slope on the Arabian side and a much steeper slope on the Iranian side. The basin is bound on the northwest and along the Iranian side by the Zagros mountain belt, which is the central part of the Alpine-Himalayan chain. During the late Cretaceous, a large compressive event caused the obduction of the Oman-UAE ophiolite on the eastern continental margin of the Arabian platform (Macklin et al. 2012). Eustatic fluctuations of sea level during the Quaternary, related to climate variations, resulted in shifting shorelines along the relatively flat Arabian Gulf (Al-Sayari and Zötl 2012).

During Pleistocene glaciations, global sea level was 100–120 m below the present level and resulted in most of the Arabian Gulf occurring as a dry basin (Purser 1973;

L. B. Brouwers (✉)
Fugro Middle East, Al Quoz Industrial Area, 2863 Dubai, United Arab Emirates
e-mail: l.brouwers@fugro.com

Gunatilaka 1986), except for a restricted area around the Straits of Hormuz (Kirkham 1998). Surface sediments exposed during this period experienced desiccation, oxidation and over-consolidation of silt and clays while evaporation of sea-water in shallow restricted basins (sabkhas) led to hypersaline conditions and deposition of evaporites. Alluvial plains, formed from the Tigris and Euphrates rivers that incised the exposed topography (Gunatilaka 1986), were a major source of aeolian siliciclastic sediment that was later blown south-eastwards by the Pleistocene Shamal winds (Glennie 1998).

Since late Pleistocene to early Holocene times, the sea level rose gradually until a maximum sea level stand 1.6–2.5 m higher than today (Gunatilaka 1986). Due to the gentle slope of the gulf on the Arabian side, a shallow marine environment with little sediment influx from the arid mainland resulted in sediments with biogenic origin and high carbonate content consisting of relatively pure carbonate clay, silt and sand that are generally unconsolidated. The Gulf then experienced the interaction of three equally important depositional systems throughout Pleistocene-Holocene time, namely, the Arabian Gulf marine carbonate system, the Mesopotamian fluvio-deltaic system, and the Arabian continental aeolian system (Walkden and Williams 1998; Williams and Walkden 2002).

1.2 Dubai Geology

A generalised overview of the Arab peninsular and stratigraphy of geology in Dubai is presented in Fig. 1. The near surface geology of coastal Dubai begins with Quaternary marine, aeolian, sabkha and fluvial deposits overlying variably cemented Pleistocene calcareous sandstone and cemented sand deposits of the Ghayathi Formation; where small changes in sea level during this period exposed the sand layers to the atmosphere leading to evaporation and chemical carbonate cementation (Williams and Walkden 2002).

Below this, is a thick succession of fluvial sediments characterized by poorly sorted conglomerates and interbedded calcisiltites belonging to the Barzaman Formation probably formed during the middle Miocene to Pliocene age (Styles et al. 2006). Uplift and erosion of the Oman mountains during this time resulted in coarse-grained sediments being deposited in wadi channels and outwash plains during wet periods; during the intervening dry season, high evaporation rates and capillary rise of dissolved carbonates resulted in variable cementation of these sediments (Macklin et al. 2012). These conglomerates are dominated by clasts of harzburgite, chert and limestone while the carbonate cement

is now composed predominately of dolomite with minor calcite and substantial portions of the clay mineral palygorskite.

Underlying the Barzaman Formation is a small component of the Fars Group also known as the Gachsaran Formation. The Gachsaran Formation is dominantly composed of thinly to thickly interbedded brownish to greenish grey siltstone and claystone (Macklin et al. 2012) with high gypsum content and thin to thick beds of gypsum also present.

1.3 Borehole Selection

A large number of boreholes have been drilled throughout the Dubai region (FME 2017). However, selection for further analysis in this paper was limited to boreholes that satisfied the following criteria:

(1) Minimum borehole depth of 40 m;
(2) Borehole groupings with small geographical clustering to be representative of ground conditions;
(3) Borehole logs containing detailed and full core descriptions (i.e. description of geological formations);
(4) Multiple laboratory results present within each borehole for a range of laboratory tests; and
(5) Author involved in the project(s).

2 Results

2.1 Overview

In total 87 boreholes satisfied the selection criteria drilled in 2016 and 2017, with core being recovered in plastic liners with guar gum drilling fluid. From the recovered core, the results for 506 uniaxial compressive strength (UCS) and 233 UCS local strain measurement laboratory tests following the ASTM D7012 standard were compiled, filtered and separated into the corresponding lithologies and geological formations. Further analysis of this separation is presented later in this paper. Figure 2 shows a histogram for the UCS results for all 739 samples and following the British standards 5930:2015, 24% of the results occur below 0.6 MPa (i.e. soil), while 11% classify as extremely weak rock, 55% classify as very weak rock and 10% classify as weak rock. Overall, for all laboratory results, the average UCS value and elastic modulus is 2.24 and 2058 MPa respectively. The average bulk and dry densities are 1960 and 1630 kg/m^3 respectively, with an average moisture content of 19%.
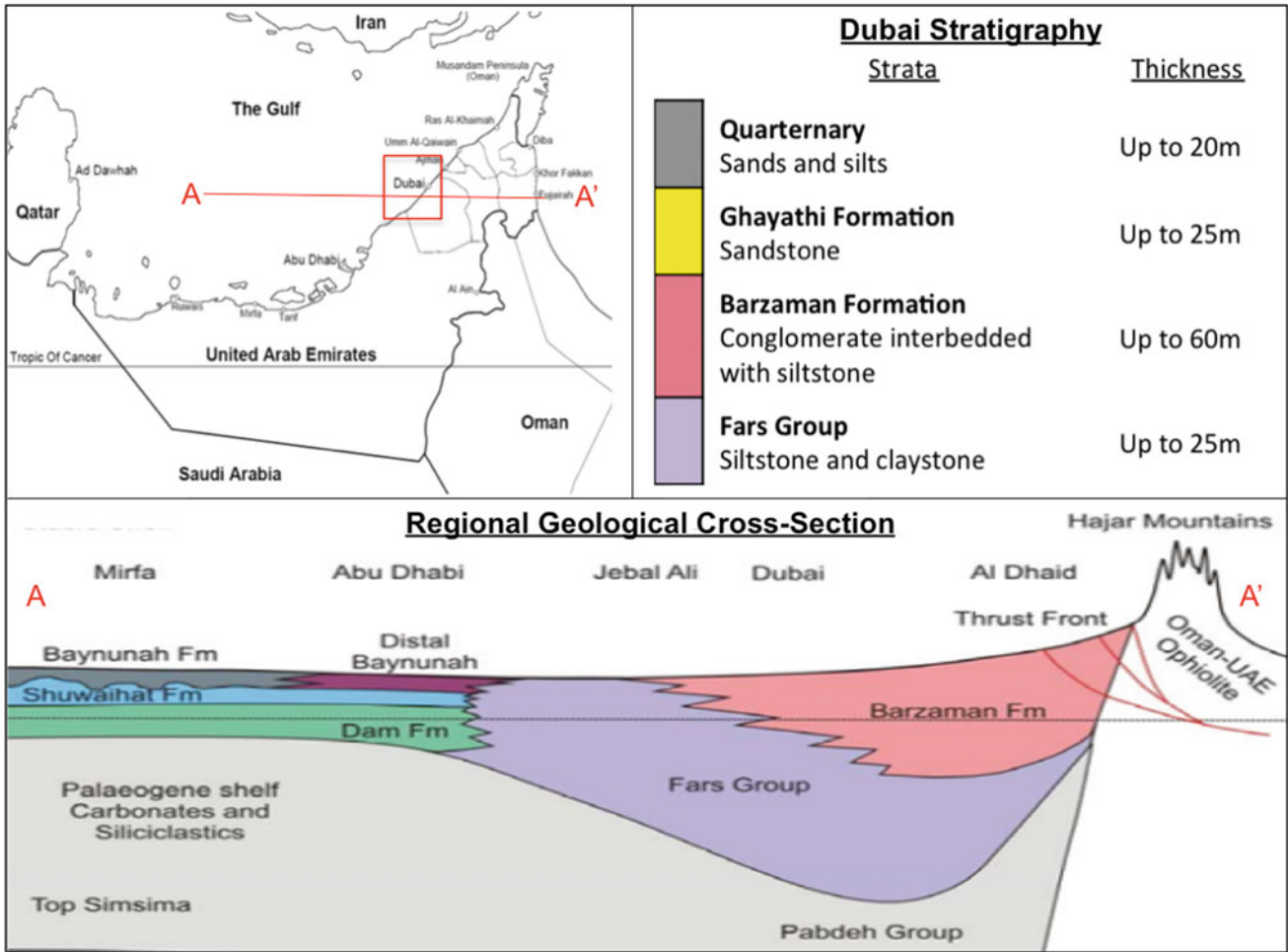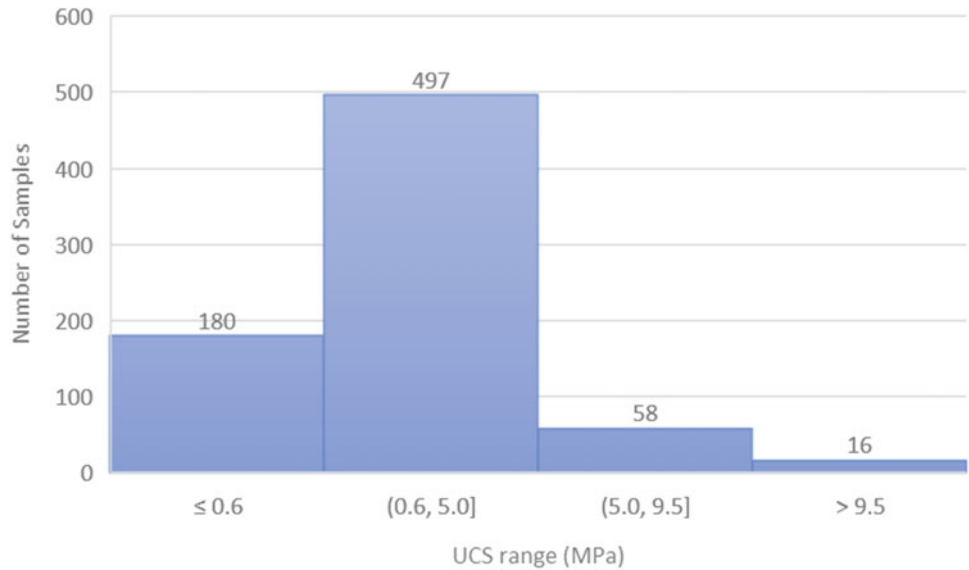
Fig. 1 Generalised overview of Dubai stratigraphy (after Macklin et al. 2012)

Fig. 2 Histogram for all UCS results

2.2 Ghayathi Formation

Samples of the Ghayathi Formation occurred in 73 boreholes with 256 UCS, 133 UCS local strain measurement and additional 40 direct shearbox tests performed. A summary of the laboratory results is presented in Table 1. Generally the Ghayathi Formation was described as: *extremely weak to very weak, light yellowish brown, fine to medium grained, highly calcareous sandstone. Partially (slightly) weathered.*

The UCS values were generally independent of moisture content. From the UCS values, 37% of the samples returned strengths less than 0.6 MPa (i.e. soil) while 13%, 45% and 5% are classified as extremely weak, very weak and weak rock respectively. The average elastic modulus determined for the Ghayathi Formation sandstones was 1987 MPa. There was moderate amount of scatter in elastic modulus values, as seen in Fig. 3, however a correlation factor of $E = 1116.7 \times UCS$ with R^2 value of 0.44 can be empirically used.

2.3 Barzaman Formation

Samples of the Barzaman Formation occurred in 41 boreholes and described as three lithologies, namely siltstone/calcisiltite, conglomerate and claystone/calcilutite. A total of 67 UCS and 26 UCS local strain measurement tests were performed on siltstone samples, 91 UCS and 33 UCS local strain measurement tests were performed on conglomerate samples and 3 UCS tests were performed on claystone samples. A summary of the laboratory results is presented in Table 2. Generally the siltstone layers was described as: *very weak, off-white to light yellowish brown mottled greyish green, siltstone/calcisiltite, partially (slightly) weathered*; and the conglomerate layers described as: *very weak, light to dark brown mottled multi-coloured, matrix dominated, polymitic conglomerate. Partially (slightly) weathered, matrix of silt and sand, clasts are, sub-angular to sub-rounded, medium to coarse gravel of different lithologies.*

The UCS values were generally independent of moisture content. From the UCS values, 14% of the siltstone samples, 11% of the conglomerate samples and 100% of the claystone samples returned strengths less than 0.6 MPa (i.e. soil). Additionally 10%, 57% and 19% of the siltstone samples classify as extremely weak, very weak and weak rock respectively; and 11%, 67% and 11% of the conglomerate samples follow the same classification. The average elastic modulus determined for the siltstone and conglomerate was 2029 and 1600 MPa respectively. There was moderate amount of scatter in elastic modulus values for both lithologies, as seen in Fig. 4, however a correlation factor of $E_{(siltstone)} = 537.49 \times UCS$ with a R^2 value of 0.33 can be empirically used for siltstone and a correlation factor of $E_{(conglomerate)} = 568.39 \times UCS$ with a R^2 value of 0.56 can be empirically used for conglomerates.

2.4 Gachsaran Formation

Samples of the Gachsaran Formation occurred in 26 boreholes with 89 UCS and 41 UCS local strain measurement tests performed. A summary of the laboratory results is presented in Table 3. Generally the Gachsaran Formation was described as: *very weak, thinly laminated, light yellowish brown to dark greenish grey mottled yellow and orange, claystone/calcilutite with occasional light greyish white thin veins and beds of gypsum. Fresh*

The UCS values were generally independent of moisture content. From the UCS values 5% of the samples returned strengths less than 0.6 MPa (i.e. soil) while 5%. 75% and 15% are classified as extremely weak, very weak and weak rock respectively. The average elastic modulus determined for the Gachsaran Formation claystone was 2516 MPa. There was high amount of scatter in elastic modulus values, as seen in Fig. 5, however a correlation factor of $E = 652.67 \times UCS$ with R^2 value of 0.36 can be empirically used.

3 Discussion—Current Challenges

Gaining knowledge on the depositional environments and geological formations encountered in the Arab gulf can be achieved through literature originating from oil and gas sector. However, as one deviates to alternative sectors, such

Table 1 Summary of Ghayathi Formation laboratory results

	Moisture content (%)	Bulk density (Mg/m³)	Dry density (Mg/m³)	UCS (MPa)	Elastic modulus (MPa)	Poisson's ratio	Direct Shearbox	
							c′ (KPa)	φ (°)
Minimum	2.3	1.40	1.21	0.03	27	0.10	0	22
Maximum	44	2.39	2.25	10.30	9793	0.47	22	34
Average	18	1.97	1.68	1.58	1987	0.26	3	30
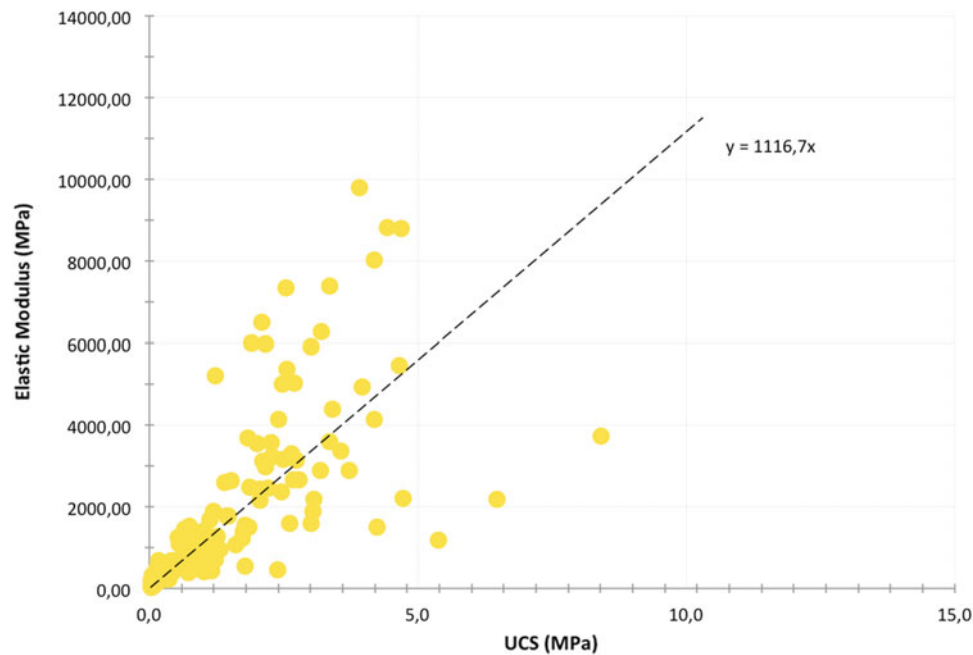
Fig. 3 Ghayathi Formation sandstone elastic modulus versus UCS

Table 2 Summary of Barzaman Formation laboratory results

		Moisture content (%)	Bulk density (Mg/m^3)	Dry density (Mg/m^3)	UCS (MPa)	Elastic modulus (MPa)	Poisson's ratio
Siltstone/calcisiltite	Minimum	2.2	1.32	0.97	0.10	79	0.14
	Maximum	56	2.21	2.04	15.70	4756	0.48
	Average	25	1.90	1.54	3.15	2029	0.33
Claystone/calcilutie	Minimum	24	1.50	1.09	0.10	–	–
	Maximum	50	2.00	1.81	0.40	–	–
	Average	37	1.72	1.27	0.23	–	–
Conglomerate	Minimum	8.9	1.56	1.21	0.10	195	0.17
	Maximum	38	2.28	2.09	12.26	4914	0.48
	Average	22	1.93	1.59	2.45	1600	0.30

as geotechnical, the available literature reduces greatly; which is a worrying scenario due to the rapid expansion of Dubai and the United Arab Emirates. The need for this invaluable knowledge on geotechnical properties and hazards is even more paramount than ever, where engineering geologists and geotechnical engineers are currently challenged to evaluate ground conditions for increasingly demanding infrastructure developments while simultaneously maintaining economic and safe designs.

Perhaps the biggest challenge currently being faced in Dubai, as indicated by the laboratory results presented in this paper, is the strength of the rocks: where, 90% of the UCS laboratory results return values of less than 5.0 MPa. This presents a two fold challenge to ground investigation

professionals, namely, sampling and deformation of the rocks encountered in Dubai. During sampling of such weak material, it is not surprising to retrieve minimal to no core recovery. Core that is recovered is further treated with great care in order to protect the rock for laboratory testing to determine geotechnical parameters. However, the applicability of standard laboratory testing techniques used can be queried due to the inherent properties of the material, which are a result of the recent geological depositional environments of the rocks. Acknowledging and understanding the unique depositional environment indicates that a separate classification scheme may be required for these rocks, where laboratory determined geotechnical parameters should be correlated to the rock mass behaviour that may exhibit

Fig. 4 Barzaman Formation conglomerate, siltstone elastic modulus versus UCS
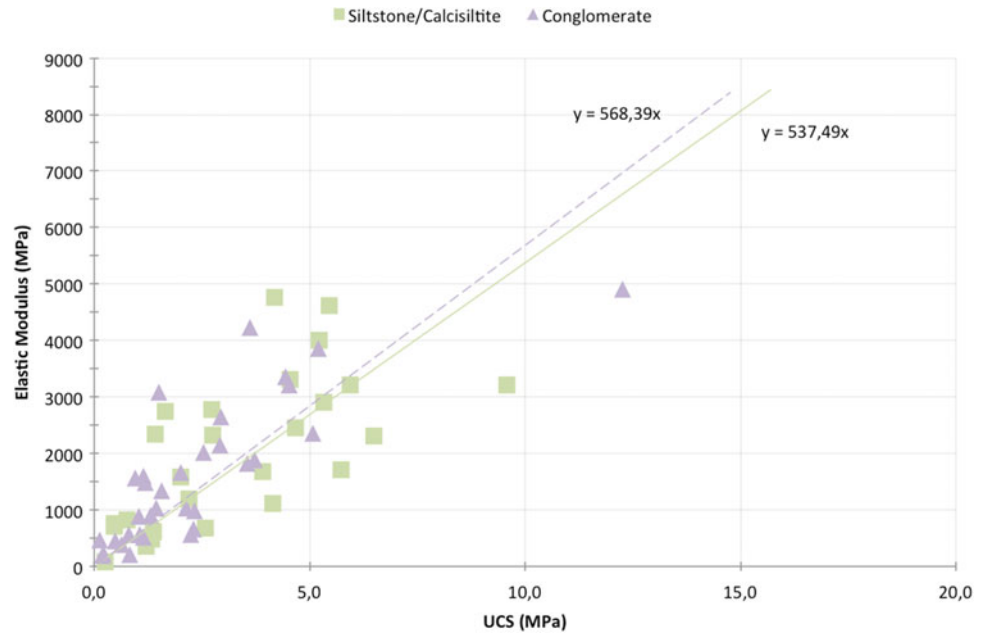
Table 3 Summary of Gachsaran Formation laboratory results

		Moisture content (%)	Bulk density (Mg/m^3)	Dry density (Mg/m^3)	UCS (MPa)	Elastic modulus (MPa)	Poisson's ratio
Claystone/calcilutite	Minimum	0.5	1.60	1.15	0.07	78	0.12
	Maximum	47	2.42	2.25	19.10	9863	0.44
	Average	24	1.94	1.58	3.21	2516	0.32

Fig. 5 Gachsaran Formation claystone elastic modulus versus UCS
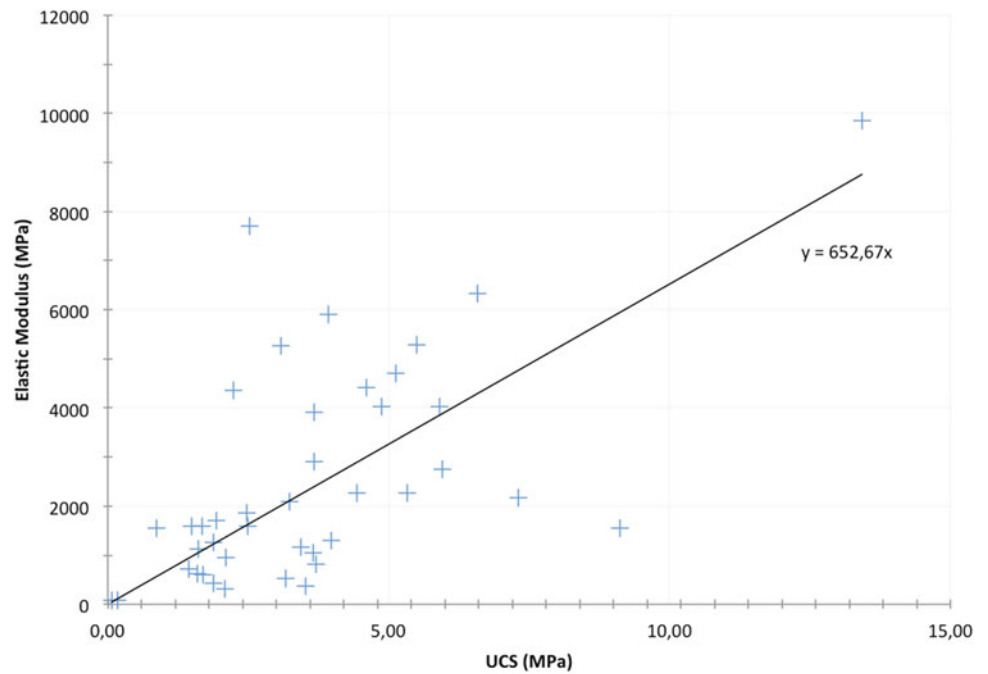
behaviour that is different to current predictions using the current classification schemes as they fail to appreciate the unique geological setting of the Arabian peninsular.

Due to the rocks lack of strength, improved sampling techniques need to be developed that maintain the in situ properties of the weak material being extracted out of the ground for further laboratory analysis. Improved laboratory testing methods also need to be developed for weak rocks with minimal sample requirement for replacing the Point Load test which becomes invalid once strength of the rock occurs below a minimum threshold as stated in ASTM D5731:16, "Test method applies to medium strength rock (compressive strength over 15 MPa)". One such potential method is the needle penetration test which shows promising applicability to weak rocks (Ulusay et al. 2013), These specialised tests for weak rocks however are not generally well known and a greater emphasis needs to be placed on educating geotechnical clients for improved interpretation of subsurface conditions. Alternatively, the use of geophysical or destructive drilling (i.e. instrumented monitored drilling) offers a potential solution to this 'lack of strength' challenge by presenting an accurate representation of ground conditions through developing a database of interpreted results and actual ground conditions post site investigation to allow back analysis to develop accurate correlations.

If sample recovery is minimal and validity of laboratory results is tentative, then perhaps all that remains is the core loggers' interpretation described in borehole log descriptions. Should a competent core logger be able to adhere accepted logging standards, then reasonable confidence can be allocated to the borehole logs in evaluation of subsurface conditions. However, the most important question that should then cross an engineering geologists' or geotechnical engineers' mind is: what is the purpose of the investigation. While it is paramount to follow internationally recognised core logging standards to ensure conformity within the geotechnical community, it is more important to have a clear understanding of the purpose of the investigation. This will influence the amount of detail afforded to core logging and core measurement such as RQD, which presents an interesting argument to this region where by blindly following logging standards, the definition of RQD may be overlooked (Deere and Deere 1989). Following the correct RQD definition could unfairly penalise the rock mass in this geological setting and not give a true representation of ground conditions. Currently, however, there is no accepted alternative measurement method available, supporting the notion for a separate classification scheme and form of measurement for materials in this geological setting.

4 Conclusion

Information available to assist engineering geologists and geotechnical engineers to evaluate potential hazards and challenges in Dubai is limited. However, the need of such information is paramount due to the rapid civil infrastructure development in Dubai. This paper compiles and presents a laboratory results and general geological descriptions of 87 boreholes drilled throughout Dubai. The general stratigraphy of Dubai consists of Quarternary Aeolian sand deposits overlying thinly bedded calcareous sandstones of the Ghayathi Formation underlain by interbedded conglomerates and siltstones of the Barzaman Formation before encountering the thinly bedded claystones of the Gachsaran Formation. Analysis of laboratory results involved separation into the appropriate identified geological units and comparison of UCS, elastic modulus, moisture content, bulk and dry density. Overall all UCS results classify 90% of the rocks as very weak or weaker with an overall average UCS value and elastic modulus of 2.24 and 2058 MPa respectively. The average bulk and dry densities are 1960 and 1630 kg/m^3 respectively, with an average moisture content of 19%. The lack of strength highlights a current challenge that needs to be addressed in accurately portraying subsurface conditions through improved sampling, classification and laboratory testing techniques in evaluating rock mass behaviour for such weak rocks. Recognition of the inherent hazards caused by subsurface conditions in Dubai emphasise the important role engineering geologists and geotechnical engineers play in ensuring that suitable site investigation methods and techniques are performed correctly to ensure that an accurate and thorough understanding of subsurface conditions is obtained to minimize the associated risk of development.

References

Al-Sayari, S.S., Zötl, J.G. (eds.): Quaternary Period in Saudi Arabia: 1: Sedimentological, Hydrogeological, Hydrochemical, Geomorphological, and Climatological Investigations in Central and Eastern Saudi Arabia. Springer Science & Business Media, Berlin (2012)

ASTM D5731-16: Standard Test Method for Determination of the Point Load Strength Index of Rock and Application to Rock Strength Classifications. ASTM International, West Conshohocken, PA (2016)

ASTM D7012-14: Standard Test Methods for Compressive Strength and Elastic Moduli of Intact Rock Core Specimens under Varying States of Stress and Temperatures. ASTM International, West Conshohocken, PA (2014)

Deere, D.U., Deere, D.W.: Rock Quality Designation (RQD) After Twenty Years. Don U Deere, Gainesville (1989)

Fugro Middle East [FME]: Geotechnical database (2017)

Glennie, K.W.: The Desert of Southeast Arabia: A Product of Quaternary Climatic Change. Quaternary Deserts and Climatic Change, pp. 279–291. Balkema, Rotterdam (1998)

Gunatilaka, A.: Kuwait and the Northern Arabian Gulf-a study in quaternary sedimentation. Episodes **9**(4), 223–231 (1986)

Kirkham, A.: A Quaternary proximal foreland ramp and its continental fringe, Arabian Gulf, UAE. Geol. Soc. Lond. Spec. Publ. **149**(1), 15–41 (1998)

Macklin, S., Ellison, R., Manning, J., Farrant, A., Lorenti, L.: Engineering geological characterisation of the Barzaman formation, with reference to coastal Dubai, UAE. Bull. Eng. Geol. Env. **71**(1), 1–19 (2012)

Purser, B.H.: Sedimentation around bathymetric highs in the southern Persian Gulf. In: The Persian Gulf, pp. 157–177. Springer, Berlin (1973)

Styles, M., Ellison, R., Arkley, S., Crowley, Q.G., Farrant, A., Goodenough, K.M., McKervey, J., Pharaoh, T., Phillips, E., Schofield, D., Thomas, R.J.: The geology and geophysics of the United Arab Emirates. vol. 2, Geology (2006)

Ulusay, R., Aydan, Ö., Erguler, Z.A., Ngan-Tillard, D.J., Seiki, T., Verwaal, W., Sasaki, Y., Sato, A.: ISRM suggested method for the needle penetration test. In: The ISRM Suggested Methods for Rock Characterization, Testing and Monitoring: 2007–2014, pp. 143–155. Springer International Publishing, Switzerland (2013)

Walkden, G., Williams, A.: Carbonate ramps and the pleistocene-recent depositional systems of the Arabian Gulf. Geol. Soc. Lond. Spec. Publ. **149**(1), 43–53 (1998)

Williams, A.H., Walkden, G.M.: Late Quaternary highstand deposits of the southern Arabian Gulf: a record of sea-level and climate change. Geol. Soc. Lond. Spec. Publ. **195**(1), 371–386 (2002)

Assessment on the Engineering Geological Conditions of the Eastern Urban Area of Thessaloniki Basin, in Northern Greece, Using a Geotechnical Database

A. Kokkala and V. Marinos

Abstract

The design and construction of underground and above ground projects in the urban environment of Thessaloniki in Northern Greece face several geological challenges. Determination of engineering geological conditions is a crucial factor for planning and designing geotechnical works. A large amount of geological and geotechnical data is being stored in a georeferenced database for that purpose. The data that are processed are based on borehole geological information, laboratory testing, geotechnical characterization and in situ field tests. The processing and assessment of this information leads to the identification of useful value ranges for several physical and mechanical geotechnical parameters, for instance SPT, uniaxial compressive strength, Atterberg limits, permeability tests and particle size analyses. Thematic maps that reference geological and geotechnical factors were constructed by means of data analysis and correlation procedures. These maps provide public and private information serving multiple purposes such as new construction projects, seismic hazard design and management of natural disasters. This study focuses on the Eastern part of urban Thessaloniki, highlighting the in situ conditions of Quaternary and Neogene deposits with the construction of 2-D profiles and 3-D models. In addition, hazardous zones are identified in order to illustrate the regions geotechnical properties. The purpose of this investigation, besides incorporating new data, is to provide a tool for summarizing data into useful information formats in order to estimate the geological conditions and geotechnical properties of formations similar to the study area while providing a detailed outline of the methodology which was followed.

A. Kokkala (✉) · V. Marinos
Department of Geology, Aristotle University of Thessaloniki, 54124 Thessaloniki, Greece
e-mail: kokkalaa@geo.auth.gr

V. Marinos
e-mail: marinosv@geo.auth.gr

1 Introduction

In the last few decades rapid development on many scales of geotechnical design in urban areas have been conducted. Site selection and risk assessment are extremely important aspects of the construction of underground and above ground engineering projects, especially in urban areas.

This paper refers to a wider research effort that focuses on the evaluation of engineering geological properties of the main formations encountered the urban areas of the city of Thessaloniki which is located in Northern Greece. This research is conducted in order to investigate the properties of the examined formations in various geotechnical investigations for structures such as building foundations, metro extension lines, deep excavations and road construction. This paper is based on geological and engineering geological data for the Eastern part of Thessaloniki which is processed and summarized from 89 boreholes. Data were provided from (Central Laboratory of Public Works, Geognosi S.A.) and the main line of Thessaloniki Metro (Attiko Metro S.A.), which was stored in a database.

The intent of this study is to build upon the current database in order to more accurately assess the geotechnical factors that contribute to improve understanding of the engineering and geological properties for the region. The data entered in and evaluated by the database came from geological and geotechnical information that was based on a large amount of laboratory tests and in situ field tests.

Explicitly, in order to achieve this scope, the following steps were conducted:

- Collection of all relevant data from existing studies, surveys, and task reports
- Selection, classification and evaluation of data regarding their accuracy, precision and utility
- Data entry into the database, analyses and correlations of the processed data
- Identification of useful ranges of values for several parameters, that are assigned for different formations
- Construction of geotechnical longitudinal profiles for specific areas
- Estimation of specific formations properties

Through a set of standard procedures, the processing and evaluation of this geotechnical information directed the research to general geotechnical properties for formations in underground and above ground projects. In addition, the paper focuses on the methodology for the classification of geological and geotechnical data. The scope of this study is based on the work of Marinos et al. (2008) which included the evaluation of the geological and geotechnical conditions of Thessaloniki metro. New data from many additional boreholes have been added to the database in order to expand and enrich the existing published study.

2 Engineering Geological Database

2.1 Description of the Database

The existing database was based on the Tunnel Information and Analysis System (TIAS), a database constructed for the Egnatia Highway tunnels in northern Greece. TIAS is a well-structured database which allows the user to access accurate information for the description of the individual data (Marinos et al. 2013).

The database is a collection of distinct geological and geotechnical data which are stored in tables and are based on an hierarchical mode. All the entries have their own identity within the database. This means that at any time, data may be divided in accordance with the field in which they are registered. The structure of the database provides a continuous connection of all the distinct data. It should be noted that any question to the database can be filtered so that the user has the option of accessing information for a particular request. These analyses can provide the user with both qualitative and quantitative outputs and the ability to correlate information that is derived from a vast amount of data relating to geological and geotechnical properties.

The processed data by the database are based on borehole geological information, laboratory testing, geotechnical characterization and in situ field tests. The current database includes thirteen tables of input data. These data refer to general and detailed geological description, in situ

permeability tests, groundwater levels, standard penetration tests (SPT) and results from laboratory tests such as particle size distributions, physical and mechanical properties from uniaxial, triaxial, shear box tests.

Conceptually the database structure can be illustrated as in Fig. 1 where nine main tables are presented and show the way the data are stored, as well as the number of inputs per file entry for the Eastern region.

3 Engineering Geological Conditions

3.1 Geology of the Research Area

The urban area of Thessaloniki is founded partly on bedrock, and partly on post alpine sediments. In detail, the underlying bedrock consists of a Mesozoic green schist-gneiss complex (Mountrakis 2010). This complex is overlain by an Upper Miocene to Lower Pliocene sedimentary sequence that covers the largest part of the city which is characterized by the presence of Neogene and Quaternary deposits. The Neogene deposits consist of a series of red clays and a series of sandstone-marl (I.G.M.E. 1978). The red clay series is composed of stiff to hard clays. The sandstone-marl series is composed of silty to clayey sand and sandy clay to sandy silt with presence of fine to medium gravels. Quaternary deposits consist mainly of sands, clays, gravel, and local presence of conglomerates. Neogene and Quaternary deposits are covered in places by fill deposits placed in different phases of the historical development of the city. The fill deposits consist mainly of loose clayey–silty materials with sand and gravel.

3.2 Analysis and Evaluation of Ground Data

The goal of this study is to evaluate the geological and geotechnical conditions for soil formations in the research area. The results of this process also contributed to a better understanding of the design and construction constraints of future geotechnical projects. Data collected between 1963 and 2011 were used and implemented for this research. Identical processes were carried out focusing on specific areas of Thessaloniki basin.

The framework of this research was data collected and analyzed from Eastern part of Thessaloniki and shown in Fig. 2. The purpose of this research is to understand the geotechnical property patterns of the study area. Detailed work based on this analysis led to the characterization of some specific geotechnical parameters. The physical and mechanical parameters that were evaluated in this study are SPT, uniaxial compressive strength (qu), Atterberg limits, groundwater level, permeability tests and particle size
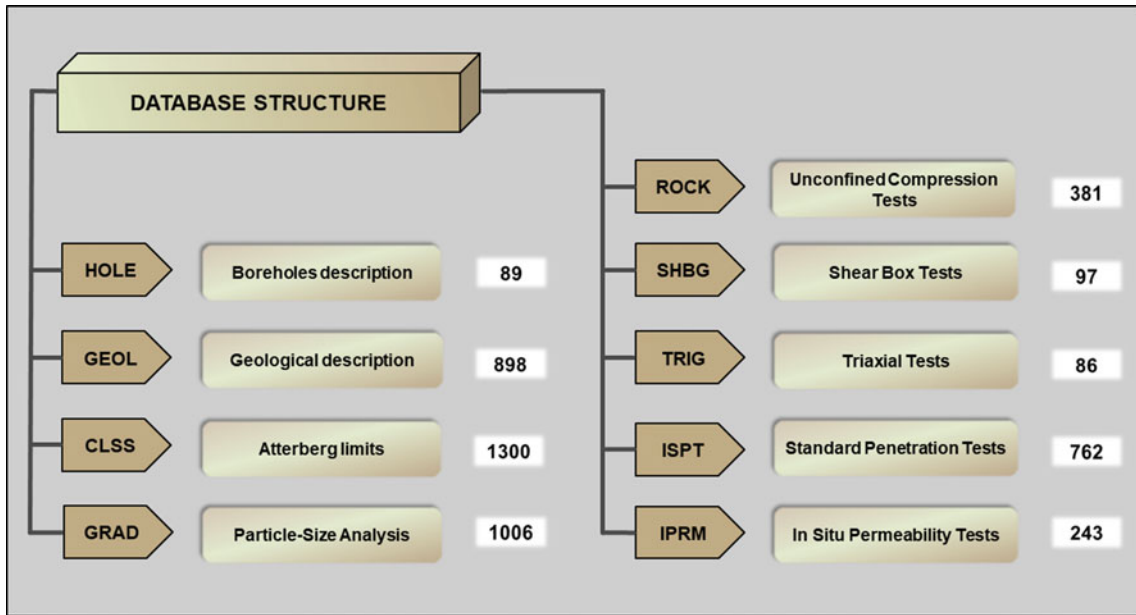
Fig. 1 A part of the database structure including the number of inputs per table entry for the Eastern research area
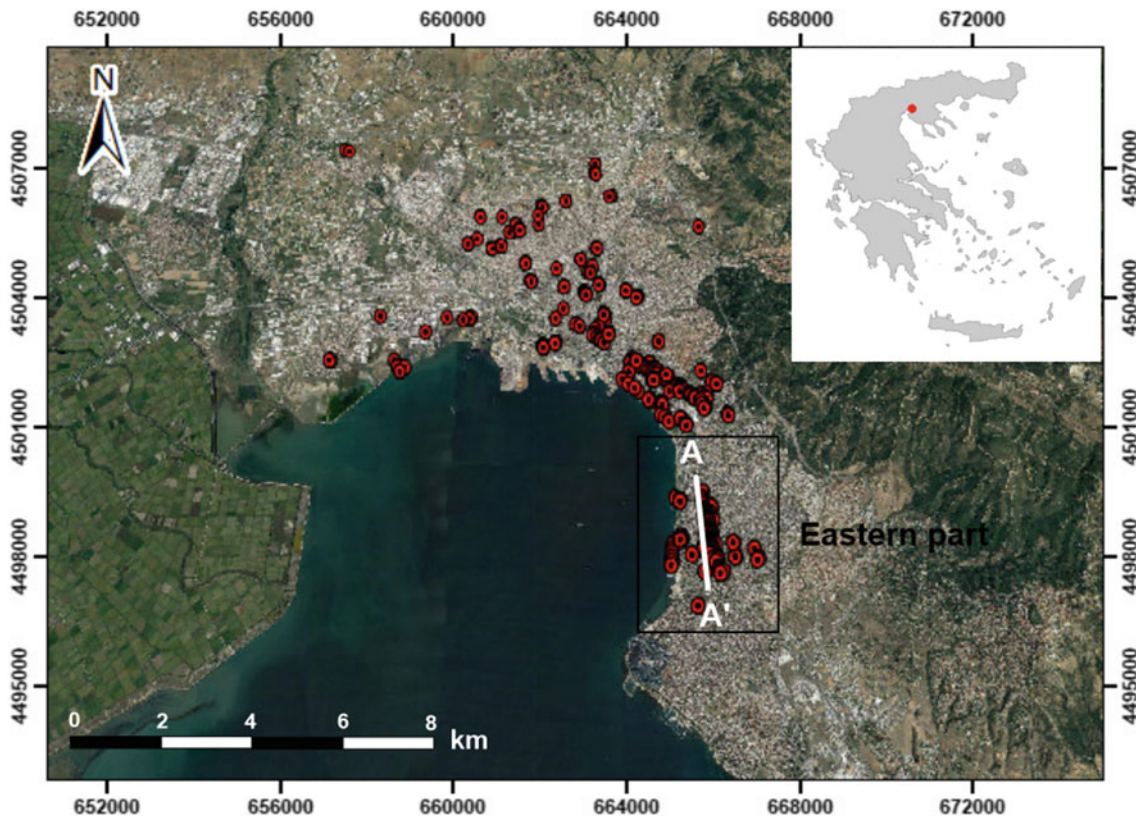
Fig. 2 Map (Google Earth) of Thessaloniki city showing the Eastern research part, the boreholes and the direction of the longitudinal section referred to Fig. 4

Fig. 3 Engineering geological
map of Thessaloniki city
illustrating the spatial distribution
of Quaternary deposits in the
research area (modified by the
authors from Rozos et al. 1998)
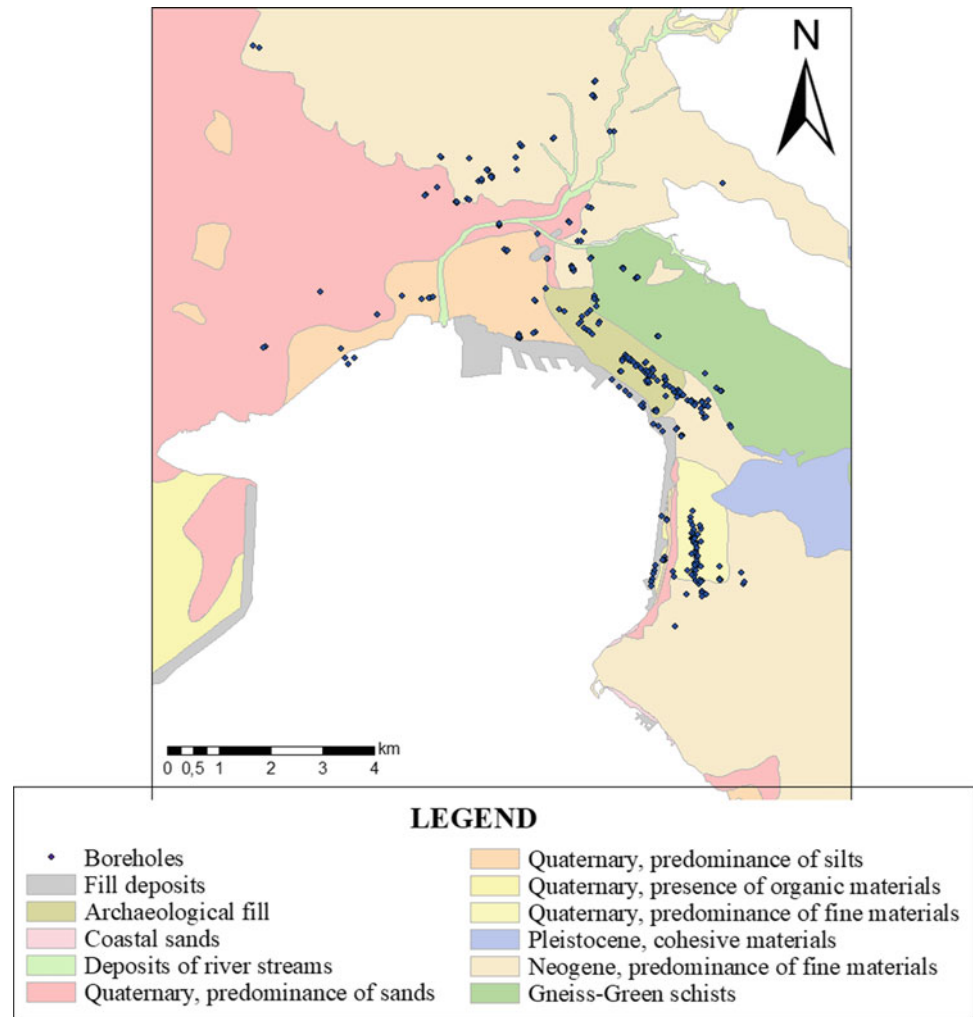
3.3 Geological-Geotechnical Ground Model

In order to demonstrate the geological conditions, several longitudinal profiles have been created. According to the longitudinal profile of the Eastern part (Fig. 4), Quaternary deposits prevail in relation to the Neogene deposits. Explicitly, Quaternary deposits consist of clayey and sandy materials. The range of spatial distribution for these sediments is large in both depth and length (Fig. 3). The existence of old stream channels in this area that possess a directional trend of southeast, are associated with recent fluvial deposits. The sandstone-marl series of Neogene deposits are mainly observed at greater depths. However, this formation can be observed at shallow depths and close to the ground surface where nearby faults exist in the area (Kokkala 2015).

3.4 Standard Penetration Tests

In addition to the longitudinal profiles, it is also necessary to evaluate physical and mechanical properties of Quaternary and Neogene deposits—the main formations that occur in the whole research area.

A significant number of SPT were executed on Quaternary and Neogene deposits for the Eastern part. Quaternary deposits exhibit a majority of values in the range of 4–30 and
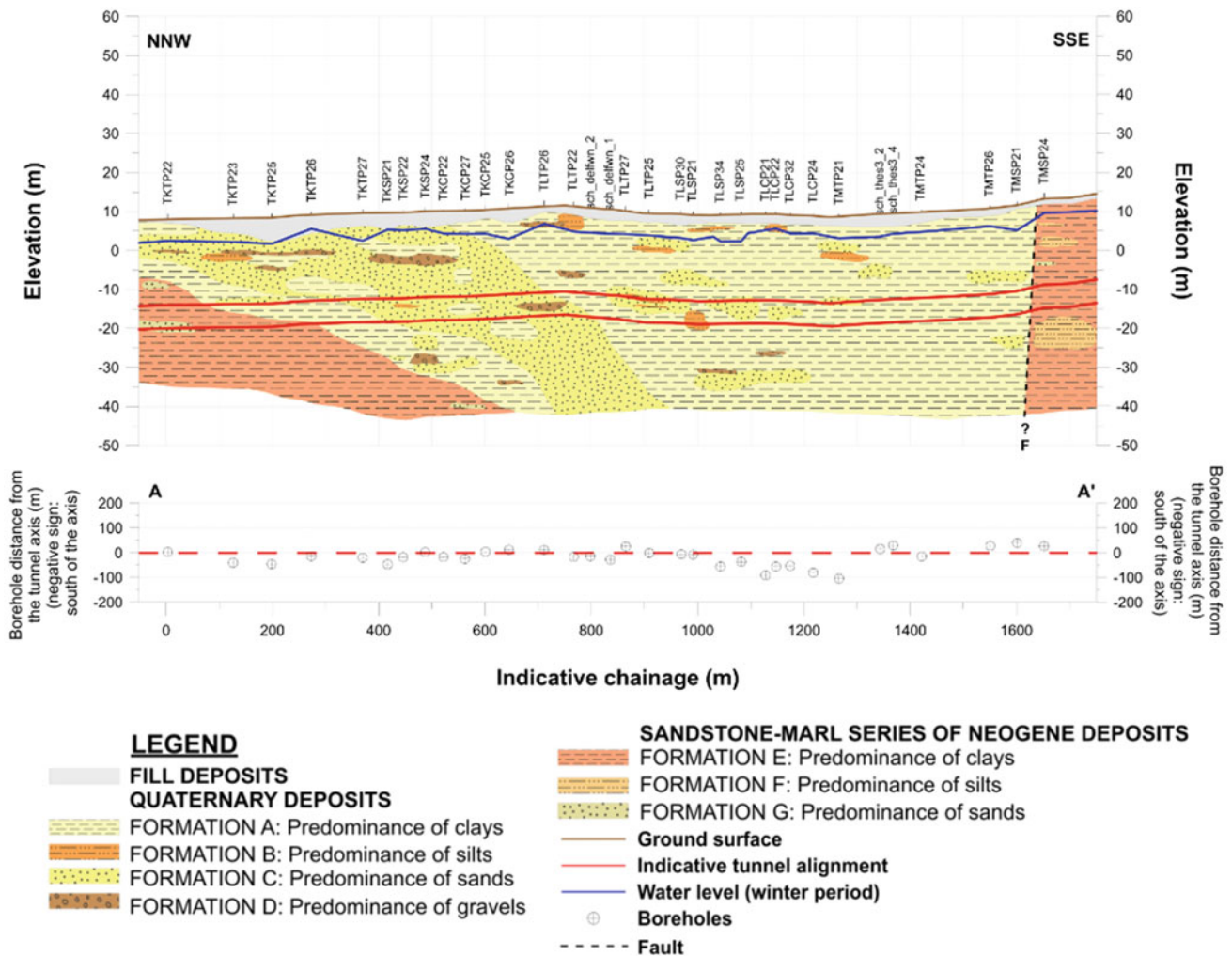
Fig. 4 Detailed geological longitudinal profile (north-northwest to south–southeast) for the Eastern part (the location of the section is shown in Fig. 2)

are characterized as loose to medium dense formation (Fig. 5a). On the other hand, the majority of the tests show greater values for Neogene values indicating a dense to very dense coarse-grained formation that is stiff to very stiff for the fine-grained formations (Fig. 5b).

3.5 Uniaxial Compressive Strength

In total 297 samples were obtained and tested from Quaternary and 70 samples from Neogene deposits. The majority of the measurements from Quaternary deposits indicate values lower than 0.25 MPa (Fig. 6a). These values indicate a low to medium strength formation. In contrast, the

Neogene deposits exhibited values mostly in the range of 0.1–1 MPa which indicate a stable to stiff formation (Fig. 6b).

3.6 Atterberg Limits

Atterberg limits, especially the liquid limit and the plasticity index provide useful information regarding the expected behaviour of the soils. Liquid limits and plasticity indices are used internationally for the identification and classification of soils in accordance with the specifications adopted by ASTM. It appears that the fine-grained geomaterials are found above the Casagrande line (Fig. 7) and
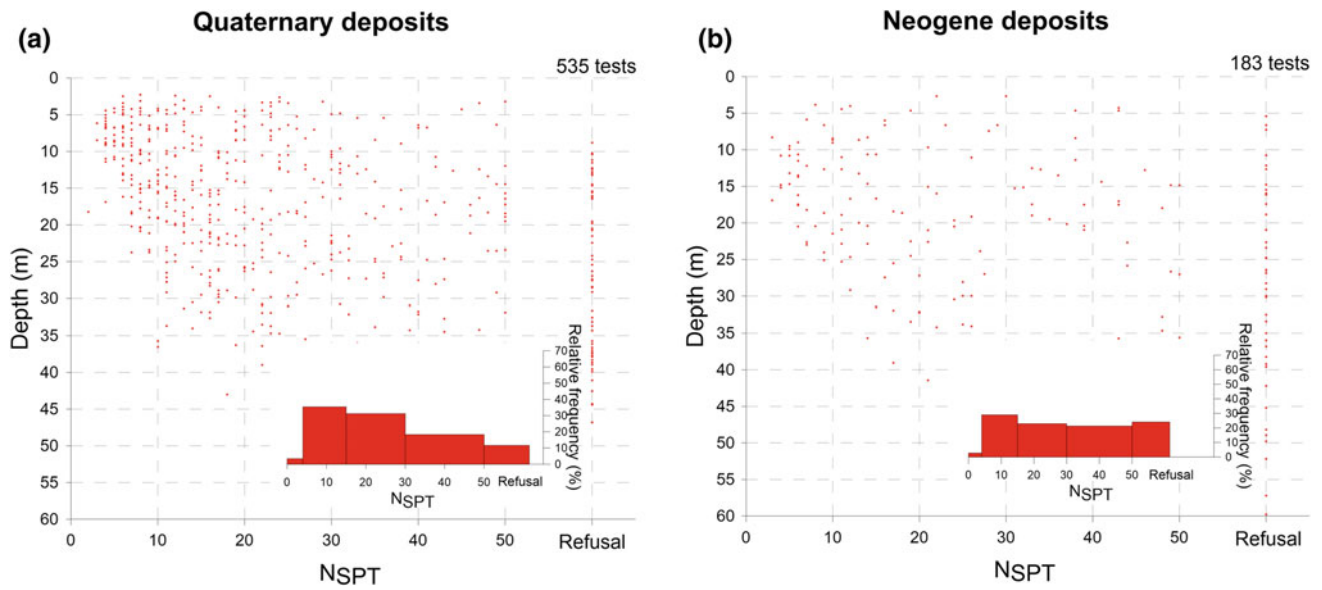
Fig. 5 Distribution charts of standard penetration test values for the Quaternary (**a**) and Neogene deposits (**b**) of the research area
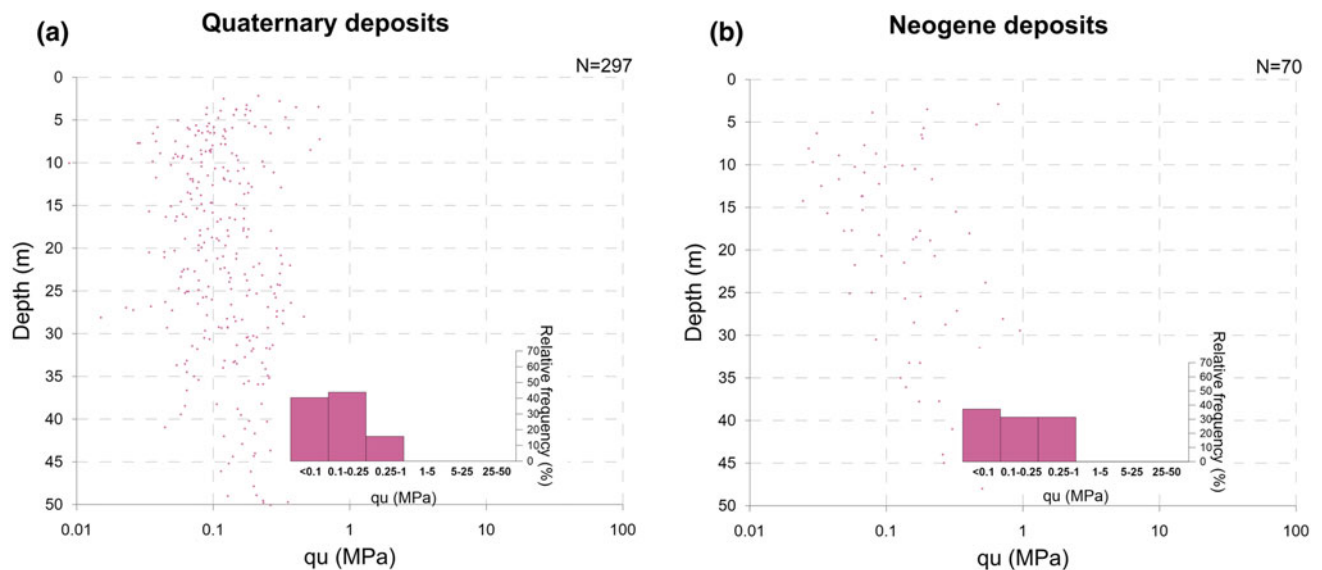
Fig. 6 Distribution charts of the uniaxial compressive strength (qu) values for the Quaternary (**a**) and Neogene deposits (**b**) of the research area

are mainly characterized as low to marginally intermediate plasticity (CL-CI). The Neogene deposits are placed also above the Casagrande line, illustrating that the fine-grained materials are low to mostly medium plasticity (CL-CI).

Particle-Size Analysis

According to the grading envelopes (Fig. 8a, b) both formations consist of sandy clays and clays with sand, sandy silts and clayey to silty sands with a variable percentage of gravels. However, considering the heterogeneous nature of soils which are fine-grained and in parts are coarse-grained,

it can be assumed that the majority of the soil curves, show a high percentage of fine material.

3.7 In-Situ Permeability Tests

The prevalence of Maag tests in both formations is notable and due to the strong presence of fine-grained soil materials. It is evident that the highest permeability values 10^{-7} to 10^{-5} m/s (meters per second) were recorded in Quaternary deposits (Fig. 9a), corresponding mainly to coarser grained materials. Within the Neogene formation, permeability
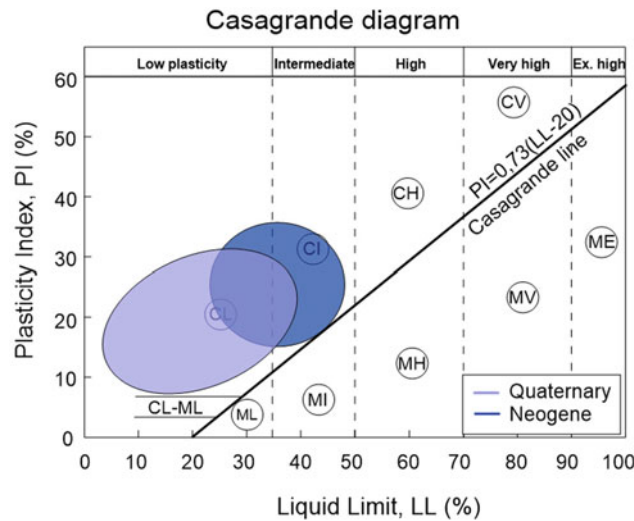
Fig. 7 Plot of Quaternary and Neogene deposits in the Casagrande diagram of the research area
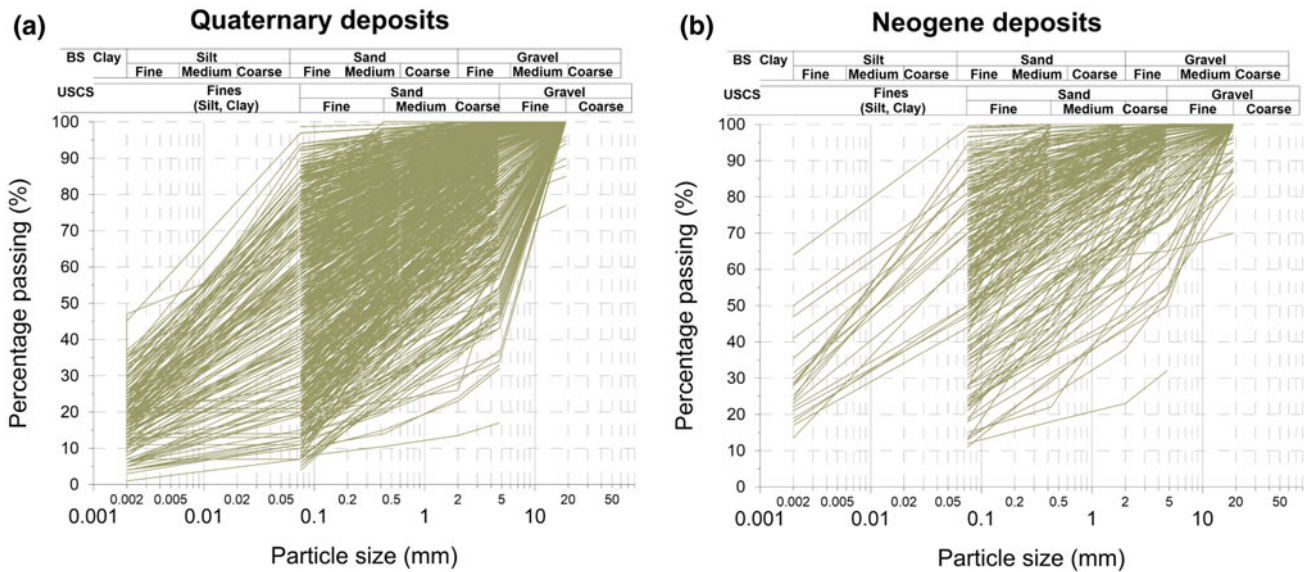
Fig. 8 Distribution grading curves of Quaternary (a) and Neogene deposits (b) of the research area

decreases (Fig. 9b), as these deposits exhibit medium to very low permeability values (lower than 10^{-6} m/s).

4 Conclusions and Discussion

This paper discusses the engineering geological conditions in the Eastern part of Thessaloniki basin that are managed and assessed in a well-structure database. The purpose of this process is to evaluate the geological response and

geotechnical properties of the formations encountered from various geotechnical investigations in order to build structures such as building foundations, metro extension lines, deep excavations and road construction. Many studies refer to the methodology of classification and evaluation of geological and geotechnical data for engineering purposes by means of investigations' results (Marinos et al. 2008; Ball et al. 2009; Sass and Burbaum 2009; Edalat et al. 2010; Azali et al. 2013; Mohammadi et al. 2016; Nasseh et al. 2018). The parameters in this study come from existing data
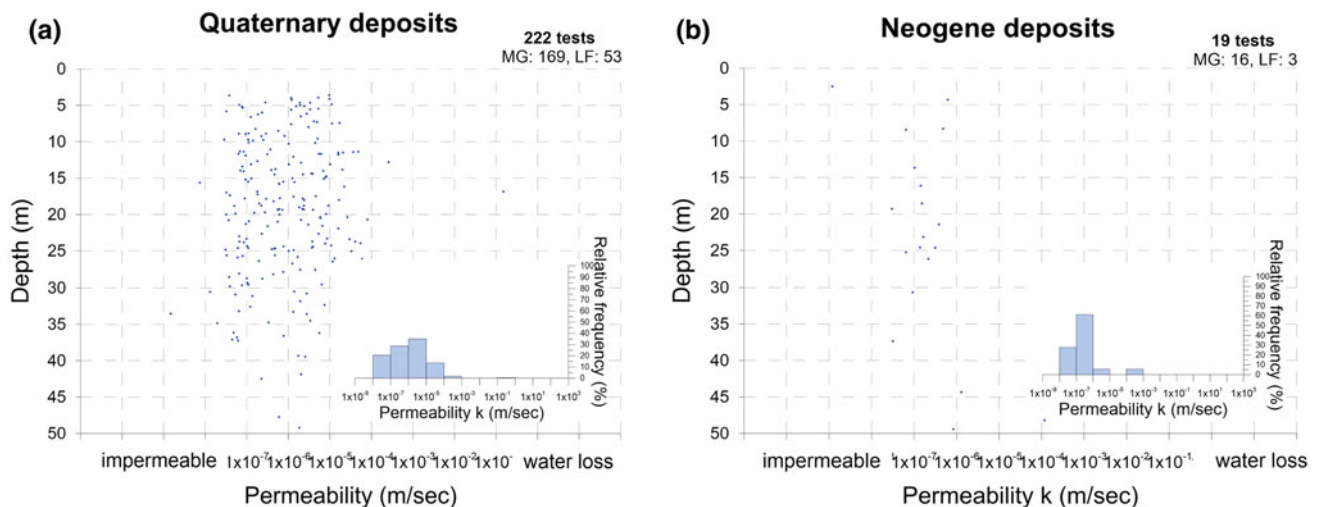
Fig. 9 Distribution charts of in situ permeability tests for the Quaternary and Neogene deposits of the research area

from numerous ground investigations and from borehole geological information, laboratory testing, geotechnical characterization, and in situ field tests.

The evaluation of physical properties and mechanical parameters demonstrates the identification of two engineering geological units with homogeneous geotechnical behavior within the area. Specifically, the Eastern part is mainly formed from the recent fluvial Quaternary deposits indicating a large property variability ranging from clayey to sandy materials. These soil materials may be prone to geotechnical challenges regarding issues such as settlement and control of ground movement, as well as seasonal changes in the water table. Correspondingly, Neogene deposits that are encountered in a more limited area constitute better geotechnical characteristics showing higher strength parameters in that formation (Rozos et al. 2004; Kokkala 2015).

The methodology proposed provides the construction of a well organized database which has a great capacity to store and represent geological and engineering geological properties. Recent literature reviews have focused on various unforeseen geological and engineering geological conditions using a geotechnical database. (Chmelina et al. 2013; Marinos et al. 2013; Rackwitz et al. 2013; Todo et al. 2013).

Results of this work will be a useful tool for developing additional procedures aimed at modelling the geological and engineering geological properties and providing the ability to integrate multiple layers of information related to the Thessaloniki's geology or comparing properties of soil types with similar depositional environment.

References

Azali, S.T., Ghafoori, M., Lashkaripour, G.R., Hassanpour, J.: Engineering geological investigations of mechanized tunneling in soft ground: a case study, East-West lot of line 7. Tehran Metro Iran Eng. Geol. **166**, 170–185 (2013). https://doi.org/10.1016/j.enggeo.2013.07.012

Ball, R.P.A., Young, D.J., Isaacson, J., Champa, J., Gause, C.: Research in soil conditioning for EPB tunneling through difficult soils. In: Proceedings—Rapid Excavation and Tunneling Conference (2009)

Chmelina, K., Rabensteiner, K., Krusche, G.: A tunnel information system for the management and utilization of geo-engineering data in Urban tunnel projects. Geotech. Geol. Eng. **31**(3), 845–859 (2013). https://doi.org/10.1016/j.enggeo.2013.07.012

Edalat, K., Vahdatirad, M.J., Ghodrat, H., Firouzian, S., Barari, A.: Choosing TBM for Tabriz subway using multi criteria method. J. Civil Eng. Manage. **16**(4), 531–539 (2010). https://doi.org/10.3846/jcem.2010.59

I.G.M.E.: Geological map of the wider Thessaloniki area, Scale 1:50.000 (1978)

Kokkala, A.: An engineering geological database for Thessaloniki basin with tunnel applications. M.Sc thesis, Aristotle University of Thessaloniki (2015)

Marinos, P., Novack, M., Benissi, M., Panteliadou, M., Papouli, D., Stoumpos, G., Marinos, V., Korkaris, K.: Ground information and selection of TBM for the Thessaloniki metro in Greece. Environ. Eng. Geosci. **XIV**(1), 17–30 (2008). https://doi.org/10.2113/gseegeosci.14.1.17

Marinos, V., Prountzopoulos, G., Fortsakis, P., Koumoutsakos, D., Korkaris, K., Papouli, D.: Tunnel information and analysis system: a geotechnical database for tunnels. Geotech. Geol. Eng. **31**(3), 891–910 (2013). https://doi.org/10.1007/s10706-012-9570-x

Mohammadi, S.D., Firuzi, M., Asghari Kaljahi, E.: Geological–geotechnical risk in the use of EPB-TBM, case study: Tabriz Metro, Iran. Bull. Eng. Geol. Environ. **75**, 1571–1583 (2016). https://doi.org/10.1007/s10064-015-0797-7

Mountrakis, D.: Geology and geotectonic evolution of Greece. University Studio Press, Thessaloniki (2010)

Nasseh, S., Moghaddas, N.H., Ghafoori, M., Asghari, O., Bazaz, J.B.: Investigation of spatial variability of SPT data in Mashhad City (NE

Iran) using a geostatistical approach. Bull. Eng. Geol. Env. **77**, 441–455 (2018). https://doi.org/10.1007/s10064-017-1136-y

Rozos, D., Apostolidis, E., Hadzinakos, I.: Engineering-geological map of the wider Thessaloniki area, Greece. Bull. Eng. Geol. Env. **63**(2), 103–108 (2004)

Rackwitz, F., Savidis, S., Rickriem, J.: Web-based data and monitoring platform for complex geotechnical engineering projects. Geotech. Geol. Eng. **31**(3), 927–939 (2013). https://doi.org/10.1007/s10706-012-9592-4

Rozos, D., Apostolidis, E., Hadzinakos, I.: Engineering-geological map of the wider Thessaloniki area, I.G.M.E. Scale 1:25.000 (1998)

Sass, I., Burbaum, U.: A method for assessing adhesion of clays to tunneling machines. Bull. Eng. Geol. Env. **68**(1), 27–34 (2009). https://doi.org/10.1007/s10064-008-0178-6

Todo, H., Yamamoto, K., Mimura, M., Yasuda, S.: Japan's nation-wide electronic geotechnical database systems by Japanese geotechnical society. Geotech. Geol. Eng. **31**(3), 941–963 (2013). https://doi.org/10.1007/s10706-012-9562-x

Comparison of Mechanical Properties of Dry, Saturated and Frozen Porous Rocks

Ákos Török, Adrienn Ficsor, Mortaza Davarpanah, and Balázs Vásárhelyi

Abstract

The mechanical properties of frozen rocks are very different from the properties of the same lithologies under ambient temperature. The goal of this paper is to describe the changes in the physical parameters of rocks caused by freezing. In addition, estimations are given on how these parameters are influenced by the intrinsic properties of rocks. For the tests, cylindrical specimens were made from highly porous Miocene limestone and porous rhyolite tuff. The samples were tested in air dry, water saturated, and frozen (−20 °C) conditions. Besides the porous stones, ice specimens were also made and used for the same tests. The laboratory tests included the determination of density, ultrasound speed propagation, porosity, capillary water absorption and strength parameters. The test results obtained under the three conditions were compared. The data set of measured physical parameters was analyzed by using regression analyses. Correlations were calculated for the measured physical parameters of air-dry, saturated, and frozen conditions. The results suggest that a stronger correlation exists between the strength and density of frozen specimens than between the strength and density of air-dry specimens. Equations were also found that describe the relationships between the density and uniaxial strength of ice and various porous rocks.

1 Introduction

Freezing is a common method for soil or rock mass stabilization in mines, or around tunnels. To apply this method, it is important to know the strength parameters of the frozen rock but very often there is not enough information on the behaviour of materials. There are several studies dealing with the influence of water on the strength of rock samples (Wong et al. 2016; Vásárhelyi and Ván 2006), and especially of limestones (Vásárhelyi 2005) and tuffs (Vásárhelyi 2002; Kleb and Vásárhelyi 2003). The mechanical problem of the frozen rock has been reviewed recently (Gambino and Harrison 2017), providing new information on the properties of frozen rocks. The current paper has another approach as it presents the latest laboratory tests results of frozen rocks. In this study, different porous rocks were analysed under different conditions; including dry, water saturated and frozen ones.

2 Materials and Methods

Two types of highly porous rocks were studied: Miocene limestone and Miocene rhyolite tuff (Fig. 1). The rhyolite tuff is a product of the Inner Carpathian volcanism (Lukács 2018) and samples from Eger represent a common lithotype of NE-Hungary with well described mechanical properties (Vásárhelyi 2002; Török and Barsi 2018). Two lithotypes of Miocene limestone from the Sóskút quarry were chosen for the tests: a medium-grained and a coarse grained bioclastic one that contains shell fragments. Detailed lithological descriptions of the porous limestone is given by Török (2003). The stone samples were compared to ice samples

Á. Török (✉) · A. Ficsor · M. Davarpanah · B. Vásárhelyi
Department of Engineering Geology and Geotechnics, Budapest University of Technology and Economics, Műegyetem rkp. 3, Budapest, 1111, Hungary
e-mail: torokakos@mail.bme.hu

A. Ficsor
e-mail: adri7.ficsor@gmail.com

M. Davarpanah
e-mail: mortaza.davarpana@epito.bme.hu

B. Vásárhelyi
e-mail: vasarhelyi.balazs@epito.bme.hu

Fig. 1 Cylindrical samples of fossiliferous Miocene limestone (left) and rhyolite tuff (right) (scale bar is 2 cm)
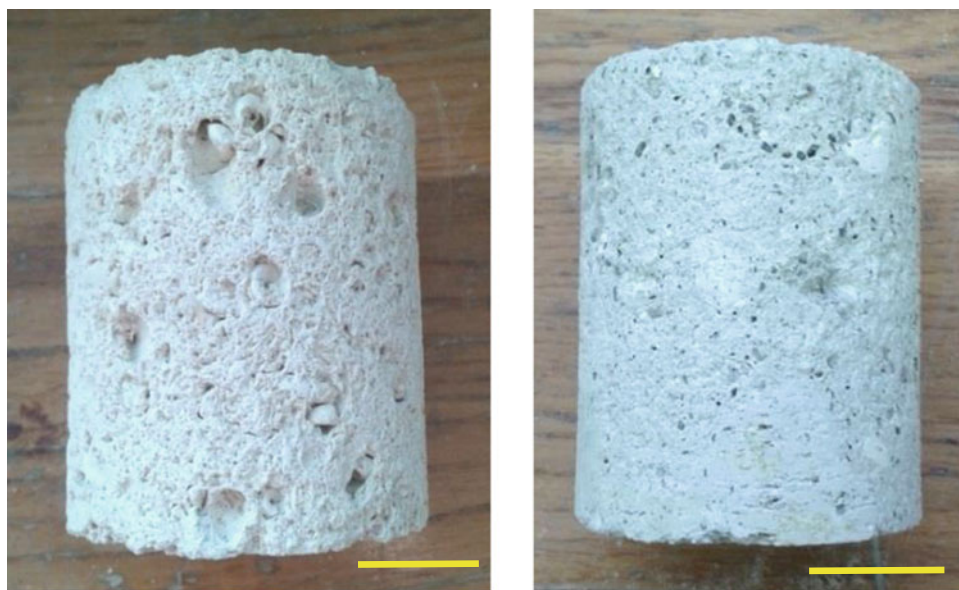
that were prepared in the laboratory. Cylindrical ice samples were made in plastic tubes. The tubes were filled with water and then it was kept in a deep freezer until the complete crystallization of ice. Altogether 30 limestone, 12 rhyolite tuff, and 7 ice samples were tested.

Cylindrical test specimens of 5 cm in diameter were used for the laboratory tests. Density and ultrasonic pulse wave velocity were measured in different petrophysical states (i.e. dry, water saturated and frozen states after water saturation). The tests on frozen samples were made on water saturated rock samples cooled to −20 °C.

Both the strength and the Young's modulus were measured by unconfined compressive tests. The laboratory investigations were carried out according to the ISRM suggested methods (Ulusay and Hudson 2006).

3 Results and Discussion

A linear relationship was found between the dry density and the saturated/frozen densities. It was possible to calculate a linear regression between the dry density of the rock and both the saturated and frozen density as calculated in:

$$\rho_i = a\rho_d + b \tag{1}$$

where ρ_d and ρ_i is the dry density and saturated or frozen density of the sample; respectively, a and b are material constants. The obtained values are summarized in Table 1.

According the regression line, the slope of Eq. (1) is around 1, i.e., these lines are basically parallel to each other.

The ultrasonic pulse wave velocity was also analysed as a function of the density, similar to a previous study on travertine (Török and Vásárhelyi 2010).

According to the published data, the ultrasonic pulse wave velocity of the ice at −4 °C is 3.25 km/s (Andersland and Ladanyi 1994). Our measured results are close to this value, but with the increasing density of the ice, the ultrasonic wave velocity increases linearly as well. There are linear regressions between the density of the rock and the ultrasonic wave velocity as well (Table 2).

The uniaxial compressive test results are analysed for the ice, Miocene limestone and rhyolitic tuff separately. The mechanical behaviour of ice depends on strain rate, temperature, porosity, crystal size, and structure. Pure ice is typically polycrystalline with random crystal orientation whose response to a deviatory stress can be represented by a power

Table 1 Calculated linear equations for the density of the sample in water saturated and frozen states

Rock type	State	a	b	R^2
Medium-grained limestone	Saturated	1.0882	0.1551	0.965
	Frozen	1.1481	0.0323	0.959
Bioclastic limestone	Saturated	1.0933	0.1112	0.989
	Frozen	1.1836	−0.0634	0.991
Rhyolitic tuff	Saturated	0.9625	0.3379	0.909
	Frozen	0.9540	0.3322	0.912

Table 2 Calculated the linear equation of ultrasonic wave velocity versus density

Rock type	a	b	R^2
Limestone	4.3486	−4.4767	0.695
Rhyolite tuff	1.5722	−0.6068	0.598
Ice	4.9942	−0.8585	0.827

law creep equation. For short periods of loading, polycrystalline ice behaves elastically with little recoverable deformation at high loading rates. Under sustained loading, micro cracking may occur under low stresses with the cracks dominating at high loading rates. When ice is loaded at small strain rates, the maximum stress initially remains the same and then decreases with rise of confining pressure (Schulson 1999).

According to the results measured by Schulson (1999), the tensile strength of ice varies between 0.7 and 3.1 MPa and the compressive strength ranges from 5 to 25 MPa over the temperature range of −10 to −20 °C. The compressive strength of ice increases with decreasing temperature and increasing strain rate, but ice tensile strength is relatively insensitive to these variables (Petrovic 2003). The measured strength is under the published values.

The strength of the porous limestone decreased after water saturation but highly increased when it is frozen (test was carried out at −20 °C).

All measured strength of the limestone samples are plotted as a function of density. Both linear and exponential functions exist (Fig. 2).

Using linear equation for determining the strength of the limestone as a function of density is as follows:

$$\sigma = a\rho + b \tag{2}$$

The calculated material constants (a and b) are summarized in Table 3. Using the exponential equation:

$$\sigma_c = ce^{d\rho} \tag{3}$$

Fig. 2 Strength of the Miocene limestone in the function of density (dry, water saturated and frozen states)
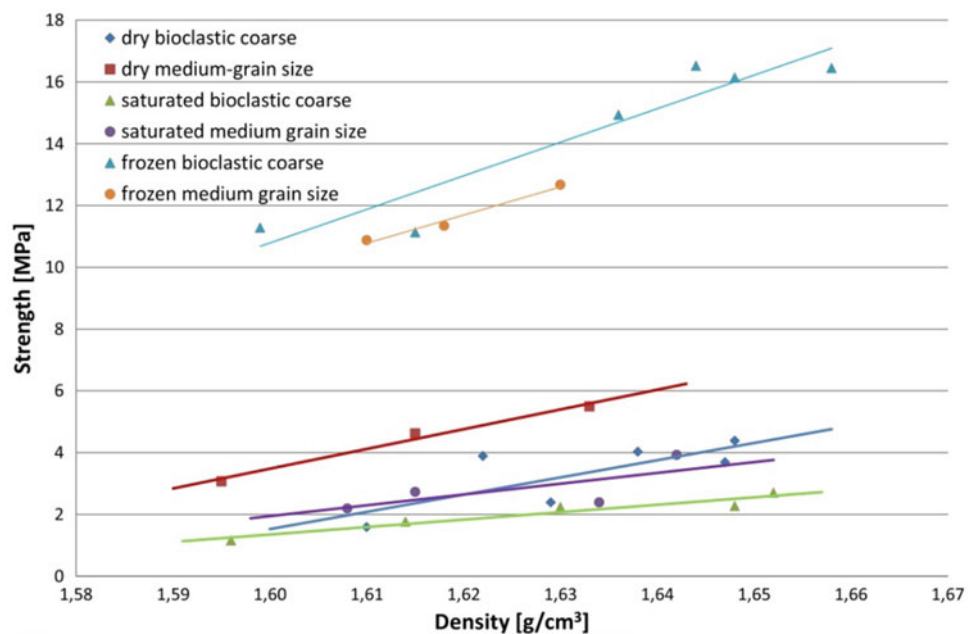
Table 3 Strength of the Miocene limestone as function of density—linear function (Eq. 2)

Rock type	State	a	b	R^2
Bioclastic lmst	Dry	55.791	−87.74	0.580
Medium-grained	Dry	64.015	−98.945	0.984
Bioclastic lmst	Saturated	24.073	−37.165	0.924
Medium-gained	Saturated	34.956	−53.986	0.511
Bioclastic lmst	Frozen	108.64	−163.04	0.895
Medium-grained	Frozen	91.184	−136.03	0.975

Table 4 Strength of the limestone in the function of density—exponential function (Eq. 3)

Rock type	State	c	d	R^2
Bioclastic lmst	Dry	8e−15	20.622	0.603
Medium-grained	Dry	7E−11	15.397	0.961
Bioclastic lmst	Saturated	8E−10	13.276	0.905
Medium-gained	Saturated	2E−08	11.494	0.505
Bioclastic lmst	Frozen	3E−05	7.979	0.891
Medium-grained	Frozen	4E−05	7.744	0.980

The material constants (c and d) are different (Table 4).

According to the measured results, the strength of the rock decreases under water saturation. This loss in strength is approximately 60% of the dry strength which is in good agreement with previously published results (Vásárhelyi 2005). The strength of the frozen saturated limestone is more than double than that of the saturated one (Fig. 2).

The dry uniaxial compressive strength of the medium grained limestone is higher than the strength of the bioclastic limestone since the former one has a more homogeneous microfabric. The opposite was observed when frozen samples were tested, namely, the bioclastic limestone has higher strength in frozen conditions. The strength of the bioclastic limestone increases 4.3 times compared to the dry strength, while the uniaxial compressive strength of the medium grain size limestone increases only 2.6 times compared to the dry strength.

R^2 values suggest that there is good correlation between the strength and density. Typical stress-strain curves of rhyolite tuff are shown on Fig. 3.

Similar to the limestone, the strength of the rhyolitic tuff can be calculated as a function of density (Fig. 4), using both linear and exponential regressions. The material constants according to Eqs. 2 and 3 are summarized in Tables 5 and 6, respectively. Additional data are required to better outline the regression.

Due to water saturation, the uniaxial compressive strength of the rhyolite tuff decreases half of the dry strength. Meanwhile, the strength of the frozen rhyolite tuff is tripled compared to the dry one. The loss in uniaxial compressive strength of rhyolite tuff was already documented (Vásárhelyi 2002). Compared to fossiliferous limestone (Fig. 2), water saturation and frost causes a smaller change in strength (Fig. 4). The difference is related to the micro-fabric of the tuff, which contains significant amount of micro-pores and very porous pumice clasts (Török et al. 2007; Stück et al. 2008). Compared to sandstones (Vásárhelyi 2003) the changes in the strength of dry and water saturated conditions are much higher. Our results show that the changes in the strength of frozen versus

Fig. 3 Typical stress-strain curves of the rhyolitic tuff (dry, water saturated and frozen states)
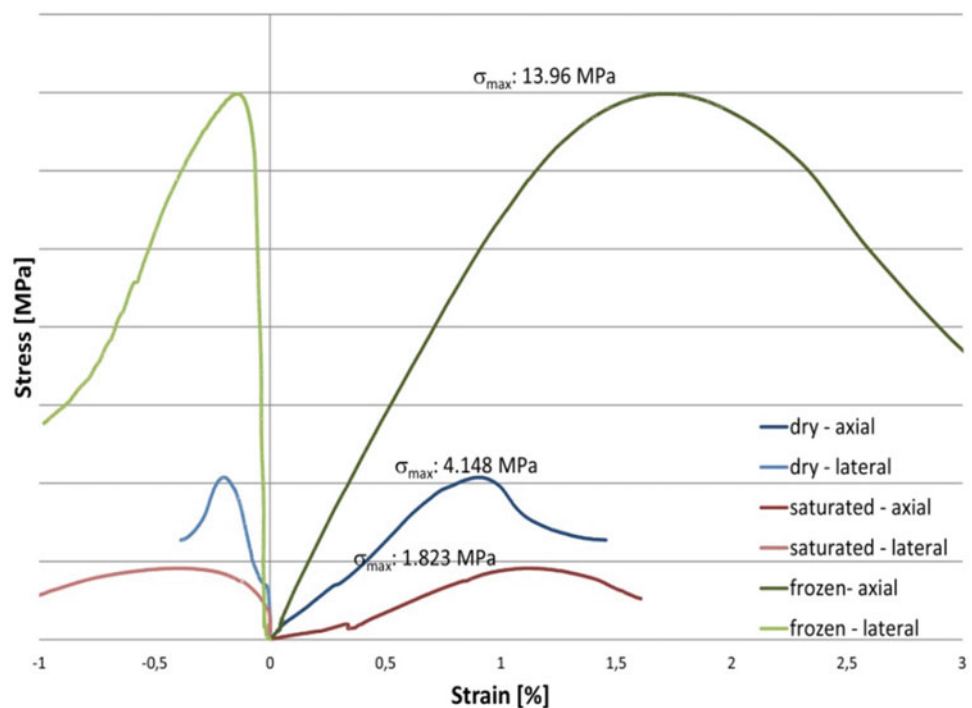
Fig. 4 Strength of the rhyolite tuff as a function of the density (dry, water saturated and frozen states)
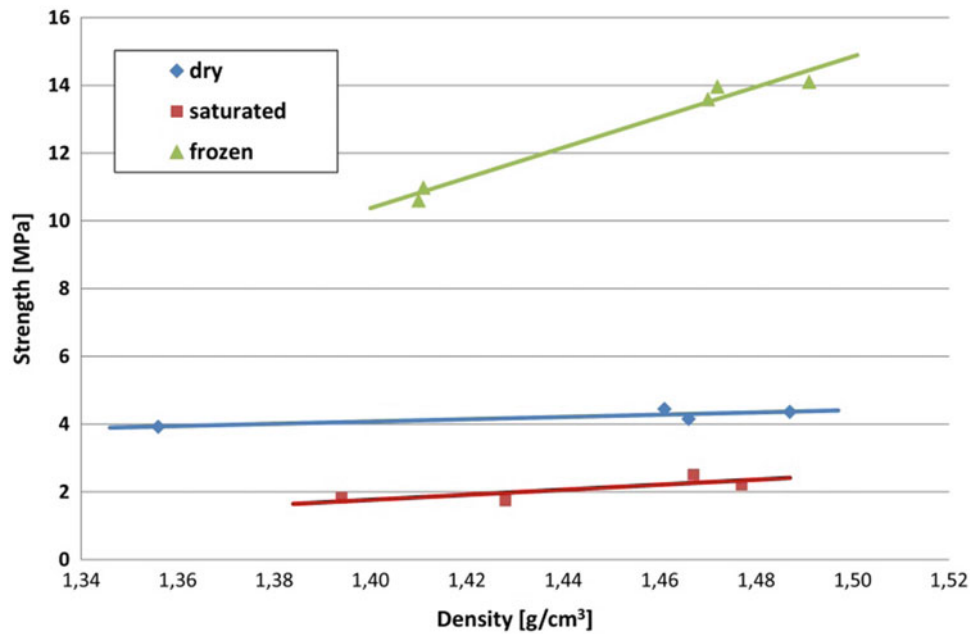
Table 5 Strength of the rhyolitic tuff in the function of the density —linear regression

State	a	b	R^2
Dry	3.3707	−0.6447	0.704
Water saturated	7.4471	−8.6623	0.6372
Frozen	44.7340	−52.2550	0.9725

Table 6 Strength of the rhyolitic tuff in the function of the density —exponential regression

State	c	d	R^2
Dry	1.2977	0.8163	0.719
Water saturated	0.0116	3.5906	0.651
Frozen	0.0640	3.6384	0.969

non-frozen specimens are higher at porous stones than that of the soils (Esmaeili-Falak et al. 1096).

4   Conclusions

The tests of frozen porous limestone and rhyolite tuff samples disprove the idea that in frozen rocks, the ice with its crystallization pressure cause micro-cracking and leads to a lower compressive strength. On the contrary, much higher strength was measured on frozen porous rocks (limestone, fossiliferous limestone, and rhyolite tuff). The ice itself has a strength that is close to the values of the water-saturated strength of the samples. Thus, the strength of ice, dry, and water saturated porous rocks are relatively low, but when the rocks are frozen, very high uniaxial strength values are measured. These experiments have proved that the uniaxial compressive strength of porous rocks can be significantly increased by freezing; accordingly, freezing can be applied to stabilize porous rock masses around tunnels or in deep foundations.

References

Andersland, O.B., Ladanyi, B.: An Introduction to Frozen Ground Engineering. Springer, USA (1994)

Esmaeili-Falak, M., Katebi, H., Javadi, A.: Experimental study of the mechanical behavior of frozen soils—a case study of Tabriz subway. Periodica Polytech. Ser. Civil Eng. (online first) (2018). https://doi.org/10.3311/PPci.10960

Gambino, F.F., Harrison, J.P.: Rock engineering design in frozen and thawing rock: current approaches and future directions. Proc. Eng. **191**, 656–665 (2017)

Kleb, B., Vásárhelyi, B.: Test results and empirical formulas of rock mechanical parameters of rhiolitic tuff samples from Eger's cellars. Acta Geol. Hung. **46**, 301–312 (2003)

Lukács, R., Harangi, S., Guillong, M., Bachmann, O., Fodor, L., Bure, Y., Dunkl, I., Sliwinski, J., von Quadt, A., Peytcheva, I., Zimmerer, M.: Early to mid-miocene syn-extensional massive silicic volcanism in the Pannonian Basin (East-Central Europe): Eruption chronology, correlation potential and geodynamic implications. Earth Sci. Rev. **179**, 1–19 (2018)

Petrovic, J.J.: Review mechanical properties of ice and snow. J. Mater. Sci. **38**(1), 1–6 (2003)

Schulson, E.M.: The structure and mechanical behaviour of ice. JOM **51**(2), 21–27 (1999)

Stück, H., Forgó, L.Z., Siegesmund, S., Rüdrich, J., Török, Á.: The behaviour of consolidated volcanic tuffs: weathering mechanisms under simulated laboratory conditions. Environ. Geol. **56**, 699–713 (2008)

Török; Á.: Surface strength and mineralogy of weathering crusts on limestone buildings in Budapest. Buil. Environ. **38**, 1185–1192 (2003)

Török, Á., Vásárhelyi, B.: Relationship between various rock mechanical parameters of Hungarian travertine and its use in monuments as replacement stones. Eng. Geol. **115**, 237–245 (2010)

Török, Á., Forgó, L.Z., Vogt, T., Löbens, S., Siegesmund, S., Weiss, T.: The influence of lithology and pore-size distribution on the durability of acid volcanic tuffs, Hungary. In: Prykril, R., Smith, J. B. (eds.) Building Stone Decay: From Diagnosis to Conservation, Geological Society, London, Special Publications, vol 271, pp 251–260 (2007)

Török, Á., Barsi, Á., Bögöly, G., Lovas,T., Somogyi, Á., Görög, P.: Slope stability and rock fall assessment of volcanic tuffs using RPAS with 2D FEM slope modelling. Nat. Hazards and Earth Syst. Sci. **18**, 583–597 (2018)

Ulusay, R., Hudson, J.A. (eds.): ISRM: The Complete ISRM Suggested Methods for Rock Characterization, Testing and Monitoring: 1974–2006 (2006)

Vásárhelyi, B.: Influence of the water saturation on the strength of volcanic tuffs. In: Eurock 2002, Madeira. Proceedings of the Workshop on Volcanic Rocks, pp. 89–96 (2002)

Vásárhelyi, B.: Some observation regarding the strength and deformability of sandstones in case of dry and saturated conditions. Bull. Eng. Geol. Environ. **62**, 245–249 (2003)

Vásárhelyi, B.: Statistical analysis of the influence of water content on the strength of the Miocene Limestone. Rock Mech. Rock Eng. **38**, 69–76 (2005)

Vásárhelyi, B., Ván, P.: Influence of the water content for the strength of the rock. Eng. Geol. **84**, 70–74 (2006)

Wong, L.N.Y., Maruvanchery, V., Liu, G.: Water effects on rock strength and stiffness degradation. Acta Geotech. **11**, 713 (2016)

Reducing Impacts Potentially Triggered by Blasting

Gregory L. Hempen

Abstract

Ore extractions, rock excavations and structures' demolitions have been quickly and cost-effectively conducted by blasting. Blasting, when cautiously performed, will have lessened the potential of vibratory impacts to nearby structures. Adverse impacts may not only affect structures, but may involve workers' harm, the public's response, historic or vibration-sensitive features, geologic hazards (slope instability, sinkhole collapse, …), and natural-resource (flora and fauna) concerns. Documented cases have noted these adverse impacts triggered by blasting. Merely monitoring air blast and vibration has no ability to identify or minimize the array of potential adverse impacts. The three primary and many secondary impacts (described in the paper) can be controlled by the blasting parameters used and, for some projects, by additional mitigating measures. Typically, the Blasting Contractor has the understanding and capability to avoid the impacts to workers and structures, and to lessen the public's response. Achieving the required goal of the blasting project may require reduced blasting efficiency to minimize the risk of inducing secondary impacts. Detailed investigations of the potential impacts, geophysical assessments of both the sites and triggering parameter levels for those potential impacts, and/or the necessity for mitigating actions may be required for some blasting projects. Two case histories cite the proper approach toward lessening the potential for human, geologic-hazard, natural-resource, and structural impacts without diminishing the capacity to effectively perform the blasting. Blasting can be conducted to achieve the project's goals with a low potential of triggering adverse impacts.

1 Introduction

Blasting is considered an extremely dangerous endeavor by the public. Blasting is very effective in moving low-tensile materials (rock and concrete) that cannot be easily excavated mechanically. It is effective, because the chemical release of energy from the blasting agent over a very short period produces a brisant detonation pulse and great gas-volume production. The detonation wavefront fractures the low-tensile material surrounding the shot hole. The near-hole fracturing is required to allow weakening of material in concrete and in massive rock units without joints and bedding planes. The confined gas production then causes tensile breakage in bending and displacement of the material.

Most experienced blasters design their initial, shot-hole and timed-delay pattern based on empirical equations and their experience with concrete or local rock units. The blaster then modifies subsequent shot-hole and timed-delay patterns relative to prior shot patterns by the: effectiveness in meeting the contract's requirements for the blasting; cost to perform the shot in labor, materials, equipment demands and time; and, caused, or risk of causing, adverse impacts. Controlled blasting, defined in Hempen (2018) and US Army Corps of Engineers (USACoE) (in press), is the desired type of blasting for all projects.

Required responsibilities of any project that may use blasting should be to resolve the adverse impacts for the project and the restriction of blasting procedures, or associated actions, to minimize adverse impacts.

G. L. Hempen (✉)
EcoBlast LC, St. Louis, MO, USA
e-mail: gregory.hempen@springer.com

2 Adverse Impacts from Blasting

Some impacts from blasting have the potential for human mortality or morbidity. Other impacts risk serious losses that either can never be made whole or cannot be returned to their original state. Projects have been delayed and significant costs have been incurred, when an adverse impact developed that was not foreseen and had appropriate limitations within the projects' contract documents.

The primary impacts from blasting are well-documented and can be controlled by an experienced, reputable Blasting Contractor. The secondary impacts may be cited, and limitations applied to minimize the risk of those impacts, in the project's blasting contract. Secondary impacts occasionally have been overlooked or were not sufficiently understood to be limited within a project's blasting contract. Some residual risk for blasting impacts will remain for any blasting program. One of the owner's or project consultant's goals should be to cite the primary and plausible secondary impacts, and to provide a metric of tolerable limits or precautions to lessen the risk of those impacts occurring.

2.1 Primary Blasting Impacts

Three primary impacts, flyrock, wave production (vibration on land or overpressure through water bodies), and air blast, require controlling measures for most blasting projects. Controlled blasting may be conducted for mineral production, tunneling, foundation development or structural demolition. Many authors have provided useful definitions of, and means to control, the primary impacts.

Flyrock. Flyrock is the launching of blasted material's projectiles from the shot pattern. The projectiles may range from innocuous small pieces [0.1 m (m) in maximum dimension or smaller] thrown a short distance (less than 5 m) to potentially damaging projectiles (larger than 0.2 m in maximum dimension) thrown further than 30 m.

Flyrock may be difficult to control for some weathered or fractured rock being shot. The blasting parameters dominantly control flyrock. Flyrock may be further controlled by not stripping the soil overburden or by soil or bagged material being placed on the surface of the shot pattern or by commercial blasting mats being laid over zones needing to be controlled. Flyrock is no issue for underwater blasting projects, where the rock or concrete collar of the shot hole exceeds 1.0 m of water depth.

The risk of damage from flyrock is project-dependent. Some project locations may be in urban areas, where practically all flyrock could cause some damage. Other project sites, for example, large mineral production operations, may have tolerable flyrock restrictions of larger blocks thrown significant distances.

Wave Production—Vibration and Overpressure. Vibrations develop from the detonation wave passing into the medium being blasted. The shock wave or ground vibration is modified and attenuated in the wave's passage to greater distances. Following the laws of optics, the shock wave is refracted and reflected at impedance boundaries, and dispersed into a lower frequency, longer total-duration wave train as distance from the blast pattern increases. The vibration in solid media is converted to pressure waves, commonly termed overpressure, at the boundary with a fluid. The fluid may be a liquid, usually water, and the overpressure wave may have an adverse impact on structural surfaces or upon flora or fauna within the fluid. The bounding fluid also may be a gas. The overpressure wave through air is air blast (or noise), and is noted as the third primary impact below. Overpressure waves may be introduced directly into the fluid by rifling ejecta from a poorly confined shot hole or by early venting of gaseous products through some weak passage of the material being blasted.

The level of vibration entering the solid medium being blasted is a function of the blasting agent's properties, its confinement, the maximum charge weight (within the entire shot pattern) per delay, the minimum delay period and the firing sequence for the shot pattern. Only blasting parameters control the source detonation wave, which then becomes the ground vibration as it passes into the solid medium being shot.

Both ground vibration on land and overpressure in water typically have greater distances of potential impact than flyrock for the same metrics of the blast pattern.

The impact of ground vibrations, which has been well-documented in the literature, is dependent upon the distance to structures from the blasting locations, the geology of the project site, and metrics of the blast pattern. The parameters of the blasting are the dominant conditions that easily may be varied to control vibrations.

The amplitude and other measures of overpressure in water, which has many remaining areas to be studied, are dependent upon the geometry and bathymetry of the water body in relation to the blasting, the distance to the wetted surfaces of structures, the geology of the project site within which the blasting occurs, and metrics of the blast pattern. The parameters of the blasting are, again, the major issues that may be varied to readily control the important measures of overpressure traveling through water.

The overpressure wave through a fluid, whether a liquid or a gas, may be diffracted by temperature or pressure stratifications of the fluid or by currents within the fluid. Amplitude attenuation and waveform modification

(in frequency and wave cycles) by travel distance are functions of the variability of the bathymetry and temperature of the water body, and of the physical properties of the bottom's or the shore's solid media.

Air Blast. Air blast or noise (or sound) is the overpressure wave production in air due to blasting. The overpressure wave is attenuated with travel distance from the blasting pattern. The air blast is the sound released from the venting gases released from the displaced blasted medium or from poor confinement.

The amplitude of the source air blast is related to the confinement of the blasting agent, the maximum charge weight (within the entire shot pattern) per delay, the minimum delay period, the firing sequence for the shot pattern, and the movement of the medium being blasted. Blasting parameters, extent of confinement and the blasted medium's displacement in time throughout the shot pattern control the source overpressure wave in air.

Air blast typically reaches the greatest distance of potential impact, as compared to the other two primary blasting impacts for the same blasting parameters. Air blast most often produces the least damage relative to other primary impacts, but may be more problematic as a nuisance issue with the public.

Overpressure may be diffracted by air temperature variations above the ground surface or intensified in the downwind direction. The air blast impact is conditioned by the distance to structures or living receptors from the blasting locations, the weather and the time of day when the shot occurs, metrics of the blast pattern, and how the blasted medium is displaced by the shot pattern. A uniform reduction of temperature with the height above the ground conducts the overpressure wave away from the ground surface, which lowers the risk of excessive airblast to structures or the occupants within the structures. Temperature inversions of warm air above cooler surficial air, which often occur with storms or at sunrise or sunset, refracts the air blast back to the ground, increasing the risk of excessive airblast. Avoiding blasting during thunderstorms, during windy conditions, and at sunrise and sunset nearly eliminates air blast as a major impact. The "noise" from a blast may tempt nearby residents to complain, especially when blasting is not anticipated or conducted outside of typical business hours or conducted on weekends.

2.2 Secondary Blasting Impacts

There are four general types of secondary impacts caused by blasting, which are due to wave production or air blast. These secondary impacts are the issues that should be resolved by the owner or the project's consulting firm as potential conditions susceptible to blasting impacts before developing contracts involving blasting. Most projects should determine whether any hazards or concerns could lead to adverse impacts when exposed to blasting on the owner's property or within 300 m of the likely blasted medium. Some instances may develop where the impact assessment range is much greater than 300 m.

Environmental Impacts. The blasting industry uses the adjective, "Environmental," to describe the better-known blasting impacts of Structural Concerns and Public Nuisance. USACoE (in press) and many others authors describe how structural concerns and public nuisance are caused by ground vibrations and air blast.

Structural Concerns. Shaking of structures by blasting may have a range of effects. The blast vibrations merely may be noticed by those within the structures or may cause unrestrained contents to rattle and shake. The ground vibrations may be severe enough to cause architectural damage, such as cracks in dry wall or plaster, or to result in masonry or foundation cracks and differential settlement. Air blast may cause windows to rattle, but it would be rare for air blast to cause more damage than the damage due to ground vibrations from blasting. The wetted face of submerged structures may be damaged by spalling from overpressure waves, when the blasting is underwater or near a water body.

Some older or poorly maintained or improperly founded structures, like mobile homes, may be very sensitive to low-amplitude horizontal vibrations in the frequency range of the blast's ground vibrations.

Public Nuisance. Humans are more sensitive to both air blast and ground vibrations than the initiation of damage to structures within which the individuals are exposed to the impacts. Complaints about the blasting may develop without any architectural or structural damage to structures.

Vibration-Sensitive Features. Guidance for minimizing blasting impacts to sensitive features is not complete. The tolerable amplitude level of ground vibration can vary over two orders of magnitude for different features at diverse distances. The frequency range of tolerable vibrations at the sensitive feature may nearly match, or may be significantly different from, the frequency range of the blast's ground vibration. Allowable ground vibrations from blasting should be assessed for all locations of vibration-sensitive features, which could reasonably be impacted.

Sensitive Devices. A variety of commercial, medical and scientific devices spin very rapidly or move over tiny, angular or displacement measures, which cause the device to be very sensitive to shaking. Equipment, machines, and instruments are likely to be sensitive to vibration, if those devices are required to be on foundations or platforms that isolate the device from the surrounding structure. Allowable base vibrations for sensitive equipment may be a small fraction of the ground vibrations that cause the onset of typical structural damage. The frequency range of the

allowable vibration is important, because the frequency of both the ground vibration and the response of the structure to the ground vibration may be very different from the frequency range of the small, allowable base vibration amplitudes for the sensitive device. Vibration-sensitive devices usually will have allowable, base vibration limits provided by the manufacturer.

Historic and Archeological Features. Poorly-maintained historic structures and archeological features may be in the vicinity of the blasting. Historic structures may not have had their foundations stabilized and improved, see Fig. 1.

Foundations and masonry parapets of historic structures and very old tombstones may be elements that have not been restored, but are quite sensitive to horizontal ground vibrations. A historic register could list structures near the project. Archeological features, such as cairns, may be impacted by ground vibrations. Archeological features, which are sensitive to blast vibrations, may not be listed in a catalogue that might easily be found or searched.

Induced Geologic Hazards. Many geologic hazards are sensitive to varied triggering mechanisms. Ground vibrations from blasting may be of sufficient amplitude to trigger a barely-stable geologic hazard. Blasting vibrations may be assessed by comparing the impacts induced by earthquakes. Kramer (1996), citing several authors, provides examples of liquefaction, lateral spreading, and varied types of mass movement induced by earthquakes. Earthquakes have caused cave accretions to break and fall.

Fig. 1 Photo of an historic building in rural United States with an enlarged inset of the stacked stone columns for the porch and the log foundation in the background (Hempen 2015). Small horizontal vibrations may be damaging to this structure

Mass Movement. Keefer (1984) meticulously cites and describes several types of mass movements, which have been induced by earthquakes. Keefer (1984) further notes the relative abundance of mass movements caused by earthquakes. This relative abundance suggests the types of landslides, which may be susceptible also to being triggered by blast vibrations. The landslides types, which were not commonly induced by earthquakes, would require somewhat larger amplitudes or greater energy to be at risk from blast shaking. Keefer (1984) provides the predominant minimum Modified Mercalli Intensity (MMI) necessary to trigger each type of landslide. The minimum MMI can be related to both a minimum triggering acceleration and particle velocity. Kramer (1996) details procedures to estimate the earthquake acceleration necessary to cause a stable, designed mass to approach the point of instability.

The information from earthquake-induced mass movement may be applied to these hazards from blasting. Simple calculations and predominant frequency histograms for three types of blasting from Dowding (1985) allows an assessment of possible peak acceleration or peak particle velocity for blast-induced triggering of landslides or designed embankments near a blasting project. Nearby, potentially unstable slopes or designed embankments should be assessed for the allowable ground motions at that location, which are unlikely to induce a failure.

Liquefaction and Lateral Spreading. Kramer (1996) develops how liquefaction may be triggered by earthquakes. Liquefaction may lead to differential settlement or lateral spreading depending upon many conditions.

Multiple variables control whether a soil mass will reach the state of initial liquefaction. Some of the variables are: soil type and particle-size distribution with depth below the surface; whether soil units have been consolidated, cemented, and/or aged; the level of the groundwater surface at the time of shaking and the saturation of the varied soils in the profile; whether there are any shear stresses on the soils due to a sloping ground surface or loading of an existing structure; and, the amplitude, duration, and frequency of the ground shaking through the soil column.

Similarly, blasting has been used to induce liquefaction for foundation improvement. Controlled blasting at a specific project is unlikely to induce initial liquefaction within a large enough soil volume near the shot pattern to allow differential settlement or lateral spreading to occur. The onset of initial liquefaction due to blast vibrations cannot be dismissed without evaluation of the soil types and groundwater surface near a project's blasting.

Karst Collapse. Spectacular sinkhole collapses and devastating releases of pond contaminants through karst groundwater channels have been documented with no known triggering mechanism. Sinkhole collapse may damage structures, buried utilities or infrastructure. Blasting can induce a sinkhole collapse beneath a structure. Williams and Vineyard (1976) cite only two documented cases of blast-induced karst collapse of 97 cases noted over a 45-year period in the state of Missouri. While documented cases of blast-induced sinkhole collapse seem to be rare, there is uncertainty in the number of actual cases. Some blast-induced sinkhole collapses must have occurred, which: were never documented as sinkholes; were noted as a new sinkhole, but not within a time period to relate the collapse to a blasting project's ground vibrations; or, were recognized as blast-induced sinkhole collapses, but either were not reported or such reporting has been destroyed or has not been found by a capable investigator.

Blasting, which may be contracted in an area of known karst conditions, should resolve whether any type of nearby structures has a potential to be founded above a karst void. If that potential exists, the location(s) of such structure(s) should be noted and an allowable ground vibration(s) specified that will minimize the likelihood of a collapse into a possible karst void.

Natural-Resource Impacts. Impacts to natural-resources are more commonly termed "environmental" hazards, but that latter term has been used in the blasting industry for the impacts cited above. Natural-resource impacts, herein, will refer to any protected flora or fauna or habitat, so listed by a regulating body, or to any commercial organisms for which a significant reduction would cause an adverse economic loss in that industry. Keevin and Hempen (1997) list general types of protected organisms, note US state regulatory concerns, and suggest some measures to mitigate blasting, particularly near a water body or underwater. Some organisms included under natural-resource concerns are terrestrial and able to move away from an active project with periodic blasting. Yet the habitat of those terrestrial organisms may be adversely impacted by the blasting or the project itself. Some blasting projects need to account for protected species of birds that may be harmed while in flight above the initiated blast or indirectly impacted by loss of habitat from blasting or the project. Many protected organisms, which may be harmed by blasting, are aquatic or marine life. For these latter organisms, overpressure waves in water should be assessed from blasting near a water body or underwater. USACoE (in press) and Hempen (2008) develop important aspects of underwater blasting and the mitigation of impacts.

The evaluation of natural-resource impacts must be taken seriously. Blasting projects have been delayed, blasting procedures have been significantly diminished or altered, difficult monitoring procedures have been required, and project objectives have be changed, because a protected organism had not been properly and fully considered in regard to blasting, or was not adequately protected in contract documents.

3   Minimizing the Risks of Adverse Impacts

Blasting can be conducted to achieve the project's goals with a low potential of triggering adverse impacts to surrounding areas. Adverse secondary impacts from blasting cannot, and will not, be minimized unless such impacts are recognized. The recognition of potential impacts will lead to a resolution whether the concern is warranted and, if warranted, what contract limitations may need to be resolved.

The recognition and assessment of secondary blasting impacts must be conducted during the design phase of the project requiring blasting to achieve the greatest effectiveness. Individuals, experienced with project contracting and management, understand that any significant change of a contract after the work begins may impact the project's objective, lengthen the project's duration, and may increase the cost to achieve the equivalent amount of work. Many projects require some education of the owner (client), the Contracting Officer, the Blasting Contractor, those who potentially could be impacted by blasting, and the general public.

The risk of all potential secondary impacts for a given project should be assessed. Some impacts may be resolved as improbable so that the risk does not warrant action. Regardless of the minimizing efforts taken to avoid a particular impact's risk, some small potential of that particular impact being caused by the project's blasting will exist. Due diligence will assure that any caused impact will be recognized immediately and will not be worsened by continued blasting without correction of the causative work.

3.1   Risks from Blasting Impacts

Confinement of the blasting agent within the shot hole is important for blasting performance and for avoiding the risk of adverse impacts being induced. The issues affecting confinement are the burden in design of the shot pattern, the use of stemming, and the weaknesses of the material being blasted. The burden is the distance between each row of shot holes. The timing of the shot pattern intends to displace the shot medium sufficiently to create a free face for each successive row, like the distance of the first shot-hole row to the original front wall (free face) before the shot is initiated. Confinement becomes excessive when the burden distance is too large for the blasting agent's charge weight to produce that row's detachment from the mass over the full wall height. Confinement is poor when the stemming's type, placement and length are inadequate to contain the blasting agent's gases. Stemming is the granular, crushed stone placed in the shot hole to contain the gases from the explosive's detonation. The gaseous products of detonation

need to be confined to perform all their work. Confinement also may be compromised when the material being blasted has weaknesses that permit venting of the gaseous products. Confinement is adequate for a blast that properly moves material being blasted.

A blast design is optimized when the largest production for the project's objective is achieved both with the lowest cost of labor, blasting and equipment usage and with no, or only tolerable, adverse impacts occurring. Hempen (2018) provides a comparative assessment of performance and of risk of an impact relative to a generalized measure of confinement, Table 1. The blasting performance is good and the risk of all adverse impacts is lowest only when the confinement is adequate. A blast design must be modified to further lessen the risk of any individual impact, which has been recognized and/or has contract limitations to minimize the risk potential.

3.2   General Procedures to Reduce the Risk of Secondary Blasting Impacts

Assessing Blasting Impacts

The design team, during a project's development that may require blasting, should include a few specialists to consider blast-induced impacts and to assist in writing the blasting specifications. The design team should assess the potential for, and rank the risk of, blasting impacts. Merely requiring vibration and air-blast monitoring is insufficient to minimize the array of potential adverse impacts without individual assessment of those impacts.

Personnel to Assess Blasting Impacts. The design team may already include a structural and geotechnical engineers and an applied geologist, each of whom may perform some assessment of potential hazards. The team should consider adding an applied geophysicist experienced in blasting and a natural-resource (environmental) professional. The assembled team will likely need to approach other governmental officers, like the State Archeologist or State or Federal Environmental Regulators, to assure the proper assessment of potential hazards or impacts.

Project-Resolved Blasting Impacts. Each project should resolve which of the adverse impacts has a potential of being induced. The following is an ordered listing of suggested actions. Assess and rank the potential for blasting to induce each of the secondary impacts. Research past similar projects in that area. Determine whether, and which of, the lowest ranking adverse impacts may be eliminated. If secondary impacts are a potential risk, assess the geophysical properties of the project site and the waveform parameter(s) that would be allowable at the hazard without triggering the impact.

Table 1 Comparative performance and risks from controlled blasting

BLASTING LOCATION	CONFINE-MENT	PERFORM-ANCE	RISK OF PRIMARY IMPACTS				RISK OF SECONDARY IMPACTS				
			Air Blast (Over-pressure)	Flyrock (Projectiles)	Underwater Over-pressure	Ground Vibration	Nuisance to the Public	Structural Damage	Sensitive Features	(Biological) Natural Resources	Induced Geologic Hazards
Terrestrial [or Land-based] **blasting**, possibly near water	EX	*P*	**L**	**L**	**L**-m	H	H	H	H	**L**	H
	A	*G*	**L**-m	m	**L**	m	**L**-m	**L**-m	m	**L**	m
	P	*P*	H	H	**L**	**L**	H	**L**	**L**	**L**	**L**
Underwater blasting with water depth greater than 0.9 m, possibly near land or structures	EX	*P*	**L**	**L**	m	H	m-H	H	H	m	H
	A	*G*	**L**	**L**	**L**-m	m	**L**	**L**-m	**L**-m	m	**L**-m
	P	*P*	m	**L**	H	**L**	**L**	m	**L**	H	**L**

[Explosives'] CONFINEMENT	EX - Excessive; **A** - Adequate; *P* - Poor
[Blasting] PERFORMANCE	**G** - Good; *P* - Poor
Potential Impact's RISK LEVEL	H - High; m - Moderate; **L** - Low

Hempen (2018) reprinted with permission

Resolve the contract limitations for each of the potential impacts to minimize the blast-induced risk. The contract limitations may be: allowable air-blast and waveform parameters, air-blast and waveform monitoring at important locations, blasting limitations, specified documentation, temporal restrictions to blasting, pre-blast structural surveys, and/or required blasting mitigation procedures. Write the blasting specifications to describe the potential blasting impact and include the contract limitations. Develop a plan for recognition, response and mitigation for the occurrence of each potential adverse impacts. Have a paper exercise at a random time for those adverse impacts, which are more serious or have a greater potential to be induced.

General Elements to Consider within a Blasting Specification. The following elements may be useful to be included within many blasting contracts, but may not necessarily be appropriate at a specific project.

Include any time or date limitations for blasting. Only allow blasts to be initiated an hour after sunrise through an hour before sunset on regular business days. Provided owner-requested time restrictions for work related concerns, such as shift changes. Include seasonal restrictions as necessary for natural-resource impacts.

Require appropriate blasting-contractor's personnel to be available for public meetings and media interviews. Require the Blasting Contractor to advertise a phone number and mailing address for complaints and damage claims. Require the Blasting Contractor to respond to, and settle, all claims as quickly as possible, and to report all damage claims to the Contracting Officer.

Require the Blasting Contractor to subcontract blast monitoring and reporting service to an independent specialty firm. Have the independent specialty firm conduct pre-blast surveys of the nearest structures that are within 150 m by azimuth about the proposed blasting area, and provide those reports to the Contracting Officer and each property owner having the pre-blast survey. Have post-blast surveys completed, if necessary, by the same independent specialty firm for reasonable damage claims. Require the independent specialty firm to monitor air blast and ground vibration at all noted locations for every blast at the project site and provide a report for each blast that compares the monitored measures to the allowable contract limitations. If underwater overpressure monitoring or mitigation measures are required, carefully select a qualified specialty firm that has successfully performed such duties.

Include a Test Blasting Program. Require the Blasting Contractor to begin with smaller charge weights and few shot holes for the first test blast at the project. The charge weights and number of shot holes only may be increased in sequential, subsequent shot patterns to production controlled-blasting levels, when the recorded air blast and vibrations have remained below the allowable contract limitations at all monitoring stations.

Require the Blasting Contractor to temporarily delay blasting until there is approval of a remedy for any induced adverse impact or misfire or blasting accident.

3.3 Project Examples of Reducing the Risk of Secondary Blasting Impacts

A Project with Potential Risks of Inducing Geologic Hazards

Project Development for Blasting. The Tennessee Valley Authority (TVA) recognized that rock blasting for a landfill surface could impact varied features near a TVA Power

Plant. Skeggs et al. (2017) cites the successfully-completed blasting program to create the uniform rock foundation of a dry-ash landfill.

The project's design team recognized the potential impacts of blast-induced sinkhole collapse under the ash ponds near the blasting, and upon an aging rock slope, historic cemeteries and archeological structures. The design team under took evaluations and field reconnaissance of each of the potential impacts. Karst conditions were known to exist within the limestone at the site. The presence of karst conditions below the extensive ash-ponds could not be confirmed due to the age, size and original construction details for the ponds. Plans were assessed to monitor the varied, potential impacts, and to respond quickly to an occurring, blast-induced impact. A physical monitoring was regularly scheduled for the entire blasting program and was conducted by the owner's consulting firm. The physical monitoring included: pond water-surface elevations, the ground-water elevation in monitoring wells, and visual inspections of the pond embankments, aging rock slope, historic cemeteries and archeological structures.

The team assessed allowable air-blast and vibration limits to reduce the risk of varied impacts. A geophysical appraisal was performed to anticipate blasting vibration parameters that could induce each hazard. The vibration limits were linked to the range of the shot pattern from the varied potential impacts. Air blast and vibration monitoring and immediate post-shot reporting were included in the specifications to assess each shot pattern's parameters relative to the contract limitations. No mitigating action for the blasting was determined necessary.

The specifications included a test blast program, which required the blasting to begin the program with small charge weights for a few loaded shot holes. The area designated for the test blasting was remote to the potential impacts. With each test blast's monitoring remaining below vibration limits, the subsequent test blast was allowed to increase the explosive's charge weight per delay and the shot pattern's number of shot holes. The test blasting program proceeded uniformly to the scale of the blaster's anticipated production blasting parameters without any restrictions and without any of the secondary impacts being triggered.

Results of the Blasting Program. The blasting program was accomplished within budget with no significant vibration limits being exceeded and no blasting impacts about the site. The blasting was conducted with only afternoon weekday shots planned around the TVA shift schedule. No complaints were received from the residential area nearest the project.

A Project with Potential Risks to Natural-Resources

Project Development for Blasting. The California Department of Transportation (CalTrans) wished to develop a program to demolish the East-span's piers of the old San Francisco-Oakland Bay Bridge (SFOBB) in the San Francisco (SF) Bay (California, USA) after the new bridge was placed into service. CalTrans recognized that blasting would be the fastest and least expensive method to remove the piers, but blasting had significant natural-resource restrictions in the water bodies throughout the state. CalTrans (California Department of Transportation 2017) reports on the beginning phase of a multi-year program to remove SFOBB piers by blast implosions.

CalTrans approached a consulting team to determine if there was a means to remove the old SFOBB piers by blasting without excessive fish kill, and with no impact to listed endangered species and to marine mammals. The consulting team proposed to: evaluate the likely controlled-blasting design to remove the first and largest pier; design a reusable Blast Attenuation System (BAS), an air-curtain system, to reflect and attenuate the water-borne overpressure waves from each pier's blast; estimate the overpressure amplitudes beyond the BAS; and, recommend an overpressure monitoring program for the early phase pier demolitions. CalTrans proposed a demonstration project for the first pier's implosion using the consulting team's study. The BAS, if proven to furnish beneficial mitigation in the first pier's implosion, would be deployed around piers for all implosions. CalTrans coordinated and modified the demonstration project with a myriad of local, state and federal stakeholders' input and acceptance.

The project required careful assessment of fish and marine mammals' impacts in the SF Bay. Coordination with, and permits from, varied agencies determined the acceptable means to: conduct the blasting in season of likely low impact to natural-resources; resolve the watch program and its coordination with the blasting to be assured of no marine mammals being near each pier's implosion; determine overpressure-parameter limits for the blasting; deploy an overpressure monitoring system; and, conduct a caged-fish study just beyond the BAS mitigation for the first pier's implosion.

The early phase of implosions included three massive piers, which were a short distance south of the active new SFOBB. Piers E3, E4 and E5 are lightly reinforced, concrete cellular caissons with a horizontal section at the SF Bay's water elevation of 25 m by 51 m. Pier E3 extend 70 m below the waterline into the bay's sediment, still 35 m above

bedrock. The demonstration implosion caisson, Pier E3, was to be removed to 21 m below the water level, just into the bay sediment. The difficulty of estimating the overpressure amplitudes beyond the BAS was being uncertain of: the explosive charge weight per delay that would actually be used by the blaster, the greatest depth of explosive placement, the physical parameters of the SF Bay sediments, and the amount of overpressure energy that would diffract beneath the BAS without being mitigated.

CalTrans contracted with a design-build joint venture to conduct the pier implosions with the potential need to modify various activities over the successive phases of SFOBB pier demolitions.

Results of the Blasting Program. The project illustrates how an owner, specialty consultant, regulating agencies, contract managers, and a design-build contractor may work cooperatively to achieve an effective, cost-controlled project without severe adverse impacts.

The joint venture effectively removed the first three massive piers in single, shot patterns on a weekend day for each pier. There was no observation of marine mammals at the time of each pier's implosion. The BAS, which was anticipated to have a 75–90% reduction in the overpressure amplitude, was found to have actually averaged 73.6% reduction. Some energy from the blast was diffracted beneath the BAS without mitigation. The BAS reduced a stipulated exposure level's impact area by 90% compared to the appraised impact without the BAS mitigation. The caged fish at four distances beyond Pier E3 should have had a range of mortality out to the greatest distance of cages, 245 m, if the BAS was not deployed. The substantiation of the BAS's effectiveness was resolved from the Fish Study's finding for Pier E3 that no mortality occurred to the caged fish beyond the BAS mitigation at any of the four distances, as assessed both by live fish immediately after the implosion and by their necropsy.

4 Conclusions

All projects have varied risks. Many projects are designed and completed by professional guidance and/or experience that considers most project impacts. Blasting has not been well developed to inform designers of potential secondary impacts, which may be triggered by blasting. Design teams can consider and rank which impacts may plausibly be induced by blasting. Just the exercise of considering these impacts prepares the design team to be more effective in contracting for blasting.

Complex or extensive blasting programs should be restricted to minimize, and preferably avoid, blast-induced adverse impacts. The small cost increase for project design, contract development and blast contracting may avoid human mortality or morbidity or other impacts that cannot be easily returned to their original state or otherwise compensated.

References

California Department of Transportation: San Francisco-Oakland Bay Bridge (SFOBB), East Span Seismic Safety Project, SFOBB Old Spans Piers E3-E5 Implosions Project Report, EA 04-01357 or EFIS#: 04-16000287, 141 p with appendices (2017)

Dowding, C.H.: Blast Vibration Monitoring and Control. Prentice-Hall, Inc., 297 p, ISBN: 0-13-078197-5 (1985)

Hempen, G.L.: Destructive water-borne pressure waves. In: Proceedings of the Sixth International Conference on Case Histories in Geotechnical Engineering, Arlington, VA, Missouri University of Science and Technology, Rolla, MO, 11 p (2008)

Hempen, G.L.: Blast-vibration consulting, picture taken during field work, personal communication (2015)

Hempen, G.L.: Blasting. In: Bobrowsky, P., Marker, B. (eds.) Encyclopedia of Engineering Geology, Encyclopedia of Earth Sciences Series, Springer, Cham, 3 p, Online ISBN: 978-3-319-12127-7 (2018)

Keefer, D.K.: Landslides Caused by Earthquakes. Geological Society of America, v 95, April 1984, pp 406–421 (1984)

Keevin, T.M., Hempen, G.L.: The Environmental Effects of Underwater Explosions with Methods to Mitigate Impacts, Legacy Report (Department of Defense study grant), U.S. Army Corps of Engineers, St. Louis District, St. Louis, MO, 145 p (1997)

Kramer, S.L.: Geotechnical Earthquake Engineering. Prentice-Hall, Inc., 653 p, ISBN: 0-13-374943-6 (1996)

Skeggs, D., Lang, G., Hempen, G.L., Combs, R., Clemmons, M.: Controlled blasting for CCP landfill construction. In: World of Coal Ash Conference, Landfill Session V, Paper 206, Lexington KY, 11 p (2017)

US Army Corps of Engineers: Systematic Drilling & Blasting for Surface Excavations, EM 1110-2-3800. Washington, DC, 260 p & 2 appendices (in press, expected September 2018)

Williams, J.H., Vineyard, J.D.: Geologic indicators of subsidence and collapse. In: Karst Terrain in Missouri. 55th Annual Meeting, Transportation Research Board, Washington, D.C., January 21, 1976, 20 p (1976)

Non-destructive Surface Strength Test—Duroskop a Forgotten Tool; Comparison to Schmidt Hammer Rebound Values of Rocks

Ákos Török

Abstract

The paper gives an overview of the test mechanism and use of Duroskop and Schmidt hammer in rock strength assessment. Duroskop is a forgotten tool that uses the same principle as a Schmidt hammer: it detects rebound values of tested surfaces. It can be applied for testing the hardness of rock surfaces to detect small scale variations in strength. Rebound values were measured on selected lithologies such as porous limestone, travertine, micro-crystalline limestone, marble, andesite tuff and basalt. The rebound values of Duroskop and 4 types of Schmidt hammer (N-34, L-9, Digi-Schmidt and PT) are compared. Not only fresh but also weathered surfaces were measured in order to assess effect of weathering on rock strength. The obtained rebound values were compared to the standardized laboratory strength test results of the same lithologies. Relationships between Duroskop rebound values and Schmidt hammer values are presented. The values of Schmidt hammer rebound and Duroskop rebound can be correlated. The latter detects minor changes in surface strength but is more sensitive to surface irregularities. Overall, these experiments indicate that special attention is needed for the interpretation of non-destructive strength test results since these tools do not provide exact data on the compressive strength or tensile strength of rocks. Nevertheless, rebound vales of Duroskop, similarly to Schmidt hammer, provide rapid information on the strength of the tested rock.

Á. Török (✉)
Department of Engineering Geology and Geotechnics, Budapest University of Technology and Economics, Műegyetem rkp. 3., Budapest, 1111, Hungary
e-mail: torokakos@mail.bme.hu

1 Introduction

Rapid on-site assessment of rock strength is an important issue in engineering geology, with wide a range of applications from rock engineering to monumental stone diagnostics. One well-known test tool is the Schmidt hammer. It was invented to test the surface strength of concrete by Swiss Ernst Schmidt in 1950, using the principle that a spring-loaded mass is released against a plunger when the hammer is pressed onto the surface and it rebounds from the test surface (Schmidt 1951). In the past 67 years, this method has been widely used for on-site testing of concrete strength and later it was also successfully applied for rocks (Kahraman 2001). It has been demonstrated that the Schmidt hammer can be used for measuring strength parameters (Aydin and Basu 2005; Yagiz 2009; Tandon and Gupta 2015; Yılmaz and Sendir 2002) and also grades of weathering (Viles et al. 2011; Török 2003). The uniaxial compressive strength of concrete can be determined from Schmidt hammer rebound values using calculations and standards. No such standardized procedures are known for calculating the strength of rocks, but recent attempts and suggestions were made to clarify methods to use this tool for rock testing (Aydin 2008). The problem of using Schmidt hammer for rock testing is related to the fact that several types of Schmidt hammer exist, and only a few of them have been standardized for stone testing. Another tool that is very similar to the Schmidt hammer and that can also be used for testing rock (Török 2010) is the Duroskop. This paper compares the test results of 4 types of Schmidt hammers with Duroskop and outlines the use and limitations of these tools in rock strength testing. The paper also emphasizes the fact that these methods provide rapid condition assessment of rocks and building stone surfaces, however, for the numerical interpretation and comparison with laboratory strength tests, large amount of rebound data and validation are needed.

2 Materials and Methods

Four types of Schmidt hammers exist, including types of N-34, L-9, and Digi-Schmidt (Fig. 1). These three types can be used on vertical, horizontal, and tilted rock surfaces. The fourth type is the PT Schmidt hammer in which the mass moves on a half-circle path providing impact values only from vertical surfaces (Fig. 2). The Duroskop was developed for testing metals, but in the past decades it has also been used for rock testing. It has a smaller pointed mass that rebounds from the surface (Fig. 2), and it is efficient when small surface strength changes need to be detected (Török 2003). For each tool, 10 readings were measured on one tested surface of 40 cm^2. On tested rock surfaces at least 10 areas of 40 cm^2 were selected and thus a minimum of 100 rebound values were measured. Mean, minimum and maximum values as well as standard deviations were calculated.

Six lithotypes were studied (Fig. 3). The first one is a highly porous Miocene limestone (Fig. 3a). This type of limestone is widely used in monuments of Hungary (House of Parliament, Mathias Church or the Basilica in Budapest) and is very similar to the ones of Austria (Vienna, St-Stephan's Church, Schönbrunn Palace) or the porous limestones of France (Castles of Loire valley) (Al-Omari et al. 2015) or UK (Oxford) (Török 2003). Tested travertine is also from Hungary and is a well-known construction material from Roman times (Al-Omari et al. 2015). This Pleistocene carbonate was deposited from lukewarm springs and was also found in lacustrine environments (Fig. 3b). It shows similarities to the travertines of Rome–Tivoli, Italy.

The third tested carbonate is a micro-crystalline red Jurassic limestone (Gerecse Mountains, Hungary). This nodular limestone (Fig. 3c) is very similar to the Ammonitico Rosso of Verona. Studied Miocene andesite tuff was formed in relation to volcanic activity of the Carpathians in Hungary. The tuff contains small lithic clasts such as pumice or andesite (Fig. 3d). It is the construction material of several castles and fortresses, such as Visegrád in north-central Hungary. The second tested igneous rock is dark grey microcrystalline basalt (Fig. 3e) with minor amounts of olivine and pyroxene phenocrysts. It forms cone shaped hills at Balaton Highland (Hungary) and is mostly used as walls or as aggregates. Carrara marble was also tested (Fig. 3f). The studied slabs were used as tombstones in a cemetery in Budapest.

3 Results and Discussion

Comparing the readings of different tools when the same stone slab was tested provided valuable information on the differences of rebound values of Duroskop and Schmidt hammer types (Table 1). A travertine slab (Fig. 4) and a porous limestone (Fig. 5) were used for testing each tool.

On cut travertine surface the mean Duroskop rebound value was 38, but this equipment has the highest scatter in data. When Schmidt hammers were compared, the highest obtained rebound values are related to PT Schmidt with a mean value of 122. It was followed by Digi-Schmidt, N-34 Schmidt and L-9 Schmidt, with mean rebound values of 57, 45 and 43, respectively. From among the Schmidt hammers the L-9 one has the largest scatter in readings (Fig. 4).

When the cut surface of porous limestone was tested with Duroskop and Schmidt hammers, a similar trend was found

Fig. 1 Schmidt hammer types. **a** N-34 and L-9; **b** Digi-Schmidt
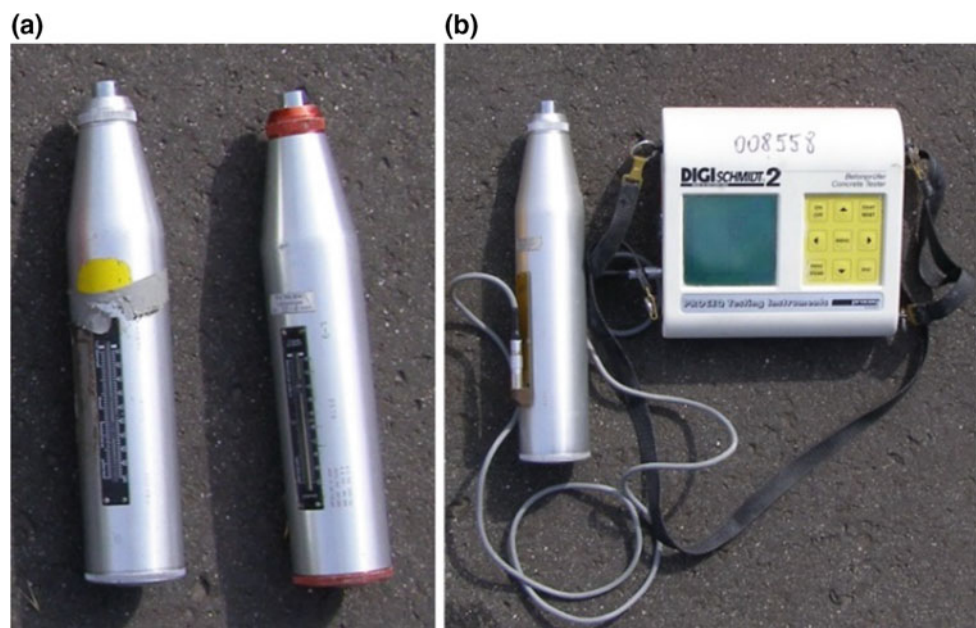
Fig. 2 PT schmidt hammer (**a**) and Duroskop (**b**)
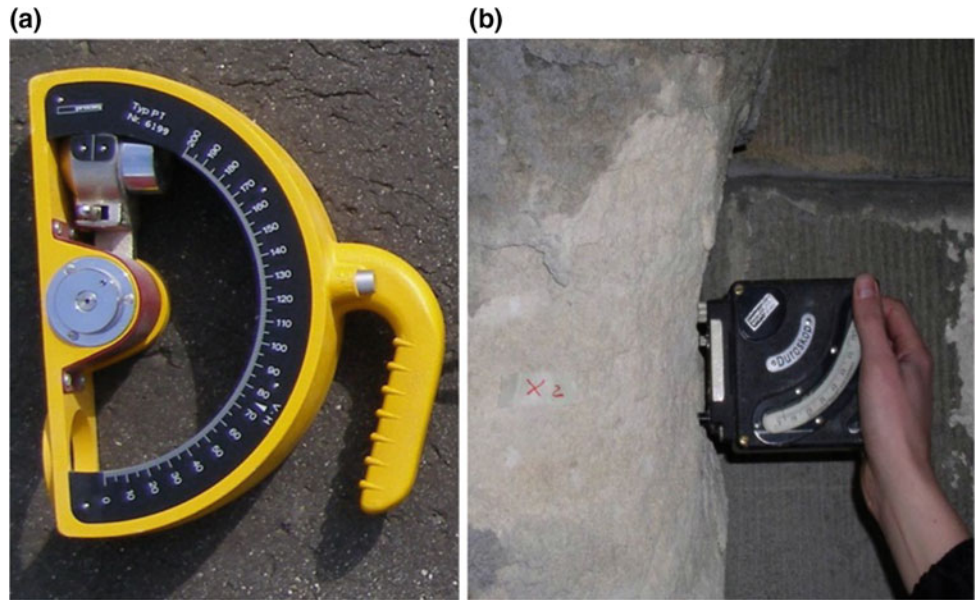
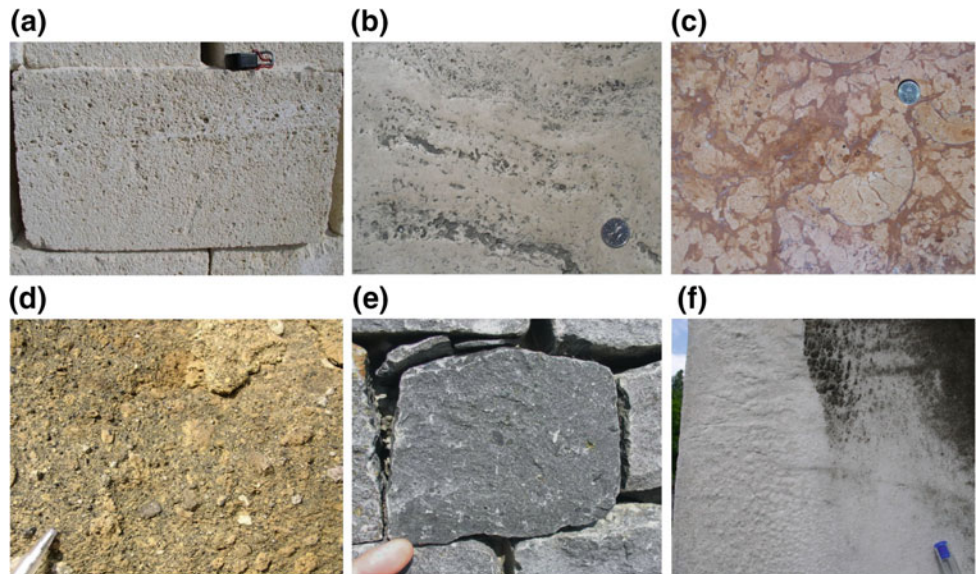**Fig. 3** Tested lithotypes: **a** porous limestone, **b** travertine, **c** micro-crystalline (compact) limestone, **d** andesite tuff, **e** basalt and **f** marble

Table 1 Comparative mean rebound values measured on travertine and on oolitic porous limestone

Test tool	Travertine		Oolitic limestone	
	Mean	Std.	Mean	Std.
Duroskop	38	6.4	17	4.6
L-9 Schmidt	43	4.5	22	2.6
N-34 Schmidt	45	1.2	37	0.7
PT Schmidt	122	2.4	84	11.9
Digi-Schmidt	57	2.8	33	1.4

Std. Standard deviations

to travertine, namely, Duroskop provided the lowest rebound values (17), which was followed by L-9 Schmidt hammer with a mean rebound value of 22. On porous limestone, the mean rebound values of N-34 Schmidt was higher (37) than that of the Digi-Schmidt (33). PT Schmidt represented the highest rebound with its mean value of 84 (Fig. 5).

Fig. 4 Comparative rebound values of travertine (Duroskop, L-9, N-34, Digi- and PT Schmidt hammer)
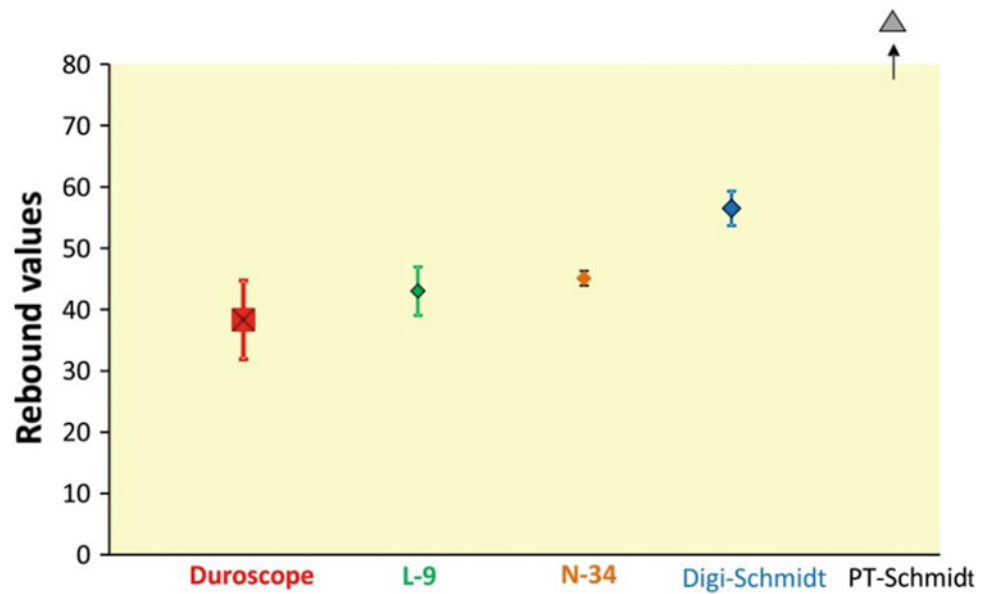
Fig. 5 Comparative rebound values of oolitic porous limestone (Duroscope, L-9, N-34, Digi- and PT Schmidt hammer)

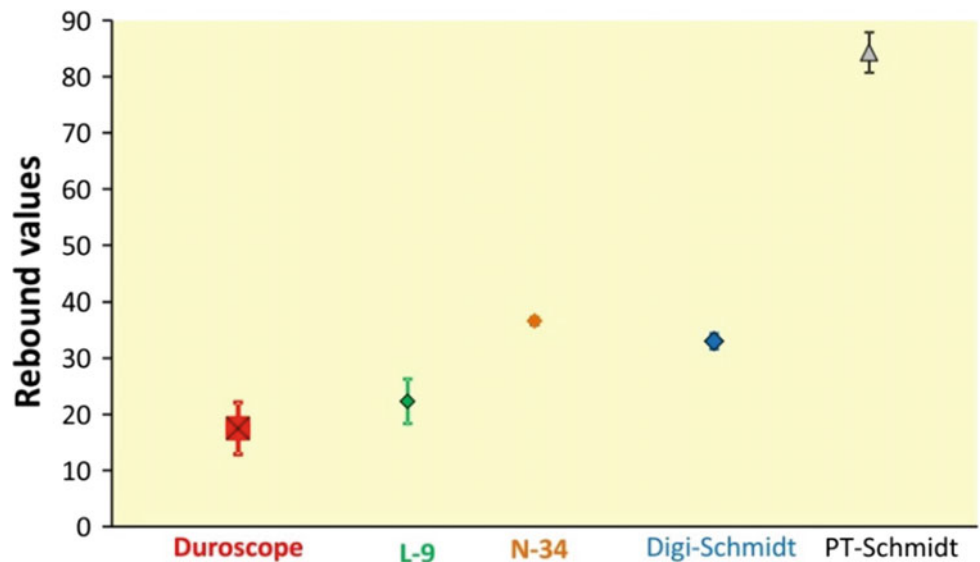These differences in rebound values of porous limestone and travertine refer to strength parameters. Namely, the uniaxial compressive strength of travertine is 40–50 MPa (Török and Vásárhelyi 2010), while that of the porous limestone is only 3–11 MPa (Török 2003). Consequently, Duroskop and Schmidt hammers provide information on the strength of materials, but the rebound values are not proportional to the results of uniaxial compressive strength tests obtained in the laboratory.

Duroskop results of the various lithotypes suggest that this tool allows the assessment of the strength of materials, and especially rocks (Table 2). According to tests performed for this study, porous limestone has the lowest rebound values which are followed by andesite tuff (Fig. 6). The highest rebound was
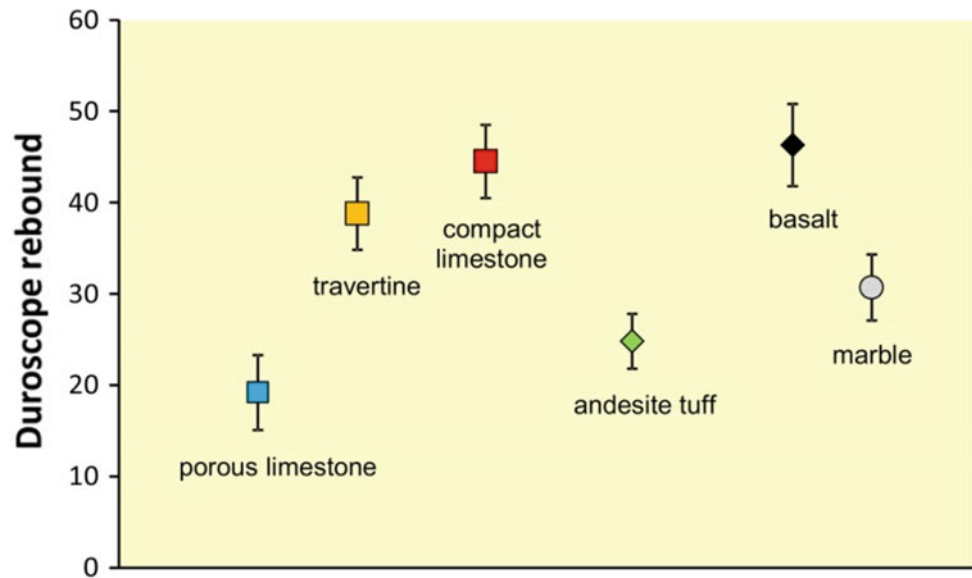
Table 2 Duroskop rebound values of different lithologies

Lithology	Duroskop rebound	
	Mean	Std.
Porous limestone	19	4.1
Travertine	39	6.4
Compact limestone	45	4.0
Andesite tuff	25	3.0
Basalt	46	4.5

Std. Standard deviations

Fig. 6 Duroskop rebound values of tested lithotypes

Table 3 Digi-Schmidt rebound values of different lithologies

Lithology	Digi-Schmidt rebound	
	Mean	Std.
Porous limestone	25	5.4
Travertine	57	2.8
Compact limestone	67	2.8
Andesite tuff	32	4.7
Basalt	71	3.0

Std. Standard deviations

measured on basalts, but micro-crystalline (compact) limestones also provided high Duroskop rebound values.

Using the Digi-Schmidt hammer for the same lithologies, the test results show similar trends (Table 3), with the lowest rebound values measured on porous limestone and the highest ones on basalt and compact limestone (Fig. 7). The differences are seen in the numerical values of the results and also in the standard deviations. Duroskop measurements have largest data scatter for most lithologies.

Our test results confirm previous studies (Török 2003, 2010) that Duroskop is able to provide information on a smaller test area. It is able to detect minor changes in strength, but it is a very sensitive tool to surface irregularities. The sensitivity is demonstrated in the higher standard deviations

Fig. 7 Digi-Schmidt rebound values of tested lithotypes
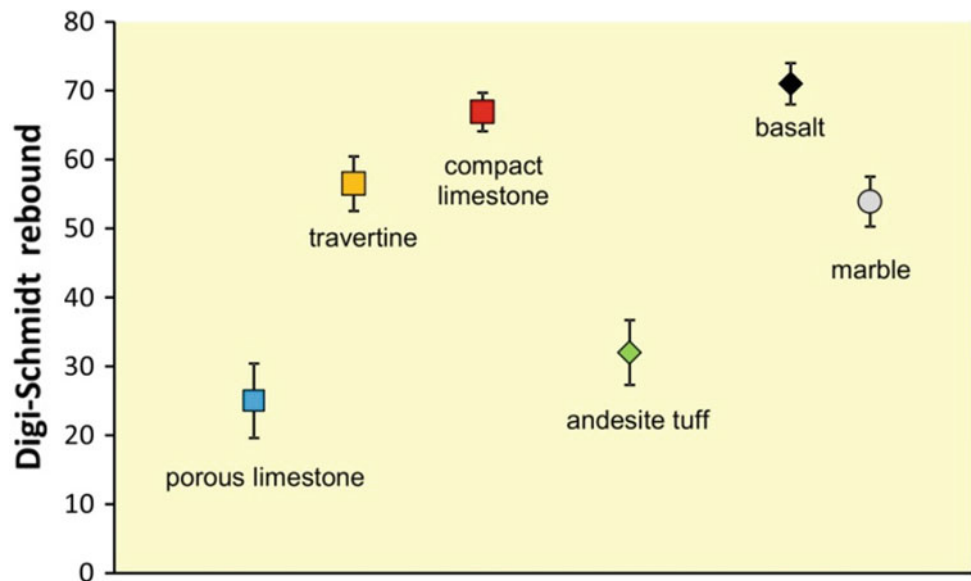
of test results measured on porous stones such as porous limestone or travertine (Table 2; Fig. 6).

4 Conclusions

Testing 6 lithotypes and measuring more than 1000 rebound values by using 5 different tools (Duroskop, L-9, N-34, Digi- and PT Schmidt hammer) the following general conclusions can be drawn:

- Several types of Schmidt hammers exist, and the obtained rebound values are generally not comparable.
- Both Duroskop and Schmidt hammers provide valuable insight to the strength of rocks, but the rebound values of the same test surfaces are different for both tools.
- The large data set presented here still does not allow for a clear conversion of rebound values to actual compressive strength, suggesting that further measurements are needed to overcome the uncertainties related to lithological heterogeneity.
- It was not possible to outline a formula that compares Duroskop and Schmidt rebound values based on the measured data set.
- Duroskop is able to detect small scale strength differences, but rebound values strongly depend on the surface irregularities.

References

Al-Omari, A., Beck, K., Brunetaud, X., Török, Á., Al-Mukhtar, M.: Critical degree of saturation: a control factor of freeze-thaw damage of porous limestones at Castle of Chambord, France. Eng. Geol. **185**, 71–80 (2015)

Aydin, A.: ISRM suggested method for determination of the Schmidt hammer rebound hardness: revised version. In: Ulusay, R. (ed.) The ISRM Suggested Methods for Rock Characterization, Testing and Monitoring: 2007–2014. Springer, Cham (2008)

Aydin, A., Basu, A.: The Schmidt hammer in rock material characterization. Eng. Geol. **81**, 1–14 (2005)

Kahraman, S.: Evaluation of simple methods for assessing the uniaxial compressive strength of rock. Int. J. Rock Mech. Min. Sci. **38**, 981–994 (2001)

Schmidt, E.: A non-destructive concrete tester. Concrete **59**, 34–35 (1951)

Tandon, R.S., Gupta, V.: Estimation of strength characteristics of different Himalayan rocks from Schmidt hammer rebound, point load index, and compressional wave velocity. Bull. Eng. Geol. Environ. **74**, 521–533 (2015)

Török, Á.: Surface strength and mineralogy of weathering crusts on limestone buildings in Budapest. Build. Environ. **38**, 1185–1192 (2003)

Török, Á.: In situ methods of testing stone monuments and the application of nondestructive physical properties testing in masonry diagnosis. In: Bostenaru Dan, M., Přikryl, R., Török, Á. (eds.)

Materials, Technologies and Practice in Historic Heritage Structures, pp. 177–193, Springer, Dordrecht (2010)

Török, Á., Vásárhelyi, B.: The influence of fabric and water content on selected rock mechanical parameters of travertine, examples from Hungary. Eng. Geol. **115**, 237–245 (2010)

Viles, H., Goudie, A., Grab, S., Lalley, J.: The use of the Schmidt hammer and Equotip for rock hardness assessment in geomorphology and heritage science: a comparative analysis. Earth Surf. Proc. Land. **36**, 320–333 (2011)

Yagiz, S.: Predicting uniaxial compressive strength, modulus of elasticity and index properties of rocks using the Schmidt hammer. Bull. Eng. Geol. Environ. **68**, 55–63 (2009)

Yılmaz, I., Sendir, H.: Correlation of Schmidt hammer rebound number with unconfined compressive strength and Young's modulus in gypsum from Sivas (Turkey). Eng. Geol. **66**, 211–219 (2002)

A Review of Some British Mixed Lithology Mudstone Sequences with Particular Emphasis on the Stability of Slopes

J. C. Cripps and M. A. Czerewko

Abstract

Ancient marine sedimentary mudstone sequences of Carboniferous to Cretaceous age account for upwards of 60% of the land surface in the UK and are frequently encountered during urban infrastructure and route-way development. These sequences often consist of alternating series of horizontally bedded, competent, well-jointed sandstone or limestone units interbedded with mudstones of an erodible nature and susceptible to rapid deterioration on exposure to surface weathering conditions. This type of mixed lithology is conducive to rock fall and slumping failures in cut slopes, whereas underground structure foundations and retaining walls may be compromised due to ground softening and development of chemically aggressive ground conditions. This paper explains some of the reasons mixed lithology formations are particularly susceptible to instability. The paper also reviews cases where the juxtaposition of units of different performance has had a significant impact and discusses ways of avoiding and overcoming the problems these conditions cause.

Keywords

Mudrocks • Slope failure • Mixed lithology sequences • Differential weathering • Rock fall

1 Introduction

Many mixed lithology sedimentary sequences outcrop in the UK, but those containing mudrocks with subsidiary beds of stronger sandstone beds or limestone are of particular widespread occurrence. Similar sequences occur elsewhere in the world (Potter et al. 1980). One of the reasons for this is that mudrocks alone underlie more than 60% of the UK (Shaw 1981) and while thick over-consolidated clay formations account for about 50% of the Mesozoic and younger sequences of southern and eastern England (Fig. 1; Table 1), mixed lithology sequences occur throughout the geological succession. The performance of these in engineering situations depends particularly upon the state of induration and geotechnical properties of the different units, as well as the contrast between these. In turn these factors depend upon their mineralogy and degree of compaction and cementation as well as the structures they contain, the structure of the overall formation and ground water conditions (Bell 1994). Dealing with ground in which it is not possible to test samples containing the different lithologies presents special challenges to the Engineering Geologist. It is necessary to base designs on geotechnical properties of the different rock types within the formation, which may not accurately anticipate the behaviour of the formation in the particular engineering situation being considered. Goodman (1993) reminds us that a combination of two rocks gives properties worse than either rock alone. As explained below, following a brief review of the geology of Britain, examples of this are all too often experienced during construction and infrastructure development, particularly with respect to the stability of slopes.

2 Geology of Britain: A Brief Overview

As illustrated in Fig. 1, the UK has a varied geology. The oldest rocks, consisting of Archaean (2700 Ma) gneiss, occur in the far northwest of Scotland and successively younger formations occur to the south and east of this, terminating with Pliocene (5.3–2.6 Ma) age deposits in south-east England. Quaternary and Recent deposits are widely distributed over these bedrock formations. The characteristics of the formations shown in Fig. 1 are summarized in Table 1.

J. C. Cripps (✉)
Department of Civil and Structural Engineering, University of Sheffield, Sheffield, S1 3JD, UK
e-mail: j.c.cripps@sheffield.ac.uk

M. A. Czerewko
AECOM, Chesterfield, S41 7SL, UK
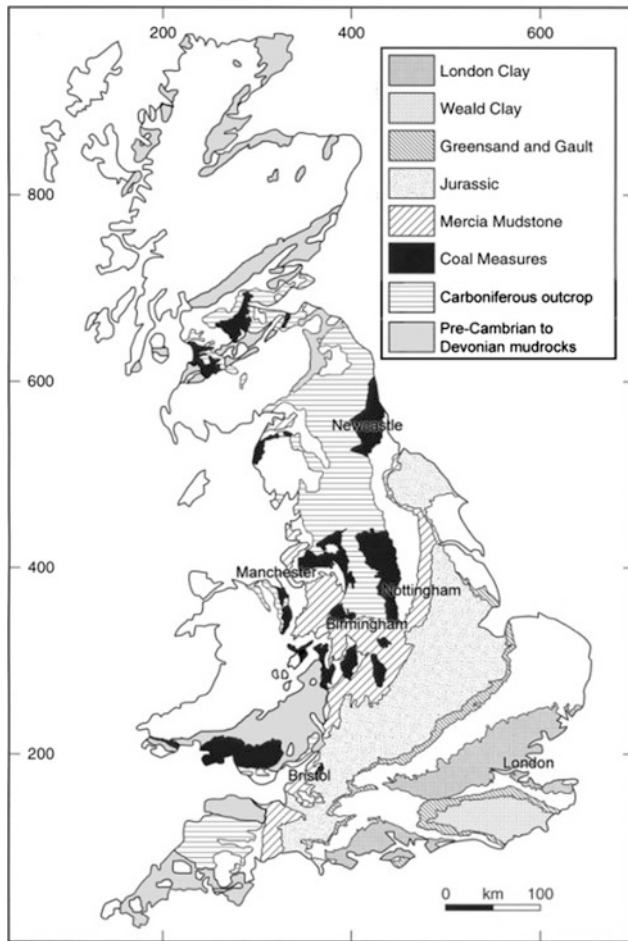
Fig. 1 General distribution of mixed-layer mudrock formations in the UK [from BGS (2007)]

Although pre-Carboniferous formations contain mudrocks, and these may cause problems in slopes and excavations, it tends to be rock mass discontinuities and structure that controls their behaviour in engineering situations. Furthermore, the higher ground and mountainous areas of the west and north are less densely populated, so there is less built in these areas. In lower Carboniferous times vast deposits of lagoonal and shelf sea limestones were formed with mudstone forming in the deeper basin areas. This sequence is succeeded by interbedded sandstone-mudstone/shale beds that now occupy high ground of the Pennine Hills of northern England (Fig. 2). This gave way in upper Carboniferous times to the Coal Measures which comprise rhythmic cycles of mudstones and shales, sandstone units and coal seams up to 2 to 3 m in thickness. The overlying Permian and Triassic sequences include limestone, sandstone and mudstone (see Fig. 3), mainly formed in lagoonal, aeolian and fluvial, hot, arid terrestrial conditions.

Jurassic and later deposits also contain significant mixed lithology formations. These tend mainly comprise weak mudrocks or stiff over-consolidated clays with sandstone or limestone units (Figs. 4 and 5). The clays or mudrocks suffer incipient weathering with fissures often opening due to near surface stress release and near-surface fabric modifications (Chandler 1972). Thick formations of stiff marine clay that contain thin discontinuous beds of nodular limestones or silty beds occur in this sequence and rhythmic alterations of lithology are also present. The Cenozoic Era comprises Tertiary deposits which includes the London Clay as well as mixed clay and subordinate sand sequences.

Table 1 Main lithologies present in the UK geological sequence (NB Upper Cretaceous and Permian strata outcrop, but are not specifically labelled on Fig. 1)

Geological period	Formation on Fig. 1	Characteristics of formations
Neogene	London clay	Stiff clay
Upper Cretaceous		Chalk and stiff clays
Lower Cretaceous	Weald clay, Greensand and Gault	Some interbedded sandstone-clay and stiff clays
Jurassic	Jurassic	Interbedded mudstone and limestone formations and limestone and stiff clays
Triassic	Mercia mudstone	Sandstones and mudstones, some mixed formations
Permian		Sandstones, limestone and mudstones
Upper Carboniferous	Coal Measures	Mixed mudstone-sandstone and sandstones
Lower Carboniferous	Carboniferous	Limestone and some mixed mudstone-limestone formations
Devonian Silurian Ordovician Cambrian Proterozoic Archean and Hadean	Pre-cambrian—Devonian	Sandstones some mudstones and meta-mudrocks, slates, well indurated greywacke sandstone, mudstone and limestones, igneous and metamorphic formations

Fig. 2 Mam Tor, Derbyshire. Upper Carboniferous Bowland Shale of alternating sandstone and mudstone beds exposed in a deep seated landslip (*Photo* MAC)

Fig. 3 Mercia Mudstone strata comprising argillaceous red-beds and light grey fine sandstone skerrie bed showing instability

Fig. 4 Interbedded mudstone, fissile mudstone and fractured limestone of the lower Jurassic Blue Lias formation

Fig. 5 Jurassic Oxford Clay strata comprising weaker soil like mudrocks with discontinuous nodular limestone beds

Significant problems arise with the mixed lithology Mesozoic and younger sequences in the south and east of England, and with mainly Carboniferous strata in the midlands, northern England, north and south Wales and central Scotland that historically provided the mineral resources for Britain's Industrial Heartlands. High levels of urbanisation and the associated infra-structure in these parts of the UK create particular challenges, especially with respect to the stability of slopes. Issues relating to both these geological situations are explored further below.

3 Engineering Implications of Mixed Lithology Sequences

The engineering implications of mixed lithology sequences and possible ameliorative and remedial actions are considered in the next two sections in which differences between older more indurated Carboniferous sequences and the Mesozoic and younger less well indurated alternating sequences are also explored.

3.1 Excavations

Unless the rock mass is heavily fractured, disturbed by faulting or weakened by weathering processes, it is usually possible to excavate stable near vertical faces in sequences of Carboniferous mudstones and sandstones. Strata dipping at angles greater than about 20° towards the excavation may experience instability due to translational or wedge sliding failures, especially if the strata have been affected by tectonic folding, valley bulge processes or mining subsidence. It is also likely that underground excavations and tunnels

will remain stable during the construction period, although support is usually required in mudstones and to prevent the fall of fracture bounded blocks in the stronger beds, including sandstones (Deaves and Cripps 1994). Some of sandstone beds are extremely strong and abrasive which can result in high rates of ware of cutting tools where mechanized methods of excavation are employed. Below the water table high rates of water ingress can be expected in the sandstone beds and permeable zones. In tunnels excavated by machines, consideration needs to be given to the possibility of the mudrock forming a slurry. In the case of the Don Valley Sewer Tunnels, the grinding action of the tunneling machine in mudstone that contained swelling clay minerals and was affected by disturbance due to mining subsidence resulted in the tunneling machine being abandoned (Varley 1990). High water pressures also contributed to the problems.

Low silt—high clay content mudrocks of Mesozoic and younger age may be sufficiently strong to remain stable during the excavation process, but may then undergo rapid deterioration before support from a lining is fully operable. The removal of confining pressure in excavations can also result in the release of stored stain energy and consequent lateral expansion of some mudrocks, especially those containing swelling clay minerals. This results in uplift and the loading of support systems and, on reloading, excessive settlement. The heave may cause failure of lightly loaded structures and instability of slopes and highway cuts. The expansion and squeezing of the mudrock may result in the opening of joints in the interbedded limestones or sandstones, which reduces strength and increases permeability, thus exacerbating the problems.

3.2 Slopes, Quarries and Road Cuts

High rainfall and seasonal freezing under periglacial conditions 80,000–10,000 years ago had significant impacts on slopes in the UK (Griffiths and Martin 2017), some of which are now mantled with layers of soliflucted material lying over shear surfaces. Examples are given in the literature of slopes shallower than 10^0 being unstable. The reactivation of this ancient instability is a common cause of problems in over-consolidated clay formations (Skempton and Weeks 1976), but problems may also arise in older mudrock dominated mixed lithology sequences. Increasing pore water pressures, loading or removal of support may result in unexpected instability of these materials.

In south west England periglacial weathering processes experienced by Jurassic age sequences of alternating limestone-mudstone sequences has resulted in extensive brittle fracturing and disturbance of the limestone beds and rapid fragmentation and slaking of the mudrocks which then degrades rapidly in slopes, and removes support from the blocky limestone beds. The ground is also subject to rapid heave if groundwater is not adequately depressurised during construction (Haydon and Hobbs 1974).

In the harder formations of the Carboniferous, periglacial weathering resulted in the formation of screes, valley cambering and non-diastrophic bulge structures. Some slopes became and still are unstable (Fig. 2) due to over-steepening of valley sides through rapid erosion. The process also resulted in the formation of sandstone escarpments along the higher flanks of the valleys, many of which are affected by cambering in which joints parallel to the valley have been opened and the sandstone bed has become tilted and displaced towards the valley. If not identified and correctly catered for in engineering works these features can cause great difficulties as changes in loading or support and surface water infiltration are apt to cause instability.

In addition to the effects on the valley sides weakening and softening of the mudstone underlying the valley floor has resulted in the deformation of the latter in features known as 'valley-bulges'. Degradation, deformation and fracturing of the strata may extend downwards for several tens of metres. The poor ground conditions caused by this process must be properly evaluated and appropriate counter measures taken in ground engineering works.

Various forms of block failure, toppling, sliding and ravelling described by Hoek and Bray (1981), commonly afflict natural and excavated slopes in mixed lithology sequences. Rapid weathering and preferential erosion of the mudrock or clayey units removes support from the stronger, more durable rock units in the sequence resulting in rock falls (Figs. 6, 7 and 8). In more indurated mudrocks the main process of removal is by ravelling or spalling in which continuous detachment and failure of small fragments of rock occurs. It is particularly prevalent in closely fractured mudrocks susceptible to slaking action and results in the accumulation of a gravelly scree (Fig. 8). In less indurated stiff clays the main mechanism of degradation is softening and lateral expansion of the unit such that it is easily eroded. In both cases the process opens joints in the overlying stronger formation which weakens it and facilitates water ingress.

In the examples considered hitherto the stratification has been dipping at angles of up to about 20° and therefore the main style of failure has been block falls. In situations in which the dip is towards the rock face and the stronger rock formation may form tall prismatic blocks, then toppling is an additional potential failure mechanism. In more steeply dipping strata the possibility of sliding on bedding planes to produce translational failures, or a combination of bedding planes and joints in wedge type failures must be considered. Failures of this type are especially likely where the downward movements of water penetrating joints within the

Fig. 6 Mudstone ravelling undermining a sandstone bed. Coal Measures, Sheffield

Fig. 7 Mass failure in overlying sandstone due to removal of mudstone support

harder units is impeded by interbedded less permeable clay or mudstone layers. The latter materials are liable to undergo degradation and softening and the raised pore water pressures have a destabilising effect on the slope as a whole.

There are many former quarries in mixed lithology bedded sequences in urban areas, especially those underlain by Carboniferous strata. In many case rock was exploited for building stone or mudstone was extracted for brick and tile manufacture. With increased urbanisation these former quarries have become engulfed in the urban area. Typically they consist of a high near vertical face in sandstone or limestone overlying weaker silty or muddy beds but in some, the face is formed out of mixed lithology beds (Figs. 6 and 9). Many of these quarry areas have been redeveloped for a variety of uses, including retails, housing, industry and recreation, that are put at risk by the presence of a potential unstable rock face.

Apart from endangering the former quarry floor area instability is liable also to remove support from land above the quarried area. In addition, the extractive process may have disturbed and weakened the rock mass making it more prone to failure than a natural or engineered rock slope.

4 Investigations and Remedial Actions

A range of engineering procedures is available for ensuring adequate protection from potential hazards posed by the failure rock slopes, as follows:

- Removal—scaling, controlled removal or re-profiling;
- Strengthening—Rock bolts, nails, buttresses, dentition;
- Protection—Masonry, shotcrete etc. protection to weaker horizons

Fig. 8 Ravelling of coal measures mudstone producing scree slopes and block falls

Fig. 9 Compound failure in alternately bedded Jurassic Blue Lias mudstone and limestone strata

- Control and containment—netting, catch fences or rock traps;
- Avoidance—move infrastructure away from the slope or vice versa.

Prevention of failure would generally be preferred but where this is impractical then debris control and containment or exclusion measures are available (Fig. 10). The reduction of pore water pressures and control of ground-and surface-waters are essential in all cases. Measures to control pore water pressures within the rock face include the provision of raking drains that intercept permeable strata and fractures (Figs. 11 and 12).

Removal of potentially unstable rock may not always be appropriate as there is the risk this may further destabilise the slopes and weathering of freshly exposed rock is likely to

lead to renewed instability. Rock bolts and nails may be used to secure individual blocks, or large zones of a rock face may be strengthened by use of pattern treatment (Fig. 13). Containment netting that holds failed rock in place (Fig. 14) is preferred to draped netting which controls the movement of loose material and therefore requires more frequent periodic maintenance.

Weathering and erosion result in a reduction in strength and the development of discontinuities in the rock mass, especially if bedding and jointing are in unfavourable directions. The likelihood and effects of reductions in strength and integrity of the rock need to be evaluated by investigation and backed up by detailed in situ examination and appropriate physical and chemical testing to evaluate the potential for deterioration. In cases where instability is likely, preventative slope remedial measures include the

Fig. 10 Undermining of sandstone blocks due to mudstone weathering, with gabion wall protecting building

Fig. 12 Inclusion of in slope raking drains to channel water from the limestone bed seen in Fig. 11 and additional weepholes

Fig. 11 Water flow from limestone horizon interbedded with mudstone

Fig. 13 Spot treatment with pre-stressed rock nails for reinforcement of individual blocks

Fig. 14 Containment netting and active drainage installed into a mixed lithology rock mass with compartmentalised groundwater domains

minimisation of exposure of the rock, drainage, ground nailing with erosion protection cover to bind together the exposed surface veneer, reduction of the slope angle, construction of benches in the more unstable horizons or rock slope cover and reinforcement by a combination of sprayed concrete (shotcrete), reinforcing mesh and rock dowels. The deterioration of poorly indurated mudrocks in exposures can be minimized by reducing the time of exposure and removal of load. Immediate shotcrete (Fig. 15) covering usually inhibits expansion and heave. Managed removal of water from sandstone or limestone horizons within a rock mass (Figs. 12 and 14) will reduce deterioration.

Determinations of the resistance to slaking (Czerewko and Cripps 2001) are useful for predicting the rate at which undercutting by the ravelling or erosion of mudrocks is liable to occur, but it is difficult to predict the rate of material loss from the face (Abderahman 2007). One approach is to

Fig. 15 Cover of exposed mudstone bed preventing air and water access

survey the performance of equivalent lithologies in slopes of known age. Factors that increase susceptibility to degradation are the presence of discontinuities, degree of cementation and the presence of swelling clay minerals. These factors also increase the susceptibility of mudrock to degrade to slurry in tunneling situations.

The possibility of instability of rock masses due to failure along structural discontinuities such as joints and bedding planes require that rock mass assessments, including the spatial distribution and spacing of discontinuities (Robotham et al. 1995; Fookes and Sweeney 1976). Discontinuity roughness and persistence should also be determined, with where necessary, measurements of the shear strength of joint or bedding plane and infill material, where present. Where possible observations should be made of the actual rock mass concerned, but otherwise assessment from trial excavations or high quality rotary core should be used. Optical survey techniques or cross-hole seismic or electrical tomography may also be considered. It can be very challenging to obtain undisturbed cores or samples of the weaker horizons with in mixed layer sequences for geotechnical testing and characterization, but geotechnical wireline coring techniques recovering S size core has been found extremely effective for such situations. Alternate rotary and thin walled pushed or percussive soil sampling have also found to be suitable.

The reactivation of ancient unstable slopes is a common cause of problems in over-consolidated clay formations, especially those of the south of England that were subject to periglacial slope failure. Avoiding this requires careful surveying of the area to identify signs of past instability, coupled with the investigation of the ground using trial pits to locate any shear surfaces.

It is essential in all cases to investigate the groundwater regime and establish seasonal variation and time lag effects of surface recharge. The potential for the generation of ground water that is aggressive to cementitious materials should also be assessed (Czerewko et al. 2016).

5 Conclusions

The UK has a varied geology but within the succession of strata, the Coal Measures of Carboniferous age and various post-Jurassic formations contain the most troublesome mixed lithology sequences. Population distribution, rock type and state of induration, rock mass structures, periglacial climatic conditions and past human activities are significant factors in determining the severity of problems that arise.

The styles of instability in these sequences include ravelling, and block falls, topping and less commonly, mass-failure depending upon the dip of the stratification and rock mass structures. The younger formations of southern

and eastern England include sequences of limestone and weakly cemented sandstones interlayered with over-consolidated, stiff clays. The latter materials in particular are subject to rapid degradation when exposed to weathering action resulting in rock falls due to loss of support for overlying blocky formations, as the stratification in these formations is mainly near horizontal. Remediation requires regrading of the slope to a stable angle, or protection and support to the weaker horizons for example by the construction of retaining walls.

In the more indurated sequences, many failures occur because ravelling of mudrock horizons creates block falls. Such slopes may be stabilized by protecting mudstone layers from weathering action and erosion with masonry or shotcrete, which will also strengthen the rock mass, with if necessary, the removal of the potentially unstable rock blocks to the rock face, or they may be secured to the rock mass using combinations of netting and rock bolts. In all cases the solution will include control and drainage of surface and ground waters. Where engineering solutions are not possible, then consideration may be given to preventing harm by catching the falling material with fences, ditches or walls.

References

Abderahman, N.: Evaluating the rate of undercutting on the stability of slopes. Bull. Eng. Geol. Environ. **66**, 303–309 (2007)

Bell, F.G.: Engineering in Rock Masses. Butterworth-Heinemann, Oxford (1994)

British Geological Survey (BGS): Bedrock Geology UK North & South Maps 1:625,000. British Geological Survey, Keyworth (2007)

Chandler, R.J.: Lias Clay: weathering processes and their effect on shear strength. Geotechnique **22**, 403–431 (1972)

Czerewko, M.A., Cripps, J.C.: Assessing the durability of mudrocks using the modified jar slake test. Q. J. Eng. Geol. Hydrogeol. **34**, 153–163 (2001)

Czerewko, M.A., Longworth, I., Reid, J.M., Cripps, J.C.: Standardized terminology and test methods for sulphur mineral phases for the assessment of construction materials and aggressive ground. Quart. J. Eng Geol. **49**, 245–265 (2016)

Deaves, A.P., Cripps, J.C.: Engineering geology investigations for the Don Valley Intercepting Sewer, Sheffield. In: 6th International Congress, International Association of Engineering Geology, Balkema, Rotterdam, vol. 5, pp. 3283–3284 (1994)

Fookes, P.G., Sweeney, S.M.: Stability and control of local rock falls and degrading rock slopes. Quart. J. Eng Geol. **9**, 37–55 (1976)

Goodman, R. E.: Engineering Geology—Rock in Engineering Construction. Wiley, USA (1993)

Griffiths, J.S., Martin, C.J.: Engineering Geology of Glacial and Periglaciated Terrains, Engineering Geology Special Publication, 28, 2017, Geological Society, London

Haydon, R.E.V., Hobbs, N.B.: The effect of uplift pressures on the performance of a heavy foundation on layered rock. In: Proceedings of Conference Rock Engineering, Newcastle, pp. 457–472 (1974)

Hoek, E., Bray, J.W.: Rock Slope Engineering, 3rd edn. Institute of Mining and Metallurgy, London, 358 p (1981)

Potter, P.E., Maynard, J.B., Pryor, W.A.: Sedimentology of Shale. Springer, New York (1980)

Robotham, M.E., Wang, H., Walton, G.: Assessment of risk from rockfall from active and abandoned quarry slopes. I.M.M. Sect. A **104**, 25–33 (1995)

Shaw, H.F.: Mineralogy and petrology of the argillaceous sedimentary rocks of the U.K. Q. J. Eng. Geol. London **14**, 277–290 (1981)

Skempton, A.W., Weeks, A.G.: The Quaternary history of the lower Greensand escarpment and Weald Clay Vale near Sevenoaks, Kent. Phil. Trans. Roy. Soc. London **A293**, 493–526 (1976)

Varley, P.M.: Susceptibility of Coal Measures mudstone to slurrying during tunneling. Q. J. Eng. Geol. Hydrol. **23**, 147–160 (1990)

Use of Borehole Shear Test to Obtain Shear Strength Data Comparison to Direct Shear Test

R. M. Sbroglia⊙, R. A. R. Higashi⊙, M. S. Espíndola⊙, V. S. Muller⊙, and P. Betiatto⊙

Abstract

The knowledge of shear strength geotechnical parameters, cohesion and friction angle, is necessary for many engineering works and slope stability analysis. Traditionally, the Direct Shear Test (DST) in the laboratory is used to determine these parameters. However, recently, the use of the Borehole Shear Test (BST) in Brazil is being evaluated to supplement or substitute for DST. The Geotechnical Mapping Laboratory of Federal University of Santa Catarina (LAMGEO-UFSC) is conducting research comparing DST and BST data which proposes to validate BST use in projects that demand a huge number of shear strength tests. Laboratory and field tests were performed to compare the parameters of shear strength of granite, migmatite, granulite, granitoid, gneiss and rhyolite residual soils from the Brazilian states of Santa Catarina and Rio de Janeiro. According to the obtained data, it was found that the failure envelope of soil samples analyzed from the same soil area (in wet states and in the same drainage and normal stress conditions) showed satisfactory correlations. The shear strength values obtained by DST and BST were similar, but the differences in the soil effective cohesion intercept parameter were more significant. Thus, BST field tests compare well with DST data with near perfect correlation.

Keywords

Shear strength data • Shear tests • Field tests

1 Introduction

In engineering works, like dams and landfills over soft soils, or even in slope stability studies, the understanding of the geotechnical parameters of shear strength, cohesion and internal friction angle is essential. Cohesion is caused by soil cementation or physical-chemical attraction between particles while the internal friction angle is the reactive strength of soil movement.

However, due to the large variability of these parameters both in space and in depth, there are some limits on collecting data in the field and also performing laboratory analysis with the necessary spatial density distributions in order to define and characterize representative values for a project area. Laboratory tests, like the Triaxial Shear Test (TST) and Direct Shear Test (DST), which are mostly used in Brazil, are methods to define these soil features but recently the Borehole Shear Test (BST) is being evaluated as an additional source of spatially distributed data.

BST is performed in the field and has many advantages when compared to other traditional laboratory equipment and testing. BST is practical because of the simple and time efficiency execution of the test and the ability to collect a significantly greater amount of spatially distributed data. Therefore, it enables a larger area to be analyzed in a shorter period of time and also provides less disruption to soil structure.

The Geotechnical Mapping Laboratory of the Federal University of Santa Catarina (LAMGEO-UFSC) is conducting research to compare DST and BST data. The goal is to validate the use of BST as a supplemental and/or surrogate-use of DST for a project in places that may require a large number of laboratory tests.

This research compares the geotechnical parameters of shear strength (cohesion and internal friction angle) between DST and BST tests from typical Brazilian residual soils and plans to validate the use of BST equipment.

R. M. Sbroglia (✉) · R. A. R. Higashi · M. S. Espíndola · V. S. Muller · P. Betiatto
Federal University of Santa Catarina, Florianópolis, SC, Brazil
e-mail: regi_sb@hotmail.com

2 Soil Shear Strength

Pinto (2002) states that the soil shear strength can be defined as the maximum shear pressure that a soil can endure without breaking or the shear pressure in the failure plane. In these conditions, the failure standard that best represents the soil's comportment is the Mohr-Coulomb Law, represented by Eq. 1.

$$\tau = c + \sigma \cdot \tan \varphi \qquad (1)$$

where τ is the shear strength in kilopascals (kPa); σ is the normal pressure to the plane (kPa); c is the cohesion strength (kPa) and φ is the internal friction angle between soil grains in degrees.

These geotechnical parameters of shear strength (c and φ) are not constant values in a soil. However, they can be determined by field tests (Borehole Shear Test, Vane Shear Test, Cone Penetration Test and Pressiometer Ménard Test), laboratory tests (Direct Shear Test, Triaxial Shear Test) or obtained by correlation with other tests, like the Standard Penetration Test (SPT).

According to Das (2012), Hachich et al. (1998), Ortigão (2007), Pinto (2002), the DST is the oldest procedure to determine the shear strength of a soil and it is based squarely on the Mohr-Coulomb Law. The objective of the DST (a laboratory test) is to determine which shear strength can cause a break in a soil sample, into a pre-defined failure plane. DST consists of putting a normal pressure into a plane and determining the strength that causes the sample to break. DST can be made under different conditions of consolidation and failure.

The BST (a field test) has been used in Brazil in the last few years by researchers since it is easy to use, fast, and has results with low variability (Lutenegger and Timian 1987). According to American Society for Testing and Materials (ASTM), BST is performed using an expandable shear probe into a pre-excavated hole, where a pressure is transmitted, making the probe expand against the hole's wall which applies pressure to the soil. Shear strength is measured by releasing the probe pressure at a measured and controlled rate. This method is similar to DST, but it has the advantage of allowing the analysis of a larger spatial area in a shorter period of time and with fewer disturbances to the soil structure.

Some authors compared the values of the shear strength parameters obtained in the BST with other tests. Lambrechts et al. (1981) compared two in situ test procedures, the BST and the Cone Penetration Test (CPT), with the laboratory Triaxial testing (TST) to evaluate shear strength of silt and varved silt soils. The authors observed that the BST procedure appeared to yield reasonable values of φ and c, and these shear strength values were close to those from the TST. Analysis of the CPT data in the varved silt showed the φ

values were slightly lower than those determined by the BST or in the laboratory TST. Lambrechts et al. (1981) concluded that both the BST and the CPT were successfully used in silt and varved silt soils to define drained shear strength parameters.

Yang (2005), with the objective to analyze two landslides in the state of Iowa (USA), determined soil resistance parameters by BST. These values were validated in laboratory by shear tests Ring Shear and DST. In his conclusions, the author indicated that BST presented significant results to the slope characterization, especially to obtain in situ parameters of soils resistance. The author also emphasized the speed in obtaining these parameters.

There exist studies that discuss the execution of BST. These other studies focus on the relation between the results and the borehole perturbation, drainage conditions, and variations of shear strength (Bechtum 2012; Lutenegger and Timian 1987). In addition, there are studies about how to improve the traditional BST method (Ballouz and Khoury 2002; Handy 1986; Handy et al. 1985; Khoury and Miller 2006; Lutenegger et al. 1981; Lutenegger and Timian 1987; Peng and Jia 2016).

3 Materials and Method

3.1 Analyzed Soils

Representative residual soil types from the Brazilian states of Rio de Janeiro (RJ) and Santa Catarina (SC) were selected for this study to compare DST and BST data and to obtain the geotechnical parameters of shear strength. Table 1 lists the soil types and their respective locations and Universal Transverse Mercator (UTM) geographical coordinates. Figure 1 shows the location of sample collection points and BST performing.

3.2 Soil Shear Strength Tests

DST were performed at UFSC's Soil Mechanics Laboratory and BST were conducted in the field.

Soil samples were selected for DST analysis at locations on adjacent slopes where BST was performed in order to minimize the potential impact of results from spatial differences (heterogeneity) between the soils.

3.2.1 Direct Shear Test—DST

According to American Society for Testing and Materials (ASTM) D3080 standard (American Society for Testing and Materials 2004), the DST is conducted in the laboratory. To perform the test for this study, two undisturbed Horizon C

Table 1 Points of sample collection and BST performing with respective soil types and their UTM coordinates

	Soil type	City	State	UTM coordinates (zone 22J)	
				Longitude (*mE*)	Latitude (*mS*)
P1	Residual granitoid	Paraty	RJ	529,433.35	7,436,495.77
P2	Residual gneiss	Angra dos Reis	RJ	571,473.32	7,457,576.64
P3	Residual migmatite	Angra dos Reis	RJ	569,757.32	7,463,043.17
P4	Residual granite A	Angra dos Reis	RJ	556,783.17	7,455,796.37
P5	Residual granite B	Florianópolis	SC	747,626.00	6,944,771.00
P6	Residual granite C	Florianópolis	SC	747,229.28	6,946,221.04
P7	Residual granite D	Florianópolis	SC	747,538.04	6,945,315.52
P8	Residual granulite	Corupá	SC	669,288.00	7,080,483.00
P9	Residual rhyolite	São Bento do Sul	SC	660,960.00	7,087,591.00

Fig. 1 Sample collection points and BST test performing location
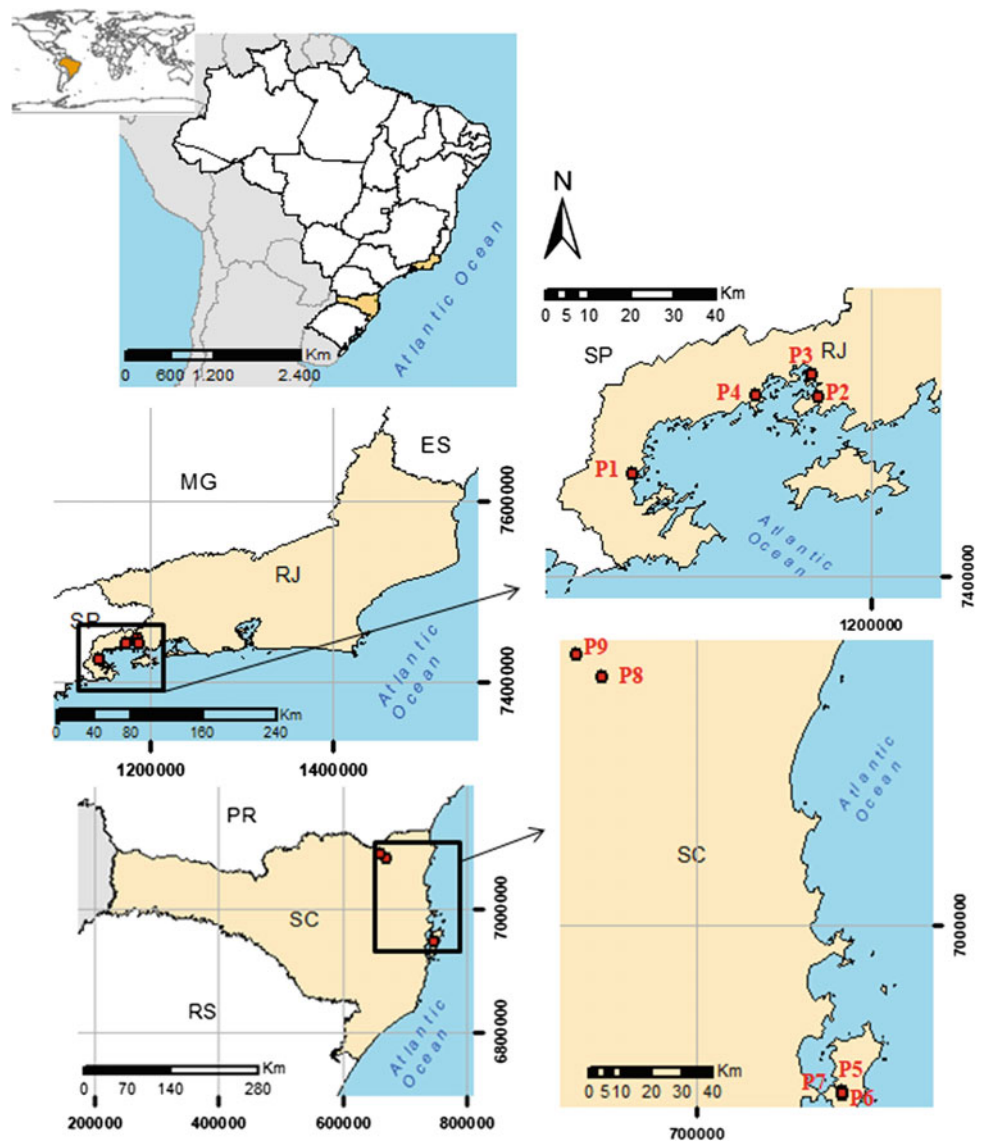
samples were collected in metallic containers (10.16 cm × 10.16 cm × 2 cm) for each soil. After collecting and laboratory preparation, each sample was placed and was flooded in the direct shear press which was activated.

The sample consolidation occurred by applying normal strength under drained conditions. Normal strengths were applied in a range of 30–150 kPa. Soil sample was considered stabilized at the time when the variations in vertical deformations stopped.

The shear part occurred after consolidation and verified the largest shear strength that a soil can endure when imposed to a failure surface. The sample shear strength occurred by the movement of the shear press case at a standard rate of 0.37 mm per second (mm/s) (see Fig. 2).

3.2.2 Borehole Shear Test (BST)

The BST was conducted in accordance with the Handy Geotechnical Instruments procedures (Handy Geotechnical Instruments 2017). Initially, a soil drilling was done by using two pedological auger holes, with a diameter of 65 and 82 mm (see Fig. 3a). The borehole depth of the BST probe varied between 50 and 90 cm, and it was located in Horizon C for each soil.

After assembly of the field equipment, the borehole was flooded and effective normal pressure was applied. The effective normal pressure varied from 20 to 170 kPa which was applied with a manual pump (see Fig. 3b). The time for the material to consolidate with the pressure that was exerted was 15 min for each borehole.

With BST, four different normal pressures were used in each soil, in order to verify the linearity of shear strengths obtained and was used to confirm the reliability of the results.
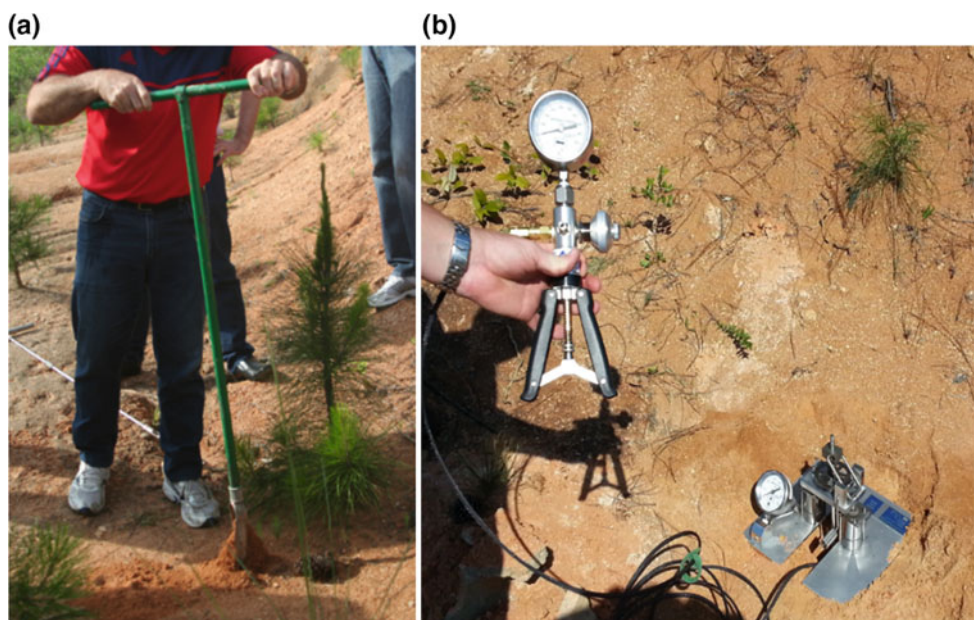
3.3 Comparison of Test Results

In order to evaluate and compare DST and BST results for the samples submitted to different normal strengths, pairs of values for normal strengths and shear strengths (σ, τ) for

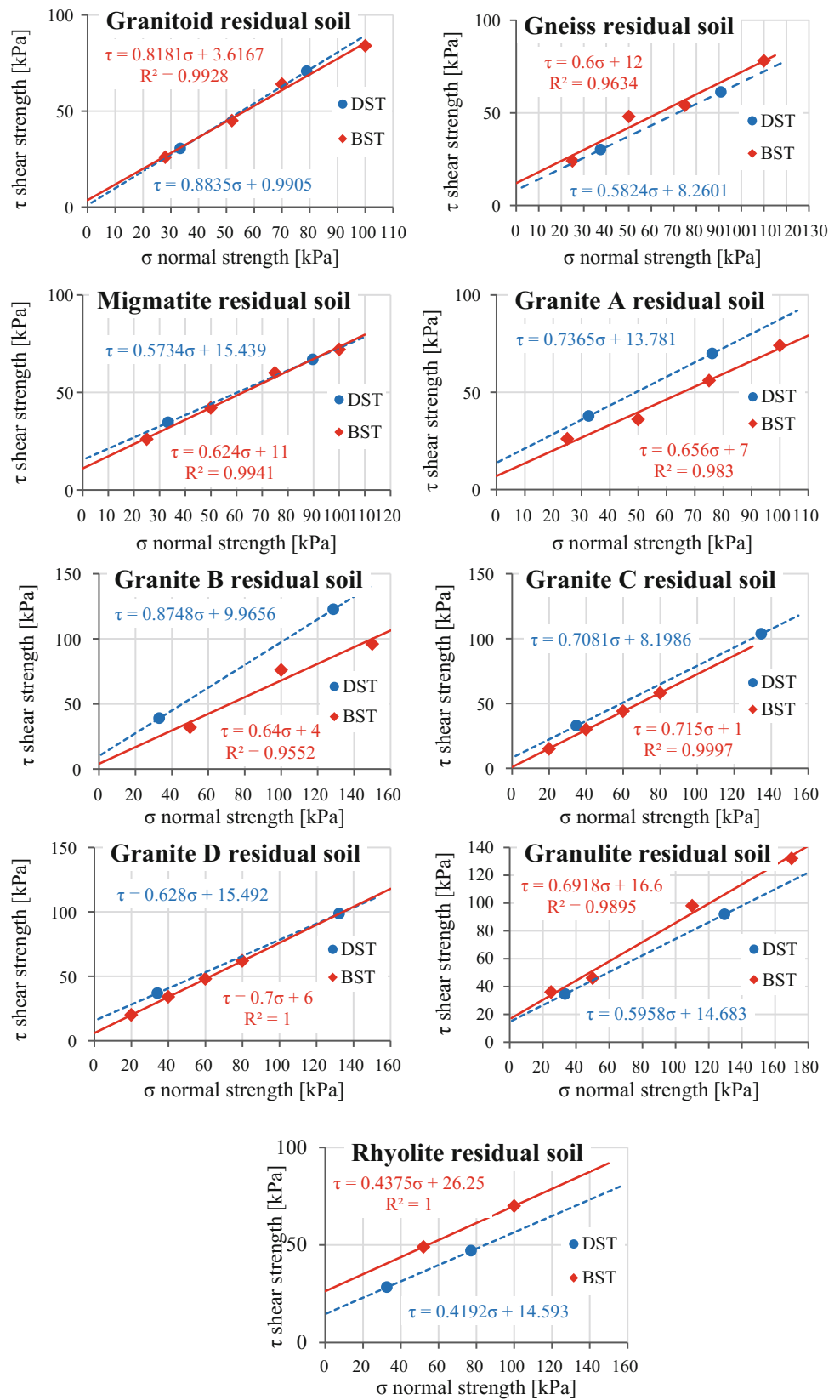**Fig. 2** Direct shear press used (**a**) and shear sample (**b**)
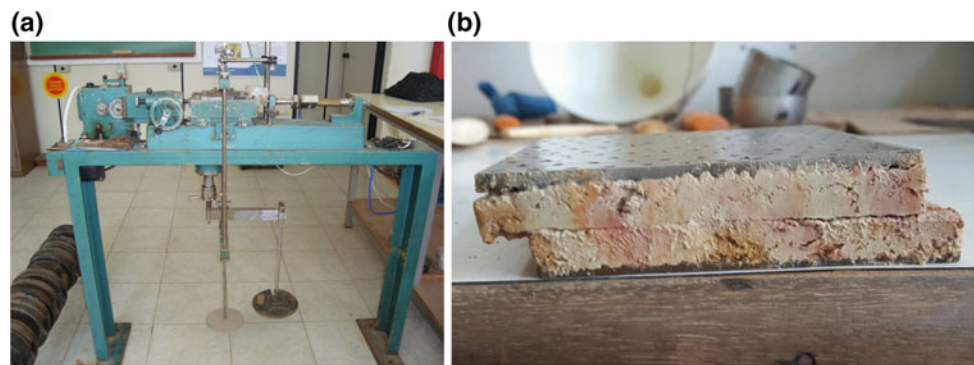
Fig. 3 Soil increment core (**a**) and BST (**b**)

Fig. 4 DST and BST results

Table 2 Shear strength parameters obtained by DST and BST

Soil types	Effective cohesion intercept				Effective friction angle			
	DST (kPa)	BST (kPa)	Variation (kPa)	Variation (%)	DST (degrees)	BST (degrees)	Variation (degrees)	Variation (%)
Granitoid	1	4	−3	−265	41.5	39.3	2.2	5
Gneiss	8	12	−4	−45	30.2	31.0	−0.7	−2
Migmatite	15	11	4	29	29.8	32.0	−2.1	−7
Granite A	14	7	7	49	36.4	33.3	3.1	9
Granite B	10	4	6	60	41.2	32.6	8.6	21
Granite C	8	1	7	88	35.3	35.6	−0.3	−1
Granite D	15	6	9	61	32.1	35.0	−2.9	−9
Granulite	15	17	−2	−13	30.8	34.7	−3.9	−13
Rhyolite	15	26	−12	−80	22.7	23.6	−0.9	−4

each phase were used. These values were plotted on a graph of maximum shear strength versus normal strength. Hence, the shear strength envelope was obtained.

From the envelope it was possible to determine the parameters c and φ. The comparison of test results was made with the shear strength envelopes and by the parameter values, evaluating the size of variations that were measured.

4 Results and Discussions

The direct shear strength test results were analyzed according to the Mohr-Coulomb Law. It was possible to obtain a shear strength envelope for each studied soil from two samples. The BST results, which were separated into four normal strength phases, were plotted on graphs. By evaluating the graphs, shown in Fig. 4, it is possible to determine the equivalent behavior of the results obtained from DST and BST and from the failure envelope overlaps.

Note that the linear regression coefficient (R) for all the soils analyzed by BST was near to unit and indicates the linearity of the results; as was desired.

In addition, the similarity between the results and acceptable correlations between the failure envelopes is also noted. The equations of the trend lines showed similar angular and linear coefficients with low representative discrepancies which were also analyzed using the values of the geotechnical parameters of shear strength. These parameters, obtained by both of the tests, are shown in Table 2.

It is shown that the shear strength values are close; being more significant, the differences in the soil effective cohesion intercept parameter. The largest variation in values occurred in residual rhyolite (12 kPa) and granite D (9 kPa).

Bechtum (2012) compared the results of the automated BST and the DST for two types of distinct soils, glacial sand and soft clay. The author also observed larger variation

between the values measured for the cohesive intercept when compared to the internal friction angle, and concluded that the BST normally provides lower values of cohesive intercept when compared to the DST.

For the effective friction angle values, these values were within a small range that varied less than 15% except for the residual soil of granite B (21%). However, for granite B soil, this difference can be attributed to the soil heterogeneity of the samples resulting in variations in the results that are inherent to the tests used.

The shear strength envelopes discovered by each one of these tests, when compared, suggests that it is not necessary to create an equivalency equation that correlates BST to DST data. The results obtained directly by BST test are acceptable.

5 Conclusions

Traditionally, it is more common to use the direct shear strength in the laboratory to determine geotechnical parameters of shear strength. However, because of the need to obtain more data in a shorter period of time and with more practical methods, this paper summarizes research about other investigation methods that use BST.

The field equipment for BST is a potential alternative that makes it possible to obtain the effective cohesion intercept and the effective friction angle in an easy way when compared to DST.

According to the comparative data obtained by DST and BST, it was possible to estimate the failure envelope of samples from the same soil in wet states and with the same drainage and normal stress conditions. These comparisons showed that satisfactory correlations and results with similar shear strength parameters were consistent with the values proposed by the residual soil literature. In addition,

variations that arise from the BST procedures are acceptable since these are not laboratory driven and high precision tests.

In this way it is possible to conclude that there is no need to create an equivalency equation that relates and corrects the BST data with DST data. The BST data are acceptable for this set of data.

It is important to conduct research about these tests and about the BST equipment, as well as to present information about the BST methodology, since there is still no standard for the test.

References

American Society for Testing and Materials: ASTM D3080: Standard Test Method for Direct Shear Test of Soils Under Consolidated Drained Conditions. ASTM, West Conshohocken, USA (2004)

Ballouz, M., Khoury, C.: ISST: In-situ Shear Test for Soil Investigations. Journees Libanaises de Geotechniques (JLG), Roumieh, Beirut. Lebanese University, Lebanon (2002)

Bechtum, T.: Automation and further development of the borehole shear test. Master of Science Dissertation, Civil Engineering, Iowa State University, Iowa (2012)

Das, B.M.: Fundamentos de engenharia geotécnica, 7th edn. Cengage Learning, São Paulo (2012)

Hachich, W., Falconi, F.F., Saes, J.L., Frota, R.G.Q., Carvalho, C.S., Niyama, S.: Fundações: teoria e prática, 2nd edn. Editora Pini, São Paulo (1998)

Handy Geotechnical Instruments, Inc.: Borehole shear tester. http://www.handygeotech.com/borehole/. Last accessed 2017/08/22

Handy, R.L.: Borehole Shear Test and Slope Stability. Use of In Situ Tests in Geotechnical Engineering. ASCE, pp. 161–175 (1986)

Handy, R.L., Schmertmann, J.H., Lutenegger, A.J.: In: Chancy, R.C., Demars, K.R. (eds.) Borehole Shear Test in a Shallow Marine Environment, Strength Testing of Marine Sediments: Laboratory and In-Situ Measurements. ASTM STP 883, American Society for Testing and Materials, Philadelphia, pp. 140–153 (1985)

Khoury, C., Miller, G.A.: Influence of flooding on Borehole Shear Test (BST) results in unsaturated soils. Unsaturated Soils **1**, 235–246 (2006)

Lambrechts, J.R., Rixner, J.J.: In: Yong, R.N., Townsend, F.C. (eds.) Comparison of Shear Strength Values Derived from Laboratory Triaxial, Borehole Shear, and Cone Penetration Tests. Laboratory Shear Strength of Soil, ASTM STP 740, American Society for Testing and Materials, pp. 551–565 (1981)

Lutenegger, A.J., Timian, D.A.: Reproducibility of borehole shear test results in marine clay. Geotech. Test. J. **10**(1), 13–18 (1987)

Lutenegger, A.J., Hallberg, G.R.: In: Yong, R.N., Townsend, F.C. (eds.) Borehole Shear Test in Geotechnical Investigations. Laboratory Shear Strength of Soil. ASTM STP 740. American Society for Testing and Materials, pp. 566–578 (1981)

Ortigão, J.A.R.: Introdução à mecânica dos solos dos estados críticos, 3rd edn. Livros técnicos e científicos S.A, Rio de Janeiro (2007)

Peng, K., Jia, R.: Development of the borehole direct shear testing apparatus. IN: International Conference on Sustainable Energy, Environment and Information Engineering, pp. 187–191 (2016)

Pinto, C.S.: Curso básico de mecânica dos solos, 2nd edn. Oficina de Textos, São Paulo (2002)

Yang, H.: Soil slope stability investigation and analysis in Iowa. Doctoral thesis, Iowa State University, Ames (2005)

A Petrographic and Geotechnical Study of the Sandstone of the Fundudzi Formation, Lake Fundudzi, South Africa

Sibonakaliso G. Chiliza and Egerton D. C. Hingston

Abstract

The Fundudzi Formation is one of five formations of the Soutpansberg Group, which consists essentially of reddish, arenaceous and minor argillaceous deposits. Little is known about the sandstone of the Fundudzi Formation apart from a massive rockslide event that occurred in the Soutpansberg Mountains approximately twenty thousand years ago, which blocked the course of the eastern flowing Mutale River forming Lake Fundudzi, the only true inland lake in South Africa. A study of the petrographic and geotechnical properties of selected samples of sandstones of the Fundudzi Formation has been undertaken in order to contribute to the geotechnical knowledge of this material. Detailed petrographic analysis has been undertaken by analyzing thin sections of selected samples of the sandstone obtained in close proximity to Lake Fundudzi. The geotechnical tests conducted include Schmidt hammer rebound test, point load test, Brazilian strength test and uniaxial compressive strength (UCS) test on representative samples of the sandstone. Based on a detailed petrographic analysis, the sandstone can best be described as quartzitic sandstone. The correlated UCS values derived from Schmidt hammer tests, point load corrected size index strength and UCS values from direct testing of the quartzitic sandstone show that the material classifies as medium to very high strength. The mineralogy, grain size, deformation, grain to grain contact (almost interlocking due to recrystallization) and silica cement were found to significantly affect the strength of Fundudzi Formation sandstone.

1 Introduction

The knowledge of mechanical properties of rocks is essential in any rock mechanics investigation connected with mining, tunnelling, drilling, blasting, cutting or crushing. The mechanical properties of a rock depend primarily on its mineral composition and constitution, i.e. its structural and textural features. They also depend upon the conditions under which testing is done (e.g. temperature, water content) (Vutukuri et al. 1974). In intact rock, the mechanical properties depend not only on the properties of the individual minerals, but also upon the way in which the minerals are assembled. The relevant information is given by a full petrographic description, which includes the mineral composition of crystals, grains, cementing materials and alteration products and also the structure and texture, including size, shape, distribution and orientation of crystals, grains, pores and cracks (Vutukuri et al. 1974).

Little is known about the petrographic and geotechnical properties of the sandstone of the Fundudzi Formation apart from a massive rockslide event that occurred in the Soutpansberg Mountains, which host the sandstone. The landslide occurred ∼20,000 years ago in the northward dipping quartzitic sandstone of the Fundudzi Formation of the Soutpansberg Group (van der Waal 1997). The landslide, which blocked the course of the eastern flowing Mutale River, formed Lake Fundudzi, the only true inland lake in South Africa. The main aim of this study was to determine the petrographic and geotechnical properties of the sandstone of the Fundudzi Formation at Lake Fundudzi. A detailed petrographic analysis of the sandstone was conducted in order to determine its mineral composition and constitution, i.e. its structural and textural features. Laboratory tests were

S. G. Chiliza (✉)
Council for Geoscience, Silverton, Pretoria 0001, South Africa
e-mail: gchiliza@geoscience.org.za

E. D. C. Hingston
College of Agriculture, Engineering and Science, University of KwaZulu-Natal, Westville Campus, Durban, 4000, South Africa

conducted on samples obtained from site in order to assess the geotechnical properties of the sandstone. The geotechnical properties determined were the density, unit weight, Schmidt hardness, point load strength, Brazilian tensile strength test, and direct unconfined compressive strength test.

2 Location of Study Area

Lake Fundudzi is located in the Mutale River valley of the eastern Soutpansberg Mountains in Limpopo Province (22° 50″ 22.08″S and 30° 18″36″E) near the Kruger National Park. The study area lies approximately 57 km north east of Makhado (Louis Trichardt) and 21 km north-west of Thohoyandou, South Africa (Fig. 1).

3 Geology of the Area

The geology of the study area is characterized by sandstone of the Fundudzi Formation. Barker et al. (2006) described the geology as sandstone and quartzitic in places, locally gritty or a conglomerate with interbedded basaltic lava, tuff, shale, agglomerate and siltstone (Fig. 2). Around the landslide area, it was observed that the rock slope is homogenous, consisting of sandstone, which is quartzitic in places. The sandstone is pinkish to reddish brown in colour, and medium- to fine-grained. The bedding is preserved and heavy jointing of the rock mass is evident.

4 Methodology

Block samples of the sandstone were taken randomly from the site for laboratory testing. From the samples obtained, several thin sections were prepared in compliance with national and international best practices as described by Allman and Lawrence (1972), and Hutchison (1974) for detailed petrographic analysis using an Olympus microscope. A total of five samples were prepared for petrographic analysis.

Laboratory tests were conducted on the samples in order to determine the geotechnical properties of the sandstone. The tests conducted include dry density, uniaxial
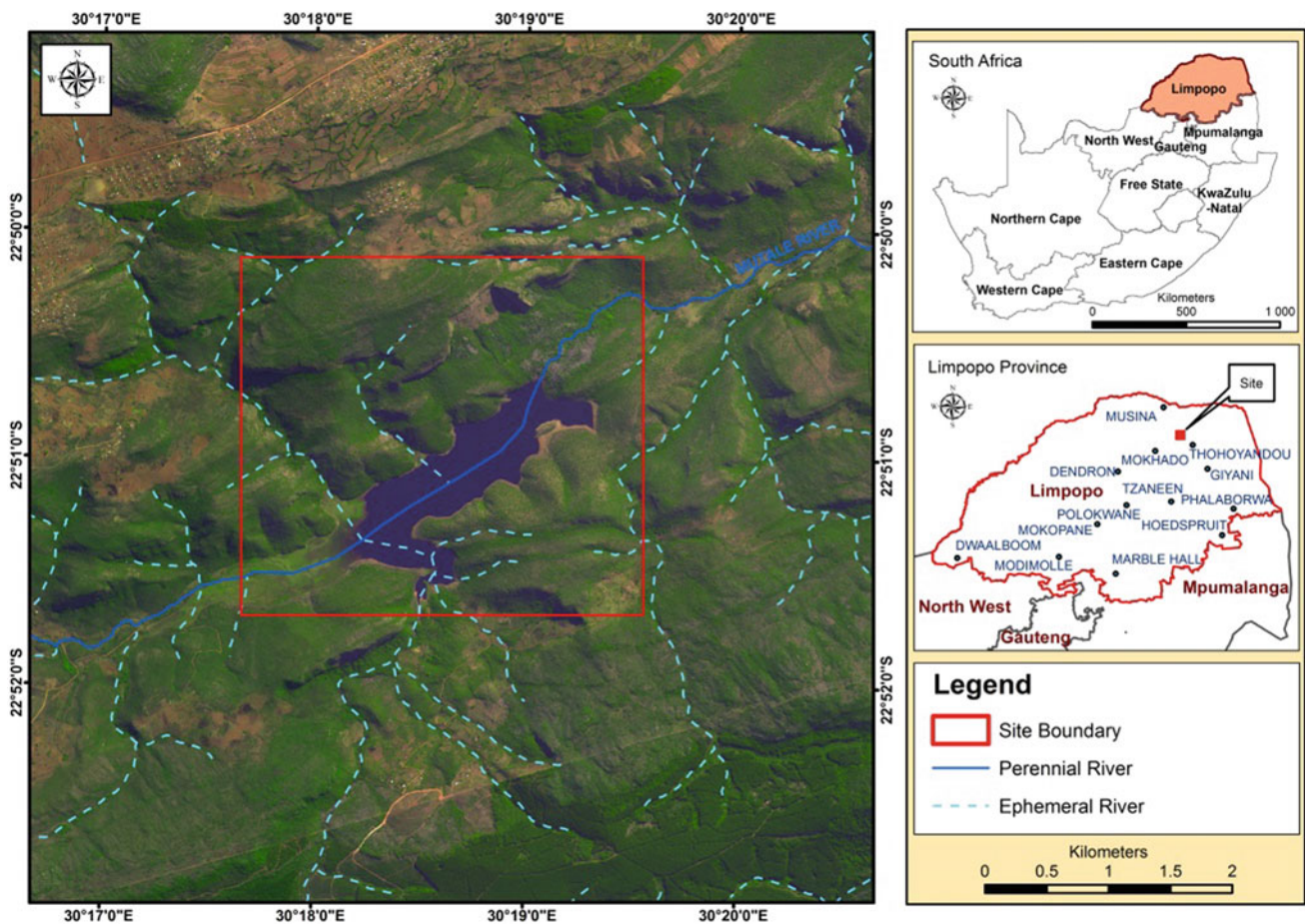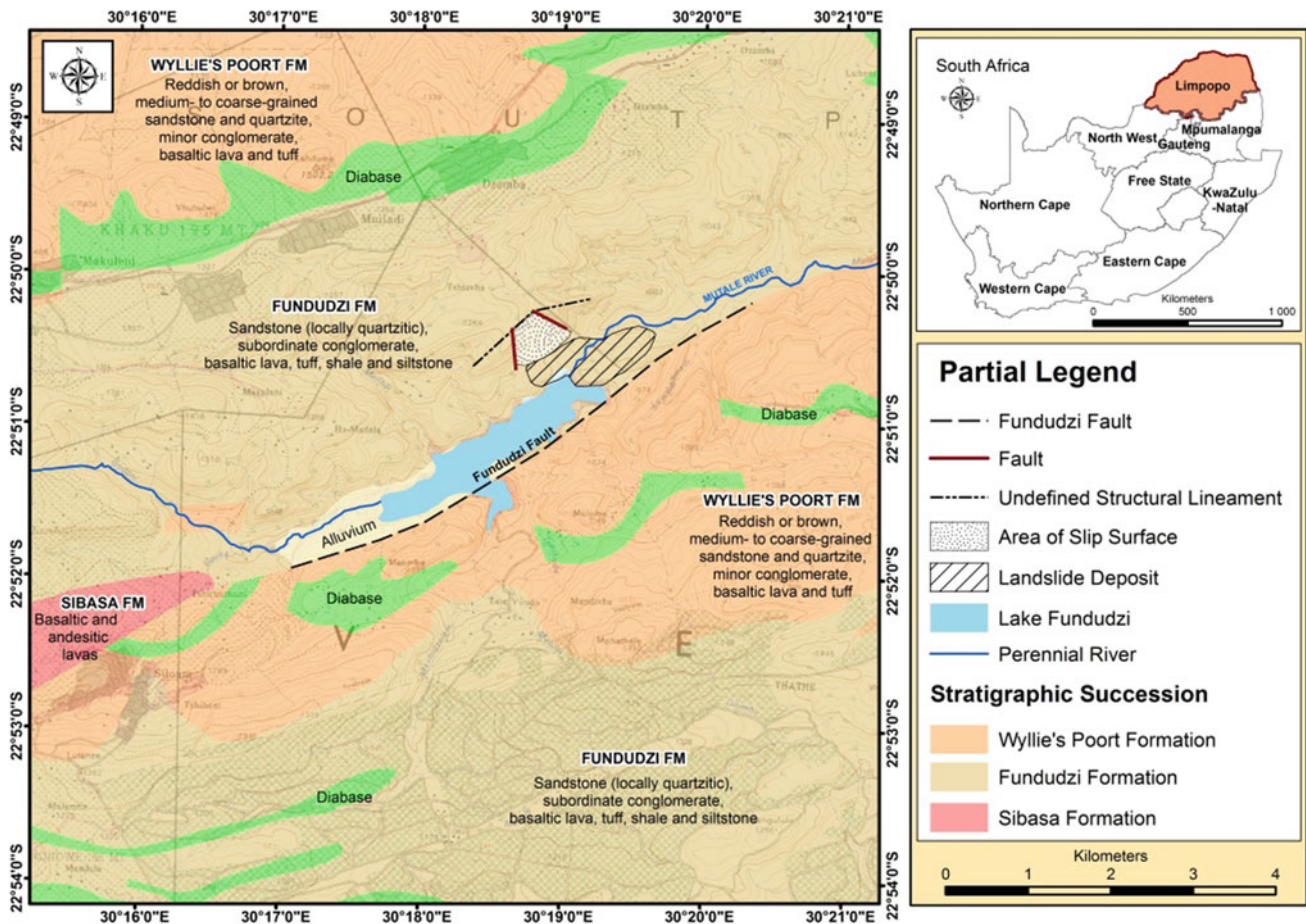

Fig. 1 Location map of Lake Fundudzi

Fig. 2 Local geological map of Lake Fundudzi

compressive strength (UCS) tests, Brazilian tensile strength tests and point load tests. All the tests were conducted in accordance with the ISRM (1981) procedures for rock testing. In the case of the UCS test, a Rothenberger rodiadrill 1800 was used to obtain NX-size diameter core samples from the block samples. The Schmidt hardness rebound test was also conducted in the field on unweathered surfaces of the sandstone from which the rebound number was obtained and then used to correlate with the UCS of the rock as described by Deere and Miller (1966).

5   Results and Discussion

Thin section microscopic analysis shows that the sandstone is composed predominantly of quartz (+95%) and trace amounts of secondary carbonate minerals (Fig. 3). Distinctly visible also on stage rotation under crossed polarized light is undulatory extinction of the quartz grains, which indicates that the quartz minerals may have undergone some amount of deformation. Grain to grain contact was evident and almost interlocking indicating recrystallization. The majority

of these sediments also reflected increased sphericity (0.7–0.9) and roundness (0.5–0.9) of the mineral grain and in general, the sorting is good. Quartz veins are also present. Silica cements around the quartz grains forming very hard rock sandstone. The original shape of many of the quartz grains may have been reworked because they are well sorted and are of equal size. The relation between different grain sizes and the variation in strength was not assessed as the grain size of the sandstone was more or less equal. The average grain size varies between 200 and 300 microns, which according to Wentworth (1922), classifies it as medium sand.

A summary of the geotechnical properties obtained from the different tests conducted on the sandstone is presented in Table 1. Schmidt hardness rebound test results show that the UCS values derived from Schmidt hammer tests ranged from 50 MPa to 135 MPa with a mean of 37 and 80 MPa respectively. According to Deere and Miller (1966) the intact rock strength of the quartzitic sandstone classifies as a strong rock.

The unit weight results showed minor variation of between 28.5 and 28.6 kN/m^3, for the five core samples

Fig. 3 Photomicrograph of sandstone; **a** under plane polarized light, **b** under crossed-polarized light
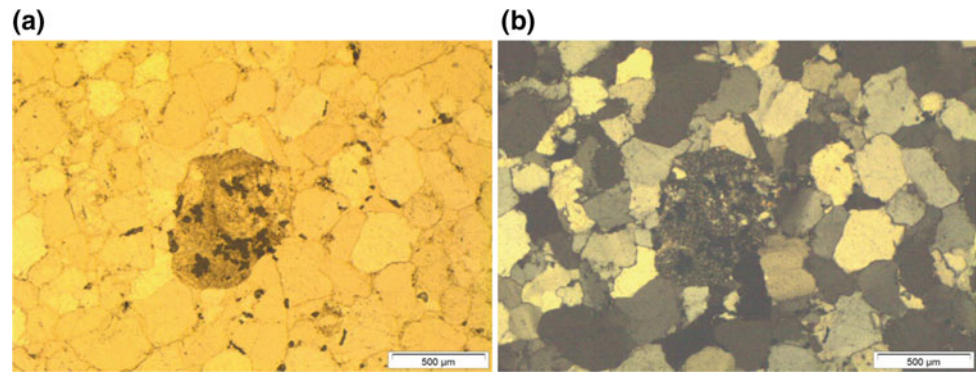
Table 1 Geotechnical properties of the sandstone obtained from laboratory testing

| Type of test	Range	Average	Number of samples tested
Schmidt hardness rebound values (R) (Vertical)	28–50	37	17
Schmidt hardness rebound values (R) (Horizontal)	28–48	37	37
UCS (MPa) correlated by Miller (1965) (Vertical)	50–135	82	17
UCS (MPa) correlated by Miller (1965) (Horizontal)	50–130	79	23
Unit weight (kN/m^3)	28.5–28.6	28.6	5
Brazilian (indirect tensile) strength (MPa)	4.1–7.8	5.7	6
Point load $Is_{(50)}$	1.37–12.28	5.51	29
Point load Correlated UCS (MPa), Broch and Franklin (1972)	31–282	126	29
Direct UCS test (MPa)	145–250	189	5

assessed (Table 1). An average unit weight value of 28.6 kN/m^3 was calculated for the quartzitic sandstone. The unit weight results for quartzitic sandstone were in agreement with those published values of hard sandstone (e.g. Hoek and Bray 1981) which range between 23 and 28 kN/m^3. This could have been controlled by reduced porosity of quartzitic sandstone due to the recrystallization which in turn increased the density.

The mode of failure from the Brazilian tensile test was roughly parallel to the loading direction (or radial stress) and they are located in the central part of the sample between the two loading lines. The results obtained for the samples tested fall within the lower range of values derived from previous studies by Bell (2007) on the Natal Group Sandstones, which are similar in composition to the sandstones tested in this study.

The failure pattern on the samples tested for the point load strength generally occurred parallel to the loading direction in a form of single extensional fracture planes. Isolated incidents of what was described as dihedral failure mode patterns were also observed whereby three extensional failure planes (i.e. triple junction) form 120° angles from the axial point load test. The results from the point load tests revealed that the corrected size index strength $Is_{(50)}$ and UCS values range from 1.37 to 12.28 MPa and 31 and 282 MPa respectively with an average of 5.51 and 126 MPa respectively. The 29 samples presented here only consist of samples with valid failure mode where the failure fracture surface passes through both loading points (ISRM 1985). According to ISRM (1979) strength classification for intact rock, the strength of the rock could be classified as medium to very high.

The uniaxial compressive strength for the quartzitic sandstone ranges from 145 to 250 MPa. Failure of the quartzitic sandstone occurred very violently and the two types of failure patterns that were evident are conical failure (Fig. 4) and axial splitting failure. Sounds of the first stage in the failure process could be heard as if micro-cracks were forming or tiny bits of rock were coming off the core surface under incremental load by the UCS machine until pronounced failure occurred.
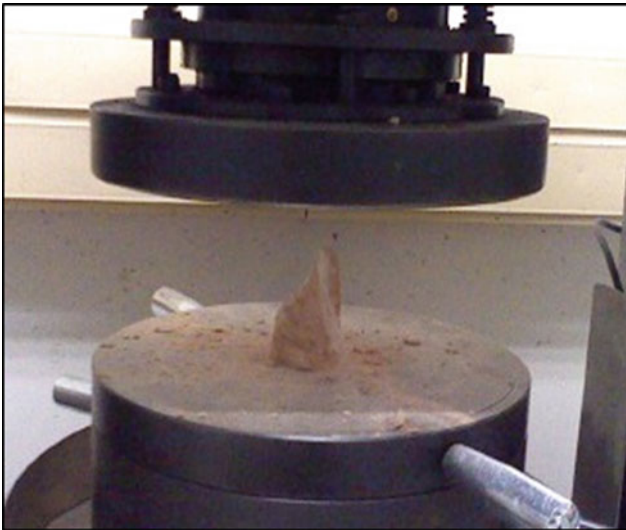
Fig. 4 Conical failure pattern from UCS testing

Based on the values obtained from the UCS tests, the strength of the quartzitic sandstone could be classified as high to very high according to the ISRM (1979) classification. This could be attributed to the mineralogy, grain size and much interlocking of the grains. The tested rock contained about 95% of quartz mineral and the binding of grains was contact to contact (almost interlocking) which could have resulted in the high compressive strength. The grain sizes of the tested sandstone material are small i.e. between 200 and 300 μm. Koncagül and Santi (1999) pointed out that small grain size results in higher grain to grain contact, thereby allowing the distribution of the load over a large surface area. According to Vutukuri et al. (1974), these factors are inter-related and they complement each other in determining the compressive strength of a rock. The interlocking and recrystallized quartz grains, also allow the rock to withstand a greater stress compared to rock with sparse grains.

Also, from the average values obtained from Schmidt hammer, point load and direct UCS tests which were 80.15, 126.71 and 189 MPa respectively, it can be concluded that the values obtained from the direct UCS test were higher than those obtained from Miller (1965) and Broch and Franklin (1972) equations. The values obtained from the Schmidt hammer rebound tests were much lower than the values obtained from the point load and UCS tests. This may be due to the fact that the Schmidt hammer rebound test is not only a function of the degree of surface weathering, but also the sample size, base material, edge effect and highly subjective to the user. The UCS test proved to be more reliable than the Schmidt hammer and point load tests.

6 Conclusion

Microscope analysis of the sandstone revealed that the sandstone is composed predominantly of quartz (+95%) and trace amounts of secondary carbonate minerals. It further showed that grains are deformed and showed evidence of re-crystallization. Therefore, the sandstone can best be described as quartzitic sandstone. The unit weight results for quartzitic sandstone were in agreement with those published values of hard sandstone (e.g. Hoek and Bray 1981). This could have been controlled by the reduced porosity of quartzitic sandstone due to the recrystallization which in turn increased density. The Brazilian tensile strength results generally fall within a range of values derived from previous studies of similar rock type for example values obtained by Bell (2007) on the Natal Group sandstone, but the values fall within the lower end of the spectrum of values derived by Bell (2007). This shows that rock material with higher strength has lower tensile strength.

The correlated UCS values derived from Schmidt hammer tests and point load corrected size index strength of the quartzitic sandstone show that the material classifies as medium to very high strength. Whilst, direct UCS tests, revealed that the strength of the quartzitic sandstone could be classified as high to very high based on the ISRM (1979) classification. The values obtained from Schmidt hammer were even lower and this may be due to the strength in this test is not only a function of the degree of surface weathering, but also the sample size, base material and edge effect. The UCS test proved to be more reliable than the Schmidt hammer and point load tests. The mineralogy, grain size, deformation, grain to grain contact (almost interlocking due to recrystallization) and silica cement were found to significantly affect the strength of the quartzitic sandstone.

References

Allman, M., Lawrence, D.F.: Geological Laboratory Techniques. Blandford, London, pp. 1–335 (1972)

Barker, O.B., Brandl, G., Callahgan, C.C., Eriksson, P.G., van der Neut M.: The Soutpansberg and Waterberg groups and the Blouberg formation. In: Johnson, M.R., Anhaeusser, C.R., Thomas, R. J. (eds.) The Geology of South Africa, Johannesburg/Council for Geosciences, Pretoria, pp. 301–319 (2006)

Bell, F.G.: Engineering Geology, 2nd edn. Butterworth-Heinemann (Elsevier), Burlington, MA. 581 p (2007)

Broch, E., Franklin, J.A.: The point load strength test. Int. J. Rock Mech. Mining Sci. **9**(6), 669–697 (1972)

Deere, D.U., Miller, R.P.: Engineering classification and index properties for intact rock. Tech. Rep. No. AFWL-TR-65-115, Air Force Weapons Lab., Kirtland Air Base, New Mexico, pp. 1–332 (1966)

Hoek, E., Bray, J.W.: Rock Slope Engineering, 3rd edn. Institute of Mineralogy and Metallurgy, London, 358 pages (1981)

Hutchison, C.S.: Laboratory Handbook of Petrographic Techniques. Wiley-Interscience, New York, xiii + 527 p (1974)

ISRM: Suggested methods for determining in situ deformability of rock. Int. J. Rock Mech. Min. Sci. Geomech. Abstr. **16**(3), 195–214 (1979)

ISRM: Suggested methods for determining hardness and abrasiveness of rocks. In: Brown, E.T. (ed.) Rock Characterization, Testing and Monitoring: ISRM Suggested Methods. Pergamon, Oxford, pp. 95–96 (1981)

ISRM: International society of rock mechanics commission on testing methods, suggested method for determining point load strength. Int. J. Rock Mech. Min. Sci. Geomech. Abstr. **22**, 51–60 (1985)

Koncagül, E.C., Santi, P.M.: Predicting the unconfined compressive strength of the Breathitt shale using slake durability, shore hardness and rock structural properties. Int. J. Rock Mech. Min. Sci. **36**, 139–153 (1999)

Miller, R.P.: Engineering classification and index properties for intact rock. Ph.D. thesis, University of Illinois (1965)

van der Waal, B.C.W.: Fundudzi, a unique, sacred and unknown South African Lake. S. Afr. J. Aquat. Sci. **23**(1), 42–55 (1997)

Vutukuri, V.S., Lama, R.D., Saluda, S.S.: Mechanical Properties of Rocks, vol. 1. Trans Tech Publications, Switzerland, 280 pages (1974)

Wentworth, C.K.: A scale of grade and class terms for clastic sediments. J. Geol. **30**(5), 377–392 (1922)

Leachate Effects on Some Index Properties of Clays

Ibrahim Adewuyi Oyediran and David Ayodele Olalusi

Abstract

Bulk disturbed samples of two clay soils were obtained from different parent rocks, mudstone and migmatite gneiss. The clays were permeated and cured with natural leachate from an old active dump site and investigated with a view to understanding the effect of leachate interaction on some engineering index properties including grain size distribution, consistency limits and specific gravity, typically used in their identification and hence classification. Results show that addition of leachate to the soils resulted in varying responses in terms of amounts of fines and clay size fraction with respect to soil type. In addition the consistency limits of the soils including liquid limit, plastic limit, plasticity index and linear shrinkage also varied with soil type. However, while variation in responses was observed for the two different soils in terms of particle size and plasticity, leachate addition lowered the specific gravity of both soils, signifying similar response by the soils to leachate contact. The responses observed are thought to be attributable to organic matter presence and varied soil structure and composition traceable to parent material influence.

1 Introduction

Index properties including the particles size, type and distribution, consistency and water content are properties that aid in the identification and classification of soils and are indicative of their engineering properties. They relate to the shear strength, compressibility, and other aspects of soil behavior. These properties are important parameters, which indicate the qualitative behavior of soils when subjected to load and are used to determine the engineering properties of clay in geotechnical design (Arasan 2010; Oyediran and Adeyemi 2011; Oyediran and Iroegbuchu 2013). In addition they help to obtain general information and are used to estimate design properties.

The generation of Leachate is an inevitable consequence of waste disposal either in engineered landfills (Sruti et al. 2014) or open dumpsites. This obnoxious liquid generated from landfill sites by hydrolysis processes and also by water penetration poses serious environmental risks to the surroundings by causing contamination of soil (Sitaram et al. 2007). Owing to their low permeability characteristics and other suitable engineering properties, clays are mostly used as barrier materials in Landfill sites to protect the environment from harmful substances especially from wastewater seepage (Amann and Martinenghi 1993) and largely to prevent groundwater contamination and untoward migration.

The preliminary design of the liner materials is done based on index properties. Furthermore as indicated by Moses et al. (2013), compatibility of a liner material with leachate is a very important consideration in the design of waste containment facilities. However perhaps much more important is an understanding of the effects and responses observed from such contact between leachate and proposed liner materials. Assertions by Chen et al. (2000), Egloffstein (2001), Frempong and Yanful (2008), that particles are highly susceptible to changes as a result of interactions with the liquid to be contained has made understanding the leachate effects on these very important properties (which can be measured by simple laboratory or field tests) used for engineering classifications of soils more imperative. Several authors have carried out investigations on the geotechnical properties of proposed barrier materials with particular reference to their suitability. Others including Sunil et al. (2008), Francisca and Glatstein (2010), Oyediran and Olalusi (2017) have indicated

I. A. Oyediran (✉) · D. A. Olalusi
Department of Geology, Faculty of Science, University of Ibadan, Ibadan, Nigeria
e-mail: oyediranibrahim2012@gmail.com;
oyediranibrahim@yahoo.com

that leachate can modify the soil properties and significantly alter the behaviour of soil. However, much more work is still required to provide a better understanding of the parent material influence on the effects of natural leachate on the engineering index properties of clay soils thereby giving an idea of materials/leachate compatibility.

2 Test Materials and Protocols

Bulk, fresh representative samples of Mudstone (AR) and Migmatite-gneiss (AB) derived clay soils were obtained from their respective deposits and sufficiently air-dried for 3 weeks. The index properties, including grain size distribution, consistency limits and specific gravity of the soils were determined in accordance with BS1377 (1990) standard test procedures. In addition the pH, Cation Exchange Capacity (CEC), Total Organic Carbon (TOC) and clay mineralogical composition (using X-ray Diffraction, XRD method) of the soils were also determined to provide pre-contamination information (Table 1). Subsequently, 10 kg of each of the soils was permeated with 5 l of natural leachate (which accumulated at the base of a 20 yr old waste

disposal site). The dark brown, malodorous smelling leachate possessed a pH of 8.2, Total Dissolved Solids (TDS) of 4.93 g/l and Total Organic Carbon (TOC) of 0.15%. The pH of the leachate according to Abbas et al. (2009) is an indication of an old dumpsite. This setup was left undisturbed in the laboratory for 21 days at a mean room temperature of 26.8 °C. All the tests initially conducted on the soils before contamination were repeated to obtain post-contamination information to enable a comparison with the pre-contamination data earlier generated.

3 Leachate Effects on Specific Gravity

The specific gravity values of AR (2.81) and AB (2.92) reduced respectively by 7 and 10% upon contamination with leachate. The decrease in specific gravity of the soils is attributed to increase in soil pH (Rakmi and Mannan 1995), influenced by higher organic waste generated from the municipal solid waste leachate on the soils (Franklin et al. 1973). The pH increased from 5.1 to 7.4 for AB while in the case of AR no noticeable change was observed. It should be noted that the no noticeable change in pH of AR is due to the

Table 1 Pre and post contamination properties of tested soils

Property	Sample label	Pre-contamination	Post-contamination
Specific gravity (g/cm^3)	AR	2.81	2.59
	AB	2.92	2.61
Liquid limit (%)	AR	46.00	65.00
	AB	64.00	45.00
Plastic limit (%)	AR	24.00	25.00
	AB	38.87	28.00
Plasticity index (%)	AR	22.00	40.00
	AB	25.13	17.00
Linear shrinkage (%)	AR	15.70	16.10
	AB	13.60	7.10
pH	AR	8.00	8.00
	AB	5.10	7.40
CEC	AR	26.60	28.00
	AB	2.00	3.70
TOC (%)	AR	0.70	0.80
	AB	0.10	0.10

Mineralogical composition

Sample	Sample type	% Composition					
		Anatase	Calcite	Hematite	Kaolinite	Quartz	Illite
AR	Uncontaminated	0.63	2.38	0.16	86.88	10.15	–
	Contaminated	1.11	1.60	0.36	78.78	18.40	–
AB	Uncontaminated	0.41	0.24	0.40	89.67	2.20	7.08
	Contaminated	0.46	0.23	0.30	90.33	1.71	6.98

fact that calcareous soils have high buffer capacity, thereby the soil pH remains at the initial after leachate addition while the pH of the acidic soils increases (Ebrahim et al. 2011). Moreover, the TOC for AR increased while that of AB showed no noticeable change. This is thought to be due to the presence and or absence of Illitic mineral in the mineralogical composition of the soils (Rakmi and Mannan 1995; Musa 2012; Evangelin and Ramprasad 2013).

4 Leachate Effects on Grain Size Distribution Characteristics

Contamination of the respective clay soils resulted in noticeable effects in the grain size distribution characteristics (Fig. 1). The grain size distribution curve pattern for the contaminated soils showed a marked difference from that of the uncontaminated soils.

Upon contamination, AR increased in clay size content by 74% while for AB clay size content decreased by 38%. However increase in amount of silts (17%) and fines (9%) was observed for AB. Change in particle size distributions of the soils is thought to depend on the nature of the soils and influence of chemicals in the leachate. Similar to chemical weathering, reactants within the leachate attack the clay mineral structure and incorporate into or remove different ions from them thereby changing the internal organization of the clay structure. This may have led to a build-up or reduction in the size distribution. In addition leachate contact with the colloids in the soil (organic and inorganic composite colloids) leads to dissolution resulting in the weakening of

strong link between the soil grains. Furthermore, Rajasekaran and Narasimha (1995) mentioned that the presence of abundant monovalent cations introduced into the soil pore water system weaken the soil. Exchange of divalent ions of soil particles by monovalent hydrogen ions of the pollutant during reaction might also have resulted into a complete loss of strong link between the soil grains. Hence, the samples dispersed easily and the amount of fines content increased as a result of contaminations (Jia et al. 2009; Musa 2012).

5 Leachate Effects on Consistency Limits

Grytan et al. (2012) did indicate that consistency limits are a basic measure of the nature of fine-grained soils. Hence, liquid limit (LL), plastic limit (PL) and plasticity Index (PI) are the most useful indicators of engineering behaviour of soils. The addition of leachate to the soils increased the LL, PL, PI and Linear shrinkage (LS) of AR by 41.30, 4.17, 81.81 and 2.55% respectively while those of AB were however reduced by 29.69, 27.97, 32.35 and 47.79% respectively (Fig. 2). Mitchell (1976) opined that organic matter addition is responsible for the changes in PL of the soils. With regards to the LL of the soils, the changes are attributed to soil-leachate interaction (Khan and Pise 1994; Puppala et al. 2007 and Sunil et al. 2009). Increase in LL and PI in AR could be attributed to the increase in the double layer thickness of the clay minerals (Shah et al. 2003) while reduction in the liquid limit as observed for AB is a function of decrease in the double layer thickness of the soil clay minerals. Moreover, nature of the pore fluids which is
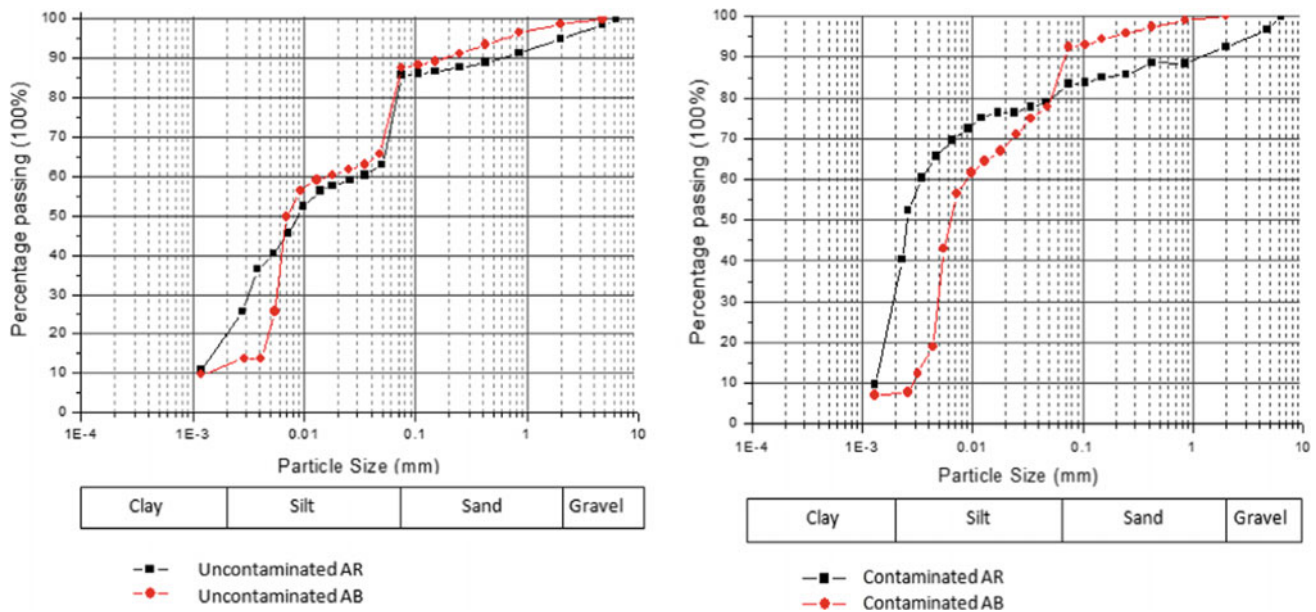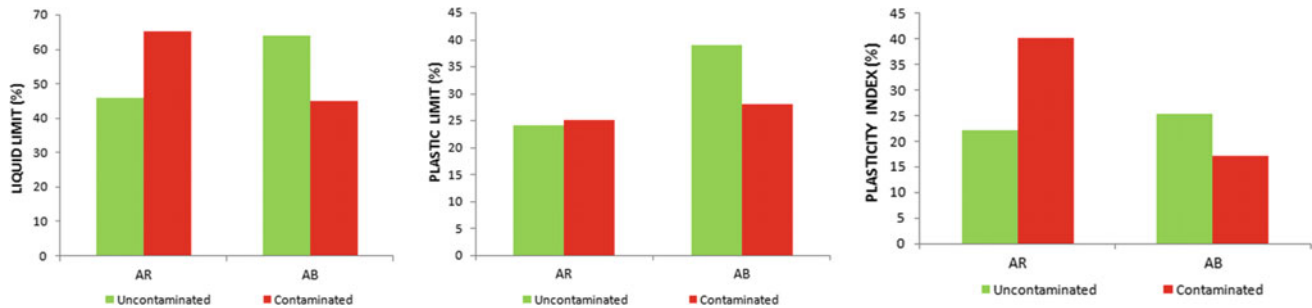

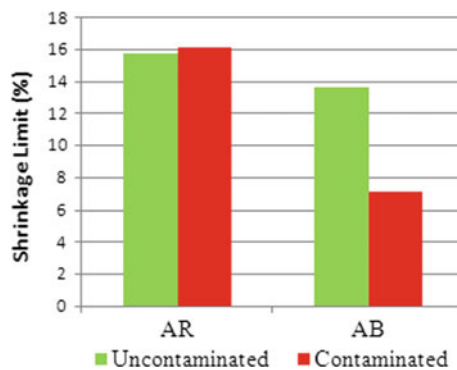**Fig. 1** Grading curves of uncontaminated and contaminated soils

Fig. 2 Consistency limits of uncontaminated and contaminated soils

reflected by the changes in the clay content of the soils as observed from the grading curves alters the specific surface area of the soil leading to high and low adsorption of water ultimately changing the limits values. In addition, the absence of Illite, increased clay contents and TOC are also thought to be responsible for the increase in LL and PI of AR while reduction in LL and PI of AB is a function of decrease in the double layer thickness of the clay minerals, presence of Illite, decreased clay content and corresponding decreased TOC. Hence, changes in LL and PI of the studied soils with leachate are directly linked to mineralogy and clay content as observed in the grain size distribution of the soils thus supporting earlier findings by Benson and Trast (1995).

Effect of leachate on LS of the soils is evident in the 2.55% increase for AR while a decrease of 47.79% occurred for AB (Fig. 3). Observed changes in LS of soils is linked to the mineralogy of the soils. Increase in LS for AR and corresponding decrease in LS for AB is attributed respectively to Illite absence, increased clay contents, increased soil consistency and high Kaolinite content, Illite presence, low clay content and reduced soil consistency. The LS observed is as a result of packing phenomenon primarily controlled by the relative grain size distribution of the soil.

Soils with flocculated structures shrink less than that with a dispersed structure. Thus, volume reduction takes place due to capillary pressures induced by the evaporation of water from the soil differs (Sridharan and Prakash 2000). Increase and decrease in LS may also be attributed to the corresponding change in the soil structure due to diffused double layer. Consideration for the possibility of existence of dangerous cracks and gaps in the liner makes it imperative to understand the response to shrinkage. In addition excessive shrinkage can cause differential settlement of structures (Jones and Jefferson 2012).

Casagrande chart classification of the soils (Fig. 4) clearly shows the influence of leachate on the soils. Leachate addition resulted in modification of AR from a soil of medium plasticity to a soil of high plasticity and above the A-line. However AB on the other hand was modified from being a soil of high plasticity to that of medium plasticity and below the A-line. El-Hajji (2006) observed this same trend and noted the obvious effect of leachate addition. Alteration of host soil properties by contaminants shows the significant effect such contaminants have as reported by several other researchers including Arasan and Yetimoglu (2008), and Yukselen-Aksoy et al. (2008).

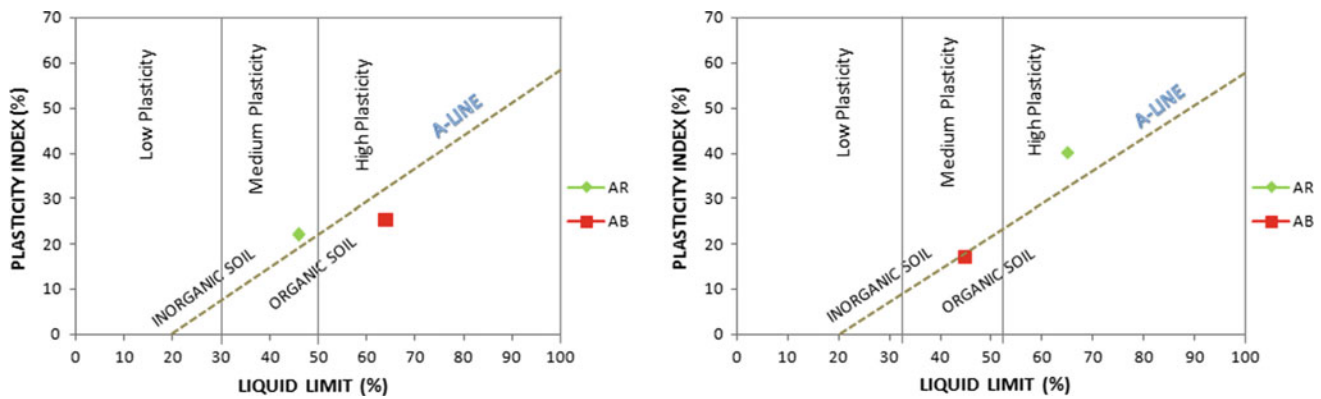**Fig. 3** Consistency limits of uncontaminated and contaminated soils

Fig. 4 Cassagrande chart classification of uncontaminated and contaminated soils

6 Conclusions

The experimental studies conducted on the engineering index properties of the two clay soils of different parent materials upon contamination with natural leachate shows that addition of leachate to the soils resulted in varying responses in terms of amounts of fines and clay size fraction with respect to soil type. Changes in the consistency limits of the soils with leachate contact are directly linked to mineralogy and clay content and also varied with soil type indicative of parent material influence. However, while variation in responses was observed for the two different soils in terms of particle size and plasticity, leachate addition lowered the specific gravity of both soils, signifying similar response by the soils to leachate contact. The responses observed are thought to be attributable to organic matter presence and varied soil structure and composition traceable to parent material influence. Hence, consideration must be given to the parent material, which produced proposed barrier soils and the inherent responses observable with leachate contact in deciding barrier soil suitability.

References

Abbas, A.A., Jingsong, G., Ping, L.Z., Ya, P.Y., Al-Rekabi, W.S.: Review on landfill leachate treatments. J. Appl. Sci. Res. **5**(5), 534–545 (2009)

Amann, P., Martinenghi, L.: Geotechnical design criteria for landfills and waste disposal sites. In: Joint CSCE-ASCE National Conference on Environmental Engineering, vol. 1, pp. 797–804 (1993)

Arasan, S.: Effect of chemicals on geotechnical properties of clay liners: a review. Res. J. Appl. Sci. Eng. Technol. **8**, 765–775 (2010)

Arasan, S., Yetimoglu, T.: Effect of inorganic salt solution on the consistency limits of two clays. Turk. J. Eng. Environ. Sci. **32**, 107–115 (2008)

Benson, C.H., Trast, J.M.: Hydraulic conductivity of thirteen compacted clays. Clays Clay Miner. **43**(6), 669–681 (1995)

British Standard Institution (BS1377): Methods of Test for Soils for Civil Engineering Purposes. British Standard Institute, London (1990)

Chen, J., Anandarajah, A., Inyang, H.: Pore fluid properties and compressibility of kaolinite. J. Geotech. ASCE **126**(9), 798–807 (2000)

Ebrahim, P., Ali, G., Amir, H.D.: Influence of garbage leachate on soil reaction, salinity and soil organic matter in East of Isfahan. World Acad. Sci. Eng. Technol. Int. J. Environ. Chem. Ecol. Geol. Geophys. Eng. **5**(9) (2011)

Egloffstein, T.: Natural bentonites—influence of the ion exchange and partial desiccation on permeability and self-healing capacity of bentonites used in GCLs. Geotext. Geomembr. **19**, 427–444 (2001)

El-Hajji, D.: Evaluation of the long term effect inorganic leachate on geosynthetic clay liners. Graduate Theses and Dissertations, 98p (2006). http://scholarcommons.usf.edu/etd/2516

Evangelin, R.S., Ramprasad, C.: Effect of dumping municipal solid waste on geotechnical properties of the soil. In: Proceedings of Indian Geotechnical Conference, 22–24 Dec 2013, Roorkee (2013)

Francisca, F.M., Glatstein, D.A.: Long term hydraulic conductivity of compacted soils permeated with landfill leachate. J. Appl. Clay Sci. **49**, 187–193 (2010). https://doi.org/10.1016/j.clay.2010.05.003

Franklin, A.G., Orozeo, L.P., Semrau, R.: Compaction and strength of slightly organic soils. J. Soil Mech. Found. Div. ASCE **99**(SM 7), 541 (1973)

Frempong, E.M., Yanful, E.K.: Interaction between three tropical soils and municipal waste landfill leachate. J. Geotech. Geoenviron. Eng. ASCE **134**(3), 379–396 (2008)

Grytan, S., Islam, M.R., Alamgir, M., Rokonuzzaman, M.: Study on the geotechnical properties of cement based composite fine-grained soil. Int. J. Adv. Struct. Geotech. Eng. **1**(2), 42–49 (2012)

Jia, Y.G., Wu, Q., Meng, X.M., Yang, X.J., Yang, Z.N., Zhang, G.C.: Case study on influences of oil contamination on geotechnical properties of coastal sediments in the Yellow River Delta. In: Proceeding of International Symposium on Geoenvironmental Engineering, Hangzhou, China (2009)

Jones, L.D., Jefferson, I.: Expansive Soils. ICE Publishing, UK, pp. 413–441 (2012)

Khan, A.K., Pise, P.J.: Effect of liquid wastes on the physico chemical properties of lateritic soils. In: Proceedings of Indian Geotechnical Conference, Dec 1994, Warangal, pp. 189–194 (1994)

Mitchell, J.K.: Fundamentals of Soil Behaviour. Willey, New York (1976)

Moses, G., Oriola, F.O.P., Afolayan, J.O.: The impact of compactive effort on the long term hydraulic conductivity of compacted foundry

sand treated with bagasse ash and permeated with municipal solid waste landfill leachate. Front. Geotech. Eng. **2**(1), 7–15 (2013)

Musa, A.: The effects of municipal solid waste on the geotechnical properties of soils. Int. J. Environ. Sci. Manage. Eng. Res. **1**(5), 204–210 (2012)

Oyediran, I.A., Adeyemi, G.O.: Geotechnical investigations of a site in Ajibode, southwestern Nigeria for landfill. Ozean J. Appl. Sci. **4**(3), 265–279 (2011)

Oyediran, I.A., Iroegbuchu, C.D.: Geotechnical characteristics of some southwestern nigerian clays as barrier soils. Ife J. Sci. **15**(1), 17–30 (2013)

Oyediran, I.A., Olalusi, D.A.: Hydraulic conductivity and leachate removal rate of genetically different compacted clays. Innovative Infrastruct. Solutions **2**(46), 1–14 (2017). https://doi.org/10.1007/s41062-017-0097-0

Puppala, A.J., Pokola, S.P., Intharasombat, N., Williammee, R.: Effects of organic matter on physical, strength, and volume change properties of compost amended expansive clay. J. Geotech. Geoenviron. Eng. **133**(11), 1449–1461 (2007)

Rajasekaran, G., Narasimha, R.S.: Cation exchange studies on a lime treated marine clay. J. SE. Asian Geotech. Soc. **26**(1), 19–35 (1995)

Rakmi, A., Mannan, M.A.: Effects of organic load on basic geotechnical properties of compacted sand-kaolinite mixture. Pertanika J. Sci. Technol. **3**(1), 87–98 (1995)

Shah, S.J., Shroff, A.V., Patel, J.V., Tiwari, K.C., Ramakrishnan, D.: Stabilization of fuel oil contamination soil: a case study. Geotech. Geol. Eng. **21**, 415–427 (2003)

Sitaram, N., Sunil, B.M., Shrihari, S.: Hydraulic and compaction characteristics of leachate-contaminated lateritic soil. J. Eng. Geol. 137–144 (2007)

Sridharan, A., Prakash, K.: Shrinkage limit of soil mixtures. Geotech. Test. J. GTJODJ **23**(1), 3–8 (2000)

Sruti, P., Anju, E.P., Sunil, B.M., Shrihari, S.: Soil pollution near a municipal solid waste disposal site in India. In: Proceedings of International Conference on Biological, Civil and Environmental Engineering (BCEE-2014), 17–18 Mar 2014, Dubai (UAE), pp. 148–152 (2014). http://dx.doi.org/10.15242/IICBE.C0314080

Sunil, B.M., Shrihari, S., Sitaram, N.: Soil-leachate interaction and their effects on hydraulic conductivity and compaction characteristics. In: Proceedings of 12th International Conference of International Association for Computer Methods and Advances in Geomechanics (IACMAG), 1–6 Oct, Allahabad, India (2008)

Sunil, B., Shrihari, S., Nayak, S.: Shear strength characteristics and chemical characteristics of leachate-contaminated lateritic soil. Eng. Geol. **106**, 20–25 (2009)

Yukselen-Aksoy, Y., Kaya, A., Oren, A.H.: Seawater effect on consistency limits and compressibility characteristics of clays. Eng. Geol. **102**, 54–61 (2008)

Mineralogical Composition and Structure of Fibrous Anthophyllite: A Case Study from Argentina

Lescano Leticia, Marfil Silvina, Sfragulla Jorge, Bonalumi Aldo, and Maiza Pedro

Abstract

In this work a multimethodological approach is taken, complementing field studies with petrographic-mineralogical, compositional and morphological analyses of anthophyllite in the "Coco Solo" mine from the province of Córdoba (Argentina). Fibrous minerals were studied by stereomicroscopy, polarizing light microscopy and SEM. The fibres have positive elongation, straight extinction and slight pleochroism. Thermogravimetric and differential scanning calorimetry (TG/DSC) data allowed the determination of the structural water content and temperature stability. X-ray diffraction was used for the characterization of the mineral fibres before and after heating at 1000 °C to identify the products of thermal decomposition. The crystal structure determined corresponds to anthophyllite. Finally, morphological analyses on acicular and fibrous phases were conducted. Particles up to ∼ 1 μm were analysed by optical microscopy, while particles up to ∼ 0.1 μm were examined by SEM. When complemented, these two techniques are useful to characterize the morphologies of the particles.

Keywords

Asbestos • Anthopyllite • Argentina

1 Introduction

In a general sense and from a commercial perspective, the term "asbestos" is defined as a group of six minerals that appear in nature forming bundles of thin and long fibres, with high tensile strength and flexibility, low thermal and electrical conductivity, high absorbance and thermal stability, and chemical resistance (Gunter et al. 2007). These minerals have been classified as a carcinogen by the U.S. Department of Health and Human Services (HHS), the Environmental Protection Agency (EPA), and the International Agency for Research on Cancer (IARC). Studies have shown that exposure to asbestos may increase the risk of lung cancer and mesothelioma (Yarborough 2006). There are several records related to health problems in miners that work in both underground and open pits, where asbestiform minerals are major or accessory constituents of the ores extracted.

Asbestos is divided into two groups (amphiboles and chrysotile) that form thin and long fibres. They are hazardous due to their morphology. The mineralogical study is essential for assessing their potential impact on human health. Chrysotile fibres have low degrees of aggressiveness as compared to amphiboles. Epidemiological studies show that long and rigid fibres (amphiboles) are more harmful than curly fibres (chrysotile) (Rigarti et al. 2003).

There is scarce information about the potential hazardousness of anthophyllite or tremolite because they have been rarely exploited in pure form. Morphological characterization in itself usually does not constitute a reliable identification criterion (Ross et al. 1984). Hence, microscopic examination methods and other analytical approaches are usually combined. The optical properties of the different types of asbestos fibres, together with information on fibre shapes, enable positive identification of all varieties of asbestos fibres. Their refractive index, colour, pleochroism, birefringence, orientation, etc. cannot always be measured, thus other methods must be employed. TG/DSC data allowed the determination of the structural water content and thermal stability.

In this work a multimethodological approach is taken, complementing field studies with petrographic-mineralogical, compositional and morphological analyses of asbestiform minerals in the "Coco Solo" mine from the province of

L. Leticia (✉) · M. Silvina · M. Pedro
Geology Department, Universidad Nacional del Sur, Bahía Blanca, Argentina
e-mail: leticia.lescano@uns.edu.ar

S. Jorge · B. Aldo
sec. de Minería de la Prov. de Córdoba, Universidad Nacional de Córdoba, Córdoba, Argentina

Córdoba (Argentina). The mine object of study was exploited until the end of the 1970s. Although it is currently abandoned, it is important to carry out detailed studies of the deposit to determine the occurrence of asbestiform minerals in the ore and associated with vermiculite, serpentine and talc, currently in operation.

The presence of minerals with asbestiform morphologies and their potential impact on human health have been a subject of study and debate for more than 40 years worldwide (Goodwin 1974; OSHA 1992; Van Gosen et al. 2004). The mineralogical analysis is important to evaluate its health hazard which depends on chemistry, resistance and the most important property: the fibre morphology. But not all asbestos are equally carcinogenic or harmful to human health. Amphibole fibres being the most harmful (Ross et al. 1993).

2 Materials and Methods

The geological setting of the Coco Solo mine is composed of an ultramafic lenticular body embedded in amphibolites, 80 m in length and with variable thickness (between 0.5 and 2 m) (Angelleli et al. 1980). Pegmatites appear crosscutting the amphibolite-ultramafic set, generating reaction halos with vermiculite development. The ultramafic talc body is crosscut by fractures filled with asbestos. The fibres crystallize perpendicular and parallel to the subhorizontal and vertical veins respectively. Although the mine is currently closed, detailed studies of the deposit indicate the presence of minerals with asbestiform morphology in the talc ore or associated with vermiculite-rich belts. The fibrous minerals were studied by optical and scanning electron microscopy, TG/DSC (heating at 1000/1100 °C), and XRD.

3 Results

3.1 Optical and Scanning Electron Microscopy (SEM)

The fibrous mineral of the Coco Solo mine presents acicular habit, with remarkable crystal development. It can reach from a few microns up to several cm in length, with a length/width ratio greater than 200.

The crystals, of asbestiform morphology, are developed along the axis c. Figure 1a shows the acicular crystals in loose grains observed with the optical microscope. They are associated with other fibrous amphiboles, calcite, dolomite and opaque minerals. The fibres are arranged in dense packages concordant with the strike of the mineralized structure as well as amphiboles and carbonates. The fibrous mineral presents brown colour, low pleochroism, high relief, second order interference colour, positive elongation and right extinction. For their optical properties and morphology they are classified as anthopyllite amphibole. Opaque minerals are concentrated mainly in the carbonatic areas. Intense flexure of the crystals, caused by tectonic processes after crystallization, is observed. Discordant and fractured prismatic crystals arranged in an irregular shape are frequently identified (Fig. 1b).

Elongated and acicular fibres were observed by SEM. Abundant smaller fibres are detached from fibre packages as can be seen in Fig. 1c. Figure 1d shows a detail of the morphological characteristics and their distribution.

3.2 Thermal Analysis (TG/DSC)

The structural changes of anthophyllite with increasing temperature can be summarized in the following steps: dehydrogenation and/or dehydroxylation accompanied by iron oxidation, structure collapse and crystallization of newly formed crystalline phases, early melting (Bloise et al. 2016).

The DSC diagram (Fig. 2) shows endothermic peaks at 260, 574 and 862 °C, and an exothermic peak at 940 °C attributed to enstatite crystallization. The loss of weight is 4.15%. These results are comparable with the anthophyllite curve shown by Bloise et al. (2016).

The weak peaks at 260 and 546 °C are attributed to the dehydration and dehydroxylation of mineral impurities in the sample.

3.3 X-Ray Diffraction (XRD)

The main reflexions of anthophyllite were identified by XRD and are comparable to ICDD card number 042-0544 (ICDD 1993). The peaks are sharp and with high intensity indicating good crystallinity (Fig. 3a).

The material obtained after the DSC analysis (heated at 1000 °C) was also analysed by this method, identifying enstatite (Fig. 3b). This result is similar to that obtained by Bloise et al. (2016).

4 Conclusions

The fibrous mineral associated whit talc and vermiculite in the Coco Solo mine (province of Córdoba, Argentina) was determined as anthopyllite.
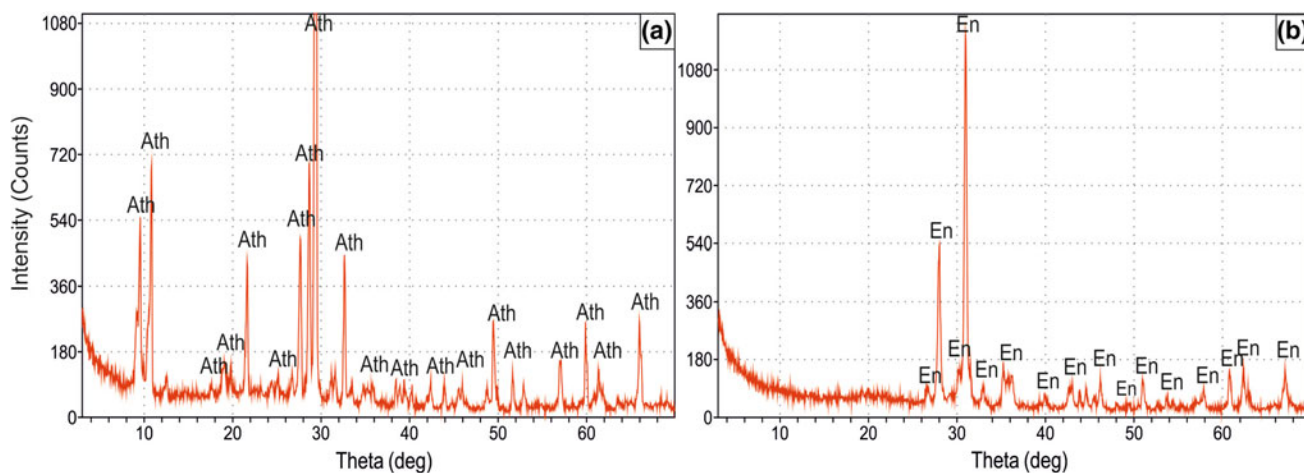
By optical and SEM microscopy the fibrous mineral presents acicular habits and asbestiform morphology, associated with other fibrous amphiboles, calcite, dolomite and opaque minerals.
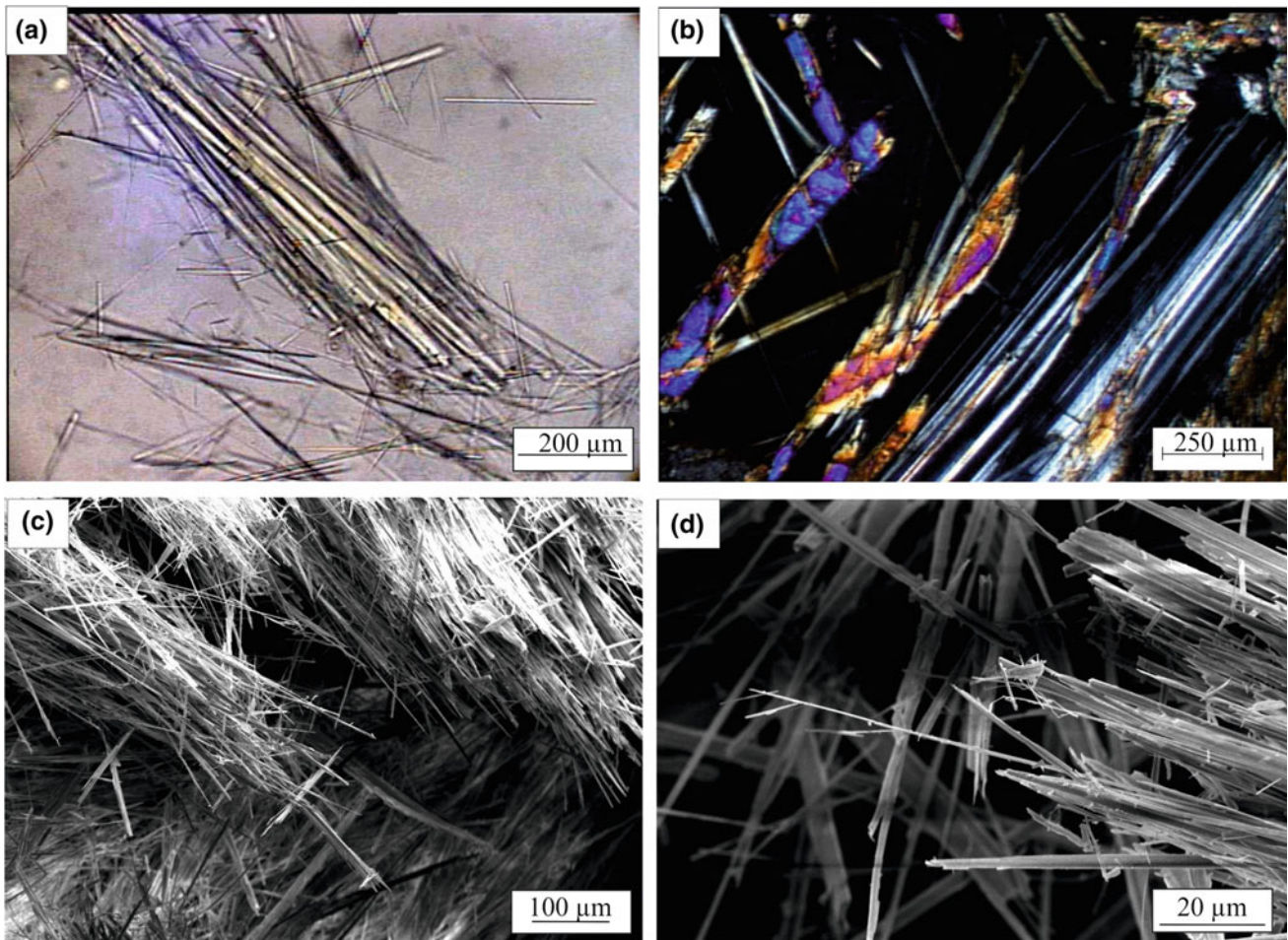
Fig. 1 **a** Acicular crystals in loose grains. **b** Anthopyllite in thin section. **c**, **d** SEM: morphological characteristics

Fig. 2 DSC-TG of fibrous mineral determined as anthophyllite
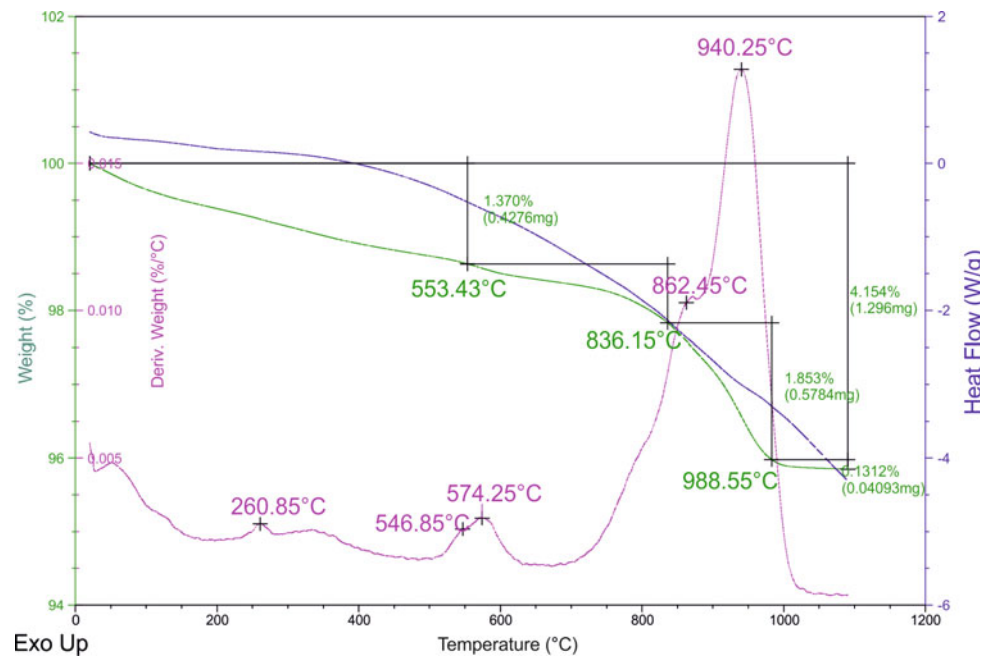
Fig. 3 XRD. **a** Natural mineral fibres. **b** Mineral fibres after heating at 1000 °C. Ath: anthophyllite. En: enstatite

By TG, the structural changes of anthophyllite with increasing temperature was determinate. The DSC shows an exothermic peak at 940 °C attributed to enstatite crystallization.

The main reflexions of anthophyllite were identified by XRD. The material obtained after the DSC analysis was identified as enstatite.

The identified amphibole asbestos may be a potential health hazard during ore mining, transportation, and grinding works.

References

Angelelli, V., Schalamuk, I., Fernández, R.: Los yacimientos no metalíferos y rocas de aplicación de la región Centro-Cuyo. Secretaría de Estado de Minería, Anales **19**, 1–261 (1980)

Bloise, A., Catalano, M., Barrese, E., Gualtieri, A., Gandolfi, N., Capella, S., Belluso, E.: TG/DSC study of the thermal behaviour of hazardous mineral fibres. J. Therm. Anal. Calorim. **123**, 2225–2239 (2016)

Goodwin, A.: Proceedings of the symposium on talc, Washington D.C. Bureau Min. Info. Circular **8639**, 102 pp (1974)

Gunter, M., Belluso, E., Mottana, A.: Amphiboles: environmental and health concerns. In: Rosso, J.J. (ed.) Reviews in mineralogy and geochemistry, pp. 453–516. Mineralogical Society of America Geochemical Society, Chantilly (2007)

International Centre for Diffraction Data (ICDD): Mineral powder diffraction file, p. 2389. Databook, Park Lane, Swarthmore. Pennsylvania (1993)

OSHA: Occupational exposure to asbestos, tremolite, anthophyllite and actinolite. Fed. Reg. **57**, 24310–24331 (1992). Department of Labor, Occupational Safety and Health Administration, US

Rigarti, C., Aldieri, E., Bergandi, L., Tomatis, M., Fenoglio, I., Costamagna, C.: Long and short fiber amosite asbestos alters at a different extent the redox metabolism in human lung epithelial cells. Toxicol. Appl. Pharmacol. **193**, 106–115 (2003)

Ross, M., Kuntze, R., Clifton, R.: A definition for asbestos, pp. 139–147. Special Technical Publication 834. American Society for Testing Materials, Philadelphia (1984)

Ross, M., Nolan, R., Langer, A., Cooper, W.: Health effects of mineral dusts other than asbestos. In: Guthrie, G.D., Mossman, B.T. (eds.) Health effects of mineral dusts. Reviews in mineralogy, vol. 28, pp. 361–407. Mining Society of America, Washington DC (1993)

Van Gosen, B., Lowers, H., Sutley, S., Gent, C.: Using the geologic setting of talc deposits as an indicator of amphibole asbestos content. Environ. Geol., 43 pp (2004)

Yarborough, C.: Chrysotile asbestos and mesothelioma. Crit. Rev. Toxicol. **36**(2), 165–187 (2006)

Effect of Lime on the Plasticity of Fine-Grained Soils of Tabriz Northern Highway Route, Iran

Mahin Salimi, Ebrahim Asghari-Kaljahi, and Masoud Hajialilue-Bonab

Abstract

Fine-grained soils with high plasticity exhibit an expansion potential when the soil moisture changes. Because of the swelling nature of the fine-grained soils, the use of lime to improve their engineering properties is common. This research investigated the effect of lime on plastic soils from Tabriz northern highway, Iran. Soil samples were taken from five locations along this highway with a length of about 17 km. The soils classification, based on USCS, is CL and plasticity index values of soils (PI) vary between 15 and 25%. The properties of soil-lime mixtures depended on the soil type, lime content were curing time. Soil samples mixed with 2, 4 and 6% lime at optimum moisture content were allowed to cure at room temperature for 2, 14, and 28 days. Test results indicate that addition of lime increases the plastic limit soils, while the plasticity index of samples decreases. Adding more lime and curing more time indicate more reduction in the plasticity index. Generally, the addition of 4% lime is good for stabilizing all soil samples and is recommended as the optimal lime content for the study soils.

M. Salimi (✉)
University of Tabriz, 5166616471 Tabriz, Iran
e-mail: salimi.mahin@yahoo.com

E. Asghari-Kaljahi
Department of Earth Sciences, University of Tabriz, Tabriz, Iran
e-mail: e-asghari@tabrizu.ac.ir

M. Hajialilue-Bonab
Faculty of Civil Engineering, University of Tabriz, Tabriz, Iran

1 Introduction

Clay soils have a wide range of mineralogical composition and they consist of various proportions of different types of clay minerals, such as Kaolinite, Illite, Montmorillonite, and etc Holtz et al. (2011). Clay soils can be stabilized by the addition of small percentage of lime. The addition of lime to soils to improve their use for construction purposes has a very long history (Bell 1996). Expansive soils show large volume change when the natural environmental conditions of the soil are altered and pose a problem to the construction engineers (Dakshanamurthy and Raman 1973). Lime stabilization is most often used in relation to road construction (Bell 1996). When lime is added to a clay soil it has an immediate effect on the properties of the soil as cation exchange begins to take place between the metallic ions associated with the surface of the clay particles are surrounded by a diffuse hydrous double layer which is modified by the ion exchange of calcium. This alters the density of the electrical charge around the clay particle which leads to them being attracted closer to each other to form flocs, the process being termed flocculation. It is this process which is primarily responsible for the modification of the engineering properties of clay soils when they are treated with lime (Sherwood 1993). The optimum addition of lime needed for maximum modification of the soil and is normally between 1 and 3% (Bell 1996). In most cases the effect of lime on the plasticity of clay soil is more or less instantaneous, the calcium ions from the lime causing a reduction in plasticity, the soils becoming more friable and more easily worked. The clay particles undergo flocculation to form aggregates. The aggregates behave like particles of silt. The plastic limit of montmorillonite increased and the plastic limit of kaolinite suffered slight reduction. When Kaolinite was treated with 2% lime it underwent an increase of some 28% in liquid limit (Bell 1996). The reduction in liquid limit and increase in plastic limit produced a considerable reduction in the plasticity index of montmorillonite.

Salimi et al. (2017) is evaluated the expansive potential of soils of Tabriz Northern Highway (TNH) by plasticity limits.

This paper presents the effect of lime on the plasticity of fine grained soils of TNH, in the north west of Iran. Swelling of soils is caused some problems for this highway.

2 Soil Sampling

Tabriz Northern Highway (TNH) with 17 km is located in the north of Tabriz city, Iran. Tabriz is one of biggest cites of Iran, with population more than 2 millions. The TNH is beside the Eynali mountain range that much of the area around TNH is covered with red mudstone, marlstone, and sandstone from Miocene and Pliocene formations. The weathering of these formations is produced red expansive fine-grained soils.

Soil samples were taken from five points along TNH. Figure 1 shows the satellite photo of TNH and location of sampling and Fig. 2 shows a photo of soil sampling.

3 Soil Testing

Based on soil particle size distribution and Atterberg limits of samples, all natural soil samples are classified as CL according to USCS. The Atterberg limits of samples (LL and PL) are determined and showed in Table 1. Fine material of soils (F) varies between 86 and 97%. The maximum dry density (γ_{dmax}) and optimum water content (ω_{opt}) were determined according to standard Proctor compaction test (ASTM D698 2000) and is showed in the Table 1.

Based on Sowers (1979) calcification that is showed in Table 2, the plasticity of soil samples are slightly to medium.

4 Lime Stabilizing

Lime is used to prepare various trial mixes at 0, 2, 4 and 6% hydrated lime content. The soil and lime are mixed manually. Water is added and mixed with mass of lime and soil. The mixed of soil and lime is placed in plastic bags and left
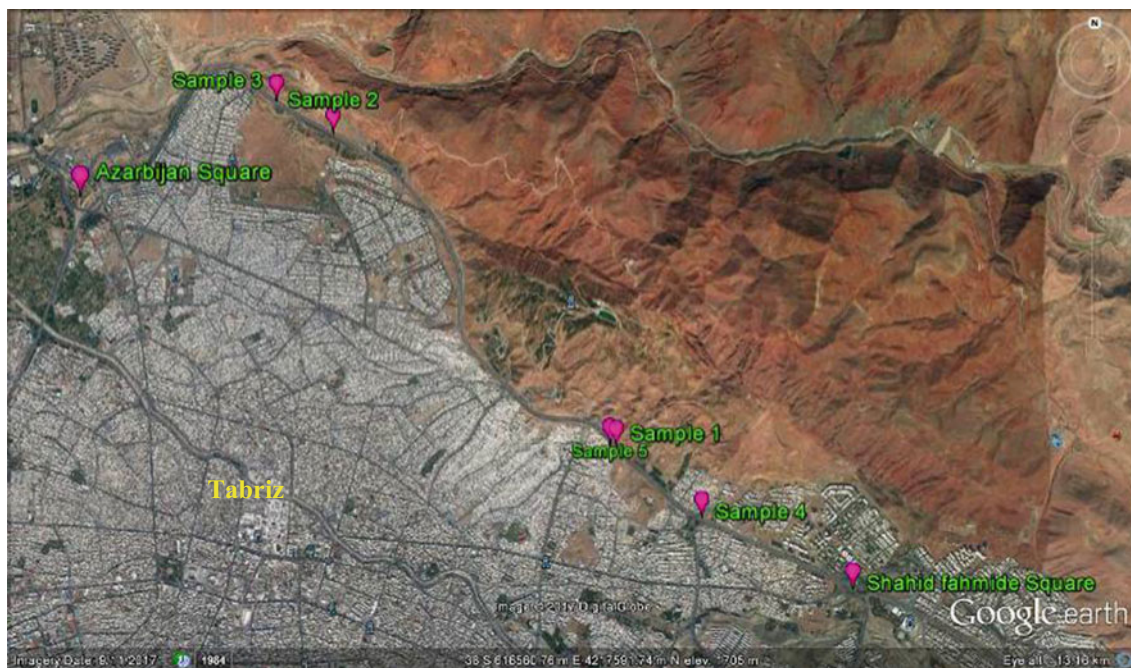

Fig. 1 Satellite photo of TNH and sampling points (Google Earth)

Fig. 2 A picture of soil sampling

Table 1 Physical properties of soil samples

Sample no.	F (%)	PL (%)	LL (%)	PI (%)	USCS	ω_{opt} (%)	γ_{dmax} (g/cm^3)	Gs
1	91	15.1	30.5	15.4	CL	14.0	1.89	2.66
2	88	21.1	31.5	10.5	CL	16.1	1.90	2.76
3	86	20.1	30.1	10.0	CL	13.0	1.93	2.74
4	94	20.1	41.1	21.0	CL	16.2	1.72	2.71
5	97	22.1	45.6	23.5	CL	14.6	1.78	2.70

Table 2 Soil classification based on plasticity (Sowers 1979)

Dry strength	Plasticity index (%)	Plasticity
Very low	0–3	Non-plastic
Slight	3–15	Slightly plastic
Medium	15–30	Medium
High	>30	Highly plastic

to cure at room temperature (about 20 °C) and are tested for determining Atterberg limits at the ages of 2, 14, and 28 days. This extended curing time was to allow for the completing of reactions between lime and clay particles. Then the samples were prepared and tested. The LL of samples was determined by the Casagrande cup and the fall cone methods (Fig. 3). The plastic limit (PL) of soils was determined by rolling soil method.

The liquid limit of soils are determined using the Casagrande apparatus, by measuring the moisture content at which a standard groove in a minus sieve No. 40, per-moistened soil pat, will flow together for a distance of 13 mm under the impact of 25 blows (ASTM D4318 2005).

The fall cone test is considered as a reliable method for determining the liquid limit than the Casagrande method (Koumoto and Houlsby 2001). The fall cone method is said to eliminate most of the drawbacks of the Casagrande method, and results in improved accuracy and repeatability (Campbell and Blackford 1984). In the fall cone method, the liquid limit is taken as the moisture content at which a

Fig. 3 The Casagrande apparatus (left) and the fall cone apparatus (right)

standard 30°, 80 g cone will penetrate the soil sample a distance of 20 mm in approximately 5 s (BS 1990).

5   Test Results and Discussion

Based on the grain-size distribution and plasticity tests results, the samples were classified as CL. The LL and PL of all samples stabilized with lime are performed by Casagrande method based on ASTM D4318. The curing effect and lime content on the plasticity index curve of samples are shown in Fig. 4. It is observed that by adding about 4% of lime the PI changes are high, but after 4%; the PI changes is slightly by adding lime.

The sample No. 2 selected for determining of LL by fall cone test method. Lime percentages in the stabilized clayey soil specimens were 2, 4, and 6%. The soil specimen was mechanically mixed with the required amount of lime homogeneously. After that the pre-determined amount of water was added to the soil and lime was mixed and whole components were thoroughly mixed once more and made ready for curing 2, 14, and 28 days. The liquid limits of sample with lime stabilized were determined with reference to BS 1337-2 standard.

In most cases the effect of lime on the plasticity of clay soil is more or less instantaneous, the calcium ions from the lime causing a reduction in plasticity, the soils becoming more friable and more easily worked (Bell 1996). Bell (1996) was showed that the plasticity index of kaolinite increase and liquid limit of montmorillonite decreased with increasing lime content. In the other hand the plasticity index of the montmorillonite decreased. The plasticity index of all samples were reduced with adding 2 and 4% hydrated lime, plasticity index of samples 1, 2, and 3 increasing with adding 6% lime, and plasticity index of samples 4 and 5 were reduced.
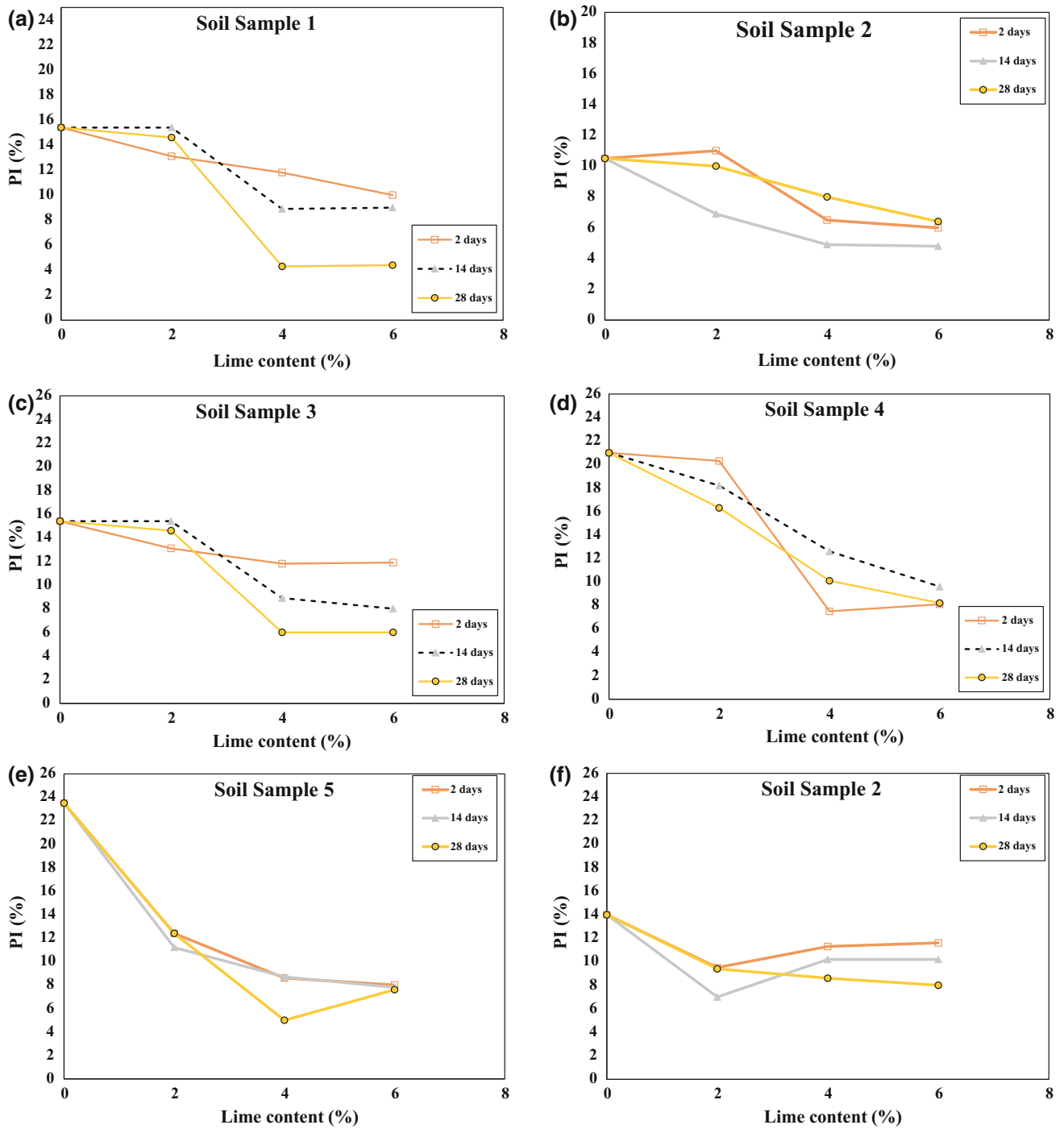
Fig. 4 Relationship between plasticity index, lime content and curing time as determined by Casagrande apparatus (**a**, **b**, **c**, **d**, **e**) and fall cone method (**f**)

6 Conclusions

The main results of this research are as follows:

- The classification of natural soil samples of Tabriz northern highway route are classified CL based on USCS. The treated soil samples with 2, 4 and 6% lime is classified ML.
- The plasticity index of soils is reduced with increasing lime content.
- The liquid limit of soils is increased with increasing lime content.
- Soil samples that had high liquid limit are shown highest reduction in the plasticity index with adding 6% lime, and samples that had medium liquid limit, adding 2% lime, the plasticity index decreases. Generally, adding 4% lime stabilizes study site soils and is recommending as optimum content.
- Almost it is constant the decrease in the plasticity index of soil curing 2, 14, and 28 days; because it has done the reactions to reduce the swelling in the soil curing 2 days.
- Using fall cone test method is more suitable than Casagrande method for determining plasticity limit of soils.

References

ASTM D698: Standard test methods for laboratory compaction characteristics of soil using standard effort. West Conshohocken, (2000)

ASTM D4318-05: Standard test methods for liquid limit, plastic limit, and plasticity index of soils. West Conshohocken, (2005)

Bell, F.G.: Lime stabilization of clay minerals and soils. Eng. Geol. **4294**, 223–237 (1996)

BS 1377-2: Methods of test for soils for engineering purposes. Classif Tests (1990)

Campbell, D.A., Blackford, J.W.: Fall cone method used to determine the liquid limit of soil. Engineering and Research Center, Denver, Colorado (1984)

Dakshanamurthy, V., Raman, V.: A simple method of identifying an expansive soil. Japan. Soil Mech. Found. Eng. **13**(1), 97–104 (1973)

Holtz, R.D., Kovacs, W.D., Sheahan, T.C.: An introduction to geotechnical engineering, 2nd edn. Perntice Hall, Upper Saddle River, NJ (2011)

Koumoto, T., Houlsby, G.T.: Theory and practice of the fall cone test. Geotechnique **51**(8), 701–712 (2001)

Salami, M., Asghari-Kaljahi, E., Hajialilue-Bonab, M.: Evaluation of soils swelling potential of Tabriz northern highways based on plasticity characteristics. In: 35th geosciences congress. GSI, Tehran, Iran, (2017)

Sherwood, P.T.: Soil stabilization with cement and lime. Transport Research Laboratory, Her Majesty's Stationery Office, London (1993)

Sowers, G.F.: Introductory soil mechanics and foundations. Geotechn. Eng. Macmillan Publication, New York, 0-02-413870-3 (1979)

Modeling Grain Size Heterogeneity Effects on Mechanical Behavior of Crystalline Rocks Under Compressive Loading

Jun Peng, Louis Ngai Yuen Wong, and Cee Ing Teh

Abstract

Strength and deformation behavior of intact rocks is influenced by a large number of factors, notably mineralogical content. If the constituent minerals are strong, the overall rock strength will be high, and vice versa. The prediction of rock properties of those composed of different types and amounts of minerals will be difficult. This paper presents a numerical approach to study the influence of material heterogeneity associated with the variation of grain size distribution and shape on the strength and deformation behavior of a felsic crystalline rock. By taking advantage of a grain-based modeling approach in two-dimensional Particle Flow Code, a heterogeneity index is defined and explicitly incorporated into the numerical models quantitatively. The numerical results reveal that the peak strength increases as the numerical model gradually changes the character of the rock from heterogeneous to homogeneous. The number of grain boundary tensile cracks gradually decreases and the number of intra-grain cracks increases at the moment of failure. The orientation of grain boundary micro-cracks is mainly controlled by the geometry of assembled grain structure of the numerical model, while the orientation of intra-grain micro-cracks is to a large degree influenced by the confinement. In addition, the development of intra-grain cracks (both tensile and shear) is much more favored in quartz than in other minerals. The findings of this study provide insights to the interpretation of rock properties, particularly those which are strongly influenced by the heterogeneous mineralogical composition.

1 Introduction

Rock is typically heterogeneous composed of different types of minerals and inherent microstructures. Laboratory test results indicate that the strength and deformation responses and the associated micro-cracking behavior of rocks are to a large extent affected by the internal microstructures-induced heterogeneity (Brace et al. 1966; Eberhardt et al. 1998; Fredrich et al. 1990; Martin and Chandler 1994). Therefore, the mineral assembly induced rock material heterogeneity is an important factor that needs to be considered when studying the micro-cracking behavior of rocks.

In general, two approaches are available for incorporating material heterogeneity into numerical models when investigating the cracking processes of rocks. In the first approach, which is known as the implicit approach, the material heterogeneity is implicitly incorporated via a stochastic distribution of rock properties, such as the Weibull distribution based models and the Lattice model (Tang et al. 2000; Blair and Cook 1998; Schlangen and Garboczi 1997). These implicit modeling methods have demonstrated that heterogeneity has a great influence on the mechanical behavior of rocks. However, the choice of input properties is to some extent subjective and highly dependent on the parameters in the statistical distribution. In the second approach, which is known as the explicit approach, the heterogeneity is explicitly described in the numerical specimen model to be simulated, such as grain-based models implemented into Universal Distinct Element Code (UDEC) (Lan et al. 2010) or two-dimensional Particle Flow Code (PFC2D) (Potyondy 2010), combined finite-discrete element

J. Peng
Wuhan University, Wuhan, China

L. N. Y. Wong (✉)
The University of Hong Kong, Hong Kong, China
e-mail: lnywong@hku.hk

C. I. Teh
Nanyang Technological University, Singapore, Singapore

method (Mahabadi et al. 2014), and explicit finite element method (Manouchehrian and Cai 2016).

In a recent study by Peng et al. (2018), the grain-based modeling approach in PFC2D was demonstrated to be promising for studying the micro-cracking behavior of crystalline granitic rocks. This model is used in this study to further investigate the influence of rock material heterogeneity on the strength and micro-cracking behavior of a crystalline rock. The heterogeneity induced by variation of grain size distribution and shape is explicitly incorporated into the numerical specimens quantitatively by a "heterogeneity index". The rock strength and deformation behavior and the associated micro-cracking process of numerical models with different heterogeneity indices are then examined and discussed.

2 Methodology

2.1 Grain-Based Modeling Approach in PFC2D

The grain-based modeling approach in PFC2D which was proposed by Potyondy (2010) is used in this study to investigate the material heterogeneity effect on rock strength and micro-cracking behavior. The micro-properties in a real rock, such as grain size distribution and mineralogical composition, can be reflected in the grain-based model. The PFC2D grain-based modeling approach generates polygonal grain structure which is representative of the crystalline rocks. Two contact models are used in the grain-based model. The discs inside the grains are bonded by parallel bonds and the discs along the grain interfaces are assigned with the smooth-joint contacts.

The details of generating a grain-based model in PFC2D are not presented here. Interested readers can refer to Potyondy (2010) or Peng et al. (2018). The PFC2D grain-based model can not only simulate the micro-crack initiation and interaction at the grain boundary, but also capture the micro-cracking behavior inside the grains which is associated with intra-granular micro-cracking. This approach has been demonstrated to be capable of simulating the failure behavior and micro-cracking process of crystalline rocks (Bahrani et al. 2014; Bewick et al. 2014; Hofmann et al. 2015).

2.2 Numerical Model Setup

In this study, the numerical model comprises four minerals (quartz, K-feldspar, plagioclase, and biotite) which is the same as that simulated by Peng et al. (2018). Grain sizes of different minerals are generally different. The average grain size R_a of a numerical model is expressed as

$$R_a = \sum_{i=1}^{m} \omega_i r_i \tag{1}$$

where ω_i and r_i are the volume fraction and mean grain size of different constituent minerals, respectively, and m is the number of associated mineral types.

In order to study the influence of material heterogeneity, which is induced by the variation of grain size distribution, on rock strength and micro-cracking behavior, a dimensionless heterogeneity index H is defined as

$$H = \sqrt{\sum_{i=1}^{m} \left(\frac{r_i}{R_a} - 1\right)^2} \tag{2}$$

By changing the grain size of different minerals that constitute a rock, numerical models with different heterogeneity indices can be generated. According to the definition of the heterogeneity index, a larger heterogeneity index represents a more heterogeneous model. Table 1 shows the mean grain sizes of minerals r_i and the heterogeneity indices H for the six different numerical models investigated in this study. The average grain sizes R_a of the numerical models are basically the same, while the heterogeneity indices range from 0 to 1.12.

In a former study by Peng et al. (2018), the micro-cracking behavior of Singapore Bukit Timah granite (BTG) was simulated using the PFC2D grain-based model. The studied BTG was composed of approximately 22.3% K-feldspar, 30.4% quartz, 36.3% plagioclase, and 10.7% biotite. It was found from previous laboratory test results that the mineralogical composition had a great influence on the mechanical properties of rocks (Güneş Yılmaz et al. 2011; Sajid et al. 2016). To avoid the influence of mineralogical composition on the simulation results in this paper, we assign the content of each mineral with equal value, i.e., 25.0%, at the early development of the model. However, due to truncation by the specimen boundary, some grains along the periphery are smaller than the designated grain size, leading to the fact that the content of each mineral is not exactly 25.0%.

The dimensions of the present generated numerical specimen models are 50 mm in length and 25 mm in width, which are the same as those simulated by Peng et al. (2018). They are smaller than those experimentally tested (100 mm long and 50 mm wide). According to Potyondy and Cundall (2004), if the particle size is relatively small as compared to the size of the model, the scale effect is not significant for modeling rocks in compressive loading conditions. Reducing the size of the numerical model will thus not significantly affect the simulation results and conclusions, but can improve the computing efficiency. The numerically-generated models of different heterogeneity indices (H) are presented in Fig. 1.

Table 1 Parameters for the generated numerical grain-based models

Specimen no.	R_a (mm)	H	Mean grain size of minerals r_i (mm)			
			K-feldspar	Quartz	Plagioclase	Biotite
HE1	2.1	1.12	3.0	1.5	3.5	0.5
HE2	1.9	1.02	2.5	1.5	3.0	0.5
HE3	2.0	0.79	2.5	1.5	3.0	1.0
HE4	1.9	0.69	2.5	1.5	2.5	1.0
HE5	2.0	0.35	2.0	2.0	2.5	1.5
HE6	2.0	0	2.0	2.0	2.0	2.0

| $H = 1.12$ | $H = 1.02$ | $H = 0.79$ | $H = 0.69$ | $H = 0.35$ | $H = 0$ |
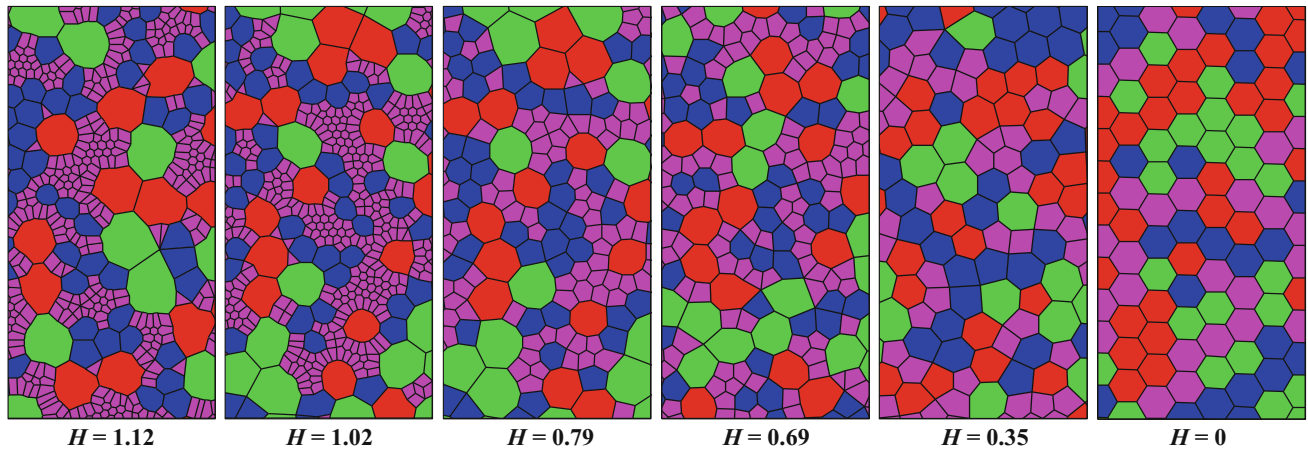
Fig. 1 Numerical models with different heterogeneity indices. The colors indicate different mineral types (red = K-feldspar, blue = quartz, green = plagioclase, magenta = biotite). The specimen dimensions are 50 mm in length and 25 mm in width

Note that when $H = 0$, the model is homogeneous, consisting of uniformly packed regular hexagons.

The micro-parameters of BTG were calibrated by Peng et al. (2018) to match a number of macro-properties of the BTG tested in the laboratory, including direct tensile strength (σ_{dt}), UCS, Young's modulus (E), and compressive strengths under various confining pressures. The results revealed that the errors between the laboratory properties and the simulated values using grain-based model were within ±6%. The well-calibrated micro-parameters are used in this study to investigate the strength and micro-cracking behavior of models processing different numbers of heterogeneity indices.

Fig. 2 Strength evolutions of numerical models with the heterogeneity index

3 Simulation Results

3.1 Rock Strength Behavior

The strength variations of the numerical models with the heterogeneity indices are illustrated in Fig. 2. The material heterogeneity also has a great effect on the rock strength under compressive loadings. The compressive strength gradually decreases as H increases from 0 to 1.12, i.e., the more heterogeneous the numerical model is, the lower the compressive strengths will be.
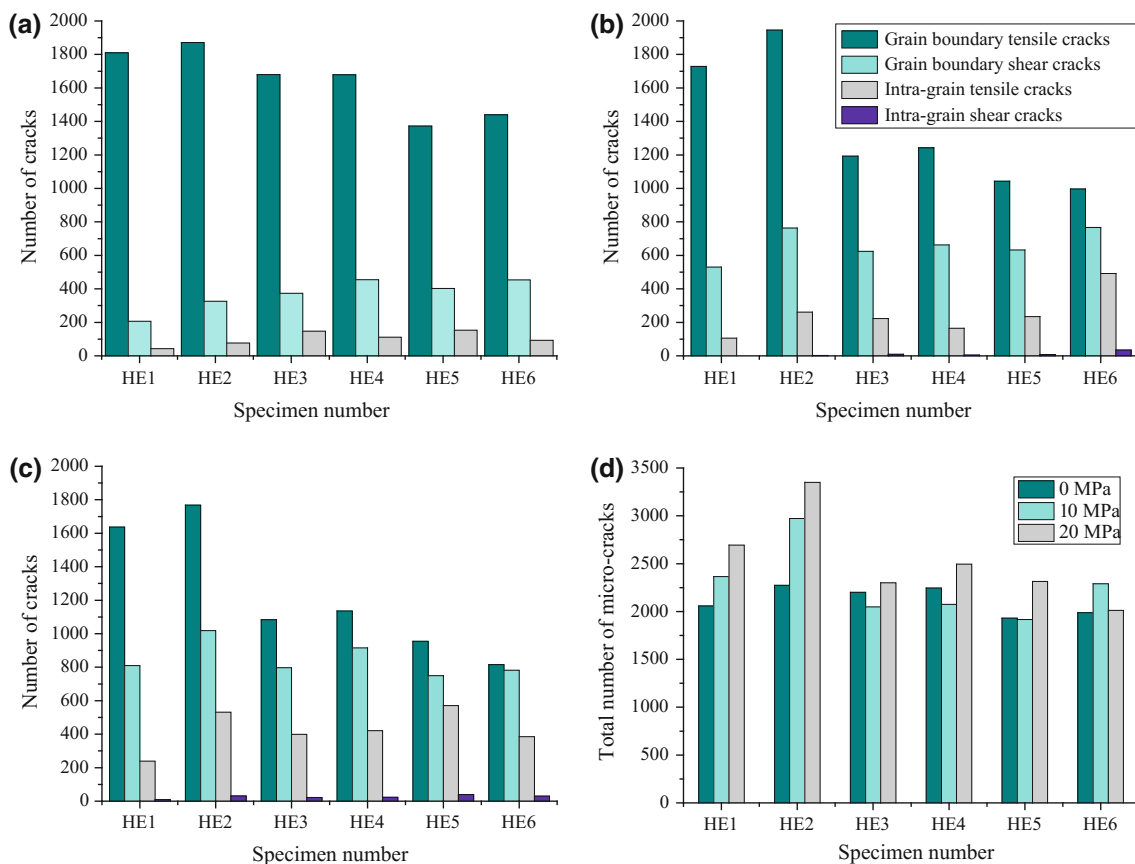
3.2 Number of Micro-cracks

Figure 3a–c presents the number of four different types of micro-cracks at the end of the loading process of the numerical models under different loading conditions. The grain boundary tensile cracks are found to dominate among the generated micro-crack types, indicating that the failure mechanism is attributed mainly to tensile cracking under low confining pressures. The number of grain boundary tensile cracks generally decreases with the decrease of H from 1.12 to 0 under compressive compression. However, there is no obvious trend for the development of other types of micro-cracks.

The total number of generated micro-cracks is also computed and summarized (Fig. 3d). The results reveal that when the heterogeneity index is large (i.e., HE1 and HE2), the total number of micro-cracks increases with the increase of confining pressure. However, as the heterogeneity index becomes lower, the total numbers of generated micro-cracks are very similar for different confining pressures.

3.3 Orientation of Micro-cracks

Figure 4 illustrates the orientation distribution of generated "**grain boundary micro-cracks**" for numerical models with different heterogeneity indices under uniaxial compression. The results reveal that the orientation of grain boundary micro-cracks is significantly affected by the grain size distribution induced heterogeneity, which is associated with the geometry of assembled grain structure of the numerical model. The following phenomena are observed:

- When the heterogeneity index is large, the grain boundary micro-cracks are mainly generated approximately parallel to the vertical direction.
- As the heterogeneity index decreases, although most of the generated grain boundary micro-cracks are oriented in the vertical direction, more and more micro-cracks are found to be inclined at about 60°–75° and 105°–120°.
- When the numerical model is homogeneous ($H = 0$), most of the grain boundary micro-cracks are generated at

Fig. 3 Number of different types of generated micro-cracks for different numerical models under confining pressure of **a** 0 MPa—uniaxial compression. **b** 10 MPa. **c** 20 MPa. **d** Total number of generated micro-cracks for different numerical models
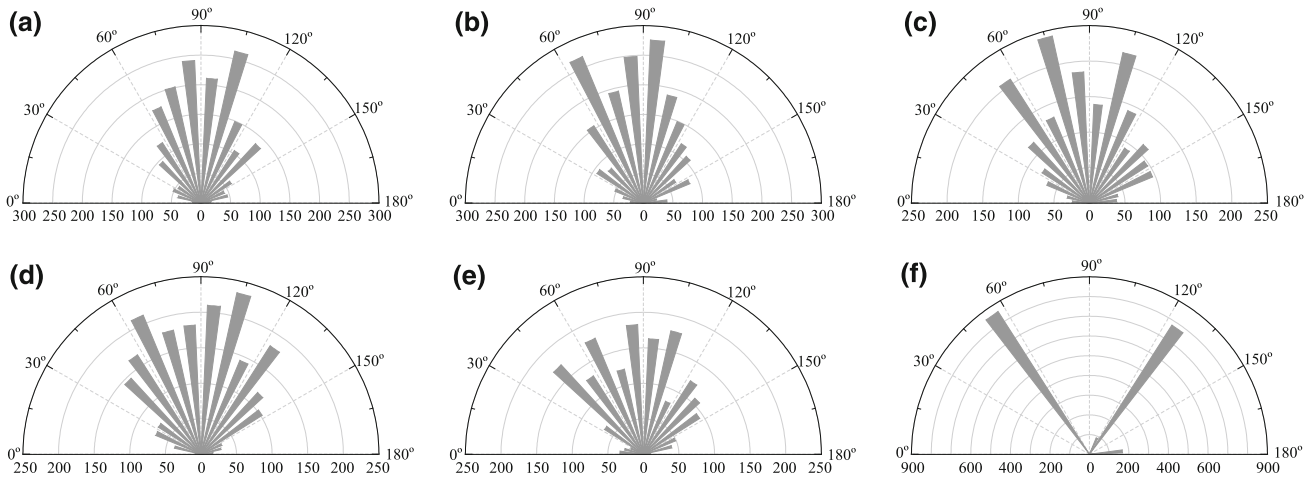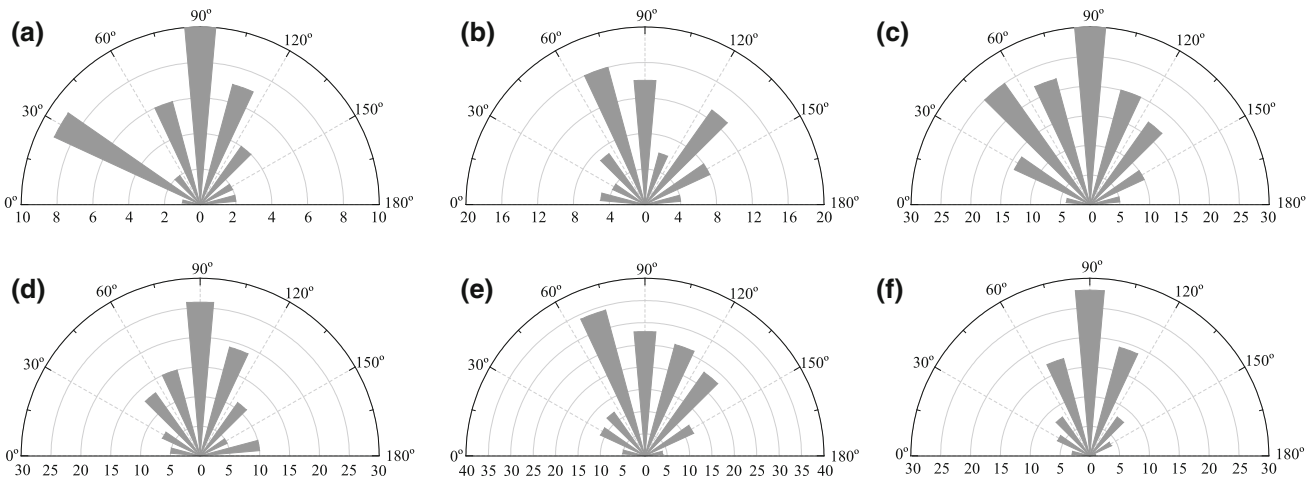
Fig. 4 Orientation distribution of the generated grain boundary micro-cracks in the numerical models with different heterogeneity indices under uniaxial compression. **a** HE1: $H = 1.12$. **b** HE2: $H = 1.02$. **c** HE3: $H = 0.79$. **d** HE4: $H = 0.69$. **e** HE5: $H = 0.35$. **f** HE6: $H = 0$

about 60° and 120°. The phenomenon is mainly due to the general association of the grain boundary micro-cracks and the grain interfaces in the generated numerical models. As shown in Fig. 1, as the numerical model becomes more homogeneous, more grain interfaces tend to be inclined at about 60°–75° and 105°–120°.

The orientation distribution of generated "**intra-grain micro-cracks**" of different numerical models under uniaxial compression are presented in Fig. 5. The heterogeneity does not have a pronounced influence on the orientation of intra-grain micro-cracks, as compared with the results of grain boundary micro-cracks. Most of the generated

intra-grain micro-cracks incline approximately parallel or slightly inclined to the vertical loading direction.

Figure 6 presents the variations of orientation of "**grain boundary micro-cracks**" and "**intra-grain micro-cracks**" with the confining pressure for the numerical model of $H = 0.69$. The rose diagrams reveal that the orientation of grain boundary micro-cracks are generally the same under different confining pressures, indicating that the influence of confinement is not significant. On the other hand, the orientation of intra-grain micro-cracks seems to be greatly affected. When the numerical model is loaded under uniaxial compression, most of the intra-grain micro-cracks are generated along the vertical direction. With increase of the

Fig. 5 Orientation distribution of the generated intra-grain micro-cracks in the numerical models with different heterogeneity indices under uniaxial compression. **a** HE1: $H = 1.12$. **b** HE2: $H = 1.02$. **c** HE3: $H = 0.79$. **d** HE4: $H = 0.69$. **e** HE5: $H = 0.35$. **f** HE6: $H = 0$
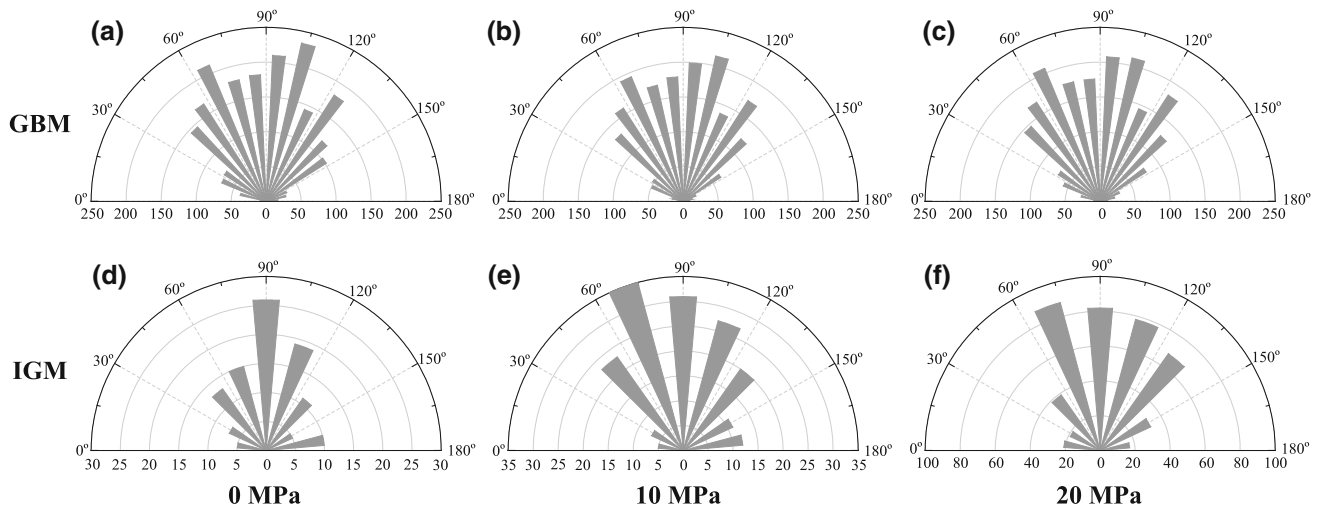
Fig. 6 Orientation distribution of two types of micro-cracks in the numerical model HE4 ($H = 0.69$) under various confining pressures. Grain boundary micro-cracks under confining pressure of **a** 0 MPa, **b** 10 MPa, **c** 20 MPa; Intra-grain micro-cracks under confining pressure of **d** 0 MPa, **e** 10 MPa, **f** 20 MPa. (GBM: grain boundary micro-crack; IGM: intra-grain micro-crack)

confining pressure, more intra-grain micro-cracks are found to incline at about 30° along the loading direction.

3.4 Pattern of Micro-cracks

The spatial distributions of different types of micro-cracks for numerical models with different heterogeneity indices under uniaxial compression are presented in Fig. 7. When the heterogeneity index is relatively high, the generated micro-cracks are generally uniformly distributed in the model, with the orientation of micro-cracks varying in a relatively large range. As the numerical model becomes more homogeneous, the interaction of generated micro-cracks tends to form more macroscopic fractures which are oriented approximately in the vertical direction. Because the homogeneous numerical model ($H = 0$) is

uniformly assembled with regular hexagons, when the numerical model is loaded, the micro-cracks are generally generated along the sub-vertical grain interfaces, which will eventually form vertical macroscopic fractures. The lateral dilation in this condition is much larger than those with large heterogeneity indices.

The distributions of different types of micro-cracks for different heterogeneity indices under the confining pressure of 20 MPa are shown in Fig. 8. As compared with the results under uniaxial compression, more intra-grain cracks develop in the model due to the higher applied confining pressure. When the crack density is sufficiently high, the interaction and coalescence of grain boundary micro-cracks and intra-grain micro-cracks lead to the formation of macroscopic shear bands. The results are in good agreement with microscopic observation of the Westerly granite by Moore and Lockner (1995). When the heterogeneity index is large, the
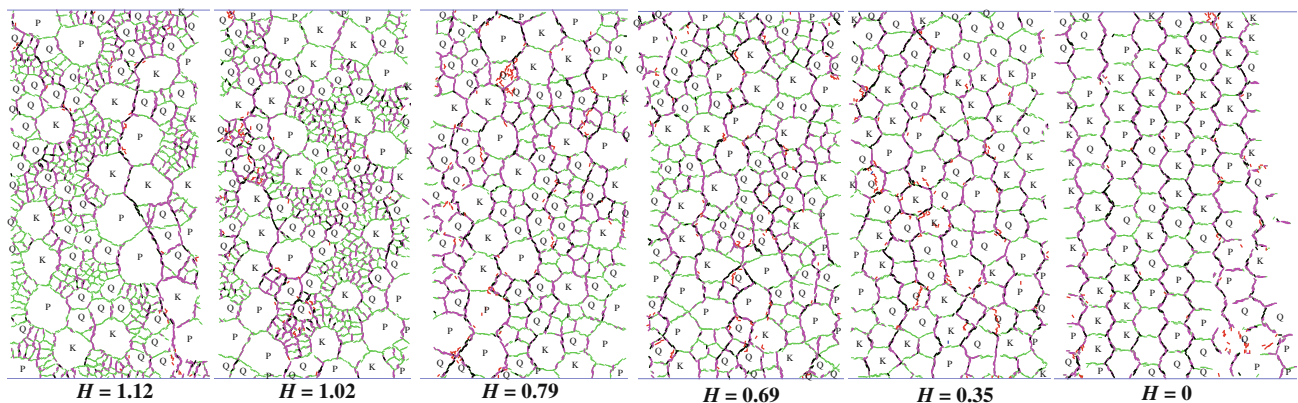
Fig. 7 Micro-cracking behavior of the numerical models with different heterogeneity indices under uniaxial compression. The different minerals are identified (Q: quartz, K: K-feldspar, P: plagioclase, and biotite is not labelled). Green segments represent grain boundaries, magenta and black segments represent grain boundary tensile and shear cracks, respectively, and red segments represent intra-grain tensile cracks

| H = 1.12 | H = 1.02 | H = 0.79 | H = 0.69 | H = 0.35 | H = 0 |
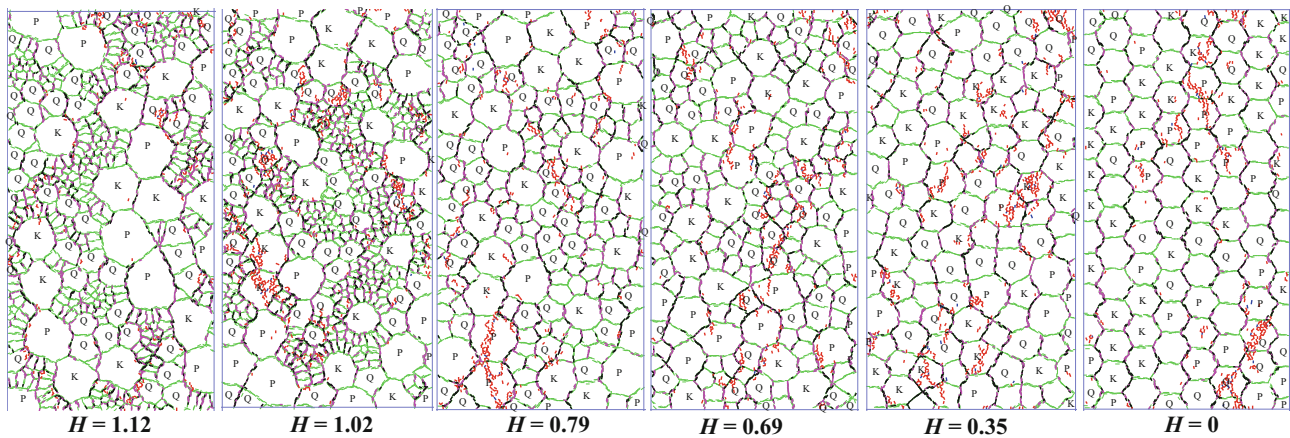
Fig. 8 Micro-cracking behavior of the numerical models with different heterogeneity indices under the confining pressure of 20 MPa. The different minerals are identified (Q: quartz, K: K-feldspar, P: plagioclase, and biotite is not labelled). Green segments represent grain boundaries, magenta and black segments represent grain boundary tensile and shear cracks, respectively, and red and blue segments represent intra-grain tensile and shear cracks, respectively

generated micro-cracks are found to be relatively uniform. As the numerical model becomes more homogeneous, more intra-grain cracks develop in the model and the induced macroscopic shear band is more prominent than the results of numerical models with much higher heterogeneity indices.

The simulation results also show that most of the intra-grain cracks (both tensile and shear) generally develop in quartz (except the numerical models with heterogeneity indices equal to 0.35 and 0.79 under the confining pressure of 20 MPa). This is mainly due to the fact that the particle-particle contact modulus, and parallel bond modulus and strength in the quartz mineral are assigned with the highest value as compared with the values of other minerals (Peng et al. 2018). Many researchers investigated the micro-cracking behavior of crystalline rocks and found that the intra-grain cracks occurred mostly in quartz grains (Tullis and Yund 1977). These observations are in good agreement with the simulation results in this study.

4 Conclusions

This paper numerically investigates the influence of grain size heterogeneity on the micro-cracking process and strength of a crystalline rock. The simulation results reveal that the peak strength generally increases as the numerical model gradually progresses from heterogeneous to homogeneous. The micro-cracking behavior is also found to be greatly affected by material heterogeneity. As the numerical model becomes more homogeneous, the number of generated grain boundary tensile cracks gradually decreases and the number of intra-grain cracks (both tensile and shear) increases. The orientation of grain boundary micro-cracks is mainly controlled by the geometry of assembled grain

structure of the numerical specimen model, while the orientation of intra-grain micro-cracks is to a large degree influenced by the confinement. The results also reveal that the development of intra-grain cracks (both tensile and shear) is much more favored in quartz than in the other minerals, which is generally in good agreement with the previous laboratory test results by other researchers.

References

Bahrani, N., Kaiser, P.K., Valley, B.: Distinct element method simulation of an analogue for a highly interlocked, non-persistently jointed rockmass. Int. J. Rock Mech. Min. **71**, 117–130 (2014)

Bewick, R.P., Kaiser, P.K., Bawden, W.F.: DEM simulation of direct shear: 2. grain boundary and mineral grain strength component influence on shear rupture. Rock Mech. Rock Eng. **47**(5), 1673–1692 (2014)

Blair, S.C., Cook, N.G.W.: Analysis of compressive fracture in rock using statistical techniques: part I. A non-linear rule-based model. Int. J. Rock Mech. Min. **35**(7), 837–848 (1998)

Brace, W.F., Paulding, B.W., Scholz, C.: Dilatancy in the fracture of crystalline rocks. J. Geophys. Res. **71**(16), 3939–3953 (1966)

Eberhardt, E., Stead, D., Stimpson, B., Read, R.: Identifying crack initiation and propagation thresholds in brittle rock. Can. Geotech. J. **35**(2), 222–233 (1998)

Fredrich, J.T., Evans, B., Wong, T.F.: Effect of grain size on brittle and semibrittle strength: implications for micromechanical modelling of failure in compression. J. Geophys. Res. Solid Earth **95**(B7), 10907–10920 (1990)

Güneş Yılmaz, N., Mete Goktan, R., Kibici, Y.: Relations between some quantitative petrographic characteristics and mechanical

strength properties of granitic building stones. Int. J. Rock Mech. Min. **48**(3), 506–513 (2011)

Hofmann, H., Babadagli, T., Yoon, J.S., Zang, A., Zimmermann, G.: A grain based modeling study of mineralogical factors affecting strength, elastic behavior and micro fracture development during compression tests in granites. Eng. Fract. Mech. **147**, 261–275 (2015)

Lan, H.X., Martin, C.D., Hu, B.: Effect of heterogeneity of brittle rock on micromechanical extensile behavior during compression loading. J. Geophys. Res. Solid Earth **115**(B01202), 1–14 (2010)

Mahabadi, O.K., Tatone, B.S.A., Grasselli, G.: Influence of microscale heterogeneity and microstructure on the tensile behavior of crystalline rocks. J. Geophys. Res. Solid Earth **119**(7), 5324–5341 (2014)

Manouchehrian, A., Cai, M.: Influence of material heterogeneity on failure intensity in unstable rock failure. Comput. Geotech. **71**, 237–246 (2016)

Martin, C.D., Chandler, N.A.: The progressive fracture of Lac du Bonnet granite. Int. J. Rock Mech. Min. Sci. Geomech. Abstr. **31**(6), 643–659 (1994)

Moore, D.E., Lockner, D.A.: The role of microcracking in shear-fracture propagation in granite. J. Struct. Geol. **17**(1), 95–114 (1995)

Peng, J., Wong, L.N.Y., Teh, C.I., Li, Z.: Modeling micro-cracking behavior of Bukit Timah granite using grain-based model. Rock Mech. Rock Eng. **51**(1), 135–154 (2018)

Potyondy, D.O., Cundall, P.A.: A bonded-particle model for rock. Int. J. Rock Mech. Min. **41**(8), 1329–1364 (2004)

Potyondy, D.O.: A grain-based model for rock: approaching the true microstructure. In: Li, C.C. (eds.) Proceedings of the rock mechanics in the Nordic countries, pp. 225–234. Norwegian Group for Rock Mechanics, Kongsberg, Norway (2010)

Sajid, M., Coggan, J., Arif, M., Andersen, J., Rollinson, G.: Petrographic features as an effective indicator for the variation in strength of granites. Eng. Geol. **202**, 44–54 (2016)

Schlangen, E., Garboczi, E.J.: Fracture simulations of concrete using lattice models: computational aspects. Eng. Fract. Mech. **57**(2–3), 319–332 (1997). https://doi.org/10.1016/S0013-7944(97)00010-6

Tang, C.A., Liu, H., Lee, P.K.K., Tsui, Y., Tham, L.G.: Numerical studies of the influence of microstructure on rock failure in uniaxial compression—part I: effect of heterogeneity. Int. J. Rock Mech. Min. **37**(4), 555–569 (2000)

Tullis, J., Yund, R.A.: Experimental deformation of dry westerly granite. J. Geophys. Res. **82**(36), 5705–5718 (1977)

The Effect of Jointing in Massive Highly Interlocked Rockmasses Under High Stresses by Using a FDEM Approach

Ioannis Vazaios, Nicholas Vlachopoulos, and Mark S. Diederichs

Abstract

In deep underground mines and deep infrastructure tunnels, spalling and strain bursting are among the most common failure mechanisms observed and reported in massive rockmasses under high stresses. Therefore, the need to be able to estimate such conditions and counter them with an economic and effective design is rising. Part of the common practice is the use of computer packages involving numerical methods based on continuum approaches. However, the failure mechanisms involved and the rockmass response observed are often difficult to capture by employing such methods and usually discontinuum approaches are better suited for this task. Additionally, discrete structures observed within the rockmass in situ, such as joints and other discontinuities, can be explicitly incorporated into the numerical model in order to investigate their effect on the overall rockmass response during an underground excavation and adjust the design if necessary. In this study, the presence of joints and their effect on the response of a hard rockmass under a high stress regime during an excavation is examined by employing a FDEM (Finite-Discrete Element Method) approach. The setup of the numerical model is based on the URL (Underground Research Laboratory) Test Tunnel located in Pinawa, Manitoba, Canada and a Discrete Fracture Network (DFN) model is implemented in order to simulate the impact of joints on brittle failure. Numerical results show that the presence of joints increases the intensity and evolution of the damage during the excavation.

1 Introduction

Within hard, massive rockmasses, brittle behaviour can cause significant problems in deep tunnelling (Kaiser and McCreath 1994; Lee et al. 2004; Diederichs et al. 2004), similarly to deep mining excavations (Hoek 1968; Hoek and Brown 1980). Spalling and strain bursting are the most common failure mechanisms observed in hard rock excavations under high stress regimes, and they are associated with complex failure mechanisms which are usually quite difficult to simulate numerically by employing continuum mechanics approaches. Additionally, challenges arise when pre-existing joints are present and they need to be incorporated into the numerical model. In such cases, discontinuum modelling techniques are usually more suitable for simulating the associated fracture phenomena that occur as a result of the joints and the brittle rock response.

For the purposes of this study, the short term mechanical response of hard rock excavations is investigated by applying a finite-discrete element method (FDEM) technique implemented into the Irazu software (Geomechanica 2017). The setup of the numerical model is based on the URL (Underground Research Laboratory) Test Tunnel located in Pinawa, Manitoba, Canada and a Discrete Fracture Network (DFN) model is implemented in order to simulate the impact of joints on brittle failure.

I. Vazaios (✉) · N. Vlachopoulos · M. S. Diederichs
Department of Geological Sciences and Geological Engineering, Queen's University, Kingston, Canada
e-mail: ioannis.vazaios87@gmail.com

N. Vlachopoulos
e-mail: vlachopoulos-n@rmc.ca

M. S. Diederichs
e-mail: diederim@queensu.ca

N. Vlachopoulos
Department of Civil Engineering, Royal Military College of Canada, Kingston, Canada

2 The Geological Setting

2.1 Intact Material Properties

For the development of the numerical model, the mechanical properties of the intact material were required to be representative of this of a hard rock which could demonstrate brittle behaviour. In order to achieve this, the well documented case of the Lac du Bonnet (LdB) granite, located in Manitoba, Canada, was selected (Martin 1994; Martin et al. 1997; Hajiabdolmajid et al. 2002, 2003). The LdB granite is a relatively undifferentiated, massive rock of Precambrian age with a relatively uniform texture and composition (Chandler 2003). The mechanical properties of the LdB granite are listed in Table 1.

2.2 Discontinuity Geometrical Properties

The LdB granite has been characterized as a relatively undisturbed rockmass (Hajiabdolmajid 2001), and for the purposes of this study it is considered as a fractured free medium, an assumption supported by field observations as well (Martin 1994). In order to investigate the effect of pre-existing joints within a brittle, hard rockmass, structural data obtained from an unsupported tunnel is used to generate a stochastic network of joints.

The discontinuity data required were acquired by utilizing point-clouds obtained from LiDAR (Light Detection and Ranging) scanning of an unlined 10 m section of a railway tunnel located in Brockville, Ontario, Canada (Fig. 1a). The point cloud was meshed to create a 3D surface model and discontinuity mapping was conducted (Fig. 1b–d) using Polyworks, which is a multipurpose range imaging processing package (Innovemetrics 2016), in order to determine the orientation of the identified sets and their fracture intensity (Vazaios et al. 2017). The discontinuity geometrical properties are listed in Table 2.

3 DFN Generation

The collection of discontinuity data described in Sect. 2.2 served as input for the generation of a stochastic discontinuity network which was used to create the joint features which were incorporated into the numerical model. In order to create the utilized DFN, the DFN generator MoFrac (Mirarco 2015) was used. Initially, a master volume is determined in order to generate the DFN. Random seeds within this volume are created and the employed propagation algorithm creates discontinuity surfaces (consisting of a triangular mesh) using the measured orientation and fracture intensity. Additionally, the mapped traces are used to create deterministic discontinuities at the specific locations that they were mapped. For more information the reader is referred to Vazaios et al. (2017).
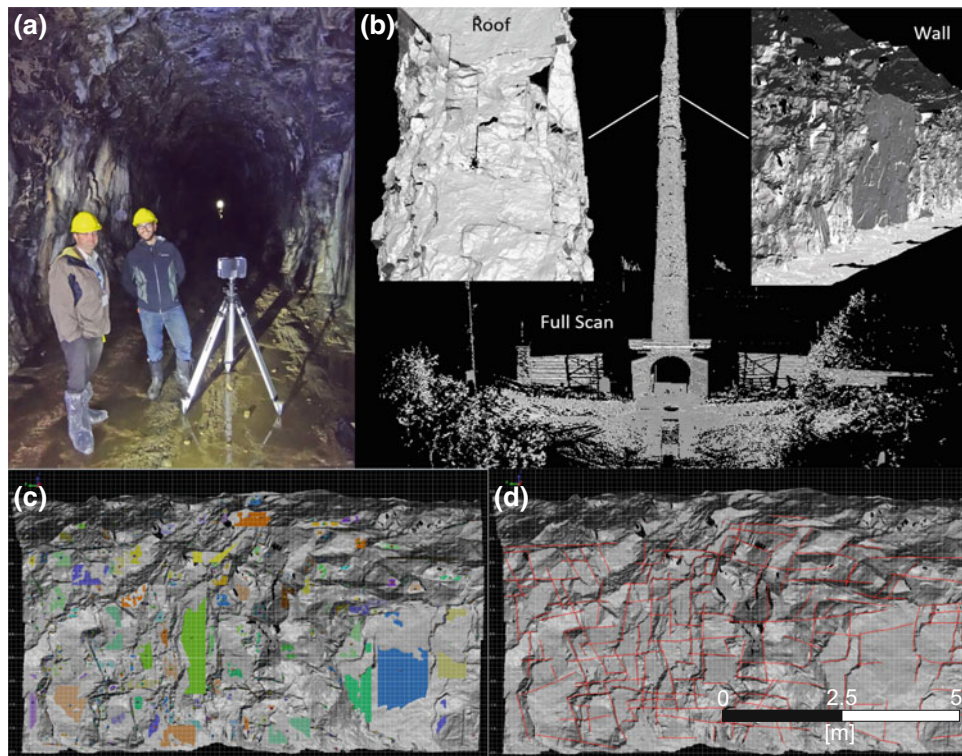
The generated DFN model used in this study consists of a volume of 60 × 60 × 60 m (Fig. 2a), in order to minimize the effect of possible boundary effects, and in order to be validated 10 random mapping windows with an equivalent area of 56 m^2 were created. Within these mapping windows, the traces were mapped and their lengths were measured for every one of the three sets in order to ensure that they follow the obtained distributions from the traces mapped within the LiDAR data (Fig. 2b). Once the DFN model was validated, a cross-section of it was extracted in order to be imported into the numerical model.

4 Development of the FDEM Numerical Model

4.1 Model Geometry, Boundary Conditions, Stress State and Excavation Sequence

The main geometrical features of the model are illustrated in Fig. 3. The model, which was built in Irazu, is made of 3-node triangular elements. It consists of a 3.50 m diameter

Table 1 Experimental values (average value and range) of the mechanical properties of the intact Lac du Bonnet granite (Martin 1994)

Mechanical property	Value
Young's modulus E (GPa)	69.0 ± 5.8
Poisson's ratio ν	0.22 ± 0.04
Unconfined compressive strength UCS (MPa)	213 ± 20
Tensile strength σ_t (MPa)	9.3 ± 1.3
Cohesion C (MPa)	30
Friction angle (°)	59

Fig. 1 **a** Terrestrial laser scanning conducted in an unlined section of the Brockville Railway Tunnel, Ontario, Canada. **b** 3D surface model of the tunnel created from the acquired LiDAR data. Discontinuity surface (**c**) and discontinuity trace (**d**) "virtual" mapping performed at a 10 m section of the tunnel

Table 2 Discontinuity geometrical data of an unlined 10 m section of the Brockville railway tunnel (Vazaios et al. 2017)

Set	Dip (°)	Dip direction (°)	Mapping area (m^2)	Trace length (m)	Areal fracture intensity (m/m^2)
1	88	285	60	71.03	1.18
2	12	077	54	91.61	1.70
3	77	207	54	62.93	1.17
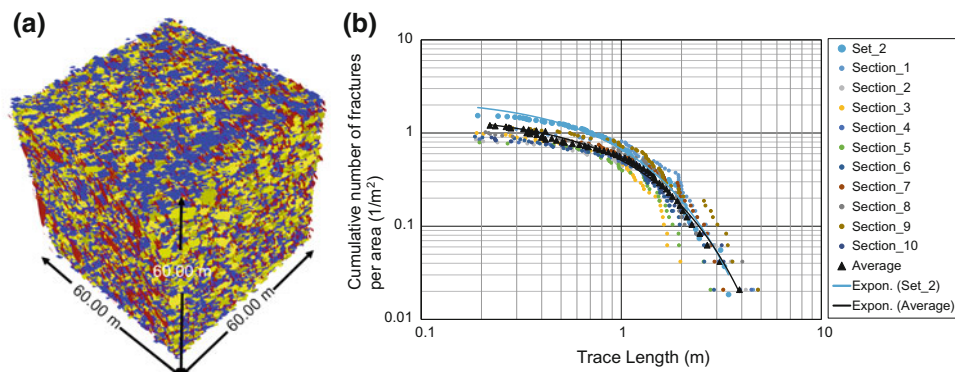
Fig. 2 **a** DFN model generated by using LiDAR data collected from a 10 m unlined section of the Brockville Railway tunnel. **b** Cumulative discontinuity trace length distributions created after field data (blue curve) and data obtained from the generated DFN model (black curve)

Fig. 3 Tunnel model configuration (geometry and stress state) created in Irazu. The different mesh domains within the model are highlighted with yellow dashed squares, showing the element size variation and transition between the excavation area (area of interest) and the model boundaries. The pre-existing discontinuities originating from the implemented DFN model are coloured red
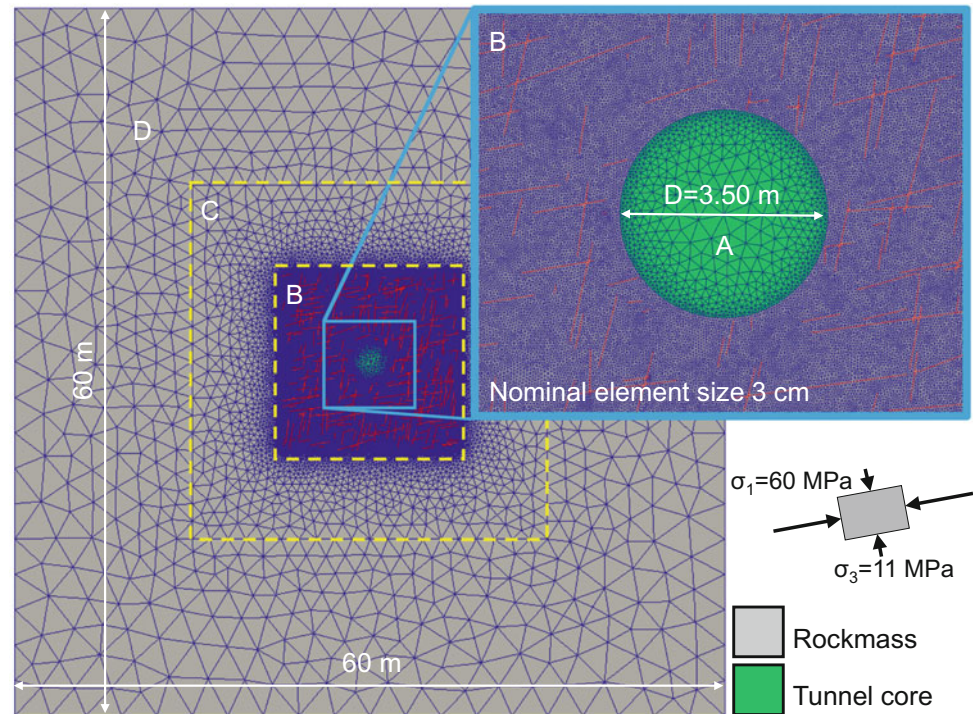
Table 3 The URL Test Tunnel stress tensor (Martin et al. 1997) and the assigned stress field to the FDEM model. All listed stresses are compressive

	Stress component	Magnitude (MPa)
URL test tunnel	σ_1	60 ± 3
	σ_2	45 ± 4
	σ_3	11 ± 4
FDEM model	σ_{xx}	58.0
	σ_{yy}	13.0
	τ_{xy}	9.2

tunnel, which corresponds to the diameter of the URL Test Tunnel and a 60×60 m square domain which is divided into four different sub-domains A, B, C and D with nominal element sizes 0.50, 0.03, 1.50 and 4.00 m respectively. Within Domain B, the mesh was refined in order to be able to capture the brittle fracturing response that the rockmass was expected to demonstrate as a result of the excavation. The model was meshed by using Gmsh (Geuzaine and Remacle 2009) and an unstructured Delaunay triangulation scheme was applied in order to minimize the effect of the mesh topology on the fracturing processes, as suggested by Mahabadi et al. (2012) and Lisjak et al. (2014). The model containing the incorporated DFN model consists of approximately 615,000 elements and the DFN-free model consists of 600,000 elements respectively.

The greater dimension of the model was selected to be 60 m (30 m from the centre of the excavation at each

direction) in order to minimize possible boundary effects. Additionally, the displacements were fixed in the X and Y direction and an absorbing boundary condition was employed. Finally, a constant stress field condition was applied to the FDEM model. The stress components used are listed in Table 3 and they correspond to the stresses measured at the URL Test Tunnel.

Following the establishment of the model geometry, a geostatic stress field was applied and the excavation of the tunnel was performed sequentially by decreasing the deformation modulus of the excavated material (softening of the core) from its initial value to zero (Vlachopoulos and Diederichs 2014). The geostatic stage of the model was established within 500,000 steps, followed by 4,000,000 excavation steps during which the softening of the core took place. Finally, 3,000,000 time steps were performed in order to establish static equilibrium conditions after the completion of the excavation.

4.2 Model Deformability and Strength Parameters

The primary form of damage within hard rockmasses is that of extensile failure, with the internal tensile strength of the geomaterial controlling the fracturing processes, especially under low confinement conditions around underground excavations in high stress environments (Diederichs 2007).

Such fracturing processes at low confinement stresses can be modelled by applying a FDEM approach in which crack initiation and propagation are explicitly simulated by adopting a cohesive-zone approach. This technique allows for the progressive failure of rock materials through the strength degradation of 4-node interface elements that are installed between the 3-node triangular elements (Lisjak et al. 2015), and therefore the use of a macroscopic failure criterion (Mohr-Coulomb, Hoek-Brown etc.) is not required. An explicit time integration scheme is employed in order to solve the motion equations of the discretized system and it updates the nodal coordinates at each simulation step (Lisjak et al. 2015).

The deformability of the system prior to any fracturing depends on the elastic properties of the triangular elements which are assigned a Young's modulus E and a Poisson's ratio v. While the interface elements are not supposed to deform before their strength is exceeded, the time-explicit formulation of the FDEM requires a finite cohesive stiffness. This artificial stiffness is introduced in the system by defining normal, tangential and fracture penalty values p_n, p_t, and p_f respectively (Munjiza 2004; Mahabadi 2012).

The strength of the interface elements is determined based on their tensile strength and their shear strength. The response in tension of the interface elements is governed by their assigned tensile strength f_t and the fracture energy in tension G_I. Similarly, their response in shearing is governed by the assigned cohesion c, the internal friction angle φ expressed as a frictional coefficient μ, and the fracture energy in shear G_{II} (Lisjak 2013).

The deformability and strength parameters adopted in this study were based on a calibrated model procedure of the URL Test Tunnel. The calibrated model replicates the brittle behaviour of the LdB granite observed during the excavation of the tunnel and the extent of the damaged material, as a result of the spalling processes taking place in a fracture free environment. For the FDEM model containing the DFN model, the discontinuities were assumed to be purely frictional for simplicity. The deformability and strength parameters used in this study are listed in Table 4.

5 Results and Discussion

In order to investigate the effect of pre-existing discontinuities on the failure mechanisms of hard, brittle rockmasses and the extent of the damaged zone around an excavation at great depths, the two numerical models were compared for various stages of the excavation process.

In Fig. 4a–d the magnitude of the deviatoric stresses is illustrated along with the fractures that have been formed as a result of the yielding of the interface elements due to the changes of the stress regime because of the excavation. In Fig. 4a, b, both models are captured before the initiation of any fracturing as a result of the excavation. Stress concentrations occur at the crown and the floor of the excavation at approximately the same locations for both models, as a result of the advancing face. However, it can be observed that the formation and the magnitude of the stress contours are not exactly the same due to the presence of the pre-existing

**Table 4** Input parameters for the FDEM simulation using Irazu

Parameter	Value
Young's Modulus E (GPa)	65
Poisson's ratio v	0.18
Viscous damping factor	1.0
Normal contact penalty p_n (GPa m)	650
Tangential contact penalty p_t (GPa/m)	650
Fracture penalty p_f (GPa)	650
Friction coefficient μ	1.7
Cohesion c (MPa)	50
Tensile strength f_t (MPa)	10
Mode I fracture energy G_I (N/m)	300
Mode II fracture energy G_{II} (N/m)	1900
Discontinuity friction coefficient μ_f	0.7
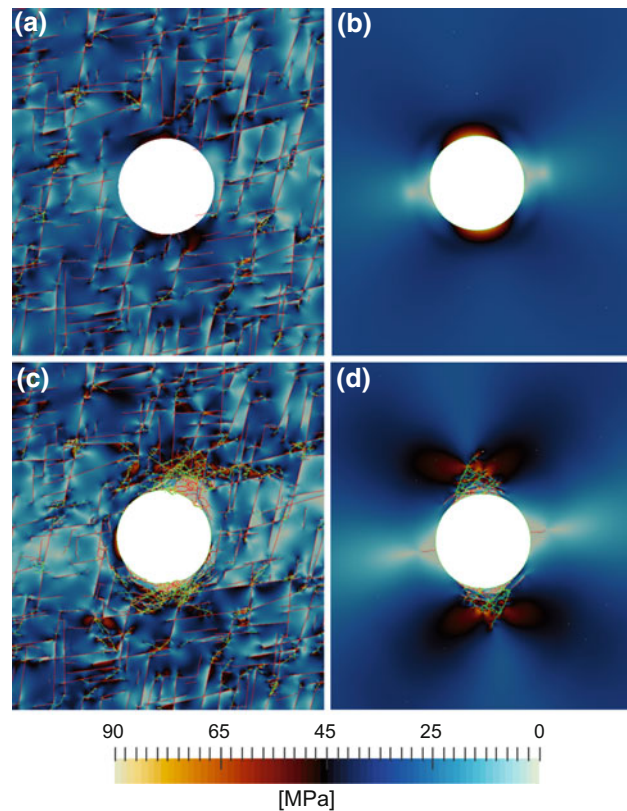
Fig. 4 Deviatoric stress contour plots for the **a** "fractured" model and **b** "intact" model prior to fracture initiation, and **c** the "fractured" and **d** "intact" model when fractures have propagated. Shear fractures are coloured green and tensile fractures are coloured red

Fig. 5 Extent of collapsed material (black curve) in **a** the FDEM and **b** the FDEM-DFN models. Tensile fractures are highlighted red and shear fractures are highlighted green
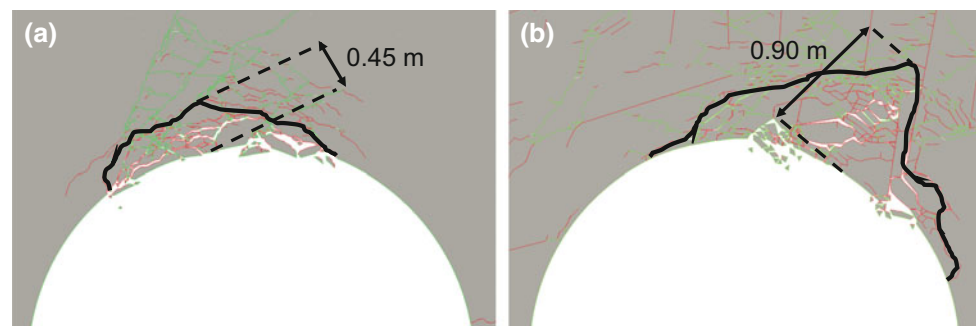
planes of weakness in the FDEM-DFN model, herein called "fractured" model. More specifically, in the "fractured" model the resultant stresses appear to have a lower magnitude than in the "intact" model. Furthermore, while stress induced fractures around the excavation are absent, it can be seen that stress concentrations at the tips of the pre-existing joints cause the initiation of fracturing and fracture interaction away from but still within the vicinity of the excavation. In Fig. 4c, further advancement of the face is leading to the interaction between stress induced fractures and pre-existing discontinuities in the "fracture" model. On the contrary, in

Fig. 4d, in the "intact" model fractures are free to propagate and their formation is dictated solely by the stresses present.

By focusing on the crown of the excavation in both models (Fig. 5), it can be observed that in the case of the "intact model" the high compressive stresses concentrating at this specific location result in the extensile failure of the material (Fig. 5a). The extensile stress induced fractures follow approximately the trajectories of the high magnitude compressive tangential stresses around the excavation boundary. That leads to the formation of a "v-shaped" notch type failure, similar to the one observed in the field at the

URL Test Tunnel (Martin et al. 1997; Diederichs 2007), as the tensile strength of the rockmass is exceeded. Additionally, the notch is formed at an angle relative to the vertical axis of the model, which is consistent with the stress tensor described in Table 3, with the extent of the collapsed material being approximately 0.45 m.

This is not the case, however, for the "fractured" model. As illustrated in Fig. 5b, the pre-existing discontinuities present re-direct the excavation induced stresses resulting in a failed area that is rotated relative to the one developing in the "intact" model. More specifically, a sub-horizontal joint located at the crown of the tunnel acts as a stress barrier preventing the formation of the notch, and it forces the stress induced fractures to move to the right. As the stress induced fractures propagate further, the sub-vertical joints "trap" the formed cracks and lead to the containment of the undergoing fracturing processes, with the extent of the collapsed material being approximately 0.90 m. While the manifestation of the failed material and the extent of the damage occurring are different between the "intact" and the "fractured" configurations, it has to be noted that the main failure mechanism in both cases is brittle, extensile failure. As seen in Fig. 5b, tensile fractures are propagating in the intact part of the rockmass encountered between the sub-vertical joints, once the tensile strength of the rockmass has been exceeded, hence leading to the collapse of the material.

6 Conclusions

In this study, the effect of pre-existing discontinuities on the response of brittle, hard rockmasses by employing a hybrid FDEM-DFN approach was investigated. From the obtained numerical results it becomes evident that while the dominant damage mechanism is extensile fracturing in both examined scenarios, the presence of pre-existing joints increases the intensity of the damage sustained to the rockmass. Additionally discontinuities can act as stress barriers and redirect the evolution of the inflicted damage on the rockmass, which is controlled by the joint network geometry.

References

Chandler, N.A.: Twenty years of underground research at Canada's URL. In: WM' 03 conference Tucson AZ (2003)

Diederichs, M.S., Kaiser, P.K., Eberhardt, E.: Damage initiation and propagation in hard rock during tunnelling and the influence of near-face stress rotation. Int. J. Rock Mech. Min. Sci. **41**(5), 785–812 (2004)

Diederichs, M.S.: The 2003 Canadian geotechnical colloquium: mechanistic interpretation and practical application of damage and spalling prediction criteria for deep tunnelling. Can. Geotech. J. **44**(9), 1082–1116 (2007)

Geomechanica Inc.: Irazu 2D Geomechanical simulation software, version 3.0 (2017)

Geuzaine, C., Remacle, J.F.: Gmsh: a three-dimensional finite element mesh generator with built-in pre- and post-processing facilities. Int. J. Numer. Meth. Eng. **79**(11), 1309–1331 (2009)

Hajiabdolmajid, V.R.: Mobilization of strength in brittle failure of rock. Ph.D. Thesis, Department of Mining Engineering, Queen's University, Kingston, Canada (2001)

Hajiabdolmajid, V.R., Kaiser, P.K., Martin, C.D.: Modelling brittle failure of rock. Int. J. Rock Mech. Min. Sci. **39**(6), 731–741 (2002)

Hajiabdolmajid, V.R., Kaiser, P.K., Martin, C.D.: Mobilized strength components in brittle failure of rock. Geotechnique **53**(3), 327–336 (2003)

Hoek, E.: Brittle failure of rock. In: Stagg, K.G., Zienkewicz, O.C. (eds.) Rock mechanics in engineering practice, pp. 99–124. Wiley, London (1968)

Hoek, E., Brown, E.T.: Underground excavations in rock. Institute of Mining and Metallurgy, London (1980)

Innovemetrics: Polyworks V 11.0.4, Quebec City: Innovemetrics (2016)

Kaiser, P.K., McCreath, D.R.: Rock mechanics considerations for drilled or bored excavations in hard rock. Tunn. Undergr. Space Technol. **9**(4), 425–437 (1994)

Lee, S.M., Park, B.S., Lee, S.W.: Analysis of rockbursts that have occurred in a waterway tunnel in Korea. Int. J. Rock Mech. Min. Sci. **41**, 911–916 (2004)

Lisjak, A.: Investigating the influence of mechanical anisotropy on the fracturing behaviour of brittle clay shales with application to deep geological repositories. Ph.D. thesis, University of Toronto, Toronto, Canada (2013)

Lisjak, A., Grasselli, G., Vietor, T.: Continuum–discontinuum analysis of failure mechanisms around unsupported circular excavations in anisotropic clay shales. Int. J. Rock Mech. Min. Sci. **65**, 96–115 (2014)

Lisjak, A., Garitte, B., Grasselli, G., Müller, H.R., Vietor, T.: The excavation of a circular tunnel in a bedded argillaceous rock (Opalinus Clay): short-term rock mass response and FDEM numerical analysis. Tunn. Undergr. Space Technol. **45**, 227–248 (2015)

Mahabadi, O.K.: Investigating the influence of micro-scale heterogeneity and microstructure on the failure and mechanical behaviour of geomaterials. Ph.D. thesis. University of Toronto. Toronto, Canada (2012)

Mahabadi, O.K., Lisjak, A., Grasselli, G., Munjiza, A.: Y-Geo: a new combined finite-discrete element numerical code for geomechanical applications. Int. J. Geomech. **12**, 676–688 (2012)

Martin, C.D.: The strength of massive Lac du Bonnet granite around underground openings. Ph.D. thesis, University of Manitoba, Winnipeg, Manitoba, Canada (1994)

Martin, C.D., Read, R.S., Martino, J.B.: Observations of brittle failure around a circular test tunnel. Int. J. Rock Mech. Min. Sci. **34**(7), 1065–1073 (1997)

MoFrac software version alpha: MIRARCO Mining Innovation, www. mofrac.com (2015)

Munjiza, A.: The combined finite-discrete element method. Wiley, Chichester, West Sussex, England (2004)

Vazaios, I., Vlachopoulos, N., Diederichs, M.S.: Integration of lidar-based structural input and discrete fracture network generation for underground applications. Geol. Geotech. Eng. **35**(5), 2227–2251 (2017)

Vlachopoulos, N., Diederichs, M.S.: Appropriate uses and practical limitations of 2D numerical analysis of tunnels and tunnel support response. Geotech. Geol. Eng. **32**(2), 469–488 (2014)

Geomechanical Model for a Higher Certainty in Finding Fluid Bearing Regions in Non-porous Carbonate Reservoirs

Georg Stockinger, Elena Mraz, Florian Menschik, and Kurosch Thuro

Abstract

The Upper Jurassic carbonate rocks, underlying the Bavarian Molasse Basin, host a hydrothermal fluid with temperatures up to 160 °C. This fluid is used for renewable and sustainable domestic heating and power generation in the area of Munich. The probability of discovering fluids, however, decreases southward—and closer to the Alps, due to a decline in porosity. This increases economic risk. A concept that could reduce this risk is targeted drilling into fractured zones within the carbonate rocks. However, the rock-mechanical understanding for stress redistribution, fracture initiation and propagation for these depths is insufficient. Although, these processes control borehole stability and durability as well as borehole connectivity with the aquifer. To assess the mechanical properties of the carbonate rocks at depths of over 4000 m, we started sampling rocks of same age and equivalent lithology from Upper Jurassic outcrops. These rocks, so-called 'analogue samples', were tested with non-destructive and destructive rock-mechanical methods in order to access their elastic and strength properties. The results from analogue samples of nine different lithologies show typical values for carbonate rocks. P-wave velocity ranges between 3669 and 5534 m/s. Poisson's ratio is fairly uniform with a mean value of 0.31. Yet, tensile strength deviates by over 4 MPa from a maximum of 10.9 MPa to a minimum of 6.5 MPa and Young's modulus varies from 40.4 to 69.0 GPa by more than 28 GPa. Thus, with a change in lithology, disparate mechanical behavior down the borehole must be expected.

Keywords

Geothermal energy • Analogue samples • Ultrasonic testing • Rock-Mechanical properties • Laboratory measures • Upper Jurassic carbonates

1 Introduction

The hydrogeothermal well in Geretsried (GEN-1), southern Germany, was drilled successfully in 2013 and reached temperatures of 160 °C in the borehole bottom. Although the drilling itself was successful considering the technical realization, the project failed since there was insufficient hot water to realize a hydrogeothermal power plant. The analysis of the lithology showed that the porosity of the Upper Jurassic limestone decreases the more southwards and thus, deeper this aquifer is located.

In 2017 a new attempt was made with the concept of targeted drilling into fault zones since fault zones are supposed to have a higher permeability than the surrounding limestone and dolostone matrix. This concept was already applied successfully in the neighboring geothermal well Traunreut (www-01 2018) where it led to a profitable flow rate of 120 l/s.

Based on this approach, the following questions arose, which are the main objectives of this research:

- How does the stress field change laterally in the formation?
- What are the changes in stress distribution with increasing depth?
- How do fractures develop and spread throughout the rock?

These rock-mechanical processes are important if we want to reflect on borehole stability (especially in fault zones) and on the borehole—aquifer connectivity. These

G. Stockinger (✉) · E. Mraz · K. Thuro
Chair of Engineering Geology, Technical University of Munich, Munich, Germany
e-mail: georg.stockinger@tum.de

F. Menschik
Laboratory Dr. Ettl & Dr. Schuh, Munich, Germany

processes must be understood for depths over 4000 m and therefore a rock-mechanical parametrization is inevitable.

Although accessing these parameters is arduous, actual rock cores from the sidetrack borehole (GEN-1ST) will be dealt with in future publications. In this work, analogue samples with a similar lithology to the main borehole (GEN-1) are used. The method of analogue sampling has been adopted earlier in geothermal researches by authors such as Tondera et al. (2013) and Homuth and Sass (2014). We improve upon this method with a larger variety of samples and thus achieve a higher resolution of the geology along the borehole.

2 Methodology

The methods, described in the following sections allow us to geomechanically characterize deep, joint-dominated aquifers. Sampling as well as laboratory methods are presented in detail.

2.1 Sampling

The selection of 'analogue samples' was based on cuttings analysis of the deep geothermal borehole GEN-1. For this purpose, this main borehole GEN-1 was analyzed in the reservoir section after micro facies according to Dunham (1962), texture, and components by using 40 thin sections of cutting material. Further, as a new approach, the different intersected Upper Jurassic carbonate rocks were grouped into five homogeneous areas, where analogue outcrops were looked for. In addition, the analogue samples were classified, as the cuttings before, within 15 thin sections, which are polished, half-side stained by Alizarin S and contain blue dye.

Figure 1 shows a generic quarry in the Franconian Alb, where actual analogue samples come from. It can be recognized that different rock types, i.e. transitions in lithology may be encountered within one quarry.

2.2 Laboratory Testing

Laboratory testing is composed of non-destructive and destructive testing. Rock samples were prepared as cylindrical test specimens after ASTM D4543 (2017). As a non-destructive testing method, Ultrasonic velocity (US) testing was conducted with longitudinal waves (p-waves) parallel and cross-wise to the specimen's longitudinal axis. This allowed, on the one hand, predictions of the samples quality, isotropy, and comparability among the specimen themselves. On the other hand, the US testing enabled a comparison of these analogue samples with in situ

core samples from former and recent drillings. In addition, a quasi-longitudinal wave (a combination of longitudinal and transversal waves) was applied in order to determine the elastic properties of the rock samples. Hence, the Dynamic Young's Modulus E_{dyn} and the Poisson's ratio ν, which are inevitable for geomechanical modelling, were determined.

As destructive testing method, Brazilian Tensile Tests (ASTM D3967 2016) were conducted to determine the tensile strength of these rock samples.

3 Results

In the first part of this section, we are using the above-mentioned methods to describe and classify the analogue samples. Subsequently, rock-mechanical parameters like p-wave velocity, elastic parameters and tensile strength of these samples are presented in the second section.

3.1 Analogue Samples

The obtained analogue samples include limestones and dolostones from the Franconian Alb and the Swabian Alb, which were deposited during the Upper Jurassic. These rocks are listed in Table 1 according to their trading name, sample code, classification after Dunham (1962), Folk (1959, 1962) and type of rock.

Figure 2 shows the locations of taken analogue samples. As seen in Sect. 2.1, Fig. 1, some quarries can reveal both limestones and dolostones.

The carbonate rocks of the analogue samples were classified by examining 15 thin sections according to Dunham (1962) and Folk (1959, 1962) (Table 1). The limestones are mainly grainstones to packstones, with varying amounts of oncoids, ooids, peloids and bioclasts such as echinoderms and tubiphyts. The dolostones cannot be further classified, as so-called ghost structures are not visible. However, the porosity of the samples was estimated by observing the visible porosity of the thin sections. Only the Wasserzeller Dolomit shows dedolomitization and must therefore be classified as a limestone.

3.2 Results of Laboratory Analyses

The mean values of p-wave velocities, elastic properties and indirect tensile strength are listed in Table 2.

For a brief overview, the maximum and minimum values of all tests are given. The p-wave velocity is separated in a parallel and a cross-wise velocity. The parallel velocities are measured along the height of the cylinders and range from 3751 m/s (BK) to 5529 m/s (DK). The cross-wise velocities

Fig. 1 Quarry in the Franconian Alb as source location for analogue samples. In the upper area of the photo, massive dolostone is exposed. Below, divided by a lithological boundary, layered limestone can be found. *Photo Credit* E. Mraz
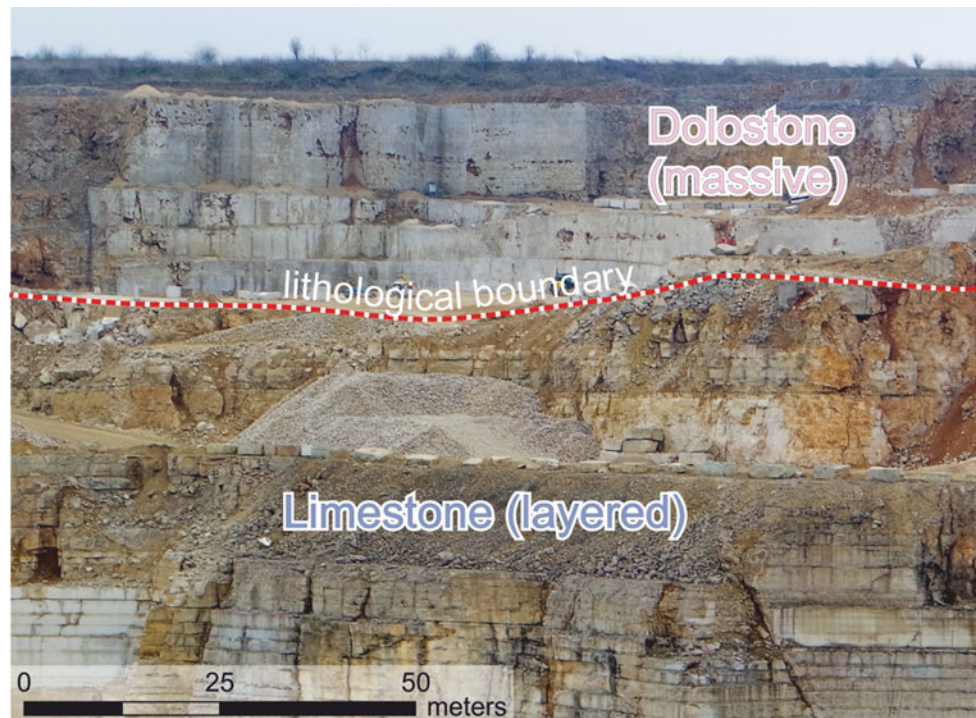
Table 1 List of the obtained analogue samples with their trade name, sample code, classification after Dunham (1962), classification after Folk (1959, 1962) and rock type

Trade name	Sample code	Classification after Dunham (1962)	Classification after Folk (1959, 1962)	Rock type
Bankkalk	BK	Packstone—Floatstone	Biosparite	Limestone
Basisoolith	BO	Packstone	Pelsparite	
Dietfurter Kalkstein	DK	Packstone—Floatstone	Pelbiosparite	
Kelheimer Auerkalk	KAK	Grainstone	Pelbiosparite	
Obere Krumme Lage	KRL	Packstone—Bindstone	Biosparite	
Wasserzeller Dolomit	WAD	[dedolomitized]		
Dietfurter Dolomit	DD			Dolostone
Pfraundorf Dunkel	PFD			
Wachenzeller Dolomit	WD			

are measured along the specimen's diameter. They range from 3669 m/s (BK) to 5534 m/s (DK). The Dynamic Young's Modulus varies between 40.4 GPa (BK) and 69.0 GPa (DD). The range of the Poisson's ratio stretches from 0.28 to 0.34. The only strength parameter, the indirect tensile strength, has a minimum of 6.5 MPa (KAK) and a maximum of 10.9 MPa (DD).

4 Discussion

In the following section, the laboratory data is examined in detail. In order to evaluate our data, we compare it to investigations by other authors. In addition, we present and discuss new insights that have emerged from this work.

4.1 Evaluation of Laboratory Results

The tested carbonate rocks have their p-wave values fall within the range of values being noted as typical p-wave values (1700 to 6600 m/s) of carbonate rocks by Eberli et al. (2003). The fact that the recorded p-wave values vary significantly can, however, be the first indicator for the heterogeneity of carbonates in general. Regarding this given range, the results lie within this range with velocities of 3669–5529 m/s. The low differences in parallel to cross direction velocities with a maximum of 3.7% implies isotropy within the specimens themselves.

Regarding the elastic parameters, we see that the Poisson's ratio varies between a value from 0.28 minimum to 0.33 as maximum. With a mean value of 0.31 the maximum

Fig. 2 Origin of analogue samples in the Swabian Alb and the Franconian Alb. The carbonate rocks are named after their trading names, not after their lithology
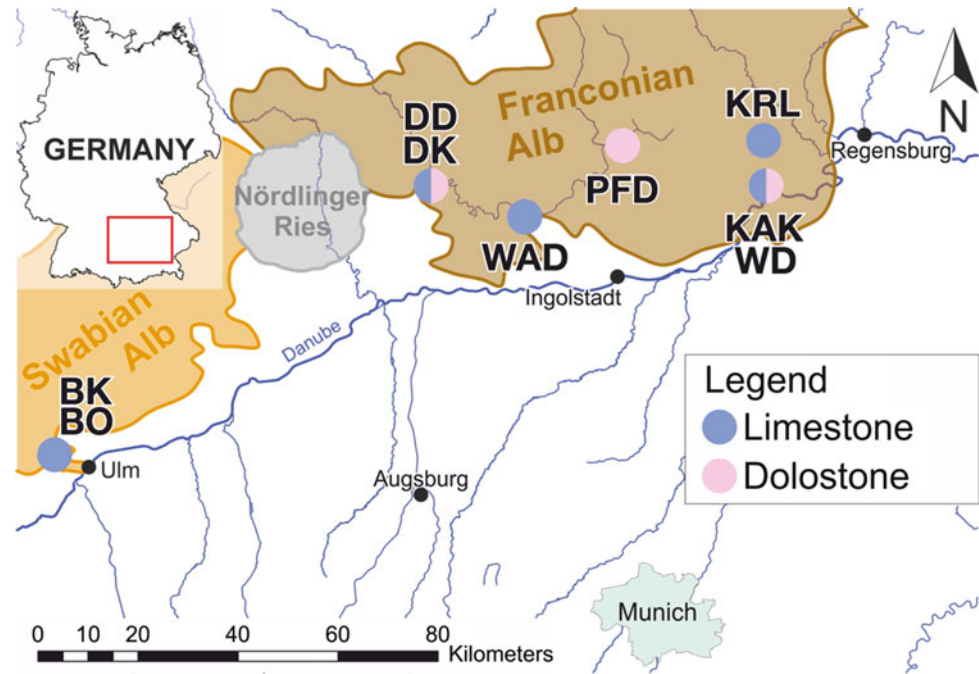
Table 2 Mean values of the rock-mechanical properties of the tested analogue samples

	Sample code	P-wave velocity (m/s)				Dyn. Young's Modulus		Poisson's ratio		Indirect tensile strength
		N	Parallel	N	Crosswise	N	(GPa)	(-)	N	(MPa)
Limestone	BK	5	3751	9	3669	5	40.4	0.28	4	5.6
	BO	16	4693	30	4615	15	66.4	0.33	11	8.4
	DK	36	5529	72	5534	12	61.2	0.34	9	10.5
	KAK	21	5108	36	4940	19	63.1	0.33	26	6.5
	KRL	7	4527	12	4693	6	42.7	0.31	6	8.7
	WAD	35	4940	22	4759	11	50.8	0.28	10	10.5
Dolostone	DD	57	5516	114	5334	16	69.0	0.33	10	10.9
	PFR	42	4787	28	4645	14	67.2	0.28	19	10.7
	WD	24	4166	16	4178	9	48.6	0.32	8	8.4

N is the number of tests conducted

deviation is 0.03 only. The results are comparable to those obtained by Bell (1981), who measured a Poisson's ratio of 0.26–0.32 for carbonate rocks. A wide variation in values is also noticed when the Dynamic Young's Moduli of the carbonates are considered.

Figure 3 shows the values of Young's Modulus from Table 2 in details. The mean values for the limestones and dolostones spread by more than 28 GPa, with the highest mean value of 69.0 GPa for the Dietfurter Dolomit (DD) and the lowest mean of 40.4 GPa for the Bankkalk (BK). Thus, the results suit well with values from carbonate rocks of 41.3–68.9 GPa as measured by Bell (1981). Moreover, the

Interquartile Range (IQR) is consistently small, whereby we can assume that the single specimen from the same rock are highly comparable. Since the carbonates as a whole show differences in the Young's Modulus and in Tensile Strength, yet no pattern can be established in the data trend, it is important to examine the reasons the limestones and dolostones have both low and high values. It is very likely that the observed differences in data and data trend are attributable to variations in component size and lithology, which will be investigated in the future. To complete the set of rock-mechanical parameters, we will add the Static Young's Modulus and UCS for each data set in future publications.

Fig. 3 Box-plot diagram of the Dynamic Young's Modulus resulting from Ultrasonic measurements on analogue samples
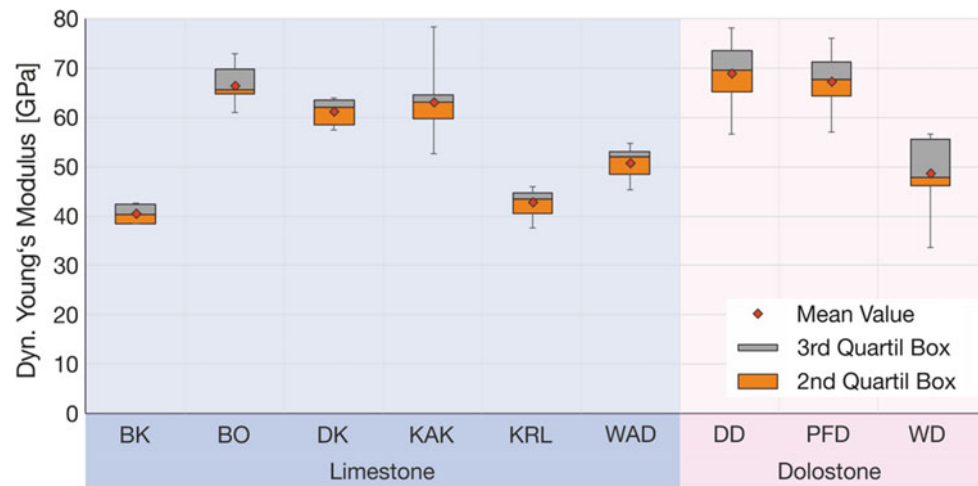
4.2 Comparison of Different Sampling Methods

As explained in Sect. 2.1, we chose analogue samples based on lithology, while several authors followed different approaches for sampling. Tondera et al. (2013) chose rocks after facies criteria. These samples covered three types of rocks, of which two represent actual geothermal reservoir rocks. However, these rocks were not addressed lithologically by Tondera et al. (2013). They also indicated that their rocks had anisotropy-dependent properties, while at the same time exhibiting a high degree of fluctuation in the measurement range, which we could not observe in our experiments. This information on rocks, however, is crucial since all the factors, such as stress distribution or simulation input parameters are highly sensitive to those. Homuth and Sass (2014) chose analogue samples according to stratigraphy, but again not after lithology. Recent research from Mraz et al. (2016) shows that the depositional environment within the Upper Jurassic changes southbound from the outcrop to the Alpine boundary. Hence, taking the huge range of laboratory results on these rocks in consideration, describing samples lithologically is a much more assuring way to produce reliable data. In addition, the main goal of Homuth and Sass (2014) was to characterize these analogue samples after permeability and heat conductivity, which does not overlap with our requirements.

A recent and related publication, Hedtmann and Alber (2017), compares dry and saturated limestones and dolostone from similar rock samples as used in this study. The Kelheimer limestone and the Wachenzeller Dolomit, which were tested by Hedtmann and Alber (2017) correspond to two of our nine rocks, 'KAK' and 'WD'. However, Hedtmann and Alber (2017) came up with different values. Comparing the results, our measured p-wave velocities of 5108 m/s for the limestone and 4178 m/s for the dolostone are 900–500 m/s lower to Hedtmann and Alber's (2017)

mean values of 6027 and 4711 m/s. In both cases the velocity is higher in the limestone than in the dolostone. On the contrary, our elasticity parameter results show a Poisson's Ratio of 0.33 and 0.32 compared to Hedtmann and Alber's (2017) 0.21 and 0.17 and an up to 2-times higher Young's Modulus of 63.1 and 48.6 GPa in contrast to their 24.7 and 31.0 GPa for both of these rock types. Furthermore, their limestone has a higher tensile strength of 9.1 MPa compared to ours which is 6.5 MPa, while the dolostone is almost the same strength (8.7 compared to 8.4 MPa). In comparison, our elastic properties fit better with data from Bell (1981) as shown in Sect. 4.1. The reasons for the discrepancy between Hedtmann and Alber's (2017) and ours may be diverse. Firstly, the tests we conducted had a different specimen geometry than Hedtmann and Alber's (2017). We conducted our tests after ASTM Standards, while Hedtmann and Alber (2017) used smaller specimen sizes, which may in general have led to differing or rather inaccurate results. Secondly, we had a well-described and well-defined lithology along with better information on porosity and grainsize. This should not be underestimated since it does, considering Fig. 3, verifiably influences the rock-mechanical parameters.

5 Conclusion

This work has shown that carbonate rocks' lithology greatly influences their mechanical properties, such as elasticity and strength. The mechanical properties that we recorded in carbonate rocks were not expected and also not identified with respect to geothermal reservoir characterization by other authors. These new insights show that we need to look at the rocks along deep drillings in a much more detailed way than has been done before. Furthermore, we gained a large pool of high quality data, which reflects plausible

values for carbonate rocks in general. In further stages of this work, this database will be complemented with examinations on porosity, component size and UCS.

However, we still face the issue that it is unknown if these samples are really representative for rocks at depths over 4000 m. Hence, it will be necessary to compare analogue samples with in situ rock cores from the drilling. If it can be shown that analogue samples represent rocks in greater depths, or at least give an empirical factor to approximate these values, it will be possible to derive rock-mechanical parameters from cuttings. Analytical calculations and numerical models fed with this data would thus become more plausible and reliable.

References

ASTM D3967-16: Standard test method for splitting tensile strength of intact rock core specimens. ASTM International, West Conshohocken, PA (2016)

ASTM D4543-08e1: Standard practices for preparing rock core as cylindrical test specimens and verifying conformance to dimensional and shape tolerances (withdrawn 2017), ASTM International, West Conshohocken, PA (2018)

Bell, F.G.: A survey of the physical properties of some carbonate rocks. In: Bulletin of the international association of engineering geology, no. 24, pp. 105–110. Aachen/Essen (1981)

Dunham, R.J.: Classification of carbonate rocks according to depositional texture. In: Ham, W.E. (eds.) Classification of carbonate rocks. Association of petroleum geologists memoir, vol. 1, pp. 108–121 (1962)

Eberli, G.P., Baechle, G.T., Anselmetti, F.S., Incze, M.L.: Factors controlling elastic properties in carbonate sediments and rocks, In: The leading edge, pp. 654–660 (2003)

Folk, R.L.: Practical petrographic classification of limestones. AAPG Bulletin **43**, 1–38 (1959)

Folk, R.L.: Spectral subdivision of limestone types. In: Ham, W.E. (ed.) Classification of carbonate rocks—a symposium, AAPG Memoir, vol. 1, pp. 62–84. American Association of Petroleum Geologists, Tulsa, Oklahoma (1962)

Hedtmann, N., Alber, M.: Investigation of water-permeability and ultrasonic wave velocities of german malm aquifer rocks for hydro-geothermal energy. Procedia Eng. **191**, 127–133 (2017)

Homuth, S., Sass, I.: Outcrop analogue vs. reservoir data: characteristics and controlling factors of physical properties of the upper jurassic geothermal carbonate reservoirs of the Molasse Basin, Germany., In: Thirty eighth workshop on geothermal reservoir engineering, 10 S. Stanford University, Stanford (2014)

Mraz, E., Wolfgramm, M., Moeck, I., Thuro, K.: Faziesabhängige Diageneseentwicklung des südlichen Weißen Jura im bayerischen Molassebecken. In: Der Geothermiekongress DGK 2016. Essen (2016)

Tondera, D., Klapperich, H., Blöcher, G., Moeck, I., Steiger, T., Bems, C., Hild, S.: Geothermie Forschungsprojekt „Allgäu 2.0"—Forschungsansätze, Untersuchungen & Planungsschritte. In: 19. Tagung für Ingenieurgeologie, S. 285–293. Munich (2013)

www-01: http://www.tiefegeothermie.de/projekte/traunreut. Last accessed 10 Mar 2018

The Development of a Geological 3D Model of the São Carlos Region, Brazil

Moisés Furtado Failache and Lázaro Valentim Zuquette

Abstract

The lithological, stratigraphic and geological structure in a three-dimensional model is an important tool to comprehend geological complexity more effectively. This paper presents a structured geological 3D model of the São Carlos region, located in the state of São Paulo, in southeastern Brazil. The structured geological 3D model was built using Subsurface View MX developed by INSIGHT. The software method is based on the Delaunay triangulation of the top and bottom layer surfaces, considering a cross-section network. The geological data were obtained from 133 groundwater well profiles, a digital terrain model (30 m resolution) and bedrock geological map (1:50,000 scale). The results show that the model represents five main geological formations of the study area, namely, Itaqueri (medium grain sandstones), Serra Geral (basalts and diabases), Botucatu (friable and silicified aeolian sandstones), Pirambóia (fluvial sandstones) and Corumbataí (shales, siltstones and claystones). The Eolian friable sandstones from the Botucatu Formation present the greatest distribution both in extent (693 km^2) and in thickness (can reach up to >250 m), as well as in terms of volume (93.928 km^3). In conclusion, the 3D geological model of the São Carlos region permits the acquisition of spatial information of geological layers with vertical sections in all directions that can be used for various purposes, such as underground excavation, groundwater management and well drilling.

M. F. Failache (✉) · L. V. Zuquette
University of São Paulo, São Carlos, SP 13566-590, Brazil
e-mail: moisesfailache@hotmail.com

1 Introduction

In recent years, geological 3D models have been widely applied in several fields such as, engineering geology, geological surveys, environmental assessment, mining and petroleum exploration (Fookes 1997; Wycisk et al. 2009; Zhu et al. 2012; Jørgensen et al. 2015; Shogenov et al. 2017). They are a powerful tool for visualizing, quantifying and communicating the geological context of a region, providing useful information to decision makers, geographers, engineers and geologists.

In Brazil, it is difficult to develop regional geological 3D models, because it is not common to find areas with reasonable quantity and quality data and maps at a suitable scale. However, in the São Carlos Region (SCR) there is a reasonable amount of data, which according to (Kessler et al. 2009) allows for the development of a 3D model for visualizing and overview the main geological formations and lithologies.

In this context, this paper aims to build a structured geological 3D model of the São Carlos Region. The SCR is located in the state of São Paulo (Fig. 1), in southeastern Brazil, between the meridians 48° 00′ and 47° 45′W and parallels 22° 00′ and 22° 15′S.

The regional context of the study area is described as follows:

- Three geomorphologically predominant units: scarps supported by basalts and silicified sandstones; plateau with the highest altitudes; and depression with the lowest altitudes, all regions are mainly composed of sedimentary rocks;
- The altitude ranges from 600 to over 1000 m;
- The relief consists of broad, medium, elongated and rounded hills, alluvial plains, slopes with local canyons and channelized slopes;
- The slope ranges from 2 to 20% in most of the SCR and over 20% in areas with the greatest slope;

Fig. 1 São Carlos region location, including drainage channels, urban area, geological formations and groundwater wells
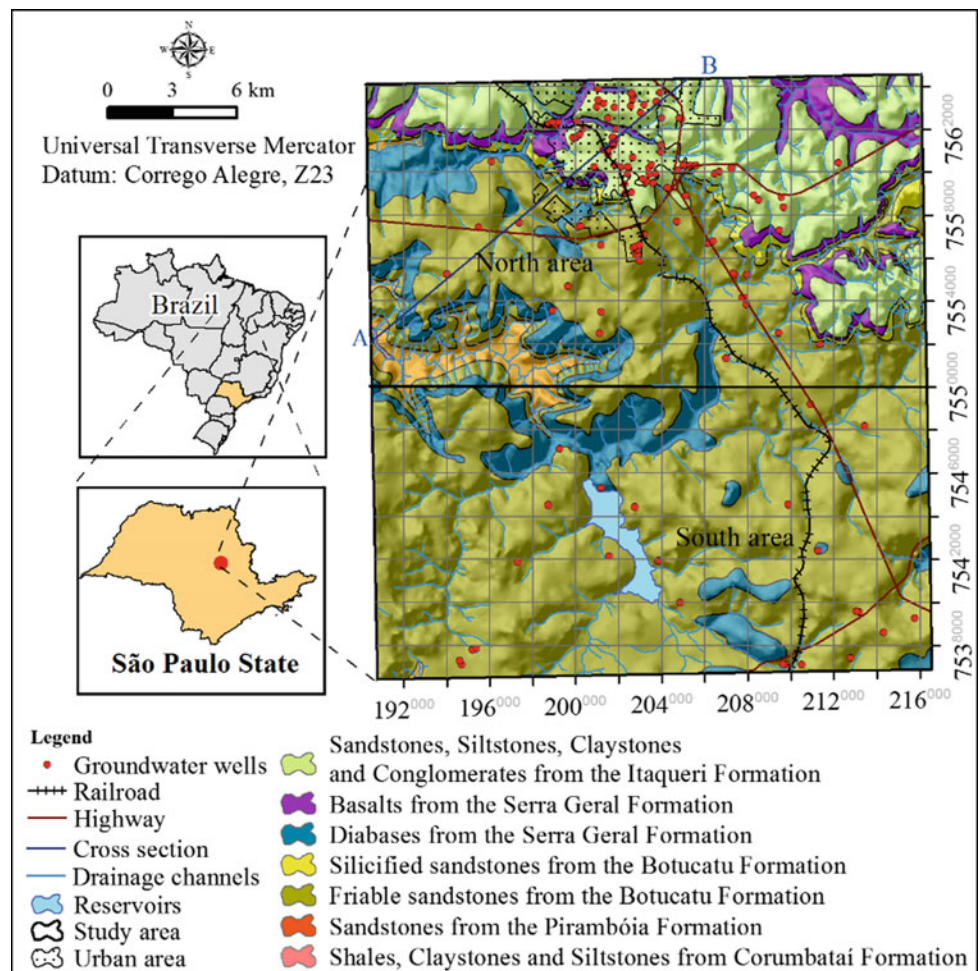
- The SCR presents a suitable bedrock geological map at a scale of 1:50,000; and;
- The study area presents 133 groundwater wells with adequate data to develop the 3D model.

2 Regional Geology

The studied region is constituted by igneous and sedimentary lithologies belonging to five geological formations distributed in different combinations, which make understanding the spatial extent of each lithology difficult. Brief descriptions of the geological formations follow:

The Itaqueri Formation is located predominantly in the northern portion of the study area occupying the highest altitudes. This formation is characterized by reddish-brown sandstones, siltstones, claystones and conglomerates with variable matrixes, poor selection and rarely occurring cross stratification.

The Serra Geral Formation is formed by basalt flow and diabase sills. The basalts occur predominantly in the northern region, while the diabases in the west and southeast. Generally, independent of mentioned lithologies, both are fractured with varying thicknesses.

The Botucatu Formation is composed of pinkish, reddish and whitish fine-grained to medium sandstones, with well selected rounded grains, a clay content of less than 10% and a cross-stratification ranging from medium to large due to its Aeolian origin. There are two types of sandstone found in the area. The first is very friable and occupies the plain regions of the studied area. It is also porous and is characterized as the main aquifer of the region. The second sandstone type is silicified sandstone, stratigraphically above the friable sandstone, outcropping in the scarps and presenting diversified fractured structures.

The Pirambóia Formation is characterized by layers of fine to medium sandstones, with relatively high percentages of clay, moderately selected, reddish, yellowish and whitish with intercalation of siltstone and argillite, of fine to medium

grain size. The predominant structure is small to medium-sized, with a plane-parallel and cross stratifications caused by fluvial deposition.

The Corumbataí Formation is composed of varied shales with gray to purple color, claystones and siltstones and they may present calcareous cementation.

3 Methods and Materials

The model was generated in Subsurface View MX, developed by INSIGHT, which is based on an older software called GSI3D, developed by the British Geological Survey (BGS). Several studies with the software were developed (Kessler et al. 2009; Sobisch 2000; Tame et al. 2013; Watson et al. 2015). Structured geological 3D model development is based on a method that relates geological cross sections forming a cross section network as a result, which is the base for model calculation. The software calculation method is based on the Delaunay triangulation, where the top and base surfaces are calculated using all nodes defined in the cross-sections and the distribution of geological layers, noting that the established quotas are preserved. During the process, triangulation is automatically limited by the lateral extent of the respective layers and the digital terrain model. It is important to note that the surfaces are calculated from top to bottom, where the layers upper boundary are used to establish the elevation values along the lateral boundary. The selection of the Delaunay triangulation is because this method shows the original control points, besides it is also possible to evaluate the uncertainty degree when distances between nodes increase.

The steps of structured geological 3D model development are shown in Fig. 2.

3.1 Data Collection

The data collection aimed at obtaining already established data, such as topographic maps, bedrock geological maps and other geological data from groundwater well profiles.

3.2 Input Data

The input data required to build the structured geological 3D model are categorized into four types: digital terrain model (DTM); bedrock geological map; groundwater well profiles and general vertical section (GVS).

The DTM was developed in ArcGIS 9.3, using a regular grid method (30 m pixel resolution) and then converted into a triangular irregular network format in Subsurface view MX. The DTM elaboration considered the drainage channel
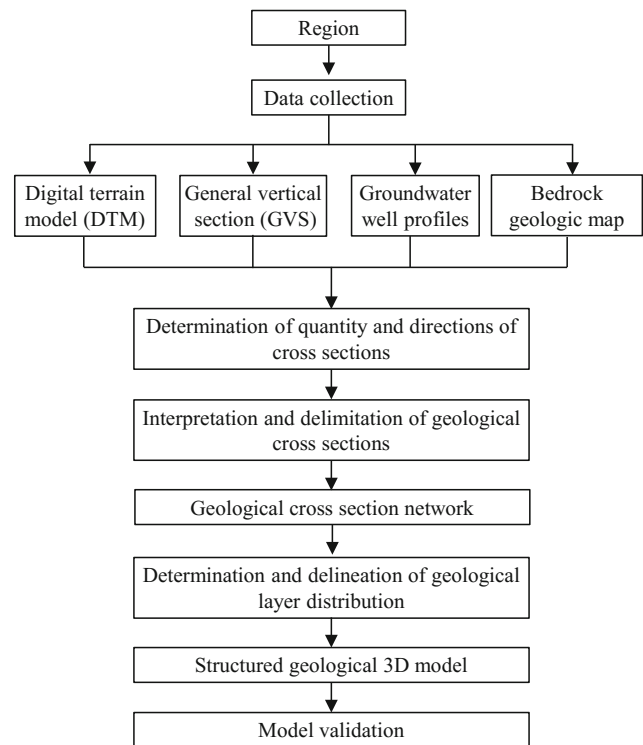
Fig. 2 Flowchart of the study steps to develop the structured geological 3D model of the São Carlos region

net, altitude lines and points obtained from a topographic map at a scale of 1:50,000 (IBGE 1971).

The bedrock geological map was obtained from (Nishiyama 1991), updated and validated with field surveys.

The groundwater well data were obtained from the SIAGAS database (SIAGAS database homepage 2017): localization and altitude, description of geological materials, thicknesses and porosities.

The GVS describes the vertical sequence of the layers and was obtained through the interpretation of groundwater well profile descriptions, a bedrock geological map and regional stratigraphic sequences.

Faults were not considered in the model development because of the tailing is small, even though they occur in the SCR.

3.3 Model Preparation

The steps for model preparation were as follows:

- Insertion of the input data.
- The number and directions of the vertical geological cross sections were based on spatial distribution of the geological materials, groundwater well profiles and areal distribution;

- Interpretation and delimitation of geological cross sections, considering the groundwater well profiles' descriptions and bedrock geological map. At the end of delimitation of all geological cross sections, the net of the intersection point was obtained that corresponded to the preliminary geological model. From the cross section network, the plausibility of the correlations was verified and interpretations were made;
- Determination and delimitation of the distribution of geological layers. The distribution was based on the analysis of the previously obtained cross section network and the bedrock geological map. The bedrock geological map determined the surface distribution, while the cross-section network that considered the groundwater wells was used to establish the lateral extent.
- Development of the structured geological 3D model.

3.4 Model Validation

The validation of the structured geological 3D model was done by comparing the layer limits delimited in interpreted geological cross sections with those generated from the calculated model and field works.

4 Results and Discussion

Based on the analysis of the bedrock geological map, stratigraphic relations, groundwater well data and the digital terrain model, a structured geological 3D model was built. The model validation revealed an average variation of ±2 m between the lithological layer bases, determined from the interpreted vertical geological cross section, and the layers obtained from the geological 3D model. In Fig. 3, the 3D model is shown with multi-view examples and Table 1 shows the distribution and volume values of the different geological layers.

The results show that the geological formations of the São Carlos region present the following basic spatial characteristics:
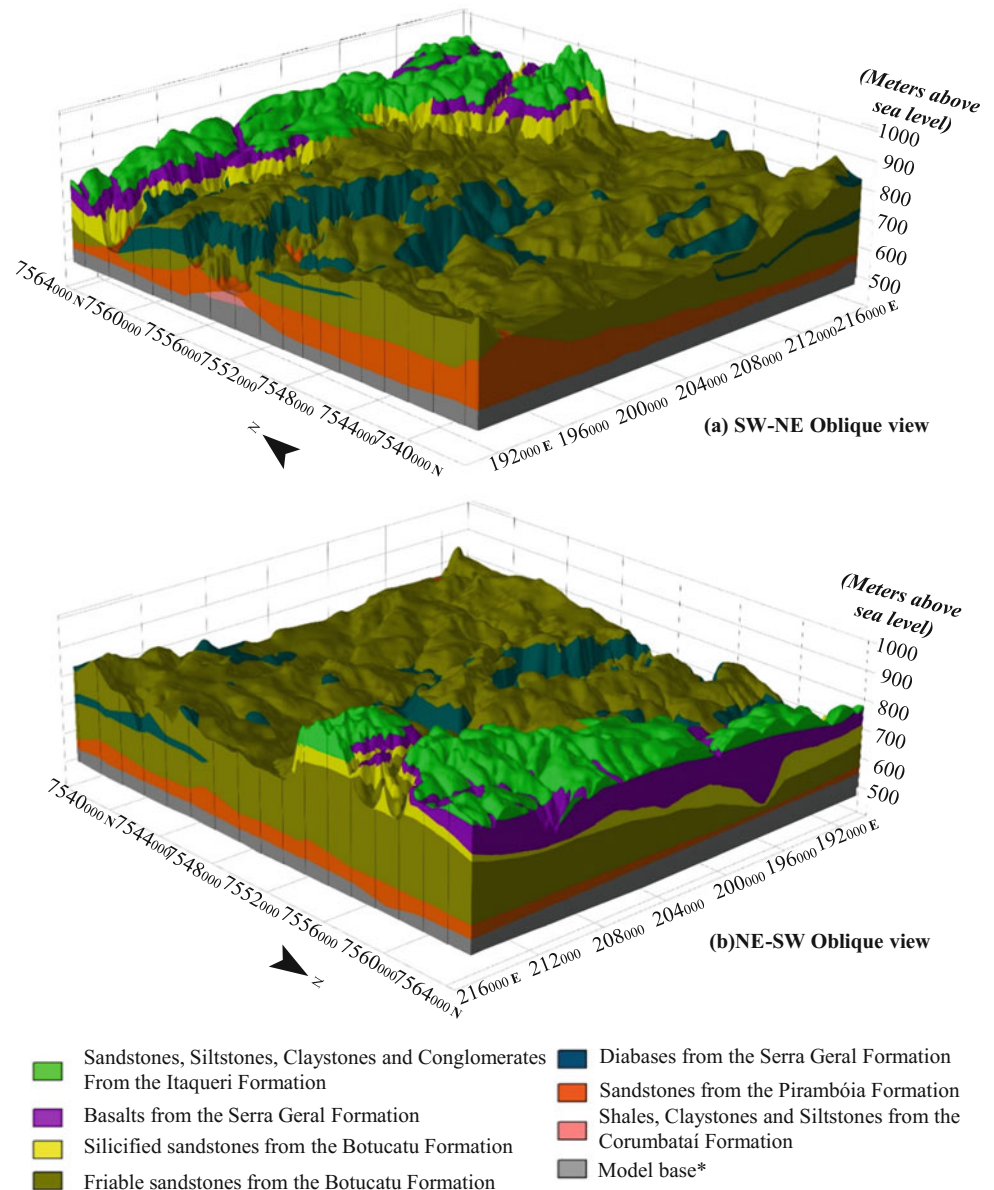
- The sandstones, siltstones, claystones and conglomerates from the Itaqueri Formation occur predominantly north of the studied area from 850 m above sea level. The maximum thickness is around 30 m at the upper slope and decreases when nearing drainage channels.
- The basalt layers from the Serra Geral Formation are distributed north of the SCR and outcrop at the base of the drainage channels and at the open slope. This

lithological layer presents the greatest thickness variability, which varied from 20 to more than 200 m
- The diabase bodies from the Serra Geral Formation occurs in several spots in the area, however they outcrop mostly in the west. The average thickness of the diabase layers is around 100 m.
- The total Botucatu Formation thickness can reach up to 150 m. The friable sandstones outcrop and are distributed in more than 60 and 95% of the SCR area. On the other hand, the silicified sandstones outcrop in 2.29% of the studied area, located on the scarps.
- The Pirambóia Formation outcrops solely in the west, but occurs in all parts of the region.
- The Corumbataí Formation outcrops in a small portion of the region located in the western area, but is still found in the region under the sandstones of the Pirambóia Formation.

The results also show that it is possible to understand the geological context of the São Carlos region, in terms of distribution, thickness and volume. The geological layers that are widely distributed in the São Carlos region are the sandstones from the Pirambóia Formation and the friable sandstones from the Botucatu Formation, occupying almost the entire region. However, those geological layers are not homogeneous throughout the studied area, because of the diabases are intruded in several depths inside of friable sandstones from the Botucatu Formation and sandstones from the Pirambóia Formation, which generated layers with distinct thickness. The friable sandstones from the Botucatu Formation have almost double the volume than that of the sandstones from the Pirambóia Formation.

From the structured geological 3D model development procedures, some potential advantages and limitations were identified. The main potential advantage is that the software allowed for new vertical geological cross sections to be attained, even though they were not used in the interpretation process to check the interpolation results of the generated model. An example is shown in Fig. 4 in which there is a vertical geological cross section with all the geological materials in the SW–NE direction.

The limitations were mainly related to the quality and quantity of input data, because the model consistency is dependent on the interpretation along cross sections that is based on the knowledge of the geology obtained from the bedrock geological map and groundwater well profiles. Thus, the global groundwater wells' density is one well per 5.37 km^2. However, the distribution of groundwater wells is not homogeneous, which influenced the degree of uncertainty in the model.

Fig. 3 Some views of the structured geological 3D model of the São Carlos region, located in the state of São Paulo, in southeastern Brazil
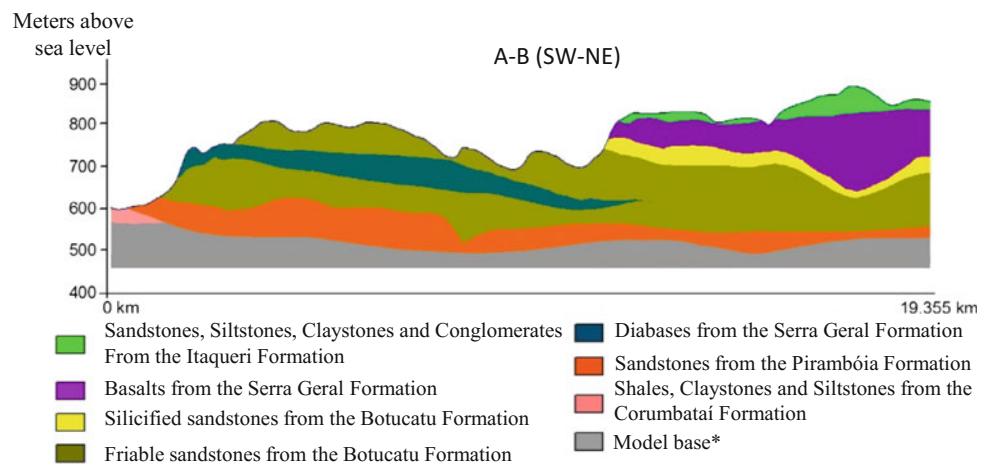

(a) SW-NE Oblique view

(b) NE-SW Oblique view

| | Sandstones, Siltstones, Claystones and Conglomerates From the Itaqueri Formation | | Diabases from the Serra Geral Formation |

Sandstones, Siltstones, Claystones and Conglomerates From the Itaqueri Formation

Basalts from the Serra Geral Formation

Silicified sandstones from the Botucatu Formation

Friable sandstones from the Botucatu Formation

Diabases from the Serra Geral Formation

Sandstones from the Pirambóia Formation

Shales, Claystones and Siltstones from the Corumbataí Formation

Model base*

*This layer has only an aesthetic function, which was delimited for the model base presented a flat aspect.

UTM projection / Datum: Córrego Alegre, Z23

Table 1 Distribution and volume of the different lithologies that occur in the São Carlos region

Geological formation and lithologies	Distribution (km^2)	Volume (km^3)	Outcrop distribution (km^2)
Sandstones, siltstones, claystones and conglomerates from the Itaqueri formation	116.40	3.662	116.74
Basalts from the Serra Geral formation	137.83	9.197	29.03
Diabases from the Serra Geral formation	429.07	17.412	77.36
Silicified sandstones from the Botucatu formation	159.04	5.560	16.33
Friable sandstones from the Botucatu formation	693.37	93.928	455.67
Sandstones from the Pirambóia formation	713.29	44.742	19.77
Shales, claystones and siltstones from the Corumbataí formation	4.197	0.101	0.35

Fig. 4 Example of a geological cross section obtained from the geological structured 3D model of the São Carlos region

Meters above sea level

A-B (SW-NE)

■ Sandstones, Siltstones, Claystones and Conglomerates From the Itaqueri Formation

■ Basalts from the Serra Geral Formation

■ Silicified sandstones from the Botucatu Formation

■ Friable sandstones from the Botucatu Formation

■ Diabases from the Serra Geral Formation

■ Sandstones from the Pirambóia Formation

■ Shales, Claystones and Siltstones from the Corumbataí Formation

■ Model base*

*This layer has only an aesthetic function, which was delimited for the model base presented a flat aspect.

If the studied area is divided into two regions, as shown in Fig. 1, one observes that the northern area presents 111 groundwater wells (a density of one well per 3.28 km^2) in comparison to the 24 (a density of one well per 14.89 km^2) in the southern region. The groundwater well locations in both areas are also different; in the northern region, the wells are distributed in greater density near the urban area and sparser going outward from the urban area. In the southern area, the groundwater water wells show a sparse distribution.

Other model uncertainty sources are associated with the sandstone from the Pirambóia Formation and the diabases from the Serra Geral Formation. In the first lithology, not all of the groundwater wells were deep enough to reach said layer, and when the layer was reached, it was not possible to identify the base in the well profiles. Because of that, in some cases, it was necessary to estimate the base layer and lateral extent based on the geological knowledge of the region, which resulted in an increase in the uncertainty of the model in relation to this lithology.

The second lithology is associated with the intrusions of the diabases, those which occur in three distinct layers found in the region. The first outcrops on the hilltops southeast of the SCR; the second outcrops in the west, but it is also distributed in subsurface to southeast; and the last one, which is a sill, is located between 580 and 620 m above sea level in the northern central region. The intrusions normally vary in terms of lateral extent. Because of that, the distance between groundwater wells was analyzed to determine their distribution. Initially, the well nearest to the diabase outcrop was considered, however, if the intrusion presence was observed, testing proceeded to the next well, which was at a maximum distance of 2 km. In dealing with the next well, if intrusion occurred, the same procedure noted before was conducted, otherwise the lateral extent would be limited to 500 m from the first well. In relation to the sill, because it did not outcrop, the analysis began at the most central groundwater well, emphasizing that to be considered a sill, the diabases should have occurred in at least three groundwater wells with a maximum of 2 km between them.

5 Conclusions

A geological structured 3D model of the São Carlos region was developed that presented different geological formations and lithological characteristics. Some of the identified geological layers are relatively homogenous in terms of distribution, thickness and boundary geometry. However, others are complex, which resulted in different geological layers and thicknesses. The groundwater well density shows that the northern portion of the SCR presents a greater consistency, with a lesser degree of uncertainty about the thickness, distribution and geometry of the geological layers when compared to the southern area. The quantity of groundwater wells present in the studied area was considered acceptable, however, to improve the model and reduce uncertainties related to the areas with a greater degree of complexity, it is necessary to obtain more groundwater well data, borehole logs and geophysical data. The proposed model allows for the improvement in the unit limit of the bedrock geological map, as well as the analysis of spatial information about geological layers that can be used for various purposes, such as underground excavation, engineering design, groundwater management and well drilling. The model can be easily accessed since Subsurface View MX provides a free version that allows for the visualization of models and performs functions such as the delineation of vertical and cross sections.

References

Fookes, P.G.: Geology for engineers: the geological model, prediction and performance. Q. J. Eng. Geol. **30**, 293–424 (1997)

IBGE.: Topographic maps. SF-23-Y-A-I-1 (São Carlos), scale 1:50,000 (1971)

Jørgensen, F., Høyer, A., Sandersen, P., He, X., Foged, N.: Combining 3D geological modelling techniques to address variations in geology, data type and density: an example from Southern Denmark. Comput. Geosci. **81**, 53–63 (2015)

Kessler, H., Mathers, S., Sobisch, H.: The capture and dissemination of integrated 3D geospatial knowledge at the British geological survey using GSI3D software and methodology. Comput. Geosci. **35**, 1311–1321 (2009)

Nishiyama, L.: Mapeamento geotécnico preliminar da quadrícula de São Carlos—SP. M.Sc. Thesis. Geotechnics Department, University of São Paulo, São Carlos (1991)

Shogenov, K., Forlin, E., Shogenova, A.: 3D geological and petrophysical numerical models of E6 structure for CO_2 storage in the Baltic Sea. Energy Procedia **114**, 3564–3571 (2017)

SIAGAS database homepage: http://siagasweb.cprm.gov.br (2017). Last Accessed 20 June 2017

Sobisch, H.: Ein Digitales Raeumliches Modell des Quartaers der GK25 Blatt 3508 Nordhorn auf der Basis vernetzter Profilschnitte (a digital spatial model of the quaternary at 1:25,000 scale of sheet 3508 Nordhorn based on intersecting cross-sections). Shaker Verlag, Aachen, 113 pp (2000)

Tame, C., Cundy, A., Royse, K., Smith, M., Moles, N.: Three-dimensional geological modelling of anthropogenic deposits at small urban sites: a case study from Sheepcote Valley, Brighton, UK. J. Environ. Manage. **129**, 628–634 (2013)

Watson, C., Richardson, J., Wood, B., Jackson, C., Hughes, A.: Improving geological and process model integration through TIN to 3D grid conversion. Comput. Geosci. **82**, 45–54 (2015)

Wycisk, P., Hubert, T., Gossel, W., Neumann, C.: High-resolution 3D spatial modelling of complex geological structures for an environmental risk assessment of abundant mining and industrial megasites. Comput. Geosci. **35**, 165–182 (2009)

Zhu, L., Zhang, C., Li, M., Pan, X., Sun, J.: Building 3D solid models of sedimentary stratigraphic system: an automatic method and case studies. Eng. Geol. **127**, 1–13 (2012)

GigaPan Image-Based 3D Reconstruction for Engineering Geological Investigations

Lee Hana, Mostegel Christian, Fraundorfer Friedrich, and Kieffer D. Scott

Abstract

Image based 3-dimensional (3D) reconstruction is a powerful technique for quantifying the shape of complex objects, and interactive gigapixel panoramic photographs provide multi-scale imagery that facilitate unprecedented long-range qualitative observations. This research examines approaches for combining these technologies with the goal of generating 3D reconstructions from multiple ultra-long range gigapixel panoramas. Because restricted access to the geological object is often an issue for a close-range observation. The overall workflow involves: (1) acquiring multiple overlapping gigapixel panoramas from various viewpoints providing a triangulation angle of approximately 5°; (2) camera calibration; and (3) creating a 3D model using specifically adapted Structure-from-Motion and subsequent Multi-View-Stereo techniques. Initial studies performed at a dolomite quarry located near Graz, Austria, show that a dense and accurate 3D point cloud can be obtained at a range of 630 m. Rock discontinuity orientations measured directly from the model are in excellent agreement with traditional compass measurements, model dimensions (lengths and slope angles) agree with actual physical quantities, and geologic features can be mapped and projected into the 3D model in very high detail. These initial results indicate the developed methodology can greatly assist engineering geologists making quantitative measurements and analyses of outcrops and exposures that are inaccessible or at such great distances so as to preclude traditional photogrammetric techniques. To better define the limits of application, ongoing research is focused on evaluating range effects, in particular the maximum range (and associated parameters) to which this methodology can be reasonably applied in the context of engineering geological investigations.

1 Introduction

Three dimensional imagery and panoramic gigapixel photography are indispensable techniques for documenting geologic field conditions. Image-based 3D reconstruction algorithms can capture and quantify physical details of geologic features, while gigapixel panoramic photography provides qualitative optical information of unprecedented detail that covers multiple observational scales. In this research, a workflow has been developed to combine these methods; namely, to create accurate long-range georeferenced 3D photogrammetric models directly from a suite of gigapixel panoramas since restricted access to the geological object is often an issue for a close-range observation. The workflow involves: (1) acquiring multiple gigapixel panoramas from various viewpoints; (2) camera calibration; and (3) 3D model generation using specifically adapted Structure-from-Motion (SfM) and Multi-View-Stereo (MVS) algorithms, hereafter referred to as "SfM-MVS". The SfM-MVS approach was tested at a dolomite quarry near Graz, Austria. The overall SfM-MVS workflow is enumerated below, together with a summary of results obtained and a comparison to reference hand-measured structural geologic measurements.

L. Hana (✉) · K. D. Scott
Institute of Applied Geosciences, Graz University of Technology, Graz, Austria
e-mail: hana.lee@tugraz.at

M. Christian · F. Friedrich
Institute of Computer Graphics and Vision, Graz University of Technology, Graz, Austria
e-mail: mostegel@icg.tugraz.at

Fig. 1 Geological map [modified from the source: Multithematische Geologische Karte von Österreich 1:1.000.000 (Geologische Bundesanstalt 2017)] and satellite image of the Quarry (Google Earth 2017)
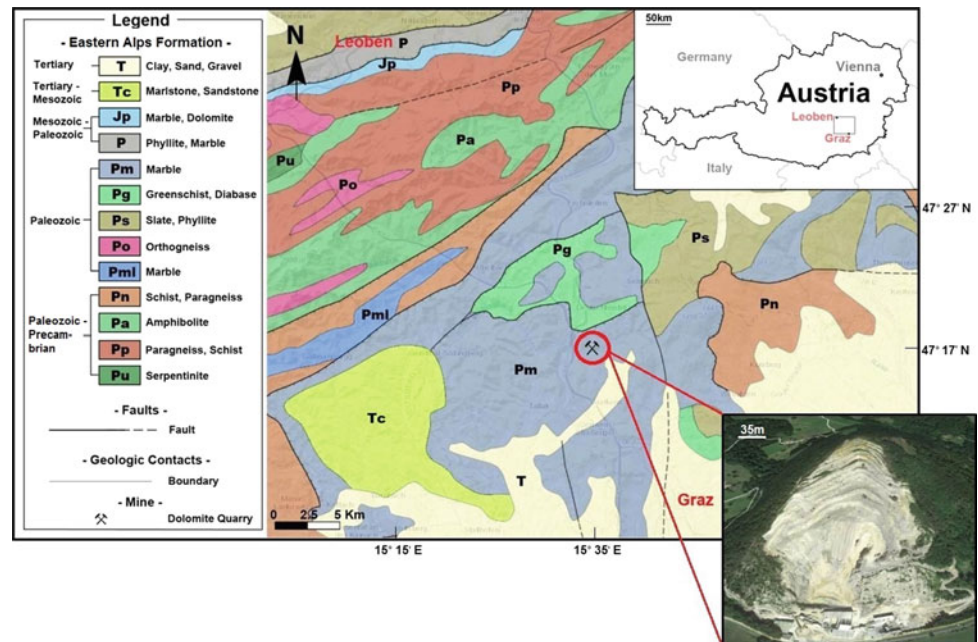
2 Geological Setting

The study site selected for testing the SfM-MVS approach is an active dolomite quarry located approximately 18 km northwest of Graz in Styria, Austria (Fig. 1). The quarry location is regionally mapped as Paleozoic Marble of the Eastern Alps Formation (Geologische Bundesanstalt 2017), and the predominant rock type outcropping in the quarry is light gray, fine to medium grained, moderately weathered to fresh dolomite.

The quarry is cut at an overall slope angle of 37° and the overall plan dimensions are about 350 m by 250 m. The highest elevation is 695 m a.s.l. and the maximum relief is 195 m. The quarry includes 14 benches ranging in height from 5 to 18 m.

3 Methods

The following sections summarize: (1) gigapixel panoramic image acquisition methods; (2) camera calibration methodology; and (3) approach for generating a 3D point cloud using SfM-MVS algorithms.

3.1 Gigapixel Image Acquisition

Panoramic gigapixel images were obtained with the GigaPan Epic Pro robotic head (www.gigapan.com), Nikon D800 camera, and 400 mm Nikon objective (Fig. 2). Hardware specifications and image acquisition settings are summarized in Table 1.

Six instrument stations were established and located as shown in Fig. 3. The triangulation angle between instrument set-ups is approximately 5° which is suitable for automatic image matching, and the average range to the quarry wall is approximately 600 m. The geographic coordinates of each instrument set-up are summarized in Table 2, along with the respective range to the quarry wall. At each instrument set-up, 110–145 photographs were made in a raster pattern, with specified vertical and horizontal overlaps of 45%.

3.2 Camera Calibration

Prior to any 3D reconstruction and measurement tasks, the interior orientation of the camera needs to be computed by camera calibration. The interior orientation parameters consist of the focal lengths f_x and f_y, the image coordinates of the principal point p_x and p_y and the 4 parameters for radial and tangential distortion. The camera model is described in detail in Daftry et al. (2013). Camera calibration has been performed using the calibration tool of our in-house I3D 3D reconstruction software. This calibration tool utilizes coded calibration targets which facilitate fully automatic control point identification and thus fully automatic camera calibration without any manual intervention involved. For camera calibration, different poses of 73 calibration images have been acquired using a checkerboard (Fig. 4).

Fig. 2 GigaPan epic pro robotic mount (left) and instrument set-up at the dolomite quarry (right)

Table 1 Hardware specifications and image acquisition settings

Camera/Lens		GigaPan	
• Camera model	Nikon D800	• Model	GigaPan Epic Pro
• Lens model	Nikon AF-S NIKKOR 70–200 mm 1:2.8GII ED with 2× teleconverter	• Mirror lock up	On (lock-up time: 1 s)
• Mode/Flash	Manual/off	• Time/Exposure	3 s
• Anti-shock	On	• Motor speed	Med
• Shutter speed	1/200	• Motor rigid	On
• ISO/AE lock	100/on	• Pre-trigger delay	2 s
• White balance	Sun	• Picture overlap	45%
• Vibration reduction	On		
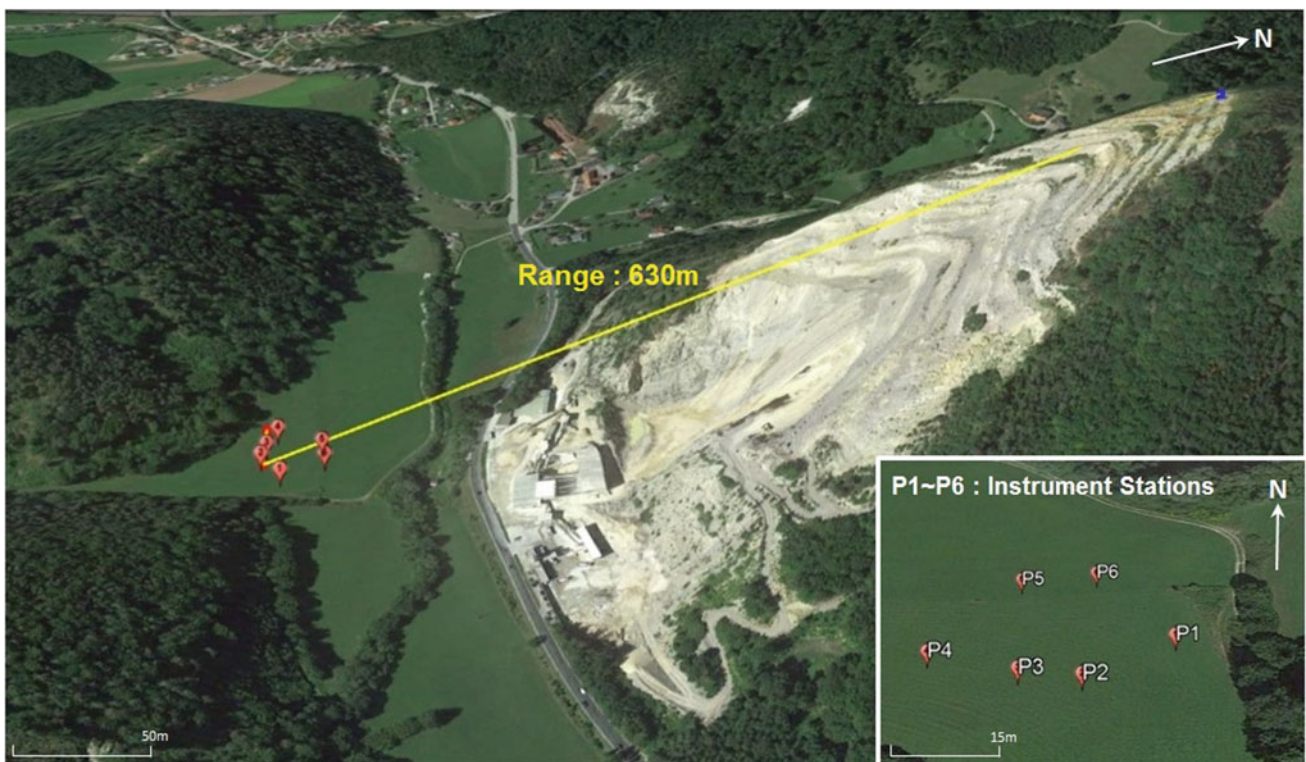
Fig. 3 Instrument set-ups (Basemap: Google Earth 2017)

Table 2 Location of instrument set-ups and the respective range to quarry

Stations	Latitude	Longitude	Elevation (m)	Range (m)
P1	47° 10′ 16.33″N	15° 21′ 6.67″E	440	607.02
P2	47° 10′ 15.87″N	15° 21′ 5.72″E	442	626.34
P3	47° 10′ 15.95″N	15° 21′ 5.06″E	441	626.64
P4	47° 10′ 16.14″N	15° 21′ 4.08″E	440	624.80
P5	47° 10′ 17.14″N	15° 21′ 4.87″E	437	584.01
P6	47° 10′ 17.23″N	15° 21′ 5.75″E	437	578.72

Fig. 4 Different poses of checkerboard for camera calibration
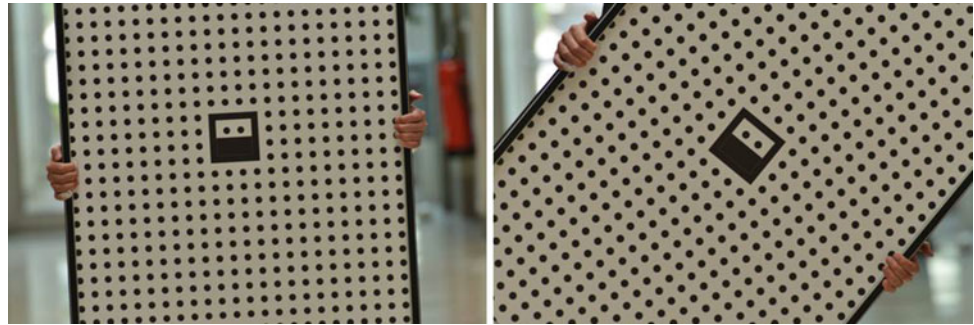
The interior calibration parameters acquired by the calibration procedure are then refined in the bundle adjustment step of the 3D reconstruction procedure. For 3D reconstruction, a set of 713 images is used which is a much larger data set than the 73 calibration images. The use of these additional images also for refining the calibration improves the accuracy of the interior parameters.

3.3 3D Reconstruction

The 3D reconstruction step computes a 3D point cloud from image data using the SfM-MVS process. The SfM step computes the exterior orientation (position and orientation) of the cameras in a fully automatic way. With the computed exterior orientation, a dense 3D reconstruction using stereo matching can be performed. Considering the availability of highly overlapping data, a MVS technique was selected.

The main steps of the SfM technique are feature extraction, feature matching, epipolar graph computation, sparse reconstruction and bundle adjustment. For efficient processing, it is crucial that these processes are performed fully automatically. Automatic processing also includes a process that finds an optimal sequence concerning the order in which images are processed. This task is performed by the epipolar graph computation and is a key ingredient for fully automatic processing. These individual steps are described in detail in Rumpler et al. (2016). For this case example our in-house software I3D and the Colmap software (https://github.com/colmap/colmap) was utilized.

The SfM process only triangulates a few 3D points for camera orientation. A dense 3D model in which a depth value for every image pixel is computed needs a dense stereo matching process. For this we chose a MVS technique as described in Schönberger et al. (2016). Visualized results of the 3D reconstructions are shown in Fig. 5.

4 Results

The results of gigapixel panorama image acquisition are summarized below, together with key aspects of the 3D point cloud model.

As shown in Fig. 6, a single panoramic image composed of 1.8 gigapixels captures a great detail of geological information, including discontinuity details and areas of talus deposition.

The final dense 3D point cloud generated from the gigapixel images consists of 10 million points. The point coordinates have been computed from MVS with a maximum baseline of 35 m. According to a theoretical analysis, this leads to a standard deviation of the measured depth of 15 cm for a distance of 600 m. Figure 7 shows the 3D point cloud in RGB and scalar fields. The model is an accurate representation of the quarry, rather than a series of qualitative representations obtained with the original gigapixel panoramic imagery. The bench surfaces, being horizontal, were largely outside of the camera's field of view (line of sight) and are thus only sparsely represented.
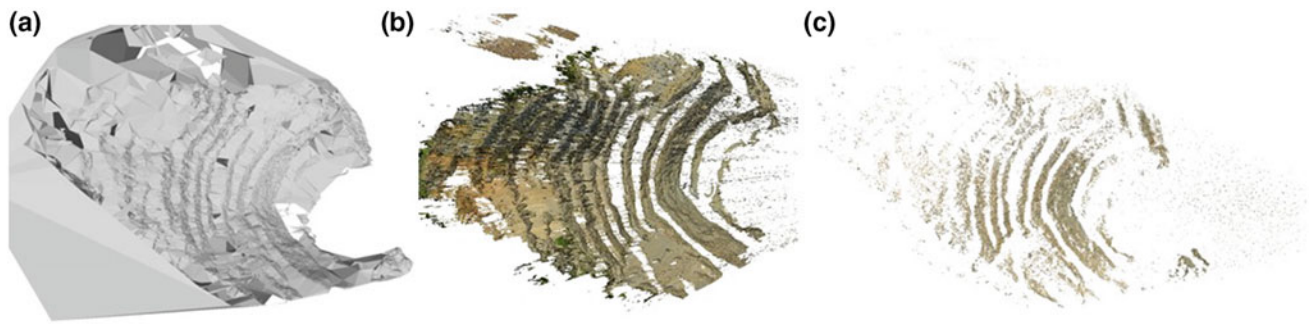
Fig. 5 Visualization of the 3D reconstruction results: **a** meshed point cloud; **b** dense 3D point cloud from MVS; and **c** sparse 3D point cloud from SfM
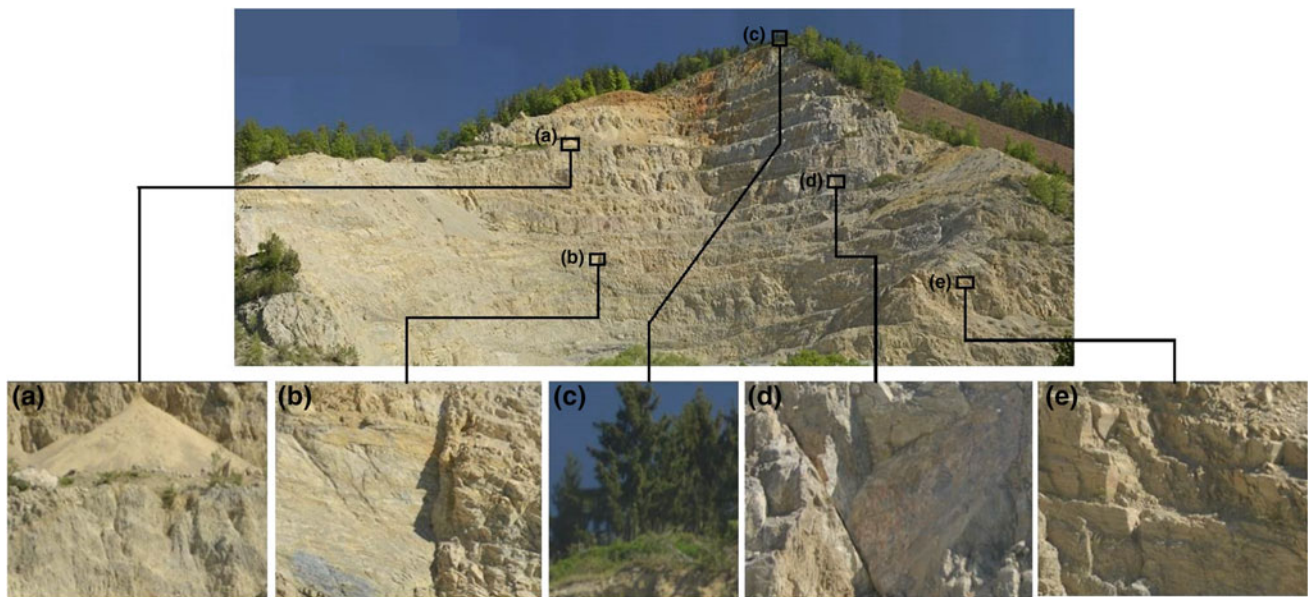
Fig. 6 Panoramic image and zoomed-in images of the quarry: **a** talus deposition; **b** planar joint surfaces; **c** soil overburden and vegetation; **d** block mould of a wedge failure; and **e** bedding planes

Fig. 7 3D point cloud model of the quarry (left: RGB, right: scalar fields of dip angle)
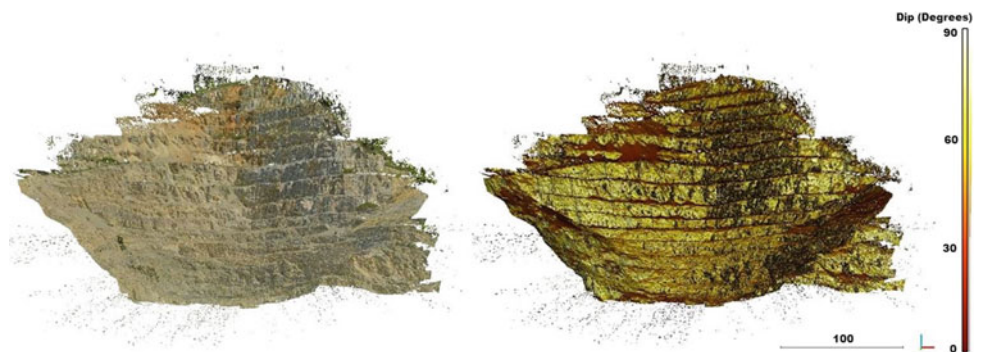
5 Model Verification

In order to verify model accuracy, orientations of rock discontinuities extracted directly from the point cloud were compared to field-based compass measurements, and model dimensions were compared to known physical dimensions.

5.1 Rock Discontinuity Orientations

Figure 8 shows all automatically detected and measured discontinuities within a selected area of the quarry wall. The automated detection was performed using the *Facets* plugin for the open source point cloud processing software *CloudCompare* (http://danielgm.net/cc). *Facets* is intended for fully automatic structural data extraction (Dewez et al. 2016), and operates by dividing the point cloud into clusters of adjacent points and implementing a least square plane fitting algorithm. Following user defined criteria of co-planarity, the clusters are reassembled in a three-step process: (1) elementary facets corresponding to small fragments of planes are computed; (2) elementary planes are then re-clustered into encompassing planes; and (3) parallel planes are merged into plane families. The end result is a number of polygons that are color coded according to their orientation. As depicted in Fig. 8, the main discontinuity sets include: two sets of near-vertical joints striking to the north and west (J1 and J2), a near-horizontal joint set (B).

Figure 9 shows the characteristics of bedding joints (B) and the two sets of near-vertical joints (J1 and J2).

Figure 10 shows the comparison of 90 joint orientations obtained with a compass in the field, and 6120 measurements automatically extracted from the point cloud. Although the hand measurements correlate in general to the results from the 3D model, the number of hand measurements is not sufficient to discriminate individual joint set clusters.

5.2 Quarry Dimensions

The dimensions (lengths and angles) of physical features appearing in the quarry model were compared to the current surveyed plan map and cross sections (Steinbruch Harrer & Harrer Gesellschaft m.b.H. & Co. KG. 2014, 2016). As test dimensions, the width, height and slope angle of 7 uppermost benches were determined on the basis of relevant survey plans, then compared to measurements made directly in the model using the software VRMesh V9.4 (https://www.vrmesh.com).

The overall plan and profile of the quarry is shown in Fig. 11, along with the dimensions measured for comparison. As indicated in Table 3, model dimensions are in excellent agreement with actual physical dimensions.

6 Discussion and Conclusions

Photographic data sets based on gigapixel panoramic imagery are challenging for fully automatic 3D image processing. One of the main difficulties relates to the typical small triangulation angles between instrument setups. For typical applications, the images are acquired at a very high range (several hundred meters) and the target field of view may
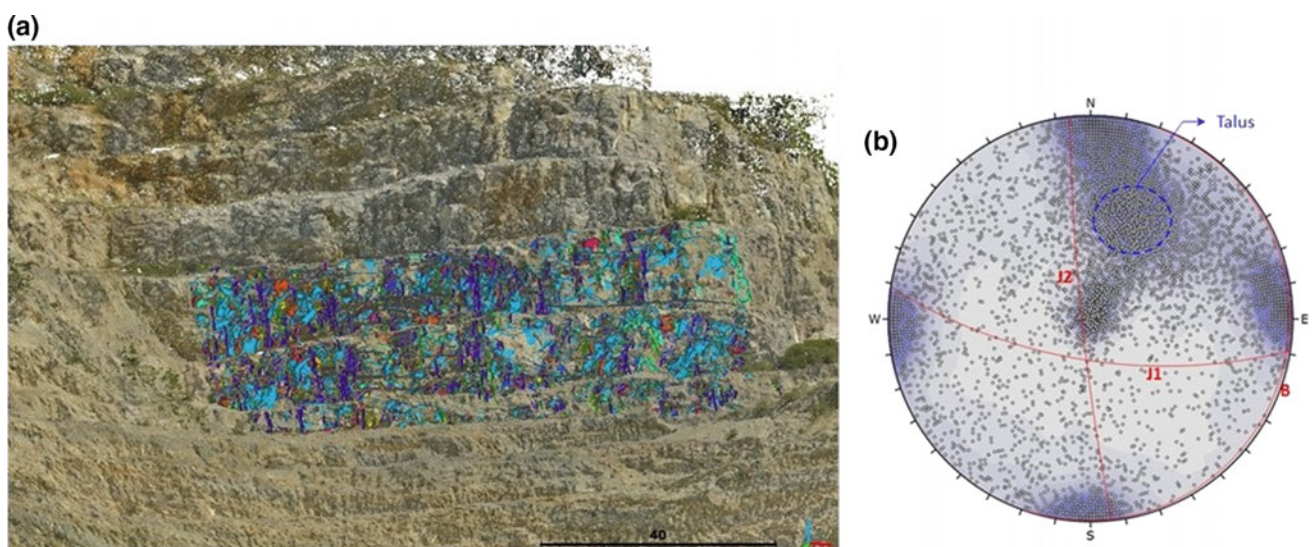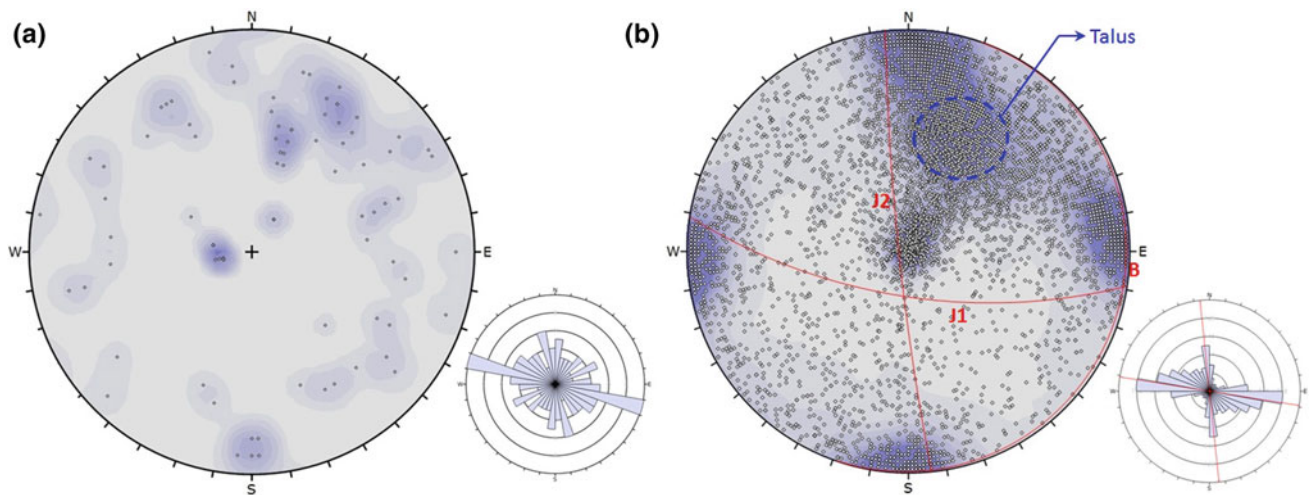

Fig. 8 **a** Automated discontinuity measurements (CloudCompare Facets plugin), **b** lower hemispherical stereonet plot of discontinuity poles (Dips 7.0 using discontinuities extracted from CloudCompare)
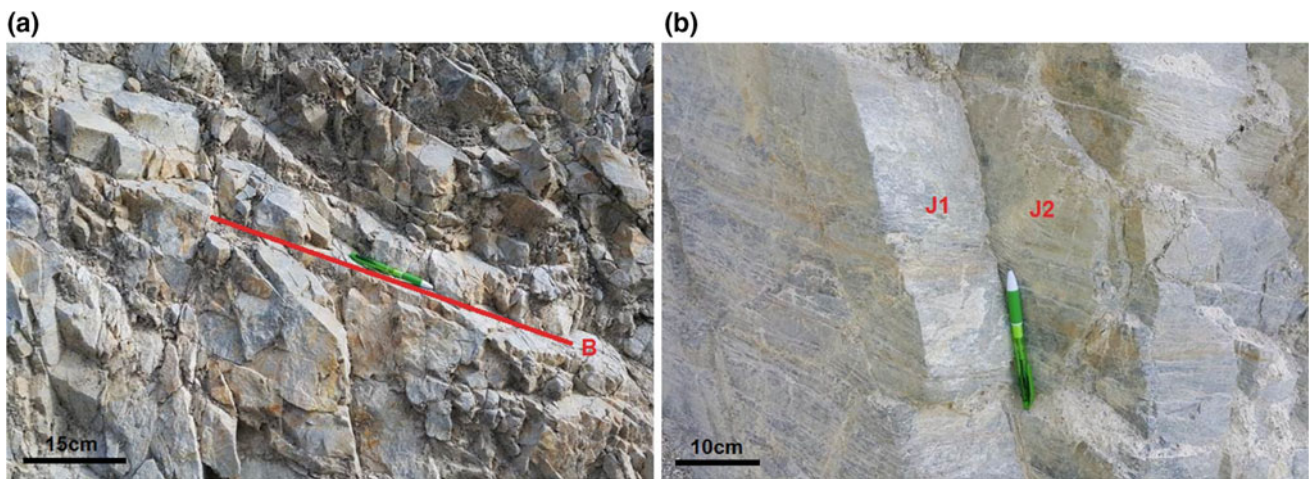
**Fig. 9** Discontinuities on site: **a** bedding joint (B); **b** two joint sets (J1, J2)

Fig. 10 Stereonet and Rosette plots of discontinuity measured by: **a** geological compass; and **b** automatically extracted from 3D point cloud. Two sets of near-vertical joints striking north and west, and a near-horizontal joint correlate in the result of (**a**) and (**b**)

only be a few degrees. For most practical applications, these conditions make it difficult to establish instrument locations that provide favorable triangulation angles (the accuracy of the 3D reconstruction depends strongly on the triangulation angle). Images for the data set presented herein were acquired at a range of over 600 m from positions only 35 m apart.

Initial studies performed at a dolomite quarry located near Graz, Austria, show that a dense and accurate 3D point cloud (without appreciable noise and artifacts) can be obtained at a range of 630 m using the SfM–MVS approach. Rock discontinuity orientations measured directly from the model are in good agreement with traditional compass measurements, and model dimensions (lengths and slope angles) are in

excellent agreement with actual physical quantities. These initial results indicate the developed methodology can greatly assist engineering geologists making quantitative measurements and analyses of outcrops and exposures that are inaccessible or at such great distances so as to preclude traditional photogrammetric techniques.

A significant implication of this research is that multiple gigapixel panoramic photographs can be successfully handled with automated 3D image reconstruction techniques. To better define the limits of application, ongoing research is focused on evaluating range effects, in particular the maximum range (and associated parameters) to which this methodology can be reasonably applied in the context of engineering geological investigations.
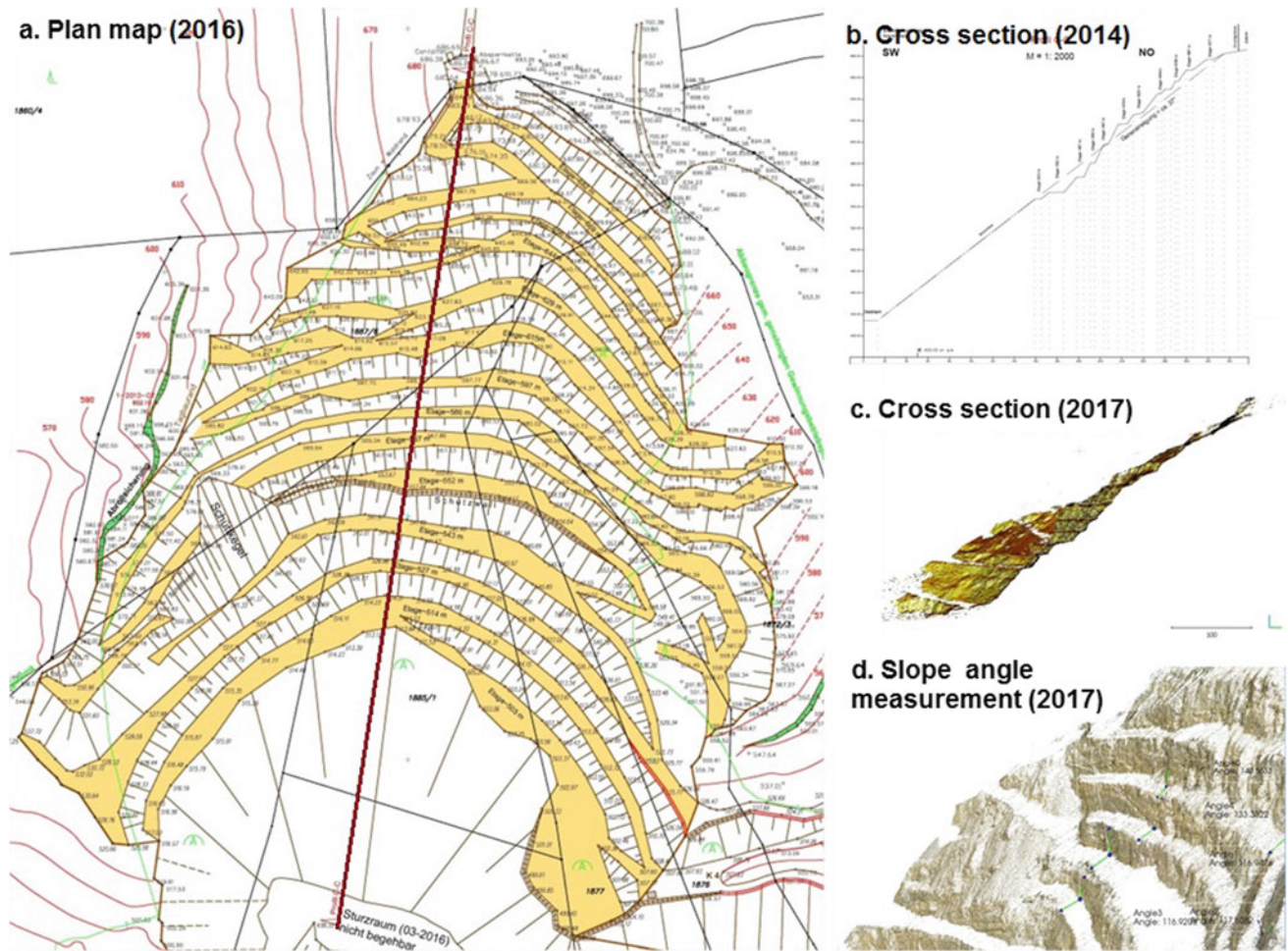
Fig. 11 a Quarry plan map and slope profile line (Tagbaustand, Steinbruch Harrer & Harrer Gesellschaft m.b.H. & Co. KG. 2016); **b** surveyed cross section from 2014 (Tagbaustand, Steinbruch Harrer & Harrer Gesellschaft m.b.H. & Co. KG. 2014); **c** modeled cross section, 2017 in CloudCompare; and **d** location of dimensional and angular measurement in VRmesh

Table 3 Comparison of physical dimensions to model dimensions

Bench no.	Physical dimensions			Model dimensions		
	Width (m)	Height (m)	Slope angle (°)	Width (m)	Height (m)	Slope angle (°)
1	5.8	13	40	5.7	13	40
2	3.1	12	65	3.2	11	65
3	6.2	15	58	6.9	14	60
4	9.4	14	58	9.8	14	60
5	8.6	18	65	8.5	18	65
6	4.3	17	64	4.7	17	60
7	4.3	13	67	4.6	13	60

References

CloudCompare software: https://danielgm.net/cc

Colmap software: https://github.com/colmap/colmap

Daftry, S., Maurer, M., Wendel, A., Bischof, H.: Flexible and user-centric camera calibration using planar fiducial markers. In: British Machine Vision Conference (BMVC) (2013)

Dewez, T.B., Girardeau-Montaut, D., Allanic, C., Rohmer, J.: Facets: a cloudcompare plugin to extract geological planes from unstructured 3D point clouds. Int. Arch. Photogramm. Remote Sens. Spat. Inf. Sci. **XLI-B5**, 799–804, https://doi.org/10.5194/isprsarchives-xli-b5-799-2016 (2016)

Dips software: https://www.rocscience.com/rocscience/products/dips

Geologische Bundesanstalt: Multithematische Geologische Karte von Österreich 1:1.000.000 (2017)

Google Earth: https://www.google.com/earth, Last accessed 2017/09/04

Rumpler, M., Tscharf, A., Mostegel, C., Daftry, S., Hoppe, C., Prettenthaler, R., Fraundorfer, F., Mayer, G., Bischof, H.: Evaluations on multi-scale camera networks for precise and geo-accurate reconstructions from aerial and terrestrial images with user guidance. In: Journal of Computer Vision and Image Understanding (CVIU), Special Issue on Large-Scale 3D Modeling of Urban Indoor or Outdoor Scenes from Images and Range Scans (2016)

Schönberger, J.L., Zheng, E., Pollefeys, M., Frahm, J.M.: Pixelwise view selection for unstructured multi-view stereo. In Proceedings European Conference on Computer Vision (ECCV) (2016)

Steinbruch Harrer & Harrer Gesellschaft m.b.H. & Co. KG: Tagbaustand 1:1000 (2014)

Steinbruch Harrer & Harrer Gesellschaft m.b.H. & Co. KG: Tagbaustand 1:1000 (2016)

VRMesh software: https://vrmesh.com

Study of Gully Erosion in South Minas Gerais (Brazil) Using Fractal and Multifractal Analysis

Ligia de Freitas Sampaio, Silvio Crestana, and Valéria Guimarães Silvestre Rodrigues

Abstract

Tropical countries experience intense rainfall; this natural process, associated with land use, influences or accelerates soil erosion due to changes in soil properties and water flow dynamics. Gullies are an expression of soil erosion caused by water and are considered an environmental problem, since their extents and depths reach hundreds of meters, and areas of gullies frequently become unusable. Gullies are present in most states of Brazil. The case study of this paper focuses on the watershed between the Grande River and Das Mortes River (in Nazareno, southern region of Minas Gerais). There are 96 gullies in this municipality in areas where the soil has low fertility and high erodibility; the origins of these gullies are linked to vegetation removal and gold mining in the 17th century, potentialized by non-conservationist farming practices and by runoff intensification due to inadequate road drainage systems. The studied Charuteiro stream watershed has 13 gullies within a 6.55 km^2 area. Therefore, we used a box-counting method with two software packages to analyze the fractality and multifractality of these gullies. The vegetated gullies presented similar values for fractal dimension, while those with bare soil presented more variability. The multifractal spectrum for each gully in the study area was obtained; these soil erosion features do not show high complexity and heterogeneity. This analysis of watersheds with intense gully erosion is a novel and promising approach, enabling mathematical modeling and recovery projects to more closely reflect reality.

1 Introduction

Fractal geometry is applied to investigate irregular or complex patterns in nature; these forms have a fragmented characteristic that could not be described adequately by Euclidean geometry (Mandelbrot 1982). Measurement of the fractal dimension is usually made by iterations of a function or law whose behavior is related to the peculiarities of the fractal image, and the fractal dimension is not an integer (Feder 1988).

The common steps used in algorithms to analyze the fractal dimension are quantifying the forms, such as lines, circles or boxes, that could cover the fractal image in different stages of measurement; then, plotting the value of this quantification versus the stages in a log-log plot and fitting the data with a least-squares regression line. The fractal dimension could be estimated by the slope of the regression line (Lopes and Betrouni 2009).

Box counting is one of the most used methods for measuring the fractal dimension. Fractal objects present a heterogeneous characteristic in reality and may have singularities, which could form fractal subsets. In this case, the analysis will relate to a variety of fractal sets and subsets, or multifractals (Feder 1988; Vicsek et al. 1992; Wang et al. 2012). The multifractals can be used to analyze the spatial patterns and the heterogeneity of those patterns (Wang et al. 2012), and the dimensions are studied as the maximum of a convex function spectrum (Lopes and Betrouni 2009), not only counting the number of boxes with pixels but using the pixel density within each box (Embrapa 2008). Multifractal spectra of environmental phenomena can be asymmetric (Szczepaniak and Macek 2008).

There is a variety of software that performs fractal and multifractal analysis using the box-counting method, and

L. de Freitas Sampaio (✉) · V. G. S. Rodrigues
São Carlos School of Engineering, University of São Paulo, São Carlos, 13566-590, Brazil
e-mail: ligia.sampaio@usp.br

V. G. S. Rodrigues
e-mail: valguima@usp.br

S. Crestana
Brazilian Agricultural Research Corporation—Embrapa, São Carlos, 13560-970, Brazil

some are free and open source. In general, this type of analysis requires an earlier image processing step, such as binarization, and is commonly used in medical images (Lopes and Betrouni 2009).

Concerning soil erosion by water, some studies focused on fractal and multifractal analysis on soil losses used field plots (Bertol et al. 2017) or satellite image processing to identify soil erosion (Oliveira et al. 2013; Tedesco et al. 2014). There have been efforts to advance erosion geometry studies (Casalí et al. 2015), but the connection between erosion and fractal geometry still needs to be evaluated.

In this context, using fractal and multifractal analysis, combined with image processing, we assessed soil erosion in a Brazilian watershed. The southern region of Brazil presents many gullies, a complex type of erosion that causes soil and economic losses. Thus, the objective of this research was to study the fractal dimension and multifractal analysis in gullies to evaluate the connection between this approach and physical erosion patterns.

2 Study Area

The study area is the Charuteiro stream watershed, an area of 6.55 km^2, located in southern Minas Gerais State, in Brazil (Nazareno municipality). Even though it is a small watershed, the presence of gully erosion is very expressive: 5.8% of the total area is lost to this process. The land in the study area is used mostly for pasture, but there are coffee crops and other cultivations in smaller proportions; consequently, this area is considered a predominantly rural area. (Ferreira 2008; Ferreira et al. 2010) observed that erosion problems were intensified by inadequate pasture management, such as overgrazing and fire, which also modified soil properties.

This region is on the São Francisco Craton, characterized by the presence of greenstone belts (Nazareno and Rio das Mortes Belts) (Toledo 2002; Nunes 2007). The main rock types in the watershed are tonalite and trondhjemite, of the Paleoproterozoic, and banded orthogneiss, of the Archaean and/or Paleoproterozoic (CODEMIG 2013).

The predominant soil is red-yellow Oxisol, which originates from granite-gneiss weathering. In this region, it is observed that pasture is principally on this type of soil, which has a clay texture and high aluminum oxide content (Silva 1990; Ferreira 2005).

The climate is classified as Cwa in the Köppen classification (rainy summers and dry winters) (Dantas et al. 2007). The natural vegetation, before applying land uses, was rainforest and cerrado (Brazilian Savana) (Embrapa 2006).

3 Materials and Methods

The 1975 topographic map SF-23-X-C-I-2, of the Brazilian Institute of Geography and Statistics was georeferenced, and the study area data were digitized using ArcMAP, from ArcGIS 9.3 (from Environmental Systems Research Institute-ESRI). Then, after the creation of a grid over the location of the Charuteiro watershed, it was possible to save the satellite images of the area from Google Earth Pro 7.1.5.1557; these images were also georeferenced in Arc-MAP for the identification of the gully boundaries (Fig. 1).

The box-counting method was used to assess the fractal dimensions of the gullies (both overall and individually) of the Charuteiro watershed. The image of the gully erosion area was binarized using the free software ImageJ 1.51j8, from the National Institutes of Health (Rasband and ImageJ 2016). With the binarized images, a region of interest was selected, as a bounding box of the images, and grids with different sizes were chosen to cover the gully images.

Fixing the size of the boxes, r, for each grid, the number of boxes used to cover the binarized image, N(r), was counted. Additionally, the fractal dimension, D_B, was estimated using Eq. 1 (Russell et al. 1980; Liebovitch and Toth 1989):

$$D_B = \lim_{r \to 0} \frac{\log N(r)}{\log\left(r^{-1}\right)} \tag{1}$$

Then, the ImageJ plugin FracLac (Karperien 2013) was used with the additional following inputs: 4 different grid calibers, 12 different positions for the grid to evaluate, minimum pixel number of 0 and maximum coverage of 45% of the images. No filters were used, and the fractal dimension analyzed was D_B (box-counting dimension).

The multifractal analysis was conducted using the software Multifractal Analysis and Scaling System version 3.0 (MASS), provided by Embrapa (Brazilian Agricultural Research Corporation) (MASS 2017). The input was a binarized image, made in ImageJ ("txt" file), of all the gullies together with 4000 × 4000 pixels, and different parameter adjustments were made to obtain the results.

The degree of multifractality and the degree of asymmetry were determined by Eqs. (2) and (3), respectively, as (Szczepaniak and Macek 2008) showed in their research:
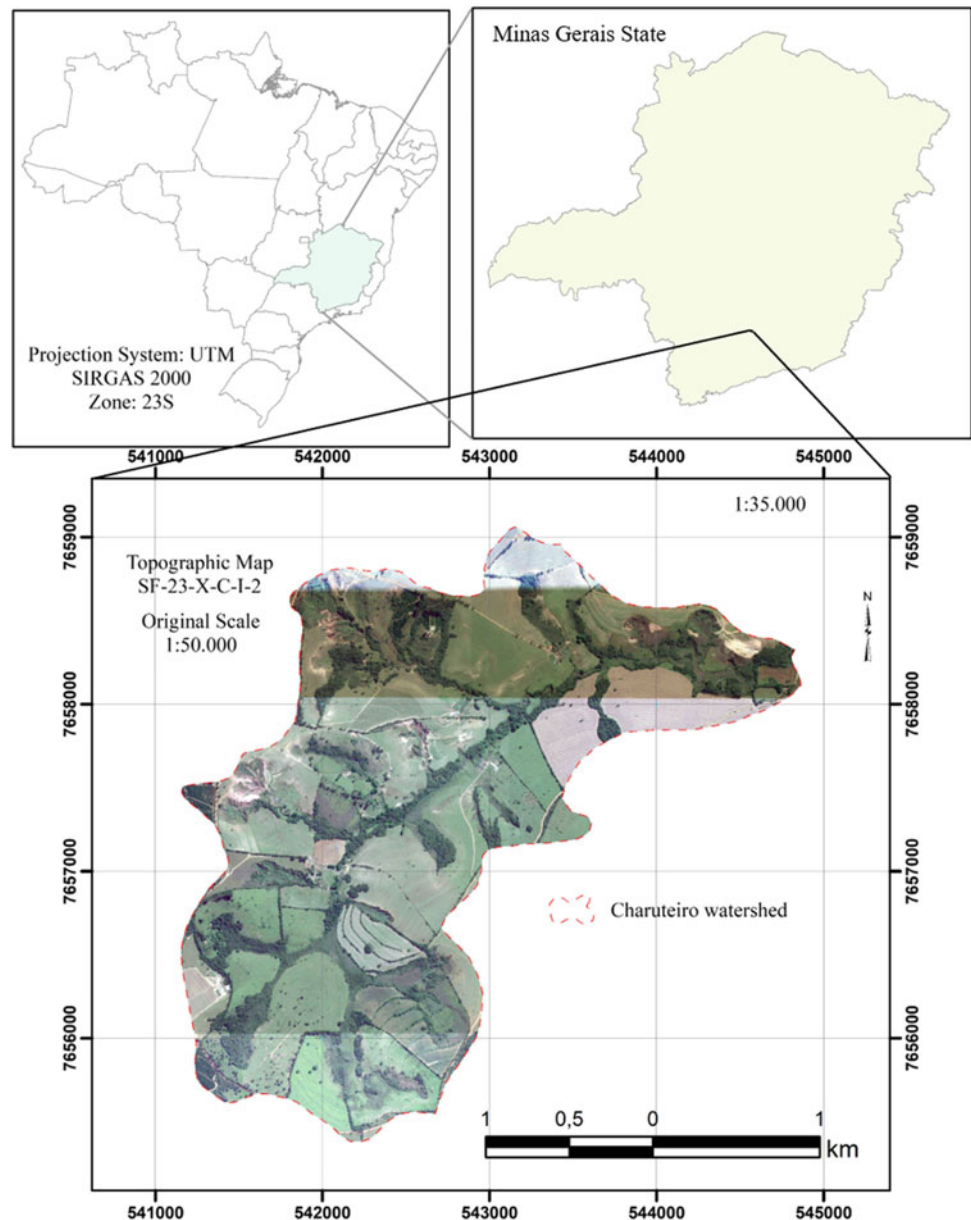
$$\Delta \equiv \alpha_{max} - \alpha_{min} \tag{2}$$

$$A = \frac{\alpha_0 - \alpha_{min}}{\alpha_{max} - \alpha_0} \tag{3}$$

The degree of multifractality is the difference between maximum and minimum Lipschitz-Hölder exponent of

Fig. 1 Charuteiro stream watershed, Southern Minas Gerais State

multifractal spectra, α; the degree of asymmetry is the ratio between the distance of α_0 from α_{max} and α_0 from α_{min}, being α_0 the exponent when the order of the probability moment, q, is zero. These parameters were obtained using MASS.

4 Results and Discussion

4.1 Fractal Dimension

The map of the Charuteiro watershed with delimited gullies is shown in Fig. 2. Numbers 1–7 are used to classify more vegetated gullies, and numbers 8–13 refer to gullies with

bare soil. The fractal dimensions for each gully are presented in Table 1 with its respective standard deviation.

The results from the FracLac calculation show a variation in the fractal dimensions (1.68 to 1.86). Connecting the results back to the images, it is verified that the vegetated gullies (1 to 7) show more homogeneity between the values of fractal dimension than that of gullies with more bare soil (8 to 13).

Gullies 7 and 8 present lower values and a similar "curve" form; gullies 1 and 13 are wider and have similar patterns of evolution stage and similar fractal dimension values. However, the similarity between form and dimensions do not correspond in the observations of gullies number 2 and 6;

Fig. 2 Gullies of the Charuteiro watershed, 2016 (Google Earth Pro)
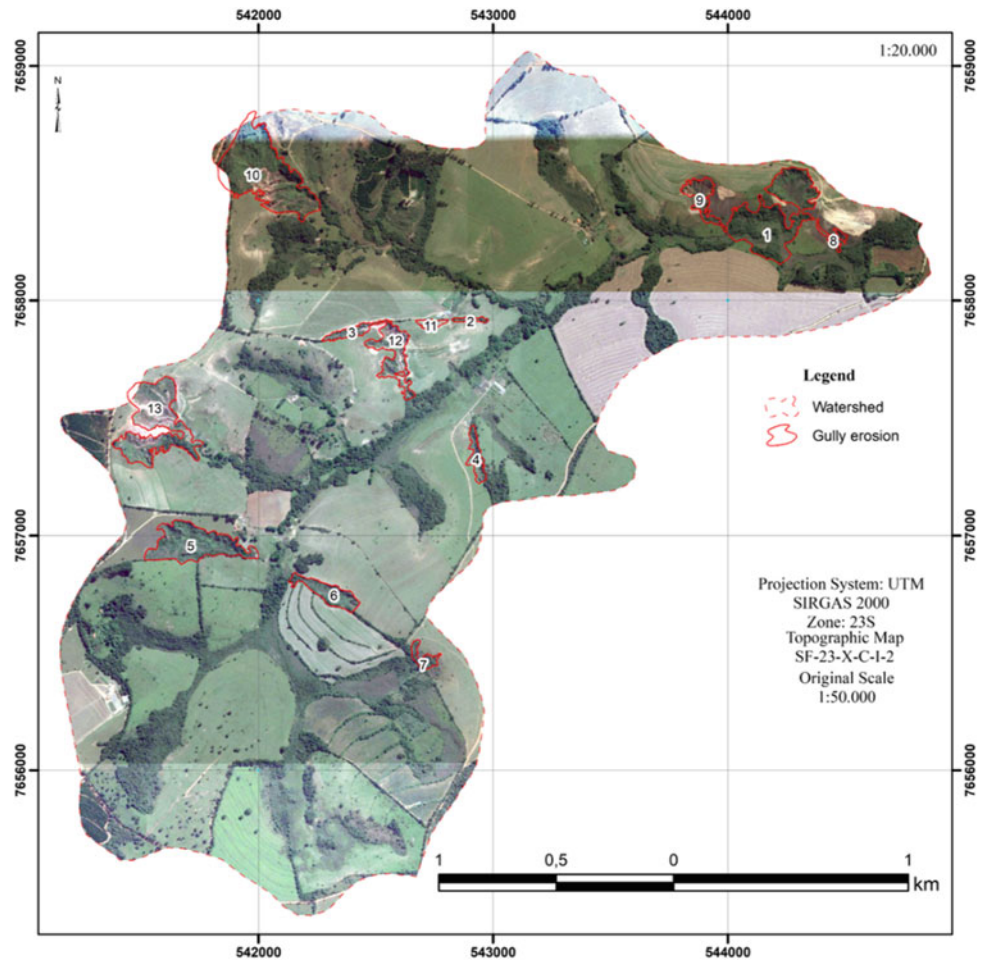
Table 1 Fractal dimension and standard deviation results for the 13 gullies of the Charuteiro watershed

Gully	D_B	Standard deviation
1	1.83	0.01
2	1.8	0.02
3	1.76	0.01
4	1.8	0.01
5	1.86	0.01
6	1.8	0.02
7	1.74	0.02
8	1.68	0.02
9	1.76	0.02
10	1.83	0.01
11	1.82	0.03
12	1.79	0.01
13	1.81	0.01
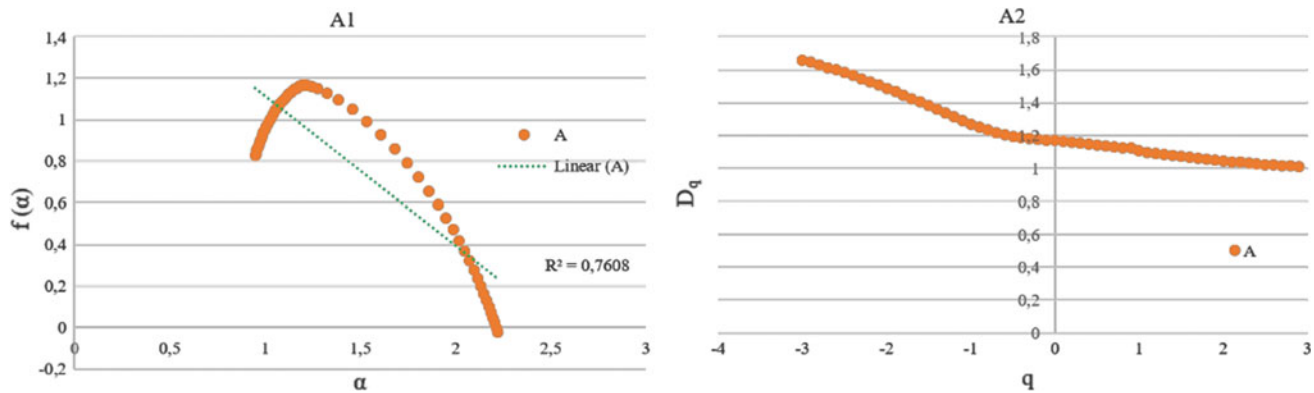
Fig. 3 Multifractal spectra for −3 < q < 3 and 4000-pixel scale—Charuteiro watershed gullies

even with the same fractal dimension, they have distinct characteristics.

Thus, more studies in other watersheds of the region should be done to compare these results and to find a statistical result of fractal dimension and gully erosion processes in the region.

4.2 Multifractal Analysis

The multifractal spectra for the 4000-pixel scale are shown in Fig. 3.

Figure 3 shows the total range analysis by MASS. The convex spectrum showed in A1 with the plot of the singularity spectra, $f(\alpha)$, and the Lipschitz-Hölder exponent, α, and the monotonous decreasing curve in A2 (generalized dimensions D_q as a function on the probability moment, q) confirmed the multifractal pattern and showed high R^2 values, but the convex function was not symmetric.

The degree of multifractality (Δ) and asymmetry (A) for the multifractal analysis of A1 is 1.27 and 0.25, respectively. The high degrees of multifractality can be associated with a complex and heterogeneous pattern, as studied by (Hu and Wang 2009). When compared to the results of (Szczepaniak and Macek 2008) of 1.75 and 1.37 for Δ and A, respectively, the degrees from A1 are lower; thus, we determine that these gullies do not present high complexity and heterogeneity.

5 Conclusion

Gully erosion in the Charuteiro watershed presented fractal dimensions and multifractal behavior. The fractal analysis showed that more of the vegetated gullies have homogeneous dimensions, and that the bare soil gullies presented heterogeneous values. Moreover, the multifractal analysis was confirmed, meaning that conventional geometry used in gully management might underestimate the real dimensions of the problem, and that the use of different scales is very important in gully studies. These considerations may help environmental managers to evaluate recovery measures for gullies.

We recommend further investigation of other watersheds and at other scales to further verify these conclusions. Additionally, it is important to use methodologies other than box counting to complement this evaluation.

References

Bertol, I., Schick, J., Bandeira, D.H., Paz-Ferreiro, J., Vidal Vázquez, E.: Multifractal and joint multifractal analysis of water and soil losses from erosion plots: a case study under subtropical conditions in Santa Catarina highlands, Brazil. Geoderma **287**, 116–125 (2017). https://doi.org/10.1016/j.geoderma.2016.08.008

Casalí, J., Giménez, R., Campo-Bescós, M.A.: Gully geometry: what are we measuring? SOIL **1**, 509–513 (2015). https://doi.org/10.5194/soil-1-509-2015

CODEMIG (Companhia De Desenvolvimento Econômico De Minas Gerais): Carta Geológica. Folha SF.23-X-C-I LAVRAS. Escala 1:100:000. Versão SIG. Projeto Sul de Minas – Etapa I. CODEMIG; Governo de Minas; Universidade Federal do Rio de Janeiro; Universidade Federal de Minas Gerais; Centro de Pesquisa Manoel Teixeira da Costa; Centro de Sensoriamento Remoto (2013). www.portalgeologia.com.br, Last accessed 2017/01/10

Dantas, A.A.A., Carvalho, L.G., Ferreira, E.: Classificação e tendências climáticas em Lavras, MG. Ciênc. agrotec., Lavras, **31**(6), 1862–1866 (2007)

Embrapa (Empresa Brasileira de Pesquisa Agropecuária - Brazilian Agricultural Research Corporation): Levantamento de reconhecimento de média intensidade dos solos da Zona Campos das Vertentes – MG. Boletim de Pesquisa e Desenvolvimento 96. Embrapa Solos, Rio de Janeiro, Brazil, p. 326 (2006)

Embrapa (Empresa Brasileira de Pesquisa Agropecuária—Brazilian Agricultural Research Corporation): Aplicação da Técnica

Multifractal para Caracterização de Manejo do Solo. Documentos, **41**. ISSN: 1518-7179 (2008)

Feder, J.: Fractals (Physics of solids and liquids). Plenum Press, New York (1988)

Ferreira, V.M.: Voçorocas no município de Nazareno, MG: origem, uso da terra e atributos do solo. Masters Dissertation, Federal University of Lavras, Brazil, p. 84 (2005)

Ferreira, R.R.M.: Qualidade física de cambissolos sobre dois materiais de origem com pastagens extensivas. Doctoral Thesis, State University of Londrina, Brazil, p. 106 (2008)

Ferreira, R.R.M., Tavares Filho, J., Ferreira, V.M., Ralisch, R.: Estabilidade física de solo sob diferentes manejos de pastagem extensiva em cambissolo. Semina: Ciências Agrárias, Londrina, **31** (3), 531–538 (2010)

Hu, M.G., Wang, J.F.: Multifractal analysis of global total column ozone image. In: AIP Conference Proceedings 1168, 390 (2009). http://doi.org/10.1063/1.3241477

Karperien, A.: FracLac for ImageJ. Homepage: http://rsb.info.nih.gov/ij/plugins/fraclac/FLHelp/Introduction.htm, (2013). Last accessed 2017/09/04

Liebovitch, L.S., Toth, T.A.: Fast algorithm to determine fractal dimensions by box counting. Phys. Lett. A, **141**(8, 9), 386–390 (1989). http://dx.doi.org/10.1016/0375-9601(89)90854-2

Lopes, R., Betrouni, N.: Fractal and multifractal analysis: a review. Med. Image Anal. **13**, 634–649 (2009). https://doi.org/10.1016/j.media.2009.05.003

Mandelbrot, B.B.: The fractal geometry of nature. Updated and augmented. W.H Freeman and Company, New York (1982)

MASS—Multifractal Analysis and Scaling System 3.0.: Software developed by Centro Internacional de La Papa (CIP), with partial support by Directoraat Generaal voor Internationale Samenwerking (DGIS) of Netherlands (Ecoregional Fund). Provided by Embrapa (Brazilian Agricultural Research Corporation) in 2017

Nunes, L.C.: Geocronologia, geoquímica isotópica e litoquímica do plutonismo diorítico-granítico entre Lavras e Conselheiro Lafaiete: implicações para a evolução paleoproterozóica da parte central do Cinturão Mineiro. Masters Dissertation, Instituto de Geociências, University of São Paulo, Brazil, p. 109 (2007)

Oliveira, B.E.N., Matricardi, E.A.T., Chaves, H.M.L., Bias, E.S.: Identificação dos processos erosivos lineares no Distrito Federal através de fotografias aéreas e geoprocessamento. São Paulo, UNESP, Geociências **32**(1), 152–165 (2013)

Rasband, W.S., ImageJ, U.S.: National Institutes of Health, Bethesda, Maryland, USA. Homepage, https://imagej.nih.gov/ij/ (2016). Last accessed 2017/08/14

Russell, D.A., Hanson, J.D., Ott, E.: Dimension of strange attractors. Phys. Rev. Lett. **45**(14), 1175–1178 (1980). https://doi.org/10.1103/PhysRevLett.45.1175

Silva, A.C.: Relação entre voçorocas e solos na região de Lavras (MG). Masters Dissertation, Escola Superior de Agricultura de Lavras (currently Federal University of Lavras), Brazil, p. 125 (1990)

Szczepaniak, A., Macek, W.M.: Asymmetric multifractal model for solar wind intermitente turbulence. Nonlin. Process. Geophys. **15**, 615–620 (2008). https://doi.org/10.5194/npg-15-615-2008

Tedesco, A., Antunes, A.F.B., Oliani, L.O.: Gully erosion detection by hierarchical classification and tree decision. Bol. Ciênc. Geod. **20** (4), 1005–1026 (2014). https://doi.org/10.1590/S1982-21702014000400055

Toledo, C.L.B.: Evolução geológica das rochas máficas e ultramáficas no Greenstone Belt Barbacena, região de Nazareno, MG. Doctoral Thesis, Instituto de Geociências, State University of Campinas, Brazil, p. 274 (2002)

Vicsek, T.: Fractal growth phenomena, 2nd edn. World Scientific Publishing Co. Pte. Ltd. (1992) http://dx.doi.org/10.1142/1407

Wang, D.L., Yu, Z.G., Anh, V.: Multifractal analysis of complex networks. Chin. Phys. B, **21**(8), 080504(1–11) (2012). https://doi.org/10.1088/1674-1056/21/8/080504

Suggested Enhancements to the Geologic Model Complexity Rating System

Jeffrey Keaton and Rosalind Munro

Abstract

The suggested Geologic Model Complexity Rating System, introduced in 2014, was developed considering the 1993 Oregon rockfall hazard rating system with four rating levels. Five of the nine Geologic Model Complexity Rating System components pertained to geologic complexity: four regional components (genetic, structural/deformation, alteration/dissolution, and weathering/erosion) and one site-scale component. The other Geologic Model Complexity Rating System components were: terrain features, information quality, geologist competency, and level of effort. A pairwise comparison of components for a landslide hazard study, using a multi-factor decision analysis procedure called Analytic Hierarchy Process (AHP), weighted geologist competency highest (20%), followed by genetic complexity and deformation (each 18%) and site-scale complexity and level of effort (each $\sim 11\%$). The other four components had weights from 8 to 3%. The 1–9 scoring for AHP, with 1 indicating that components are equal and 9 indicating one is extremely more important, appeared to be useful for objective comparisons. The AHP matrix configuration lists components in the same order in rows and columns. Regional complexity is now being considered as a single four-element component that depends not only on the basic geology of the site area, but also on the purpose of the geologic evaluation. Thus, the suggested enhancements streamline the Geologic Model Complexity Rating System, reducing it from nine components to six, but also complicates it by considering basic geology and purpose of evaluation as fundamentally important to the geologic model. These enhancements bring the suggested Geologic Model Complexity Rating System into alignment with the Oregon rockfall hazard rating system, which included facility components (i.e., what is at risk) for which the hazard was being rated.

1 Introduction

The objectives of this paper are to describe enhancements to the Geologic Model Complexity Rating System (Keaton 2014) that may be useful in quantifying variability and uncertainty in geologic mapping and introduce a multi-factor decision analysis procedure called Analytic Hierarchy Process (AHP; Saaty 2008). The Geologic Model Complexity Rating System recognized that a geologic map or section is a type of geologic model, which is an artistic representation of one interpretation of geologic features and relationships inferred from limited observations of the distribution of rock types, surficial deposits, and geologic structures often with little or no subsurface data or laboratory test results (Keaton 2013). A geologic model relevant to a proposed project that includes pertinent engineering aspects is an engineering geologic model. Engineering projects, particularly those that employ reliability-based design (RBD), need geologic complexity to be expressed in quantitative terms. Geologists use solid, dashed, dotted, and queried lines on geologic maps and sections to convey confidence in interpretation, but this interpretation confidence is not quantified.

In the United States, general purpose geologic maps produced by or for federal agencies are made to satisfy a wide range of needs, consequently digital geologic maps do not have specified target values for what are called zones of confidence (FGDC 2006). Therefore, the solid, dashed,

J. Keaton (✉) · R. Munro
Wood, Plc, 6001 Rickenbacker Road, Los Angeles, CA 90040, USA
e-mail: jeff.keaton@woodplc.com

R. Munro
e-mail: rosalind.munro@woodplc.com

dotted, and queried lines on geologic maps and sections represent unspecified location error related to map scale, terrain, vegetation, and field methods, and unspecified uncertainty related to competency of the geologist, degree of complexity of the regional and local geology, and time allotted for field mapping.

Engineering geologic maps made by consulting geologists for specific engineering projects address all relevant aspects of the projects, such as excavations, foundations, borrow-material sources, and tunnels. However, it is relatively common for these engineering geologic maps to use traditional geologic symbols and explanations, without descriptions of location errors or references to uncertainty, beyond what is implied by solid, dashed, dotted, and queried lines. It is also relatively common for engineering geologic maps to be made in complex areas where the mapping geologist can support multiple interpretations about the geologic history of the site or area, and even in the distribution of geologic materials between bore holes or test pits. It is essentially unheard of that a consulting or research project will include more than a single geologic or engineering geologic map to indicate uncertainty in interpretation. However, it is common for the interpretation displayed in the geologic map and sections to be defended in the report text with some discussion of alternative hypotheses and why the displayed interpretation is the preferred, therefore, the correct interpretation to be used as the basis for design.

Consulting geotechnical and geological companies in the United States are sensitive to the potential for legal challenges regarding their recommendations, particularly if cost overruns or failures occur during construction or operation. Variability and uncertainty in geologic or geotechnical materials tends to be expressed by disclaimer sentences that are printed on boring logs and cross sections. These disclaimers indicate that the descriptions are valid for the location of the borings at the time the boring was drilled, and that projections between borings shown on sections are illustrative and have not been verified. Variability in geo-materials for RBD projects tends to be connected to the relevant engineering properties, such as lateral earth pressure or bearing capacity, or even limited to the geotechnical parameters, such as unit weight, Atterberg Limits, and undrained shear strength. Uncertainty tends to be dismissed as a consideration separate from variability by being considered to be adequately incorporated as part of global factors of safety, the selection of engineering properties, and the disclaimers on boring logs and cross sections.

Engineering geologists may have an opportunity to quantify some aspects of uncertainty and variability by using the AHP semi-quantitative decision-making approach. This process uses a straightforward, 1-to-9 scoring system based on value, contribution, membership, or preference in a pairwise comparison of factors that are considered relevant

to the issue being considered or items being compared. The pairwise comparison allows systematic evaluation of aspects that are challenging to compare, such as level of effort allocated to a mapping project and alteration of geologic units.

The remaining sections of this paper contain descriptions of the AHP, the Geologic Model Complexity Rating System, and suggested enhancements to the rating system.

2 Analytic Hierarchy Process Overview and Example

Saaty's (2008) description of the AHP uses decisions that involve trade-offs of factors that can include many aspects, some of which are tangible and others intangible. How well each factor serves the decision-maker's objectives is evaluated by considering each factor against the others, one at a time, in a systematic pairwise approach using matrix algebra (Fig. 1) and a straightforward judgement-based 1-to-9 priority scoring system (Table 1) that allow intangibles to be expressed quantitatively in relative terms. The factor pairs are displayed in a square matrix with the same factor order in both rows and columns. The example in Fig. 1 represents three alternative geological interpretations, labeled A, B, and C, for a hypothetical site. It can be seen in Fig. 1 that the weighting factors converge in the second iteration (at the fifth decimal place), considering the initial calculation to be the first iteration, which is simply the sum of each row divided by the total sum of all cells in the matrix. Subsequent iterations are based on the square of the previous matrix. The matrix calculations in Fig. 1 were done with Microsoft Excel® with the Analysis ToolPak enabled to allow matrix multiplication.

The example in Fig. 1 represents three alternative geologic interpretations of a hypothetical site. Presumably, the interpretations would affect some characteristic of the site that controls an engineering decision for a RBD project. The weighting factors for the three alternatives are "crisp" even though the geologist's considerations of factors may be "fuzzy". Had geologic reasoning supported elimination of Alternative C from consideration, Alternatives A and B would have weights of 0.833 (A) and 0.167 (B).

Saaty (2008) points out that the process of paired comparisons has broad uses for making decisions from four different perspectives: the benefits (B) that the decision brings, the opportunities (O) it creates, the costs (C) that it incurs, and the risks (R) that it might have to face. Saaty refers to these merits considered together as BOCR and compares them to a similar use in strategic planning known as SWOT (strengths, weaknesses, opportunities and threats), which may be more familiar than BOCR. The alternatives must be ranked for each of the four merits, which then may

Geologic Interpretation	Column A	Column B	Column C		Row sum	Initial weight	Second iteration	Third iteration	Fourth iteration
Row A	1	5	7	Input	13	0.604	0.725	0.725	0.725
Row B	1/5	1	6	Input	7 1/5	0.335	0.220	0.220	0.220
Row C	1/7	1/6	1	Fixed	1 1/3	0.061	0.054	0.054	0.054
	Calculated		Fixed	sum =	21 1/2	1.000	1.000	1.000	1.000

Fig. 1 Example AHP calculation for three geologic interpretations (A, B, C) in rows and columns. Left half is the square matrix with scores indexed to Table 1; right half is columns showing row sum, initial weight, and iterative weights, with column sums in bottom row. This figure is an extraction from a Microsoft Excel® worksheet in which numbers in the matrix are displayed as rational fractions for easy checking by inspection. The matrix was setup for input in cells above the diagonal with reciprocal values calculated in cells below the diagonal. Iterations were performed by successive squaring of the matrix

Table 1 Scale of importance of value, contribution, membership, preference, or degree of belief in row-column pairwise comparison. Based on Saaty (2008, Table 1)

Score	Basic definition	Explanation
0	Not applicable	Pairwise comparison does not apply
1	Equal importance	Row and column pair are equal
2	Slight	Row has slightly higher value than column
3	Moderate importance	Row has moderately higher value than column
4	Moderate to strong	–
5	Strong importance	Row has strongly higher value than column
6	Strong to very strong	–
7	Very strong importance	Row has very strongly higher value than column
8	Very strong to extreme	–
9	Extreme importance	Row has extremely higher value than column
Reciprocal	Value in the cell corresponding to reversed row-column pair	Column has some value compared to row for non-zero value of row; if row score is zero, then corresponding column score is defined as zero

be combined into a single overall ranking by rating the best alternative in each of the BOCR perspectives on strategic criteria that an individual or a project uses to decide whether or not to implement one or the other of the numerous decisions that are being faced. Engineering geologists who can engage in discussions of this type may add substantial value to the projects in which they participate.

3 Geologic Model Complexity Rating System Overview

The Oregon Rockfall Hazard Rating System (Pierson and van Vickle 1993) was recognized by Hoek (1999) for its simple, comprehensive, and quantitative nature, which contained relevant elements of cut slopes and traffic conditions on highways at the cut-slope locations. The rating system uses a four-level, exponential scoring system; 3 points for favorable conditions, 9 points (3^2) for moderately favorable, 27 points (3^3) for moderately unfavorable, and 81 points (3^4) for unfavorable conditions. Keaton (2014) used this framework for a Geologic Model Complexity Rating System consisting of nine factors, of which five are regional or site-specific geology (Fig. 2). The logic of the rating system is embodied in the key words used to describe the condition for each of the criteria. The possible range of scores was used to define a coefficient of variation (COV) in a way that seemed reasonable because low scores indicated favorable conditions. However, the nine components in the rating system all have equal weight, yet some seemed intuitively to be more important than others. It became clear that enhancements to the Rating System were needed (Keaton and Munro 2017).

Fig. 2 Geologic model complexity rating system, rating criteria, and scores. Adapted from Keaton (2014)

Category Component		Rating Criteria and Score			
	Points	**3**	**9**	**27**	**81**
Regional Geologic Complexity — Genetic - deposition or emplacement		Simple, uniform conditions	Generally simple, predictable conditions	Somewhat complex, generally predictable	Highly complex and variable conditions
Epigenetic - structural or deformational		No faulting or folding observed or expected	One episode of faulting and folding expected	Two episodes of faulting and folding expected	Two+ episodes of major faulting and folding expected
Epigenetic - alteration or dissolution		Unlikely because of geologic setting	Possible because of geologic setting	Likely because of geologic setting	Known to exist
Epigenetic - weathering and erosion		Uniform weathering profile; minor erosion	Generally regular weathering profile; some erosion	Irregular weathering profile; moderate erosion	Highly irregular weathering; extensive erosion, buried valleys
Site-scale geologic complexity		Vertically and laterally uniform over project site	Generally regular over project site	Irregular over project site	Highly irregular over project site
Terrain features		Some relief; many good exposures	Some relief; some good exposures	Strong relief; poor exposures	Heavy vegetation; few or very poor exposures
Information quality		Extensive data from multiple sources	Limited data from few sources	Reconnaissance level information only	Existing information only; desktop study
Geologist competency level		Professional Geologist; local field experience	Professional Geologist; non-local field experience	Geology degree or training; some field experience	No geology training or field experience
Allotted time or level of effort		Ample time; well-developed interpretation	Adequate time; thoughtful interpretation	Brief time; thoughtful interpretation	Brief time; rushed interpretation

4 Suggested Enhancements to the Rating System

The recognition that the Geologic Model Complexity Rating System was composed of factors that had different weights led to the idea that the Analytic Hierarchy Process could be used to assign weights to the components. Therefore, we constructed a 9 × 9 matrix of the components and came to consensus on preference scores (Fig. 3) for an application of the rating system on landslide studies. The resulting weights converged within three or four iterations (Table 2; Fig. 4). As we began to consider preference scores, we realized two things: (1) we

needed project context for our selection of preference scores and (2) the Oregon Rockfall Hazard Rating System was developed with a specific context: cut slopes above highways. Both authors of this paper are consulting engineering geologists; we happened to be working on a project that included landslide hazards. Therefore, we chose 'landslide studies' as context for our preference scores. However, the complexity of a geologic model should be independent of the project.

The results of the AHP analysis summarized in Table 2 and Fig. 4 demonstrate the importance of geologist competence with the highest weight (0.20); a good geologist can overcome challenges with other factors, such as information quality and allotted time. Regional genetic and deformation

Landslide Study	Complexity-Genetic	Complexity-Structural	Complexity-Alteration	Complexity-Weathering	Complexity-Site scale	Terrain Features	Information Quality	Geologist Competency	Allotted Time	Explanation of Cells
Complexity-Genetic	1	1	3	3	1	2	3	3	2	Input
Complexity-Structural	1	1	3	3	1	2	3	3	2	Fixed
Complexity-Alteration	1/3	1/3	1	2	1/2	1/3	3	1/2	1/2	Calculated
Complexity-Weathering	1/3	1/3	1/2	1	1/3	1/3	3	1/3	1/2	
Complexity-Site scale	1	1	2	3	1	1	3	1	1	
Terrain Features	1/2	1/2	3	3	1	1	3	1/5	1/4	
Information Quality	1/3	1/3	1/3	1/3	1/3	1/3	1	1/7	1/5	
Geologist Competency	1/3	1/3	2	3	1	5	7	1	7	
Allotted Time	1/2	1/2	2	2	1	4	5	1/7	1	

Fig. 3 AHP matrix of preference scores for components of the Geologic Model Complexity Rating System for application to landslide studies

Table 2 Calculated weights from the AHP matrix in Fig. 3

Landslide study	Row sum	Initial weight	Second iteration	Third iteration	Fourth iteration	Fifth iteration
Complexity—genetic	19.000	0.151	0.179	0.180	0.180	0.180
Complexity—structural	19.000	0.151	0.179	0.180	0.180	0.180
Complexity—alteration	8.500	0.068	0.056	0.058	0.058	0.058
Complexity—weathering	6.667	0.053	0.043	0.046	0.046	0.046
Complexity—site scale	14.000	0.111	0.113	0.118	0.117	0.117
Terrain features	12.450	0.099	0.081	0.082	0.082	0.082
Information quality	3.343	0.027	0.027	0.029	0.029	0.029
Geologist competency	26.667	0.212	0.212	0.199	0.200	0.200
Allotted time	16.143	0.128	0.110	0.108	0.108	0.108
Sum	125.769	1.000	1.000	1.000	1.000	1.000

complexity ranked equal to each other (0.18). Site-scale geologic complexity and level of effort ranked third (0.12) and fourth (0.11). These five components had nearly 80% of the AHP factor weight. The four regional components comprised 46% of the total weight, the three site components had 23% of the weight, and the two field components had 31% of the weight. Geologic complexity seemed to have more weight than warranted, so the four regional factors were combined into a single geologic complexity component in the enhanced rating system (Fig. 5).
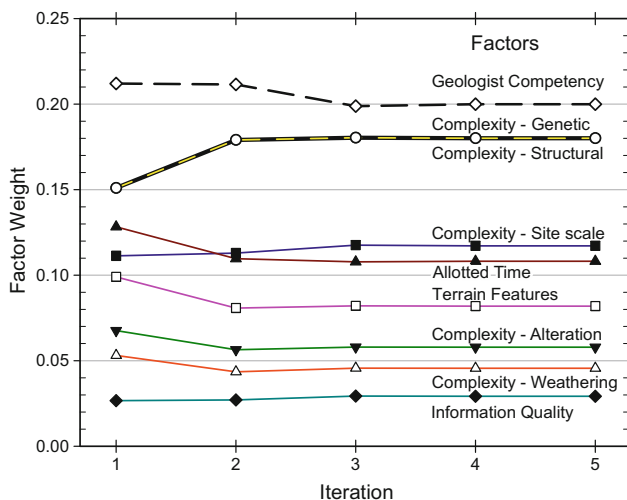
Fig. 4 Graph showing convergence of AHP factor weights listed in Table 2

Fig. 5 Enhanced geologic model complexity rating system

Category or Component		Rating Criteria and Score			
	Points	3	9	27	81
Regional – Genetic and epigenetic geologic complexity; deposition or emplacement; deformation; alteration or dissolution; weathering and erosion		Simple, uniform conditions without faults, folds, alteration, or dissolution; uniform weathering profile; minor erosion	Generally simple, predictable conditions with minor faulting and folding; possible minor alteration or dissolution; regular weathering profile, some erosion	Somewhat complex, generally predictable conditions with moderate faulting or folding; likely alteration or dissolution; irregular weathering, moderate erosion	Highly complex and variable conditions with multiple faulting and folding episodes; alteration or dissolution is known to exist; highly irregular weathering; extensive erosion, buried valleys
Site – Geologic complexity		Vertically and laterally uniform over project site	Generally regular over project site	Irregular over project site	Highly irregular over project site
Site – Terrain features		Some relief; many good exposures	Some relief; some good exposures	Strong relief; poor exposures	Heavy vegetation; few or very poor exposures
Site – Information quality		Extensive data from multiple sources	Limited data from few sources	Reconnaissance level information only	Existing information only; desktop study
Field – Geologist competency level		Professional Geologist; local field experience	Professional Geologist; non-local field experience	Geology degree or training; some field experience	No geology training or field experience
Field – Allotted time or level of effort		Ample time; well-developed interpretation	Adequate time; thoughtful interpretation	Brief time; thoughtful interpretation	Brief time; rushed interpretation

5 Conclusions

The Geologic Model Complexity Rating System seems to have merit for identifying factors that contribute to variability and uncertainty in geologic conditions and interpretations. The initial Rating System treated all nine factors as equal contributors to Rating System result. Five of the factors pertained directly to geology. The suggested enhancement to the Rating System (Fig. 5) groups the Rating System into Regional, Site, and Field components, with weights of 46, 23, and 31%, respectively, using the AHP pairwise factor-analysis tool. The groupings in the enhanced Rating System suggest that regional complexity could be used independently, possibly as an index of geologic complexity that could have broad applicability in land-use planning and civil engineering.

The Oregon Rockfall Hazard Rating System, on which the Geologic Model Complexity Rating System was based, includes the project context, thus, making it a risk rating system, too. Having the Geologic Model Complexity Rating System packaged for different project contexts appears to be logical, too. The example in Fig. 3 was for landslide studies. We have not evaluated different project elements, such as shallow foundations and deep excavations, or project types, such as transportation tunnels and electrical substations, and therefore do not know how the results vary. Additional consideration and experience with the Rating System are needed for this topic. The rockfall hazard rating system was for a specific geologic process and a specific project element.

Our expectation had been for the Geologic Model Complexity Rating System to be a backward-looking tool that enabled uncertainty and variability to be quantified at the analysis and reporting phase of a project based on the geologic conditions at the site, encountered in an investigation, and interpreted by the geologist. The results described in this paper allowed us to realize that the Rating System also could be a forward-looking tool at the proposal phase of a project because a fast-track project in complex geology deserves one or more highly competent geologists with a substantial level of effort. Perhaps the Rating System quantified with the AHP can help make this clear in terms that are tangible, such as reduction of the sizes of foundation elements that may be justified by improved confidence in geologic interpretation that is integrated by the project engineer into a coefficient of variation for ground conditions, and thereby contributes to lower project costs. The two Field group components (Fig. 5) suggest that the Rating System could be used to defend assigning senior geologists to more time in the field on some projects and having a larger level of effort in the office analysis phase because of the geologic complexity of the project site.

Thus, the suggested enhancements (Fig. 5) streamline the initial Geologic Model Complexity Rating System, reducing it from nine components to six, but also complicate it by considering purpose of evaluation as fundamentally important to the geologic model, thus making it an engineering geologic model. These enhancements bring the suggested Geologic Model Complexity Rating System into conceptual alignment with the Oregon rockfall hazard rating system, which included facility components (i.e., what is at risk) for which the hazard was being rated. Possible future enhancements to be evaluated include adding relevant project parameters to the Rating System similar to parameters in the rockfall hazard rating system for driver sight distance.

References

FGDC: FGDC digital cartographic standard for geologic map symbolization. US geological survey geologic data subcommittee, Federal geographic data committee document number FGDC-STD-013-2006, 33 (plus 250 pages of appendices) (2006)

Hoek, E.: Putting numbers to geology—an engineer's viewpoint (Second Glossop Lecture). Q. J. Eng. Geol. **32**, 1–19 (1999)

Keaton, J.: Engineering geology: fundamental input or random variable? In: Withiam, J.L., Phoon, K.K., Hussein, M.H. (eds.) Foundation engineering in the face of uncertainty: Geotechnical Special Publication 229, pp. 232–253. VA, ASCE, Reston (2013)

Keaton, J.: A suggested geologic model complexity rating system. In: Lollino, G., Giordan, D., Thuro, K., Carranza-Torres, C., Wu, F., Marinos, P., and Delgado, C. (eds.) Engineering Geology for Society and Territory: Proceedings of XII IAEG Congress, Torino, Italy, Vol. 6, Applied Geology for Major Engineering Projects, Springer, Switzerland, 363–366 (2014)

Keaton, J., Munro, R.: Analytic hierarchy process: a possible semi-quantitative alternative to "on the other hand…" for Geologic Complexity (abstract). AEG Annual Meeting Program with Abstracts Colorado Springs, CO, 68, (2017)

Pierson, L.A., van Vickle, R.: Rockfall hazard rating system—participants' manual. Federal Highway Administration Publication No. FHWA-SA-93-057, Washington, D.C. (1993)

Saaty, T.: Decision making with the analytic hierarchy process. Int. J. Services Sciences **1**(1), 83–98 (2008)

Identification of Anomalous Morphological Landforms and Structures Based on Large Scale Discrete Wavelet Analysis

Angelo Doglioni

Abstract

The identification and delineation of morphological patterns through a quantitative approach constitutes an important stage both for the geomorphological characterization of a region and for the interpretation of landforms for engineering geological purposes. This task is usually based on the expert judgment of terrestrial and aerial surveys or of thematic maps. This is potentially a cause of uncertainty, since personal and empirical opinions may bias the procedure. Here an automatic numerical approach, based on 2D discrete wavelet transform of the digital elevation model, is applied in order to map the anomalies of the topographic surface at large scale. The approach focuses on the digital elevation model of the Salento peninsula in Southern Italy denoted by a widespread outcropping of Quaternary sedimentary units largely covering an intensively fractured Cretaceous limestones substratum. The data-mining used procedure allowed for emphasizing details related to morphological structures.

Keywords

Discrete wavelet analysis • Landform delineation • Geomorphology • Digital elevation model • Data-mining

1 Introduction

The delineation and classification of landforms and morphological structures is of paramount importance for the analysis and knowledge of the regional geology and geomorphology for engineering geological purposes. These analyses are commonly based on observations made during site and aerial surveys, and examination of the available cartography. However, the large and easy availability of numerical cartography is fostering the development of automatic approaches to the extraction of data and consequently this produces new scientific knowledge. Here, starting from a medium resolution digital elevation model, an extensive analysis of a region in southeast Italy is presented. The approach is based on discrete wavelet transform (Daubechies 1992), which is able to extract the topographical anomalies from a digital elevation models, thus allowing them to be mapped and classified (Doglioni and Simeone 2014). For instance, this permits identification of anomalous patterns in the topography potentially correlated to faults, cracks or landslides. Moreover, the proposed approach is able to provide a classification of the anomalies with respect to the neighbourhood (Doglioni 2013, 2015). This methodology is herein applied to the Salento peninsula, which is a peninsula at the extreme southeast of the Apulian Region in southern Italy. This locality is quite flat with respect to other areas of the Apulia region and is characterized by a widespread outcropping of Quaternary sedimentary units covering a substratum of intensively fractured Cretaceous limestones, which are sometimes visible in outcrops. The morphology of Salento is representative of a complex geologic history, highly conditioned by tectonics, which produced peculiar landforms and caused deep and frequent faults of the carbonatic bedrock (Ciaranfi et al. 1988; Festa 2003; Tozzi 1993).

2 The Investigated Region

Salento is situated in the extreme south-east area of Italy. It is an elongated peninsula, with a relatively flat morphology, sometimes interrupted by small limestone ridges. The main lithotypes outcropping in this area are Cretaceous limestones and Quaternary deposits, mostly made of clayey sediments and sands, which can vary from weakly to moderately

A. Doglioni (✉)
Department of Civil, Environmental and Construction Engineering and Chemistry, Technical University of Bari, via E. Orabona 4, 70125 Bari, Italy
e-mail: angelo.doglioni@poliba.it

cemented, i.e. calcarenitic formations. These sediments cover the substratum of Cretaceous limestones and dolomitic limestones that sometimes outcrop and break the continuity of the landscape with small ridges. These ridges are mostly oriented SSE—NNW. This bedrock constitutes the carbonatic bedrock of the Apulian foreland, in this area intensively karstified and fractured, with many discontinuities, mostly faults, due to the tectonic stresses it underwent until the late Pleistocene (Forte and Pennetta 2007). These geologic conditions created scarps and typical sinkholes besides faults, which together characterize the landscape of Salento (Selleri et al. 2003).

Figure 1 represents a generalized geological map of the investigated area, reconstructed from geological map of central-southern Apulia by Ciaranfi et al. (1988). For the entire area of Salento a medium resolution, 20 m, grid-based digital elevation model is available and was used of the following processing approach.

3 The Methodological Approach

Wavelet transform is the decomposition of a sequence of discrete or continuous data into a series of irregular shaped wave functions. This decomposition allows for smoothing a series of data by extracting details and generating approximations of data. This kind of transformation is made by scaling and translating data using proper irregular wave functions, referred to as wavelets (Daubechies 1992). Figure 2 represents the detail coefficients along a transect. It is noteworthy that whereas the topography does not shot changes of slope, detail coefficients have very low values. Conversely, where the shallow topography shows sudden

changes of slopes, detail coefficients have high values. In particular, detail coefficients increase when the variation of slope is higher between two adjacent elements of the grid of the digital elevation model.

This approach can be easily adapted to distributed data, in particular elevation data coming from a grid-based description of land surface, like a Digital Elevation Model (DEM). Discrete Wavelet Transform (DWT) is an orthogonal function applied to a finite set of data. DWT is orthogonal: a signal passed twice through the transformation is unchanged, and it is assumed the input signal as a set of discrete-time samples (Doglioni and Simeone 2014). Detail coefficients of 2D DWT applied to a DEM are here analyzed, since their variations represent discontinuities of DEM. 2D DWT can be pushed to further levels, assuming a higher scale number of the transform. This approach emphasizes sharp changes in relief, creating maps highlighting topographical features at large scale, which can be used as a starting point for successive and more localized analysis, based on traditional methodologies (Doglioni et al. 2016).

4 Results and Discussion

The 2D discrete wavelet transform based on the biorthogonal 1.3 function was applied to the DEM of Salento 4 times in succession, thus obtaining 4 levels of transformation. In particular, here the results are presented as maps of the values of post-processed detail coefficients. These are processed as squared root of the composition of the sum of the squares of detail coefficients obtained along the N-S and W-E directions. This choice allows for composing the

Fig. 1 Geological map of the Salento area (after Ciaranfi et al. 1988, modified)
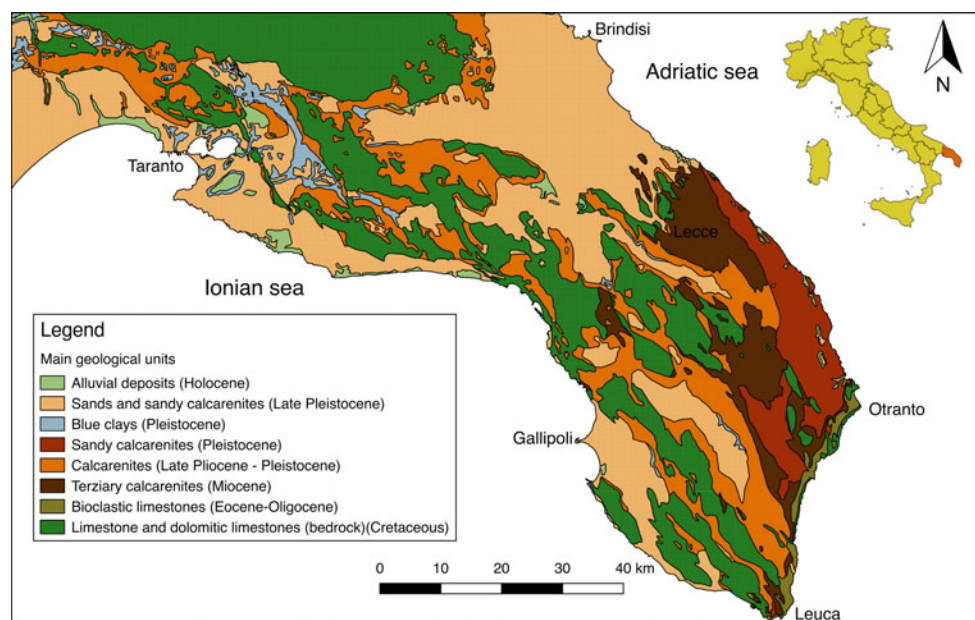
Fig. 2 Detail coefficients estimated by 2D DWT on a transect. Red dotted lines confine zones with similar slope features (after Doglioni and Simeone [2014](#), modified)
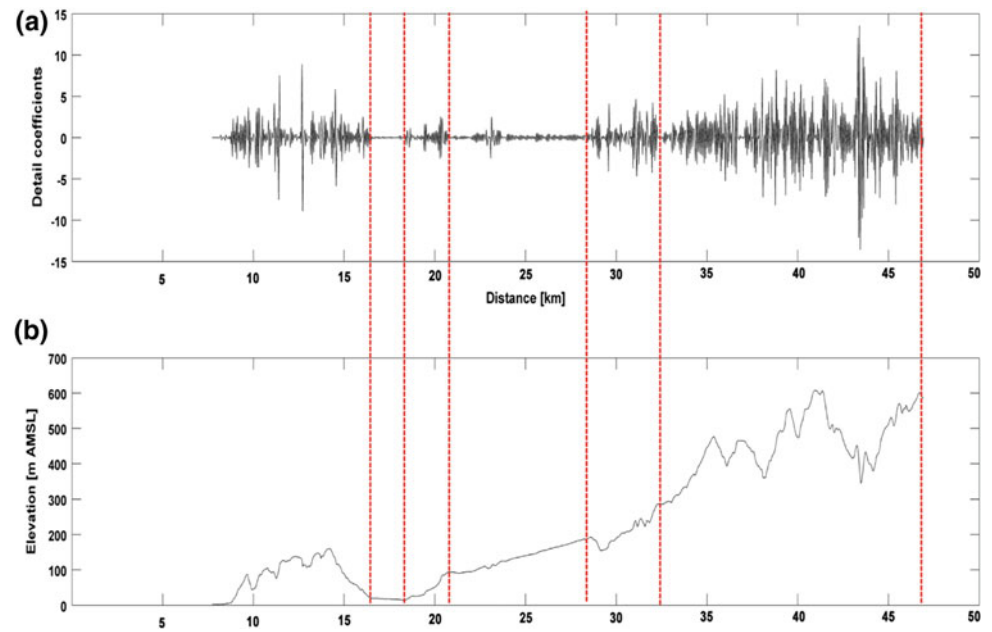
horizontal and vertical components of the transformation as well as for filtering the negative values of the detail coefficients. Therefore, the outcome of this process is a new grid of values, with a lower number of elements than the initial DEM, where high values of detail coefficients clearly denote persisting anomalies of the topography. This essentially means sudden changes of slopes of the topography are possibly related to the emphasized discontinuity of the earth surface. Figure 3 shows the most significant result, in terms of composition of detail coefficients. It corresponds to the map of 2nd level detail coefficients. The result emphasizes that the higher values of detail coefficients corresponds to the zones where the carbonatic bedrock outcrops and to those areas where particular structures exists, like paleo dunes, terraces, or coastlines.

It is also interesting to observe that overlapping the map of detail coefficients to the geological and geomorphological map of Salento, see Fig. 3a, the high values of detail coefficients corresponds to the boundaries of the geological formations. It is also possible to observe that high values of detail coefficients correspond to the main faults known in this area. Once again, this supports how the map of detail coefficients provides a representation of the morphology of a large area, without a preliminary interpretation. This does not mean that no interpretation is needed, but the expert judgment becomes the second stage of the procedure, when a general morphological numerical map is available.

Differently from the analyses based on slopes or aspects, 2D DWT produces maps where the anomalies are clearly identified. In particular, those anomalies, which are not clearly readable from slope or aspect maps, are more visible, thus landforms are more efficiently delineated than with simple GIS analyses.

Looking at the values of detail coefficients, it is possible to assume a classification of the discontinuities of the topography. In particular, here detail coefficients are classified according the categories: 0 to 300, higher than 300. In order to filter those values related to poorly significant variations of slope, the classes higher than 300 are highlighted with blue colour on Fig. 3. The values higher than 300 correspond to the limestone ridges, in the area between Gallipoli and Leuca: in particular to their boundaries and to fractures, which are mostly oriented NNW-SSE. They also show in the area located east than Taranto, where there is a calcareous horst and a half circular paleo dune, see Fig. 3b. Values higher than 300 correspond also to coastal cliffs and to some faults in the Quaternary calcarenitic formations to the extreme southeast of Salento, close to Otranto, see Fig. 3c. It is finally noteworthy to observe values higher than 300 in the area close to the town of Brindisi, in an apparently uniform formation of Pleistocene clayey sand, see Fig. 3a. These are probably related to the presence of some areas where sands become more cemented, creating calcarenitic formations.

Fig. 3 **a** 2nd level detail coefficients of Salento; **b** detail of the paleo-dune located at east than Taranto; **c** detail of the faults located in the neighbourhood of Otranto
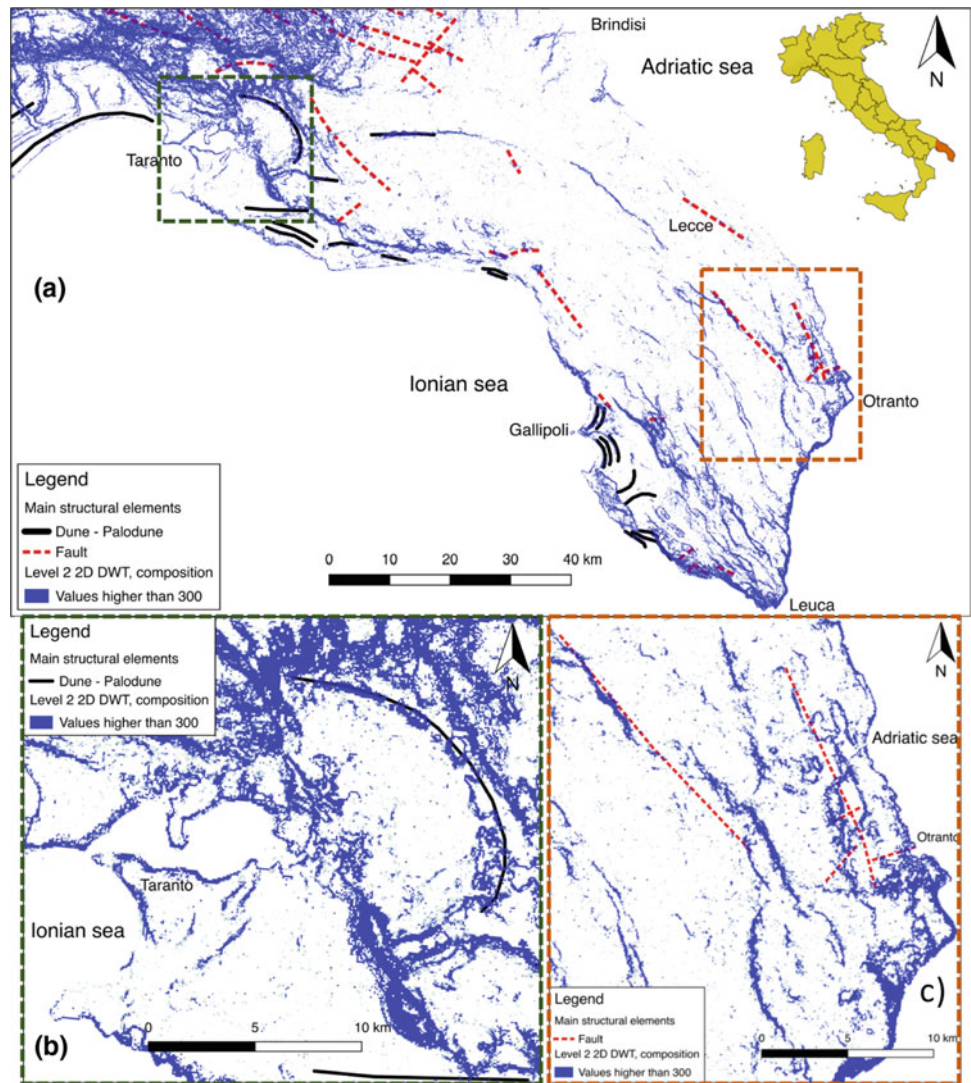
5 Conclusions

This work presented the outcomes of a geomorphic numerical analysis at regional scale, based on 2D discrete wavelet transform of a DEM. The approach proved to be quite effective at mapping the topographical anomalies, related to discontinuities like faults, scarps, terraces, contacts between different outcropping units. Moreover, the numerical classification based on the numerical values of detail coefficients is helpful for discriminating the insignificant anomalies from those actually related to morphological structures. In addition, the possibility of performing a hierarchical analysis, based on iterative 2D DWTs, enables further filtering secondary or local anomalies of the topographic surface.

2D DWT is alternative to conventional GIS-based analysis, where for instance slope and aspects maps are analysed. In fact 2D DWT starts from a different approach, based on the separation of detailed information from general information. Therefore, it can be more efficient than conventional GIS-based analysis, allowing for quicker delineations of the morphological anomalies.

For these reasons, the proposed approach, together with a posteriori interpretation, based on the expert judgment, can be an effective instrument for geological and geomorphological mapping at medium-large scale.

References

Ciaranfi, N., Pieri, P., Ricchetti, G.: Note alla Carta Geologica delle Murge e del Salento (Puglia centromeridionale). Mem Soc. Geol. It **41**, 449–460 (1988)

Daubechies, I.: Ten lectures on wavelets, p. 357. SIAM, Philadelphia (1992)

Doglioni, A.: The use of discrete wavelet transform for the analysis of topographic surface for geological purposes. Rend. Online Soc. Geol. It. **24**, 104–106 (2013)

Doglioni, A.: Analysis of a complex tectonic scenario based on 2D discrete wavelet analysis. Rend. Online Soc. Geol. It. **35**, 113–116 (2015). https://doi.org/10.3301/ROL.2015.77

Doglioni, A., Simeone, V.: Geomorphometric analysis based on discrete wavelet transform. Environ. Earth Sci. **71**(7), 3095–3108 (2014). https://doi.org/10.1007/s12665-013-2686-3

Doglioni, A., Berardi, C., Simeone, V.: Multi temporal 2D discrete wavelet analysis of a large and deep landslide. Rend. Online Soc. Geol. It. **41**, 143–146 (2016). https://doi.org/10.3301/ROL.2016.114

Festa, V.: Cretaceous structural features of the Murge area (Apulian Foreland, Southern Italy). Eclogae Geol. Helv. **96**, 11–22 (2003)

Forte, F., Pennetta, L.: Geomorphological Map of the Salento Peninsula (southern Italy). J. Maps **3**(1), 173–180 (2007). https://doi.org/10.1080/jom.2007.9710836

Selleri, G., Sansò, P., Walsh, N.: The karst of Salento Region (Apulia, southern Italy): constraints for management. Acta Carsologica **32**(1), 19–28 (2003). https://doi.org/10.3986/ac.v32i1.361

Tozzi, M.: Assetto tettonico dell'Avampaese Apulo meridionale (Murge Meridionali – Salento) sulla base dei dati strutturali. Geol. Romana **29**, 95–111 (1993)

Engineering Geological, Geotechnical and Geohazard Modelling for Offshore Abu Dhabi, UAE

Andrew Farrant, Ricky Terrington, Gareth Carter, Matthew Free,
Esad Porovic, Jason Manning, Yannis Fourniadis, Richard Lagesse,
Charlene Ting, and Tarek Omar

Abstract

This paper presents the development of an engineering geological, geotechnical and geohazard model for four oil and gas fields offshore of Abu Dhabi in the Arabian Gulf. The purpose of the model was to characterize the shallow ground conditions for the design of offshore platforms and other infrastructure. The model was developed based on the interpretation of nearly 60 years of ground engineering data including a vast amount of boreholes, laboratory test and cone penetration test data. Carbonate-rich sediments dominate the shallow geology of Abu Dhabi offshore region. The main lithological units of Miocene to Pleistocene age comprise weak carbonate rocks, calcarenite and calcisiltite, with frequent lenses and pockets of gypsum. These units are overlain by recent carbonate marine deposits. The geological models for the region were developed using the software package GSI3D™. Geostatistical methods were applied in the treatment of geological uncertainty in the model, and the analysis of the associated geotechnical design recommendations. The model also includes a detailed review of local and regional natural hazards, including seismic and submarine geohazards, with the potential to affect existing and proposed offshore infrastructure. Interrogation of the model enables effective decision-making on oil and gas development issues related to offshore ground investigation for the siting of new developments. This model can allow these works to be optimized at the advanced stages of planning, saving on time, cost and significantly reducing health, safety and environmental risks.

1 Introduction

The offshore region of Abu Dhabi comprises several major deep oil and natural gas reserves operated by the Abu Dhabi Marine Operating Company (ADMA-OPCO) with the area of interest covering approximately fifteen times the area of Greater London. Since exploitation of the reserves commenced in the late 1950s, a vast amount of ground engineering information has been collected for the development of offshore platforms, artificial islands and associated infrastructure. The data includes boreholes, laboratory test results, cone penetration tests, geophysical and topographic surveys. Over decades the information has been compiled in various formats; from paper through to modern electronic data exchange formats resulting in a significant variation in quality and reliability. An interpretation of the information has not been attempted for over 30 years and subsequent attempts to use the information has become time consuming and expensive, making effective decision making inefficient.

This paper presents the development of a ground engineering model based on a comprehensive review and interpretation of all the available information. This includes the development of three-dimensional (3D) geological models for each field and a review of local and regional geohazards. The ground engineering model data was integrated into an interactive GIS-based platform, and used for the derivation of geotechnical parameters, and for indicative design of geotechnical elements, including shallow and deep foundations for offshore structures.

A. Farrant · R. Terrington · G. Carter
British Geological Survey, Nottingham, NG12 5GG, UK

M. Free · E. Porovic · J. Manning · Y. Fourniadis (✉)
R. Lagesse · C. Ting
Arup, London, W1T 4BQ, UK
e-mail: yannis.fourniadis@arup.com

T. Omar
Abu Dhabi Marine Operating Company, Abu Dhabi, P.O.
Box 303 United Arab Emirates

1.1 Project Area Location

The study area comprises four offshore oil and gas fields, namely NR, UL, US and ZK fields (Fig. 1). The oil and gas fields are located in the Arabian Gulf offshore of the United Arab Emirates (UAE) coastline to the northwest of Abu Dhabi. The UL field is closest to the coastline, approximately 25 km offshore, while NR and US fields are approximately 130 km offshore.

1.2 Geological and Tectonic Setting

The four oil and gas fields are located offshore of the UAE in the southern part of the Arabian Gulf. This area is located on the southern edge of the Zagros foreland basin, which occupies much of the present-day Arabian Gulf. Up to 11 km of sediments has been deposited over the Proterozoic (Late Precambrian) metamorphic basement of the Arabian Shield (Farrant et al. 2012). It is within this thick sedimentary succession that the large oil and gas reserves have accumulated. However, most of the oil and gas field infrastructure is founded within the near-surface Miocene

and Quaternary sediments. As such, these are the focus of this study.

During the Miocene, significant changes in global climate facilitated the transition of the Zagros foreland basin from a shallow marine environment in the Aquitanian through to an evaporitic basin and ultimately a terrestrial environment during the Burdigalian. The sediments deposited within this basin comprise the Fars Group. In the Early Miocene, carbonate muds (the Gachsaran Formation) were deposited in the central part of the basin. These thin towards the southern margin of the basin, and change character, becoming more marginal with the deposition of shallow marine to freshwater carbonates (Dam Formation). This upward shallowing trend continued into the Middle Miocene (Serravallian) when the Abu Dhabi region became a terrestrial semi-arid environment. A sequence of fluvial and aeolian terrestrial sediments were deposited across the western Emirates (Shuwaihat Formation). In the Late Miocene (Tortonian or Messinian), regional tilting and climatic change led to the development of large river systems draining the Arabian highlands to the south, which deposited fluvial sandstones across the region. These sandstones (Baynunah Formation) are well exposed in the western UAE. This regional tilting heralded a period of

Fig. 1 Study area location plan
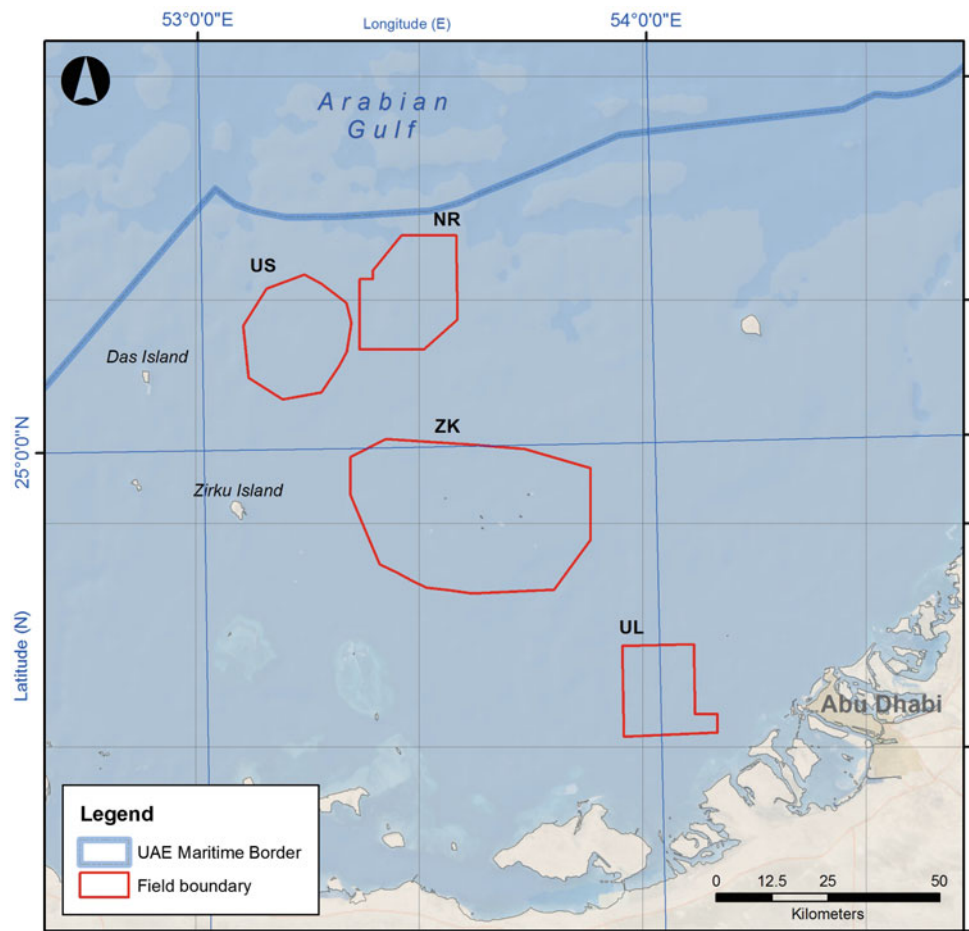
uplift and non-deposition during the Pliocene. These sediments have undergone relatively minor flexuring to create a series of shallow anticlines and synclines. In addition, halokinesis has created a series of salt domes across the region, some of which form offshore islands.

During the Quaternary, renewed subsidence in the Zagros fore-deep initiated marine deposition in the Arabian Gulf. Carbonate sedimentation in the shallower parts of the Gulf, including around Abu Dhabi, was limited by periods of low global sea-level during glacial periods, notably during the last glacial-interglacial cycle. Periods of emergence during these low sea-level stands may have enabled some erosion and incision of the Miocene bedrock, creating bathymetric highs. During the Holocene marine transgression, a complex succession of carbonate sediments including mudstones, limestones and reef complexes have been deposited across the region which form a thin accretionary wedge draped over an irregular bedrock topography (Evans 2011).

2 Project Data

The project data comprised reports, drawings, maps and other information dating from 1959 to 2015; this data was supplemented by publicly available information.

2.1 Ground Engineering Data

Most of the detailed research on the geology and geotechnics of Abu Dhabi has been conducted onshore. The first detailed studies were produced in the 1970s, largely on the basis of aerial photograph interpretation coupled with limited field mapping. Subsequent detailed geological maps and memoirs were produced by the British Geological Survey (BGS) for the Abu Dhabi Ministry of Energy between 2002 and 2012. Detailed study of the Neogene and Quaternary materials and successions have been documented in a number of studies including Farrant et al. (2012) and Alsharan and Kendall (2003).

In contrast, the shallow subsurface of the offshore region has been poorly studied. Williams and Walkden (2002) examined Quaternary carbonate sediments of the southern Arabian Gulf which included an analysis of a few selected boreholes from Umm Shaif and Zakum fields. Most geological and geotechnical information for the offshore area was derived from ground investigation data in factual and interpretive reports from previous site investigations provided by ADMA-OPCO. This data comprised exploratory hole information, in situ testing and laboratory testing data.

2.2 Other Project Data

Regional-scale bathymetric data was available for the study area as well as locally obtained high resolution bathymetry for the oil and gas fields. The regional scale data for the Arabian Gulf was obtained from a global dataset compiled by the General Bathymetric Chart of the Oceans (GEBCO) project. The locally obtained bathymetric data for the oil and gas fields was provided by ADMA-OPCO.

3 Modelling and Design

The modelling for the project comprised three principal components: the geological model, geotechnical interpretation and geohazard assessment. These three components were compiled into geotechnical zoning models for each field from which geotechnical analysis and design charts could be generated based on the full range of ground engineering information integrated into the model. The outputs from the analysis and design were then disseminated through a fully interactive GIS-based platform and a series of hard-copy map sheets. The project workflow is illustrated in Fig. 2.

3.1 Geological Model

The 3D geological model was developed using the software GSI3D™. This software is an established approach for modelling Quaternary and undeformed bedrock horizons at the British Geological Survey (Kessler et al. 2009; Aldiss et al. 2009; Mathers et al. 2014; De Beer et al. 2012; Price et al. 2012). This methodology relies on the construction of an interlocking network of manually created cross sections, which is then used to generate surfaces. Cross-sections are manually correlated between physical data such as boreholes, seismic data and topographical features and constrained by geological maps where available. The 3D geological models were calculated by combining the correlated units present on cross-sections with envelopes defining the plan distribution of those units. The modelling calculation in GSI3D™ uses a Triangular Irregular Network (TIN) algorithm. An illustration of the 3D geological model development workflow is presented in Fig. 3.

The GSI3D™ methodology provides the flexibility to incorporate the geoscientist's interpretation where borehole or other data may be sparse or not available. For example, where borehole density is low or where boreholes do not penetrate geological rockhead, the modeler can enhance the

Fig. 2 Project workflow
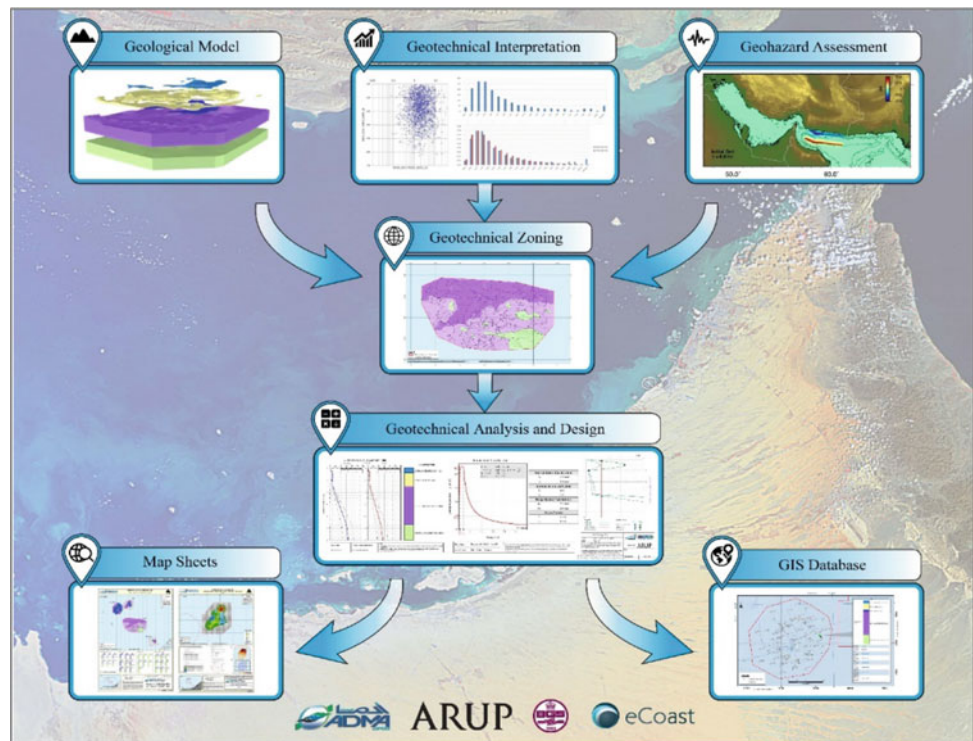
Fig. 3 Workflow for development of 3D geological model
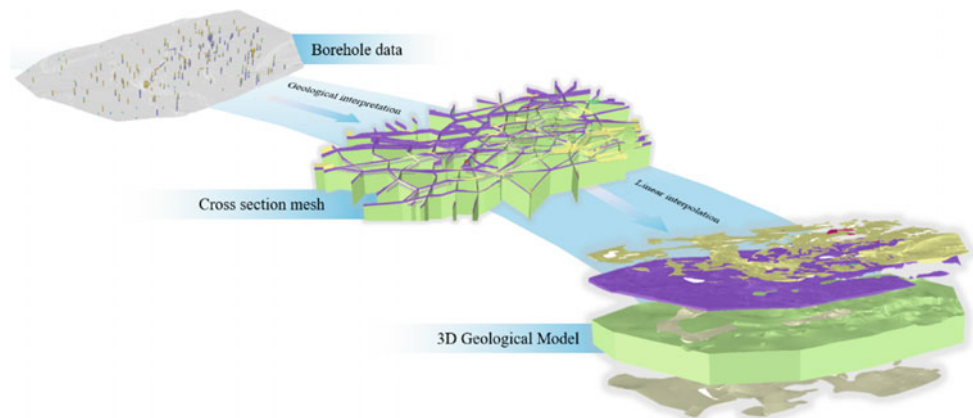
3D model, by using surrounding borehole data or locally derived knowledge, to define and interpret the thickness or geometry of the geological unit.

The final geological model was exported as a series of 3D surfaces in ASCII grid format with 20 m spatial resolution. Each surface represents the top and base elevation as well as the thickness of each geological unit. Integration of the outputs into the GIS-based platform allowed interrogation of the data to generate synthetic boreholes, geological cross-sections and 3D surfaces showing elevation or thickness.

The assessment of uncertainty in the 3D geological models was undertaken in order to communicate the relative accuracy of the model and its derived outputs. A quantitative method for assessing the uncertainty related to GSI3D™-derived geological surfaces was developed and applied for the geological models, by using kriging interpolation and reporting the associated variation in elevation values of the geological surfaces generated by the kriging model compared to the elevation values of the geological surfaces obtained from the GSI3D™ model.

3.2 Geotechnical Interpretation and Design

The reliability of the geotechnical design calculations is dependent on the uncertainty of the modelled geological surfaces and variability of the input parameters to the

analyses. Due to the large spatial extent of the study area and the variability in data density, it was considered appropriate to employ probabilistic methods for the geotechnical design calculations. As such, recommended geotechnical design parameters for use in the design calculations were determined using statistical methods based on recommended practice given in DNV (2012) to determine mean, standard deviation and probability density function (PDF) for the parameters.

Probabilistic analyses of foundation capacity, foundation performance and jack-up platform leg penetration were performed using Monte Carlo simulation and checked using deterministic calculations on upper and lower bound parameters. The analyses provided indicative foundation design charts to inform the geotechnical design of foundations for proposed platforms and infrastructure.

The geotechnical interpretation and design outputs were incorporated into the project GIS-based platform and disseminated as a series of hard-copy map sheets for use by the project team and other stakeholders. An example map showing the summary geotechnical zonation for NR field is shown in Fig. 4.

3.3 Geohazard Assessment

Geohazards are those geological states that represent or have the potential to develop further into a situation leading to damage or uncontrolled risk (ISO 17776, 2002). Jack-up rigs are especially susceptible to marine geohazards as they are based upon foundations that are embedded in the seafloor and are therefore vulnerable to natural seabed and subsurface processes. Mapping of seafloor features was undertaken using the available data, including multi-beam bathymetric surveys and geotechnical parameters (particularly relevant for submarine slope stability assessment).

Fig. 4 Example geotechnical zoning plan for NR field
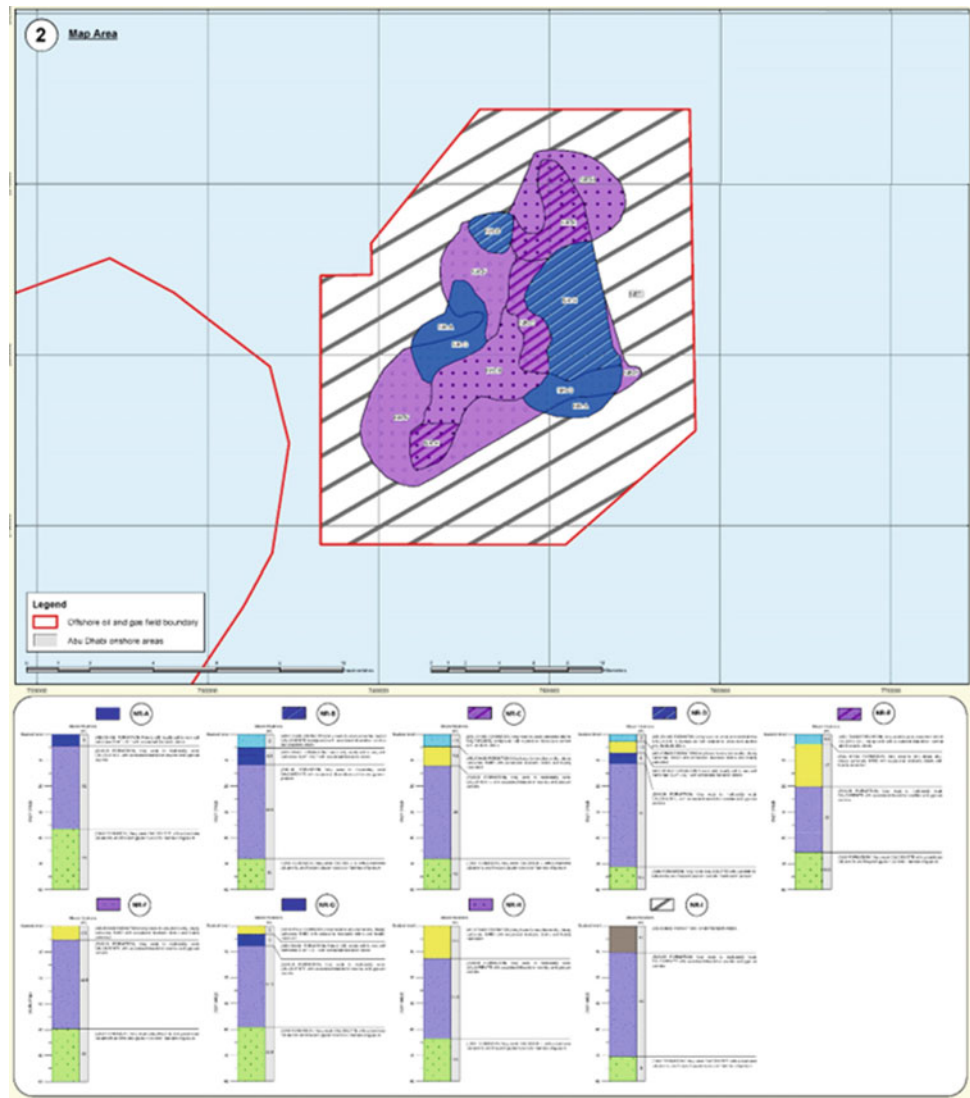
Fig. 5 Example of pockmark identification
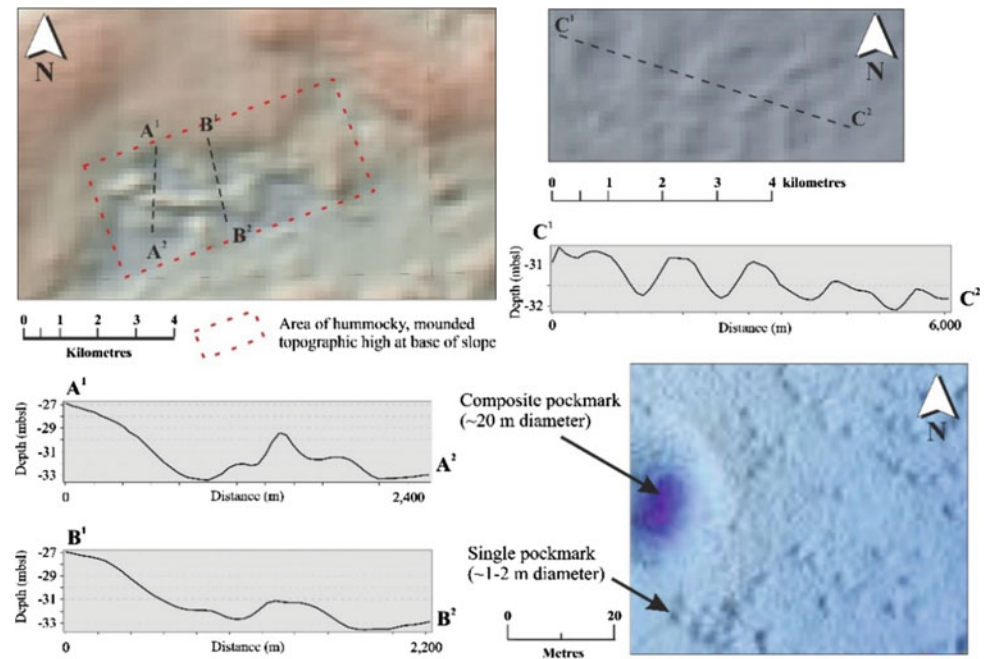
In the Arabian Gulf area, there is little recorded evidence of submarine mass movement events. Within the four field areas, the maximum slope angles are generally within the range of 4–6°, with the steeper gradient slopes of the ZK field influenced by the areas of made ground and reefs. For the submarine slopes that were composed of unconsolidated, cohesionless sediments, a simple translational slope stability model was generated in order to produce a Factor of Safety (FoS) map. For all four fields, the FoS model produced values greater than two, indicating that, under normal stress conditions [i.e. no seismic loading], the seabed slopes in these areas appear to be in a stable state.

Two pockmark fields were mapped on the NW perimeters of the US and NS fields (Fig. 5). These pockmarks typically consist of composite pockmarks, with diameters of up to ~300 m and depths of >2 m below seafloor (mbsf), formed from the amalgamation of several smaller depressions caused by gas seeps. It is unknown whether any of these vents are still active. Localized occurrences of seabed hazards, such as historical mass movement deposit, areas of scour and sandwave bedforms were identified in the study area. These geohazard features were schematically included in conceptual ground models of the four fields (Fig. 6 presents the conceptual ground model of ZK field showing the location of geohazards).

Detailed seismic hazard assessments were also undertaken for the four field areas including the probabilistic assessment of earthquake ground motions, liquefaction susceptibility and tsunami hazard.

Fig. 6 Schematic conceptual ground model of ZK field illustrating key geological and local geohazard features
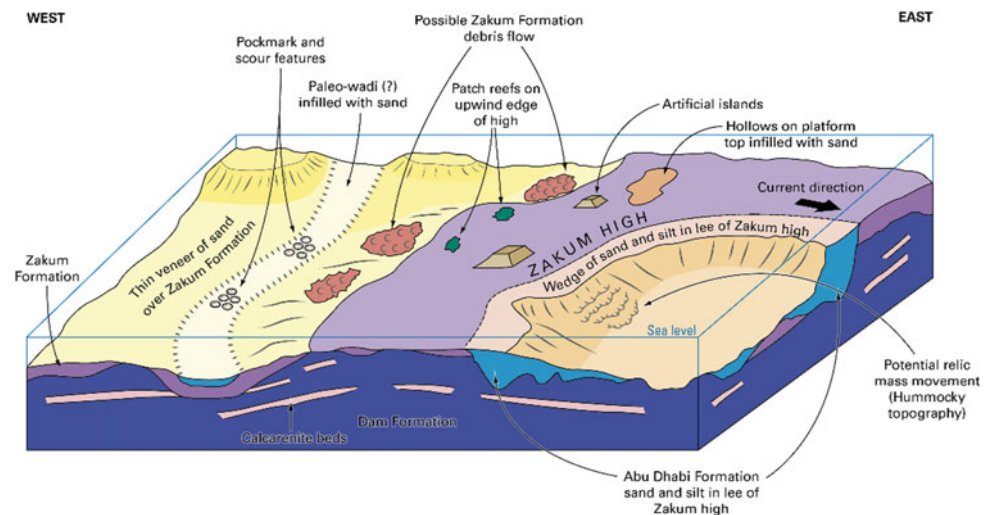
4   Conclusions

The geology of the shallow subsurface influences the type and style of geohazards encountered during the construction, operation and decommissioning of offshore installations. Getting the geology correct is a key part of reducing the potential risk from geotechnical and submarine geohazards. In this study, a large quantity of geological data including boreholes, bathymetric, seismic and geophysical data acquired of many decades were synthesized to create 3D geological models for four offshore oilfields of the coast of Abu Dhabi.

These geological models provided the basis for a more detailed, quantitative geotechnical assessment of the shallow subsurface, down to depths of c. 100 m below sea-level. The engineering geological models for offshore Abu Dhabi developed for the project have proven to have provided significant benefits to ADMA-OPCO including program efficiency and cost savings, and an enhancement of health, safety and environmental performance. Offshore ground investigations are hugely expensive and require a mobilization of equipment under conditions of very severe access and health, safety and environmental requirements. The engineering geological model allows these works to be optimized at the advanced stages of planning thus saving on time and cost and significantly reducing health, safety and environmental risks.

References

Aldiss, D.T., Black, M.G., Entwisle, D.C., Page, D.P., Terrington, R.L.: Benefits of a 3D geological model for major tunnelling works: an example from Farringdon, east-central London, UK. Q. J. Eng. Geol.Hydrogeol. **45**(4), 405–414 (2012). https://doi.org/10.1144/qjegh2011-066

Alsharhan, A.S., Kendall, C.S.C.: Holocene coastal carbonates and evaporites of the southern Arabian Gulf and their ancient analogues. Earth Sci. Rev. **61**(3), 191–243 (2003)

De Beer, J., Price, S.J., Ford, R.: 3D modelling of geological and anthropogenic deposits at the World Heritage Site of Bryggen in Bergen, Norway. Quat. Int. **251**, 107–116 (2012). https://doi.org/10.1016/j.quaint.2011.06.015

DNV: DNV-RP-207 Statistical representation of soil data (2012)

Evans, G., (Ed.): An historical review of the Quaternary sedimentology of the Gulf (Arabian/Persian Gulf) and its geological impact. Quaternary carbonate and evaporite sedimentary facies and their ancient analogues. A tribute to Douglas James Shearman. Special Publication Number 43 of the International Association of Sedimentologists, Wiley, Hoboken (2011)

Farrant, A.R., Ellison, R.A., Thomas, R.J., Pharaoh, T.C., Newell, A.J., Goodenough, K.M., Lee, J.R., Kinbell, G., Knox, R.O'B.: The geology and geophysics of the United Arab Emirates, vol 6. In: Geology of the western and central United Arab Emirates, pp. 339. British Geological Survey, Keyworth, Nottingham (2012)

International Organization for Standardization (ISO): Petroleum and natural gas industries-offshore production installations-guidelines on tools and techniques for hazard identification and risk assessment (Report No. 17776). International Organization for Standardization, Geneva (2002)

Kessler, H., Mathers, S., Sobisch, H.G.: The capture and dissemination of integrated 3D geospatial knowledge at the British Geological Survey using GSI3D software and methodology. Comput. Geosci. **35**(6), 1311–1321 (2009)

Mathers, S.J., Terrington, R.L., Waters, C.N., Leslie, A.G.: GB3D: a framework for the bedrock geology of Great Britain. Geosci. Data J. **1**(1), 30–42 (2014). https://doi.org/10.1002/gdj3.9

Price, S.J., Farrant, A.R., Leslie, A., Terrington, R.L., Merritt, J., Entwisle, D., Thorpe, S., Horabin, C., Gow, H., Self, S., McCormick, T.: A 3D superficial and bedrock geological model of the Abu Dhabi urban area, United Arab Emirates. British Geological Survey Commercial Report, CR/11/138, pp. 74 (2012)

Williams, A.H., Walkden, G.M.: Late quaternary highstand deposits of the Southern Arabian Gulf: a record of sea-level and climate change. Geol. Soc. London, Special Publications **195**(1), 371–386 (2002)

A 3D Geological Fault Model for Characterisation of Geological Faults at the Proposed Site for the Wylfa Newydd Nuclear Power Plant, Wales

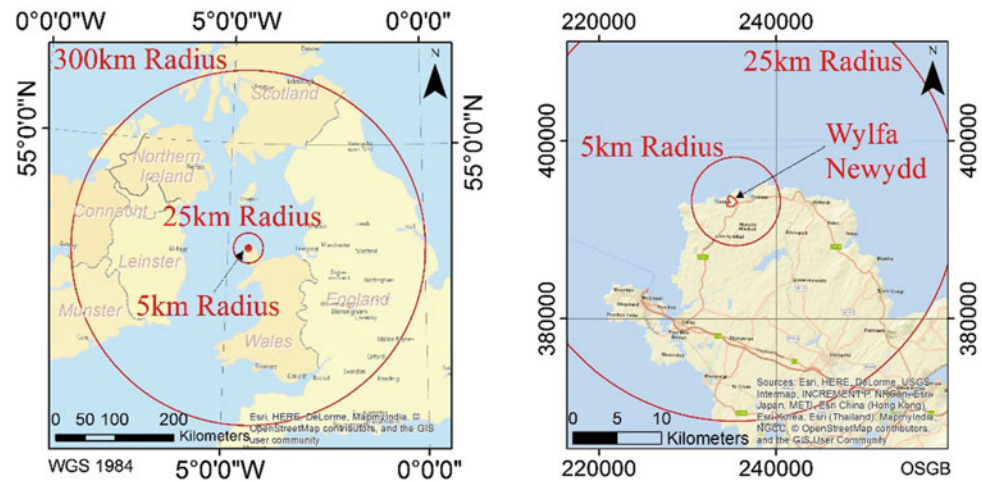Matthew Free, Ben Gilson, Jason Manning, Richard Hosker, David Schofield, Martin Walsh, and Mark Doherty

Abstract

Nuclear energy is an important part of a sustainable, economic and secure energy balance for the United Kingdom (UK). Horizon Nuclear Power commissioned Arup to provide seismic hazard assessment (SHA) consultancy services for the proposed Wylfa Newydd Nuclear Power Station in Anglesey, Wales, UK. Advanced Boiling Water Reactors are proposed to provide at least 5400 MW, enough to power around 10 million homes. The SHA comprises a probabilistic seismic hazard assessment of ground motion, a tsunami hazard assessment and a capable faulting assessment. The capable faulting assessment included thoroughly identifying and investigating geological faults at the site, with due consideration of the geological, seismological and tectonic setting. The objective of the capable faulting assessment was to demonstrate that faults are not capable of surface rupture within the current tectonic setting. Should evidence suggest that faults with the potential to affect the safety of the nuclear installation are capable, IAEA guidance dictates that an alternative site shall be considered. A project 3D Geological Fault Model was developed to characterise geological faulting at the site for the capable faulting assessment. A systematic methodology that incorporates expert judgment was developed and applied to the investigation and correlation of geological faults between site investigation data points. A total of 36 geological faults were mapped across the site and three fault sets were identified. Absolute age dating of the fault gouge on a representative selection of samples was subsequently undertaken to demonstrate that faults at the site are not capable in accordance with IAEA guidelines.

Keywords

Capable faulting · Nuclear industry · Geological modelling · Anglesey · Surface rupture

1 Introduction

Nuclear energy is an important part of a sustainable, economic and secure energy balance for the United Kingdom (UK) (HM Government 2013). Ove Arup and Partners Ltd. (Arup), supported by the British Geological Survey (BGS), was appointed by Horizon Nuclear Power (Horizon) to provide Seismic Hazard Assessment (SHA) Consultancy Services for the proposed Wylfa Newydd Nuclear Power Plant on the Isle of Anglesey, North Wales, shown in Fig. 1.

The assessment followed International Atomic Energy Agency (IAEA) guidance for site evaluation of nuclear installations and relevant guidance from the Office for Nuclear Regulation (ONR), the UK regulator for nuclear installations, as well as relevant good practice in the UK context.

The capable faulting assessment requires geological faults at the proposed site to be thoroughly investigated and, with due consideration of the geological, seismological and tectonic setting, to demonstrate that faults are not capable of

M. Free (✉) · B. Gilson (✉) · J. Manning
Arup, London, UK
e-mail: matthew.free@arup.com

B. Gilson
e-mail: ben.gilson@arup.com

J. Manning
e-mail: jason.manning@arup.com

R. Hosker (✉)
Arup, Nottingham, UK
e-mail: richard.hosker@arup.com

D. Schofield
British Geological Survey, Edinburgh, UK
e-mail: dis@bgs.ac.uk

M. Walsh · M. Doherty
Horizon Nuclear Power, Gloucester, UK
e-mail: martin.walsh@horizonnuclearpower.com

M. Doherty
e-mail: mark.doherty@horizonnuclearpower.com

Fig. 1 Regional location of
Wylfa Newydd including the
regional (300 km) near regional
(25 km) and site vicinity (5 km)
study area radii

Fig. 1 Regional location of Wylfa Newydd including the regional (300 km) near regional (25 km) and site vicinity (5 km) study area radii

surface rupture within an appropriate time frame, in this case within the current tectonic regime of the local region (from five to eight million years ago to present). Should evidence suggest that faults with the potential to affect the safety of the nuclear installation are capable, IAEA standards dictate that an alternative site shall be considered.

This paper describes the process by which geological faults were identified, visualised in the three-dimensional (3D) Geological Fault Model and mapped across the site to characterise the faults spatially and geometrically. Following this process, age dating of fault gouge was undertaken on representative samples to constrain the last age of movement on the faults in order to demonstrate whether faults are capable in accordance with IAEA guidelines.

The SHA comprised a Geological, Tectonic and Capable Faulting Assessment (GTCFA); a Probabilistic Seismic Hazard Assessment (PSHA); and a Tsunami Hazard Assessment (THA). This paper focuses on the GTCFA element of the SHA.

2 Capable Faulting Assessment Process and Regulatory Guidance

2.1 Regulatory Guidance

In the regulation of the UK nuclear industry, dutyholders are required to characterise and assess hazards in terms of their severity and frequency of occurrence and, through the design process, minimise the direct effect of initiating events in Structures, Systems and Components. They are required to apply the As Low As Reasonably Practicable (ALARP) principle to risk assessment as outlined in the Safety Assessment Principles (SAPs) for Nuclear Facilities (ONR 2014a) and UK Health and Safety Executive (HSE) technical guidelines (ONR 2014b).

IAEA guidance (International Atomic Energy Agency (IAEA) 2016) on the assessment of capable faults at a site recommends that the assessment should be based on a compiled geological and seismological database presented as interpretative modeling including fault rock age dating if needed. Based on this information, a geological fault at the site is considered capable in accordance with the IAEA guidance (International Atomic Energy Agency (IAEA) 2016) if it shows (1) evidence of past movement(s), (2) a structural relationship with a known capable fault can be demonstrated, and (3) movement at or near the surface could be induced due to the maximum potential earthquake associated with a seismogenic structure within the regional seismotectonic model. The UK is located within a tectonically "less active area" in IAEA terms and in the UK it is considered appropriate to investigate for evidence of fault capability within the "current tectonic regime", interpreted to be approximately the last 8 million years ago (Ma) (Mallard et al. 1991). Further IAEA (International Atomic Energy Agency (IAEA) 2010) guidance provides extensive recommendations on how surface and subsurface data should be gathered.

2.2 Outline of the Capable Faulting Assessment Process

In the light of this guidance, the GTCFA process adopted for the site comprised the following components:

Stage 1: Compilation of a desk study and project geographical information system (GIS) database containing geological, tectonic and geological faulting for the site and surrounding region from published sources, field reconnaissance and mapping, ground investigations and previous fault interpretations at the site.

Stage 2:   Evaluation of geological fault observation, development of a 3D Geological Fault Model and age dating of geological fault gouge to provide technically defensible interpretations to constrain the last age of fault movement, in the context of regional and near regional geology, tectonics and seismicity.

Stage 3:   Reporting on the process and provision of a summary of the findings.

Stage 4:   Expert review by team members, client and their independent peer reviewers and subject matter experts, and ongoing review by the ONR and their subject matter experts, throughout stages 1–3.

This paper focuses on Stage 2 of the GTCFA process, with the exception of age dating studies that will be reported separately.

3   Site Geological Setting

The Isle of Anglesey's geological and tectonic history covers the late Precambrian to the Quaternary. It is highly complex and has been the subject of scientific research since the mid-19th Century (Greenly 1919) which is continuing with detailed multidisciplinary mapping and reinterpretation being carried out by the BGS (Phillips 2010). The understanding of the current regional tectonic setting is an area of evolving consensus as researchers continue to refine models for the complex geological history of the British Isles and the circum Atlantic region. The more active tectonic phases occurred very early in the geological history of the region and include: Late Neoproterozoic accretionary events forming the igneous and metamorphic basement rocks of Anglesey; the Caledonian and Variscan Orogenic episodes; Atlantic Ocean formation and seafloor spreading from the Jurassic onwards; and Alpine orogenesis from the Palaeocene to present (Hunter and Easterbrook 2004; Woodcock and Strachan 2012). The resulting main tectonic terranes have a prominent north–east to south–west orientation. The major fault systems in north Wales and Anglesey, the Menai Strait Fault System located approximately 28 km to the south–east, follows this trend with some evidence suggesting that Paleocene transpression may have reactivated some of these faults and reactivated/initiated north–northwest to south–southeast oriented faulting (Cooper et al. 2012).

Basement rocks exposed at the site comprise low-grade metamorphic New Harbour Group and Gwna Group rocks (metasediments) of the Mona Complex (Institute of Geological Sciences 1974a; Institute of Geological Sciences 1974b) of Cambrian age to Lower Ordovician age (Phillips 2010), being part of the Monian Supergroup.

The British Isles was subjected to Quaternary glaciations with ice sheets passing across the Irish Sea and Anglesey from north–east to south–west, eroding a significant thickness of younger rocks; depositing glacial soils; causing glaciotectonic deformation; and resulting in isostatic rebound following ice removal (Bradley et al. 2009). No evidence for glaciotectonic deformation of the emplaced Glacial Till was observed in the Wylfa area (Harris 1991), although this process has been identified in the near region.

4   Site Investigations

Multiple stages of ground investigations (see Fig. 2) have been undertaken at the Wylfa site, prior to the current scheme and as the current scheme progressed from preliminary through to detailed phase assessments. These comprised intrusive works (including rotary boreholes and observation trenches) and non-intrusive works (including geophysical surveys such as magnetic, electrical resistivity, seismic refraction and seismic reflection). In total six stages of ground investigation were undertaken for Wylfa Newydd, with approximately 25 km of borehole core from 520 boreholes, in the onshore and nearshore Wylfa site area, focusing on the proposed Development Area. Boreholes and trenches in two of these stages were undertaken specifically for the SHA.

Aerial photography interpretation has been undertaken in addition to geological reconnaissance focusing on the coastal areas where the geology is very well exposed in the vicinity of the site.

Vertical and inclined boreholes up to 150 m long and up to 45° to the horizontal was the principal investigation technique used. The 3D Geological Fault Model was used to plan and design the investigation and evaluate the effectiveness of particular borehole locations and orientations. Wireline downhole optical and acoustic televiewer geologging was used to interpret fault geometry. Due to borehole annulus instability in faulted rock, staged casing removal was required during geologging.

5   Fault Identification, Description and Classification

Given the multiple stages and methods of site investigation that provided information on geological faults, a systematic fault classification system was required to compare faults based on a predefined set of criteria. Relevant fault characteristics were: (i) fault aperture and orientation, (ii) infill texture including fabric (referred to as fault rock), (iii) infilling mineralization, and (iv) the nature of the surrounding rock (i.e. fragmented or intact).

Fig. 2 Site layout and historical and project specific exploratory hole locations
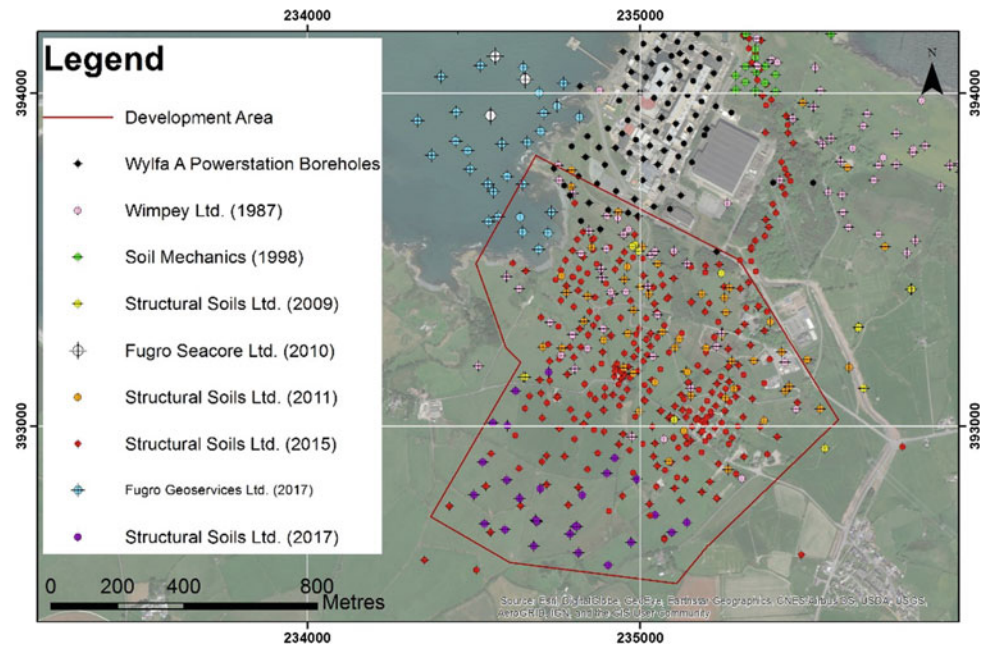
The classification system used prior to Arup's involvement on the project was based on the following three criteria: (i) thickness of fault rock in the following four classes (Class 1: <5 mm; Class 2: 5–100 mm; Class 3: >100 mm and Zone faults: >1 m zones of multiple fault rocks separated, in part, by fragmented rock or jointed core); (ii) presence of fault gouge; and (iii) presence of associated fragmented zones. This fault classification system was maintained to facilitate consistent characterisation of faults identified in all previous site investigation stages based on the key characteristics of fault thickness, fault rock texture and the presence of surrounding fragmented rock. This basis, together with expert judgement, provided a robust framework for correlating between faults across the site.

In addition, the BGS scheme for classifying discontinuities and in fillings, including geological faults, was used for core logging by the Arup/BGS team (Gillespie et al. 2011) to provide an improved basis for descriptions of faults and to determine whether fractured rock was interpreted to be related to faulting or other mechanisms, e.g. drilling disturbance.

Discontinuities identified by the ground investigation contractor as "possible faults" were set aside and inspected by the Arup/BGS team. Discontinuities which were classified to be faults were added to a schedule of faults and detailed observations and visual records made. For each confirmed fault, orientation data (dip/dip-direction) was gathered by interpreting televiewer records which was added to the fault schedule. From these schedules of faults, the 3D Geological Fault Model was populated.

6 Geological Fault Modelling

6.1 3D Geological Fault Data Visualisation

Geovisonary software produced by Virtalis (2016) was used to create the 3D Geological Fault Model by visualising various primarily sub-surface datasets to enable manual correlations to be made between interpreted or possible geological fault data points. Regional earthquakes and near regional faults were interpreted and modelled in 3D in order to provide context to the fault modelling at the site, and to compare seismicity with fault structures. At a site scale, striplogs (sticks) presented a simplified understanding of the geology encountered in boreholes and trenches. Figure 3 illustrates how interpreted faults from various sources were visualised.

Faults in boreholes were represented in the model using discs orientated according to interpreted fault geometry data, e.g. using optical televiewer imaging within boreholes, and spheres represented faults without geometry. The disc thickness represented fault rock thickness and the disc diameter emphasised fault data points interpreted by Arup/BGS which had greater confidence compared with previous ground investigation stages. The colour of discs and spheres was used to distinguish fault class [Class 3 and Zone (red), Class 2 (orange); and Class 1 (yellow)].

Faults mapped at coastal exposures were represented in the model by rectangular planes aligned with the mapped strike and dip of the fault. Three colours illustrated the

Fig. 3 Illustrative visualisation of the datasets
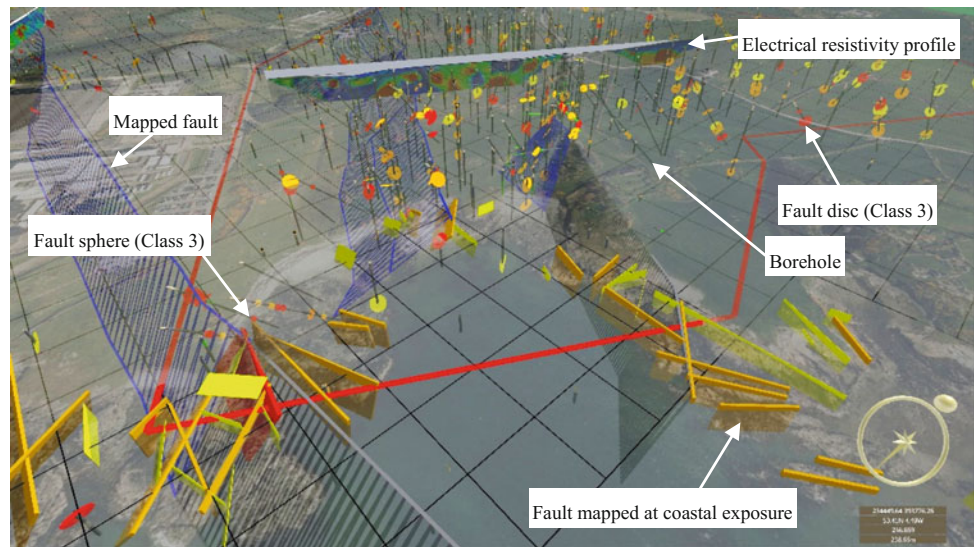
thickness of the fault rock, or inferred fault rock: greater than 3.0 m (red), between 0.5 and 3.0 m (orange); and less than 0.5 m (yellow). Longer inclined plane lengths below ground level were used to differentiate faults containing directly observed fault rock from faults inferred from topographic lineaments or other means.

Electrical resistivity and seismic reflection surface geophysical profiles were imported into the model as vertical image planes. Interpreted anomalies provided by the geo-physical contractor were included in a version of the profile images imported, however, the correlations were not limited to these anomalies. Magnetometer survey plots were geo-referenced in ArcGIS (GIS software) and imported as images draped onto the digital surface model (DSM). Rockhead contours updated by the geotechnical consultant at each new stage of ground investigation were imported as 3D contour polygons in order to correlate lineaments identified in the rock head with other fault data points. Contextual information including an aerial photograph draped on the DSM, bathymetry data, and a model of Wylfa A Power Station was added to aid visualisation.

6.2 Fault Correlation Methodology

Over 700 faults observations were identified in boreholes and trenches from recent phases of ground investigation including over 330 faults observations mapped at coastal exposures. Therefore, a systematic approach was needed to correlate between fault data observation points in boreholes, trenches and exposures and geophysical survey plot anomalies. It was not feasible to follow a robust correlation process by displaying all data at once in the 3D Geological Fault Model. Therefore, combinations of datasets in three

main strands were specified in advance to ensure that data in which greater confidence is placed (e.g. direct observations in boreholes, trenches and coastal mapping) were emphasised compared with data treated with lower confidence (e.g. early ground investigation records without accurate orientation measurement and early geophysical investigation anomalies) in the process of identifying correlations.

Repeatability and transparency were key, to be able to re-visit interpretations when new data becomes available, and to demonstrate the process undertaken.

Each combination of data was viewed in the 3D model from a consistent, oblique angle, panning horizontally around 360°. For the first iteration, the model was spun automatically at 0.2° per frame, at one frame per second. When a possible correlation was identified, the rotation was stopped and the view angle and zoom adjusted to be exactly perpendicular to the fault disc or plane, to allow any possible fault or anomaly aligned with the plane to be considered for correlation.

The fault data point location, viewing angle and an assessment of the confidence placed in the correlation were recorded, a screen shot taken and the process of visualising combinations of data continued. A higher confidence was placed in faults with known geometry correlated between two or more boreholes or trenches and a lower confidence was placed in faults correlated between a fault disc in a single borehole or trench and coastal mapping, geophysics etc. (grey surfaces) or a fault in a borehole or trench without orientation data.

Once the combinations of fault related datasets were assessed, correlations were in-vestigated further. All datasets aligned with the extrapolated plane of the fault were viewed to assess whether relevant datasets in the 3D Geological Fault Model (boreholes, trenches, geophysics profiles etc.)

Fig. 4 Conceptual geological fault model
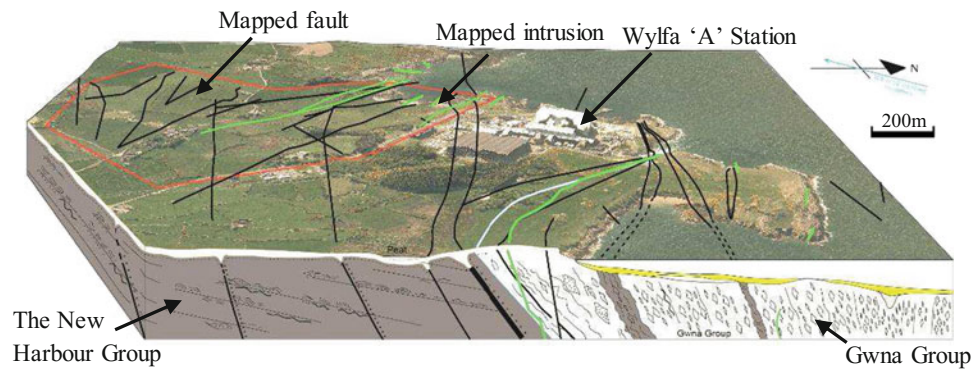
confirm or contradict the extrapolation of the fault. Approximate differences in geological fault dip and angle were noted, from which a conclusion was drawn as to whether the identified locations were interpreted to be part of the same fault.

Each correlation set was compared with other correlations in a tabular form to identify duplicates to be joined, removed or taken forward as two possibilities to be reviewed in the 3D Geological Fault Model.

Draft 3D fault surfaces were then created by extrapolating from coordinates calculated from the easting, northing, elevation, dip angle and dip orientation of each correlated fault data point to an elevation of 0 m Ordnance Datum (OD) and −100 mOD. Dip angle and dip orientation were averaged from adjacent correlated fault data points when not available, for example when correlating a geophysical profile between two fault discs. The draft fault surfaces were reviewed in the 3D Geological Fault Model and joined with adjacent surfaces, curtailed or amended as deemed appropriate following a thorough review of each source of data.

6.3 Summary Output of the 3D Geological Model

In the vicinity of the site 36 geological faults correlated between two or more ground investigation point locations over tens to thousands of metres were identified. Numerous other minor geological faults were identified in exploratory holes and coastal mapping that could not be correlated; this is assumed to indicate the relatively limited persistence of these features but may also indicate more complicated alignments and arrangements of faults that are not easily visualised with only limited reference points. Figure 4 presents the Conceptual Geological Fault Model for the site following the modelling.

Plots of geological fault geometry indicate the principal dip direction of faults is in a north–east direction, dipping between 30° and 75° which is the dominate metamorphic foliation orientation of the Monian Supergroup. A fault geometry data assessment identified the following fault sets:

1. Principal north–west to south–east striking faults (dip/dip-direction: 46–76°/030°);
2. Secondary east–west striking (dip/dip-direction: 47–68°/000°); and
3. Minor north–south striking (dip/dip-direction: 65°/080°).

7 Fault Movement Age Dating

Age dating of representative fault samples from drill core and trenches was undertaken and will be reported separately. On the basis of petrographic mineralogical investigations and geological reconnaissance studies, the fracturing, faulting and associated mineralisation at the site was categorised within a chronological sequence of 11 "Fracturing Events" (FE). The mineralogical investigations demonstrated that illite clay growth on fracture surfaces from the most recent faulting fracture event could be dated to constrain the timing of most recent fault displacement.

Absolute age dating investigations using potassium argon (K-Ar) dating were undertaken on fault breccia and gouge samples. The interpreted youngest ages of these clays that post-date shearing on the geological faults, and therefore the last age of movement on the faults, are significantly older than the current tectonic regime in the UK (i.e. older than 8 Ma) (Mallard et al. 1991).

8 Conclusions

A 3D Geological Fault Model has been developed for characterisation of geological faults at the proposed site for Wylfa Newydd Nuclear Power Plant in Wales in the UK.

A systematic methodology was developed and implemented using 3D geological modelling to identify, classify

and map geological faults at the site. These were reviewed and logged by specialist geologists from the Arup/BGS team. The use of 3D visualization software was effective in allowing the team to identify significant faults and identify fault correlations between data points. A total 36 geological faults were correlated across the site and this was used to develop an age dating testing programme which identified the most recent movement on the faults at the site occurred outside the current tectonic regime. None of the faults are assessed to be capable. The 3D Geological Fault Model is an asset that the client can maintain and update to confirm and enhance the understanding of the geological faulting at the site as further investigation works take place, including geotechnical investigation and mapping of foundation excavations during construction.

References

Bradley, S., Milne, G., Teferle, F.N., Bingley, R., Orliac, E.: Glacial isostatic adjustments of the British Isles: new constraints from GPS measurements of crustal motion. Geophys. J. Int. **178**, 14–22 (2009)

Cooper, M.R., Anderson, H., Walsh, J.J., Van Dam, C.L., Young, M. E., Earls, G., Walker, A.: Paleogene Alpine tectonics and Icelandic plume-related magmatism and deformation in Northern Ireland. J. Geol. Soc. **169**, 29–36 (2012)

Greenly, E.: Memoirs of the Geological Survey—Anglesey (1919)

Gillespie, M.R., Barnes, R.P., Milodowski, A.E.: British Geological Survey Scheme for Classifying Discontinuities and Fillings. British Geological Survey Research Report, RR/10/05. 56 pp (2011)

Harris, C.: Glacially deformed bedrock at Wylfa head, Anglesey. Geol. Soc. Eng. Geol. Spec. Pub. **7**, 135–142 (1991)

HM Government: Long-Term Nuclear Energy Strategy. BIS/13/630 (2013)

Hunter, A., Easterbrook, G.: The Geological History of the British Isles. The Open University, Milton Keynes (2004)

International Atomic Energy Agency (IAEA): Seismic Hazards in Site Evaluation for Nuclear Installations. IAEA Specific Safety Guide Series No. SSG-9, IAEA, Vienna (2010)

International Atomic Energy Agency (IAEA): Site Evaluation for Nuclear Installations. IAEA Specific Safety Standard Series No. NS-R-3 (Rev. 1), IAEA, Vienna (2016)

Institute of Geological Sciences: Anglesey 1:50,000 Scale Solid and Drift Geology Map. Prepared by Dunham, K, Geological Survey of Great Britain (1974a)

Institute of Geological Sciences: Anglesey 1:50,000 Scale Solid Geology Map. Prepared by Dunham, K, Geological Survey of Great Britain (1974b)

Mallard, D.J., Higginbottom, I.E., Wood, R.M., Skipp, B.O.: Recent developments in the methodology of seismic hazard assessment. In: Dexter-Smith, R. (ed.) Civil Engineering in the Nuclear Industry. Thomas Telford, London (1991)

ONR: Safety Assessment Principles for Nuclear Facilities. Revision 0 (2014a)

ONR: ONR Guide, External Hazards, Nuclear Safety Technical Assessment Guide, NS-TAST-GD-013 Revision 5 (2014b)

Phillips, E.: The Geology of Anglesey, North Wales: Project Scoping Study. British Geological Survey Internal Report, IR/09/05 (2010)

Virtalis: Geovisionary. Version used: 3.0.15 (2016)

Woodcock, N.H., Strachan, R.A.: Geological History of Britain and Ireland, 2nd edn. London, Blackwell (2012)

Modelling Soil Desiccation Cracking Using a Hybrid Continuum-Discrete Element Method

Y. L. Gui, W. Hu, and X. Zhu

Abstract

Shrinkage induced crack pattern is a universal phenomenon, soil cracking due to drying shrinkage is not an exception. In geotechnical engineering, desiccation shrinkage induced cracking has a profound effect on the engineering properties of soils as it can considerably increase the hydraulic conductivity and decreases the shear strength of a soil. Thus, it poses a significant threat to the hydraulic and structural integrity of earthworks. This paper presents the application of the hybrid continuum-discrete element method to simulate soil desiccation shrinkage and cracking with a mix-mode cohesive fracture model. The applicability of the proposed approach is demonstrated through numerical simulation of laboratory and field desiccation tests. The simulation results have shown good agreements with the laboratory and field observations.

Keywords

Soil • Desiccation • Cracking • Simulation

1 Introduction

Desiccation cracking is a commonly occurring phenomenon in unsaturated soil with a high degree of saturation. Its occurrence has a significant effect on the engineering properties of soils as it can considerably increase the hydraulic conductivity and decreases the shear strength of a soil. Thus, it can pose a significant threat to the hydraulic and structural integrity of

earthworks (Peron et al. 2009), dykes (Philip et al. 2014), embankments (Peron et al. 2009; Sima et al. 2014), engineered barriers (Dixon et al. 2002; Rayhani et al. 2007) and can increase the erosion potential of surface soils (Intharasombat et al. 2007; Peron et al. 2009). Understanding of the phenomenon is also important in the field of agricultural engineering due to its role in the transportation of near-surface water, air and nutrients (Arnold et al. 2005) and its potential to increase ground water pollution (Kissel et al. 1974; Arnold et al. 2005; Gui and Zhao 2015). Even in other areas, such as food engineering (Inazu et al. 2005), material engineering (Scherer 1999; Lee and Routh 2004) and chemical engineering (Singh and Tirumkudulu 2007), a clear and robust explanation of desiccation-induced cracking also has great influence.

Many researches have been done to investigate desiccation cracking in soil by experimental study, analytical interpretation and numerical simulation. However, the insight into the phenomenon is still limited. The aim of the paper is to simulate soil desiccation cracking by employing a hybrid continuum-discrete method with a cohesive fracture model. Compared with pure continuum or non-continuum methods, the hybrid method is capable of handling multiple fracture and deformation problems in materials, a considerable advantage over other methods such as finite element method (FEM) and discrete element method (DEM). This is because the traditional FEM has a problem of handling multiple fractures, and the particle deformation is not possible to be considered in conventional DEM (Gui et al. 2015, 2016a, b, 2018) due to the particle's rigidity. In this study, the laboratory and field desiccation tests from literature are simulated. The simulation results show that the fracture model is capable of modelling desiccation cracking.

2 The Theory of the Model

The theory of the hybrid continuum-discrete element method can be found in Gui et al. (2015). The cohesive fracture model presented herein is an extension and application of the

Y. L. Gui (✉)
School of Engineering, Newcastle University,
Newcastle upon Tyne, NE1 7RU, UK
e-mail: yilin.gui@ncl.ac.uk

Y. L. Gui · W. Hu · X. Zhu
State Key Laboratory of Geohazard Prevention and
Geoenvironmental Protection, Chengdu University
of Technology, Chengdu, 610059, China
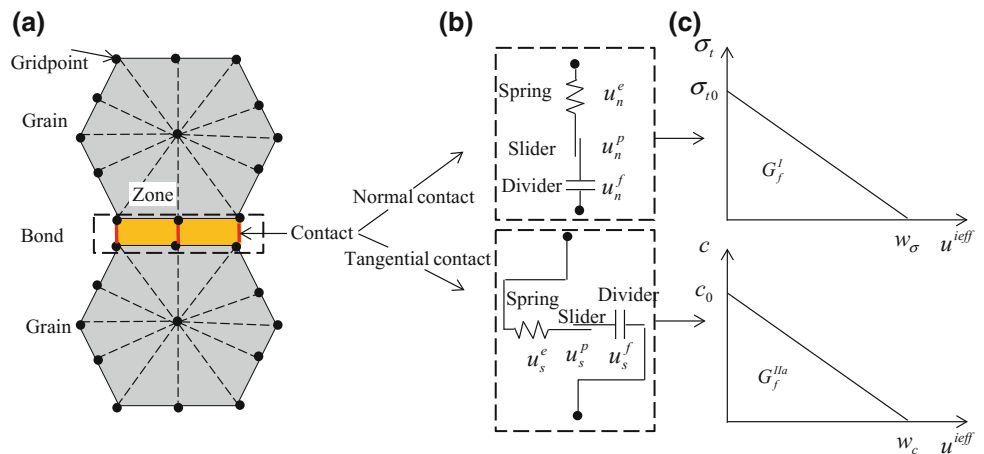
elastic-plastic-damage interface constitutive framework originally presented by Galvez et al. (2002). It takes into account the cohesive effect on both tension and shear. In the model, the fracture interface (i.e., cohesive contact bond between neighbouring grains) is idealised with zero thickness, in other words there is no layer of element embedded at the shared boundary of the two adjacent grains. Figure 1 illustrates the hybrid continuum-discrete element method and the fracture model used in this paper. More information about it can be found in Gui et al. (2015).

3 Modelling of Laboratory Desiccation Test

To investigate mechanism of desiccation induced shrinkage and cracking in fine-grained soils, a series of experimental tests with three different fine-grained materials including Bioley silt, Sion silt and La frasse clay were performed by Peron et al. (2009). The Bioley silt is adopted as experimental result to which the numerical simulations are compared. Three types of tests were performed: unconstrained desiccation, linearly-constrained desiccation and crack pattern tests. Only linearly-constrained desiccation tests are investigated in this simulation. For the experimental test, soil slurry prepared with a water content of 1.5 times liquid limit was poured into a mould with dimension: 295 mm (length) × 49 mm (width) × 12 mm (thickness), and put on a notched metallic base (Fig. 2a). The test was performed in a climate chamber with temperature and humidity controlled in a climate chamber. The temperature used was 19 °C with a variation of 1 °C. The relative humidity was 40%. Due to the existence of these notches, a constraint along the axial direction of the soil sample was created. Therefore, soil samples desiccated under linear constraint experienced paralleled one-directional cracks. These cracks were perpendicular to the sample's longitudinal direction as show in Fig. 4b. An average of 7 cracks occurred.

The linearly-constrained desiccation test was modelled using the parameters presented in Table 1. The experimental sample size (i.e., 295 mm × 12 mm) and the shape of the notched metallic base are followed in the modelling as shown in Fig. 2a. To capture the randomness of crack initiation and propagation, Voronoi tessellation technique was adopted. The average size of the Voronoi grains was 1 mm (Fig. 2a) with total of 3760 blocks included in the soil model (excluding the block of steel base). The shared boundary of each pair of blocks was modelled using the mix-mode cohesive fracture model presented in Fig. 1. For each block, it is meshed into a few finite difference zones and they are linear elastic. For the boundary condition applied in the simulation, the bottom of the metallic base is fixed along the vertical direction while it is free along the horizontal direction. Considering the geometry of the soil sample, plane-stress mode was adopted. A total isotropic strain of 5% was applied on each zone of all soil blocks along horizontal and vertical direction, separately, during the whole simulation through 50 steps, which means an isotropic strain of 0.1% was applied on each soil grain in each step.

Figure 2 shows the desiccation cracking process at different time steps. It can be seen that the cracks generally start from the top surface of the soil model. The cracking path is generally not straight due to the discrete nature of the numerical method. It is noted that the first crack is initiated randomly and a few primary cracks are formed first. The primary soil cells bounded by the primary cracks are then segregated by the secondary cracks. At the end of the desiccation, 9 fully propagated cracks are formed which are close to the experimental result although the material properties used in the paper are not same as the real experimental parameters. Diffuse cracking which occurred at the end of the model is also observed in the simulation (right end of Fig. 2f). During the simulation, the displacement at the right end of the model was monitored as shown in Fig. 3. It can be

Fig. 2 Desiccation cracking process of Bioley silt: **a** step 0; **b** step 10; **c** step 20; **d** step 30; **e** step 40; **f** step 50 (final crack pattern) (Gui et al. 2016b)
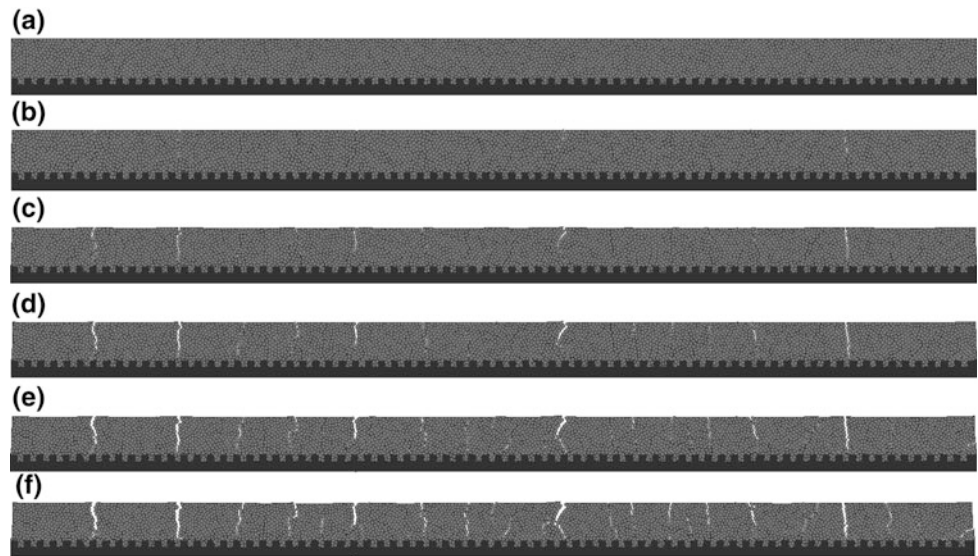

Table 1 Summary of material parameters used in the linearly-constrained desiccation simulation of Bioley silt (Gui et al. 2016b)

Property	Soil	Base
Density (kg/m^3)	1440	8000
Elastic modulus (MPa)	4.0	200×10^3
Poisson's ratio	0.2	0.2
Friction angle (°)	20	5
Cohesion (kPa)	10.0	1.4
Tensile strength (kPa)	4.0	0.7
Fracture toughness in mode-I (kPa/m$^{0.5}$)	1.0	–
Fracture toughness in mode-II (kPa/m$^{0.5}$)	1.5	–

Note The cohesion, friction and tensile strength for the base on the above table are the soil-base interface parameters

seen that the displacement increases as the desiccation progresses. The displacement at the end of modelling is 6.64×10^{-4} m considering the symmetric geometry, the calculated strain along horizontal direction is 4.5% and it is smaller than the input strain (i.e., 5%). This can be explained by the occurrence of the cracks. More specifically, the displacement at the model end can be decreased by the occurrence of cracks. Thus, with the time progressing or with more and more cracks occurred, the rate of strain increases reduces. In order to investigate the influence of the base-soil interface properties, a soil-slab siting on non-notched base was simulated. The obtained final number of cracks from the simulation is shown in Fig. 4. Again, the results have demonstrated the influence of base-soil interface properties on desiccation cracking.
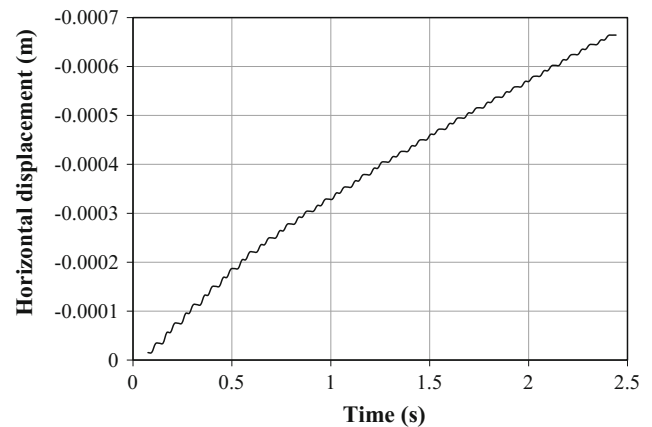
Fig. 3 Simulated horizontal displacement at the right end of the sample (Gui et al. 2016b)
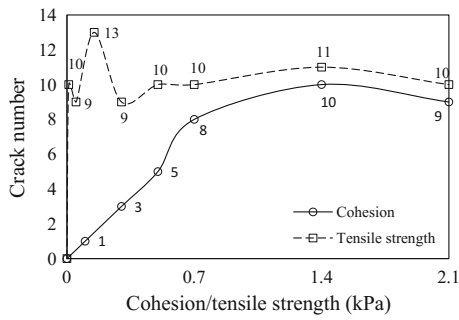
Fig. 4 The evolution of crack number with the change of cohesion and tensile strength of soil-base interface (Gui et al. 2016b)

4 Modeling of Field Desiccation Test

4.1 Numerical Model

A field experiment by excavation to three different levels from top to bottom to investigate desiccation cracking in top soil, weathered and intact clay under restrained conditions, respectively, was carried out by Konrad and Ayad (1997) at the experimental site of Saint-Alban, Quebec, Canada. In their investigation, the moisture content and suction profiles were recorded. It was found that the gravimetric water content decreased significantly in the soil close to the surface, while the deeper soil had a much smaller decrease in water content. This effect was most pronounced in the upper 40 cm. The suction profile was similar to the water content. Figure 5 show the suction profile monitored in the whole desiccation test. It was also found that desiccation cracking occurred in less than 17 h after the start of the test for both intact and weathered clays with average crack spacing of 20–24 cm for the intact clay. It was also found that horizontal crack can occur and propagate horizontally at certain

depth in the intact clay, thereby soil wedges forming and they being easily removed.

A 2-dimensional model with length of 1.2 m and depth of 0.7 m is built, as shown in Fig. 6. Plane-stress mode is used. The model is discretized using Voronoi polygon. The interface of the polygons is treated using the cohesive fracture model. The left, bottom and right boundaries are fixed using roller boundary. The model is divided into six layers bounded by the levels where the suction history was measured in the field desiccation test. In each layer the suction is interpolated linearly. Since the soil becomes harder and harder during desiccation, the elastic modulus of the soil is calculated based on the initial suction value (289 Pa) measured in the field through the following equation (Amarasiri and Kodikara 2013).

$$E = E_0 + 24(1 - 2\upsilon)(s - s_0) \tag{1}$$

where E and E_0 are the updated elastic modulus and initial elastic modulus, respectively. υ is the Poisson's ratio. s and s_0 are the updated suction and initial suction. The increase of

Fig. 5 The measured suction profile during the field desiccation test (Konrad and Ayad 1997)
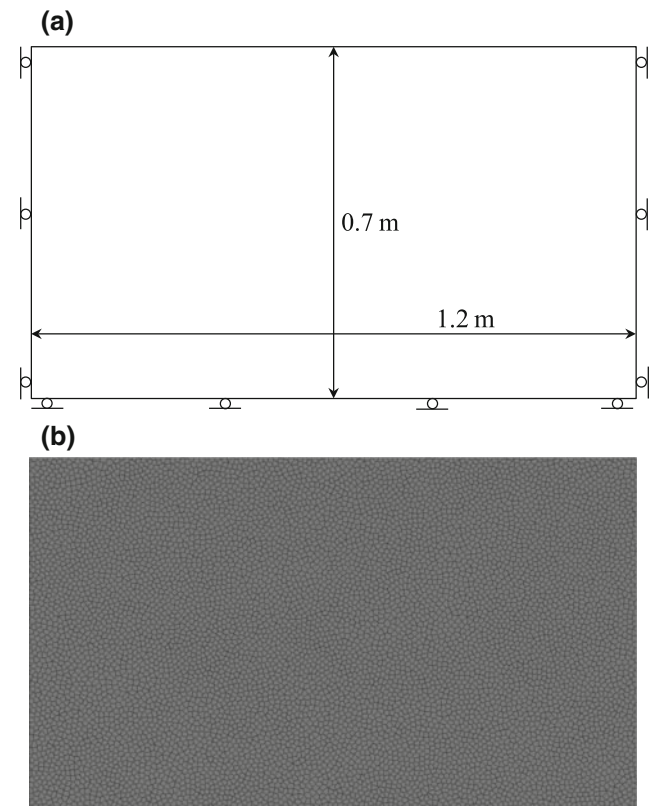
Fig. 6 **a** Physical model and **b** numerical model of the soil sample (Gui et al. 2018)

Table 2 Summary of soil parameters used in the desiccation simulation (Gui et al. 2018)

Density (kg/m³)	1440
Elastic modulus (MPa)	5.0
Poisson's ratio	0.3
Friction angle (°)	19
Cohesion (kPa)	30.0
Tensile strength (kPa)	15.0
Normal stiffness (Pa/m)	4×10^{10}
Shear stiffness (Pa/m)	2×10^{10}
w_σ(m)	1.875×10^{-6}
w_c(m)	7.5×10^{-6}

the effective stress due to desiccation is following the effective stress principle as

$$\Delta\sigma' = \Delta\sigma_{net} + \chi\Delta s \qquad (2)$$

where σ', σ_{net} and χ are the effective stress, net stress and effective stress parameter accounting the contribution of suction to the value of effective stress. During the soil desiccation shrinkage, the soil is almost saturated, even after cracking. Therefore, in this note, the effective stress parameter is set to $\chi = 1$ (Khalili et al. 2004). Due to that the value of the net stress has no change, the effective stress change is only contributed to by the increase of the suction. The initial parameters used in the modelling are listed in Table 2. During the simulation, the settlements at various depth are monitored, and the crack initiation time and crack propagation pattern are recorded.

4.2 Results and Discussions

Figure 7 shows the micro-crack initiation and propagation. It can be seen that the desiccation crack starts from the ground surface. At some locations, the cracks initiate prior to other locations. These first occurred cracks are referred to as primary crack in soil desiccation (Fig. 4a). With desiccation progressing, more cracks (secondary cracks) are initiated within the aggregates formed by the primary cracks. The cracks propagate into the deeper level, majorly vertically. Due to the discrete nature of the method, the crack propagating path is not straight. Some of the cracks bifurcate when they propagate (Fig. 7d, e). The branches of the bifurcated cracks propagate nearly horizontally and meet each other, resulting in the formation of horizontal cracks. Therefore, soil wedges are formed close to the surface (Fig. 7f). The final crack can reach as deep as more than 60 cm from the surface. Figure 8 investigates the surface crack pattern in the field soil desiccation modelling. The parameters used are shown in Table 2. Two different shaped models are used: rectangular and circular, with roller boundary. In both simulations, desiccation-induced soil polygons are formed. However, there are more cracks are formed in the circular model.

5 Conclusions

The paper presents the numerical simulation of soil desiccation tests in both laboratory and field using a hybrid continuum-discrete element method with a mix-mode cohesive fracture model. In the simulation, the desiccation induced soil hardening is considered by adopting an empirical equation for soil elastic modulus for field desiccation test. It is found that the desiccation phenomena can be reasonably replicated, especially, the sub-horizontal crack is successfully reproduced. The present findings demonstrate that the mix-mode cohesive fracture model is able to handle desiccation induced multi-cracks in the field soil desiccation using the hybrid continuum-discrete element method.
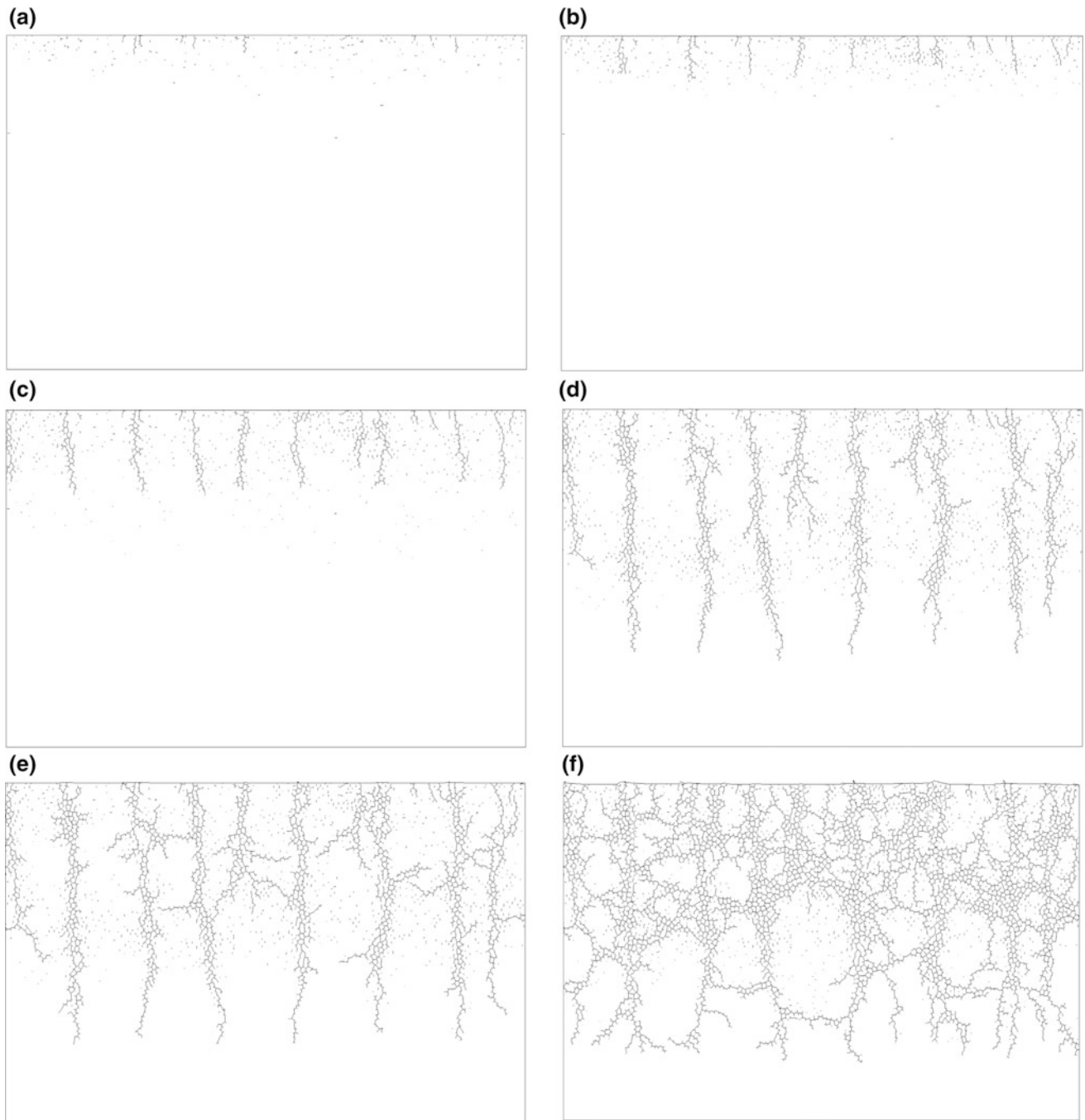
Fig. 7 Modelled micro-crack evolution during the field soil desiccation (Gui et al. 2018)

(a)

(b)
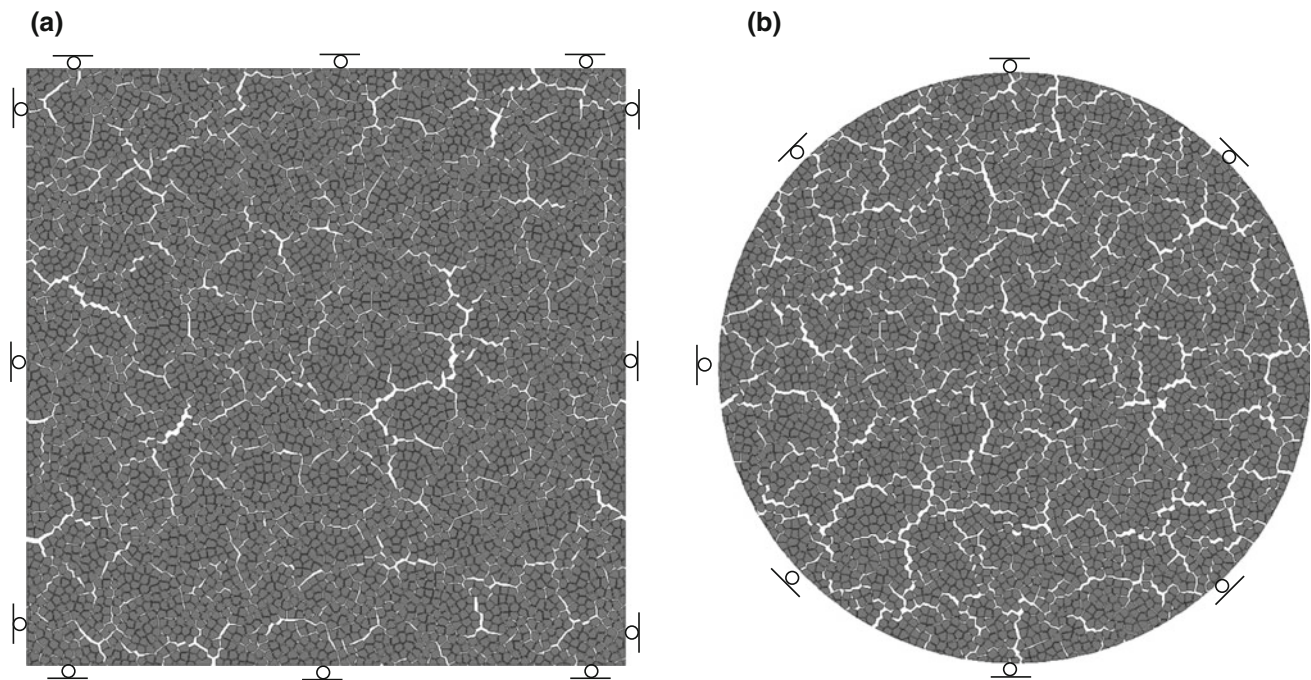
Fig. 8 Numerical final crack pattern obtained by different boundary condition

References

Amarasiri, A.L., Kodikara, J.K.: Numerical modelling of a field desiccation test. Geotechnique **63**(11), 983–986 (2013)

Arnold, J.G., Potter, K.N., King, K.W., Allen, P.M.: Estimation of soil cracking and the effect on surface runoff in a Texas Blackland Prairie watershed. Hydrol. Process. **19**, 589–603 (2005)

Dixon, D., Chandler, J., Graham, J., Gray, M.N.: Two large-scale sealing tests conducted at atomic energy of Canada's underground research laboratory: the buffer-container experiment and the isothermal test. Can. Geotech. J. **39**(3), 503–518 (2002)

Galvez, J.C., Cervenka, J., Cendon, D.A., Saouma, V.: A discrete crack approach to normal/shear cracking of concrete. Cem. Concr. Res. **32**, 1567–1585 (2002)

Gui, Y., Ha, H.H., Kodikara, J.: An application of a cohesive fracture model combining compression, tension and shear in soft rocks. Comput. Geotech. **66**, 142–157 (2015)

Gui, Y., Ha, H.H., Kodikara, J., Zhang, Q.B., Zhao, J., Rabczuk, T.: Modelling the dynamic failure of brittle rocks using a hybrid continuum-discrete element method with a mixed-mode cohesive fracture model. Int. J. Impact Eng **87**, 146–155 (2016a)

Gui, Y.L., Zhao, Z.Y., Kodikara, J., Ha, H.H., Yang, S.Q.: Numerical modelling of laboratory soil desiccation cracking using UDEC with a mix-mode cohesive fracture model. Eng. Geol. **202**, 14–23 (2016b)

Gui, Y., Zhao, G.F.: Modelling of laboratory soil desiccation cracking using DLSM with a two-phase bond model. Comput. Geotech. **69**, 578–587 (2015)

Gui, Y., Hu, W., Zhao, Z.Y., Zhu, X.: Numerical modelling of a field soil desiccation test using a cohesive fracture model with Voronoi tessellations. Acta Geotech. **13**, 87–102 (2018)

Inazu, T., Iwasaki, K., Furuta, T.: Stress and crack prediction during drying of Japanese noodle (udon). Int. J. Food Sci. Tech. **40**, 621–630 (2005)

Intharasombat, N., Puppala, A.J., Williammee, R.: Compost amended soil treatment for mitigating highway shoulder desiccation cracks. J. Intrastruct. Syst. **13**(4), 287–298 (2007)

Khalili, N., Geiser, F., Blight, G.E.: Effective stress in unsaturated soils: review with new evidence. Int. J. Geomech. **4**(2), 115–126 (2004)

Kissel, D.E., Ritchie, J.T., Burnett, E.: Nitrate and chloride leaching in a swelling soil. J. Environ. Qual. **3**(4), 401–404 (1974)

Konrad, J.M., Ayad, R.: Desiccation of a sensitive clay: field experimental observations. Can. Geotech. J. **34**, 929–942 (1997)

Lee, W.P., Routh, A.F.: Why do drying films crack? Langmuir **20**(23), 9885–9888 (2004)

Peron, H., Hueckel, T., Laloui, L., Hu, L.B.: Fundamentals of desiccation cracking of fine-grained soils: experimental characterisation and mechanisms identification. Can. Geotech. J. **46**(10), 1177–1201 (2009)

Philip, L.K., Shimell, H., Hewitt, P.J., Ellard, H.T.: A field-based tests cell examining clay desiccation in landfill liners. Q. J. Eng. Geol. Hydrogeol. **35**, 345–354 (2014)

Rayhani, M.H.T., Yanful, E.K., Fakher, A.: Desiccation-induced cracking and its effect on the hydraulic conductivity of clayey soils from Iran. Can. Geotech. J. **44**, 276–283 (2007)

Scherer, G.W.: Structures and properties of gels. Cem. Concr. Res. **29** (1999), 1149–1157 (1999)

Sima, J., Jiang, M., Zhou, C.: Numerical simulation of desiccation cracking in a thin clay layer using 3D discrete element modelling. Comput. Geotech. **56**, 168–180 (2014)

Singh, K.B., Tirumkudulu, M.S.: Cracking in drying colloidal films. Phys. Rev. Lett. **98**(21) (2007). https://doi.org/10.1103/physrevlett.98.218302

Conceptual Engineering Geological Models

Steve Parry, Fred Baynes, and Jan Novotný

Abstract

Engineering geological models should form a fundamental component of any geotechnical project as they provide a systematic methodology to support all of the engineering geological thought processes that must be worked through for successful project completion. The use of models as an approach to solving engineering geological problems, with the inherent requirement for prediction and verification, is also ideally suited to training and education. IAEG Commission C25 (Parry et al. in Bull Eng Geol Environ 73:689–706, 2014) proposed that engineering geological models could be divided into two profoundly different approaches and therefore different model types. Observational and Conceptual. However, the C25 Report perhaps lacks clarity regarding the differences between these two types of models and the way in which they work together. The conceptual approach is based on understanding the relationships between engineering geological units, their likely geometry, and anticipated distribution. This approach, and the models formed, are based on concepts formulated from knowledge and experience. When these models are proficiently developed they provide an extremely powerful tool for appreciating and communicating what is known about a site, what is conjectured and where significant uncertainties may remain. The conceptual model provides a framework for the evaluation of observational data which then forms an observational model which is constrained by real data in 3D space and time. The development of conceptual models should be a core activity for engineering geologists. The paper discusses the generation of conceptual models, gives examples of the problems that can arise when they are not used, and provides guidelines for their development.

1 Engineering Geological Models

The subject of engineering geological models was discussed in a report produced by IAEG Commission 25 (Parry et al. 2014) where an engineering geological model was defined as "any approximation of the geological conditions, at varying scales, created for the purpose of solving an engineering problem".

The C25 Report (ibid) recommended that engineering geological models should form a fundamental component of any geotechnical project as they provide a systematic methodology to support all of the engineering geological thought processes that must be worked through for successful project completion. The use of models as an approach to solving engineering geological problems, with the inherent requirement for prediction and verification, is also ideally suited to training and education. In particular, the C25 Report concluded that engineering geological models provide:

- an essential tool for engineering and geological quality control;
- a transparent way of identifying project-specific, critical engineering geological issues, parameters and risks; and
- the basis for designing the scope, the method and assessing the effectiveness of site investigations.

S. Parry (✉)
Parry Engineering Geological Services Ltd., Derbyshire, UK
e-mail: parrysteve@gmail.com

F. Baynes
Baynes Geologic Pty Ltd., Subiaco, Australia

J. Novotný
Czech Geological Survey, Prague, Czech Republic

J. Novotný
Faculty of Science, Charles University, Prague, Czech Republic

Despite the fact that models form a core part of engineering geological practice, Sullivan (2010) noted that the subject is not well covered in the literature, is rarely taught in universities and that a paucity of information exists about models, what they should depict or contain and how they should be prepared. Furthermore, they are either poorly defined or absent from many important guidelines and specifications e.g. they are not discussed in the relevant Eurocodes relating to geotechnical design. (BS EN 1997-2: 2007).

2 Engineering Geological Model Types

The IAEG Commission 25 Report (Parry et al. 2014) proposed that the development of engineering geological models could be divided into two profoundly different approaches and therefore different model types.

The conceptual approach is based on understanding the relationships between engineering geological units, their likely geometry and anticipated distribution. This approach, and the models that are created, are based on concepts formulated from geological knowledge and experience. Such models potentially involve a relatively high degree of uncertainty which is directly related to the type and amount of existing data and the knowledge and experience of those involved. However, when these models are proficiently developed they provide an extremely powerful tool for appreciating and communicating what is known about a site, what is conjectured and where significant uncertainties may remain.

The observational approach is based on understanding the observed and measured distribution of engineering geological units and processes. These models are therefore based on data that relates to actual 3D space or time and are thus constrained by surface or sub-surface observations. Importantly, they should verify or refine the conceptual engineering geological model. In particular, they should focus on potential engineering issues and risks identified in the conceptual engineering geological model but about which little or nothing is known for the specific site. Observational engineering geological models are particularly relevant at the engineering design stage. Later stage verification and refinement of the observational engineering geological model should take place during construction. If observational models are developed initially using high quality conceptual models, the uncertainties associated with observational models should be reduced. However, the derivation of an appropriate observational model is still dependent upon the knowledge and experience of those involved.

Whilst the two approaches are fundamentally different, both are based on an understanding of the geological conditions on a variety of scales, with the conceptual model providing a framework for the evaluation of observational data. The development of conceptual models should be a core component of what engineering geologists do. Their geological training allows them to understand how the ground conditions at a particular site formed and what geological variations may be present, often on limited data, and their engineering understanding allows them to evaluate which geological conditions, if present, could have an engineering significance to the project. As such, the development of engineering geological models requires as its basis a thorough understanding of geological science.

In the C25 Report there was, perhaps, a lack of clarity regarding the differences between these two types of models and the way in which they work together. In practice these two types of model are part of a spectrum of models which should be developed. What is clear is that a good engineering geological model contains more than just observations—it includes the concepts that tie these observations together and increases their value and applicability. It is postulated that there is an "engine" that drives any engineering geological modelling process which involves consideration of the entirety of the model and the assessment of the levels of "harmony" and the identification of "anomalies" within the model (Fig. 1). A good model can be identified by the level of agreement between the conceptual and observational models and it is only when there is a good model that it is appropriate to simplifying the model for the purpose of analysis and design.

3 Examples of Getting the Conceptual Model Wrong

The following two cases studies show what can happen if the conceptual model is incorrect.

Case A—Cut Slopes in Clay

Cut slopes were designed for two sites in clay of different geological ages, based on the assumption that the clay at both sites was homogenous, with analytical modelling assuming high effective cohesion resulting in deep seated failures. However, conceptual models based on knowledge and experience suggest that at neither site were such assumptions appropriate.

Figure 2 illustrates how a zone of reduced shear strength and increased secondary permeability are typically present and influence slope stability. This weathering zone typically penetrates 1–2 m below the ground surface. Landslides are commonly controlled by this zone and are typically shallow and translational. The use of this model together with the shear strength of the zone with an effective cohesion equal to
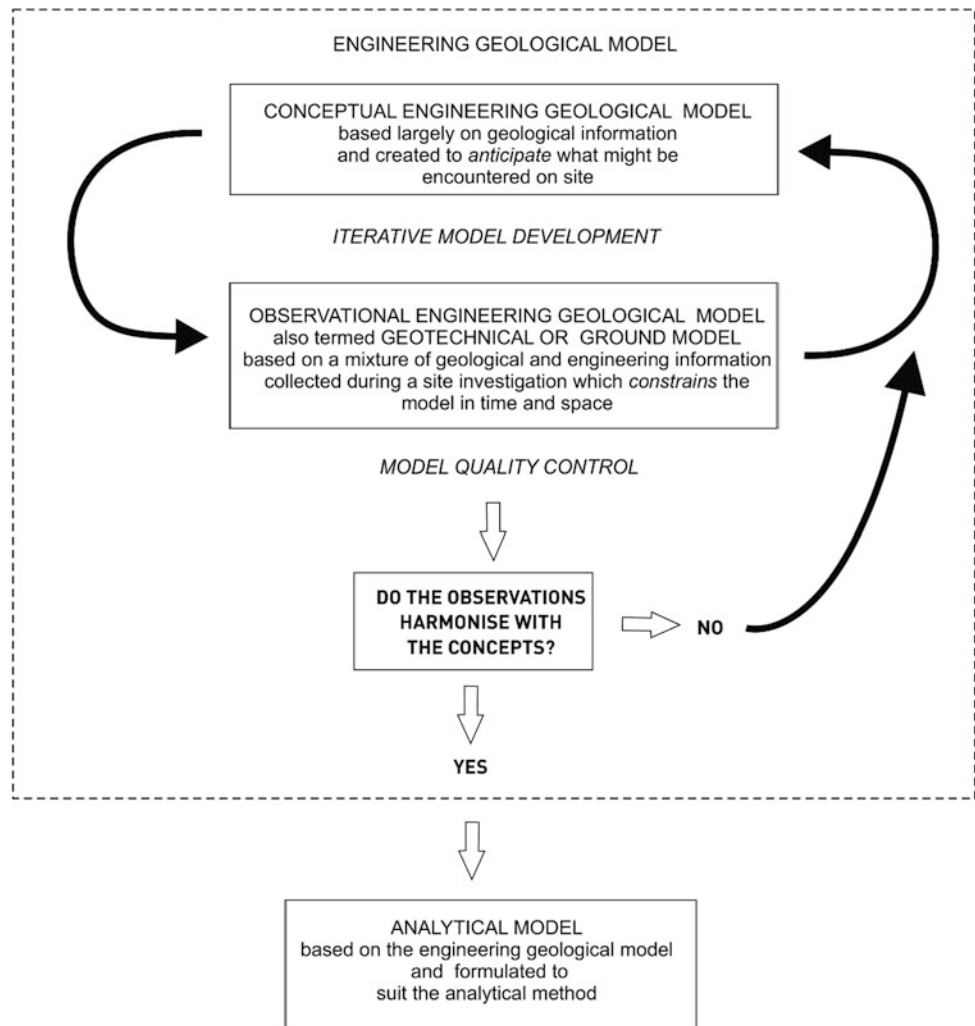
zero, results in more appropriate shallow failures being generated during analysis calculated.

Figure 3 illustrates the influence of discontinuities on cut slopes in Tertiary clay. The discontinuities are a result of syn-depositional, tectonic and gravitational processes. If the clay is assumed to be homogenous, such discontinuities are often over looked in the ground investigation resulting in inappropriate strength values and incorrect methods of analysis. The discontinuities result in the clay effectively behaving as a rock mass. In addition, the discontinuities often have slickensides resulting in their shear strength being at or close to residual strength.

This case study demonstrates how the incorrect conceptual model has a cumulative effect throughout the project by influencing the selection of ground investigation methods (sampling and laboratory testing), the interpretation and the geotechnical analysis and in the worst case scenario resulting in inappropriate design and failure.

Case B Tunnelling induced Settlement, Hong Kong. During offshore tunnelling associated with the Harbour Area Treatment Scheme (HATS), unexpected settlement occurred at Tseung Kwan O, a town founded on reclaimed land.

Initially the cause of the settlement was unclear as there was no immediate link to the HATS project which was over 1 km away. A subsequent investigation determined that over 20 m of ground water pressure loss within the rock mass overlying the tunnel due to construction inflows was the only credible cause of the settlement. This event led to a study of other monitoring data in the general area of Tseung Kwan O and settlement was noted up to 2 km from the tunnel.

Figure 4 shows the hydrogeological setting of Tseung Kwan O Bay and the HATS Tunnel. A review of the tunnelling records revealed that in the first 1700 m of tunnel large water inflows were encountered through the generally highly fractured tuffs, despite significant pre-grouting and back-grouting efforts to control water ingress.

Although some peaks in water inflow rate appeared to be related to faulting and joint frequency, the average water inflow rate steadily increased to about 7000 litres per minute by the time the tunnel had been progressed to chainage 1700.

Fig. 2 Conceptual engineering geological model for slope stability evaluation in clays affected by weathering (Novotný 2015)
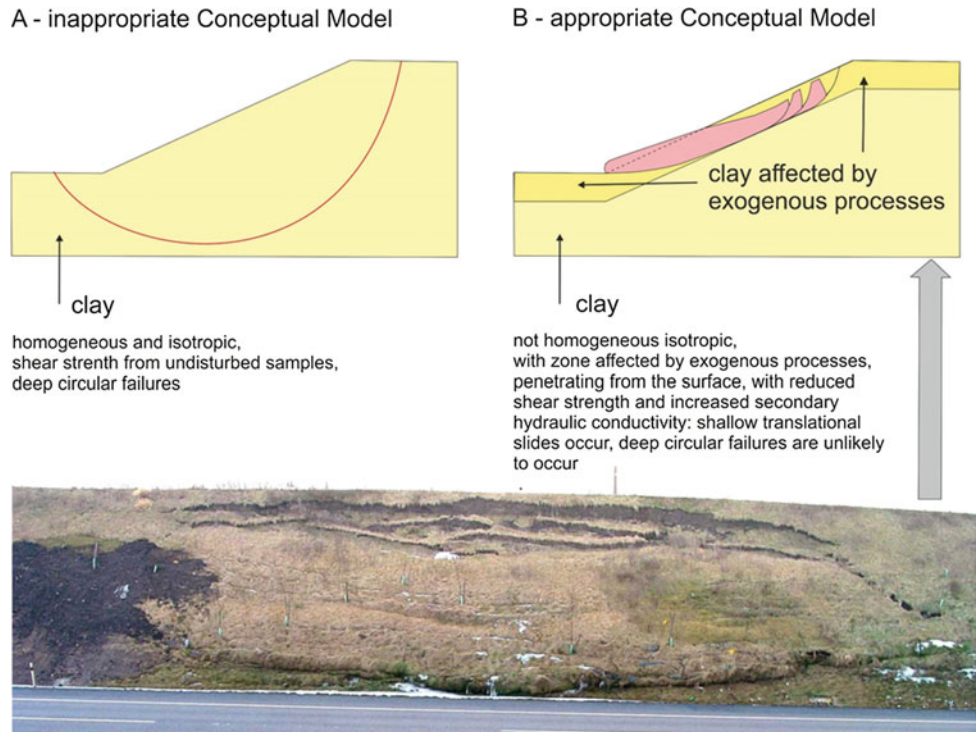
Fig. 3 Conceptual engineering geological model for slope stability evaluation in Tertiary clays, containing discontinuities (Novotný 2015)
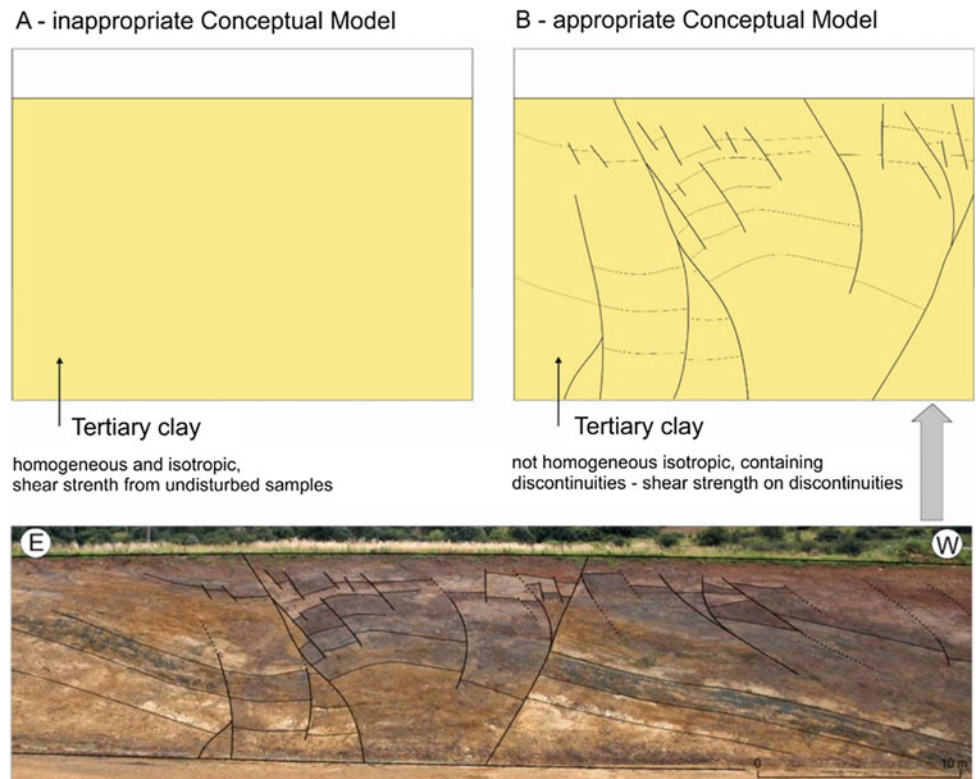
The geological model and inferred groundwater drawdown mechanisms are shown in Fig. 5. Tseung Kwan O Bay is a palaeovalley which has probably been influenced by weathering along a system of NNW-trending faults (Fig. 4) in the generally closely-jointed tuff rock mass. Alluvial sand/cobble channels run along the axis of the valley which are overlain by clayey alluvium and/or marine deposits upon which the reclamation has been placed. The water inflows

into the tunnel and the prevention of effective recharge by the marine deposits led to under-drainage of the reclamation via pathways through the rock mass, saprolite and alluvial sand channels resulting in significant settlement.

That such embayments in Hong Kong are fault control was known, as was the fact that significant paleo valleys extend offshore from the present day coastline. During the Pleistocene sea level low stand these valleys were occupied by major braided river systems (these sand bodies are exploited as a major sources of offshore fill) and were subsequently draped with marine clay during the Holocene marine transgression. However, the combined implications of such features on groundwater drawdown due to the tunnel construction was not recognised largely due to the lack of robust conceptual models.

4 Developing Conceptual Models

Four fundamental inputs should be considered when developing conceptual models:

- Setting. This is the general nature of the area surrounding the site. This should include consideration of both "big

picture" information including geographical location, tectonic setting, climate (past, present and future) as well as site specific information such as landforms and geomorphological processes. It is based on a review of all relevant information including topographic and geological maps, data bases, memoirs etc.

- Stratigraphy. This relates to the geological units that are anticipated to be present at the site and is most commonly extracted from the legend of geological maps. A geological map is a 2D representation of 3D situation as such maps are geological models based on both conceptual and observational approaches. Geological maps, and more importantly their interpretation in terms of engineering geological issues, are a fundamental building block of engineering geological models. Geological maps indicate rock types present and their age. This enables environments of formation to be evaluated which allows estimates of geological variability in terms of rock types, extent, thickness and form. Information on age allows an evaluation of subsequent modification since formation in terms of tectonics and weathering.

- Structure. These include both the bounding surfaces of engineering geological units and their nature but also discontinuities within the units. In addition to material
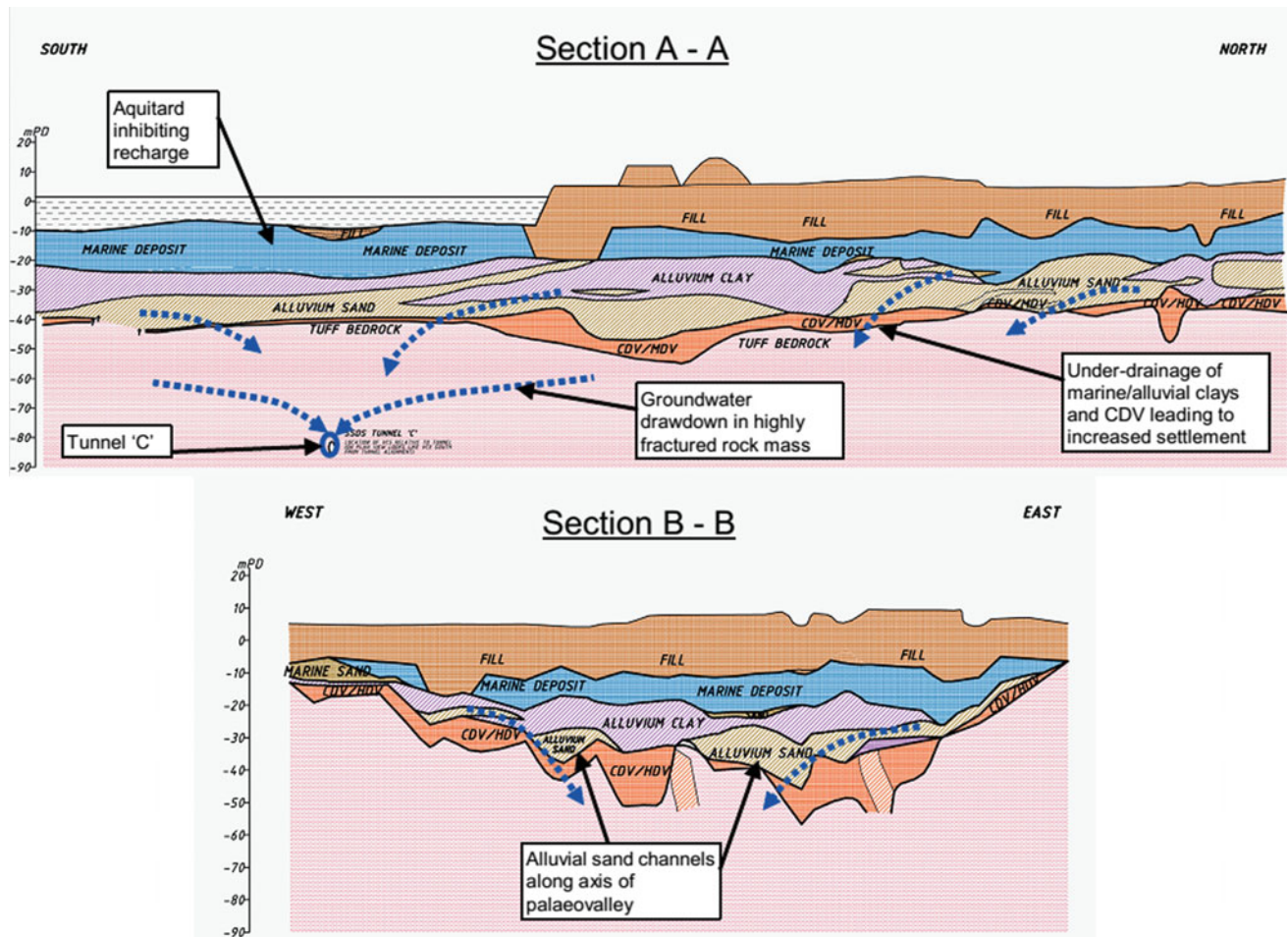
Fig. 5 Cross sections showing the inferred mechanism of under drainage during tunnelling (GEO 2000). Refer to Fig. 4 for locations

types, an understanding of boundary conditions is critical to the development of good engineering geological models. Bounding surfaces can take many forms including bedding planes, joints, faults, unconformities, igneous contacts etc. Each type of boundary is associated with different modifying geological conditions and result in distinct variations in geotechnical parameters.

- Surface and sub-surfaces processes and levels of activity. In addition to the evaluation of static geology on going geological process require identifying and evaluating. These include landslides, floods, swelling soils, earthquakes, gas etc.

However, a desk study is insufficient on its own to develop an engineering geological model. The extent to which potential variations at a site can be identified from the available information will be dependent on the geological and engineering geological knowledge and experience of the team of people involved in the project. This will affect both the identification of individual geological factors that could potentially affect the project, as well as the interaction between each individual factor.

In essence, the conceptual model tells the story of how the site came to be. Putting together that story provides accesses to the entirety of the model, the sum of which is considerably more powerful than its individual parts. It is this story that allows the identification of potential problematic ground conditions that may exist at a site prior to observations being made.

5 Conclusions

The generation of models should be a fundamental component of engineering geological practice and as such is required for all sites regardless of project type of geological complexity. Such models provide the fundamental framework for the assessment of baseline conditions and their quantification. As such any deviations away from the model will equate to areas of uncertainty and potential geotechnical risk.

Conceptual models are formulated from knowledge and experience and potentially involve a relatively high degree of uncertainty which is directly related to the type and amount of existing data and the knowledge and experience of those involved. However, when such models are proficiently developed they provide an extremely powerful tool for appreciating and communicating what is known about a site, what is conjectured and where significant uncertainties may remain.

The conceptual model tells a story, the sum of which is considerably more powerful than its individual parts. It is this story that allows the identification of potential problematic ground conditions that may exist at a site prior to observations being made.

Observational models are based on the observed and measured distribution of engineering geological units and processes that have been anticipated in the conceptual model. These data are related to actual space or time and are constrained by surface or sub-surface observations. Whilst observational data, such as boundaries in boreholes, are constrained in x, y, z space, the conceptual model is used to establish the relationships that support interpretation of geological surfaces between such points.

References

Eurocode BS EN 1997-2:2007: Eurocode 7. Geotechnical design. Ground investigation and testing (2007)

GEO: Engineering geological practice in Hong Kong geotechnical engineering office. Hong Kong Government (2000)

Novotný, J.: Geological approach to landslide evaluation. Prague Geotechnical Days 2015, 11–12 May 2015, Prague (2015)

Parry, S., Baynes, F.J., Culshaw, M.G., Eggers, M., Keaton, J.F., Lentfer, K., Novotný, J., Paul, D.: Engineering geological models—an introduction: IAEG Commission 25. Bull. Eng. Geol. Environ. **73**(3), 689–706 (2014)

Sullivan, T.D.: The geological model. In: Williams, A.L., Pinches, G.M., Chin, C.Y., McMorran, T.J., Massey, C.I. (eds.) Geologically active. In: Proceedings of the 11th Congress of the International Association for Engineering Geology and the Environment, Auckland, New Zealand. CRC Press, London, pp. 155–170

Pitfalls in Generating an Engineering Geological Model, Using a Landslide on the D8 Motorway near Dobkovičky, Czech Republic, as an Example

Pavel Pospisil, Naďa Rapantova, Petr Kycl, and Jan Novotny

Abstract

The variability of ground conditions resulting from different types of rocks with a varying origin, degree of weathering, tectonic deformation, hydrogeological conditions, and other factors poses considerable problems for engineering geological model generation and the subsequent analysis of rock mass behaviour. The authors demonstrate, through a case study of the D8 motorway in the Czech Republic, the problems that can occur during construction if the engineering geological model generation is not applied correctly during construction. It demonstrates the importance of the conceptual model and its application at the beginning of the project. The case study is also used to present experience with an observational engineering geological model generation. The simplification of the complex geological setting represented the key problem of the observational model generation for engineering purposes. The authors critically assessed the available archive data, the ability to generate 3D models using various software (RockWorks, GMS), and transferring engineering geological model to simulation software (MIDAS GTS NX). It is very demanding to construct the geometry of individual lithostratigraphic units and to define quasi-homogeneous engineering geological units based on their characteristic values for the simulation of the slope stability of the rock massif.

P. Pospisil (✉) · N. Rapantova
VSB-Technical University of Ostrava, Ostrava, Czech Republic
e-mail: pavel.pospisil@vsb.cz

P. Kycl · J. Novotny
Czech Geological Survey, Prague, Czech Republic

J. Novotny
Faculty of Science, Charles University, Prague, Czech Republic

1 Introduction—Theoretical Approach to Engineering Geological Model Generation

Engineering geological models should be the basic element of each geotechnical project. These models provide a systematic methodology for the description and understanding of all engineering geological processes that must be integrated for the successful completion of a project (Parry et al. 2014). The IAEG C25 commission, which deals with the development of engineering geological models, distinguishes conceptual and observational engineering geological models (Parry et al. 2014). The conceptual approach is based on understanding the relationships between engineering geological units, their likely geometry, and anticipated distribution. The observational approach is based on the observed and measured distribution of engineering geological units and processes.

In a general, the geotechnical risk faced by an engineering project is inversely proportional to the level of details and accuracy contained in an engineering geological model. The better the model reflects actual conditions, the lower the residual risk. However, it is not possible to define each detail of the geological environment (Parry et al. 2014).

Independently of the type of model, various authors formulated some basic principles for the correct compilation of engineering geological models (Stapledon 1982; Varnes 1974; Schumm 1991; Baynes 2010; Sullivan 2010; Parry et al. 2014):

1. To generate the conceptual model as soon as possible, otherwise it is not possible to test and improve the model when more details become available.
2. Understanding the "geology" (i.e. the origin, structure, properties, and mechanical behaviour of a rock massif), which is based on basic principles such as the principle of uniformitarianism and the law of superposition must be kept.

3. It is always necessary to move from a wider view to specific details of the project site (from a broad scale to the particular details—from far field to near field).

4. To focus on the geological conditions that are relevant for project implementation and then make a simplification appropriate for the model.

5. It is necessary to continuously test and challenge the model at all project stages and, as necessary, to review and edit the model. In addition, it is critical to use the method of multiple working hypotheses to avoid the exclusion of the correct explanation.

6. It is necessary to specify and adhere to all important geological details and to try to simplify and clearly communicate critical aspects (but not to lose any important details).

Of key importance is the application of conceptual engineering geological models as these provide the basis to define key questions with respect to the interaction of the geological environment and the construction, and to evaluate uncertainties and unknowns. If a conceptual model is compiled incorrectly, all consequential engineering geological work may be incorrect, such as the observational model and design work (Parry et al., in print). Based on the conceptual approach, the general properties and behaviour of the engineering geological units can be assumed. Rocks are heterogeneous, i.e. they have various material properties (strength, deformation, hydraulic, and other properties) and they are often anisotropic. The properties of the geological environment are influenced by endogenic processes (volcanism, brittle deformation—joints, discontinuities, faults, micro- and macroscopic fabrics, and plastic deformational structures such as folds and flexures). The geologic environment is also affected by exogenic processes including chemical and mechanical weathering (variable depth as far as the bedrock), erosion, groundwater flow, karst phenomena, and slope deformations.

Only by achieving conformity between conceptual and observational models can an appropriate basis for selecting a suitable calculation model.

The paper describes the method of generation an engineering geological model for the construction of the D8 motorway in the north of the Czech Republic leading from Prague to Dresden. Unfortunately, this method was not used during the design work and the result was a landslide that blocked the motorway (Fig. 1). Following the landslide, the area was thoroughly examined, and an observational engineering geological model was generated which is presented in this paper.

2 Conceptual Model

To comprehensively assess the engineering geological setting in the area of interest, it was necessary when generating the conceptual model to use all available data of the wider surroundings; in particular archival data from the Czech Geological Survey. The time interval for this needs to be significantly extended compared to typical evaluations, i.e. the total geological history approach has to be applied. It was necessary to understand and evaluate all geological processes from the Mesozoic to the present time. This includes, the character of sedimentation of Upper Cretaceous sedimentary rocks, their tectonic deformation, if any, and degree of weathering, and erosion. The same applies to superposed Tertiary Formations, primarily volcanoclastic and effusive rocks, and the overlying Quaternary Formations, which are very heterogeneous.

The study area is located in the Central Bohemian Uplands, where it is possible to identify by careful morphological analysis a large number of slope deformations that have been activate from the end of Pleistocene to the present (Pašek and Janek 1972). The study area is made up of layered basalt flows separated by tectonics into blocks, that overly the beds of plastic rocks. The blocks of rigid basalt are slowly creeping down the slope and they are often accompanied by landslides in plastic rocks (Rybář and Nemčok 1968). The conceptual model of this type of failure is discussed in detail in Novotný (2014). Figure 2 shows an example of this type of failures near Prackovice nad Labem located to the north of the area of interest.

The papers by Pašek and Janek (1972), see Fig. 3, and by Pašek et al. (1972) were written following initial studies of the route. These reports and, many others, formed the background data of our conceptual model. They present, among others, ideas about the type and spatial distribution of landslides and concluded that a detailed determination of the residual shear strength of clays was required. According to the tests the shear strengths are in the order of $\varphi r' = 14°$. In the conclusion, Pašek and Janek (1972) state that although the D8 motorway route is technically demanding, it is feasible. At the time of the detailed investigation for the motorway construction, sufficient information was available for the development of an appropriate conceptual model, which should have necessarily contained information on the fact that the study area had been affected by landslides of various ages. This information could have been used when generating an observational model in the following project stage.
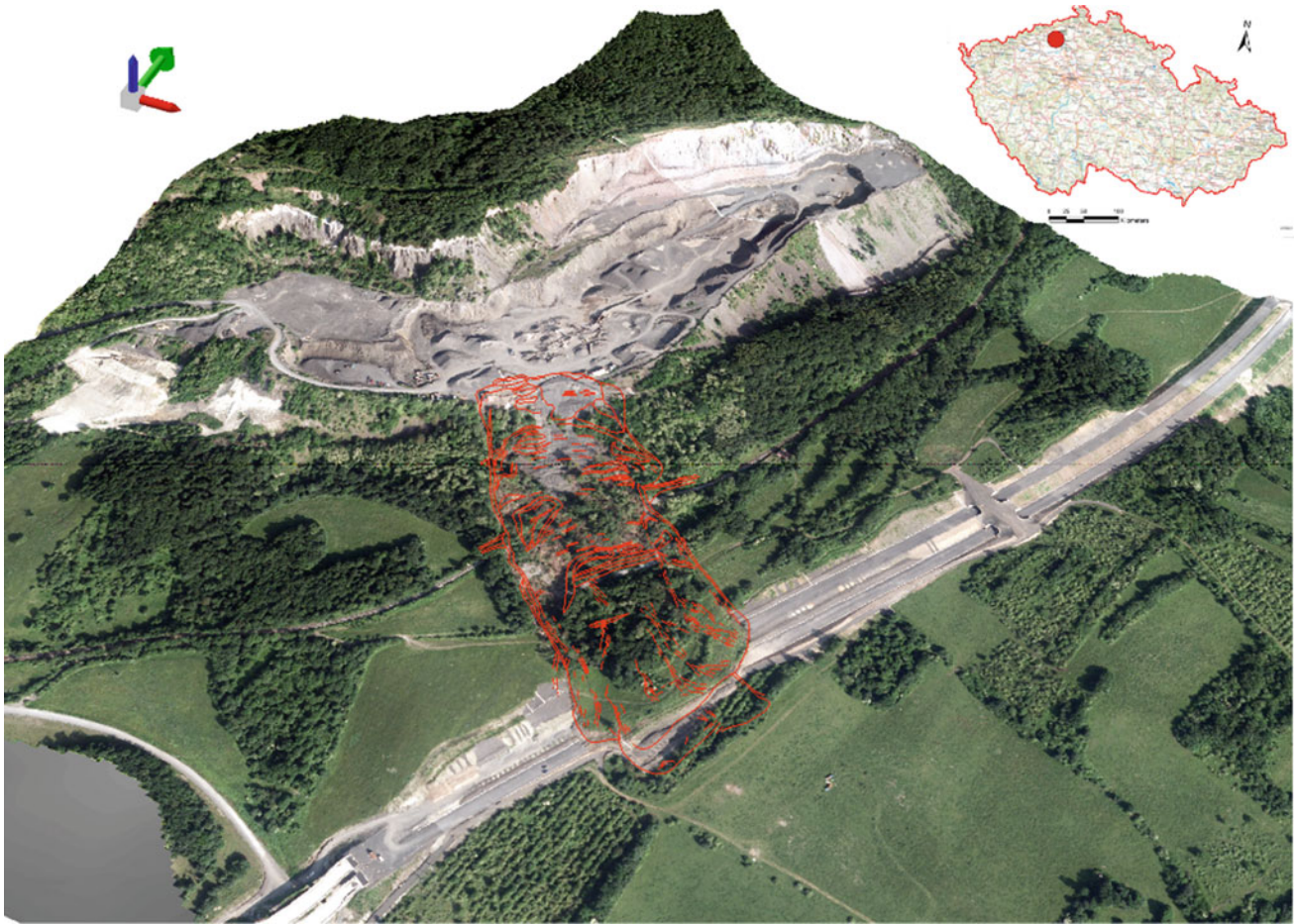
Fig. 1 3D morphological model of the area of interest and its location in the Czech Republic. *Data source* ČÚZK (*Czech Land Surveying and Cadastre Office*)

Fig. 2 Conceptual model of the Prackovice slide area according to Rybář (2005)
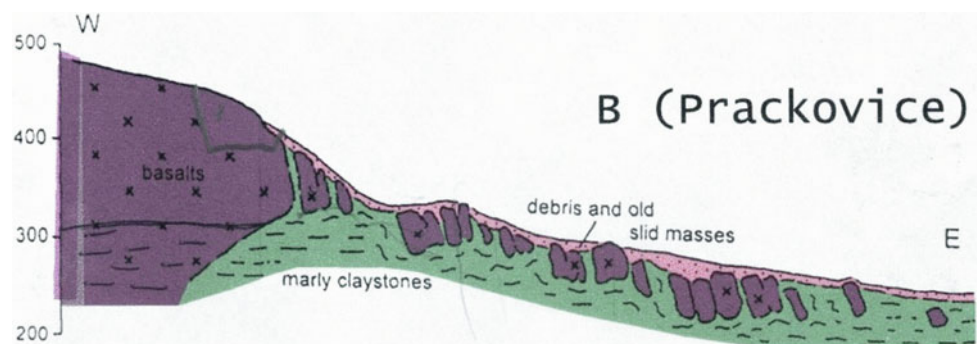
Unfortunately, investigations for D8 motorway construction did not use the above-mentioned conceptual model, which warns about the instability of slopes, as it can be seen from the distribution of exploratory boreholes of these investigations (Fig. 4). The boreholes are distributed unsuitably in a regular manner only within the strip of the body of motorway with spacing of 200 m and, in addition, with an insufficient depth (from 6 to 12 m). Consequently, in the area of the landslide there was only one exploratory borehole J646, 12 m deep which was insufficient. At other investigation stages the investor required calculations of the local stability of road cuts only. The investigation did not

Fig. 3 Cut-out of the engineering geological map manuscript (Pašek and Janek 1972) with the already known partial landslide (red) approximately in the area of the future slide of Dobkovičky (black) geo-referenced over the map of 1:10 000 scale with the apparent course of the motorway

Fig. 4 Distribution of exploratory boreholes in detailed and additional surveys for the construction of D8 motorway
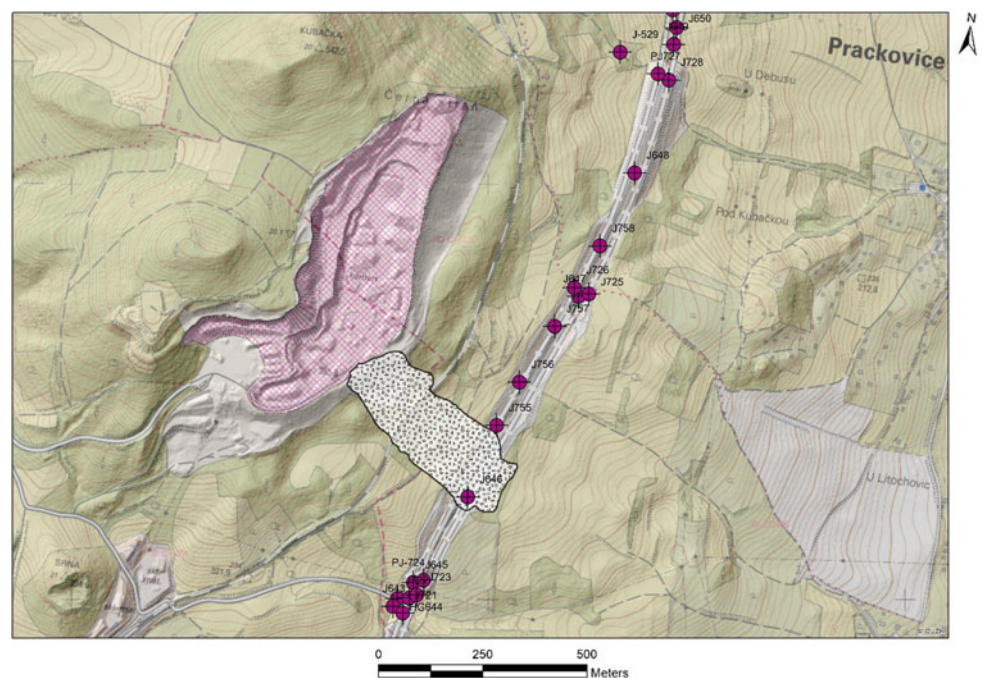
assess interaction of the construction with the larger-scale terrain, but it only dealt with the immediate ground in the vicinity of the construction sites. Therefore, the subsequent calculation models of the slope stability were evaluated in the context of the local stability of cut slopes and not in the context of the wider surroundings.

3 Description of the Dobkovičky Slope Deformation

Ground investigations for the construction of D8 motorway was carried out in a routine manner (see above), and did not use the conceptual approach during either the investigation or design phase. This oversight resulted in the landslide occurring during construction. The "Dobkovičky" landslide occurred on a southeast facing slope to the north of the town of Dobkovičky, during the night of 6/7 June 2013. The final form of the landslide was a flow slide ca. 180–200 m wide and ca. 500 m long with a flat, in some places composite shear surface at a depth of 3–8 m. The head scarp of the slide was situated at an elevation of ca. 375 m above sea level and the toe reached approximately 285 m above sea level. At the time of its occurrence, the landslide block was saturated as evidenced by ponded water in topographic depressions. A spring appeared at the toe of landslide and its yield was 3 l/s for a period of ca. 3 months. The landslide was characterized by an expressive head scarp in a horseshoe shape, as well as with a significant toe of the landslide (Fig. 5).

The slide affected equipment of the Dobkovičky quarry, including a part of the crushed aggregate storage facility. It destroyed a section of the Lovosice—Teplice railway line (the railway was moved downslope by ca. 40 m) and it blocked the D8 motorway which was under construction at the stationing from km 56.300 to 56.500. The total horizontal shift in the landslide longitudinal body axis was approximately 50 m in the centreline and 46 m at the north edge and 55 m at the south edge. The landslide block continued to move for 4 days. During the first day, the block crept by ca. 20 m and it filled the motorway cut (Figs. 6 and 7), the next day the block moved at a constant speed of ca. 1 m/h. When the movement stopped, it was apparent that initially the landslide toe first filled the motorway cutting but subsequently a shear surface developed below the motorway. The construction work of the motorway was interrupted for a period of 29 months.

On the basis of the results of the archival data study, it was apparent that the current landslide followed the older mapped slope deformation (Pašek et al. 1972).

4 Observational Model Generation

The observational model generated after the landslide occurred was designed to describe, as exactly as possible, the genesis, properties, and behaviour of the engineering geological setting, particularly the landslide and its near surroundings. In addition, the model integrated the wider area in relation to the areas of predisposition for slope movements. The overall geological structure taking into account its origin in the wider surroundings was first evaluated and then, by following the rules for the 3D model generation, quasi-homogeneous units were determined. These units represented the geology in the required detail to allow for individual subsequent models to simulate specific processes in the area of interest.

Fig. 5 Detailed manuscript map of geomorphologic shapes of the Dobkovičky landslide (Kycl 2014)
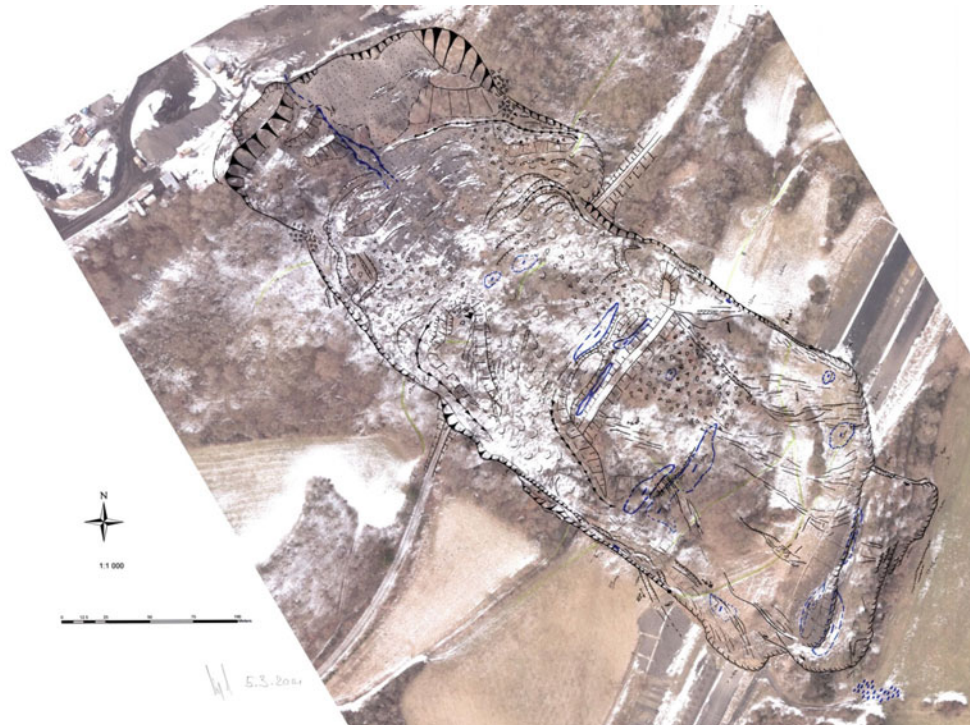
Fig. 6 Aerial view of the Dobkovičky landslide on 7th June 2013 (photo by F. Zukerstein)

Fig. 7 Landslide toe filled the motorway cut on the first day of sliding. Further movement of aprox. 35 m took place over the following three days

Data sources included exploratory boreholes as well as satellite radar interferometry and LiDAR. The area was first modelled without the motorway cutting and the landslide. It was then modelled with motorway cutting and landslide. The authors of the engineering geological model, in collaboration with the authors of the subsequent numerical model, proposed characteristic engineering geological values for each engineering geological unit.

The basis for studying the rock environment are the morphological models of the area of interest—DTM before and after the landslide (ČÚZK Digital Terrain Model 5th generation). 51 exploratory boreholes were selected to generate the observational engineering geological model.

Many of the selected boreholes, were drilled over a time range of ca. 20 years by various entities and the description of lithological units was of varying detail and in some cases, was later shown to be incorrect.

Before generating the model, it was necessary to consult specialists who would use the model for subsequent numerical models. These consultations included discussions of how detailed the description of lithostratigraphic units should be when developing the quasi-homogeneous units.

Based on these discussions and the character of the lithostratigraphic units documented in individual boreholes, it was decided that 6 basic lithologic units would be used. These include (with decreasing depth): marlstone, weathered marlstone, tuff, basalt, coarse-grained colluvium, and fine-grained colluvium. For the subsequent numerical model, very coarse grained (debris) colluvium was used as a separate unit in the coarse-grained colluvium. This very coarse-grained colluvium consisted of highly weathered and fractured rocks located in the faulted shallow zone of the basalt mass on the steep slope below the edge of the Dobkovičky quarry.

The very complicated structure is caused by the fact that in the geological past the quasi-homogenous unit of the weathered marlstone was affected by ancient slope movements in various places several times. Therefore, a unit of the lower fine-grained colluvium, created from transferred masses of weathered marlstone and, locally, also from tuffaceous rocks, was defined.

Another complication was that the irregular distribution of exploratory boreholes and their variable depth ranges were not ideal for generating the 3D model geometry. This was solved by inserting hypothetical boreholes in the areas not covered by exploratory boreholes, where the application of geostatistics methods would not provide correct results. Before generating a 3D model, it was first necessary to start a partial interpretation of dozens of 2D sections between selected boreholes, and only then to start generating a comprehensive 3D geometry of quasi-homogeneous units of the engineering geological model.

Individual pre-Quaternary lithostratigraphic units, representing the quasi-homogeneous units of the model, are shown in Fig. 8 (left side). The geometry of the model was constructed in software GMS (Aquaveo, USA) and transferred into geotechnical quasihomogenous units in geotechnical software MIDAS GTS NX. A full geometry of the rock environment model including Quaternary Formations is shown in Fig. 8 to the right (MIDAS GTS NX).

The investigations undertaken before the landslide did not encounter groundwater level and it was assumed to be at a depth of 25 m. The conceptual model suggests that this assumption was incorrect, and this was confirmed by the observational model.

The observational model included the determination of geotechnical values for the calculation model. The determination of geomechanical properties, particularly in
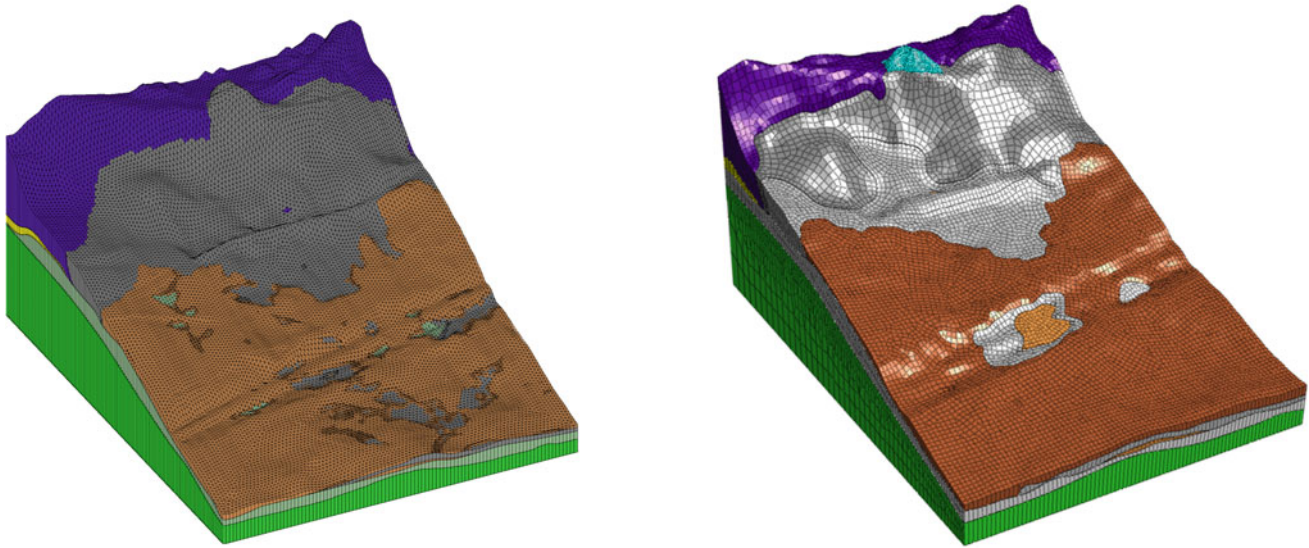
colluvial deposits, which are quite variable as to grain size, was very problematic. Effective residual values $\phi r = 14$ ($cr = 0$ kPa) were determined using laboratory analyses taking into account the experience with similar materials for lower fine-grained colluvium representing soil, where a shear surface was developed.

The engineering geological model described above was compiled with regard to the overall conception of solving the landslide remediation, and to assist with other modelling in particular, a hydrological precipitation-drain model, a hydrogeological model, and calculation models of slope stability.

5 Conclusion

Failure to apply an appropriate conceptual model during the investigation and design work led to a landslide which significantly delayed the construction of the D8 motorway. The information on the hazard of the area to instability was known prior to construction. A correctly applied conceptual model taking the hazard of the area to instability into consideration would have served for a functional and effective design for the site investigation which would have not been concentrated only along the road centreline. The application of the correct conceptual model would have also helped in communication with the investor as it could have been explained that in such geological conditions it is not appropriate to assume a routine site assessment and that sufficient time would be required to evaluate the complex geologic and geomorphologic issues. An important factor is the collaboration with the specialists preparing the subsequent numerical models, as well as the determination of appropriate geotechnical parameters. Only by using the described approach was it possible to generate the engineering geological model, which characterizes the interaction of the geological environment with the construction.

References

Baynes, F.J: Sources of geotechnical risk. Q. J. Eng. Geol. Hydrogeol. Geol. Soc. London, **43**(3), 321–331 (2010). https://doi.org/10.1144/1470-9236/08-003. ISSN 1470-9236

Digital Terrain Model 5th Generation: [on line]. ČÚZK [cit. 25.11.2017] (2016) Accessible from http://ags.cuzk.cz/dmr/

Kycl, P.: Geomorphological Map of Dobkovičky Landslide, Manuscript March 2014. CGS (2014)

Novotný, J.: Engineering geological models—some examples of use for landslide assessments. In: Lollino, G. et al. (eds.) 12th IAEG Congress Torino 2014, Engineering Geology for Society and Territory, vol. 7, pp. 11–15. Springer International Publishing Switzerland (2014). https://doi.org/10.1007/978-3-319-09303-1_2

Parry, S., Baynes, F.J., Culshaw, M.G., Eggers, M., Keaton, J.F., Lentfer, K., Novotný, J., Paul, D.: Engineering geological models: an introduction. Bull. Eng. Geol. Environ. [online]. **73**(3), 689–706 (2014). [cit. 2017-06-04]. https://doi.org/10.1007/s10064-014-0576-x. ISSN 14359529. Accessible from: http://link.springer.com/10.1007/s10064-014-0576-x

Parry, S. Baynes, J.F., Novotný, J. (in print): Conceptual engineering geological models. In: XIII IAEG Congress—San Francisco 2018. Engineering Geology for a Sustainable World, San Francisco, 17–21 Sept 2018

Pašek, J., Janek, J., Hroch, Z., Francek, J.: Engineering Geological Survey of D8 Motorway in part Chotiměř—Radejčín, km 62.2–67.8, II. stage. Final Report of Geological Institute of Czechoslovak Academy of Sciences Praha and (in Czech) Inženýrskogeologický průzkum dálnice D8 v úseku Chotiměř—Radejčín, km 62.2–67.8. II. etapa. MS Geologický ústav ČSAV—Stavební geologie, n. p. Praha (1972)

Pašek, J., Janek, J.: Engineering Geological Survey of D8 Motorway in part Chotiměř—Radejčín, km 62.2—67.8, I. stage. Final Report of Geological Institute of Czechoslovak Academy of Sciences Prague (in Czech) Inženýrskogeologický průzkum dálnice D8 v úseku Chotiměř—Radejčín, km 62.2—67.8. I. etapa. MS Geologický ústav ČSAV Praha (1972)

Rybář, J., Nemčok, A.: Landslide investigation in Czechoslovakia. In: Proceedings of the 1st Session of the International Association of Engineering Geology, pp. 183–198, Prague (1968)

Rybář, J.: Examples of deep-seated slope movements in Bohemian Massif. In: Moser, M. (ed.) Proceedings of 15th Conference on Engineering Geology, Erlangen, 06–09 Apr 2005

Schumm, S.A.: To Interpret the Earth: Ten Ways to Be Wrong. Cambridge University Press, Cambridge (1991)

Stapledon, D.H.: Subsurface engineering—in search of a rational approach. Aust. Geomech. News. **4**, 26–33 (1982)

Sullivan, T.D.: The geological model. In: Williams, A.L. et al. Geologically Active: Proceedings of the 11th Congress of the International Association for Engineering Geology and the Environment, Auckland, New Zealand, pp. 155–170. CRC Press, London (2010)

Varnes, D.J.: The Logic of Geological Maps, with Reference to Their Interpretation and use for Engineering Purposes.: Professional Paper 837. United States Geological Survey, Washington (1974)

Author Index